THE PRO-INFLAMMATORY ROLE OF COPPER IN CHEMOKINE MULTIMERISATION AND THE POTENTIAL OF COPPER CHELATORS AS ANTI-INFLAMMATORY AGENTS

Helen Jane MacGregor

This thesis is submitted in partial fulfilment of the requirements for the award of the degree of Doctor of Philosophy of the University of Portsmouth

May 2009

University of Portsmouth

Doctor of Philosophy

THE PRO-INFLAMMATORY ROLE OF COPPER IN CHEMOKINE MULTIMERISATION AND THE POTENTIAL OF COPPER CHELATORS AS ANTI-INFLAMMATORY AGENTS

By Helen Jane MacGregor

Abstract

During inflammatory reactions, leukocytes migrate from the circulation into extra-vascular tissues. Chemokines, 7-10 KDa proteins, immobilised on the endothelial cell surface bound to glycosaminoglycans, such as heparan sulphate, on proteoglycans have been implicated in this process. Evidence suggests that chemokines are functional in multimeric form bound to heparan sulphate. In this form, endothelial bound RANTES is a T-cell, monocyte and eosinophil chemoattractant. T-cell accumulation in respiratory tissue is a feature of asthma, cystic fibrosis and chronic obstructive pulmonary disease where T-cell derived cytokines orchestrate the inflammatory response. Central to inflammation, platelets migrate into tissues, augmenting the inflammatory response by degranulating and releasing their contents, including RANTES on activation. Since both copper and dityrosine links have been implicated in the multimerisation of the amyloid protein in Alzheimer's disease, chemokines including RANTES, IL-8 and ENA-78 were investigated for the possibility of copper-induced dityrosine formation within chemokine multimers. The addition of $CuCl_2$ and H_2O_2 to human recombinant RANTES induces multimerisation and dityrosine cross-linking, confirmed by fluorimetry, liquid chromatography mass spectroscopy and staining Western blots with a dityrosine specific monoclonal antibody. In addition, RANTES multimers actively induce chemotaxis in Boyden chambers. This finding led to the investigation of the T-cell response to endothelial and platelet derived RANTES in the absence and presence of copper chelators as potential anti-inflammatory agents in transendothelial migration assays, a physiological model of the vascular endothelium. Migration of activated T-cells across monolayers of human lung microvascular endothelial cells was RANTES-dependent and RANTES derived from thrombin stimulated platelets is active as a T-cell chemoattractant in this model of the lung microvascular endothelium. The copper chelators neocuproine, bathocuproine, D-penicillamine and tobramycin significantly inhibited T-cell migration indicating a pro-inflammatory role for copper and suggesting the use of copper chelators as potential anti-inflammatory agents.

Publications

MacGregor, H., Kato, Y., Nevell, T. and Shute J. K (2008). Copper induces dityrosine cross-linked oligomers of RANTES. *Am. J. Resp. Crit. Care Med.*, **177**: A76.

MacGregor, H., Kato, Y., Marshall, L. J., Laight, D., Nevell T. and Shute, J. K. (2009). Platelet-derived RANTES-induced T-cell migration is copper dependent and inhibited by the copper chelators tobramycin and D-penicillamine. *Nat. Med.,* Submitted.

Presentations

MacGregor, H., Kato, Y., Nevell, T., Shute, J. K. (2009). Platelet-derived RANTES-induced T-cell migration is copper dependent. *Biochemical Society meeting; The biochemical basis of Respiratory Disease.*

Declaration

I declare that while registered as a candidate for the degree of Doctor of Philosophy of the University of Portsmouth, I have not been registered for any other research award. The results and conclusions embodied in this thesis are the work of the named candidate and have not been submitted for any other academic award.

Helen MacGregor

May 2009

Acknowledgements

I would firstly like to sincerely thank Dr. Jan Shute for her supervision, help, guidance and critical evaluation of my work during the undertaking of this project. Thanks go to the Institute of Biomedical and Biomolecular Sciences for funding this research and also to Dr. Yoji Kato for his input to the study. I would also like to thank Dr. Brian Carpenter, Dr. Roz Gibbs, Dr. Andy Holt and Dr. David Laight for their assistance and advice. In addition, I would like to thank my friends and family for their support and also all of my volunteer blood donors, without whom this research would not have been possible.

Table of Contents

List of Figures

List of Tables

Abbreviations

2-ME:	2-mercaptoethanol
ABTS:	2,2'-Azino-bis(3-ethylbenzthiazoline-6-sulfonic acid
AD:	Alzheimer's disease
ADP:	Adenine diphosphate
ANOVA:	Analysis of variance
AP-1:	Activator protein-1
APC:	Antigen presenting cell
APP:	Amyloid protein precursor
APS:	Ammonium persulphate
ARDS:	Adult respiratory distress syndrome
ATP:	Adenine triphosphate
Aβ:	Amyloid-beta
BCA:	B-cell attracting chemokine
BCDS:	Bathocuproine disodium salt
BSA:	Bovine serum albumin
BSE:	Bovine spongiform encephalopathy
CCL:	CC Ligand
CCR:	CC Receptor
CF:	Cystic fibrosis
CJD:	Creutzfeldt-Jakob Disease
CK:	Chemokine
CLA:	Conjugated linoleic acid
COPD:	Chronic obstructive pulmonary disease
CTL:	Cytotoxic T-lymphocyte
CX3CL:	CX3C Ligand
CX3CR:	CX3C Receptor
CXCL:	CXC Ligand
CXCR:	CXC Receptor
DARC:	Duffy antigen receptor complex
DC:	Dendritic cell
DiY:	Dityrosine
DMSO:	Dimethyl sulphoxide
dp:	depolymerisation
D-Pen:	D-penicillamine
DTT:	Dithiothreitol
EBM:	Endothelial basal medium
ECL:	Enhanced chemiluminescence
ECM:	Extracellular matrix
EDTA:	Ethylenediaminetetraacetic acid
EGF:	Epidermal growth factor
EGM:	Endothelial growth medium
ELC:	EBI1 ligand chemokine
ELISA:	Enzyme-linked immunosorbent assay
ENA-78:	Epithelial cell derived neutrophil attractant-78
EPC:	Endothelial progenitor cell
ESI:	Electrospray ionisation
ESL-1:	E-selectin ligand-1
EtOH:	Ethanol
FCS:	Foetal calf serum

GAG:	Glycosaminoglycan
GCP:	Granulocyte chemotactic protein
G-HCl:	Guanidine hydrochloride
GPCR:	G-protein-coupled receptor
GRO:	Growth regulated oncogene
HBSS:	Hanks balanced salt solution
HLMVEC:	Human lung microvascular endothelial cell
HMMEC:	Human mucosal microvascular endothelial cell
hpf:	High powered field
HPLC:	High performance liquid chromatography
HRP:	Horseradish peroxidase
HS:	Heparan sulphate
HSPG:	Heparan sulphate proteoglycan
HUVEC:	Human umbilical vein endothelial cell
ICAM:	Intracellular adhesion molecule
IFN:	Interferon
Ig:	Immunoglubulin
IKK:	I kappa B kinase complex
IL:	Interleukin
IP-10:	Interferon-inducible protein-10
IS:	Internal standard
JAM:	Junctional adhesion molecule
JNK:	c-Jun N-terminal kinase
LARC:	Liver and activation-related chemokine
LCMS/MS:	Liquid chromatography mass spectroscopy/mass spectroscopy
LDH:	Lactase dehydrogenase
LFA-1:	Lymphocyte-associated function antigen-1
LPS:	Lipopolysaccharide
MAC-1:	Macrophage antigen-1
MAPK:	Mitogen-activated protein kinase
MCP:	Monocyte chemotactic protein
MDC:	Macrophage-derived chemokine
MHC:	Major histocompatibility complex
MIP:	Macrophage inflammatory protein
MMP:	Metalloprotease
MRM:	Multiple reaction monitoring
NADPH:	Nicotinamide adenine dinucleotide phosphate
NAP-2:	Neutrophil-activating peptide-2
NC:	Neocuproine
NDST:	N-deacetylase/N-sulphotransferase
NF-kB:	Nuclear factor kappa B
NO:	Nitric oxide
NOS:	Nitric oxide synthase
PA:	Plasminogen activator
PAF:	Platelet activating factor
PAI-1:	Plasminogen activator inhibitor-1
PAR:	Protease-activated receptor
PBMC:	Peripheral blood mononuclear cell
PBS:	Phosphate buffered saline
PECAM-1:	Platelet/endothelial-cell adhesion molecule-1
PET:	Polyethylene terephthalate

PHA:	Phytohaemagglutinin
PI:	Phosphatidylinositol
PrP^{C}:	Prion protein (normal)
PrP^{SC}	Prion protein (scrapie)
PSGL-1:	P-selectin glycoprotein ligand-1
PTK:	Protein tyrosine kinase
RA:	Rheumatoid Arthritis
RANTES:	Regulated on Activation T-cell expressed and Secreted
ROS:	Reactive oxygen species
SC:	Sodium chlorate
SDF:	Stromal cell derived factor
SDS:	Sodium dodecyl sulphate
SDS-PAGE:	Sodium dodecyl sulphate polyacrylamide gel electrophoresis
SLC:	Secondary lymphoid tissue chemokine
SOD:	Superoxide dismutase
SSAO:	Semicarbazide sensitive amine oxidase
TARC:	Thymus and activation-regulated chemokine
Tc1:	Cytotoxic T-cell type 1
Tc2:	Cytotoxic T-cell type 2
TE:	Trypsin/EDTA
TEMED:	N,N,N',N' – tetramethylethylenediamine
TFA:	Tetrafluoroacetic acid
Th1:	T-helper cell type 1
Th2:	T-helper cell type 2
TIMP:	Tissue inhibitor of matrix metalloproteinase
TMB:	Tetramethylbenzidine
TNF:	Tumor necrosis factor
TNS:	Trypsin neutralising solution
Tob:	Tobramycin
TTM:	Tetrathiomolybdate
Tyr:	Tyrosine
UHQ:	Ultra high quality water
VAP-1:	Vascular adhesion protein-1
VCAM:	Vascular cellular adhesion molecule
VLA-4:	Very late antigen-4
WR:	Working reagent
Y:	Tyrosine

Chapter 1

General Introduction

1. General Introduction

1.1. Leukocyte recruitment across the vascular endothelium

The endothelium is the first barrier to leukocyte recruitment to tissue sites of inflammation, a process that is mediated through the interaction of inflammatory cells with endothelial cell adhesion molecules and chemoattractants (Butcher, 1991). The transendothelial migration of leukocytes from the blood, across the endothelial monolayer and basement membrane into the underlying tissue is an important component of the normal inflammatory process, and is also important for some inflammatory disease states.

The vascular endothelium is a continuous single-cell lining of the cardiovascular system that forms a critical interface between the blood and its components on one side and the tissues and organs on the other (Gimbrone, 1987). The vascular endothelium is central to the cellular and molecular events that initiate the response of the body to infection, immune reactions and tissue injury (Rao *et al*, 2007). Endothelial cell activation by a variety of stimuli including the pro-inflammatory cytokines interleukin (IL)-β1, tumor necrosis factor (TNF)-α and interferon (IFN)-γ leads to local thrombosis, loss of vessel barrier function and leukocyte recruitment, a fundamental event in the inflammatory response that localises blood leukocyte subsets to tissues and organs through endothelial mechanisms (Gimbrone, 1999).

Leukocyte recruitment is a multi-step process (see Figure 1.1) involving adhesion molecules that support leukocyte tethering (step 1), firm adhesion (step 2) and transmigration (step 3). The migration of leukocytes across the endothelium is referred to as chemotaxis. This is the directional motility of leukocytes along a gradient of cellular adhesion sites or toward a chemical attractant (chemoattractant). Chemotaxis is the sum of the cell migration induced by soluble (chemotactic) and surface bound (haptotactic) gradients of the attractant. Haptotaxis refers to the side-side movements of cells in response to surface-bound chemoattractant (Rot, 1993).

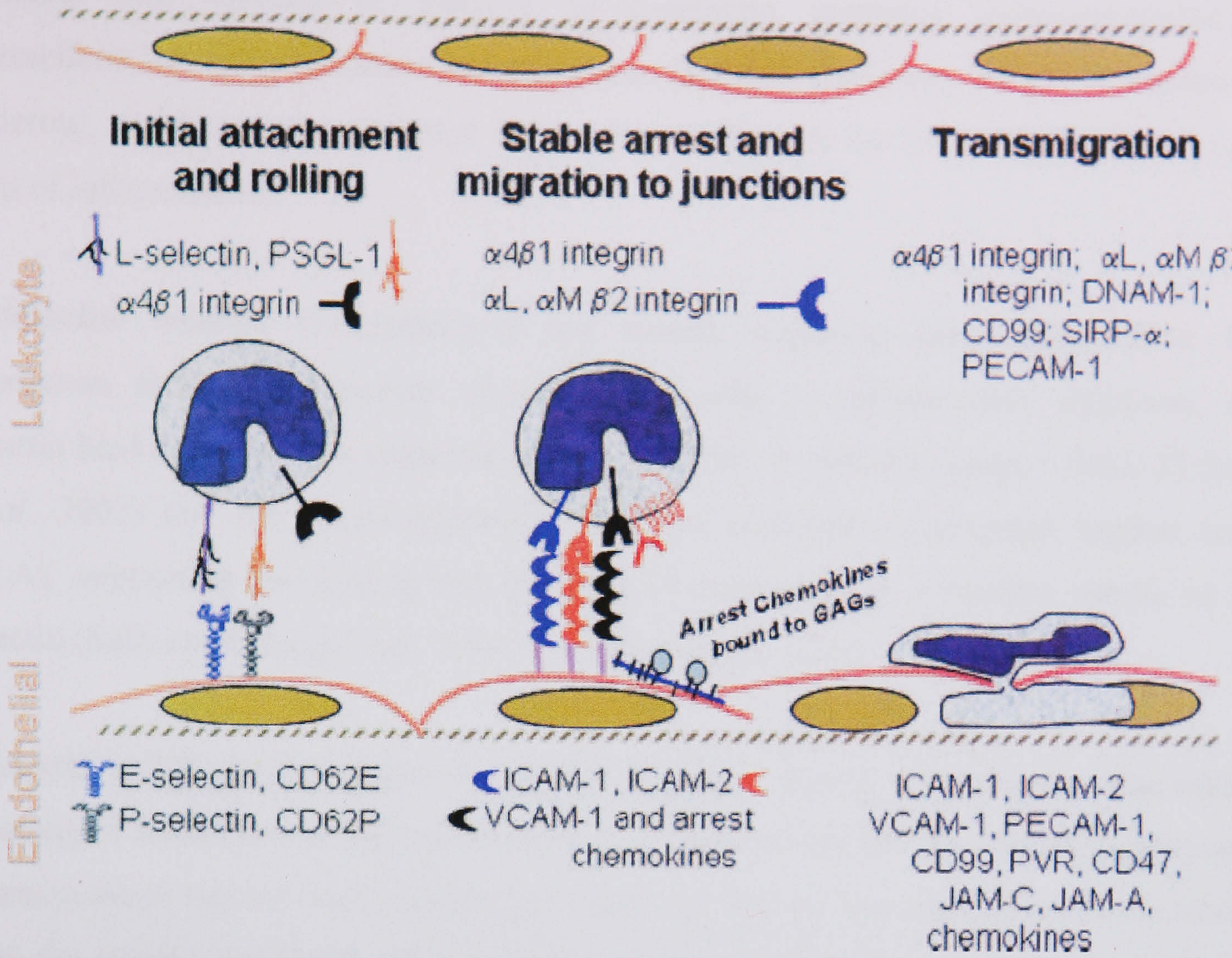

Figure 1.1. The multistep process of leukocyte recruitment. Initial attachment and rolling, arrest, and migration to cell–cell borders and transmigration across the vascular endothelium, shown here for monocytes. The leukocytes initially attach via selectin-mediated mechanisms along with contributions from the α4 and β2 integrins interacting with their ligands VCAM-1 and ICAM-1, respectively. The next step is stable arrest; β2-integrins become activated by arrest chemokines and trigger cell arrest at or near cell–cell junctions. Leukocytes then migrate to junctions and transmigrate across the vascular endothelium at both junctional and nonjunctional locations. The symbols used to represent adhesion molecules in endothelial cells are identified below each component of the figure (Rao *et al*, 2007).

The first event to occur in chemotaxis is leukocyte tethering and rolling on the endothelium (step 1), which is classically mediated by endothelial cell expressed selectins, and interactions with their leukocyte expressed ligands. There are three types of selectin. Leukocyte selectin (L-selectin) is found on leukocytes, and binds to endothelial ligands such as CD34, a sialomucin highly expressed in lymph nodes. Endothelial ligands are often induced by lipopolysaccharide (LPS) or cytokine exposure (Wagner & Roth, 2000). Platelet selectin (P-selectin) is expressed by endothelial cells in response to inflammatory stimuli. Stored intra-cellularly in endothelial cells and also in platelets, it is mobilised to the cell surface, and binds to P-selectin glycoprotein ligand-1 (PSGL-1) on leukocytes, although PSGL-1 has a dominant role as a ligand for all three selectins (Ley *et al*, 2007). L-selectin binding occurs first and is more rapid and short lived than P-selectin binding and reversible if additional adhesive events are not soon

invoked. The binding of PSGL-1 to L-selectin mediates leukocyte-leukocyte interactions, by which adherent leukocytes can facilitate secondary leukocyte capture or tethering, enabling leukocytes that do not express ligands for E- or P-selectin to reach sites of inflammation.

Endothelial selectin (E-selectin) is not stored, requiring gene transcription for expression following exposure of endothelial cells to inflammatory cytokines. E-selectin binds to leukocyte expressed PSGL-1, CD44, E-selectin ligand-1 (ESL-1) (Ley *et al*, 2007) and the T-cell expressed adhesion molecule, conjugated linoleic acid (CLA), supporting the rolling and tethering of leukocytes in a fashion similar to P-selectin (Sallusto & Baggiolini, 2008; Wagner & Roth, 2000).

L-selectin and P-selectin initiate the migration process during inflammation. The initial tethering of leukocytes to the endothelium is a weak interaction that, without additional adhesion steps, cannot lead to leukocyte migration. Due to the shear stress of the blood flow, the selectin-mediated adhesion results in leukocyte rolling on the endothelial cell surface (Rot *et al*, 1996). These reversible selectin-ligand interactions allow time for leukocytes to associate with endothelial cells and respond to stimuli on the endothelial surface.

The interactions of selectins with their ligands enables leukocytes to adhere to inflamed endothelium under conditions of flow as they bind with high on- and off-rates, the speed at which bonds are formed and broken (Ley *et al*, 2007). Chemokines, a large super-family of proteins with chemotactic properties and molecular masses of between 7 and 10 KDa, are immobilised on the luminal endothelial cell surface, bound by glycosaminoglycans and presented to the rolling leukocytes. This mechanism allows the exposure to chemokines of only those leukocytes that have already established their first adhesive interaction with the endothelium. Soluble chemokines would activate leukocytes in the circulation before their adhesion to the endothelial surface, blocking migration (Rot *et al*, 1996). Chemokine signalling through G-protein coupled receptors (GPCRs) leads to expression and activation of leukocyte integrins and results in firm adhesion (step 2).

Integrins are glycoproteins found on leukocytes that mediate cell-cell adhesion during cell recruitment. The CD18 containing integrins (β2-integrins) such as the T-cell expressed lymphocyte-associated function antigen-1 (LFA-1) mediate binding to activated endothelium. Intercellular adhesion molecules (ICAMs) on endothelial cells are ligands for integrins on leukocytes. The intercellular adhesion molecules ICAM-1 and ICAM-2 can bind to the β2-integrins such as macrophage antigen-1 (MAC-1) or the T-cell expressed integrin LFA-1 (Wagner & Roth, 2000). Vascular cell adhesion molecule-1 (VCAM-1) is another Ig-like molecule found on endothelial cells, binding selectively to β1-integrins (CD29) such as VLA-4, or $\alpha_4\beta_1$ expressed by T-cells, rather than β2-integrins (CD18) (Davenpeck *et al*, 1998; Reinhardt *et al*, 1997; Sallusto & Baggiolini, 2008).

L-selectin and T-cell PSGL-1 can activate CD18 (β2) integrins on inflammatory cells. Prolonged engagement of endothelial ICAM-1 with integrin ligands causes further expression of both ICAM-1 and VCAM-1 on endothelial cells (Clayton *et al*, 1998). Thus, T-cell migration *in vivo* might involve both ICAM-1 and VCAM-1 adhesive pathways.

Following arrest, leukocytes migrate into tissues either through or between the endothelial cell barrier and its associated basement membrane and pericyte sheath, a process known as transmigration (step 3). The ligation of intercellular adhesion molecules and integrins triggers the extension of leukocyte membrane protrusions into the endothelial cell body and endothelial cell junctions. Leukocyte migration can occur through the paracellular or transcellular route.

Paracellular migration through endothelial junctions involves the release of endothelial-expressed vascular endothelial cadherin (VE-cadherin) and is facilitated by endothelial cell junctional molecules localised at the borders between adjacent endothelial cells such as platelet/endothelial-cell adhesion molecule-1 (PECAM-1), the junctional adhesion molecules (JAM) A, B and C or ICAM-2 (Marelli-Berg *et al*, 2008). Leukocytes migrate through endothelial cell monolayers at tricellular junctions. Transmigration occurs through leukocyte spreading and diapedesis, associated with pseudopod formation (Sallusto & Baggiolini, 2008).

Transcellular migration occurs in thin parts of the endothelium where there is less distance to migrate and involves actin and caveolae containing ICAM-1 molecules that form an intracellular channel through which leukocytes can migrate. The paracellular route is generally considered the principal route of leukocyte extravasation. Migration through the basement membrane and pericyte sheath can occur through gaps between adjacent pericytes and regions of low protein disposition within the extracellular matrix (ECM) (Ley *et al*, 2007). This response is facilitated by $\alpha_6\beta_1$-integrin and proteases since adhesion and migration is accompanied by release of leukocyte proteases, such as matrix metalloproteases (MMPs) and heparanases. These enzymes are capable of digesting collagen, laminin and proteoglycans of the dense basement membrane amongst other extracellular components present in the vascular wall.

1.2. Chemokines

The chemotaxis process is predominantly directed by chemokines. These molecules play a key role in the selective activation and recruitment of a large variety of cell types in inflammation, inducing changes in shape, a transient rise in intracellular free Ca^{2+}, granule exocytosis, integrin upregulation, formation of bioactive lipids and mediating the respiratory burst (Wells *et al*, 1996).

Chemokines can be divided into subfamilies on the basis of structural motifs and are sub-classified according to the number and spacing of the conserved cysteines near the N terminus within their primary structure (Murphy, 2002). There are two major groups known as the CC and CXC classes, and two minor groups, the C and CX3C classes. The CXC, CC and CX3C chemokines all have four conserved cysteines, whereas C chemokines have only two, corresponding to the second and fourth cysteines in the other groups. CXC and CX3C chemokines are distinguished by the presence of one (CXC) or three (CX3C) amino acids between the first and second cysteines, whereas the first two cysteines of the CC chemokines are adjacent (Murphy *et al*, 2000).

The CXC cytokines, including interleukin-8 (IL-8), have been shown to have pro-inflammatory properties mainly through their actions on neutrophils, (Schall, 1991). The discovery of the neutrophil-targeted chemokine, IL-8, in 1987 represents a landmark in immunology because it was the first leukocyte subtype-selective chemoattractant to be found (Baggiolini & Dahinden, 1994; Walz *et al*, 1987;

Yoshimura *et al*, 1987). The discovery of IL-8 stimulated the search for new family members and functions for other chemokines in leukocyte chemotaxis (Murphy *et al*, 2000). Interest in the field grew with subsequent reports of monocyte chemotactic protein-1 (MCP-1), RANTES and eotaxin, the first important monocyte-, T-cell-, and eosinophil-directed chemokines (chemotactic cytokines), respectively (Jose *et al*, 1994; Matsushima *et al*, 1989; Schall *et al*, 1990; Yoshimura *et al*, 1989).

The majority of chemokines are highly potent and bind their receptors at nanomolar concentrations, exerting their physiological responses in the subnanomolar concentration range. Chemokines have been implicated in a variety of clinically important inflammatory diseases to include chronic diseases such as allergic asthma, psoriasis, atopic dermatitis, arthritis and atheroma (Wells *et al*, 1996).

1.3. Chemokine receptors

The *Bordella pertussis* (PT) toxin which specifically inhibits GTP-binding proteins prevents the responses of basophils, T-cells, eosinophils and monocytes to CC chemokines suggesting that this class of chemokines mediate their biological effects via interactions with GTP-protein coupled 7-transmembrane domain receptors (GPCRs) present on these cells. These receptors are comprised of approximately 350 amino acids, have a molecular weight of around 40 kDa and have a core domain consisting of seven trans-membrane helices (Baggiolini & Dahinden, 1994; Mellado *et al*, 2001).

The extra-cellular domain consists of the N-terminus and three extracellular loops that act together to bind the chemokine ligand. The intracellular region is comprised of three loops and the C-terminus which collaborate to transduce the chemokine signal (Mellado *et al*, 2001). Based on the amino acid sequence, GPCRs belong to the class A rhodopsin-like family. Chemokine receptors have a number of conserved motifs, including the DRYLAIV motif in the second intracellular loop domain which is necessary for receptor G-protein coupling and signal transduction events leading to a chemotactic response (Ward *et al*, 1998). As with the chemokines, chemokine receptors can be classified according to their structure. The four major families, CR, CCR, CXCR and CX3CR interact with C, CC, CXC and CX3C chemokines, respectively (Mellado *et al*, 2001). Following chemokine-receptor binding, a number of responses occur

including gene expression, cell polarisation and chemotaxis. Conformational changes in the trans-membrane domain are believed to be responsible for receptor activation.

A large variety of molecular mechanisms induce activation since these conformational changes are elicited by a wide variety of ligands including light, Ca^{2+}, pheromones, and small molecules (amino acids, amines, nucleotides, prostaglandins, peptides) or proteins (glycoproteins, interleukins and chemokines). It has been observed that chemokine receptors, like other GPCRs initiate their ligand-induced signalling cascades by receptor dimerisation and that many chemokine receptors induce signalling cascades via G-coupling and JAK/STAT as well as tyrosine and Ser/Thr kinase pathways (Mellado *et al*, 2001).

Receptor specificity is restricted to some extent by chemokine subfamily name (C, CC, CXC, CX3C). In general, the CXC chemokines such as IL-8, GRO-α, ENA-78 or platelet factor-4 (PF4) are potent chemoattractants and activators of neutrophils but not monocytes, whereas the CC chemokines such as MIP-1ß/1α, MCP-1 and RANTES exhibit chemoattractant potential for monocytes and lymphocytes but not neutrophils (Clore & Gronenborn, 1995). However, each receptor subtype typically binds multiple chemokines, and therefore receptor selectivity is more likely due to the distribution of hydrophobic sequences on the monomer surface since analysis of hydrophobicity shows that the distribution of hydrophobic regions is preserved in CC or CXC chemokines (Wells *et al*, 1996). Table 1.1 outlines the known chemokine receptors and their ligands, and shows that RANTES binds to CCR1, 3 and 5 receptors, mediating chemotaxis and activation of the various cell types bearing these receptors.

Table 1
CXC, C, CX_3C and CC chemokine/receptor families

Systematic name	Human chromosome	Human ligand	Mouse ligand	Chemokine receptor(s)
CXC chemokine/receptor family				
CXCL1	4q21.1	GROα/MGSA-α	GRO/MIP-2/KC?	CXCR2 > CXCR1
CXCL2	4q21.1	GROβ/MGSA-β	GRO/MIP-2/KC?	CXCR2
CXCL3	4q21.1	GROγ/MGSA-γ	GRO/MIP-2/KC?	CXCR2
CXCL4	4q21.1	PF4	PF4	Unknown
CXCL5	4q21.1	ENA-78	GCP-2/LIX?	CXCR2
CXCL6	4q21.1	GCP-2	GCP-2/LIX?	CXCR1, CXCR2
CXCL7	4q21.1	NAP-2	Unknown	CXCR2
CXCL8	4q21.1	IL-8	Unknown	CXCR1, CXCR2
CXCL9	4q21.1	Mig	Mig	CXCR3[a]
CXCL10	4q21.1	IP-10	IP-10/CRG-2	CXCR3[a]
CXCL11	4q21.1	I-TAC	I-TAC	CXCR3[a]
CXCL12	10q11.21	SDF-1 α/β	SDF-1/PBSF	CXCR4[b]
CXCL13	4q21.1	BCA-1	BLC	CXCR5
CXCL14	5q31.1	BRAK/bolekine	BRAK	Unknown
(CXCL15)		Unknown	Lungkine/WECHE	Unknown
CXCL16	17p13			CXCR6
C chemokine/receptor family				
XCL1	1q24.2	Lymphotactin/SCM-1α/ ATAC	Lymphotactin	XCR1
XCL2	1q24.2	SCM-1β	Unknown	XCR1
CX_3C *chemokine/receptor family*				
CX3CL1	16q13	Fractalkine	Neurotactin/ABCD-3	CX3CR1
CC chemokine/receptor family				
CCL1	17q11.2	I-309	TCA-3/P500	CCR8
CCL2	17q11.2	MCP-1/MCAF/TDCF	JE?	CCR2
CCL3	17q12	MIP-1α/LD78α	MIP-1α	CCR1, CCR5
CCL3L1	17q12	LD78β	Unknown	CCR1, CCR5
CCL4	17q12	MIP-1β	MIP-1β	CCR5[3]
CCL5	17q12	RANTES	RANTES	CCR1, CCR3, CCR5[c]
(CCL6)		Unknown	C10/MRP-1	Unknown
CCL7	17q11.2	MCP-3	MARC?	CCR1, CCR2, CCR3
CCL8	17q11.2	MCP-2	MCP-2?	CCR3, CCR5[c]
(CCL9/10)		Unknown	MRP-2/CCF18/MIP-1γ	CCR1
CCL11	17q11.2	Eotaxin	Eotaxin	CCR3
(CCL12)		Unknown	MCP-5	CCR2
CCL13	17q11.2	MCP-4	Unknown	CCR2, CCR3
CCL14	17q12	HCC-1	Unknown	CCR1, CCR5
CCL15	17q12	HCC-2/Lkn-1/MIP-1	Unknown	CCR1, CCR3
CCL16	17q12	HCC-4/LEC/LCC-1	Unknown	CCR1, CCR2
CCL17	16q13	TARC	TARC/ABCD-2	CCR4
CCL18	17q12	DC-CK1/PARC/AMAC-1	Unknown	Unknown
CCL19	9p13.3	MIP-3β/ELC/exodus-3	MIP-3β/ELC/exodus-3	CCR7[d]
CCL20	2q36.3	MIP-3α/LARC/exodus-1	MIP-3α/LARC/exodus-1	CCR6
CCL21	9p13.3	6Ckine/SLC/exodus-2	6Ckine/SLC/exodus-2/ TCA-4	CCR7[d]
CCL22	16q13	MDC/STCP-1	ABCD-1	CCR4
CCL23	17q12	MPIF-1/CKβ8/CKβ8-1	Unknown	CCR1
CCL24	7q11.23	Eotaxin-2/MPIF-2	MPIF-2	CCR3
CCL25	19p13.3	TECK	TECK	CCR9
CCL26	7q11.23	Eotaxin-3	Unknown	CCR3
CCL27	9p13.3	CTACK/ILC	ALP/CTACK/ILC/ESkine	CCR10
CCL28	5p12	MEC		CCR3/CCR10

[a] CD183.
[b] CD184.
[c] CD195.
[d] CD_w 197.

Table 1.1. Human chemokine receptor expression and ligand specificity (Murphy *et al*, 2003).

The following table (table 1.2.) outlines chemokine ligand-receptor specificity and inflammatory cell expression for some of the best known chemokines and inflammatory cells, to include B-cell attracting chemokine-1 (BCA-1); dendritic cells (DC); EBI1 ligand chemokine (ELC); epithelial-cell-derived neutrophil attractant-78 (ENA-78); granulocyte chemotactic protein-2 (GCP-2); growth-related oncogene (GRO); interleukin-8 (IL-8); interferon-inducible protein-10 (IP-10); interferon-inducible T-cell alpha chemoattractant (I-TAC); liver and activation-regulated chemokine (LARC); monocyte chemotactic protein-1 (MCP-1); macrophage-derived chemokine (MDC); monokine induced by interferon-γ (Mig); macrophage inflammatory protein-1α (MIP-1α); neutrophil-activating peptide-2 (NAP-2); stromal cell derived factor-1α (SDF-1α); secondary lymphoid tissue chemokine (SLC); thymus and activation-regulated chemokine (TARC); T-helper type 1 cell (Th1) and T-helper type 2 cell (Th2) (Sallusto *et al*, 1998a).

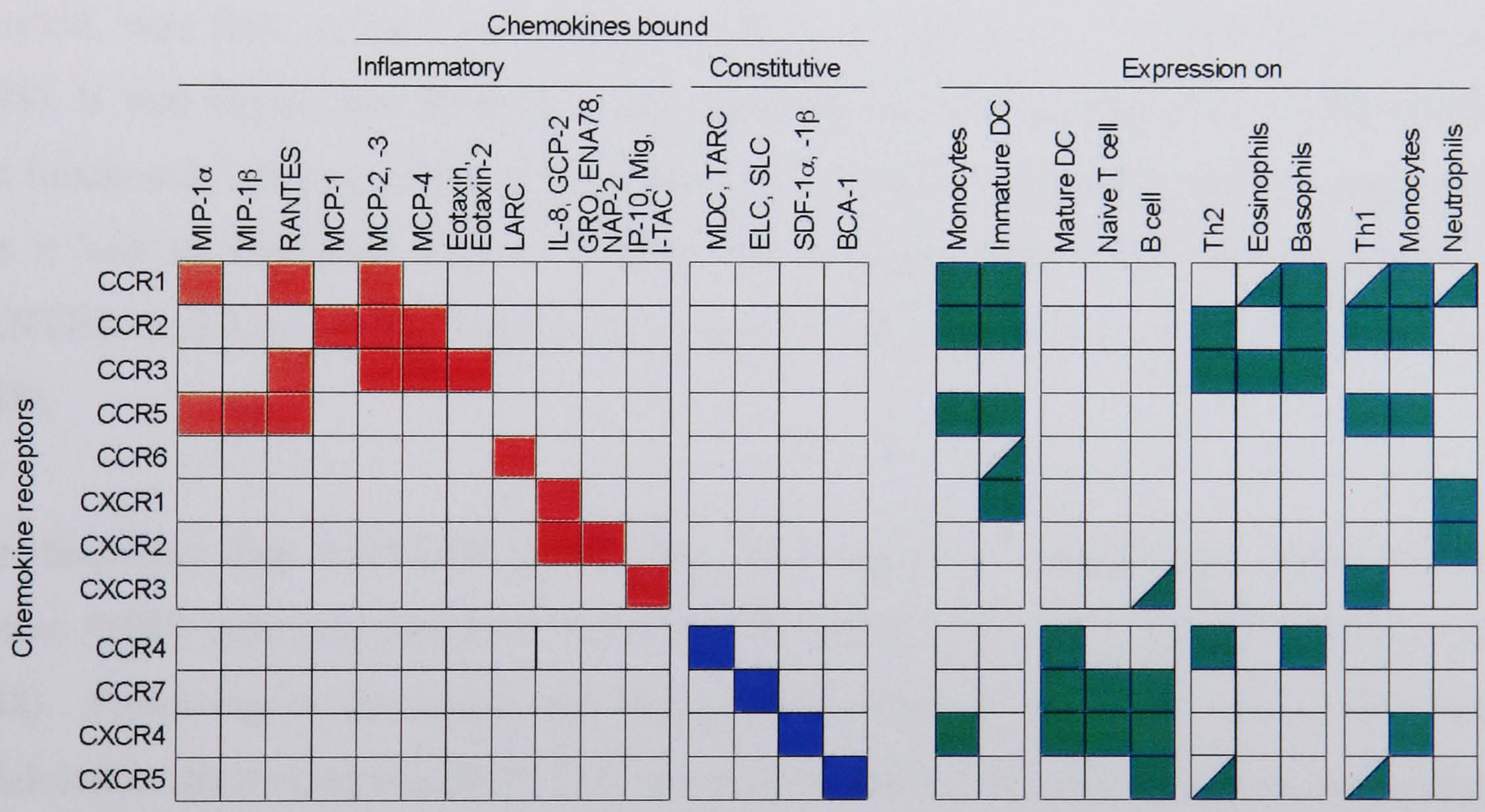

Table 1.2. Receptor expression and ligand specifities (Sallusto *et al*, 1998a)

Within the CC chemokine family, RANTES is most effective as a chemoattractant for T-cells, monocytes, eosinophils and basophils than as a stimulator of mediator release, whereas monocyte chemotactic protein-3 (MCP-3) and MCP-1 are effective as inducers of mediator release in basophils as well as effective chemoattractants for T-cells, monocytes, eosinphils and basophils. Whilst MCP-3 has the same chemoattractant properties as RANTES, it shares only 25 % sequence identity. Divergent effects were observed for the highly homologous pair macrophage inflammatory protein-1α (MIP-

1α) and MIP-1ß, of which only MIP-1α activates basophils and eosinophils and MIP-1ß is inactive. This suggests that sequence similarity is not necessarily predictive for the capacity of different chemokines to elicit one or other effector functions (Baggiolini & Dahinden, 1994.) The table shows that RANTES is not constitutively expressed, but when induced can recruit immature dendritic cells, monocytes, eosinophils, basophils, and both Th1 and Th2 type T-cells, but not neutrophils or B-cells through interactions with CCR1, 3 and 5 receptors expressed on these cells.

The focus of this thesis is the chemokine RANTES and its structure and function.

1.4. Discovery of Regulated on Activation Normal T-cell Expressed and Secreted (RANTES)

The chemokine regulated and normal T-cell expressed and secreted (RANTES), now more commonly known as regulated on activation normal T-cell expressed and secreted, was first isolated and characterised by Schall *et al.*, in 1988 (Schall *et al*, 1988). It was shown that RANTES was expressed by mitogen-activated T-cell clones that function *in vitro* as helper or cytotoxic cells. Several of its characteristics suggested that it had an important role in lymphocyte regulation and differentiation and that RANTES transcription in T-cells was regulated by cellular activation (Schall *et al*, 1988).

The discovery that RANTES was highly homologous to macrophage inflammatory protein (MIP) indicated that both molecules belonged to the same family (Schall *et al*, 1988). Following its discovery, the biological function of RANTES was investigated which led to the finding that RANTES belonged to the CC class of cytokines, associated by primary structure similarities and by the conservation of the four cysteine motif.

1.5. RANTES in inflammation

The synthesis and release of RANTES was initially identified in a search for genes expressed late (3-5 days) after T-cell activation with an antigen or mitogen (Schall et al, 1988). It has since been demonstrated that naïve ($CD45RA^+$) $CD4^+$ (helper) and $CD8^+$ (cytotoxic/killer) T-cells constitutively express RANTES and that RANTES expression is also further inducible in mature ($CD45RO^+$) $CD4^+$ T-cells of the Th1 phenotype and

$CD8^+$ T-cells upon activation with the mitogen, phytohaemagglutinin (PHA) (Nelson *et al*, 1993). However, the $CD45RO^+/CD4^+$ cells of the Th2 phenotype express RANTES constitutively and do not show inducibility (Kawai et al, 1999; Nelson et al, 1993). It has also been shown that $CD45RO^+/CD8^+$ T-cells are the more dominant source of RANTES over $CD45RO^+/CD4^+$ T-cells (Catalfamo et al, 2004; Conlon et al, 1995).

Many other cell types have also been shown to synthesise and release RANTES. RANTES is reported to be inducible in macrophages upon stimulation with IFN-γ or TNF-α, monocytes upon stimulation with TNF-α (Devergne *et al*, 1994; Fattal-German *et al*, 1998; Lane *et al*, 1999), eosinophils upon stimulation with IFN-γ (Ying *et al*, 1996), normal human bronchial epithelial cells and nasal epithelial cells upon stimulation with IFN-γ and TNF-α respectively (Olszewska-Pazdrak *et al*, 1998; Terada *et al*, 1996), the endothelium including human lung-microvascular, human umbilical vein and human mucosal microvascular endothelial cells upon stimulation with IL-1β or TNF-α plus IFN-γ (Ebnet *et al*, 1996; Kawai *et al*, 1999; Marfaing-Koka *et al*, 1995; Sundstrom *et al*, 2001; Terada *et al*, 1996) and in fibroblasts upon stimulation with IL-1β, TNF- α or IFN- γ (Meyer *et al*, 1998; Teran *et al*, 1999). RANTES is expressed early (12-24 hours) and RANTES mRNA is quickly up-regulated in these cells after stimulation with proinflammatory soluble mediators such as IL-1β, TNF- α or IFN-γ in contrast to the late expression of RANTES in T-cells, 3-5 days after activation, implying that RANTES is more likely involved in late T-cell activation events or development of late T-cell effector function.

Unusually, RANTES mRNA levels are reduced on T-cell activation (Fitzgerald, 2001) but an increase in mRNA levels 3-7 days after T-cell activation (figure 1.2) suggests that human peripheral blood T-cells secrete chemokines for prolonged periods after activation, thus recruiting fresh cells to inflammatory sites (Conlon *et al*, 1995).

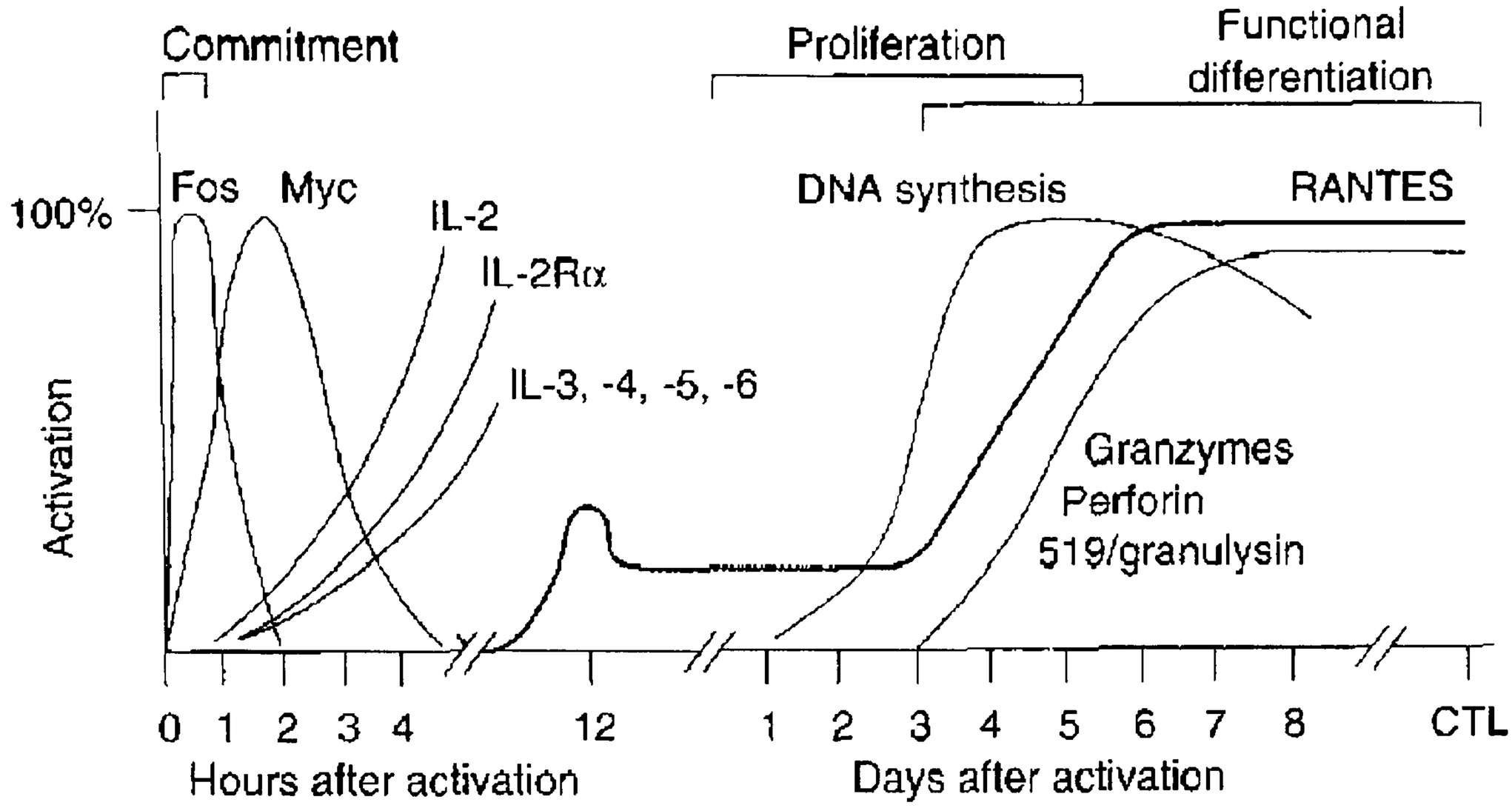

Figure 1.2. RANTES is up-regulated late after T-cell activation. The figure shows the sequence of gene expression events after T-cell triggering by antigen. Abbreviations: CTL (cytotoxic T-lymphocyte), IL (interleukin) and IL-2Rα (IL-2 receptor α chain) (Ortiz *et al*, 1997).

RANTES is also released from thrombin-stimulated platelets (Kameyoshi *et al*, 1992; Schroder *et al*, 1994) and constitutively produced by natural killer (NK) cells and megakaryocytes (Nelson *et al*, 1993).

It has been proposed that during inflammatory responses, RANTES is produced mainly by macrophages and endothelial cells (Devergne *et al*, 1994; Marfaing-Koka *et al*, 1995). Endothelial cells are known sources of both CXC and CC chemokines and the production of such chemokines may serve to initiate, augment and modify inflammatory responses (Thienel *et al*, 1999). Activated vascular endothelial cells are also known to affect the development of excessive inflammatory responses by secreting proinflammatory cytokines and chemokines (Dinarello *et al*, 1993).

Increased chemotactic activity and raised RANTES production has been associated with a wide range of inflammatory disorders and pathologies. The list is extensive, and includes allogenic transplant rejection (Sekine *et al*, 2000), atherosclerosis (Pattison *et al*, 1996), atopic dermatitis (Kaburagi *et al*, 2001), inflammatory airway disorders such as bronchial asthma (Conti & DiGioacchino, 2001; Devalia *et al*, 1999), cystic fibrosis (CF) (Schwiebert *et al*, 1999), sarcoidosis (Ziora *et al*, 1999), chronic eosinophilic pneumonia (Kurashima *et al*, 1997), idiopathic interstitial pneumonia (Panoskaltsis-Mortari *et al*, 2000) and chronic obstructive pulmonary disease (COPD) (Barnes, 2008;

O'Donnell *et al*, 2006), viral infections including respiratory syncytial virus infection (Culley *et al*, 2006), delayed-type hypersensitivity reactions (Devergne *et al*, 1994), glomerulonephritis, endometriosis, neurological diseases such as Alzheimer's disease (Tripathy *et al*, 2008), angiogenesis, rheumatoid arthritis (Volin *et al*, 1998) and certain malignancies (Hebert, 1999; Reale *et al*, 2002; Sugasawa *et al*, 2008; Tsukishiro *et al*, 2006; Vaday *et al*, 2006). In all of these pathologies, RANTES is thought to act by promoting leukocyte infiltration to sites of inflammation.

1.6. RANTES structure

RANTES is present in normal healthy tissues at physiological concentrations in the nanomolar range (Vives *et al*, 2002) and in normal plasma, physiological concentrations of 708 pg/ml have been reported (Lumpkins *et al*, 2008). The monomeric form is the major species found at physiological concentrations. RANTES is a highly basic non-glycosylated 7.8 kDa, 68 amino acid polypeptide (figure 1.3). Monomers consist of a 3-stranded anti-parallel ß-sheet with the C-terminal α-helix packed across the sheet by hydrophobic interactions (figure 1.4) (Chung *et al*, 1995). The N-terminal region is the most important for high affinity chemokine-receptor interactions of individual monomers for both the CC and CXC chemokines. The N-terminal amino acids preceding the first conserved cysteine have a large degree of movement.

The highly charged amino acids in the α-helix at the carboxyl terminus appear to be important for low affinity binding and are known as the heparin or glycosaminoglycan binding domain (McFadden & Kelvin, 1997).

1	SP**Y**SSDTTP<u>C</u>	<u>C</u>FA**Y**IARPLP	RA<u>H</u>IKE**Y**F**Y**T
31	SGK<u>C</u>SNPAVV	FVTRKNRQV<u>C</u>	ANPEKKWVRE
61	**Y**INSLEMS		

Figure 1.3. The amino acid sequence of the 68 amino acid chemokine human RANTES.

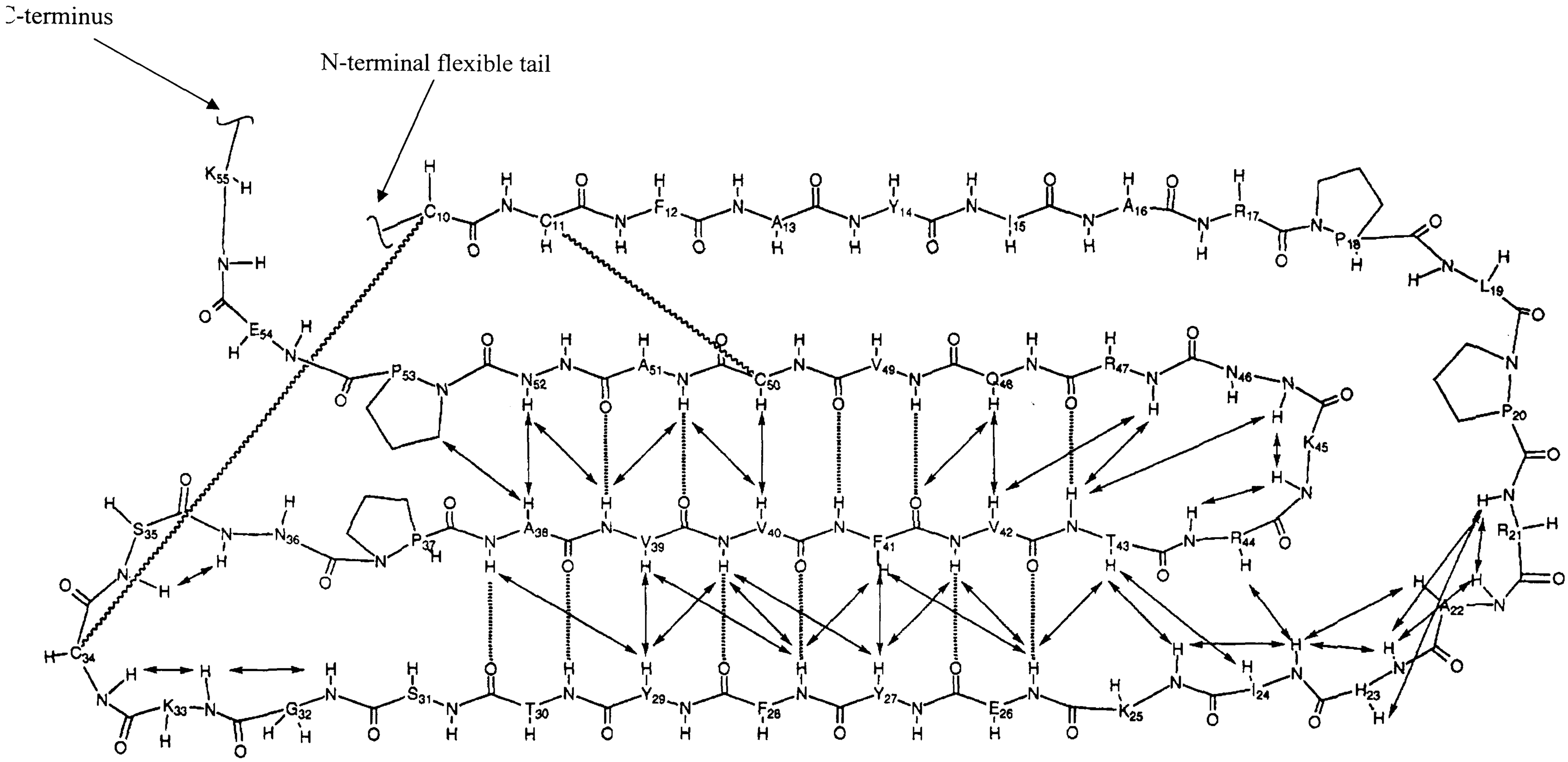

Figure 1.4. A schematic representation of the antiparallel ß-sheet structure of RANTES. Hydrogen bonds are indicated by thick broken lines. The two disulfide bridges are shown in wavy lines between Cys 10 and Cys 34 and Cys 11 and Cys 50, respectively (Chung *et al*, 1995). The N-terminus flexible tail is indicated by an arrow.

1.7. RANTES binding to chemokine receptors

Chemokines utilise both high affinity and low affinity interactions to elicit full biological activity (McFadden & Kelvin, 1997). The binding of chemokine ligands to high affinity (500 pM to 10 nM) cell surface 7-transmembrane chemokine receptors is a two step process involving two spatially distinct sites on the ligand, one necessary for receptor binding and the other necessary for signal transduction (Ward & Westwick, 1998).

The first step is the binding of the core of the ligand to the outer surface of the receptor, and the second is the orientation of the flexible tail of the ligand. RANTES can interact with each of its receptors CCR1, 3 and 5 in a distinct and specific manner. Thus Arg-17 is necessary for binding to CCR1, Phe-12 for CCR3 and both Phe-12 and Ile-15 for CCR5 binding (Ward & Westwick, 1998).

The proposed interaction between the RANTES core and its receptors involves firstly the interaction of the amino terminus of the receptor with the structured portion of the chemokine (the region beyond the first disulphide bridge) which is believed to be driven by electrostatic interactions between the acidic portion of the receptor amino terminus and the basic regions of the chemokine. In addition, the outer edge of the chemokine ß-sheet is also involved in the interaction. This first interaction results in the orientation of the flexible amino terminus of the chemokine, effectively raising its local concentration and causing it to interact at a second site inside the receptor. The flexible amino terminal regions of both CC and CXC chemokines are important for the activity of the ligand. Specific residues near the N-terminus have been identified that are involved in activating signal transduction via CCR1 (Pro-2, Asp-6, Thr-7), CCR3 (Pro-2 and Tyr-3) and CCR5 (Tyr-3 and Asp-6) (Ward & Westwick, 1998; Wells *et al*, 1995)

RANTES induces T-cell expression of adhesion molecules during chemotaxis and regulates T-cell cytokine release and T-cell proliferation. The mechanism involves biphasic calcium mobilisation. Following the binding of RANTES to its receptor, a rapid and transient rise in intracellular calcium $[Ca^{2+}]i$ is observed as one of the early events associated with the chemotaxis functional response. This initial calcium elevation is initiated by nanomolar concentrations and mediated by a heterotrimeric G-protein coupled pathway. The second peak of calcium influx is sustained, elicited by

micromolar concentrations of RANTES and protein tyrosine kinase (PTK) dependent pathways. This second peak is associated with Ca^{2+} channel opening, cytokine release, IL-2 receptor expression and T-cell proliferation. PTK activation by RANTES results in a number of downstream biochemical events that influence T-cell activation, chemotaxis, gene transcription, mediator release and cell cycle progression (Figure 1.5). RANTES induced calcium mobilisation is dependent on CD3 expression. The $[Ca^{2+}]i$ changes induced by different CC chemokines are similar in extent and kinetics and coincide with receptor activation (Ward *et al*, 1998).

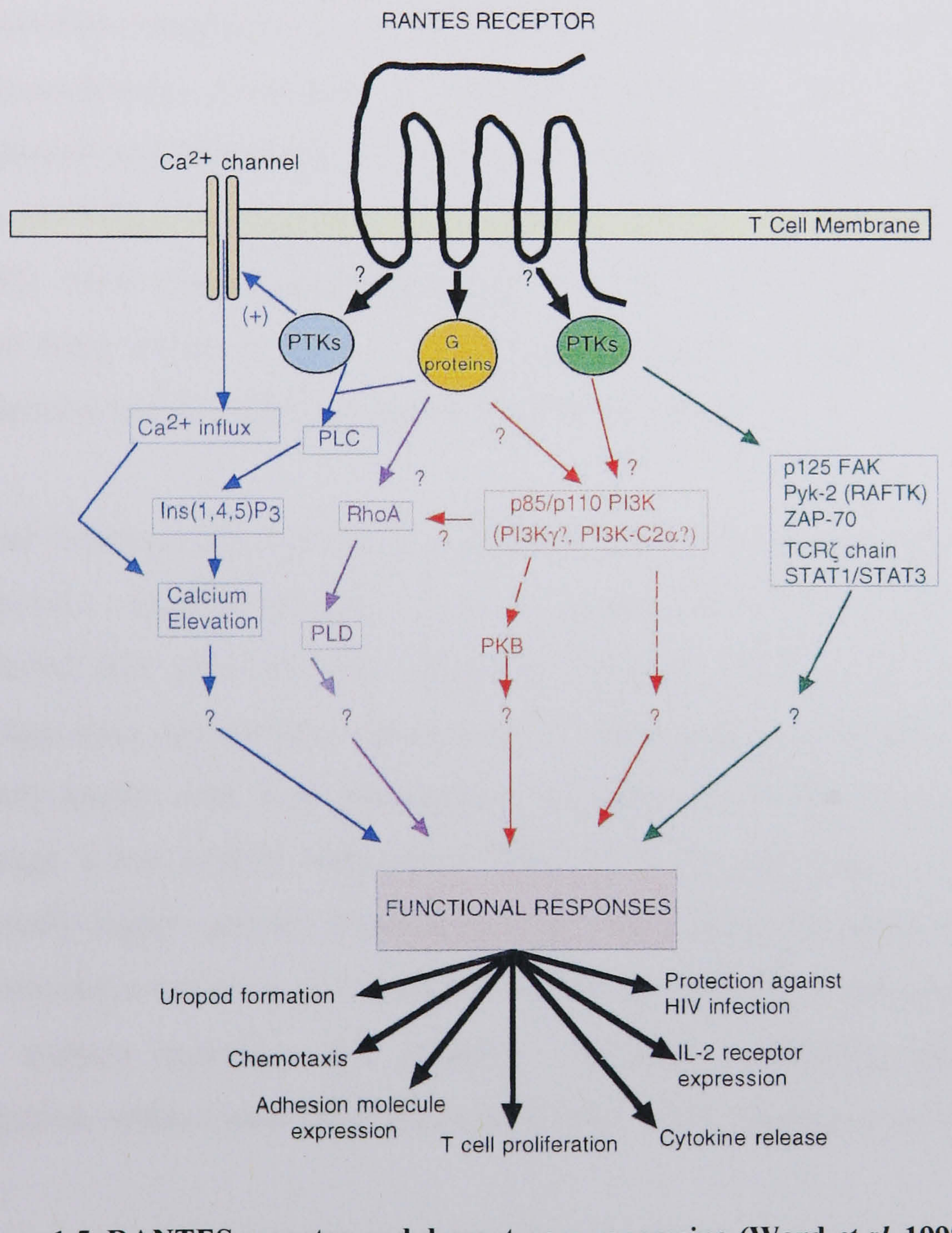

Figure 1.5. RANTES receptor and downstream processing (Ward *et al*, 1998)

1.8. Glycosaminoglycans

In order to activate integrins only on those leukocytes that have already established their initial interaction with the endothelium, chemokines must be bound to the surface of endothelial cells (Rot, 1996). The ECM surrounding human cells is a complex structure

containing carbohydrates and proteins, and important complex macromolecules called proteoglycans (Carter *et al*, 2003). Proteoglycans are expressed in all tissues and play a vital role in cell function and connective tissue formation. They are found within the cell plasma membrane, the basement membrane and the ECM (Cockwell *et al*, 1996).

The proteoglycans are a diverse family consisting of a core protein containing a membrane spanning domain to which one or more oligosaccharide members of the glycosaminoglycan (GAG) family are attached, linked to the core protein via a serine residue (Carter *et al*, 2003). GAGs are the side chains of proteoglycans and are ubiquitous components of cell surfaces (Goger *et al*, 2002). GAGs are long un-branched polysaccharides containing a repeating disaccharide unit and are generally highly sulphated and negatively charged, their rigidity providing structural integrity to cells and providing passageways between cells for cell migration (Yanagishita & Hascall, 1992). Their primary role is believed to be functional interactions with proteins. They have been shown to bind a variety of chemokines, cytokines, extra-cellular matrix molecules and growth factors (Cockwell *et al*, 1996).

When bound to the endothelial cell surface, RANTES is pro-inflammatory, stimulating leukocyte migration across a layer of endothelial cells (Proudfoot *et al*, 2003). It is believed that proteoglycans protect chemokine molecules from degradation, act as storage sites and present chemokines to their receptors (Bernfield *et al*, 1999). It is widely known that most chemokines, including RANTES, bind to cell surface GAGs through a low-affinity interaction (500 nM to 10 mM range). These interactions are normally highly specific (Spillmann *et al*, 1998) and an important aspect in maintaining a chemokine concentration gradient for the presentation of chemokines to high-affinity cell surface receptors and selective leukocyte trafficking during diapedesis and migration within tissue (McFadden & Kelvin, 1997; Skelton *et al*, 1995).

There are four classes of glycosaminoglycans, including heparin/heparan sulphate (HS), chondroitin sulphate/dermatan sulphate, keratan sulphate and hyaluronan (Frevert *et al*, 2003). All four classes are found in normal human lungs, and with the exception of hyaluronan, all are present as side chains on the core proteins of the proteoglycans. RANTES binds selectively to GAG families with different affinities: heparin >

dermatan sulphate > heparan sulphate > chondroitin sulphate (Kuschert *et al*, 1999; Martin *et al*, 2001).

In the lungs, proteoglycans are found on the surface of endothelial cells (eg. syndecan), in the extracellular matrix (eg. Decorin, perlecan and versican) and also in the intracellular locations (eg. serglycin). RANTES binds mainly to HS side chains of proteoglycans (Hillyer & Male, 2005) and HS is the most ubiquitous GAG (50 – 90 % of all GAGs) and the most predominant GAG found in the lungs, followed by chondroitin sulphate/dermatan sulphate, hyaluronan and heparin (Cockwell *et al*, 1996; Frevert *et al*, 2003; Ihrcke *et al*, 1993).

1.9. Chemokine binding to Heparan Sulphate

Highly specific cell surface receptors often use cell surface HS to recognise their ligands or to regulate their activation. The association of a number of chemokines including RANTES with heparan sulphate has been demonstrated and in this form it is presented to specific receptors (Ali *et al*, 2002; Hillyer & Male, 2005; Kuschert *et al*, 1999; Proudfoot *et al*, 2001; Proudfoot *et al*, 2003). The binding of RANTES to HS possibly induces self aggregation and allows a higher surface concentration of the chemokine (Skelton *et al*, 1995).

Chemokines are highly basic, and all are able to bind heparin with varying affinities. In addition, nearly all chemokines bind to HS which has an average molecular weight of 29 KDa with a range of 5 to 50 KDa and a structure similar to heparin, except heparin is more uniformly sulphated making it the most negatively charged molecule in the body (Hileman *et al*, 1998). Like heparin, HS is a strongly anionic linear polysaccharide, synthesized in the Golgi apparatus as a repeating linear co-polymer of variably sulphated uronic acid and glucosamine residues. HS has an average of one sulphate per disaccharide and is predominantly composed of glucuronic acid 1-4 linked to glucosamine. HS contains greater structural variation than is present in heparin (Yanagishita & Hascall, 1992).

Although HS contains all of the disaccharide sequences found in heparin, the amount of these minor sequences is greater in HS making it structurally and sequentially more complex. HS N-deacetylase/N-sulphotransferase (NDST) enzymes catalyse the reaction

that initiates sulphation and subsequent modification of HS. The sulphation pattern of GAGs is of great importance and plays a role in the regulation of cellular function and immunity and the extent and distribution of sulphation on HS is vital to regulate the range of proteins that it can bind. Specific sulphated disaccharides on heparan sulphate expressed by human microvascular endothelial cells provide the low-affinity binding site for RANTES (Carter *et al*, 2003).

The interaction between chemokines and sulphated domains on HS is ionic in nature and forms between basic amino acid sequences near the C-terminus of the chemokine and anionic sulphated domains on the GAG. RANTES has a higher affinity for HS compared to other CC chemokines (Kuschert *et al*, 1999). A conserved concensus sequence of basic amino acids has been described in the form of the BBXB motif which is found on the 40s loop of RANTES, where B represents either of the basic amino acids arginine or lysine, and X represents any other amino acid. In addition, a BBXXB sequence has been described further upstream toward the C terminal in RANTES. These sequences have been shown to play a major role in the specific low-affinity binding of RANTES to HS (Ali *et al*, 2002; Proudfoot *et al*, 2001).

HS is found consistently on two major families of membrane bound proteoglycans (PGs), the syndecans and the glypicans (Bernfield *et al*, 1999). These are referred to as heparan sulphate proteoglycans (HSPGs). The syndecans carry the bulk of the HS (Kainulainen *et al*, 1998). By way of their HS chains, syndecans and glypicans can bind a wide variety of soluble and insoluble extracellular ligands. Glypicans are covalently linked to phosphatidyl inositol in the outer leaflet of the plasma membrane and the HS chains are likely located near the plasma membrane bound to an extended protein domain (figure 1.6) (Bernfield *et al.,* 1999).

Syndecans are trans-membrane proteins that bear ligand-binding HS chains distal from the plasma membrane. There are four types of syndecan, syndecan-1 through to syndecan-4. Syndecan-1 is predominantly expressed by epithelial cells and plasma cells, and to a lesser extent by endothelial cells, monocytes and fibroblasts among other cell types. Syndecan-2 is abundantly expressed by endothelial cells and mesenchymal cells whilst syndecan-3 expression is mostly restricted to cells of neural crest origin. Syndecan-4 is expressed ubiquitously, although at lower levels than any of the other

syndecans. RANTES binds to syndecan-1 and syndecan-4 (Bartlett *et al*, 2007), and syndecans localise at adherens junctions (Bernfield *et al*, 1999).

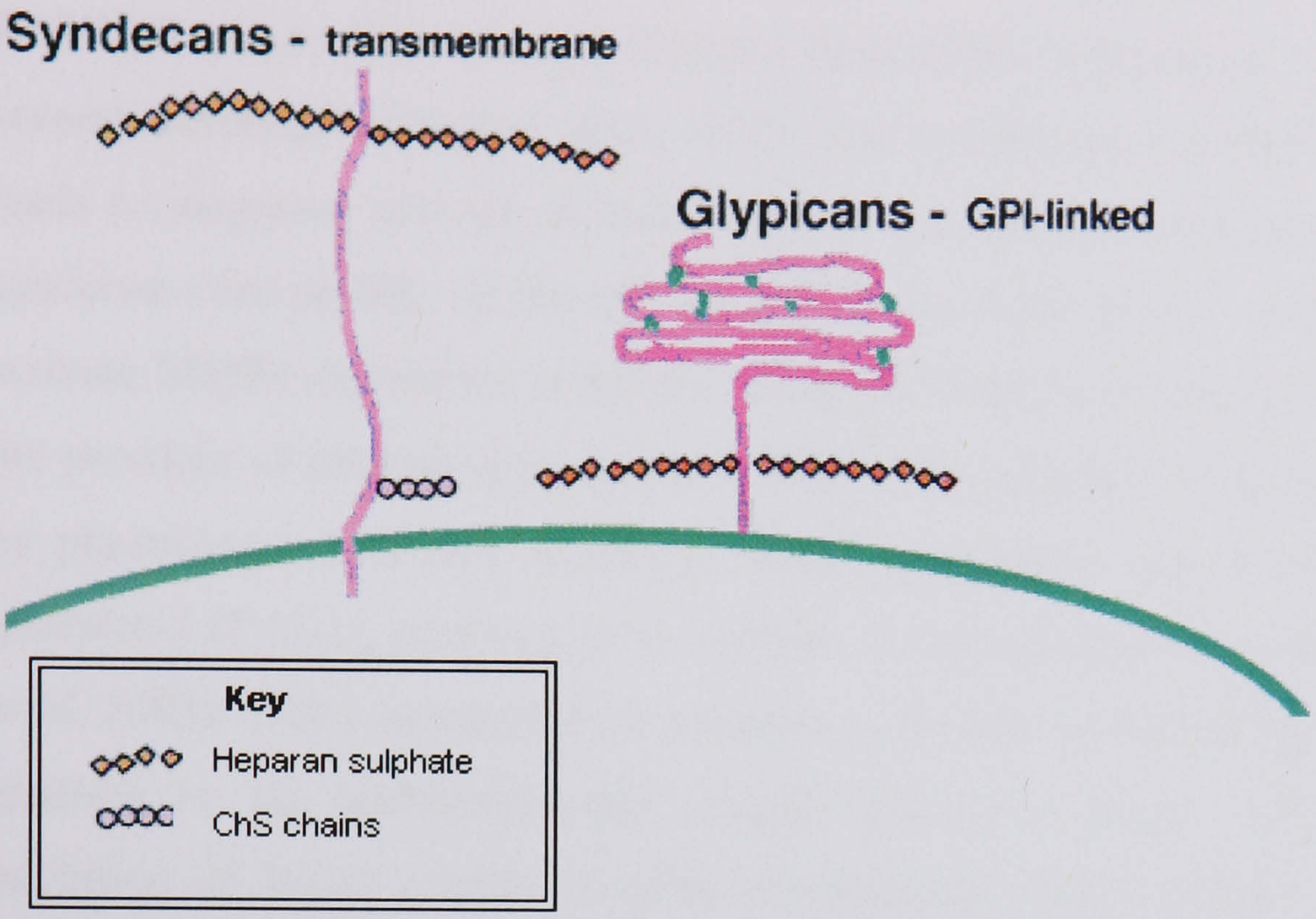

Figure 1.6. Schematic depiction of cell surface heparan sulphate (HS) proteoglcans (Bernfield et al., 1999).

Virtually all adhesive cells express at least one of the four syndecans (syndecans 1-4) and most express multiple syndecans. Glypicans are expressed predominantly in the central nervous system. Proteoglycans act as co-receptors for both insoluble (e.g. extra-cellular matrix components) and soluble ligands (e.g. growth factors and chemokines), have involvement in the internalisation of receptors, and also play a role as soluble paracrine effectors, produced by the shedding of the HSPG from the cell surface (Bernfield *et al*, 1999).

Although immobilised GAGs may aid in the presentation of chemokines, soluble GAGs can form complexes with chemokines and play a specific inhibitory role (Kuschert *et al*, 1999; Martin *et al*, 2001). All four syndecans can exist as soluble HSPGs as they can be proteolytically cleaved and secreted into the ectodomain environment by ectodomain shedding. This is not unique to syndecans and occurs in the secretion of many other cell surface components. Cultured cells shed syndecan ectodomains as a part of normal turnover, and this shedding is regulated as an inflammatory mechanism by several inflammatory factors, and activated under certain inflammatory conditions (Bartlett *et*

al, 2007). Shedding is accelerated by agonists that enhance the activity of a tissue inhibitor of matrix metalloproteinase (TIMP)-3 sensitive metalloproteinase (Fitzgerald *et al*, 2000). Agonists of syndecan cleavage include the EGF family growth factors (protein tyrosine kinase receptor mediated), thrombin and chemokines including RANTES (G-protein coupled receptor mediated), heparanase, stress mediators and second messengers (Bartlett *et al*, 2007). The activation of multiple signaling pathways leads to increased activity of membrane-bound metalloproteinase and cleavage of the syndecan core protein on the cell surface, close to the plasma membrane. Plasmin can activate MMPs and induce syndecan shedding. Plasmin is cleaved from plasminogen in the presence of plasminogen activator (PA). The activation of plasminogen is inhibited by plasminogen activator inhibitors including platelet derived plasminogen activator inhibitor-1 (PAI-1), resulting in an increase in cell associated chemokine (Kucharewicz *et al*, 2003). PAI-1 released from platelets is capable of stabilising the chemoattractant gradient on the endothelial cell surface (Taylor & Gallo, 2006). Conversely, the inhibition of PAI-1 results in syndecan shedding, and a reduction in cell-associated chemokine (Marshall *et al*, 2003).

Shedding of syndecans into the extra-cellular environment reduces the concentration of chemokines on the endothelial cell surface. Soluble HSPGs, although no longer able to bind and localise chemokines on the endothelial cell surface, can compete with endothelial bound HSPGs for soluble chemokines, playing an inhibitory role and indicating a requirement for chemokine presentation to high-affinity receptors by endothelial cell associated GAGs (Cockwell *et al*, 1996; Kuschert *et al*, 1999; Martin *et al*, 2001). Soluble chemokines can also bind leukocytes, desensitising specific receptors and preventing their adherence to endothelial cells and consequently their transendothelial migration.

GAGs are also present on leukocytes, and may therefore play a role in the presentation of chemokines to the GPCRs on the same cell (Kuschert *et al.,* 1999), or possibly cells of the same type. Following interaction with an immobilised GAG, a chemokine can be presented in either cis or trans fashion. In cis mode, the chemokine, GAG and specific receptor are all present on the same cell surface whereas the trans mode occurs when a chemokine binds to a GAG within the ECM or on an adjacent cell and then presented to a second cell expressing a specific receptor (Ali *et al*, 2002).

The presence of IFN-γ and TNF-α has been shown to up-regulate HS expression compared to other GAGS. It has been shown that cytokine activation of the endothelium increases RANTES binding to the endothelial cell surface and therefore it is likely that endothelial cell activation is necessary for efficient chemokine sequestration and presentation by the endothelium leading to leukocyte migration from the apical to the basal surface of the endothelium (Kennedy *et al*, 1998; von Hundelshausen *et al*, 2001). In addition, HSPGs are found on both the luminal and basal endothelial cell surface and have been implicated in the binding and transcytosis of chemokines across the endothelial cell barrier from the abluminal to the luminal surface of endothelial cells (Parish, 2005).

Almost all chemokines studied to date appear to bind to HS, suggesting that this interaction represents a fundamental aspect of these proteins (Vives *et al*, 2002). It has been shown that T-cells secrete CC chemokines including RANTES *in vivo* as a complex with PGs (Wagner *et al*, 1998a). This would strongly suggest that this form is physiologically relevant. It has been clearly demonstrated that GAG expression is not necessary for the biological function of RANTES *in vitro*, but the presence of cell surface GAGs does enhance the activity of low concentrations of these chemokines, indicating that the immobilisation of GAGs is functionally important (Ali *et al*, 2002).

In addition, loss of cell surface GAGs reduces the affinity of leukocytes for many chemokines (Kuschert *et al.,* 1999). RANTES mutants that cannot bind to GAGs were unable to induce leukocyte migration *in vivo*, even at 10,000 fold higher doses than those at which the wild type RANTES was able to induce statistically significant recruitment (Proudfoot *et al*, 2003). This confirms that RANTES must interact with GAGs to elicit cell migration *in vivo*. Without this mechanism, chemokines would be washed away from the local production site, especially under flow conditions and diluted to a concentration below the threshold required for receptor binding. They would become widely distributed such that no localised chemotactic signal would be generated for leukocytes to follow (Proudfoot *et al*, 2003).

1.10. Chemokine dimerisation

A characteristic feature of chemokines is the observation that they are able to form dimers and higher order multimers. Growing evidence suggests that GAGs facilitate the chemokine-receptor binding process by inducing chemokine self-aggregation, referred to as oligomerisation or multimerisation (Hoogewerf *et al*, 1997; Proudfoot *et al*, 2003; Vives *et al*, 2002). The aggregation of RANTES is not unique among the CC chemokines. Both MIP-1α and MIP-1ß have been shown to form high molecular weight aggregates in solution at neutral pH (Skelton *et al*, 1995). In fact many CC and CXC chemokines including IL-8, RANTES and MCP-1 multimerise on interaction with cell surface HS (Bernfield *et al*, 1999; Hoogewerf *et al*, 1997).

It is believed that chemokines dimerise and multimerise as a regulation mechanism for activity. GAG binding reduces the chemokine dimerisation constant, enhancing surface-bound dimer formation (Williams *et al*, 2005). Cell surface GAGs, including heparin and heparan sulphate (HS) sequester chemokines and induce chemokine multimerisation at the cell surface (Hoogewerf *et al*, 1997; Vives *et al*, 2002), thus promoting local high concentrations and establishing a stable chemotactic gradient in the vicinity of GPCRs and facilitating chemokine-receptor binding on leukocytes. The formation of stable chemotactic gradients gives a longer duration of action by preventing diffusion into the bloodstream (figures 1.7a and b). In addition, chemokine multimerisation and GAG binding may protect chemokines from proteolytic degradation (Hoogewerf *et al*, 1997; Proudfoot, 2006; Proudfoot *et al*, 2003).

Fig. 1.7a

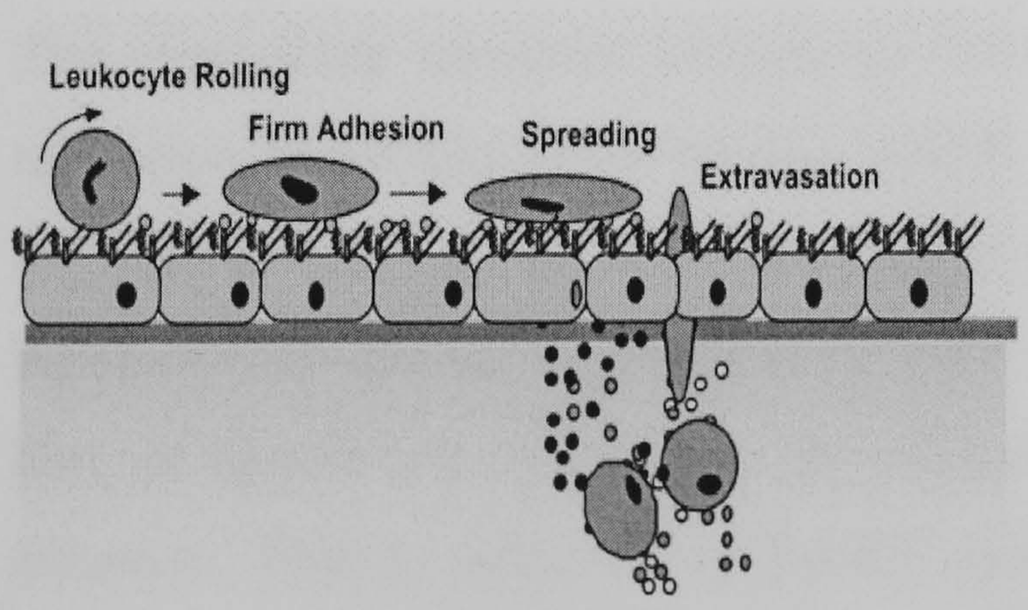

Fig. 1.7b

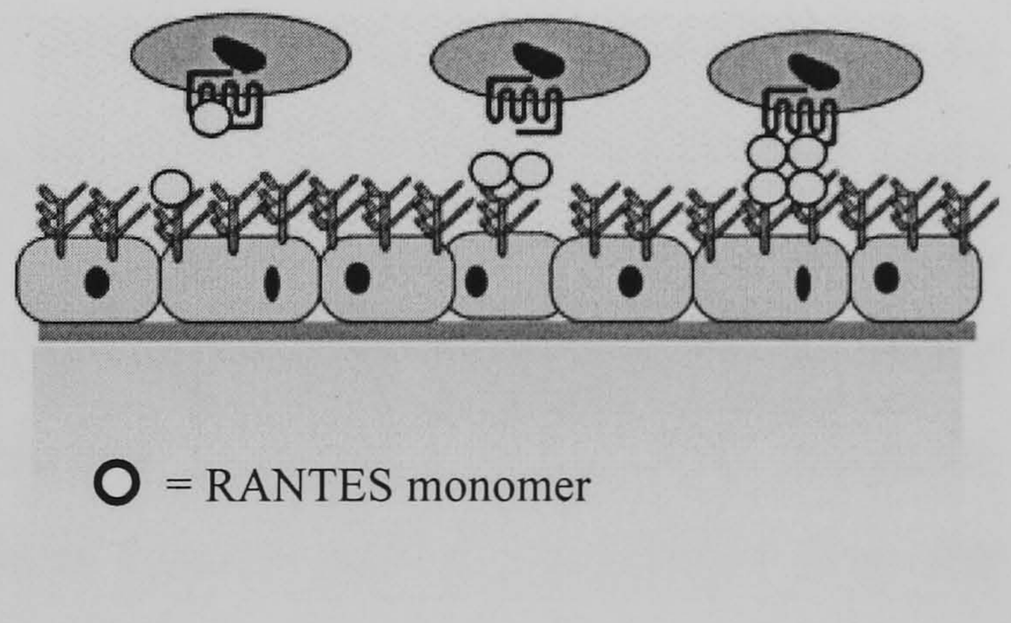

Figure 1.7a; Chemokines require immobilisation on cell-surface GAGs in order to initiate the transmigration process from the circulation (Proudfoot, 2006).

Figure 1.7b; RANTES requires a minimal tetrameric structure in order to provide a directional signal to circulating leucocytes (Proudfoot, 2006).

Maintaining a RANTES gradient that is sufficient for the pro-inflammatory stimulation of leukocyte migration across endothelial cells into tissues is crucial for their recruitment to an inflammatory site. The formation of aggregates may also have a physiological role in limiting the amount of active RANTES circulating in the blood stream (Proudfoot, 2006; Skelton *et al*, 1995).

1.11. Duffy antigen receptor for chemokines (DARC)

RANTES can also bind to the Duffy antigen receptor for chemokines (DARC) (Choe *et al*, 2005; Neote *et al*, 1994). DARC is a 48 KDa protein that belongs to the family of 'silent' chemokine receptors known also as interceptors (internalising receptors). These are 7 trans-membrane molecules present on endothelial cells and erythrocytes with high homology to the GPCRs (Colditz *et al*, 2007; Rot, 2005).

DARC binds a broad spectrum of chemokines of the CXC and CC groups but, just like other chemokine interceptors, does not activate G-protein mediated signalling cascades (Colditz *et al*, 2007; Ward *et al*, 1998) as it lacks the DRYLAIV motif in the second intracellular loop and therefore cannot couple to G-proteins and does not elicit any detectable signal transduction events (Ward *et al*, 1998). DARC has less than 20 % amino acid identity with CXC and CC chemokine receptors and is the only known chemokine receptor that can bind both CC and CXC chemokines. However, DARC is clearly distinct from the chemokine interceptor D6, which binds chemokines and leads to chemokine degradation (Pruenster & Rot, 2006).

The chemokine transport activity of DARC enhances chemokine-induced leukocyte migration across biological barriers which express this interceptor, and may play a role in inflammation since evidence suggests that DARC is up-regulated in many inflammatory diseases (Colditz *et al*, 2007). Chemokines that are produced in the tissue have to appear on the luminal endothelial surface in order to induce firm leukocyte adhesion. This is achieved by DARC mediated transcytosis of chemokines from the abluminal to the luminal surface of the endothelium.

The binding of chemokines to DARC on the endothelial cell surface also results in their neutralisation and thus prevents the systemic stimulation of circulating leukocytes

which would result in leukocyte desensitisation and temporary loss of their ability to migrate. Erythrocyte expressed DARC has been well documented as a chemokine sink, and in addition, prevents the loss of chemokines from the blood into the kidneys and other organs thus DARC also functions as a chemokine depot (Colditz *et al*, 2007).

1.12. T-cell recruitment

T-cells are normally present in almost every tissue of the body. They scan dendritic cells in lymphoid organs in search of specific antigens and, after priming, they migrate to follicles to help B-cells produce antibodies and to sites of antigen exposure to deliver the appropriate effector or regulatory function, thus inducing or dampening inflammation. Once the antigen is eradicated, central memory and effector memory T-cells remain in lymphoid organs and peripheral tissue to react rapidly if a second exposure to antigen should occur (Sallusto & Baggiolini, 2008).

The migratory pattern of T-cells changes during the transition from naïve T-cells to memory T-cells. Naïve T-cells traffic through lymphoid tissue waiting to be primed, whereas memory T-cells have acquired the ability to infiltrate non-lymphoid sites where antigen is located. In addition, primed T-cells are able to establish homing receptors for tissue-selective molecules and chemokines that allow them access to specific tissues (Marelli-Berg *et al*, 2008).

1.13. T-cell activation

It is generally accepted that the mitotic activation of T-cells *in vivo* is a result of a two-step signalling mechanism, initially triggered by a specific antigen presented in association with products of the major histocompatibility complex (MHC) at the surface of an antigen presenting cell. Binding of antigen-MHC to the clonotypic T-cell antigen receptor triggers the T-cell to express receptors for the second mitotic signal, the growth factor interleukin-2 (IL-2) (Mire-Sluis *et al*, 1987). IL-2 is secreted by T-cells in response to IL-1, which is produced by cells of the monocyte-macrophage lineage in response to an antigen-dependent interaction between monocytes and T-cells (Mire-Sluis *et al*, 1987; Mizel, 1982).

However *in vitro*, the initial signal for polyclonal activation of T-cells can be achieved by substituting a variety of agents, including the lectin phytohaemagglutinin (PHA) for

antigen-MHC and the second signal can be delivered by recombinant IL-2 (Mire-Sluis et al, 1987; Palacios, 1982). The stimulation of naïve T-cells results in activation, maturation, proliferation and cytokine release (Dairaghi *et al*, 1998; Loetscher *et al*, 1996). Activation involves the up-regulation of T-cell surface receptors.

1.14. T-cell differentiation

The maturation of resting cells into specific effector $CD4^+$ Th1 and Th2 phenotype T-helper cells is a process of maturation that takes 3-7 days and involves the influence of cytokines. Interferon-α (IFN-α) promotes the Th1 phenotype, whereas transforming growth factor-ß (TGF- ß) promotes differentiation into the Th2 phenotype (Ortiz *et al*, 1997; Ward *et al*, 1998).

There has been intense effort to determine which chemokine receptors (CCR) are expressed on different leukocytes. It is now established that T-cells express most of the known CC, CXC and CX3C chemokine receptors (table 1.1.) The precise pattern of chemokine expression depends entirely on the activation state of the T-cell. Following mitogenic stimulation/activation and/or prolonged treatment with interleukin-2 (IL-2), the chemokine receptors CCR1, CCR2, CCR5, CXCR4 and CX3CR1 are markedly up-regulated (Loetscher et al, 1996; Ward & Westwick, 1998) (see table 1.1). Some receptors are restricted to activated T-cells, such as CXCR3. Chemokine receptor expression correlates well with the known chemotactic effects of the respective ligands on T lymphocyte subsets. For example, the CXCR4 receptor is predominantly expressed on $CD45RA^+$ naïve T-cells. Its ligand, stromal cell derived factor-1 (SDF-1), is involved in the basal trafficking of naïve lymphocytes.

In contrast, CCR5 is expressed mainly on mature $CD45RO^+$ $CD4^+$ T-cells, which migrate in response to RANTES, the major ligand for CCR5 (Bleul *et al*, 1997). The expression of CCR4, CCR3 and CCR7 has been observed specifically on differentiating Th2 type T-helper cells following activation and differentiation (Gerber *et al*, 1997) whereas CCR5 and CXCR3 is preferentially expressed on Th1 type T-helper cells (Loetscher *et al*, 1998; Sallusto *et al*, 1998b). CXCR4, CCR1 and CCR2 are expressed on both Th1 and Th2 type cells (figure 1.8). In addition, $CD8^+$ cytotoxic T-cells of the Tc2 subtype also express CCR1 and CCR3, with CCR1 and CCR5 expressed by $CD8^+$

cytotoxic T-cells of the Tc1 subtype (D'Ambrosio *et al*, 1998; Sallusto *et al*, 1998b; Ward & Westwick, 1998; Weber *et al*, 2001).

The pattern of receptor expression on Th1 and Th2 T-cells correlates with the efficient attraction of Th1 T-cells by the T-cell ligands MIP-1a, MIP-1b and RANTES. SDF-1 and MCP-1 bind to CXCR-4 and CCR-2 respectively and exert chemotactic effects on both Th1 and Th2 type T-cells (Ward *et al*, 1998). However, there is evidence to suggest that differential expression of chemokine receptors may influence functional T-cell responses other than chemotaxis, since RANTES, MIP-1α and MCP-1 also promote lymphocyte activation and differentiation (Ward *et al*, 1998).

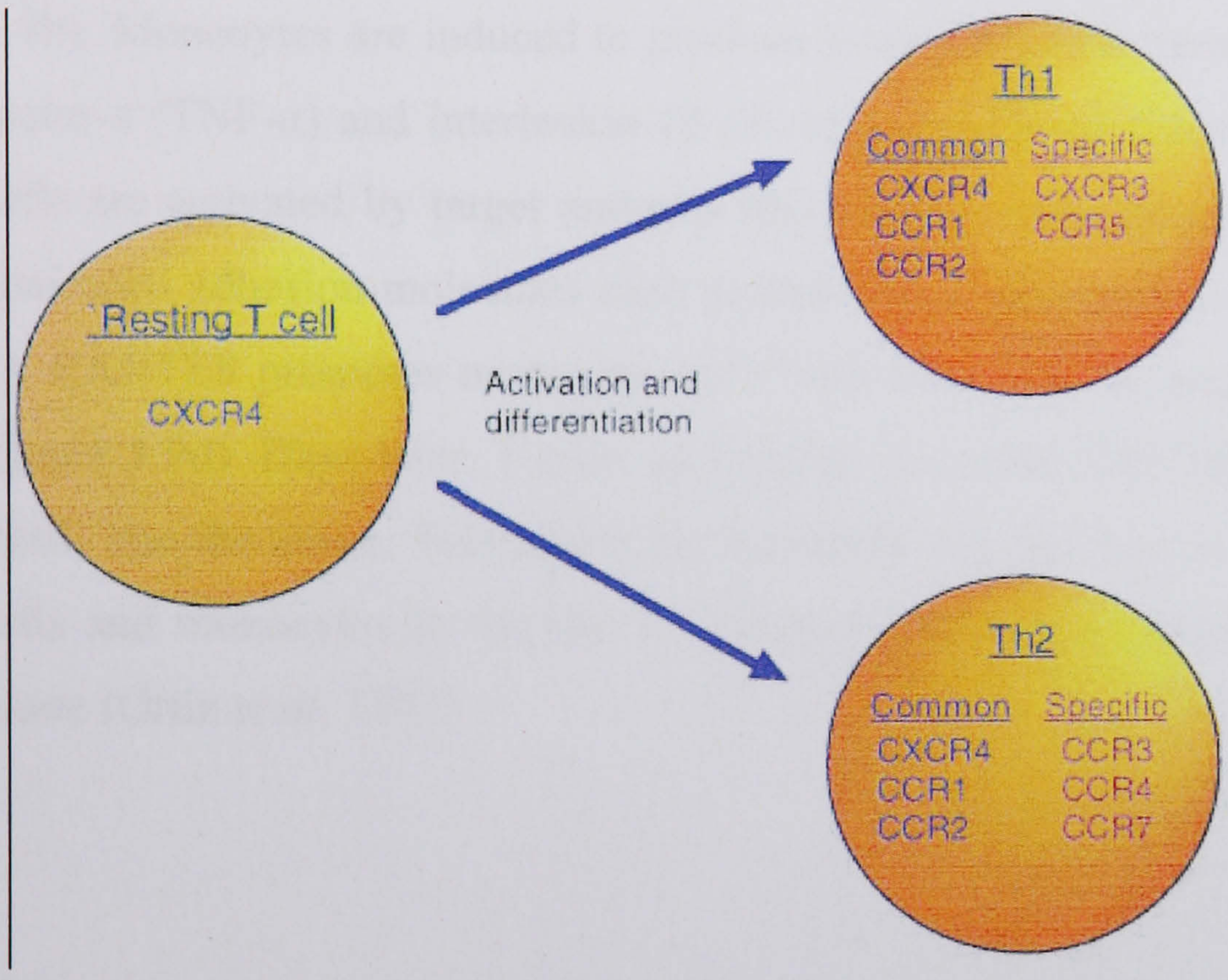

Figure 1.8. Schematic model for chemokine receptors as markers of T-cell differentiation (Ward *et al*, 1998).

1.15. The role of RANTES in T-cell migration

As an immediate early response to stress, RANTES is produced by inflamed tissues and deposited on the endothelium as a solid phase gradient (Figure 1.9a). It is proposed that chemokines induce the transition from selectin-mediated tethering and rolling to integrin-mediated firm attachment and spreading. Chemokines present on both the luminal and abluminal endothelial cell side can induce transendothelial migration, and in addition are required for the interaction of VLA-4 with fibronectin, which is important for migration of T-cells into the tissue (Sallusto *et al*, 1998a).

Chemokines induce the surface expression of endothelial cell adhesion molecules including P- and E-selectins, and Ig superfamily members, but this is an indirect effect. Chemokines trigger other cells, e.g. mast cells, T-cells or monocytes to degranulate and release multiple inflammatory mediators to include histamine and TNF-α which binds to receptors on the surface of the same cells, resulting in their activation and the expression of P- and E- selectin respectively (Colditz *et al*, 2007). TNF-α also induces the strong expression of intercellular adhesion molecules including ICAM-1. ICAM-1 expressed on the macrophage surface interacts with its ligand LFA-1 on resting T-cells, resulting in their activation and proliferation (Fattal-German *et al*, 1998).

RANTES on the endothelial cell surface is recognised by passing monocytes (figure 1.9b). Monocytes are induced to produce more RANTES transiently by tumor necrosis factor-a (TNF-α) and interleukin-1β (IL-1β), amplifying the response (figure 1.9c). T-cells are activated by target antigens and produce early genes such as IL-2 receptor-α chain and adhesion molecules such as leukocyte function-associated molecule-1 (LFA-1). RANTES promotes monocyte and T-cell adherence to, and entrance into the tissue (figure 1.9d). Days later, T-cells up-regulate sustained RANTES production, creating a 'trail' into the tissue. This assists the formation of a gradient in order to recruit more T-cells and monocytes to the site of inflammation and promotes their entrance into the tissue (Ortiz *et al*, 1997).

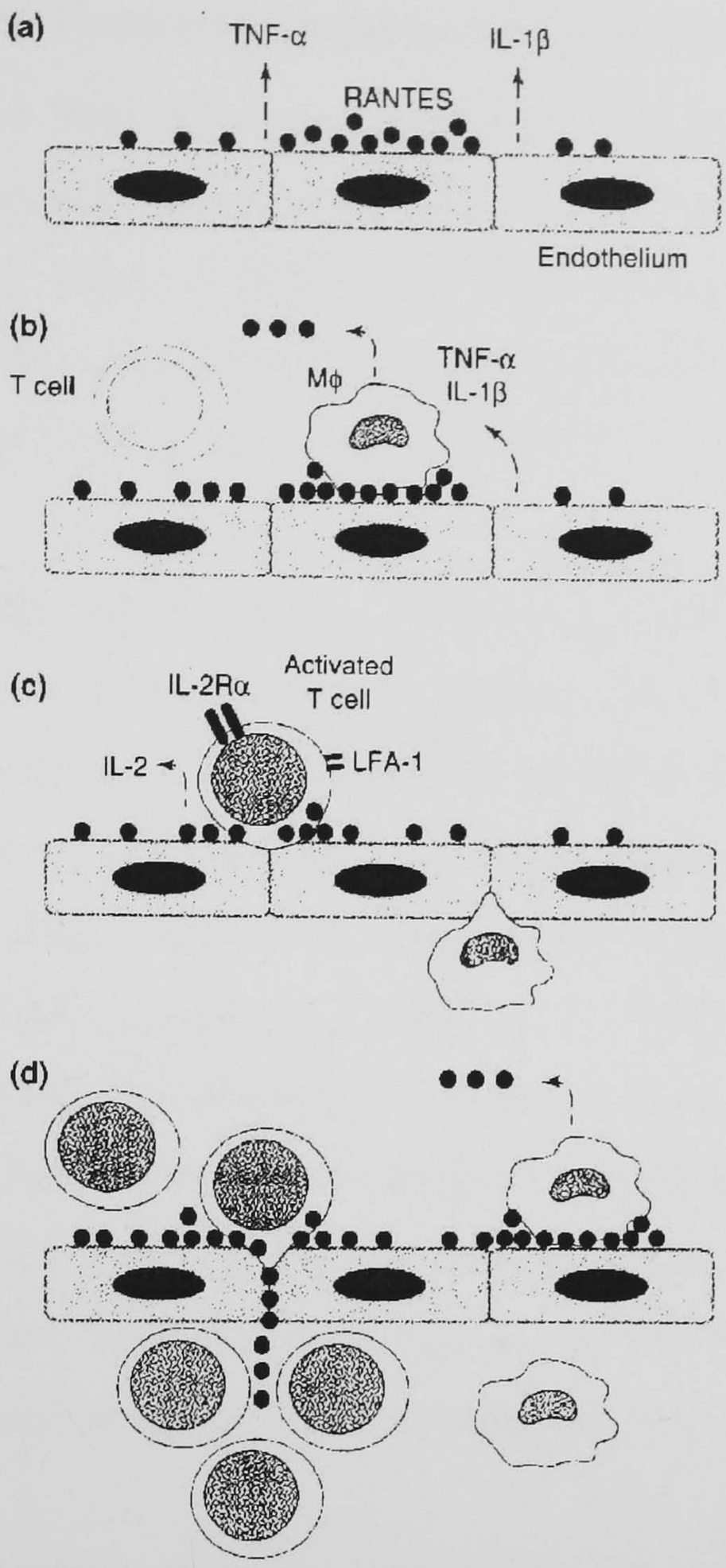

Figure 1.9. The role of RANTES in inflammatory responses (Ortiz *et al*, 1997)

For a T-cell cell to migrate, it must first acquire polarised morphology that will allow locomotion. This morphology is also required for a number of other processes including cell differentiation, recognition and binding of antigen presenting cells (APCs) by T-cells and cytolytic granule secretion for cell-killing. Chemokines induce T-cell polarisation, which is a change in cell distribution of filamentous F-actin from a radial symmetrical pattern to concentration in specific cell regions. As a result, two differentiated edges are established within the cell, namely, the leading edge and the uropod. The leading edge concentrates several chemoattractant receptors including CCR3, and CCR5. A number of adhesion molecules are concentrated in the uropod, including ICAMs, L-selectin, and PSGL-1. This serves as a method to promote the binding of other cells to enhance leukocyte recruitment and trans-endothelial migration (Mellado *et al*, 2001).

1.16. RANTES induced T-cell accumulation in lung inflammation

RANTES monomers have been shown to be functional ligands of CCR1, CCR3 and CCR5 *in vitro*, the biological activity dependent on the integrity of the N-terminal domain (Proudfoot *et al*, 2003). RANTES has been shown to stimulate T-cell and monocyte migration *in vitro* at an optimal concentration of 10 nM (Ali *et al*, 2002) and half-maximal migration at 2 nM (Kameyoshi *et al*, 1994).

RANTES can selectively attract naïve ($CD45RA^+$) $CD4^+$ (helper) and mature ($CD45RO^+$) human $CD4^+$ T-cells including Th1 (Kawai *et al*, 1999) and Th2 subtypes (Gerber *et al*, 1997; Sallusto *et al*, 1997) and $CD8^+$ (cytotoxic/killer) T-cells of the Tc1 and Tc2 subtype (Iijima *et al*, 2003; Sallusto *et al*, 1998a; Sallusto *et al*, 1998b), natural killer cells and immature DCs (Appay & Rowland-Jones, 2001; Barnes, 2008; Conti *et al*, 2001; O'Neill *et al*, 2004), monocytes (Schall *et al*, 1990), eosinophils (Rot *et al*, 1992; Schroder *et al*, 1994) and basophils (Yoshimura *et al*, 1987) and could be of particular importance in those inflammatory diseases in which these cells are present in affected tissues. However, T-cell infiltration during inflammation is of particular importance since T-cells are central to adaptive immunity, establishing and maximising the immune response by activating and directing other immune cells.

In addition to RANTES, many other CC chemokines may induce the chemotaxis of $CD4^+$ and $CD8^+$ T-cells through binding to CCR1 expressed on $CD4^+$ and $CD8^+$ T-cells (MIP-1α, MCP-2, MCP-3, MIP-5, MIP-1β, MIP-1γ and MCP-1), CCR2 expressed on activated memory T-cells (MCP-1 and MCP-5), CCR3 expressed on $CD4^+$ Th2 and $CD8^+$ Tc2 T-cells (eotaxin, eotaxin-2, eotaxin-3, MCP-2, MCP-3, MCP-4 and MIP-5) and CCR5 expressed on $CD4^+$ Th1 and $CD8^+$ Tc1 T-cells (MIP-1 α, MIP-1β and MCP-2, MCP-4, MCP-1 and eotaxin) (Murphy *et al*, 2000).

T-cell infiltration is associated in particular with several major inflammatory diseases of the lung. Bronchial biopsies from asthmatics show infiltration with eosinophils, activated mast cells, and activated T-helper ($CD4^+$) T-cells that are predominantly Th2 cells. $CD4^+$ lymphocytes predominate over $CD8^+$ cells and neutrophils are sparse (reviewed in Barnes, 2008, Holgate, 2007 and Jeffery, 1999). In bronchial biopsies from patients with COPD, it has been reported that there is an infiltration of activated T-helper ($CD4^+$) T-cells (predominantly Th1 and cytotoxic Tc1 cells) and increased

numbers of neutrophils and macrophages (Barnes, 2008). $CD8^+$ lymphocytes predominate over $CD4^+$ cells and there are increased numbers of subepithelial macrophages and intra-epithelial neutrophils (reviewed in Barnes, 2008 and Jeffery, 1999). In addition, the infiltration of T-cells of the $CD8^+$ subset again predominates in severe peribronchiolitis (Jeffery, 1999) and analysis of infiltrate in the CF airway implicates neutrophils, B-cells and T-cells, with increased numbers of $CD4^+$ T-cells appearing as the most encountered population in the CF bronchial wall (Hausler *et al*, 2002; Hubeau *et al*, 2001).

There is much evidence to suggest that RANTES predominantly induces T-cell transendothelial migration in the lung during inflammation. Using inhibitors of RANTES function and also by measuring RANTES expression, studies have shown that RANTES is a major chemoattractant in the asthmatic lung (Venge *et al*, 1996) and that RANTES induces the migration of T-cells into lung tissue in sarcoidosis, COPD, asthma, interstitial lung disease and fibrosing alveolitis (Barnes, 2008; Brozyna *et al*, 2009; Petrek *et al*, 1997; Psarras *et al*, 2005; Saetta *et al*, 1998; Ziora *et al*, 1999). T-cell accumulation in the lung has been associated with increased levels of RANTES detected in the bronchoalveolar lavage fluid of patients with diffuse panbronchiolitis (Kadota *et al*, 2001) and in addition, the neutralisation of RANTES receptors with receptor antagonists significantly decreases T-cell infiltration into lung tissue and decreases RANTES mRNA expression (Gonzalo *et al*, 1998).

1.17. Chemokine clearance

Chemokines which diffuse in blood and appear in plasma can be bound by DARC on red blood cells, which internalises from the cell surface following ligand binding. DARC serves as a chemokine reservoir in the blood circulation but DARC may also contribute to chemokine clearance from tissues into blood (Colditz *et al*, 2007; Rot, 2005). However, more likely, chemokines passively diffuse into the lymphatic vessels along pressure gradients and are cleared into the lymph nodes. Evidence shows that chemokines can induce leukocyte migration from the blood into the lymph nodes. Chemokines may also be scavenged by enzymes or by chemokine interceptor D6 expressed on lymphatic endothelium and leukocytes. D6 binds multiple inflammatory CC chemokines and aids degradation by facilitating transport into lysosomal compartments (Colditz *et al*, 2007; Ward *et al*, 1998). In addition to chemokine

interceptors, GPCRs may also be involved in chemokine clearance through uncoupling from conventional signalling responses (Colditz *et al*, 2007).

1.18. Copper

Copper (Cu) is an essential trace element existing in divalent, oxidised (Cu II) and reduced (Cu I) states. Widely distributed in the body, it is required for human survival, incorporated into organic complexes such as metallo-protein enzymes which are involved in such fundamental functions as redox reactions, iron absorption, free radical scavenging (superoxide dismutase), the cytochrome chain of mitochondrial oxidation (cytochrome oxidase), the synthesis of complex proteins of collagenous tissues in the skeleton and blood vessels, the synthesis of neurotransmitters and elastin cross-linking by lysyl oxidase. The total content of Cu in the human body is around 50-120 mg, 40 % of which is located in muscle and the highest concentration of 6.6 μg/g is found in the liver (Garrow, 2000; Osterberg, 1980). In plasma, over 90 % of Cu is bound to caeruloplasmin, 10 % to albumin and the rest to transcuprein, and amino acids (Tapiero *et al*, 2003; Twomey *et al*, 2007). In blood, Cu is bound into the metalloenzyme superoxide dismutase, which is involved in free radical scavenging. Caeruloplasmin binding to Cu occurs in the liver whereas albumin can bind and release Cu outside the liver (Garrow, 2000).

Total normal plasma or serum levels of Cu have been estimated using many different analytical techniques. The reported values range between 8.3 and 26.48 μM (Gonzalez *et al*, 1999; Versieck, 1980). In biological systems including water, free Cu tends to be in the cupric (divalent) state, although it is also found as Cu (I). However, in plasma, there is little or no free Cu in solution (Brewer, 2007). Free Cu (II) is estimated in plasma at 10^{-7} μM (Linder & Hazegh-Azam, 1996) and in eukaryotic cells at 10^{-18} M (Jackson *et al*, 2001), which is less than a single atom per cell (10^{-10} M). Caeruloplasmin bound Cu is not available as part of the exchangeable plasma copper pool, and cannot directly bind Cu ions in the plasma. Cu is only added during caeruloplasmin synthesis in the liver.

Cu appears to be exchanged directly between albumin and transcuprein which, of the two, has higher affinity for Cu. Cu bound to either of these two proteins is available as part of the exchangeable plasma Cu pool. Amino acids and small peptides in blood and

plasma are not a significant source of copper for cells (Linder & Hazegh-Azam, 1996). Cells can take up Cu from both caerulpolasmin (caeruloplasmin-Cu complex) and non-caeruloplasmin sources like albumin, transcuprein, Cu-cysteine and Cu-histidine complexes. The uptake of Cu is thought to involve interaction with cell surface receptors and metallochaperones. Within cells, copper is mostly bound to macromolecules including metallothionein and glutathione and it is thought that very few free Cu ions exist in the cytoplasm (Leary & Winge, 2007; Tapiero *et al*, 2003).

Dietary Cu is known to be essential for cardiovascular function and haemostasis, which is associated with over 30 Cu-dependent enzymes. A Cu deficient diet has major effects on both structural and functional aspects of the heart and vasculature. Interactions between endothelial cells and blood components in the microcirculation are intricately involved with Cu dependent processes. Cu deficiency results in prolonged haemostasis and inhibition of NO-dependent vasodilation (Schuschke, 1997). Some studies have indicated that Cu is required for the maintenance of appropriate signal transduction processes that are essential for the physiological function of platelets in haemostasis and thrombosis. Cu deficiency causes an increase in granule secretion from thrombin-activated platelets and it has been indicated that it is the direct effect of Cu deficiency on signalling pathways that leads to secretion (Johnson, 1999). Cu deficiency also leads to diminished platelet adhesion to endothelial cells and inhibits thrombus formation (Schuschke, 1997) but increases platelet aggregation, possibly the result of decreased platelet vWF and increased fibrinogen (Lominadze *et al*, 1996). It is clear that Cu is important for normal platelet aggregation and is involved in numerous microvascular functions. In excess, Cu can cause cellular damage. As a result, free Cu is normally present at very low levels in cells, approximately 10^{-13} – 10^{-18} M (Jackson *et al*, 2001; Linder & Hazegh-Azam, 1996).

1.19. Hydrogen Peroxide (H_2O_2)

Hydrogen peroxide (H_2O_2) is a covalent liquid that is generated *in vivo* by the dismutation of the superoxide radical (O_2^-) and can cross cell membranes readily. H_2O_2 is generated during oxidative stress and also released at sites of inflammation by the endothelium (Kinnula *et al*, 1992c), activated phagocytes and other inflammatory cells during inflammation (Halliwell *et al*, 2000a; Halliwell *et al*, 2000b).

High levels of H_2O_2 (>50 μM) are cytotoxic and it is widely thought that H_2O_2 is very toxic *in vivo* and is rapidly eliminated by enzymes such as catalases, peroxidases and thioredoxin linked systems (Halliwell *et al*, 2000a). However, H_2O_2 is poorly reactive in chemical terms, and can act as a mild oxidising or reducing agent but does not oxidise lipids, DNA or proteins readily.

The toxicity of H_2O_2 arises from its ability to form the highly reactive hydroxyl radical ($OH^{\cdot}$) either by exposure to ultraviolet light or by interaction with transition metal ions *in vivo* (Halliwell *et al*, 2000a). Transition metal ions are usually sequestered into protein-bound forms that cannot catalyse the formation of $OH^{\cdot}$ radicals, but H_2O_2 still contributes to redox chemistry by liberating transition metals from haem proteins. The addition of H_2O_2 can lead to transition metal mediated oxidative damage in cultured cells, however levels of H_2O_2 at or below 20-50 μM appear to have limited cytotoxicity to many cell types (Halliwell *et al*, 2000a) and some studies have claimed levels of H_2O_2 of up to 35 μM in human plasma (Deskur *et al*, 1998; Lacy *et al*, 1998; Varma & Devamanoharan, 1991). H_2O_2 can activate NF-κB, modulating the inflammatory process by up-regulating adhesion molecule expression and platelet aggregation (Halliwell *et al*, 2000b).

1.20. Copper and inflammation

Raised circulating Cu levels and mildly acidic conditions are common during inflammation (Atwood, *et al.,* 1998). Abnormally high Cu levels are seen in inflammation, infection, cancer and angiogenesis, cardiovascular diseases, rheumatoid arthritis, Alzheimer's disease and cystic fibrosis, chronic obstructive pulmonary disease, adult respiratory distress syndrome and asthma indicating that Cu is pro-inflammatory (Brewer, 2005; Karadag *et al*, 2004; Madaric *et al*, 1994; Milanino & Buchner, 2006; Percival *et al*, 1999; Rice *et al*, 2001; Squitti *et al*, 2002; Tapiero *et al*, 2003).

Particulate air pollution results in an increase in respiratory symptoms including the exacerbation of bronchoconstriction in asthma sufferers, increased hospitalisation rates for respiratory disorders and decreased lung function (Pope, 1989; Pope *et al*, 1991). Cu has been shown to be highly toxic for the lung when instilled in the airway, and it has been shown that Cu ions cause some of the effects of inhaled air pollution through NF-kB activation which results in cytokine (IL-6) and chemokine (IL-8) production,

indicating that pollutant-induced lung inflammation is Cu-dependent (Hirano *et al*, 1993; Hirano *et al*, 1990; Kennedy *et al*, 1998).

Furthermore, acute and chronic inflammation have been characterised by a significant increase of total serum copper, which can be regarded as a factor capable of worsening pathological processes, including oxidative stress (Milanino & Buchner, 2006) and Cu also induces endothelial IL-8 synthesis (Bar-Or *et al*, 2003).

1.21. Copper and peptide multimerisation

Copper, especially in the presence of H_2O_2 has been shown to induce aggregation and cross-linking of the amyloid-β peptide and prion protein (PrP^C). The multimerisation of the fragment amyloid-β (Aβ) by incubation with Cu was found to induce a fluorescent signal characteristic of tyrosine cross-linking (Atwood *et al*, 2004). The addition of H_2O_2 strongly promoted Cu-induced dityrosine cross-linking of Aβ 1-28, Aβ1-40 and Aβ1-42, suggesting that the oxidative coupling is induced by a Cu/H_2O_2 oxidative mechanism. In addition, it was previously shown that the binding of the PrP^C to GAGs is Cu dependent (Gonzalez-Iglesias *et al*, 2002), suggesting a possible role for Cu in the binding of chemokines to GAGs.

These findings have led to the hypothesis tested in this thesis that Cu may play a role in the multimerisation of chemokines through Cu-mediated dityrosine cross-links. It is proposed that the generation of H_2O_2 in inflammation, and its interaction with Cu coordinated to tyrosine residues of chemokines oxidises these residues through reactions that lead to covalent cross-linking, resulting in the formation of dityrosine cross-linked active chemokine multimers.

As yet there has been no documentation on the involvement of Cu forming covalent links with chemokines and GAGs, or the involvement of tyrosine residues in chemokine multimers. Recent therapeutic strategies have been directed to limiting excessive cytokine secretion from endothelial cells (Bar-Or, Thomas *et al.* 2003).

As well as providing a new therapeutic angle for the treatment of conditions such as rheumatoid arthritis, COPD, and CF, the theory that Cu is causative of chemokine

multimerisation and inflammation also provides insight to the possibility of treating other diseases.

1.22. Copper chelators

Cu chelators have been implemented for the treatment of many inflammatory disorders. Cu has been implicated in tumour growth and angiogenesis and the Cu chelator tetrathiomolybdate has been studied extensively in clinical trials as a therapy for cancer and angiogenesis. The anti-angiogenic mechanism of tetrathiomolybdate was found to involve the inhibition of angiogenic promoting cytokines, which led to the hypothesis that Cu chelators may inhibit cytokines that are associated with excessive fibrosis and inflammation (Brewer, 2005; Brewer, 2008). The mechanism is thought to be due to NF-κB inhibition resulting in reduced chemokine synthesis. Tetrathiomolybdate has also been shown in clinical trials to be successful in treating many other diseases of inflammation and fibrosis to include pulmonary fibrosis, hepatitis and liver cirrhosis (Brewer, 2005). Other Cu complexes, including Cu complexed to Cu-binding proteins have also been shown to attenuate redox reactions and subsequent NF-κB activation (Rael *et al*, 2007).

Cu chelators such as tetrathiomolybdate, D-penicillamine and trientine are clinically effective in the treatment of Wilson's disease, an inherited disease of copper toxicity. These drugs are known to remove excess copper accumulated in the liver and other organs in Wilson's disease patients (Cui *et al*, 2005; Gupte & Mumper, 2007; Schilsky, 1996). The accumulation results in neurologic symptoms of tremors, spasticity, rigidity and chorea, dystonia, unsteady gait and psychosis (Cui *et al*, 2005). Specific Cu chelators have also been shown to strongly inhibit protein oxidation that occurs in the presence of Cu (Zhu *et al*, 2002).

Copper chelators have also been shown to be effective in the treatment of rheumatoid arthritis. The active forms of anti-arthritic drugs are complexes extemporaneously formed with endogenous Cu *in vivo.* These include the current drugs, D-penicillamine, salicylate, aspirin, and trientine (Cui *et al*, 2005; Milanino & Buchner, 2006).

The Cu chelators trientine, D-penicillamine, bathocuproine and bathophenanthroline were reported to be effective in solubilising brain Aβ (Cherny *et al*, 2000) and in

addition, the metal chelation of Cu with clioquinol markedly inhibits Aβ aggregation in Alzheimer's disease transgenic mice (Cherny *et al*, 2001).

It has been found that Cu chelation delays the onset of prion disease in mice, and it has been suggested that the removal of Cu reduces the interaction of PrP^C with GAGs (Sigurdsson *et al*, 2003). From a clinical perspective, this suggests a possible role for chelators in AD and prion disease, and also potential for Cu chelators as anti-inflammatory agents. Since Cu is an essential trace element, Cu-lowering therapy must decrease Cu levels to a midrange therapeutic window where Cu deficiency does not occur (Brewer, 2005).

In addition, GAGs such as heparin and hyaluronic acid have been shown to exhibit antioxidant capacity and have a protective effect against Cu induced lipid peroxidation and oxidative damage in fibroblast and liposome cultures (Albertini *et al*, 2000; Albertini *et al*, 1996; Balogh *et al*, 2003; Campo *et al*, 2004; Volpi & Tarugi, 1999).

1.23. Hypothesis

This thesis tests the hypothesis that Cu is pro-inflammatory and promotes chemokine multimerisation, inducing covalent dityrosine cross-linking between chemokine monomers in the presence of H_2O_2.

1.24. Aims

To identify a proinflammatory role for Cu and investigate the potential for Cu chelators as anti-inflammatory therapy.

1.25. Objectives

1. To establish the effect of Cu and H_2O_2 on chemokine multimerisation
2. To determine the biochemical nature of chemokine-chemokine interactions
3. To detect the formation of dityrosine cross-links between chemokine multimers
4. To test the effect of chemokine multimers in lymphocyte migration assays
5. To determine the effect of Cu and H_2O_2 on RANTES synthesis and release by endothelial cells, T-cells and platelets
6. To establish assays for T-cell transendothelial migration and investigate the effect of Cu chelators on lymphocyte migration
7. With reference to the scientific literature, put the results into context and indicate the therapeutic potential for Cu chelators with particular reference to pulmonary inflammatory diseases

Chapter 2

The effect of $CuCl_2$ and H_2O_2 on multimerisation of isolated recombinant chemokines

2. The effect of $CuCl_2$ and H_2O_2 on multimerisation of isolated recombinant chemokines

2.1. Introduction

2.1.1. Chemokine multimerisation on endothelial cell surfaces

The immobilisation of chemokines to endothelial cell surfaces by proteoglycans has been demonstrated both *in vitro* (Hoogewerf *et al*, 1997) and *in vivo* (Rot, 1993).The interaction is thought to facilitate the retention of chemokines on cell surfaces and enable the localisation of high concentrations of chemokines under shear blood flow conditions (Proudfoot *et al*, 2003). RANTES is immediately bound to HS *in vitro* and rapidly dissociates in equilibrium. The immediate binding of RANTES to HS may be necessary for localisation of activity at the site of secretion but it can also be mobilised to extend the concentration gradient at the cell surface, an aspect of functional importance (Vives *et al*, 2002).

Growing evidence suggests that proteoglycans facilitate chemokine-receptor binding by inducing chemokine self-aggregation, also known as oligomerisation or multimerisation which may increase the local concentration of chemokines on cell surfaces (Hoogewerf *et al*, 1997; Vives *et al*, 2002).

RANTES binds to HS at a length of dp16 - dp18 (no. of saccharides upon depolymerisation (dp) of HS). Such a length suggests that optimum binding occurs with multimers of the chemokine. Binding studies have shown that RANTES multimerises along the GAG chain and that the binding of RANTES monomers depends on one another indicating a cooperative mechanism (Vives *et al*, 2002).

RANTES binds to HS in the nanomolar range, at physiological concentrations. Since the dimer dissociation constant of RANTES is 35 μM in the absence of HS (Skelton *et al*, 1995), this suggests RANTES is predominantly monomeric at physiological concentrations. Evidence shows that at nanomolar concentrations, chemokine multimers form on cell surface GAGs (Vives *et al*, 2002), and therefore it is likely that those chemokines that are monomeric at physiological concentrations may dimerise or

multimerise under physiological conditions but only in the presence of glycosaminoglycans (GAGs) *in vivo* (Proudfoot, 2006).

It is suggested that this may be a method of collecting and dimerising RANTES at low and physiological concentrations (Vives *et al*, 2002). However, it has also been suggested that the formation of high molecular weight aggregates *in vivo* may have a physiological role in limiting the amount of active chemokines circulating in the bloodstream since aggregation probably reduces the number of surface sites on chemokines that are accessible to receptors (Skelton *et al*, 1995).

Chemokines do not need to multimerise to elicit a chemotactic response *in vitro*, as mutant monomeric variants of RANTES, IL-8, MIP-1β, MCP-1 and MCP-3 are able to interact with receptors and induce leukocyte recruitment *in vitro* (Czaplewski *et al*, 1999; Laurence *et al*, 2000; Paavola *et al*, 1998; Proudfoot *et al*, 2003; Rajarathnam *et al*, 1994). However *in vivo*, these mutants do not induce leukocyte recruitment (Proudfoot *et al*, 2003) indicating that multimerisation is required for the *in vivo* chemotactic activity of these chemokines.

It has also been shown that wild-type RANTES binds to heparin and HS as a tetramer *in vitro* (Hoogewerf *et al*, 1997) and using RANTES mutants that are not able to multimerise it has been shown that RANTES has a minimal tetrameric quaternary structure for cell attractant activity *in vivo.* Both the monomeric and dimeric forms of RANTES are devoid of *in vivo* chemotactic activity (Proudfoot *et al*, 2003) indicating that multimerisation to the tetramer may be required for *in vivo* RANTES activity. In addition, a RANTES mutant that is unable to bind to immobilised GAGs was also unable to induce leukocyte recruitment *in vivo,* although it retained wild-type receptor binding to CCR1 and CCR5 *in vitro* (Proudfoot *et al*, 2003). This indicates that both multimerisation and GAG binding are necessary for the *in vivo* activity of RANTES.

Interestingly, chemokines that occur naturally as monomers such as eotaxin and MCP-3 have not been reported to multimerise as shown by structural and biophysical studies (Crump *et al*, 1998; Keizer *et al*, 2000; Kim *et al*, 1996), but both are able to recruit leukocytes *in vivo,* although it is not known whether or not these chemokines multimerise on cell surface proteoglycans (Proudfoot *et al*, 2003). However, it is

possible that these chemokines can achieve higher order multimers *in vivo* due to GAG induced multimerisation and they may interact with leukocyte receptors as dimers, trimers or tetramers.

2.1.2. Chemokine multimerisation in solution

The CXC and CC chemokines IL-8, MIP-1α, RANTES and MCP-1 all multimerise on interaction with cell surface HS (Bernfield *et al*, 1999; Hoogewerf *et al*, 1997) but many chemokines can also aggregate in the absence of proteoglycans. Such chemokines include human IL-8, RANTES, MIP-1α and MIP-1ß all of which have been shown to self associate and form stable high molecular weight aggregates in solution at neutral pH (Burrows *et al*, 1994; Clore *et al*, 1990; Czaplewski *et al*, 1999; Schnitzel *et al*, 1994; Skelton *et al*, 1995).

Most chemokines are reported to be present in normal healthy tissues at physiological concentrations in the nanomolar range (Burrows *et al*, 1994; Vives *et al*, 2002) and many chemokines exist in dimeric form at these nanomolar concentrations.

Multimer formation has been shown to be concentration and pH dependent. At concentrations greater than 1 mM (Skelton *et al*, 1995) larger aggregates of RANTES are predominant and chemokines have been shown to participate in monomer-multimer equilibrium in solution (Burrows *et al*, 1994; Mayo & Chen, 1989). Both the dilution of RANTES from 3.9 to 0.08 mM and the lowering of the pH below 3.7 results in dimer dissociation. Evidence shows that RANTES dimers are very stable at neutral pH and also very soluble (Skelton *et al*, 1995).

Whilst RANTES is predominantly monomeric at physiological concentrations *in vitro,* studies have revealed that IL-8 exists as both a monomer and dimer at nanomolar concentrations with dimer dissociation constants in the region of 100 nM – 100 μM (Williams *et al*, 2005). Structural studies have revealed that whilst the monomeric tertiary structure of the chemokines is very similar, the dimeric structure of members of the CC and CXC subfamilies is completely different, as typified by MIP-1β and IL-8 respectively. The MIP-1β dimer is elongated and cylindrical whereas the IL-8 dimer is globular in shape (Clore & Gronenborn, 1995). The structure of the monomers of CC and CXC chemokines appears to be similar despite the low level of sequence identity

between the two classes of chemokines and although the C-terminal helices are shorter for the CC chemokines.

The dimer topologies of both RANTES and MIP-1ß are completely different from those of the CXC chemokines. The RANTES dimer most closely resembles that of MIP-1ß. For the CC chemokines, the dimer interface is formed by the N-terminal ß-strand of the protein rather than the second ß-strand in CXC chemokines (Clore & Gronenborn, 1995). In RANTES, dimerisation occurs through interaction of the region N-terminal to the CC motif of one monomer with residues in the 30s loop and strand-ß3 of the other monomer (figure 2.1). Key hydrophobic residues at the N termini dictate the mode of dimerisation. Evidence shows that for MIP-1α, MIP-1β and RANTES the substitution of Glu26 or Glu66 causes substantial disaggregation, suggesting that these residues are key elements in the self-association process (Czaplewski *et al*, 1999). All CC chemokines dimerise in a fashion similar to that of RANTES. The CXC chemokines dimerise through hydrophobic residues in strand ß1 (Skelton *et al*, 1995).

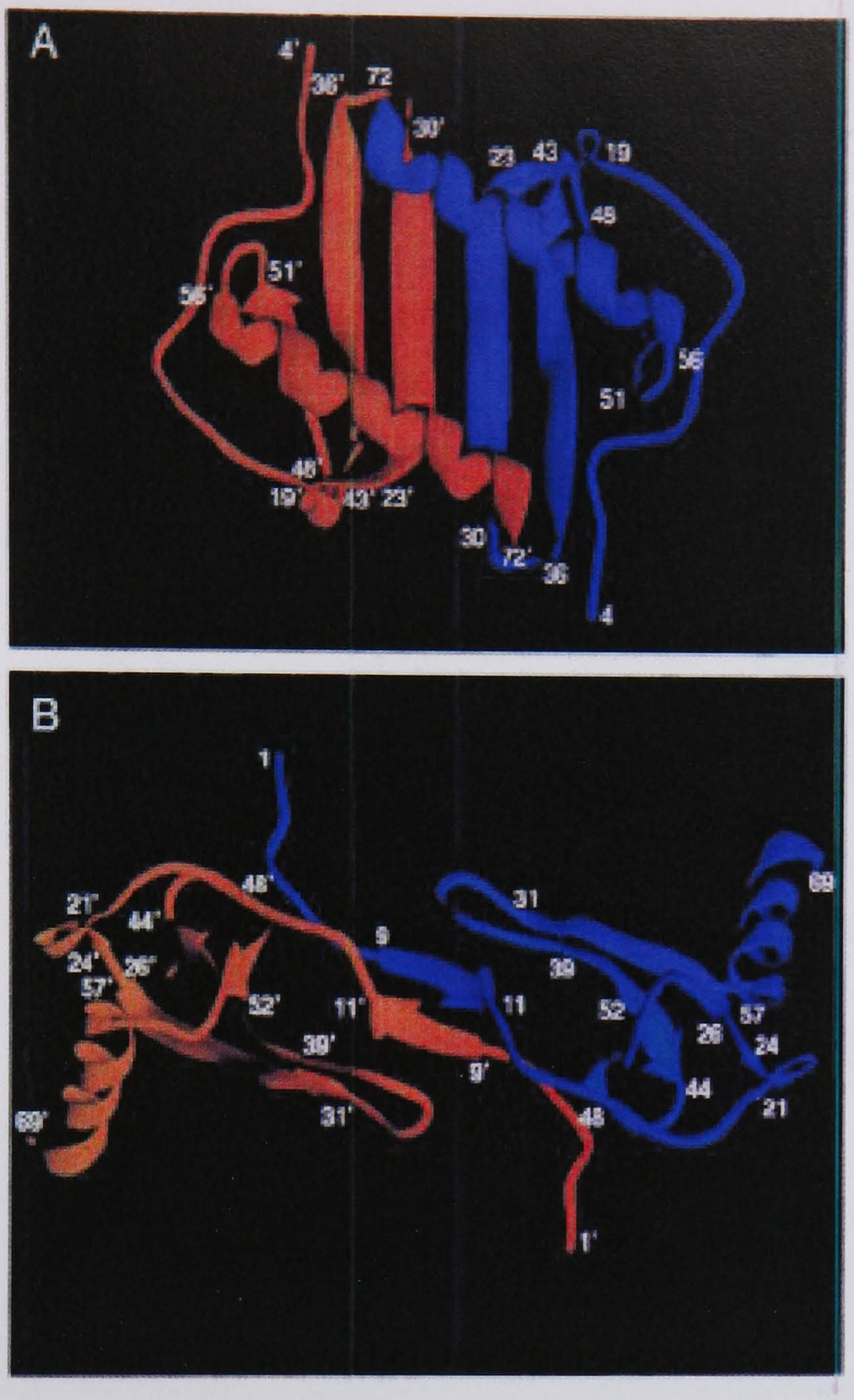

Figure 2.1. Schematic ribbon drawings of the IL-8 dimer (A) and the RANTES dimer (B). One subunit is shown in blue and the other in red (Clore & Gronenborn, 1995).

2.1.3. Amyloid-β peptide multimers

Alzheimer's disease is the most common senile dementing disorder, characterised pathologically by the accumulation of neurofibrillary tangles and senile plaques in the neocortex and cerebral vasculature (Huang *et al*, 2000b; Squitti *et al*, 2002). The Aβ-peptide (Aβ) is the main constituent of senile plaques, a 4 KDa protein consisting of 39-43 amino acid residues that is produced from its precursor, the amyloid protein precursor (APP).

The Aβ-peptides are a group of soluble proteins of considerable amino and carboxyl terminal heterogeneity found in all biological fluids. Aβ1 – 40 is the major soluble Aβ species and Aβ1-42 the minor but more fibrillogenic species (Huang *et al*, 2004; Huang *et al*, 2000b). The cortical deposition of the amyloid-β peptide (Aβ) that occurs in AD also occurs in Down's syndrome, head injury and normal ageing (Atwood *et al*, 1998).

Although Aβ-peptide from biological fluids is a 4 KDa monomeric protein, Aβ-peptide extracted from post mortem brain specimens is found as formic acid resistant oligomers and both Aβ1-40 and Aβ1-42 form multimers upon incubation.

It was found that Cu is detectable within the neuropil (the region between neuronal cell bodies in the gray matter of the brain and spinal cord) of the AD-affected brain, where it is highly concentrated within amyloid plaque deposits and neurofibrillary tangles with total concentrations reaching 0.4 mM. It was also found that Cu (II) and oxidative systems promote the oligomerisation/aggregation of Aβ-peptide in a reaction that is reversible with Cu chelation (Atwood *et al*, 2000a; Atwood *et al*, 2004; Huang *et al*, 1999). It was observed that Cu induced Aβ-peptide aggregation is enhanced in the presence of H_2O_2 and the involvement of a Cu/H_2O_2 oxidative system has been suggested (Liu *et al*, 2006). In addition, covalent links between Aβ-peptide monomers have been confirmed as dityrosine cross-links (Atwood *et al*, 2004).

2.1.4. Prion Protein multimers

Like the Aβ-peptide, the prion protein (PrP) has been shown to aggregate and form multimers in the presence of Cu. PrP has a monomeric molecular weight of 35-36 KDa. Prion proteins trigger a group of neurodegenerative diseases. A conformational isomer of the normal prion protein (PrP^C), denoted as PrP^{SC} is thought to be responsible for fatal diseases such as bovine spongiform encephalopathy (BSE) in cattle and Creutzfeldt-Jakob disease (CJD) in humans.

The prion protein is characterised by the presence of a flexible and 'unstructured' region, roughly 100-residue N terminal 'tail', and of a globular domain of nearly identical size (Brown *et al*, 2004). As yet the function of the protein is unknown, but has been identified that Cu plays a key role in the biology of PrP^C.

It is well documented that the prion protein interacts with GAGs. HS binding sites in the PrP^C have been identified. It has been reported that 2-0-sulphate groups are essential for heparin recognition, and that there are three regions of the prion protein capable of independent binding to heparin and heparan sulphate (Warner *et al*, 2002).

The interaction of the prion protein with GAGs occurs due to the formation of oligomeric complexes stabilised by Cu (II) bridges (Gonzalez-Iglesias *et al*, 2002). The interaction of the octapeptide spanning peptide motif with heparin, interestingly, is enhanced by Cu (II) ions. A peptide with the same motif (residues 53-93) inhibits the binding of the full-length prion protein to GAGs (Warner *et al*, 2002).

2.1.5. A possible role for Cu in chemokine multimerisation

Chemokines are essential for directing the inflammatory response, mediating leukocyte chemotaxis and migration from the bloodstream into the tissues at sites of inflammation. Previous findings have suggested that aggregation and multimerisation is important for chemokine binding and presentation on endothelial cell surfaces and that multimer formation is mediated by cell surface GAGs. It is also suggested that chemokine multimer formation and GAG binding is necessary to induce chemotaxis *in vivo* under shear blood flow conditions and that the binding of multimers to cell-surface GAGs concentrates and localises chemokine gradients to prevent diffusion into the bloodstream.

Chemokines self-aggregate and also bind to endothelial cell surface GAGs including HS. Previous research directed to both the amyloid-β peptide and the prion protein has revealed that Cu promotes amyloid-β peptide aggregation and dityrosine formation, which is enhanced by H_2O_2, and that Cu has a role in the formation of oligomeric PrP complexes and their binding to GAGs including heparin.

The discovery of these proinflammatory roles for Cu has led to the current investigation of the ability of Cu to induce chemokine aggregation and chemokine-GAG binding. The number of tyrosine residues in the primary sequence varies depending on the chemokine. There are none in ENA-78, one in IL-8 and five in RANTES, suggesting the chemokines may oligomerise differently under the same Cu and H_2O_2 redox conditions. Therefore, the experiments described in this chapter also investigate the possible involvement of dityrosine cross-linking in chemokine multimerisation.

2.2. Materials

Recombinant human RANTES, human IL-8 and human ENA-78 were obtained from Peprotech EC, London, UK. Dimethyl sulphoxide (DMSO), guanidine hydrochloride (G-HCl), copper chloride ($CuCl_2$), hydrogen peroxide (H_2O_2), heparan sulphate (HS) from pig mucosa, TRIS, glycine, sodium dodecyl sulphate (SDS), ammonium persulphate (APS), coloured MLW markers (Colorburst) and biotinylated SDS markers were obtained from Sigma-Aldrich Inc., Poole, Dorset, UK.

Polyacrylamide mini-gels were cast using the Bio-Rad Protean II system. The polymerising catalyst solution N,N,N',N' – tetramethylethylenediamine (TEMED), 45 μm nitrocellulose and a 30 % acrylamide solution containing 0.8 % bis-acrylamide were obtained from Bio-Rad Laboratories Ltd, Hemel Hempstead, Hertfordshire, UK. Phosphate buffered Saline (PBS) without added calcium or magnesium was obtained from Invitrogen Ltd, Paisley, UK. Methanol, ethanol and acetone were obtained from Fisher Scientific UK Ltd., Loughborough, Leicestershire, UK. All buffers and reagents were prepared in ultra-high quality (UHQ) water unless otherwise stated.

Biotinylated primary IL-8, RANTES and ENA-78 antibodies were obtained from Peprotech EC, London, UK. A streptavidin-biotinylated horseradish peroxidase complex (StreptABC) was obtained from Dako UK Ltd, Ely, Cambridgeshire, UK. A commercial enhanced chemiluminescence (ECL) kit, SuperSignal, was obtained from Pierce Biotechnology Inc., Rockford, IL 61105, USA. Tween-20, PBS ($-Ca^{2+}/Mg^{2+}$) and Super RX Fuji medical X-Ray film were obtained from Fisher Scientific, Loughborough, Leicestershire, UK.

2.3. Methods

2.3.1. Sample preparation

IL-8, RANTES and ENA-78 were incubated at 37 °C in 0.5 ml Safe-Lock eppendorf tubes for 1 (IL-8 and ENA-78) or 2 days (RANTES) at a final concentration of 5 x 10^{-7} M in PBS (-Ca^{2+}/Mg^{2+}), final volume 40 µl with $CuCl_2$ (1.25 - 100 µM), H_2O_2 (0.5 - 400µM) and HS (0.1 mg/ml) final concentration. Safe-Lock eppendorf tubes eliminate the risk of sample evaporation during incubation. Following incubation, chemokines were analysed using SDS polyacrylamide gel electrophoresis (SDS-PAGE) and Western blotting.

2.3.2. Dimethyl sulphoxide

The hydroxyl radical scavenger, DMSO (0.4, 2 and 4 µl), was added to 0.5 ml eppendorfs, followed by the addition of chemokines, $CuCl_2$, H_2O_2 and HS as described in section 2.3.1. The final concentration of DMSO was 1, 5 and 10 % (v/v) respectively, in a final volume of 40 µl.

2.3.3. Guanidine hydrochloride and ethanol precipitation

Guanidine hydrochloride (GHCl) was added to samples following 1 or 2 day incubation at 37 °C. An equal volume (40 µl, referred to as volume A) of 12 M guanidine hydrochloride (G-HCl) in PBS (-Ca^{2+}/Mg^{2+}) was added to the samples resulting in a final concentration of 6 M G-HCl and the samples were incubated overnight at 4°C. 360 µl of cold 100 % (v/v) ethanol (kept at -20 °C) was added to the protein solution (80 µl) – the final volume (400 µl) was referred to as volume B. The protein/ethanol solution was incubated at -20 °C for at least 1 hr, or left overnight. Following incubation, samples were centrifuged for 15 minutes at 4 °C in a micro-centrifuge at maximum speed (15,000 g). The supernatant was discarded and the pellet retained. The pellet was washed by re-suspending in 90 % (v/v) cold ethanol (kept at -20°C) - the final volume was equal to volume B. Samples were vortexed and re-pelleted by centrifugation at 15,000 g for 15 minutes. 90 % of the supernatant was removed by aspiration. The remaining 10 % of the samples was dried in a rotary evaporator for 30 minutes at 45 °C. The pellet was reconstituted in volume A (40 µl), of 1x sample buffer.

2.3.4. Sodium dodecyl sulphate polyacrylamide gel electrophoresis (SDS-PAGE)

Proteins were separated by electrophoresis on 1 mm thick 14 % polyacrylamide gels. Resolving gels were prepared with 2.33 ml 30 % acrylamide solution, 1.5 ml 1.5 M TRIS-resolving gel buffer (18.17 g TRIS in 100 ml H_2O, adjusted to pH 8.8 with concentrated HCl), 1.35 ml UHQ water, 50 µl 10 % (w/v) SDS, 25 µl 10 % (w/v) APS (both prepared by adding 1g to 10 ml deionised water. APS was stored in 1 ml aliquots at -20 °C and SDS stored at room temperature), and 2.5 µl TEMED per 1 gel. The resolving gel solution was poured between the glass plates and the solution was overlaid with 100% ethanol or water to ensure a flat interface. Resolving gels were allowed to set for 30 minutes before the addition of the stacking gel. At this stage, gels were either used straight away or stored at 4 °C prior to the addition of a stacking gel, overlaid in resolving gel buffer diluted 1:4.

Stacking gels were prepared with 0.65 ml 30 % acrylamide solution, 1.25 ml 0.5 M TRIS-stacking gel buffer (6.057 g TRIS in 100 ml H_2O, adjusted to pH 6.8 with concentrated HCl), 3.05 ml UHQ water, 50 µl 10 % (w/v) SDS, 50 µl 10 % (w/v) APS and 5 µl TEMED per 1 gel. The buffer overlay was removed and approximately 5 ml of stacking gel was added to the top of each resolving gel. A clean plastic spacer was immediately added to form 10 sample wells.

A 10x concentrated (1 M) TRIS-glycine running buffer was prepared by dissolving 15.15 g TRIS, 72 g glycine and 5 g SDS in 500 ml deionised water. The 10x solution was diluted 1:10 to 100 mM on the day of the experiment. A 4x non-reducing sample buffer containing bromophenol blue as a tracer dye allowed visualisation of samples in the resolving gel (8 ml of 4x running buffer, 2 ml glycerol and 1 mg bromophenol blue) The 4x running buffer was prepared by adding 4 ml of 10x running buffer to 6 ml deionised H_2O. The samples were prepared by the addition of 5 µl 4x non-reducing sample buffer to 15 µl of sample, diluting the buffer to a final concentration of 1x and pH 8.3. The 4x non-reducing sample buffer was stored at –20 °C in 0.5 ml aliquots. Samples were loaded in the sample wells in the stacking gel (15 µl per well.) One lane of biotinylated molecular weight markers and one lane of colour markers (Sigma-Aldrich Inc., Poole, Dorset, UK) was analysed on each gel (5-10 µl per lane.)

The samples were run slowly through the stacking gel at 40 V for 15 minutes. When the dye front reached the resolving gel the voltage was increased to 120 V. Electrophoresis was terminated when the bromophenol blue dye front reached the bottom of the gel, after approximately 1.5 hours.

2.3.5. Western blotting

Following electrophoresis, the stacking gel was removed and discarded. The resolving gel was equilibrated in SDS-PAGE running buffer containing 20 % (v/v) methanol and placed onto a 45 μm nitrocellulose membrane, between 2 paper filters pre-soaked in SDS-PAGE running buffer containing 20 % (v/v) methanol. The gel was marked by removing the corner of the gel on one side. This ensured it was transferred the correct way round.

Proteins were transferred by BioRad semi-dry electrophoretic transfer at 15 V, current limit 1.76 A, for 15 minutes per mini-gel at room temperature. Following transfer, the non-specific binding of antibodies to the membrane during staining was blocked by the immersion of Western blots in blocking buffer (PBS -Ca/Mg / 2 % (v/v) Tween-20) and overnight incubation at 4 ^{o}C.

Prior to staining, the membranes were washed three times for 10 minutes each in 1x PBS (-Ca^{2+}/Mg^{2+}) /0.05 % (v/v) Tween-20 (Sigma, UK). They were then incubated in biotinylated primary antibody (rabbit polyclonal anti-human RANTES, goat polyclonal anti-human IL-8 or rabbit polyclonal anti-human ENA-78), at 0.1 μg/ml in PBS / 2 % (v/v) Tween-20, 5 ml per blot) for 90 minutes at room temperature. The membranes were washed three times as before, and then incubated with a 1:20,000 (v/v) dilution (1 μl of each of tubes A and B in 10 ml 2 % (v/v) Tween-20 / PBS) of a streptavidin-biotinylated horseradish peroxidase complex (StreptABC, DAKO, UK) for 45 minutes at room temperature.

Following incubation with StreptABC, membranes were washed five times in 1x PBS (-Ca^{2+}/Mg^{2+}) /0.05 % (v/v) Tween-20 for 10 minutes each and the blots developed using SuperSignal ECL kit (Pierce) and placed against X-Ray film for 1 and 5 minutes, and overnight to visualise results. 2.5 ml of each of the developer and enhancer were mixed

together, 5 ml per blot. Chemiluminescence is a chemical reaction between an enzyme (horseradish peroxidase, HRP), and a chemiluminescent chemical, such as luminol, resulting in emission of light. HRP is oxidised in the presence of H_2O_2, the oxidised HRP is then capable of oxidising the luminol. Once oxidised the luminol exists in an excited state, which then decays to its ground state via the emission of light. In the kit used, an enhancer has been added allowing increased intensity and duration of light production.

2.3.6. Scanning and density analysis

If the intensity of staining was sufficiently consistent to allow for semi-quantitative analysis, the blots were scanned using Quantiscan software.

2.4. Statistical analysis

Data were compared with a 1 or 2-way ANOVA followed by either a Dunnet's or Tukey's *post-hoc* test where $p < 0.05$ was the minimum accepted level of significance.

2.5. Results

2.5.1. RANTES

To investigate the form of freshly prepared RANTES prior to incubation, recombinant human RANTES (Peprotech, UK) was prepared in the concentration range 10^{-10} – 10^{-6} M in PBS (-Ca^{2+}/Mg^{2+}), in a final volume of 40 µl, and analysed by SDS-PAGE. The Western blot was stained for human RANTES (figure 2.2). RANTES has a dimer dissociation constant of 35 µM, and therefore it was expected that RANTES would be predominantly monomeric.

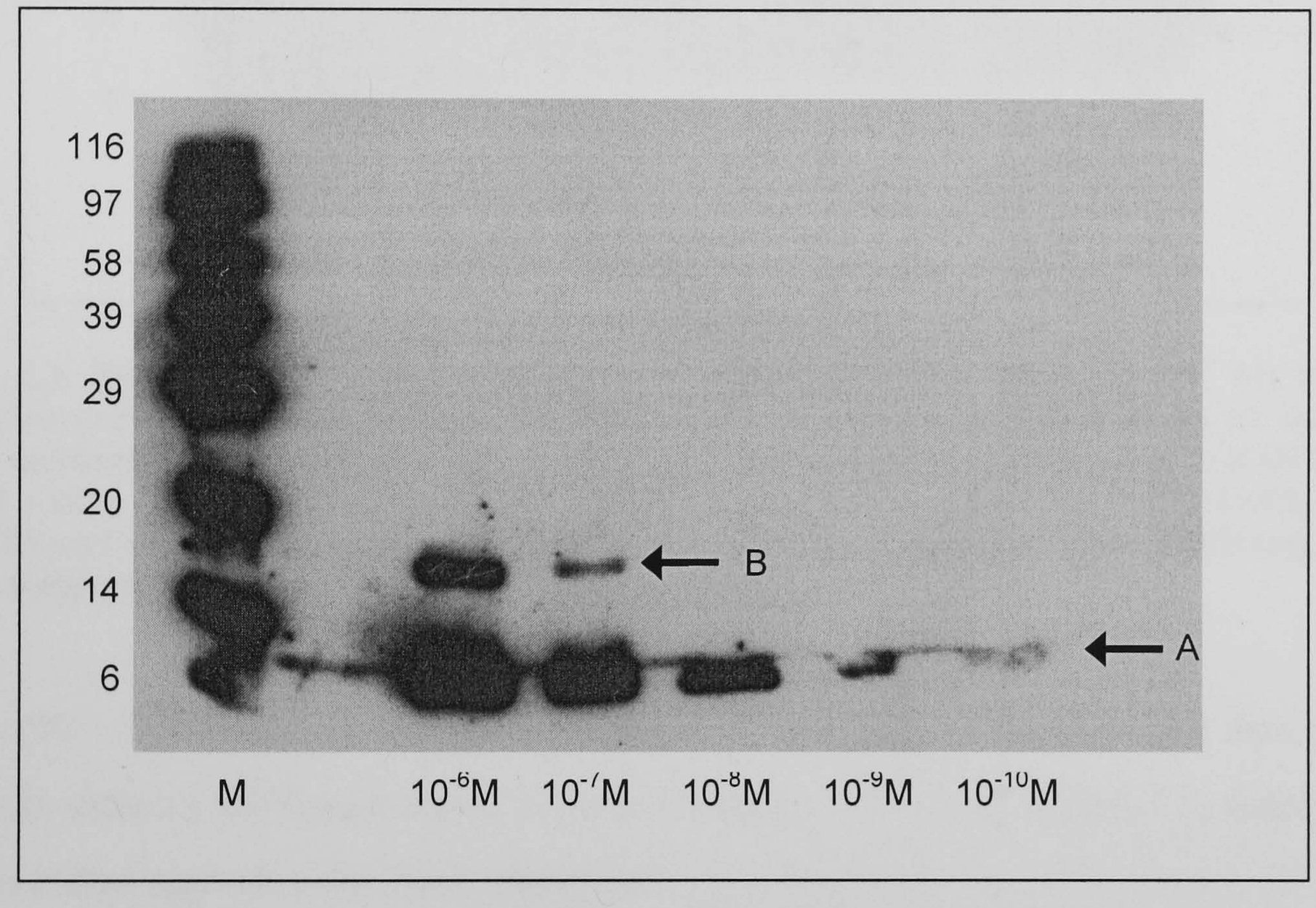

Figure 2.2. The form of recombinant RANTES in solution at 10^{-10} M to 10^{-6} M, analysed by SDS-PAGE on a 14 % polyacrylamide gel. Arrows show 8 KDa monomers (A) and 16 KDa dimers (B). M: Molecular weight markers. Representative of two independent experiments.

RANTES was present in monomeric form (8 KDa) at 10^{-10} – 10^{-8} M (figure 2.2). Dimers (16 KDa) appeared at the higher concentrations of 10^{-7} and 10^{-6} M RANTES, with maximum dimer formation seen at 10^{-6} M. No higher order multimers greater than dimer were seen. A concentration of 5 x 10^{-7} M RANTES was used in all further experiments to test the effect of Cu and H_2O_2 on multimerisation.

To investigate the effect of copper on RANTES multimerisation, RANTES (5 x 10^{-7} M) was incubated with $CuCl_2$. Incubation of RANTES with $CuCl_2$ for 1 day did not induce multimer formation above the dimer present in the sample (data not shown). Therefore

RANTES (5×10^{-7} M) was incubated at 37 °C for 2 days in the presence of increasing concentrations of $CuCl_2$ (1.25 – 100 μM).

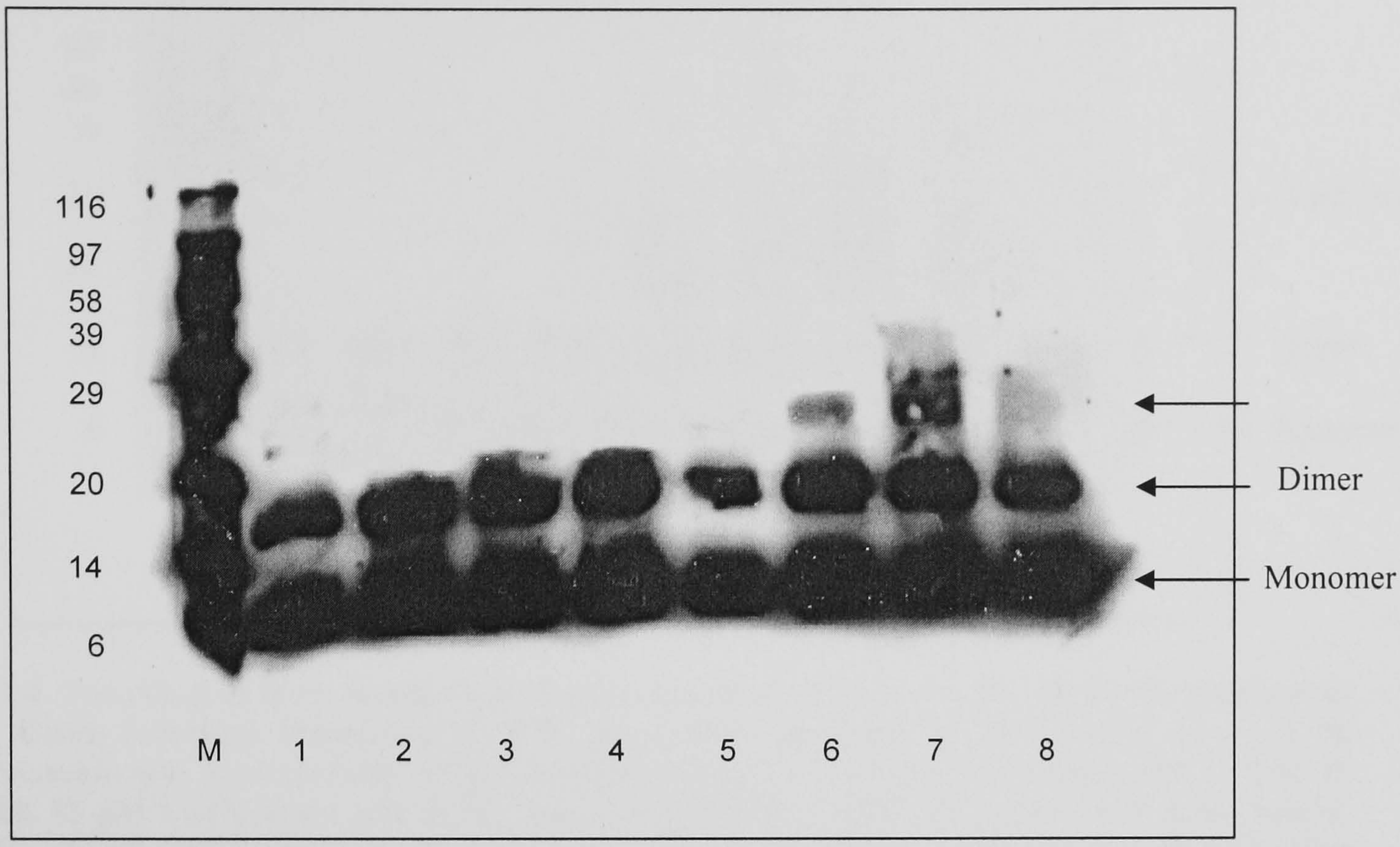

Figure 2.3. The effect of $CuCl_2$ on the form of recombinant RANTES (5×10^{-7} M) following incubation at 37°C for 2 days analysed by SDS-PAGE on a 14 % polyacrylamide gel. M: molecular weight markers. Lane 1: RANTES only, lane 2: RANTES and 1.25 μM $CuCl_2$, lane 3: RANTES and 2.5 μM $CuCl_2$, lane 4: RANTES and 12.5 μM $CuCl_2$, lane 5: RANTES and 25 μM $CuCl_2$, lane 6: RANTES and 50 μM $CuCl_2$, lane 7: RANTES and 75 μM $CuCl_2$ and lane 8: RANTES and 100 μM $CuCl_2$. Representative of two independent experiments.

$CuCl_2$ (50 – 100 μM) induced the appearance of multimers of higher order than dimers. Analysis showed the formation of RANTES trimers (24 KDa) (figure 2.3, lanes 6 - 8), and the effect appears to be dose dependent.

A $CuCl_2$ / H_2O_2 redox mechanism has been implicated in the formation of amyloid-β multimers (Atwood *et al*, 2004; Kato *et al*, 2001), and therefore H_2O_2 (1 – 400 μM) was added to the samples, in the presence of 25 μM $CuCl_2$. This concentration of $CuCl_2$ is a physiological concentration (Versieck, 1980).

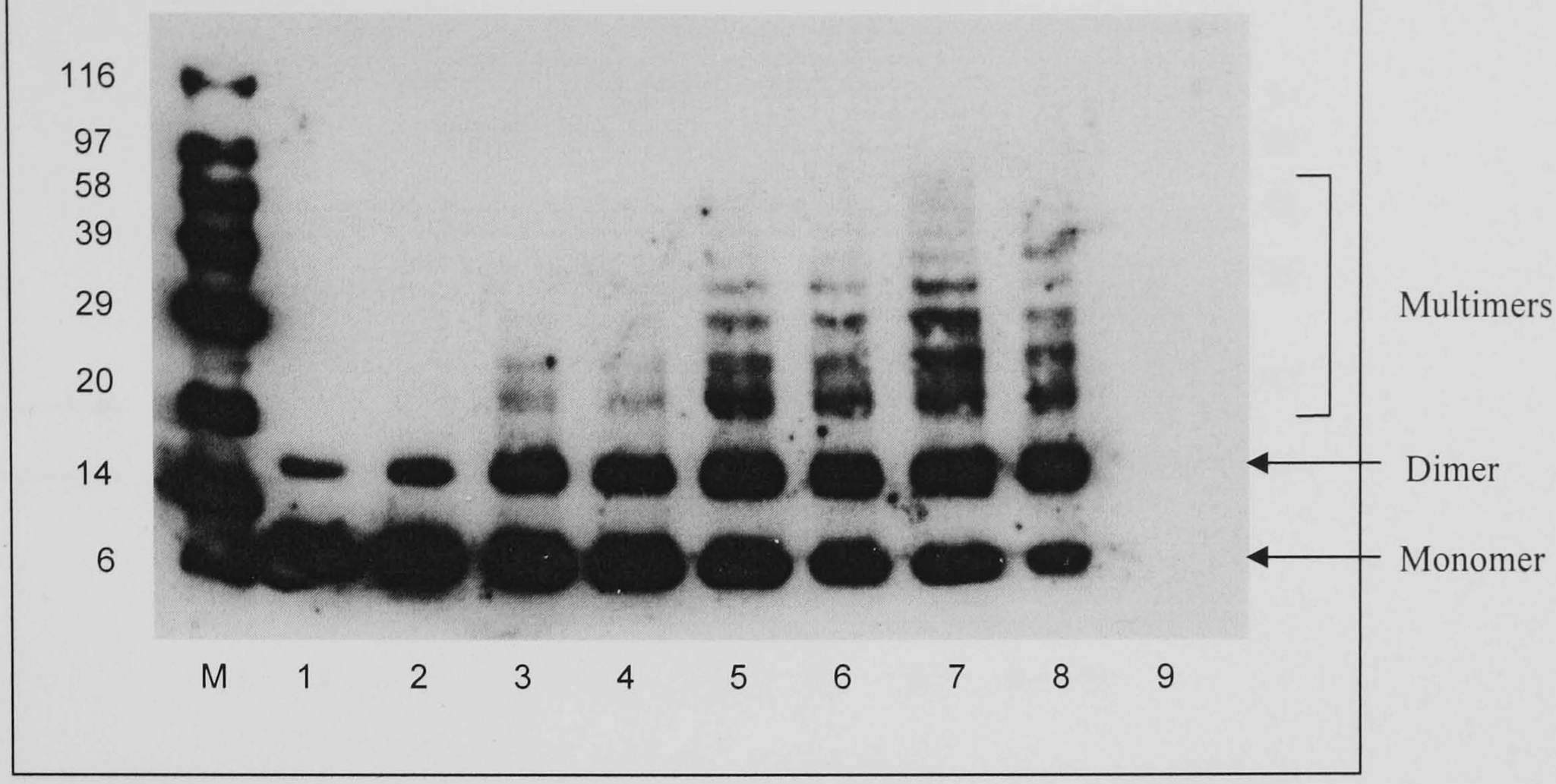

Figure 2.4. The effect of H_2O_2 on the form of recombinant RANTES (5×10^{-7} M) in the presence of 25 μM $CuCl_2$ following incubation at 37°C for 2 days analysed by SDS-PAGE on a 14 % polyacrylamide gel. M: molecular weight markers. Lane 1: RANTES and 25 μM $CuCl_2$, lane 2: RANTES, 25 μM $CuCl_2$ and 1 μM H_2O_2, lane 3: RANTES, 25 μM $CuCl_2$ and 5 μM H_2O_2, lane 4: RANTES, 25 μM $CuCl_2$ and 12.5 μM H_2O_2, lane 5: RANTES, 25 μM $CuCl_2$ and 25 μM H_2O_2, lane 6: RANTES, 25 μM $CuCl_2$ and 50 μM H_2O_2, lane 7: RANTES, 25 μM $CuCl_2$ and 100 μM H_2O_2, lane 8: RANTES, 25 μM $CuCl_2$ and 200 μM H_2O_2 and lane 9: RANTES, 25 μM $CuCl_2$ and 400 μM H_2O_2. Representative of two independent experiments.

In the absence of H_2O_2, RANTES was seen in the presence of 25 μM $CuCl_2$ predominantly as a monomer with a small proportion of dimer (figure 2.4, lane 1). Multimerisation of RANTES was strongly enhanced with increasing concentrations of H_2O_2. At physiological concentrations, Cu (25 μM) and H_2O_2 (5-25 μM) promote the higher order multimerisation of chemokines in a dose dependent manner (lanes 3-5) and promote dimer formation at the expense of the monomer (lanes 1-8). Increased H_2O_2 concentrations (50 – 200 μM) resulted in further dose-dependent multimer formation (lanes 6 – 8). Multimerisation is maximal at 100 μM H_2O_2 (lane 7). At 200 μM H_2O_2 (lane 8), RANTES multimers were diminished and at 400 μM H_2O_2 (lane 9), the monomer, dimer and multimers were completely destroyed.

Since chemokines bind to heparan sulphate (HS), the effect of HS on $CuCl_2$ induced multimer formation was investigated. RANTES was incubated in the presence of $CuCl_2$ (0.5 – 100 μM) and HS (0.1 mg/ml).

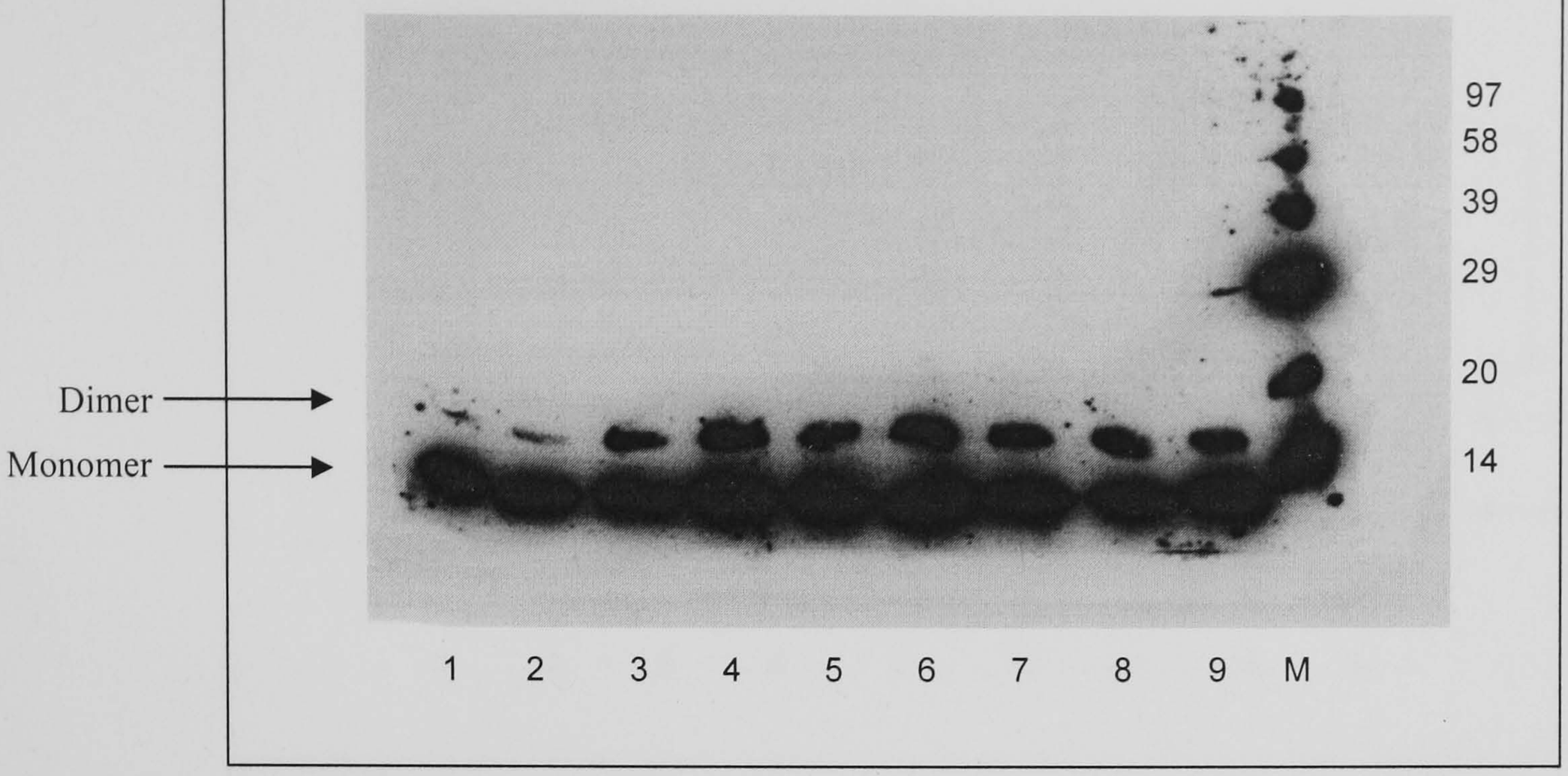

Figure 2.5. The effect of $CuCl_2$ on the form of recombinant RANTES (5×10^{-7} M) in the presence of HS (0.1 mg/ml) following incubation at 37°C for 2 days, final volume 40 µl and analysis by SDS-PAGE on a 14 % polyacrylamide gel. M: molecular weight markers. Lane 1: RANTES and HS, lane 2: RANTES, HS and 0.5 µM $CuCl_2$, lane 3: RANTES, HS and 1.25 µM $CuCl_2$, lane 4: RANTES, HS and 2.5 µM $CuCl_2$, lane 5: RANTES, HS and 12.5 µM $CuCl_2$, lane 6: RANTES, HS and 25 µM $CuCl_2$, lane 7: RANTES, HS and 50 µM $CuCl_2$, lane 8: RANTES, HS and 75 µM $CuCl_2$ and lane 9: RANTES, HS and 100 µM $CuCl_2$. Representative of two independent experiments.

The addition of HS (0.1 mg/ml) resulted in the attenuation of $CuCl_2$ induced RANTES multimer and dimer formation. The addition of 1.25 – 400 µM $CuCl_2$ resulted in an increase in RANTES dimer (16 KDa) formation but there was no higher order multimer formation (trimer (24 KDa) and above). The proportion of dimer is reduced and RANTES exists mainly in monomeric (8 KDa) and dimeric (16 KDa) form in the presence of HS (0.1 mg/ml) and 0.5 – 100 µM $CuCl_2$ (figure 2.5 lanes 2 – 9). It appears that HS has attenuated multimer formation compared with the effect of $CuCl_2$ in the absence of HS (figure 2.3).

As a further investigation of the effect of HS on RANTES multimer formation, RANTES was incubated with 25 µM $CuCl_2$ and increasing concentrations of H_2O_2 (1 – 400 µM) in the presence of HS (0.1 mg/ml).

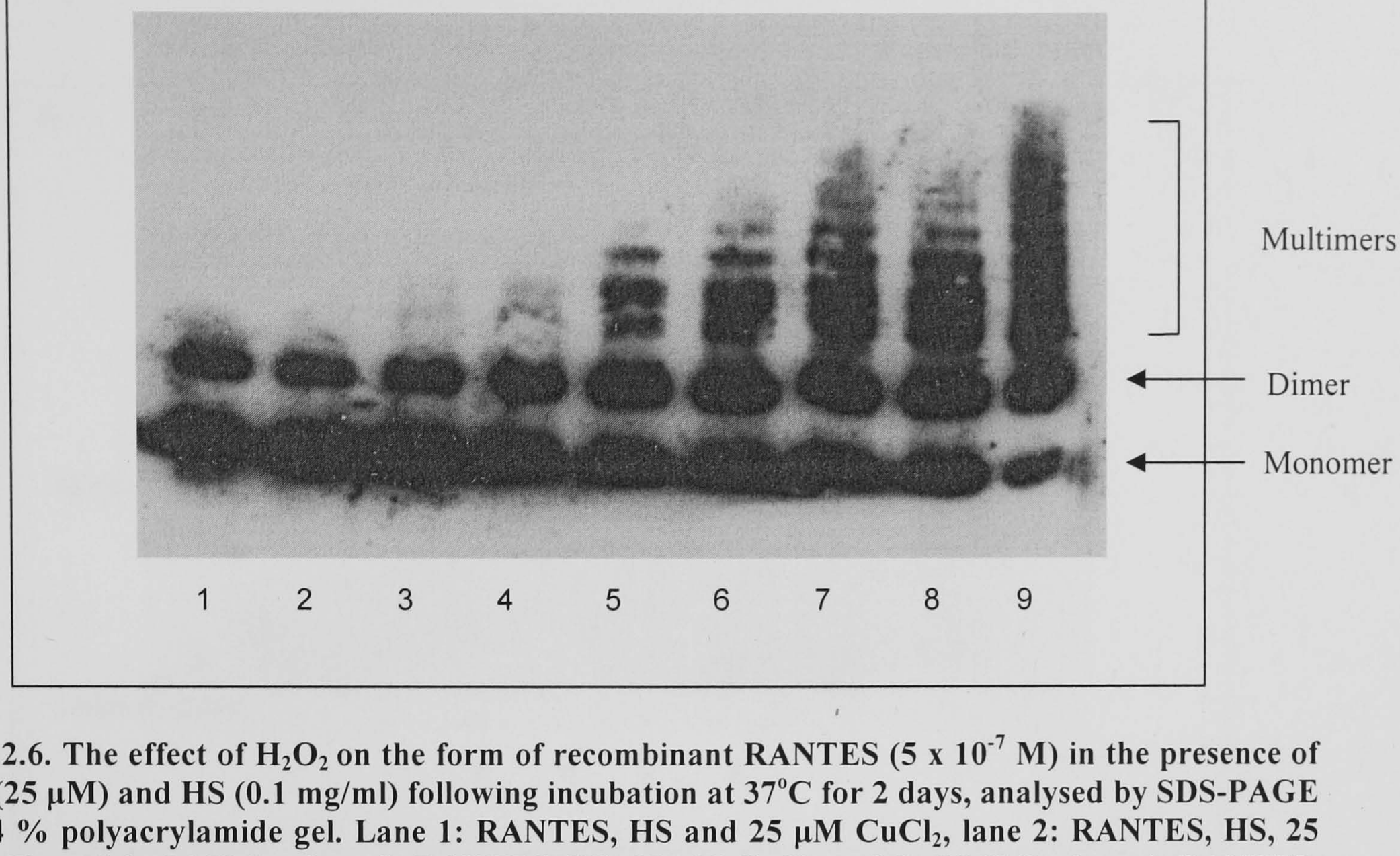

Figure 2.6. The effect of H_2O_2 on the form of recombinant RANTES (5×10^{-7} M) in the presence of $CuCl_2$ (25 μM) and HS (0.1 mg/ml) following incubation at 37°C for 2 days, analysed by SDS-PAGE on a 14 % polyacrylamide gel. Lane 1: RANTES, HS and 25 μM $CuCl_2$, lane 2: RANTES, HS, 25 μM $CuCl_2$ and 1 μM H_2O_2, lane 3: RANTES, HS, 25 μM $CuCl_2$ and 5 μM H_2O_2, lane 4: RANTES, HS, 25 μM $CuCl_2$ and 12.5 μM H_2O_2, lane 5: RANTES, HS, 25 μM $CuCl_2$ and 25 μM H_2O_2, lane 6: RANTES, HS, 25 μM $CuCl_2$ and 50 μM H_2O_2, lane 7: RANTES, HS, 25 μM $CuCl_2$ and 100 μM H_2O_2, lane 8: RANTES, HS, 25 μM $CuCl_2$ and 200 μM H_2O_2 and lane 9: RANTES, HS, 25 μM $CuCl_2$ and 400 μM H_2O_2. Representative of two independent experiments.

In the presence of HS (figure 2.6), H_2O_2 (5 – 400 μM) promoted RANTES multimer formation in a dose-dependent manner in the presence of 25 μM $CuCl_2$. In both the presence (figure 2.6) and absence (figure 2.4) of HS (0.1 mg/ml), RANTES trimers (24 KDa) occurred at 25 μM $CuCl_2$ and 5 – 12.5 μM H_2O_2 (figures 2.4 and 2.6, lanes 3 - 4). In the absence of HS (figure 2.4), RANTES tetramers (32 KDa) and higher order multimers appeared at 25 – 200 μM H_2O_2 (figure 2.4, lanes 5 – 8), but were diminished at 200 μM and absent at 400 μM H_2O_2 (lane 9). However, in the presence of HS (0.1 mg/ml), RANTES tetramers and higher order multimers were seen at 25 – 400 μM H_2O_2 (figure 2.6 lanes 5 – 9) and were not diminished even at 400 μM H_2O_2 (lane 9). Thus, multimers were able to withstand higher concentrations of H_2O_2 in the presence of 0.1 mg/ml HS (figure 2.6, lane 9) compared to in the absence of HS (figure 2.4, lane 9).

In order to quantify the degree of multimerisation, RANTES was incubated in the presence and absence of physiological concentrations of $CuCl_2$ (25 μM) and H_2O_2 (50 μM), and in the presence and absence of HS (0.1 mg/ml). Multimers of higher order

than dimer were quantified by scanning densitometry and presented as the % of total RANTES including the monomer.

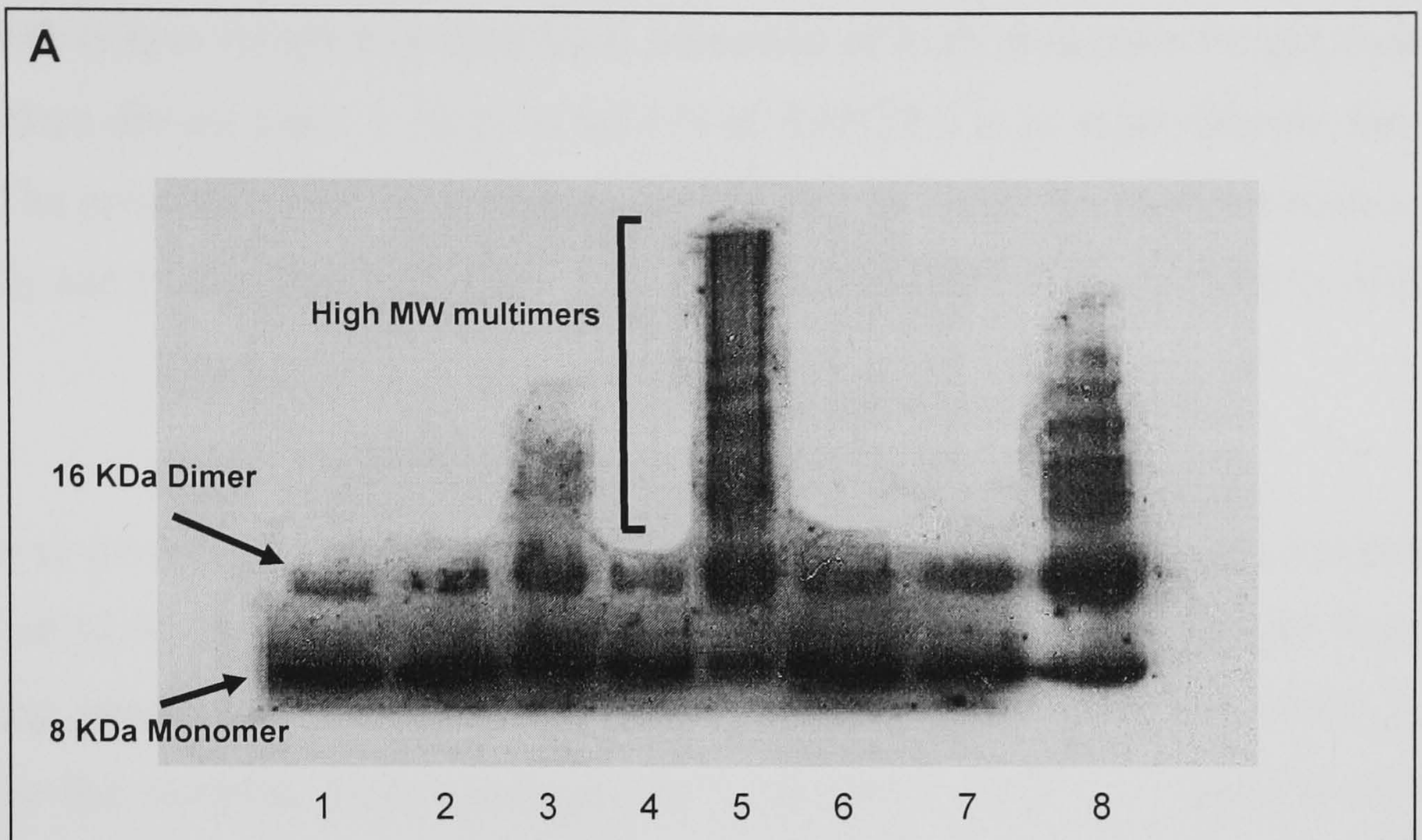

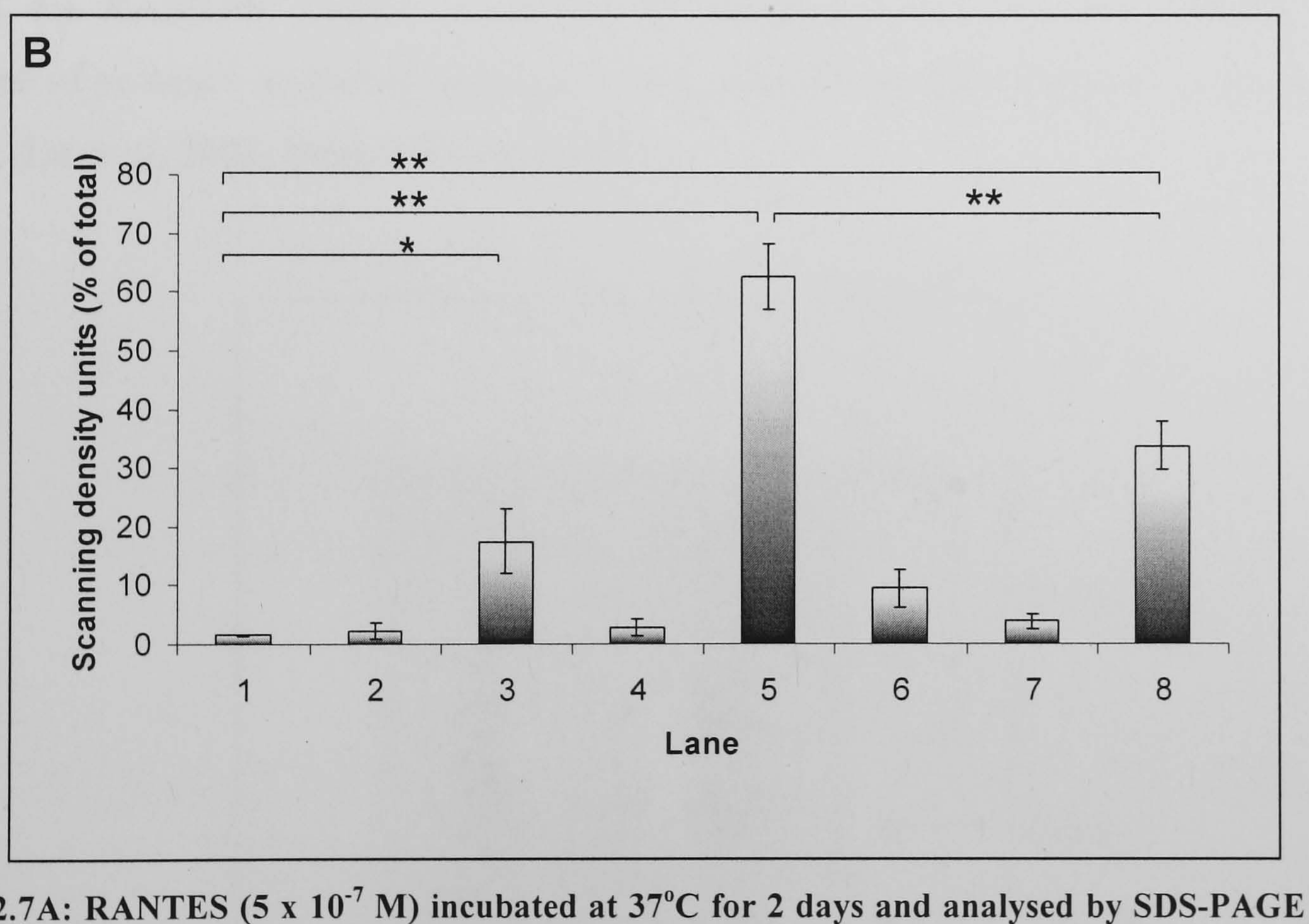

Figure 2.7A: RANTES (5×10^{-7} M) incubated at 37°C for 2 days and analysed by SDS-PAGE on a 14 % polyacrylamide gel. ± $CuCl_2$ (25 μM), H_2O_2 (50 μM) and HS (0.1 mg/ml). Lane 1: RANTES only, lane 2: RANTES + HS, lane 3: RANTES + $CuCl_2$, lane 4: RANTES + H_2O_2, lane 5: RANTES + $CuCl_2$ and H_2O_2, lane 6: RANTES + HS + $CuCl_2$, lane 7: RANTES + HS + H_2O_2 and lane 8: RANTES + HS, $CuCl_2$ and H_2O_2. Representative of three independent experiments.

Figure 2.7B: Quantitative analysis of supra-dimeric RANTES intensity (higher order complexes of RANTES including tetramer (24 KDa) as % of total analysed using density analysis (Quantiscan). Lane 1: RANTES only, lane 2: RANTES + HS, lane 3: RANES + $CuCl_2$, lane 4: RANTES + H_2O_2, lane 5: RANTES + $CuCl_2$ and H_2O_2, lane 6: RANTES + HS + $CuCl_2$, lane 7: RANTES + HS + H_2O_2 and lane 8: RANTES + HS, $CuCl_2$ and H_2O_2. * indicates $p < 0.05$, ** indicates $p < 0.01$, (n = 3).

Formation of RANTES multimers greater than the dimer increased significantly in the presence of 25 μM $CuCl_2$ (lane 3, 17.52 ± 9.46 % of total RANTES is in supra-dimeric form, $p < 0.05$) compared to the control (RANTES only, lane 1). The addition of 50 μM H_2O_2 with copper resulted in significant formation of high molecular weight multimers greater than dimers (lane 5, 62.51 ± 9.76 % of RANTES is in supra-dimeric form, $p < 0.01$). The presence of HS (0.1 mg/ml) significantly reduced the multimerisation effect of $CuCl_2$ and H_2O_2 (lane 8, 33.78 ± 7.22 % of RANTES is in supra-dimeric form, $p < 0.01$).

In order to investigate the stability of RANTES multimers, RANTES was incubated for 2 days at 37 °C in the presence and absence of 25 μM $CuCl_2$ and 50 μM H_2O_2 and, following incubation, the chaotropic agent, guanidine hydrochloride (G-HCl), was added to the samples, final concentration 6 M. The G-HCl was removed by EtOH precipitation before the samples were analysed by SDS-PAGE and Western blots stained for RANTES. G-HCl is capable of disrupting non-covalent 3-dimensional structure of proteins, including hydrogen bonds, van der Waals forces and hydrophobic effects (Lu *et al*, 2001; Neet & Timm, 1994).

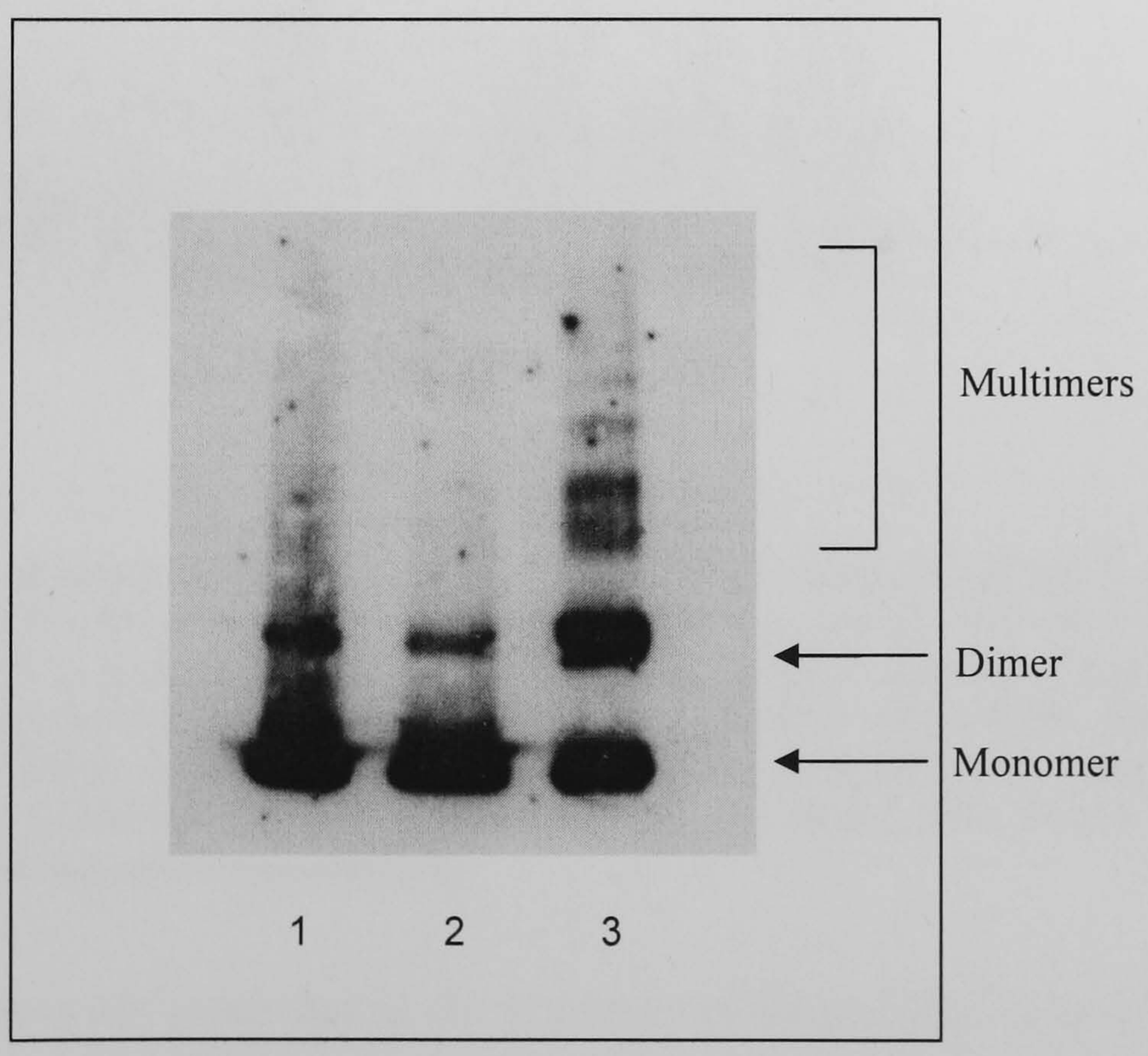

Figure 2.8. The effect of G-HCl (6 M) and EtOH precipitation on the form of recombinant RANTES (5×10^{-7} M) in the presence of $CuCl_2$ (25 μM) plus H_2O_2 (50 μM) following incubation at 37°C for 2 days, analysed by SDS-PAGE on a 14 % polyacrylamide gel. Lane 1: RANTES only with G-HCl and EtOH precipitation, lane 2: RANTES and 25 μM $CuCl_2$ with G-HCl and EtOH precipitation, lane 3: RANTES, 25 μM $CuCl_2$ and 50 μM H_2O_2 with G-HCl and EtOH precipitation. Representative of two independent experiments.

Monomers, dimers and higher order RANTES multimers (trimers (24 KDa) and tetramers (32 KDa)) generated in the presence of 25 μM $CuCl_2$ plus 50 μM H_2O_2 were found to remain following treatment with G-HCl (6 M) (figure 2.8, lane 3), indicating that the links in RANTES multimers were covalent.

To ensure that the technique of EtOH precipitation had not affected the stability of RANTES multimers, RANTES was incubated with 25 μM $CuCl_2$ plus 50 μM H_2O_2 to generate higher order multimers, which were then EtOH precipitated, dried, reconstituted in 1x sample buffer and analysed by SDS-PAGE, Western blotting and staining for RANTES.

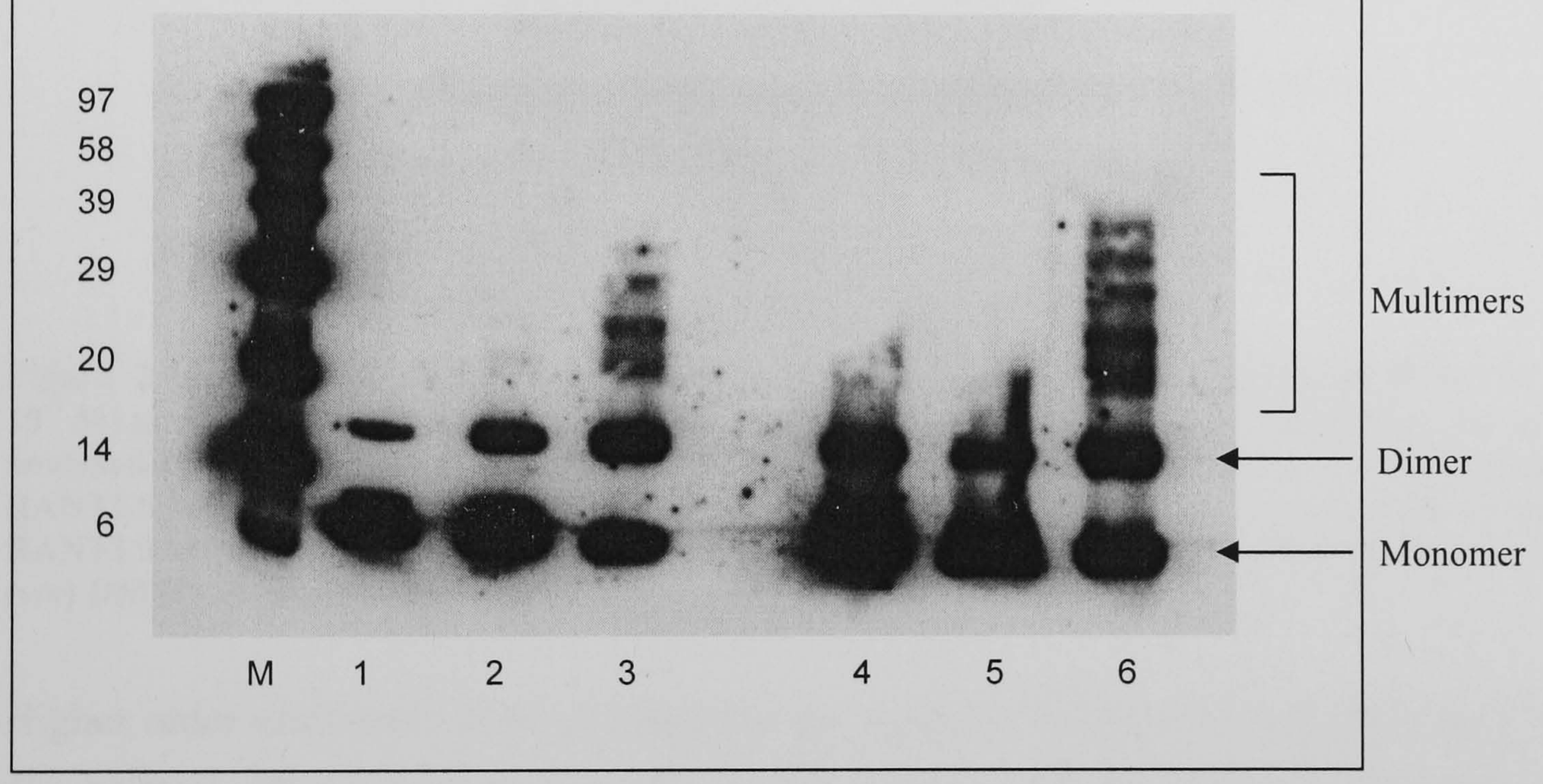

Figure 2.9. The effect of EtOH precipitation on the form of recombinant RANTES (5 x 10^{-7} M) in the presence of $CuCl_2$ (25 μM) plus H_2O_2 (50 μM) following incubation at 37°C for 2 days, analysed by SDS-PAGE on a 14 % polyacrylamide gel. M: molecular weight markers. Lane 1: RANTES only, lane 2: RANTES and 25 μM $CuCl_2$, lane 3: RANTES, 25 μM $CuCl_2$ and 50 μM H_2O_2, lane 4: RANTES only with EtOH precipitation, lane 5: RANTES and 25 μM $CuCl_2$ with EtOH precipitation, lane 6: RANTES, 25 μM $CuCl_2$ and 50 μM H_2O_2 with EtOH precipitation. Representative of two independent experiments.

Higher order multimers are generated in the presence of 25 μM $CuCl_2$ plus 50 μM H_2O_2 (figure 2.9, lane 3). It appears that EtOH precipitation does not affect the stability of RANTES multimers, which remain after the RANTES multimers are precipitated.

As further investigation into the mechanism of multimer generation by the Cu/H_2O_2 system, RANTES multimers were generated by the incubation of RANTES for 2 days at 37 °C with 25 μM $CuCl_2$ plus 50 μM H_2O_2 in the presence of the hydroxyl radical scavenger, dimethyl sulphoxide (DMSO) at final concentrations of 1, 5 and 10 % (v/v). DMSO was used to discern which radicals were involved in the mechanism.

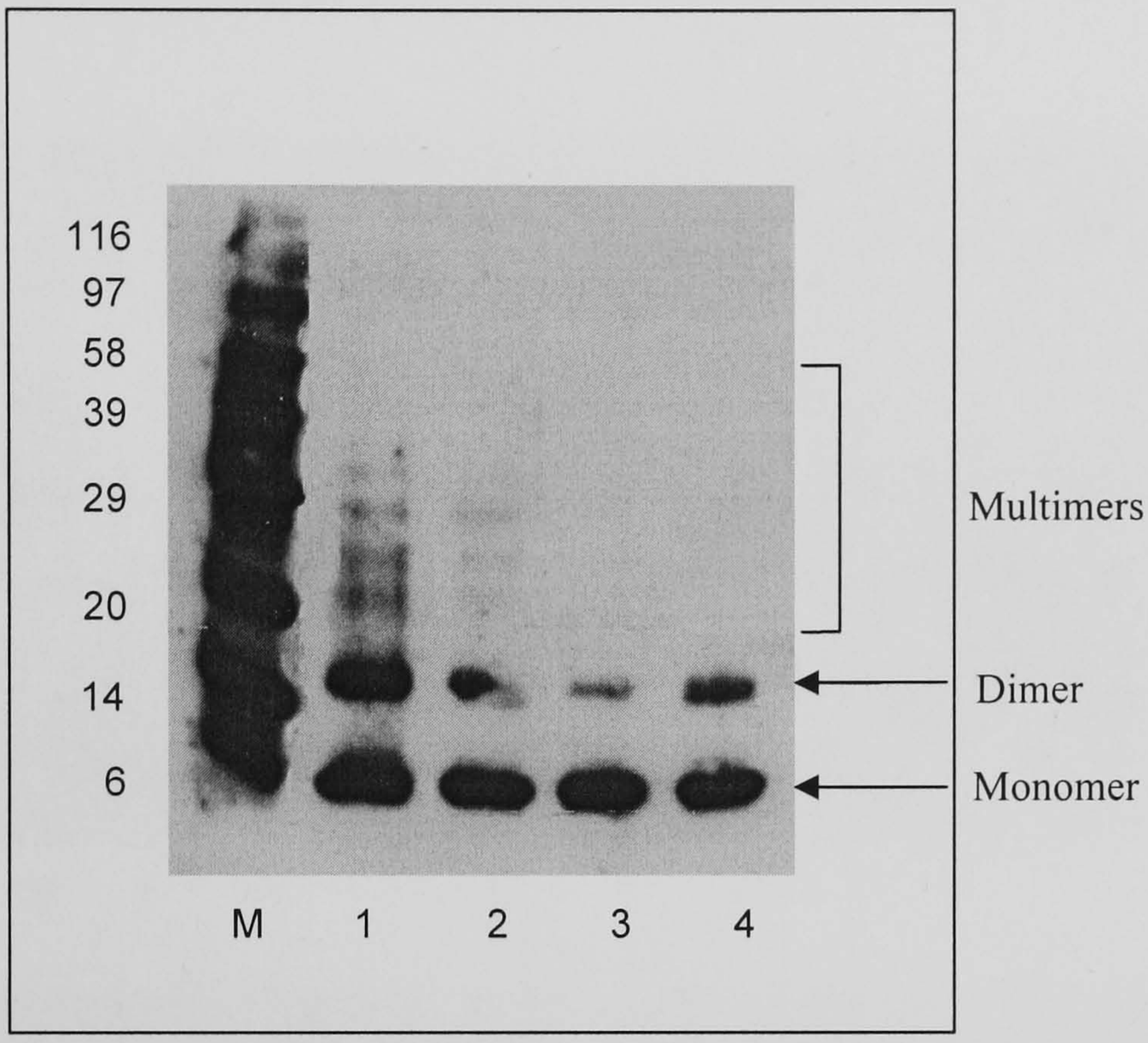

Figure 2.10. The effect of DMSO (1, 5 and 10 % (v/v)) on the form of recombinant RANTES (5 x 10^{-7} M) in the presence of $CuCl_2$ (25 μM) plus H_2O_2 (50 μM) following incubation at 37°C for 2 days, analysed by SDS-PAGE on a 14 % polyacrylamide gel. M: molecular weight markers. Lane 1: RANTES with $CuCl_2$ plus H_2O_2, lane 2: RANTES with $CuCl_2$, H_2O_2 and 1 % (v/v) DMSO, lane 3: RANTES with $CuCl_2$, H_2O_2 and 5 % (v/v) DMSO, lane 4: RANTES with $CuCl_2$, H_2O_2 and 10 % (v/v) DMSO. Representative of two independent experiments.

Higher order multimers were generated in the absence of DMSO by 25 μM $CuCl_2$ plus 50 μM H_2O_2 (figure 2.10, lane 1). Trimers and tetramers are diminished upon treatment with 1 % (v/v) DMSO (lane 2) and are not generated in the presence of 5 and 10 % (v/v) DMSO (lanes 3 and 4).

2.5.2. IL-8

The neutrophil chemoattractant, IL-8, was of significant interest as this chemokine has only one tyrosine residue compared to five in the amino acid sequence of RANTES. Therefore, if tyrosine was involved in multimerisation of chemokines it was expected that IL-8 should be less sensitive to $CuCl_2$ and H_2O_2 than RANTES. First, the effect of $CuCl_2$ on IL-8 multimer formation was investigated. Recombinant human IL-8

(Peprotech, UK) was incubated with $CuCl_2$ (1.25 – 100 μM) at the same concentration as RANTES (5×10^{-7} M) at 37 °C but for 1 day only, as it was found that multimers were diminished after 2 days, unlike RANTES where maximum multimer formation was seen after 2 days of incubation. IL-8 multimers were analysed by SDS-PAGE, and Western blots were stained with anti-human IL-8 antibody (Peprotech, UK).

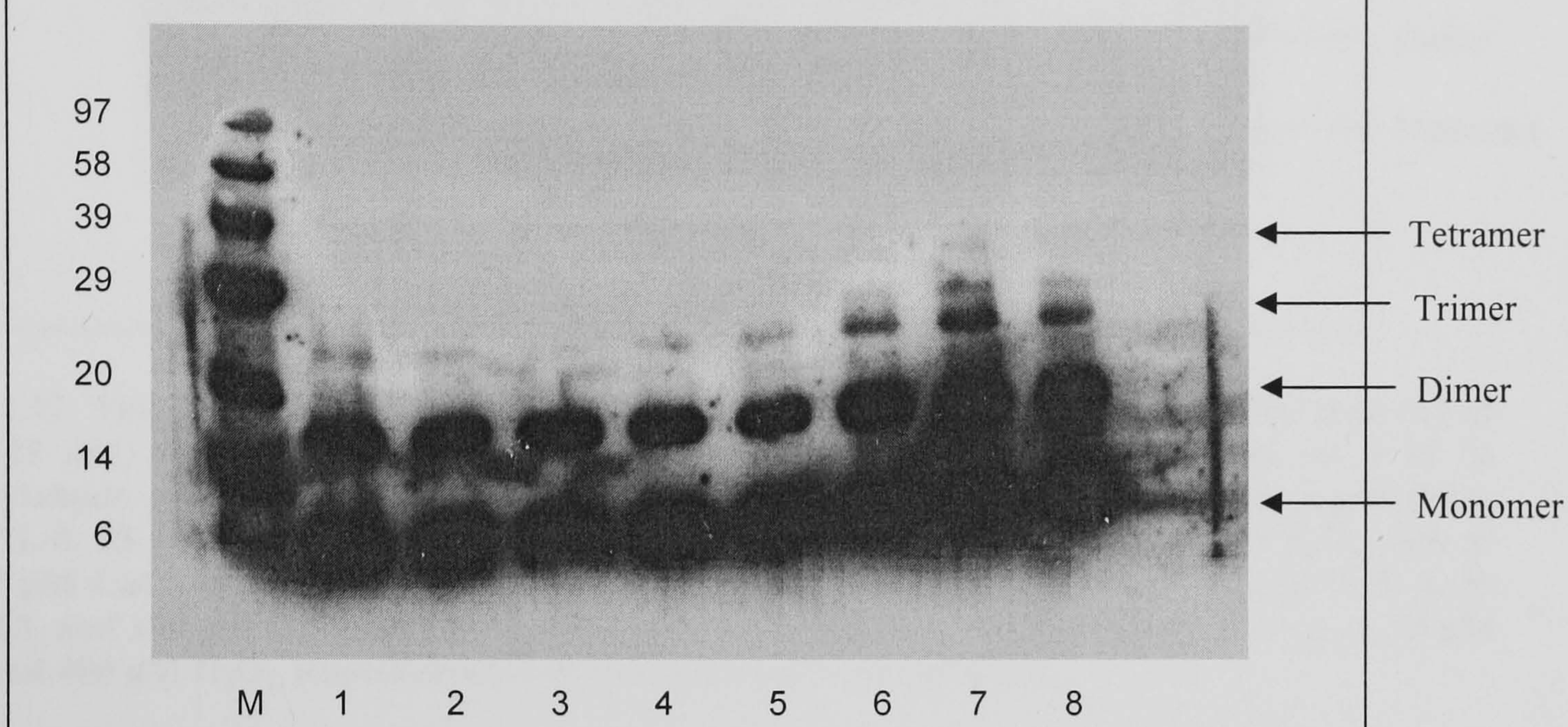

Figure 2.11. The effect of $CuCl_2$ on the form of recombinant IL-8 (5×10^{-7} M) following incubation at 37°C for 1 day, analysed by SDS-PAGE on a 14 % polyacrylamide gel. M: molecular weight markers. Lane 1: IL-8 only, lane 2: IL-8 and 1.25 μM $CuCl_2$, lane 3: IL-8 and 2.5 μM $CuCl_2$, lane 4: IL-8 and 12.5 μM $CuCl_2$, lane 5: IL-8 and 25 μM $CuCl_2$, lane 6: IL-8 and 50 μM $CuCl_2$, lane 7: IL-8 and 75 μM $CuCl_2$ and lane 8: IL-8 and 100 μM $CuCl_2$. Representative of two independent experiments.

IL-8 (5×10^{-7} M) in the absence of $CuCl_2$ exists mainly as a monomer and dimer with some appearance of trimers (figure 2.11, lane 1). $CuCl_2$ alone (50 – 100 μM) induced a small increase in higher order multimers, resulting in an increase in the formation of IL-8 trimers (figure 2.11, lanes 6 – 8) and tetramers (75 μM $CuCl_2$ lane 7). The effect appears to be dose dependent with maximum multimer formation occurring at 75 μM $CuCl_2$ (lane 7).

Subsequently, the effect of H_2O_2 (1 – 400 μM) in the presence of 25 μM $CuCl_2$ on IL-8 multimer formation was investigated.

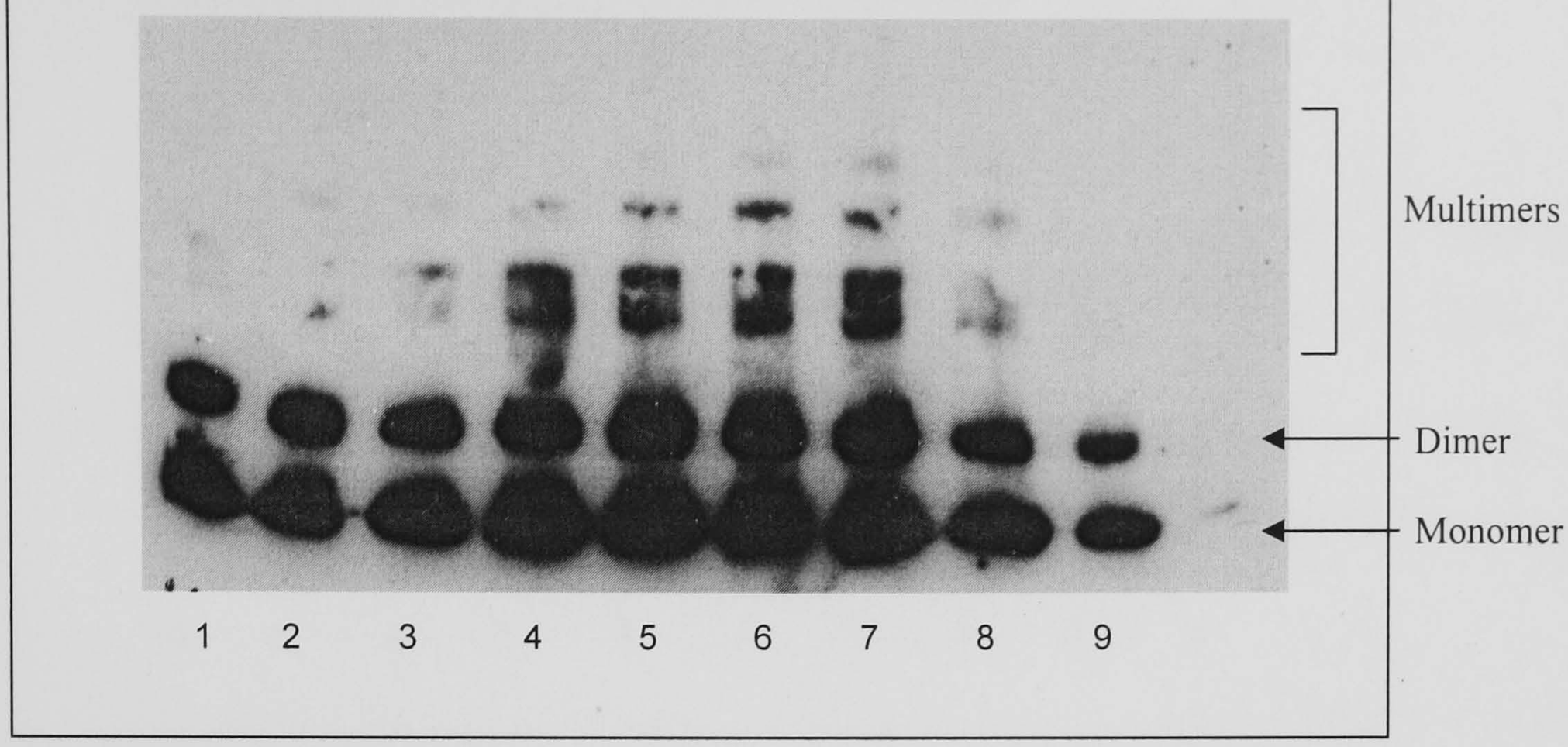

Figure 2.12. The effect of H_2O_2 on the form of recombinant IL-8 (5×10^{-7} M) in the presence of $CuCl_2$ (25 μM) following incubation at 37°C for 1 day, analysed by SDS-PAGE on a 14 % polyacrylamide gel. Lane 1: IL-8 and 25 μM $CuCl_2$, lane 2: IL-8, 25 μM $CuCl_2$ and 1 μM H_2O_2, lane 3: IL-8, 25 μM $CuCl_2$ and 5 μM H_2O_2, lane 4: IL-8, 25 μM $CuCl_2$ and 12.5 μM H_2O_2, lane 5: IL-8, 25 μM $CuCl_2$ and 25 μM H_2O_2, lane 6: IL-8, 25 μM $CuCl_2$ and 50 μM H_2O_2, lane 7: IL-8, 25 μM $CuCl_2$ and 100 μM H_2O_2, lane 8: IL-8, 25 μM $CuCl_2$ and 200 μM H_2O_2 and lane 9: IL-8, 25 μM $CuCl_2$ and 400 μM H_2O_2. Representative of two independent experiments.

In the absence of H_2O_2, IL-8 was seen predominantly as a monomer and dimer (lane 1). In the presence of 25 μM $CuCl_2$ with increasing concentrations of H_2O_2, IL-8 multimerisation was strongly enhanced (fig 2.12). At physiological concentrations, Cu (25 μM) and H_2O_2 (5 - 25 μM) promoted the multimerisation of chemokines to higher order multimers (trimers and tetramers - lanes 3 - 5). Increasing H_2O_2 concentrations above physiological plasma levels (50 – 100 μM) also resulted in higher order multimer formation (lanes 6 – 7). Multimerisation was maximal at 100 μM H_2O_2 (lane 7). At 200 μM H_2O_2 (lane 8), IL-8 multimers were diminished and at 400 μM H_2O_2 (lane 9), the higher order multimers were destroyed.

The effect of heparan sulphate (HS) on $CuCl_2$ induced multimer formation was then investigated. IL-8 was incubated in the presence of $CuCl_2$ (0.5 – 100 μM) and HS (0.1 mg/ml).

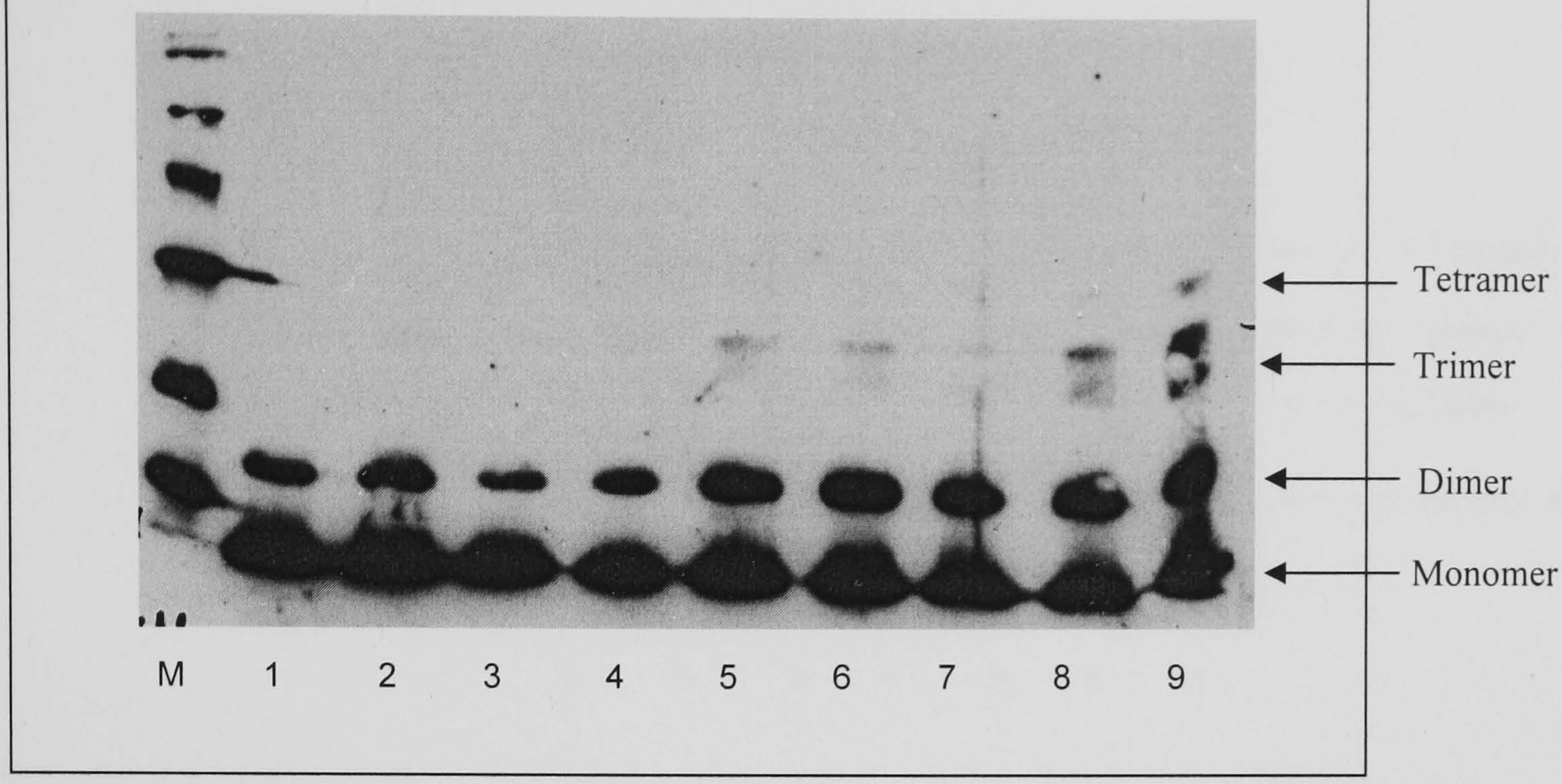

Figure 2.13. The effect of $CuCl_2$ on the form of recombinant IL-8 (5×10^{-7} M) in the presence of HS (0.1 mg/ml) following incubation at 37°C for 1 day, analysed by SDS-PAGE on a 14 % polyacrylamide gel. M: molecular weight markers. Lane 1: IL-8 and HS, lane 2: IL-8, HS and 1.25 μM $CuCl_2$, lane 3: IL-8, HS and 2.5 μM $CuCl_2$, lane 4: IL-8, HS and 5 μM $CuCl_2$, lane 5: IL-8, HS and 12.5 μM $CuCl_2$, lane 6: IL-8, HS and 25 μM $CuCl_2$, lane 7: IL-8, HS and 50 μM $CuCl_2$, lane 8: IL-8, HS and 75 μM $CuCl_2$ and lane 9: IL-8, HS and 100 μM $CuCl_2$. Representative of two independent experiments.

The addition of HS (0.1 mg/ml) resulted in the attenuation of $CuCl_2$ induced IL-8 multimer formation. Trimers were less predominant in the presence of HS (figure 2.13) than in the absence of HS (figure 2.11). The addition of 12.5 – 75 μM $CuCl_2$ resulted in an increase in IL-8 trimer formation (figure 2.13, lanes 5 – 8) and at 100 μM $CuCl_2$, tetramers were formed (lane 9). However, IL-8 remained monomeric and dimeric in the presence of HS (0.1 mg/ml) and 1.5 – 5 μM $CuCl_2$ (lanes 2 – 4). As observed with RANTES, it appears that HS attenuated IL-8 multimer formation.

Subsequently the effect of HS (0.1 mg/ml) on IL-8 multimerisation in the presence of 25 μM $CuCl_2$ and increasing concentrations of H_2O_2 (0.5 – 400 μM) was investigated.

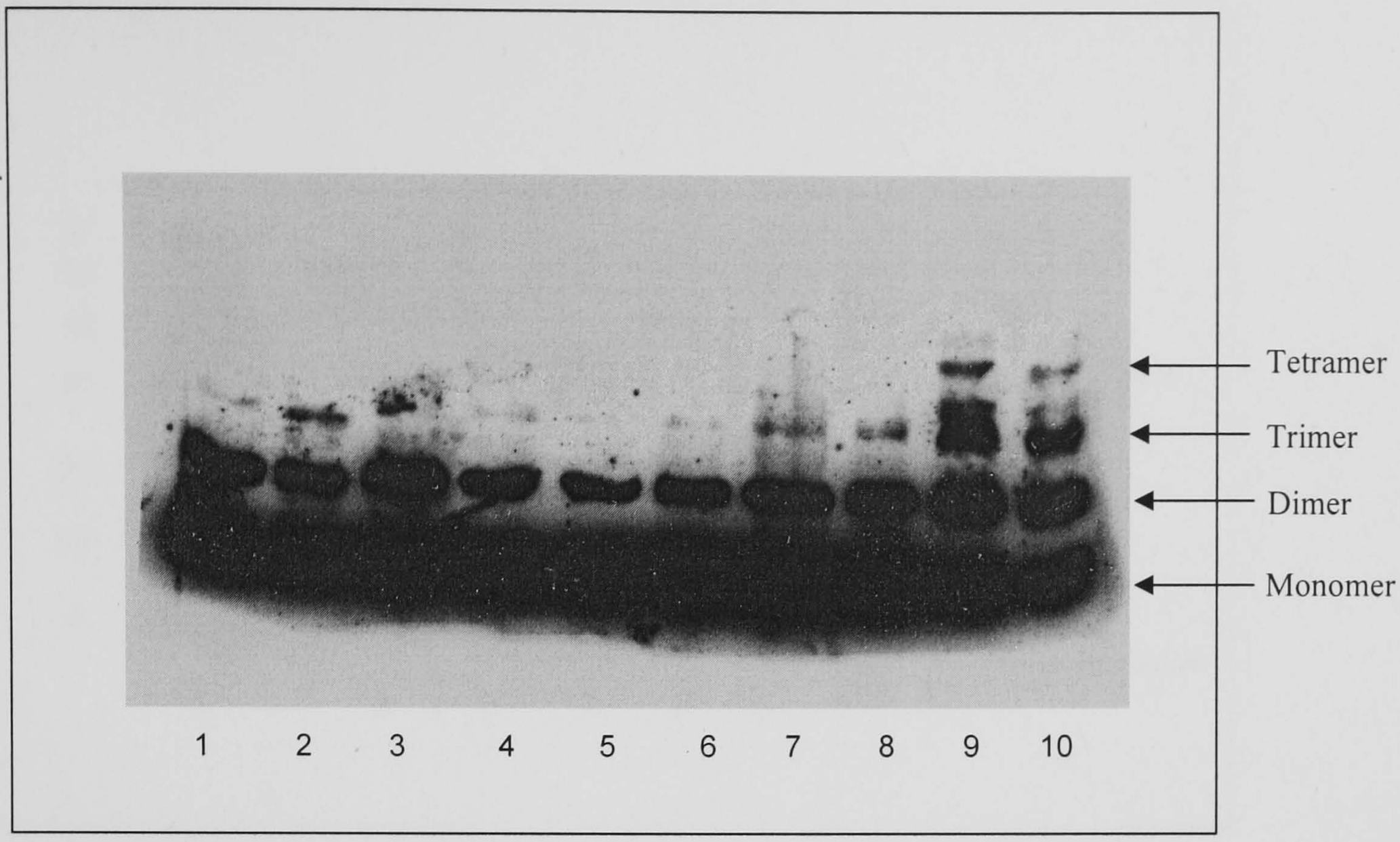

Figure 2.14. The effect of H_2O_2 (0.5 – 400 μM) on the form of recombinant IL-8 (5 x 10^{-7} M) in the presence of $CuCl_2$ (25 μM) and HS (0.1 mg/ml) following incubation at 37°C for 1 day, analysed by SDS-PAGE on a 14 % polyacrylamide gel. Lane 1: IL-8, HS and 25 μM $CuCl_2$, lane 2: IL-8, HS, 25 μM $CuCl_2$ and 0.5 μM H_2O_2, lane 3: IL-8, HS, 25 μM $CuCl_2$ and 1 μM H_2O_2, lane 4: IL-8, HS, 25 μM $CuCl_2$ and 5 μM H_2O_2, lane 5: IL-8, HS, 25 μM $CuCl_2$ and 12.5 μM H_2O_2, lane 6: IL-8, HS, 25 μM $CuCl_2$ and 25 μM H_2O_2, lane 7: IL-8, HS, 25 μM $CuCl_2$ and 50 μM H_2O_2, lane 8: IL-8, HS, 25 μM $CuCl_2$ and 100 μM H_2O_2, lane 9: IL-8, HS, 25 μM $CuCl_2$ and 200 μM H_2O_2 and lane 10: IL-8, HS, 25 μM $CuCl_2$ and 400 μM H_2O_2. Representative of two independent experiments.

In the absence of HS (figure 2.12), H_2O_2 (12.5 – 50 μM) promoted IL-8 trimer and tetramer formation in the presence of 25 μM $CuCl_2$ (figure 2.12, lanes 4 – 6) In the presence of HS (0.1 mg/ml), IL-8 trimers and tetramers did not occur at 12.5 – 50 μM H_2O_2, but only at higher concentrations of H_2O_2 (50 - 200 μM, figure 2.14, lanes 7 -9). In the absence of HS (figure 2.12), IL-8 tetramers (32 KDa) were diminished at 200 - 400 μM H_2O_2 (figure 2.12, lanes 8 - 9). However, in the presence of HS (0.1 mg/ml), IL-8 tetramers occured at 200 – 400 μM H_2O_2 (figure 2.14 lanes 9 – 10) and were not diminished by 400 μM H_2O_2 (lane 9). The multimers were able to withstand higher concentrations of H_2O_2 in the presence of 0.1 mg/ml HS (figure 2.14, lane 10). This suggests that HS was protecting high order multimers from damage by high concentrations of H_2O_2.

In order to quantify the degree of multimerisation, IL-8 was incubated in the presence and absence of physiological concentrations of $CuCl_2$ (25 μM) and H_2O_2 (50 μM), and in the presence and absence of HS (0.1 mg/ml). Multimers of higher order than dimer were quantified by scanning densitometry and presented as the % of total RANTES including the monomer.

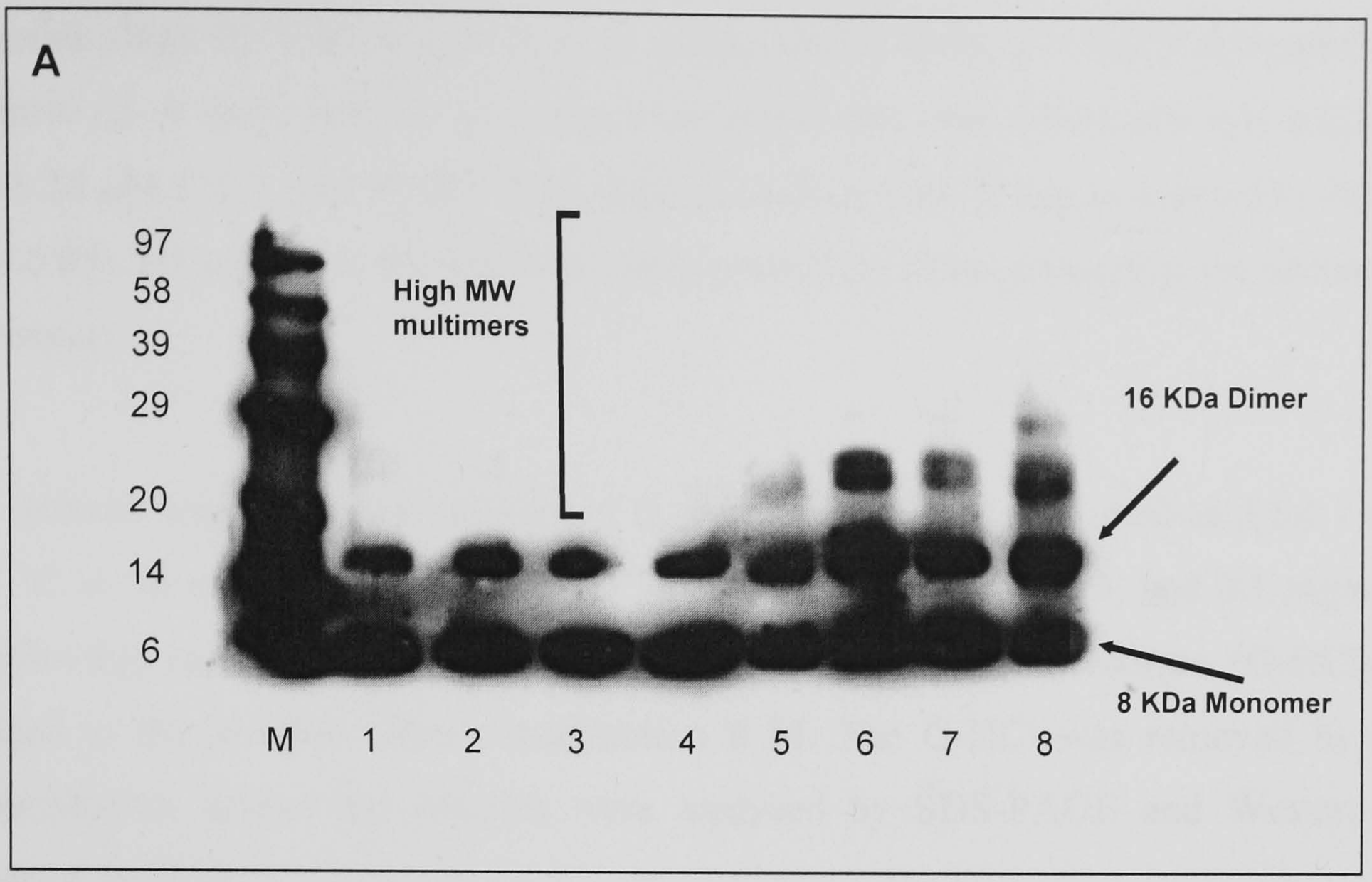

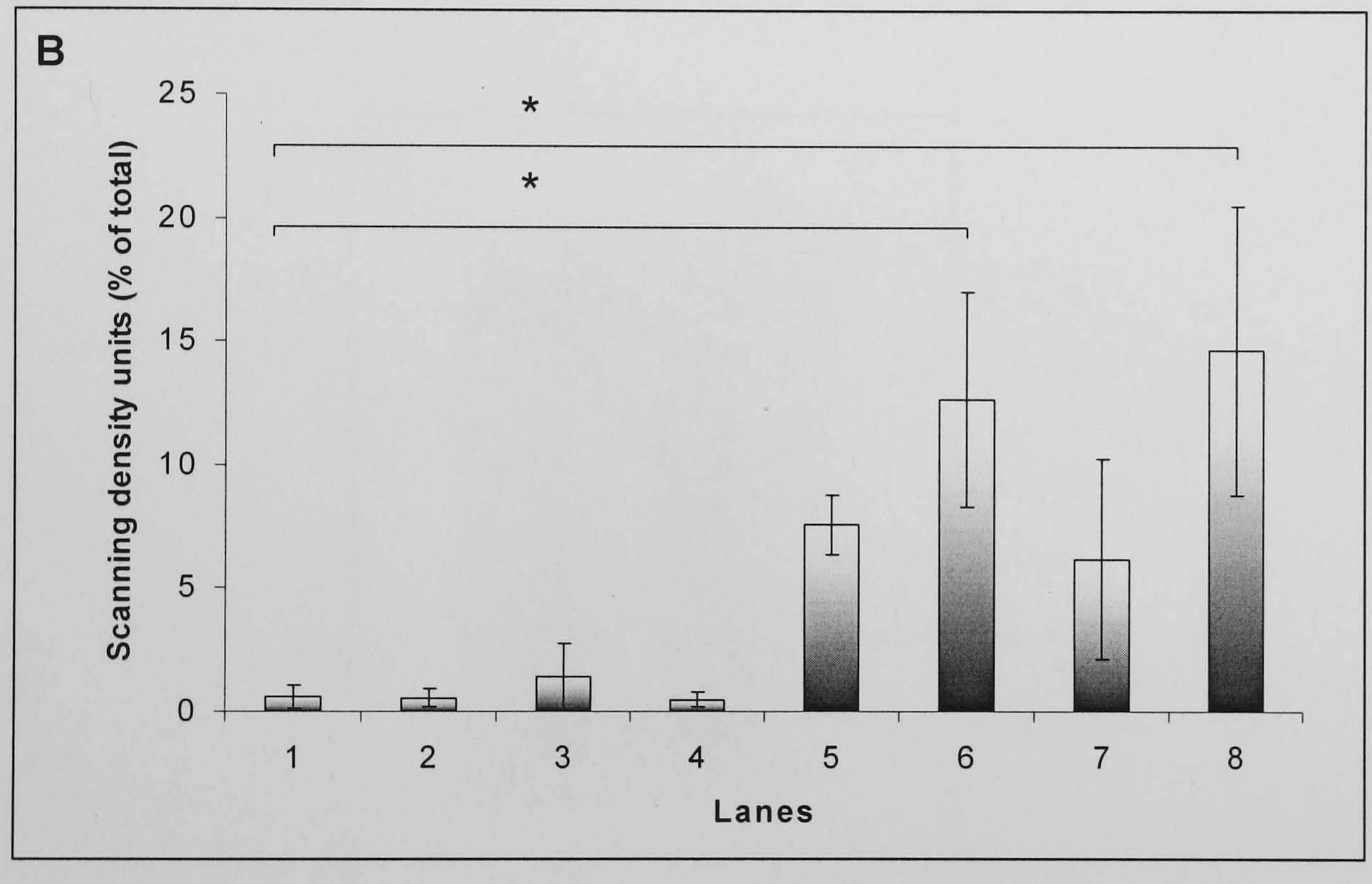

Figure 2.15A. IL-8 (5 x 10^{-7} M) incubated at 37°C for 1 day and analysed by SDS-PAGE on a 14 % polyacrylamide gel. ± $CuCl_2$ (25 μM), H_2O_2 (50 μM) and HS (0.1 mg/ml). M: molecular weight markers. Lane 1: IL-8 only, lane 2: IL-8 + HS, lane 3: IL-8 + $CuCl_2$, lane 4: IL-8 + H_2O_2, lane 5: IL-8 + $CuCl_2$ and H_2O_2, lane 6: IL-8 + HS + $CuCl_2$, lane 7: IL-8 + HS + H_2O_2 and lane 8: IL-8 + HS, $CuCl_2$ and H_2O_2. Representative of three independent experiments.

Figure 2.15B: Quantitative analysis of supra-dimeric IL-8 intensity (higher order complexes of IL-8 including tetramer (24 KDa) as % of total analysed using density analysis (Quantiscan). Lane 1: IL-8 only, lane 2: IL-8 + HS, lane 3: RANES + $CuCl_2$, lane 4: IL-8 + H_2O_2, lane 5: IL-8 + $CuCl_2$ and H_2O_2, lane 6: IL-8 + HS + $CuCl_2$, lane 7: IL-8 + HS + H_2O_2 and lane 8: IL-8 + HS, $CuCl_2$ and H_2O_2. * indicates $p < 0.05$, (n = 3).

The addition of 25 μM $CuCl_2$ plus 50 μM H_2O_2 increased trimer formation (lane 5). The addition of 0.1 mg/ml HS with 50 μM H_2O_2 decreased multimerisation (lane 7). Multimerisation was significantly increased by adding 0.1 mg/ml HS and 25 μM $CuCl_2$

together (lane 6, 12.67 ± 4.36 % is in supra-dimeric form, $p < 0.05$) compared to the control (IL-8 only, lane 1). The maximum effect was seen where HS was added with both 25 μM $CuCl_2$ and 50 μM H_2O_2 (lane 8, 14.65 ± 5.86 % was in supra-dimeric form, $p < 0.05$). HS enhanced the effect of $CuCl_2$ plus H_2O_2 alone, promoting the formation of tetramers.

In order to investigate the stability of IL-8 multimers, IL-8 was incubated for 1 day at 37 °C in the presence and absence of 25 μM $CuCl_2$, 50 μM H_2O_2 and 0.1 mg/ml HS. Following incubation, the chaotropic agent, guanidine hydrochloride (G-HCl), was added to the samples, final concentration 6 M. The G-HCl was removed by EtOH precipitation before the samples were analysed by SDS-PAGE and Western blots stained for IL-8.

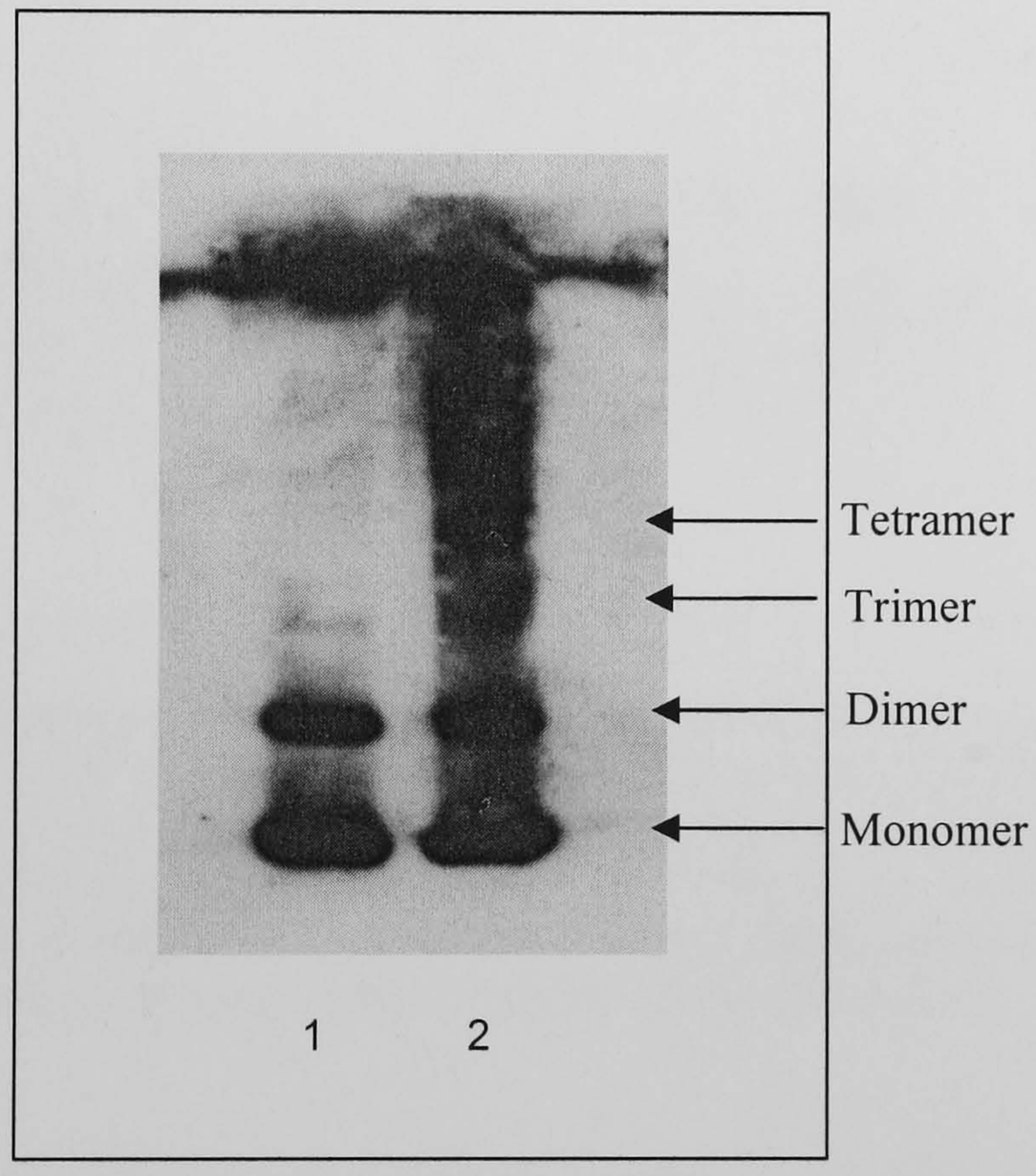

Figure 2.16. The effect of G-HCl (6 M) and EtOH precipitation on the form of recombinant IL-8 (5 x 10^{-7} M) in the presence of $CuCl_2$ (25 μM) plus H_2O_2 (50 μM) following incubation at 37°C for 1 day, analysed by SDS-PAGE on a 14 % polyacrylamide gel. Lane 1: IL-8 + G-HCl, lane 2: IL-8, 25 μM $CuCl_2$ and 25 μM H_2O_2 with G-HCl and EtOH precipitation. Representative of two independent experiments.

The higher order IL-8 multimers (above and including trimers) generated in the presence of 25 μM $CuCl_2$ plus 50 μM H_2O_2 were found to remain following treatment with G-HCl (6 M) (figure 2.16, lane 2). Monomers and dimers were also found to

remain following treatment with G-HCl, indicating that the 3-dimensional structure of IL-8 was not disrupted and that multimers are highly stable.

The effect of the hydroxyl radical scavenger DMSO on IL-8 multimerisation was then investigated. IL-8 multimers were generated by the incubation of IL-8 for 1 day at 37 °C with 25 μM $CuCl_2$ plus 50 μM H_2O_2 in the presence of the hydroxyl radical scavenger, dimethyl sulphoxide (DMSO) at concentrations 1, 5 and 10 % (v/v).

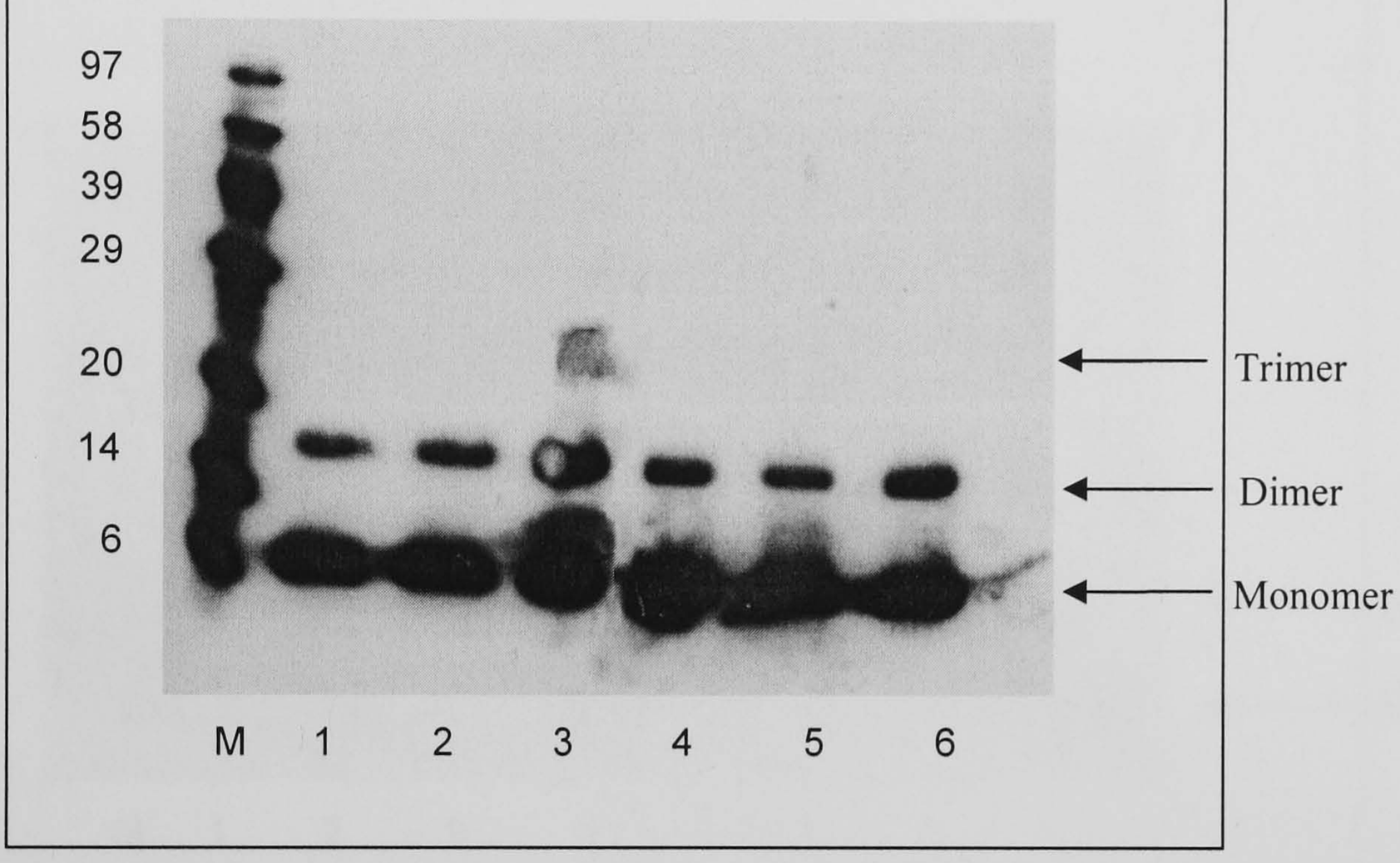

Figure 2.17. The effect of DMSO (1, 5 and 10 % (v/v)) on the form of recombinant IL-8 (5 x 10^{-7} M) in the presence of $CuCl_2$ (25 μM) plus H_2O_2 (25 μM) following incubation at 37°C for 1 day, analysed by SDS-PAGE on a 14 % polyacrylamide gel. M: molecular weight markers. Lane 1: IL-8 only, lane 2: IL-8 with $CuCl_2$, lane 3: IL-8 with $CuCl_2$ and H_2O_2, lane 4: IL-8 with $CuCl_2$, H_2O_2 and 1 % (v/v) DMSO, lane 5: IL-8 with $CuCl_2$, H_2O_2 and 5 % (v/v) DMSO, lane 6: IL-8 with $CuCl_2$, H_2O_2 and 10 % (v/v) DMSO. Representative of two independent experiments.

IL-8 trimers were generated in the absence of DMSO by 25 μM $CuCl_2$ plus 50 μM H_2O_2 (figure 2.17, lane 3) but were diminished upon treatment with 1, 5 and 10 % (v/v) DMSO (lanes 4 -6) indicating that hydroxyl radicals may be involved in the mechanism of multimer formation.

2.5.3. ENA-78

ENA-78, another neutrophil chemoattractant, was also of interest as this chemokine has no tyrosine residues in its amino acid sequence. Since it was suspected that dityrosine cross-linking could be involved in the mechanism of multimerisation, and as there are

no tyrosine residues in ENA-78, it was expected that ENA-78 should not be sensitive to $CuCl_2$ and H_2O_2. First, the effect of $CuCl_2$ on ENA-78 multimer formation was investigated. Recombinant human ENA-78 (Peprotech, UK) was incubated with $CuCl_2$ (1.25 – 100 μM) at the same concentration as RANTES and IL-8 (5 x 10^{-7} M) at 37 °C for 1 day only, as it was found that multimers are diminished after 2 days, as with IL-8. ENA-78 was analysed by SDS-PAGE, and Western blots were stained with anti-human ENA-78 antibody (Peprotech, UK).

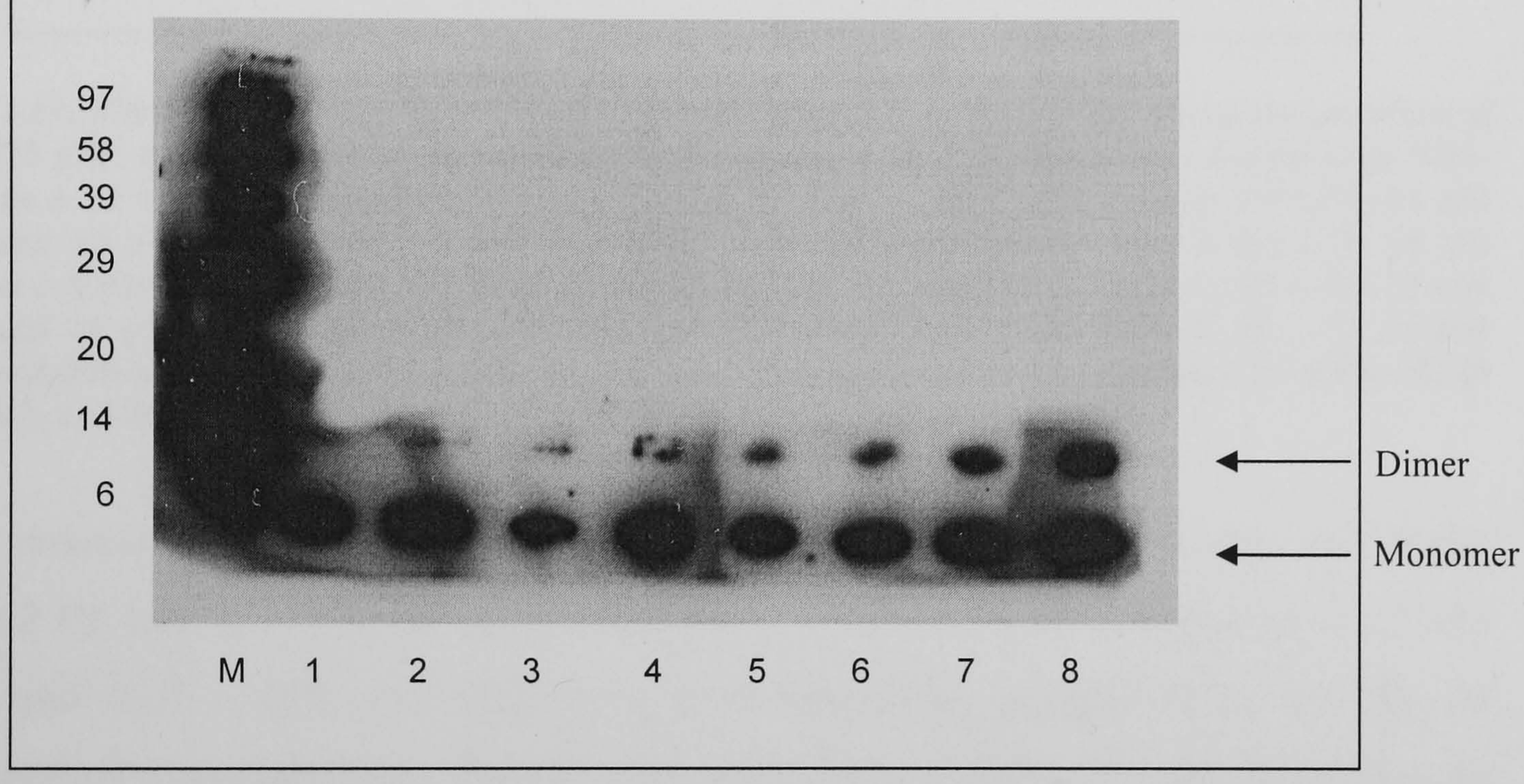

Figure 2.18. The effect of $CuCl_2$ on the form of recombinant ENA-78 (5 x 10^{-7} M) following incubation at 37°C for 1 day, analysed by SDS-PAGE on a 14 % polyacrylamide gel. M: molecular weight markers. Lane 1: ENA-78 only, lane 2: ENA-78 and 1.25 μM $CuCl_2$, lane 3: ENA-78 and 2.5 μM $CuCl_2$, lane 4: ENA-78 and 12.5 μM $CuCl_2$, lane 5: ENA-78 and 25 μM $CuCl_2$, lane 6: ENA-78 and 50 μM $CuCl_2$, lane 7: ENA-78 and 75 μM $CuCl_2$ and lane 8: ENA-78 and 100 μM $CuCl_2$. Representative of two independent experiments.

It was observed that $CuCl_2$ alone had no effect on ENA-78 multimer formation. ENA-78 was monomeric and dimeric in the presence of 1.25 – 100 μM $CuCl_2$.

The effect of H_2O_2 (1 – 400 μM) on multimerisation of ENA-78 in the presence of 25 μM $CuCl_2$ was then investigated.

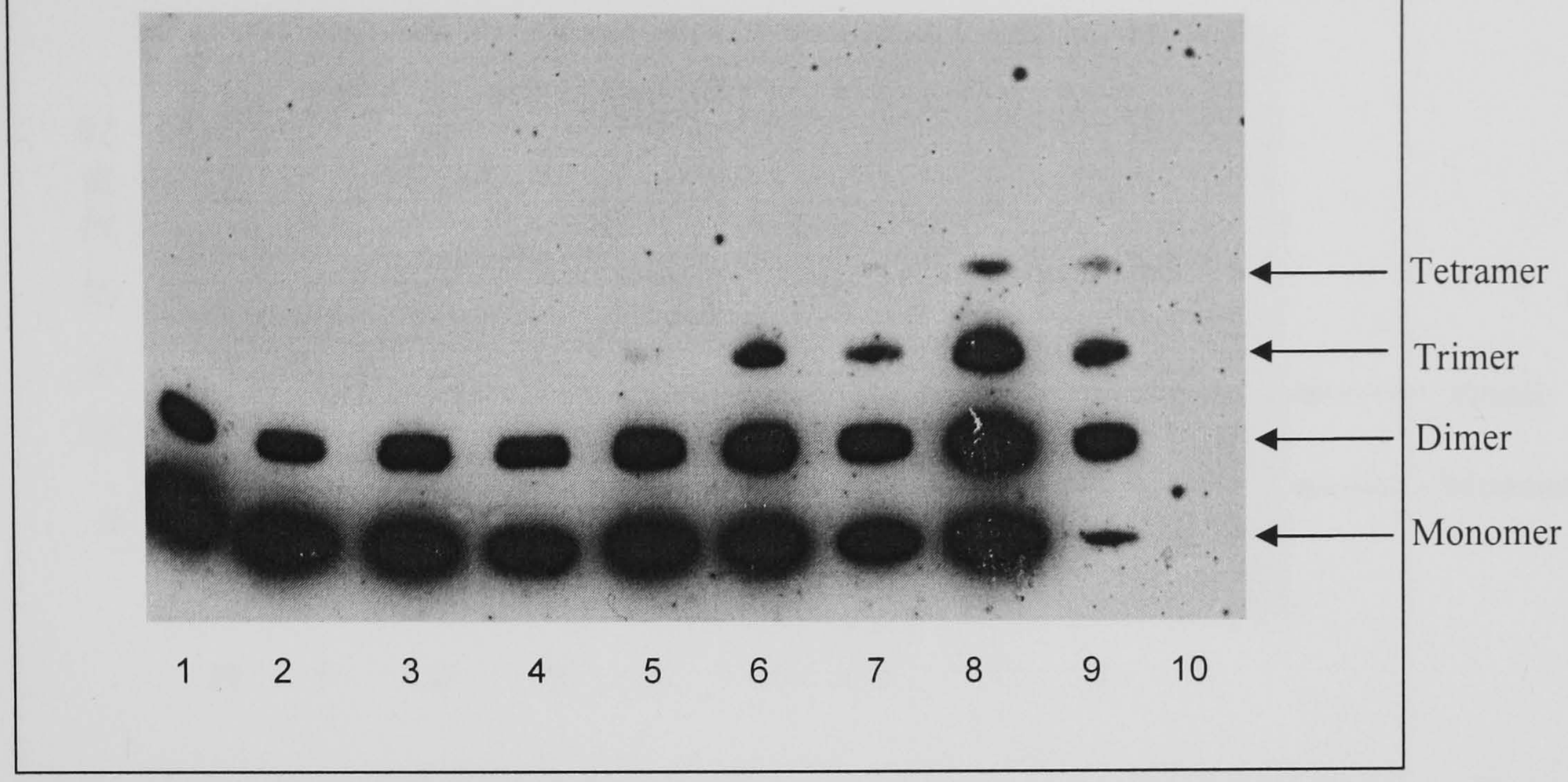

Figure 2.19. The effect of H_2O_2 on the form of recombinant ENA-78 (5×10^{-7} M) in the presence of $CuCl_2$ (25 μM) and H_2O_2 (1 – 400 μM) following incubation at 37°C for 1 day, analysed by SDS-PAGE on a 14 % polyacrylamide gel. Lane 1: ENA-78 and 25 μM $CuCl_2$, lane 2: ENA-78, 25 μM $CuCl_2$ and 0.5 μM H_2O_2,, lane 3: ENA-78, 25 μM $CuCl_2$ and 1 μM H_2O_2,, lane 4: ENA-78, 25 μM $CuCl_2$ and 5 μM H_2O_2, lane 5: ENA-78, 25 μM $CuCl_2$ and 12.5 μM H_2O_2, lane 6: ENA-78, 25 μM $CuCl_2$ and 25 μM H_2O_2, lane 7: ENA-78, 25 μM $CuCl_2$ and 50 μM H_2O_2, lane 8: ENA-78, 25 μM $CuCl_2$ and 100 μM H_2O_2, lane 9: ENA-78, 25 μM $CuCl_2$ and 200 μM H_2O_2 and lane 10: ENA-78, 25 μM $CuCl_2$ and 400 μM H_2O_2. Representative of two independent experiments.

In the absence of H_2O_2, ENA-78 was seen predominantly as a monomer and dimer (figure 2.19, lane 2). ENA-78 multimerisation was enhanced in the presence of 25 μM $CuCl_2$ and 12.5 – 100 μM H_2O_2 in a dose dependent manner (lanes 5 – 8). At physiological concentrations, Cu (25 μM) plus H_2O_2 (12.5 - 25 μM, lanes 5 - 6) promote the multimerisation of ENA-78 to tetramers - lanes 5 - 6). Increased H_2O_2 concentrations (50 – 200 μM) resulted in further higher order multimer formation (lanes 6 – 9). Multimerisation is maximal at 100 μM H_2O_2 (lane 8). At 200 μM H_2O_2 ENA-78 multimers were diminished and at 400 μM H_2O_2 ENA-78 multimers were destroyed.

The effect of heparan sulphate (HS) on $CuCl_2$ induced multimer formation was then investigated. ENA-78 was incubated in the presence of $CuCl_2$ (0.5 – 100 μM) and HS (0.1 mg/ml).

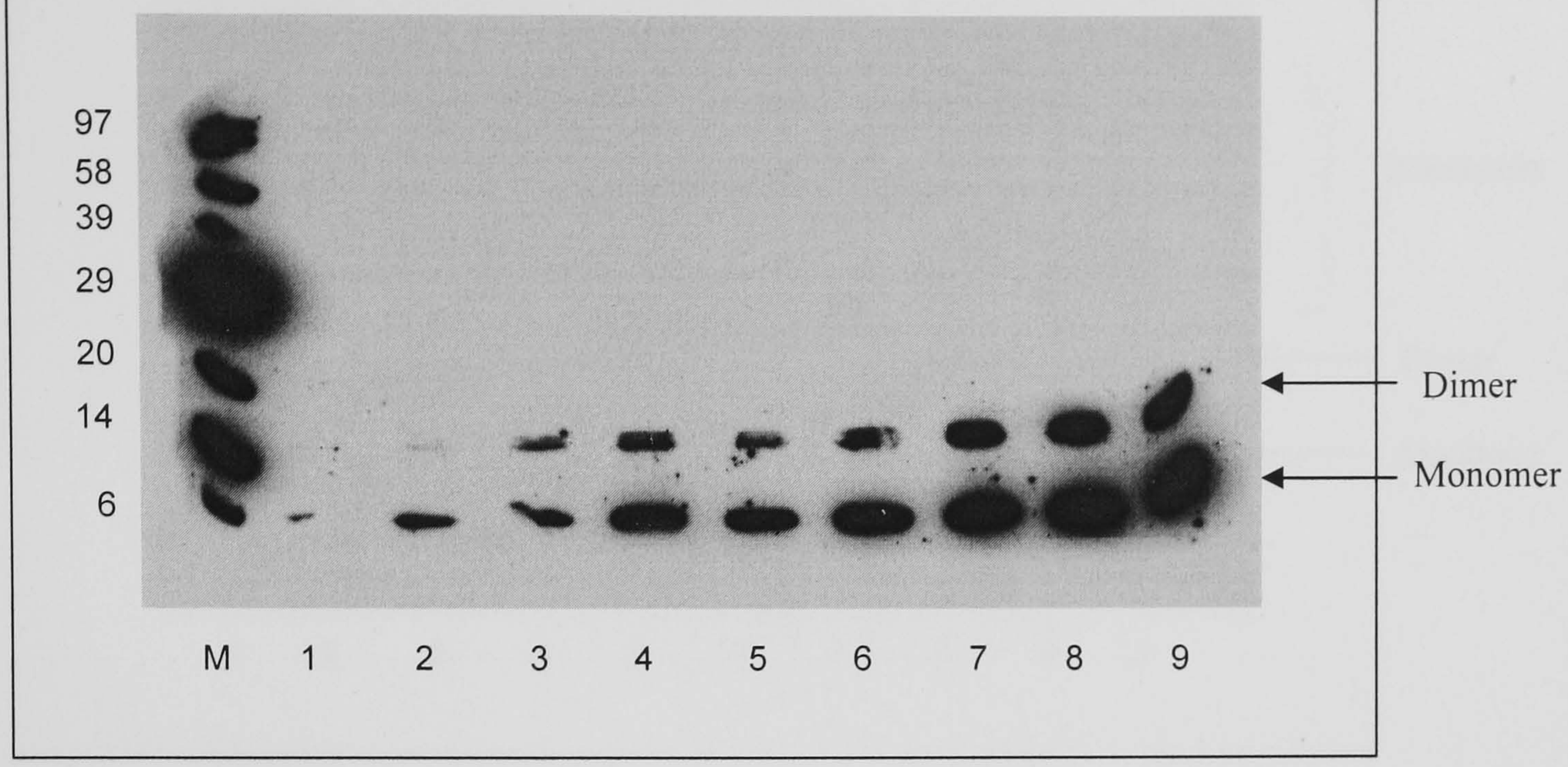

Figure 2.20. The effect of $CuCl_2$ on the form of recombinant ENA-78 (5×10^{-7} M) in the presence of HS (0.1 mg/ml) following incubation at 37°C for 1 day, analysed by SDS-PAGE on a 14 % polyacrylamide gel. M: molecular weight markers. Lane 1: ENA-78 and HS, lane 2: ENA-78, HS and 1.25 µM $CuCl_2$, lane 3: ENA-78, HS and 2.5 µM $CuCl_2$, lane 4: ENA-78, HS and 5 µM $CuCl_2$, lane 5: ENA-78, HS and 12.5 µM $CuCl_2$, lane 6: ENA-78, HS and 25 µM $CuCl_2$, lane 7: ENA-78, HS and 50 µM $CuCl_2$, lane 8: ENA-78, HS and 75 µM $CuCl_2$ and lane 9: ENA-78, HS and 100 µM $CuCl_2$. Representative of two independent experiments.

In the presence of HS (figure 2.20), there was little change in the form of ENA-78 in the presence of $CuCl_2$ compared to the absence of HS (figure 2.18). ENA-78 appeared only in monomeric and dimeric form.

Subsequently, the effect of HS (0.1 mg/ml) on ENA-78 multimer formation in the presence of 25 µM $CuCl_2$ and increasing concentrations of H_2O_2 (1 – 400 µM) was investigated.

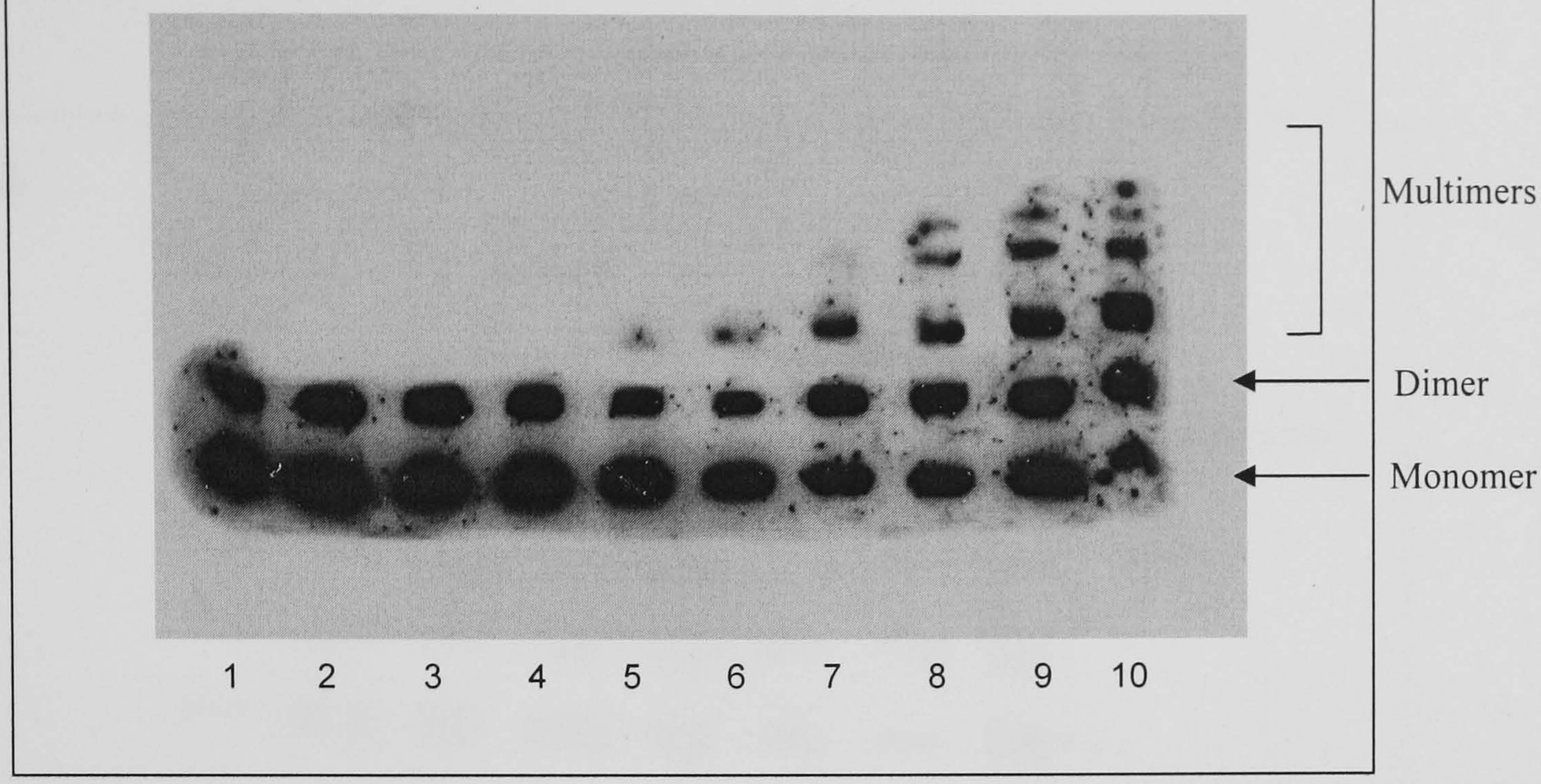

Figure 2.21. The effect of H_2O_2 on the form of recombinant ENA-78 (5×10^{-7} M) in the presence of $CuCl_2$ (25 μM) and HS (0.1 mg/ml) following incubation at 37°C for 1 day, analysed by SDS-PAGE on a 14 % polyacrylamide gel. Lane 1: ENA-78, HS and 25 μM $CuCl_2$, lane 2: ENA-78, HS, 25 μM $CuCl_2$ and 0.5 μM H_2O_2, lane 3: ENA-78, HS, 25 μM $CuCl_2$ and 1 μM H_2O_2, lane 4: ENA-78, HS, 25 μM $CuCl_2$ and 5 μM H_2O_2, lane 5: ENA-78, HS, 25 μM $CuCl_2$ and 12.5 μM H_2O_2, lane 6: ENA-78, HS, 25 μM $CuCl_2$ and 25 μM H_2O_2, lane 7: ENA-78, HS, 25 μM $CuCl_2$ and 50 μM H_2O_2, lane 8: ENA-78, HS, 25 μM $CuCl_2$ and 100 μM H_2O_2, lane 9: ENA-78, HS, 25 μM $CuCl_2$ and 200 μM H_2O_2 and lane 10: ENA-78, HS, 25 μM $CuCl_2$ and 400 μM H_2O_2. Representative of two independent experiments.

In the absence of HS (figure 2.19), higher order multimer formation occurred in the presence of 25 μM $CuCl_2$ plus 12.5 – 100 μM H_2O_2 in a dose dependent manner (figure 2.19, lanes 5 – 8) and multimerisation was maximal at 100 μM H_2O_2 (figure 2.19, lane 8). In the presence of HS (0.1 mg/ml), higher order multimer formation also occurred in the presence of 25 μM $CuCl_2$ plus 12.5 – 100 μM H_2O_2 in a dose dependent manner (figure 2.21, lanes 5 – 8), but at 200 – 400 μM H_2O_2, multimers remained and were protected by HS. In the presence of 0.1 mg/ml HS, multimerisation was maximal at 200 - 400 μM rather than at 100 μM H_2O_2 in the absence of 0.1 mg/ml HS (figure 2.19). HS appeared to protect high order multimers from damage by high concentrations of H_2O_2. The multimers were able to withstand higher concentrations of H_2O_2 (200 – 400 μM) in the presence of 0.1 mg/ml HS (figure 2.21, lanes 9 and 10).

In order to quantify the degree of multimerisation, ENA-78 was incubated in the presence and absence of physiological concentrations of $CuCl_2$ (25 μM) plus H_2O_2 (50 μM), and in the presence and absence of HS (0.1 mg/ml). Multimers of higher order

than dimer were quantified by scanning densitometry and presented as the % of total RANTES including the monomer.

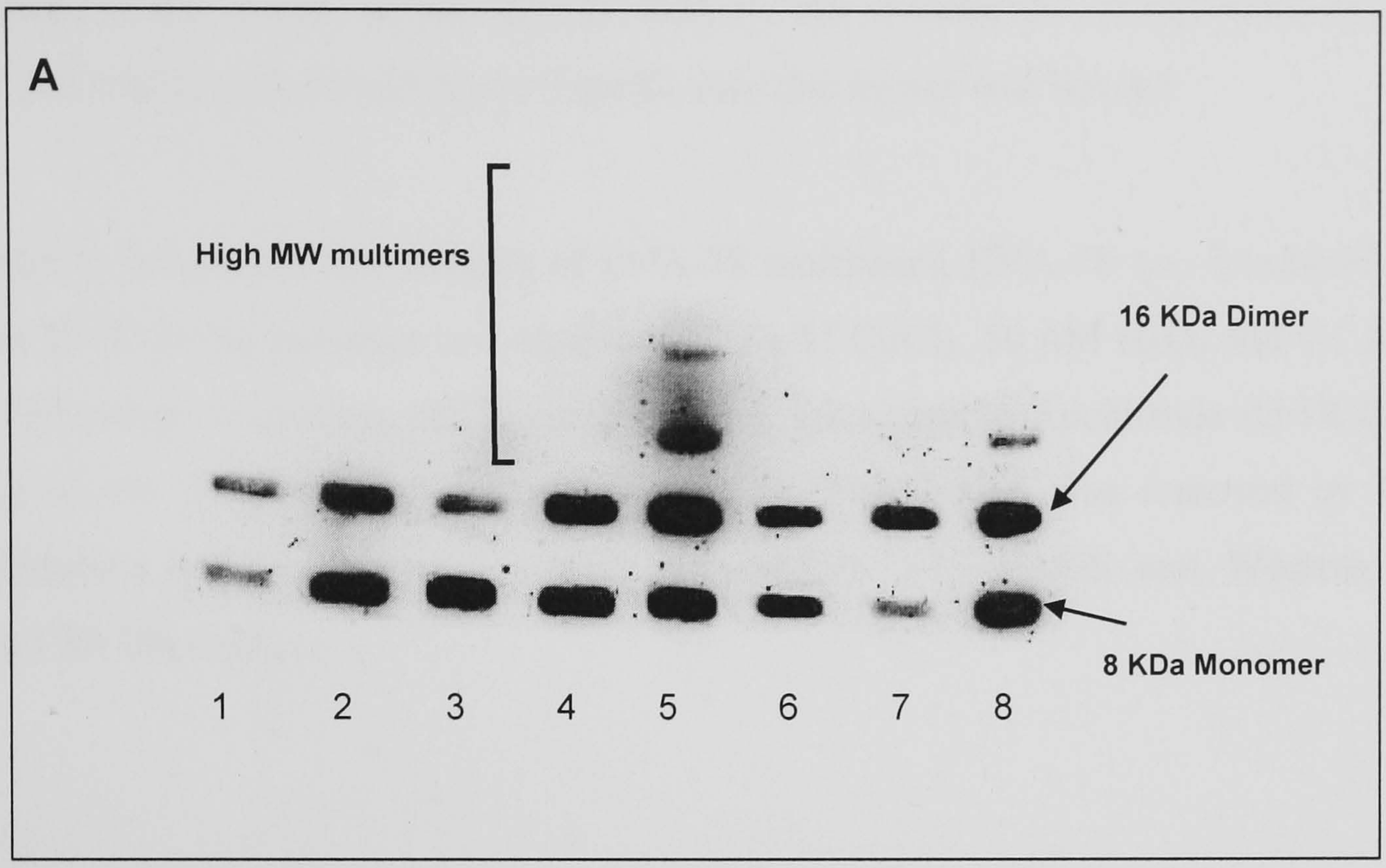

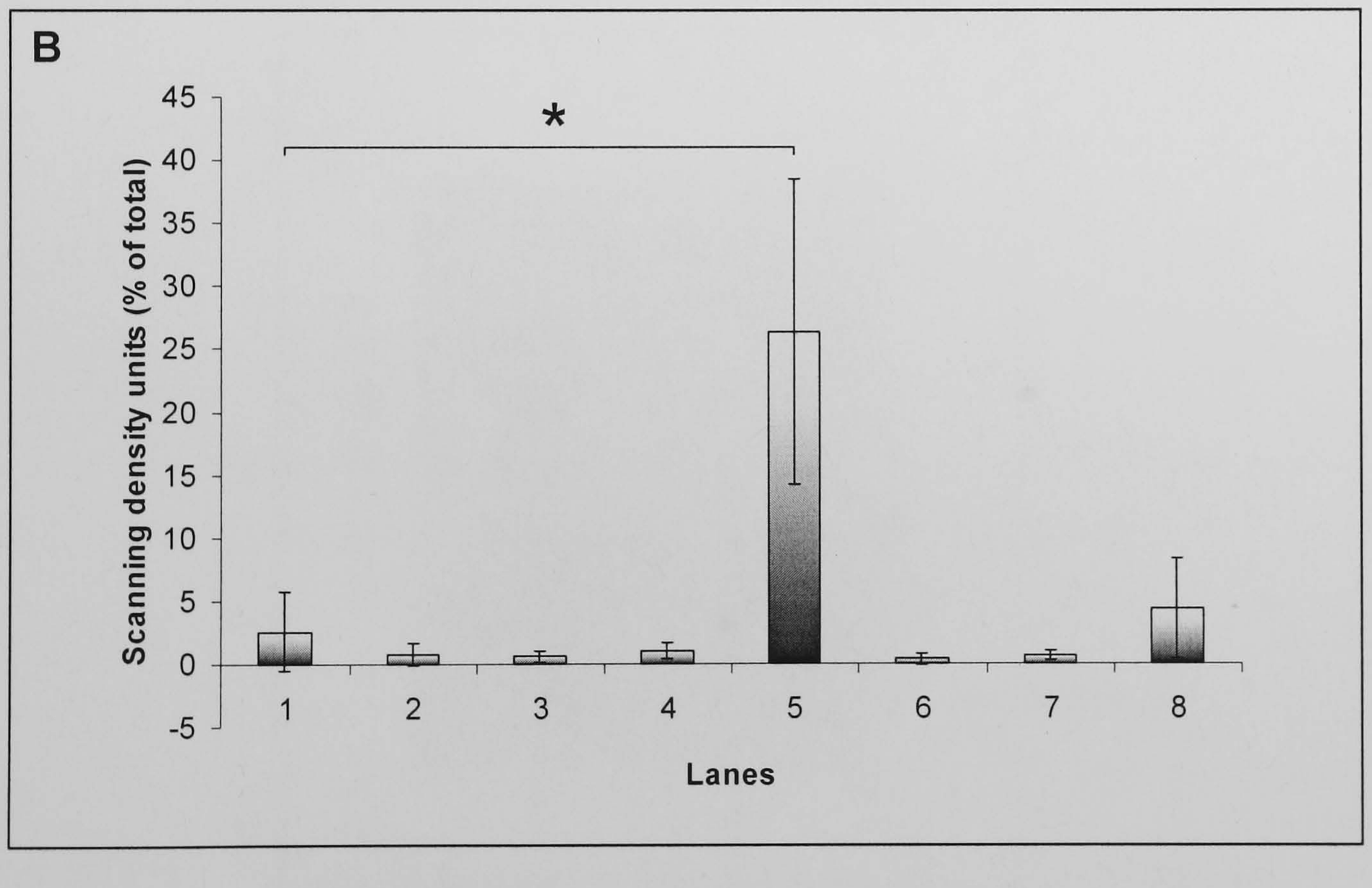

Figure 2.22A. ENA-78 (5×10^{-7} M) incubated at 37°C for 1 day and analysed by SDS-PAGE on a 14 % polyacrylamide gel. ± $CuCl_2$ (25 µM), H_2O_2 (50 µM) and HS (0.1 mg/ml). Lane 1: ENA-78 only, lane 2: ENA-78 + HS, lane 3: ENA-78 + $CuCl_2$, lane 4: ENA-78 + H_2O_2, lane 5: ENA-78 + $CuCl_2$ and H_2O_2, lane 6: ENA-78 + HS + $CuCl_2$, lane 7: ENA-78 + HS + H_2O_2 and lane 8: ENA-78 + HS, $CuCl_2$ and H_2O_2. Representative of three independent experiments.

Figure 2.22B: Quantitative analysis of supra-dimeric ENA-78 intensity (higher order complexes of ENA-78 including tetramer (24 KDa) as % of total analysed using density analysis (Quantiscan). Lane 1: ENA-78 only, lane 2: ENA-78 + HS, lane 3: RANES + $CuCl_2$, lane 4: ENA-78 + H_2O_2, lane 5: ENA-78 + $CuCl_2$ and H_2O_2, lane 6: IL-8 + HS + $CuCl_2$, lane 7: IL-8 + HS + H_2O_2 and lane 8: IL-8 + HS, $CuCl_2$ and H_2O_2. * indicates $p < 0.05$, ($n = 3$).

The addition of 25 μM $CuCl_2$ plus 50 μM H_2O_2 significantly promoted trimer and tetramer formation (lane 5, 26.32 ± 12.11 % is in supra-dimeric form, $p < 0.05$) compared to the control (ENA-78 only, lane 1). HS reduced the multimerisation effect of 25 μM $CuCl_2$ with 50 μM H_2O_2 (lane 8), only the trimer was formed.

In order to investigate the stability of ENA-78 multimers, ENA-78 was incubated for 1 day at 37 °C in the presence and absence of 25 μM $CuCl_2$, 50 μM H_2O_2 and 0.1 mg/ml HS. Following incubation, the chaotropic agent, guanidine hydrochloride (G-HCl), was added to the samples, final concentration 6 M. The G-HCl was removed by EtOH precipitation before the samples were analysed by SDS-PAGE and Western blots stained for ENA-78.

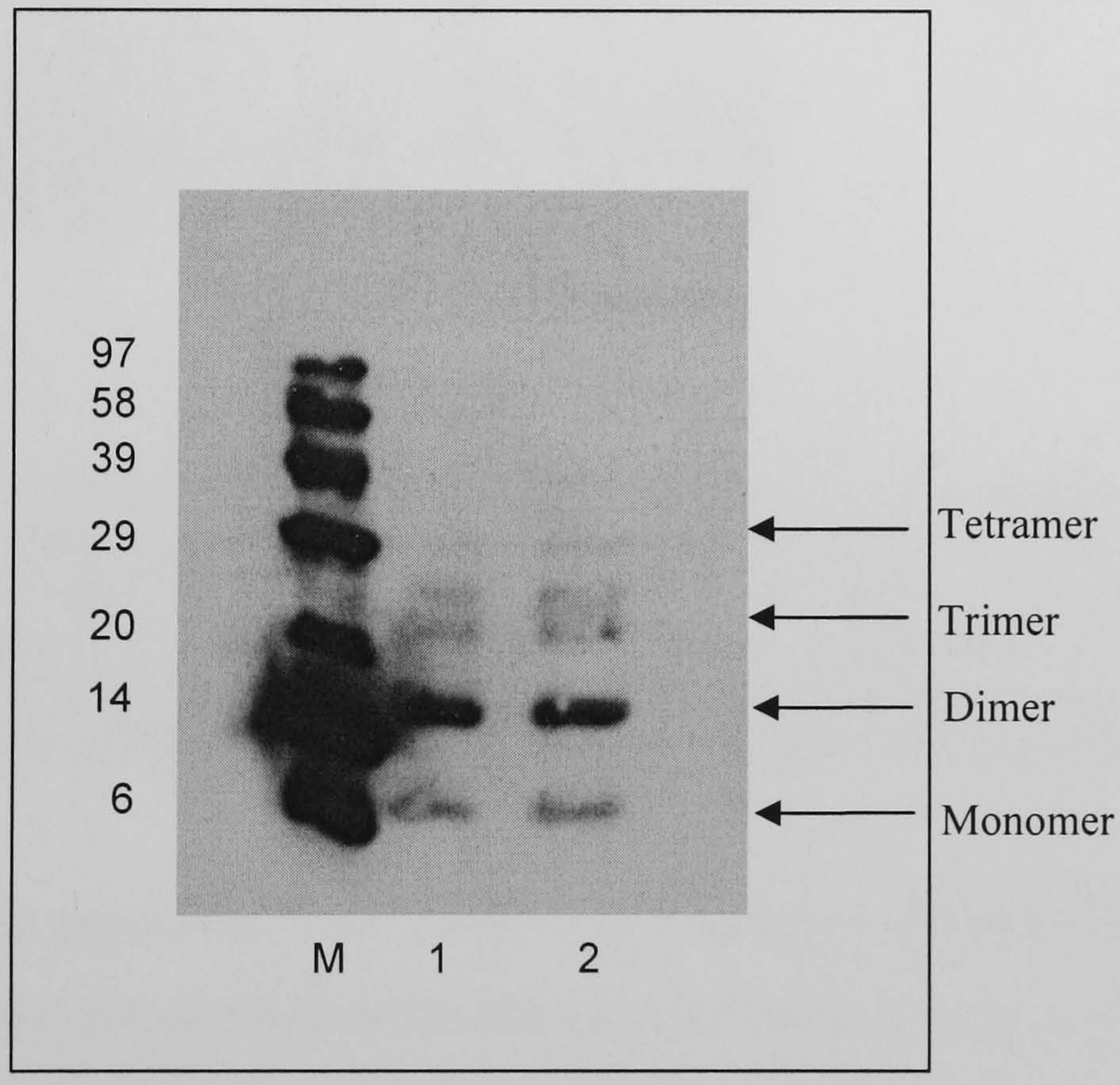

Figure 2.23. The effect of G-HCl (6 M) and EtOH precipitation on the form of recombinant ENA-78 (5×10^{-7} M) in the presence of $CuCl_2$ (25 μM) plus H_2O_2 (50 μM) following incubation at 37°C for 1 day, analysed by SDS-PAGE on a 14 % polyacrylamide gel. M: molecular weight markers. Lane 1: ENA-78 with 25 μM $CuCl_2$ and 25 μM H_2O_2, lane 2: ENA-78, 25 μM $CuCl_2$ and 25 μM H_2O_2 with 6 M GHCl and EtOH precipitation. Representative of two independent experiments.

The higher order ENA-78 multimers (above and including trimers) generated in the presence of 25 μM $CuCl_2$ plus 50 μM H_2O_2 were found to remain following treatment

with G-HCl (6 M) (figure 2.23, lane 2) compared to the control (ENA-78 in the presence of 25 μM $CuCl_2$ and 50 μM H_2O_2 but in the absence of G-HCl, lane 1). Monomers and dimers were also found to remain following treatment with G-HCl, indicating that the 3-dimensional structure of ENA-78 was not disrupted.

The effect of the hydroxyl radical scavenger, dimethyl sulphoxide (DMSO) at concentrations 1, 5 and 10 % (v/v) on ENA-78 multimerisation in the presence of 25 μM $CuCl_2$ plus 50 μM H_2O_2 was then investigated.

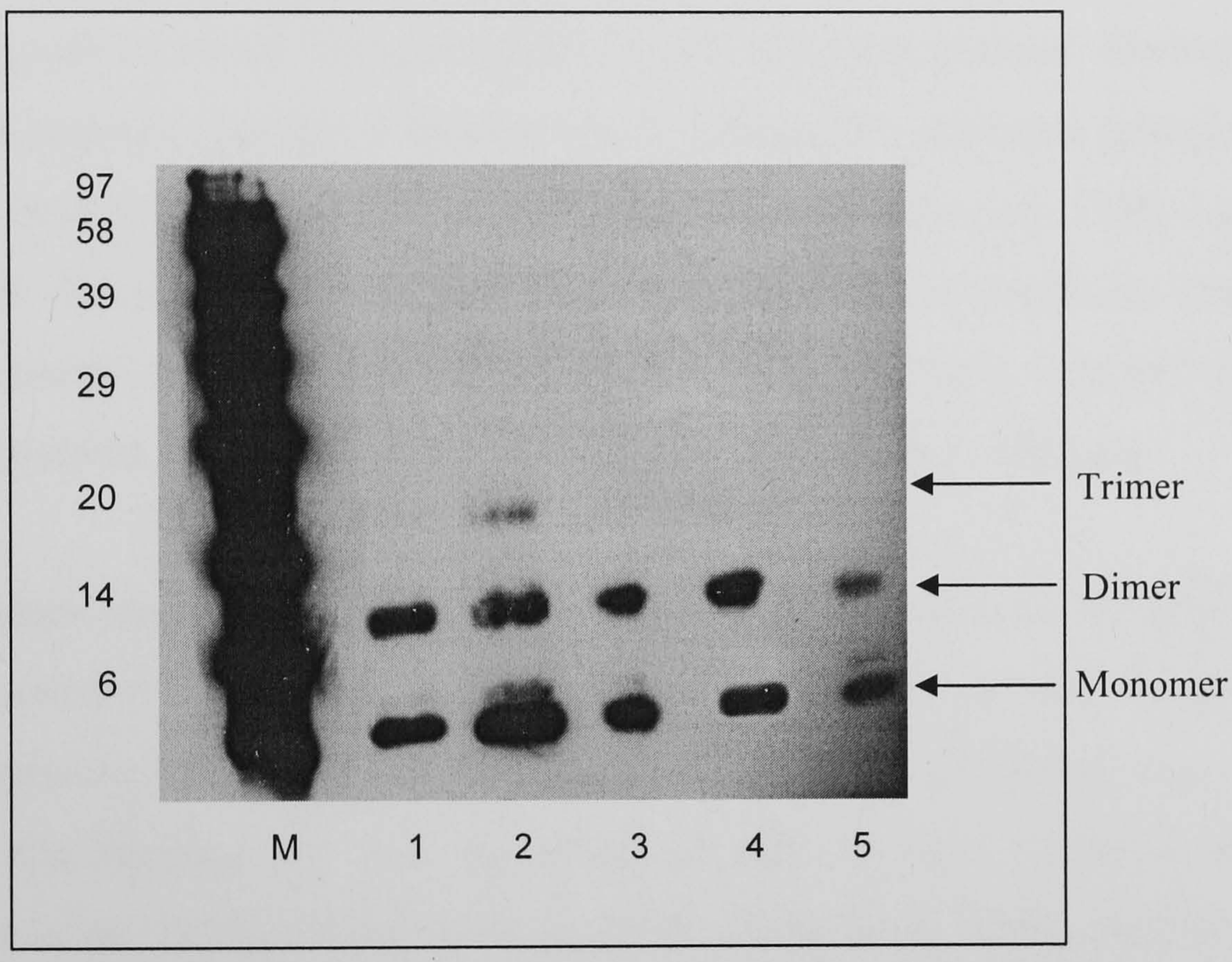

Figure 2.24. The effect of DMSO (1, 5 and 10 % (v/v)) on the form of recombinant ENA-78 (5×10^{-7} M) in the presence of $CuCl_2$ (25 μM) plus H_2O_2 (50 μM) following incubation at 37°C for 1 day, analysed by SDS-PAGE on a 14 % polyacrylamide gel. M: molecular weight markers. Lane 1: ENA-78 with $CuCl_2$, lane 2: ENA-78 with $CuCl_2$ and H_2O_2, lane 3: ENA-78 with $CuCl_2$, H_2O_2 and 1 % (v/v) DMSO, lane 4: ENA-78 with $CuCl_2$, H_2O_2 and 5 % (v/v) DMSO, lane 5: ENA-78 with $CuCl_2$, H_2O_2 and 10 % (v/v) DMSO. Representative of two independent experiments.

ENA-78 trimers were generated in the absence of DMSO by 25 μM $CuCl_2$ plus 50 μM H_2O_2 (figure 2.24, lane 2) but were diminished upon treatment with 1, 5 and 10 % (v/v) DMSO (lanes 4 -5) indicating that hydroxyl radicals may be involved in the mechanism of multimer formation.

2.6. Discussion

$CuCl_2$ alone induces the formation of RANTES and IL-8 multimers of higher order than the dimer. In the presence of physiological concentrations of $CuCl_2$ the addition of H_2O_2 further enhances the formation of higher order chemokine multimers in a dose-dependent manner. With the addition of Cu plus increasing concentrations of H_2O_2, dimer formation increases at the expense of the monomer (figure 2.4).

Physiological levels of Cu in plasma have been reported ranging between 8.3 and 26.48 μM (Gonzalez *et al*, 1999; Versieck, 1980) and some studies have claimed physiological levels of H_2O_2 of up to 35 μM in human plasma. During inflammatory reactions pathophysiological levels of H_2O_2 released by activated granulocytes of up to 100 μM have been reported (Bucchieri *et al*, 2002; Deskur *et al*, 1998; Lacy *et al*, 1998; Varma & Devamanoharan, 1991). The observation that chemokines multimerise with optimal conditions of 25 μM $CuCl_2$ plus 50 – 100 μM H_2O_2 indicates that chemokine multimerisation should occur *in vivo*, under inflammatory conditions.

Chemokines appear to multimerise via a mechanism similar to the self-aggregation of the amyloid-β (Aβ) peptide. Evidence for an interaction between Cu and Aβ1-40 was first observed by the stabilisation of an Aβ dimer by Cu (II) (Bush *et al*, 1994). A high affinity Cu binding site was observed on Aβ1-42 that mediates self-aggregation (Atwood *et al*, 2000b; Burrows *et al*, 1994; Clore *et al*, 1990; Schnitzel *et al*, 1994; Skelton *et al*, 1995).

Chemokine multimerisation was found to occur optimally after 1 day for IL-8 and ENA-78 and 2 days of incubation for RANTES at 37 °C. Similarly, the Aβ peptide was found to multimerise optimally following 5 day incubation. This observation indicates the involvement of a slow oxidative system, with a requirement for the accumulation of free radicals. In addition, the hydroxyl radical scavenger DMSO attenuates chemokine multimerisation in a dose-dependent manner, indicating that hydroxyl radicals and therefore a redox mechanism may be involved in multimer formation. IL-8 and ENA-78 may have a different mechanism of cross-linking to RANTES. Dityrosine formation was investigated and results reported in Chapter 3.

All Cu plus H_2O_2-induced higher order chemokine multimers were resistant to SDS and G-HCl (6 M). The G-HCl and SDS resistance of chemokine multimers indicates that multimers are covalently linked and highly stable.

It is possible that in these *in vitro* conditions Cu contributes to the generation of free radicals/reactive oxygen species and mediates chemokine oligomerisation in a fashion similar to the mechanism involved in Cu-mediated Aβ peptide oligomerisation.

Evidence suggests that Cu firstly binds to the Aβ-peptide via histidine residues and secondly, forms links between tyrosine residues (tyrosine-tyrosine links) that are covalent (Atwood *et al*, 2000a; Atwood *et al*, 1998; Atwood *et al*, 2000b). Senile plaques isolated from AD brain are predominantly composed of Aβ-peptide bound to Cu (II) via high affinity interactions with histidine residues (Atwood *et al*, 2004). Cu-histidine binding is abolished by acidic pH or chemical blocking of histidine residues (Atwood *et al*, 2000a; Cuajungco *et al*, 2000). It has also been shown that Cu induced oxidative conditions promote the modification of both histidine and tyrosine residues in Aβ. One of the oxidation products was identified as dityrosine by both fluorescence detection and detection with a specific dityrosine antibody (Atwood *et al*, 2000a; Atwood *et al*, 2004).

It has been reported that following the binding of Cu (II) to histidine residues, Aβ-peptide multimerisation is mediated through oxidation of tyrosine residues with the subsequent reduction of Cu (II) to Cu (I) (Atwood *et al*, 2000b; Huang *et al*, 1999), and it has now been shown that the β-amyloid protein reduces Cu (II) to Cu (I) with concurrent generation of H_2O_2 and hydroxyl radicals from O_2 (Liu *et al*, 2006). It was confirmed that through this mechanism, Cu (II) induces the generation of dityrosine cross-linked, SDS-resistant multimers of human Aβ peptide of 8.6, 13 and 17 KDa (Atwood *et al*, 2004; Huang *et al*, 1999), see figure 2.25.

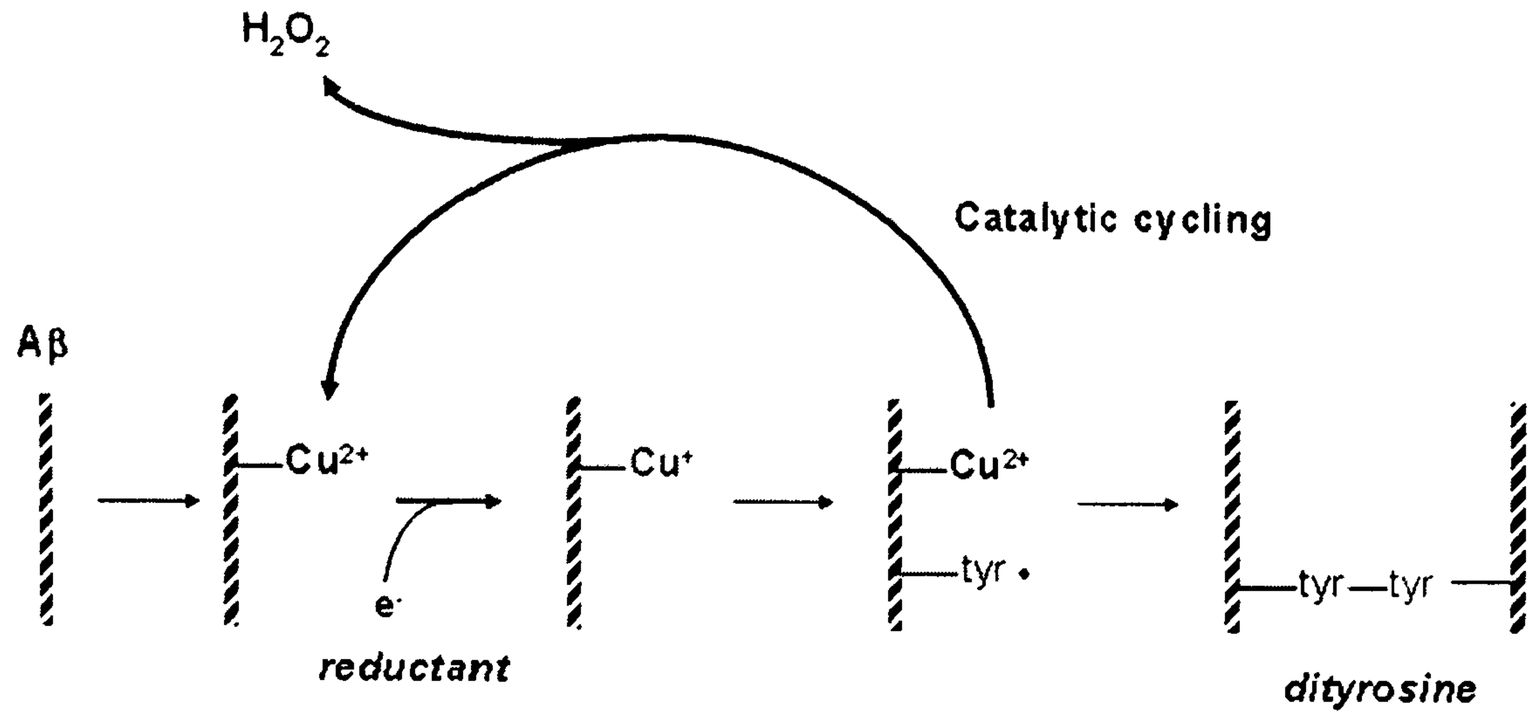

Figure 2.25. A simple model depicting the redox chemistry of dityrosine formation in Aβ oligomerisation (Smith *et al*, 2007). The origin of the electron(s) could be the peptide itself or from other biological reducing agents such as dopamine and ascorbate (Opazo *et al*, 2002). Cu (II) binds Aβ via histidine residues. Aβ-peptide multimerisation is mediated through the oxidation of adjacent tyrosine residues with the subsequent reduction of Cu (II) to Cu (I) and concurrent generation of H_2O_2. As a consequence of the formation of a tyrosyl radical, dityrosine cross-links are generated giving rise to covalently linked soluble Aβ oligomers (Atwood *et al*, 2000b; Huang *et al*, 1999; Liu *et al*, 2006; Smith *et al*, 2007).

These findings reveal the requirement for both tyrosine and histidine residues for metal-mediated Aβ-peptide assembly (Atwood *et al*, 2000b), which are both known to coordinate Cu in Aβ (Atwood *et al*, 2004).

The hypothesis for the involvement of Cu in chemokine multimerisation is based on the known mechanism for dityrosine cross-link formation in the multimerisation of the β-amyloid protein. The covalent binding of Cu and the formation of dityrosine cross-links is likely promoted by the presence of H_2O_2. The suggested mechanism is a Cu-redox system that occurs in the presence of Cu plus H_2O_2.

The hypothesis is that Cu (II) binds and subsequently oxidises the chemokine (CK) to form oligomers, whilst Cu (II) is subsequently reduced to Cu (I).

$$CK + Cu^{2+} \longrightarrow Cu^{+} + CK{:}CK^{+}$$

Reduced Cu (I) reacts with molecular oxygen (O_2) generating the superoxide anion (O_2^-). This recycles Cu (I) back to Cu (II).

$$Cu^{+} + O_2 \longrightarrow Cu^{2+} + O_2^-$$

The O_2^- generated in the recycling of Cu (I) back to Cu (II) undergoes dismutation to H_2O_2 and O_2 spontaneously.

$$O_2^- + O_2^- + 2H^+ \longrightarrow H_2O_2 + O_2$$

This shows that chemokines could multimerise without the addition of H_2O_2 to the reaction, as it is generated spontaneously in the presence of molecular oxygen. Indeed, Cu alone induced multimerisation of RANTES and IL-8, but not ENA-78, which implicates the tyrosine residue in the reaction. Similarly, it has been suggested that in the absence of added H_2O_2, the Aβ-peptide directly produces H_2O_2 in the presence of $CuCl_2$ alone through Cu (II) reduction and redox in the presence of molecular oxygen (Huang *et al*, 1999).

However, in the presence of H_2O_2 Cu (I) can be more efficiently oxidised back to Cu (II) in the Fenton reaction, providing more Cu (II) for the reaction and resulting in further multimerisation of CK. All chemokines were found to multimerise in the presence of Cu plus H_2O_2, indicating the involvement of other residues in the formation of stable covalent cross-links in ENA-78.

Haber Weiss – Fenton reaction

$$H_2O_2 + Cu^+ \longrightarrow Cu^{2+} + OH^- + OH\cdot$$

$$Cu^{2+} + O_2^- \longrightarrow O_2 + Cu^+$$

When both reactions above combine, further ROS are generated causing the redox to propagate:

$$H_2O_2 + O_2^- \xrightarrow{Cu^+/Cu^{2+}} O_2 + OH^- + OH\cdot$$

DMSO scavenges OH· radicals and inhibits chemokine multimerisation, indicating the involvement of OH· radicals. Interestingly, investigation using lens proteins has shown that the H_2O_2/Cu ion system but not other metal-catalysed oxidation systems such as H_2O_2/Fe-EDTA produces protein-bound dityrosine (Kato *et al*, 2001).

Chemokine multimer formation is enhanced in the presence of H_2O_2 but the effect does not occur in the presence of H_2O_2 alone. This is also true for the Aβ-peptide (Atwood *et al*, 2004; Atwood *et al*, 2000b). The Cu is required for redox cycling to occur, and it is the redox that drives the reaction leading to multimer formation.

Since multimerisation in the presence of Cu plus H_2O_2 occurs in ENA-78 which has no tyrosine residues in its primary structure, there must be an additional mechanism that does not involve dityrosine formation (figure 2.18). As suggested with Aβ-peptide multimer formation (Atwood *et al*, 2000a), chemokine multimerisation could occur via the involvement of histidine residues, of which ENA-78 has one, RANTES has one and IL-8 has two. Cu has been shown to bind to histidine residues with high affinity (Camakaris *et al*, 1999). Evidence implies that in addition to the involvement of Cu (II) in dityrosine formation, Cu (II) is coordinated to Aβ via 3 histidine residues, with the formation of an intermolecular histidine bridge between Cu (II) atoms (Atwood *et al*, 2000a; Huang *et al*, 2004; Smith *et al*, 2006). Binding of Cu to histidine may also explain the multimerisation of ENA-78 in the absence of tyrosine residues.

Oligomer formation is also observed with the prion protein (PrP). Since 1995, investigations on Cu binding to PrP^C have been focussed on peptides from the unstructured N-terminal segment of PrP^C, consisting of a highly conserved repeat of four octarepeat units containing histidine and glycine residues with the concensus sequence PHGGGWGQ. Four Cu (II) ions have been found to bind in this region whilst a fifth Cu (II) ion has been proposed to bind to the prion protein in the region connecting the unstructured segment with the globular portion of the protein. This portion of the protein is characterised by the presence of helices.

Cu (II) dependent PrP aggregation has been reported to occur through the coordination of Cu to His-111 as the key residue together with His-96, Met-112 and the N-terminal amino group (Brown *et al*, 2004; Jackson *et al*, 2001; Jobling *et al*, 2001; Kramer *et al*, 2001; Qin *et al*, 2002; Wadsworth *et al*, 1999). This indicates the possible involvement of methionine residues in conjunction with histidine residues. Evidence suggests that the mechanism for PrP multimerisation involves Cu (II) ions coordinated with histidine to form a complex that also involves a tyrosine residue (Stanczak *et al*, 2005a; Stanczak *et al*, 2005b).

This mechanism of Cu (II) – PrP histidine/methionine/tyrosine coordination is similar to the histidine/tyrosine involvement in Aβ-peptide multimerisation, and this could also be a possible mechanism for chemokine multimerisation in those chemokines which contain histidine, methionine and tyrosine residues. This also explains why chemokines

with a higher number of tyrosine residues may multimerise more effectively than those with few or no tyrosine residues. Dityrosine cross-links may occur in addition to histidine bridges in those chemokines that have one or more tyrosine residues in their primary structure.

There is also evidence suggesting that the prion-like protein 'Doppel' binds Cu. Doppel exhibits 26 % sequence identity with the prion protein, but lacks the octarepeat region implicated as the major Cu-binding domain. Matrix-assisted laser desorption ionisation mass spectrometry of a doppel peptide revealed binding of Cu but not other metals (Qin *et al*, 2003)

Alternatively, chemokine multimerisation may involve cysteine residues, since Cu is also known to bind cysteine residues as well as methionine and histidine with high affinity (Bopp *et al*, 2008). In addition, homocysteine, a thiol containing derivative of cysteine has been shown to interact with Cu (II) and reduce it to Cu (I) with subsequent H_2O_2 generation (White *et al*, 2001). ENA-78 has 4 cysteine residues and both IL-8 and RANTES have 5 in their primary structure. ENA-78 and RANTES have 1 methionine residue whilst IL-8 has none. Other amino acid residues may also be involved in multimerisation effects in conjunction with histidine, methionine or cysteine residues.

It was speculated that the interaction of chemokines with GAGs may be via a similar mechanism to the interaction of the PrP with GAGs, i.e. through the covalent binding of Cu. PrP multimers stabilised by Cu (II) bridges interact with glycosaminoglycans (GAGs) and this protein-GAG interaction is mediated largely by protonated and Cu (II)-bound histidine side chains of PrP, occurring with the formation of a multimeric PrP complex (Gonzalez-Iglesias *et al*, 2002).

The previous work of others leading to the discovery that Cu (II) coordinates the binding of PrP multimers to GAGs, together with the knowledge that chemokines bind to GAGs led to the investigation of heparan sulphate (HS) binding to chemokine multimers in the presence of Cu. It was speculated that the addition of HS to chemokines, in the presence of 25 μM $CuCl_2$ and increasing concentrations of H_2O_2 would result in the formation of higher molecular weight GAG-chemokine multimer complexes.

However, no such complexes were detected. Instead, the evidence suggested that HS is acting as a free radical scavenger. GAGs including HS are well known as free radical scavengers and have been shown to have protective effects against Cu induced peroxidation and oxidative damage in fibroblast and liposome cultures (Albertini *et al*, 2000; Albertini *et al*, 1996; Balogh *et al*, 2003; Campo *et al*, 2004; Volpi & Tarugi, 1999). Following the addition of HS, higher concentrations of H_2O_2 were required for optimal multimer formation indicating that HS limits the availability of free radicals and the extent of multimerisation at any given H_2O_2 concentration. In addition, higher order multimers were protected from damage at high concentrations of H_2O_2 in the presence of HS. GAGs have also been shown to have a protective effect against lipid peroxidation in endothelial cells (Section 4.5.1, figure 4.13).

The multimer limiting and protective effects of HS as a scavenger mirror the observation that the hydroxyl radical scavenger DMSO also limits chemokine multimer formation. Again, this indicates the involvement of free radicals and redox in the mechanism of chemokine multimer formation.

It appears that HS has a biphasic effect dependent on the H_2O_2 concentration. Chemokines appear to have different susceptibilities to oxidative degradation induced by free radical attack at high H_2O_2 concentrations with IL-8 more susceptible than RANTES and ENA-78 (figures 2.7A, 2.15A and 2.22A). Chemokines such as RANTES or ENA-78 appear less susceptible to oxidative degradation by free radical attack at high concentrations of H_2O_2 and therefore the addition of HS attenuates multimer formation as the availability of free radicals is limited by HS. Chemokines such as IL-8 appear to multimerise more effectively in the presence of HS and therefore may be more susceptible to oxidative degradation. The protective effect of HS may promote rather than attenuate IL-8 multimer formation. This may be why RANTES multimer formation was optimal after 2 days of incubation and IL-8 and ENA-78 multimer formation was optimal after 1 day of incubation, i.e. the multimers were more unstable and degraded after 2 days.

High MW HS-chemokine complexes were not observed following the addition of 0.1 mg/ml HS in the presence of $CuCl_2$ and H_2O_2. A possible explanation is that HS-

chemokine binding is electrostatic and disrupted in SDS-containing gels. Another explanation is that the addition of soluble HS is not a model of the endothelial bound HS that is present *in vivo*, but a model of the effect of soluble GAGs shed at sites of inflammation. IL-8 has been shown to bind to HS on endothelial cells, and shedding results in an IL-8 complex with HS-containing syndecan-1 ectodomains, a trimolecular complex with a mass of 140 KDa (Marshall *et al*, 2003). However it is possible that chemokines may not bind soluble HS in the absence of the core protein, and that soluble HS may be presented to chemokines in a form that causes the chemokine binding site to be inaccessible.

Given the observation that $CuCl_2$ and H_2O_2 induce multimerisation in the chemokines RANTES, IL-8 and ENA-78 it seems likely that other chemokines may multimerise in a similar way. The most likely chemokines to form multimers in the presence of $CuCl_2$ and H_2O_2 are those that contain tyrosine and histidine residues, in light of the previous reports that Cu induces multimer formation in Aβ and PrP via coordination with histidine and tyrosine residues. Such chemokines include the monocyte, T-cell and basophil chemoattractant, monocyte chemoattractant protein (MCP)-1 (contains 3 tyrosines and 1 histidine), the monocyte, pre-B cell and T-cell chemoattractant stromal cell-derived factor (SDF)-1 (contains 2 tyrosines and 2 histidines) and the neutrophil chemoattractants haemoinfiltrate CC chemokine (HCC)-1 (contains 6 tyrosines and 2 histidines) and macrophage inflammatory protein (MIP)-2β (contains 2 histidines). These are some examples but the list is not exhaustive.

Chapter 3

The contribution of dityrosines to RANTES, IL-8 and ENA-78 multimer formation under redox conditions

3. The contribution of dityrosines to RANTES, IL-8 and ENA-78 multimer formation under redox conditions

3.1. Introduction

3.1.1. Dityrosine formation

Dityrosine cross-links occur naturally in proteins isolated from the elastic ligaments of insects, the cell walls of *candida albicans* and the fertilisation envelope of the sea urchin egg (Andersen, 1963; Foerder & Shapiro, 1977; Smail *et al*, 1995). Vertebrate animal proteins known to contain dityrosine links include elastin, collagen and a storage form of the prothyroid hormone, thyroglobulin (Herzog *et al*, 1992; LaBella *et al*, 1967; LaBella *et al*, 1968). Hydroxyl radicals have been shown to induce dityrosine formation (Karam *et al*, 1984) and dityrosine may be a useful marker for assessing oxidative damage to proteins (Giulivi & Davies, 1993; Giulivi & Davies, 1994). Exposure of metmyoglobin or oxyhaemoglobin to H_2O_2 results in the conversion of tyrosyl radicals to dityrosine (Giulivi & Davies, 1993; Tew & Ortiz de Montellano, 1988).

The formation of dityrosine adducts *in vivo* is a sign of oxidative stress and a result of free radical reactions. The formation of dityrosine arises from the reaction of two tyrosine residues which form carbon centred radicals in the aromatic ring under redox conditions (figure 3.1). The formation of dityrosine results in the creation of a very stable, irreversible covalent bond (Smith *et al*, 2007).

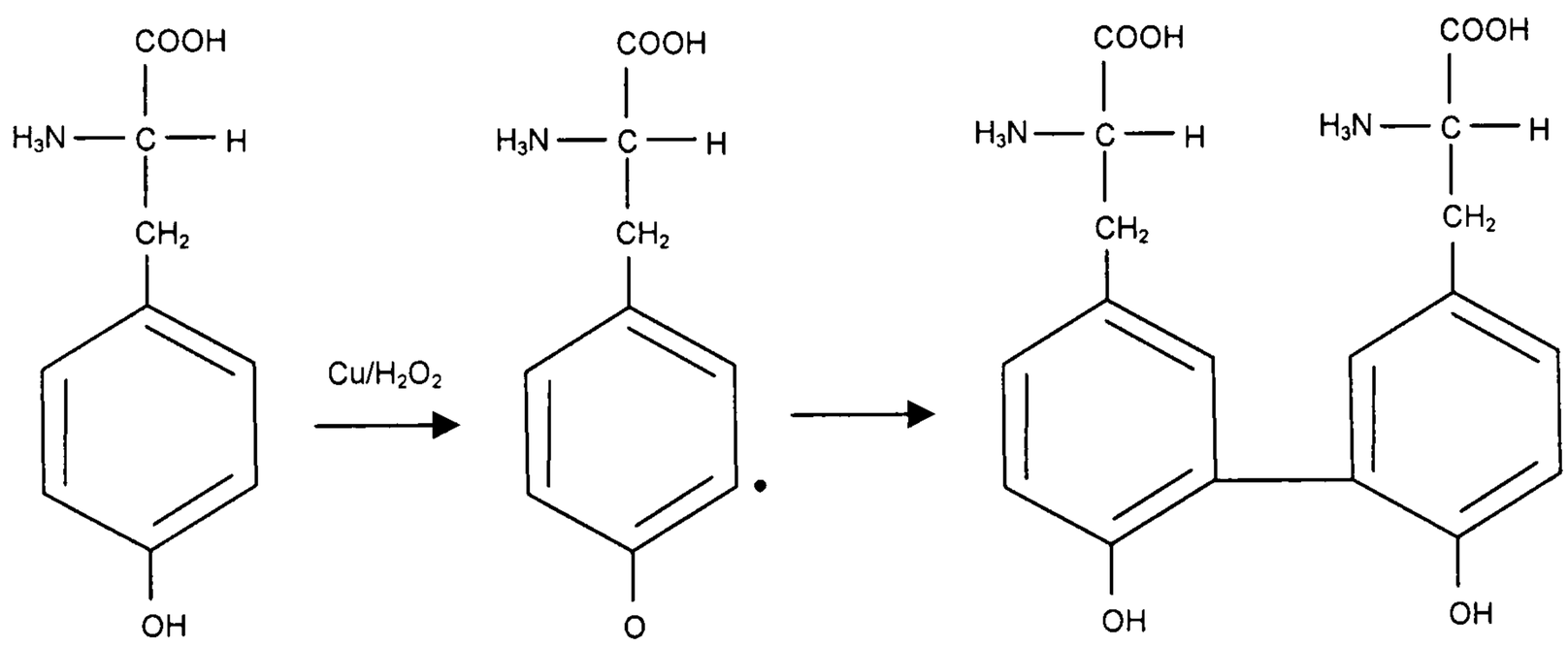

Figure 3.1. Dityrosine formation under oxidative conditions. Adapted from (Smith *et al*, 2007). The tyrosyl radical is formed under oxidative conditions in the presence of Cu and H_2O_2, and leads to stable dityrosine formation.

The addition of H_2O_2 strongly promotes Cu-induced dityrosine cross-linking of amyloid peptides Aβ1-28, Aβ1-40 and Aβ1-42 and it is suggested that dityrosine cross-linking is dependent on a Cu (II) mediated oxidative mechanism (Atwood *et al*, 2004). It is proposed that Cu (II) binds to histidine residues of Aβ, which acts as the reductant, reducing Cu (II) to Cu (I). Tyrosine residues in the vicinity of neighbouring histidine residues allows the extraction of an electron from Cu (I) to form a carbon centred radical which can then covalently link to another adjacent tyrosyl radical, forming a stable dityrosine cross-link (Malencik *et al*, 1996).

3.1.2. Detecting dityrosines by fluorimetry

Both isolated and protein bound dityrosines have characteristic emission spectra of 350-500 nm upon excitation at 284-315 nm (Andersen, 1964), and emission spectra of 460 and 538 nm upon excitation at 460 and 538 nm respectively (Ali *et al*, 2006; Ali *et al*, 2005). Excitation wavelengths of 280 and 320 nm have also been shown to be effective for detecting dityrosines with emission wavelengths in the 350-500 nm range at acidic and alkaline pH respectively, and an excitation wavelength of 301 nm has been shown to effective for detecting dityrosines in boric acid/sodium-borate buffers with emission spectra in the 350-500 nm range (Malencik *et al*, 1996). The emission spectra are quite distinct from those of tyrosine and trytophan which do not fluoresce at these wavelengths. With an excitation wavelength of 280 nm, tyrosine fluoresces at an emission of 300-305 nm (Malencik *et al*, 1996).

The oligomerisation of Aβ by incubation with Cu was found to induce a fluorescent signal characteristic of tyrosine cross-linking (Atwood *et al*, 2004). Using an excitation wavelength of 300 nm it has been shown that there is a linear increase in fluorescence at 400 nm with increasing dityrosine concentrations between 0-5 μM (Atwood *et al*, 2004). Dityrosines have been detected in Aβ-peptide oligomers using this method and in addition, dityrosine cross-linked oligomers of Aβ have been detected using excitation wavelengths of 355 and 485, with emission spectra of 460 and 538 nm respectively (Ali *et al*, 2006; Ali *et al*, 2005).

3.1.3. Detecting dityrosines using a specific monoclonal antibody

The specific monoclonal antibody IC3 has been used to detect protein bound dityrosine in isolated bovine lens proteins exposed to Cu plus H_2O_2 *in vitro* by enzyme-linked immunosorbent assay (ELISA) and in mouse atherosclerotic tissue using an

immunohistochemical method (Kato *et al*, 2001; Kato *et al*, 2000). IC3 preferentially recognises protein bound dityrosines compared to free dityrosines (Kato *et al*, 2000). IC3 was also successful in detecting Cu/H_2O_2 induced dityrosine cross-links formed in recombinant Aβ-peptide oligomers *in vitro* and analysed by Western blot (Atwood *et al*, 2004).

The IC3 antibody was used in the experiments described in this chapter, and was a kind gift from Yoji Kato, University of Hyogo, JAPAN.

3.1.4. Detecting dityrosines using liquid chromatography-mass spectroscopy/mass spectroscopy (LC-MS/MS)

Protein dityrosines have been well characterised by liquid chromatography-mass spectroscopy/mass spectroscopy (LC-MS/MS) analysis. The collision-induced dissociation of protonated native dityrosine (mass 361.2, contains 18 x carbon atoms) produced product ions of 315, 298, 283, 269, 254 and 237, detected by mass spectroscopy. Multiple-reaction monitoring (MRM) transitions of 361/315 and 361/237 were used to detect protein dityrosines in oxidised wheat-flour dough. The pairings of 361/315 and 361/237 among the product ions showed outstanding sensitivity and selectivity (Takasaki et al, 2005).

A stable isotopic standard was required to quantify dityrosines in wheat-flour dough by LC-MS/MS. Stable isotopic dityrosine (C^{13} x 18) was prepared from isotopic tyrosine (C^{13} x 9). The MRM transitions for the internal standard of C^{13} x 18 dityrosine were selected as 379.2/332.1 and 379.2/253.1, which corresponds respectively to 361.2/315.1 and 361.2/237.1 for native (C^{12} x 18) dityrosine (Takasaki et al, 2005).

3.1.5. Other metals

It may be possible for other metals to substitute for Cu in free radical generation via the mechanism discussed in Chapter 2, Section 2.6. Lead, cadmium, silver, mercury, copper and nickel have all been shown to stimulate lipid peroxidation and tissue damage through redox mechanisms (Horton & Fairhurst, 1987).

Metals with a variety of oxidative properties were compared with Cu using LC-MS/MS, namely, iron (Fe), zinc (Zn), mercury (Hg) and nickel (Ni), all of which are found in the

d-block of the periodic table, often referred to as the transition metals. Unlike the metals of group 1 and group 2, ions of the transition elements can exist in multiple stable oxidation states. They are capable of losing *d* electrons without a high energetic penalty. A transition metal is defined as an element whose atom has an incomplete d sub-shell, or which can give rise to cations with an incomplete d sub-shell. Although Cu, Fe and Ni are true transition metals, Zn and Hg could be excluded from this category as they have a complete d sub-shell configuration (d^{10}). Whilst Zn exists only in one oxidation state (oxidation state 2), Hg can exist in oxidation states 1 and 2, but both elements retain the d^{10} configuration.

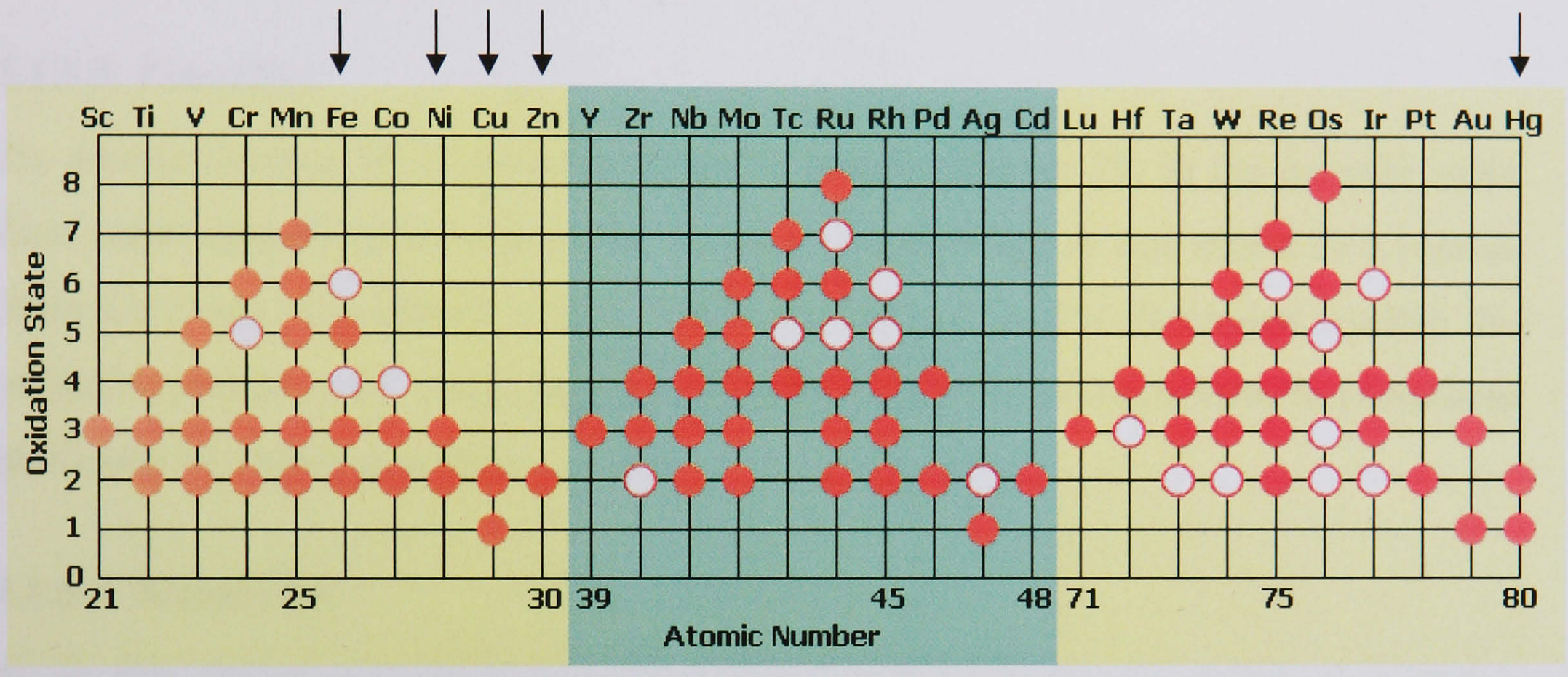

Table 3.1. Some of the oxidation states found in compounds of the transition-metal elements. A solid circle represents a common oxidation state, and a ring represents a less common (less energetically favourable) oxidation state (Wikipedia 2008, Transition metal, retrieved on Dec 19th, 2008). Arrows indicate the metals used in the experiments described in this chapter for comparison with Cu.

3.1.5.1. Iron (Fe)

Fe exists in five possible oxidation states. Fe can exist as Fe^{2+}, Fe^{3+}, Fe^{4+} Fe^{5+} and Fe^{6+} although oxidation states 4 and 6 are rare. It is well established that Fe generates free radicals, and plays a significant part in redox cycling. Fe (II) has been shown to react with H_2O_2 or molecular oxygen itself to generate the superoxide ion, and hydroxyl radical. The iron-dependent decomposition of H_2O_2 was originally postulated by Fenton, and has become known as the Fenton reaction (Imlay *et al*, 1988).

The Fenton reaction

$$Fe^{2+} + H_2O_2 \longrightarrow Fe^{3+} + OH^- + OH^{\cdot}$$

Because Fe is fundamental to redox cycling and peroxidation, and because of its ability to exist in many oxidation states, it was important to investigate its effect on dityrosine formation in RANTES.

3.1.5.2. Mercury (Hg)

Hg has very similar oxidative properties to Cu. Hg, like Cu, exists in oxidation states 1 and 2, and is one of 2 elements to do so. The other is silver (Ag), which can exist in oxidation states 1 and 2. However oxidation state 2 in Ag is uncommon and so Hg was used in preference, to equate with Cu.

3.1.5.3. Zinc (Zn)

Zn, atomic number 30, is found next to Cu, atomic number 29, in the periodic table. Zinc exists almost exclusively in the +2 state and therefore it was useful as a control. Since Cu exists in oxidation states 1 and 2, Zn (II) was used to determine whether this oxidative property of Cu was paramount for the formation of dityrosines in chemokine multimers by means of a redox system.

3.1.5.4. Nickel (Ni)

Ni is also found next to Cu in the periodic table, but having different oxidative properties to Cu, existing predominantly in oxidation states 2 (Ni II) and 3 (Ni III). Interestingly, Ni (II) is known to induce oxidative stress. Studies have indicated that reactive oxygen species (ROS) are generated as one of the main mechanisms in the carcinogenicity and cytotoxicity of Ni (II) exposure (Jia & Chen, 2008). Nickel induced oxidative stress has also been shown to result in the activation of lymphocyte death signalling pathways (M'Bemba-Meka *et al*, 2005). Considering the reported generation of ROS caused by nickel, and similarities of nickel and copper, it was speculated that nickel might generate free radicals and participate in redox cycling

3.1.6. Chemokine multimerisation

Cu plus H_2O_2 were shown to induce chemokine multimerisation in RANTES, IL-8 and ENA-78 (Chapter 2). A redox mechanism involving dityrosine cross-links was suggested as a potential mechanism for chemokine multimer formation. RANTES has five tyrosine residues, IL-8 has one and ENA-78 none and therefore it was expected that dityrosines should be detectable in RANTES and possibly IL-8 multimers but not in ENA-78 multimers.

The contribution of dityrosine cross-links to multimer formation was investigated using fluorimetry, Western blotting and liquid chromatography mass spectroscopy/mass spectroscopy (LCMS/MS).

3.2. Materials

Bovine serum albumin, copper chloride ($CuCl_2$), hydrogen peroxide (H_2O_2, 30 % (v/v)), $CuCl_2$, $NiCl_2$, $HgCl_2$, $FeCl_3$, $ZnCl_2$ sodium dihydrogen phosphate, disodium hydrogen phosphate, heparan sulphate (HS) from pig mucosa and glutaraldehyde were obtained from Sigma-Aldrich Inc., Poole, Dorset, UK. Phosphate buffered saline (PBS) (-Ca^{2+}/Mg^{2+}), guanidine hydrochloride (G-HCl) and 2-mercaptoethanol (2-ME) were obtained from Invitrogen Ltd, Paisely, UK). A Far UV quartz 10 x 4 mm light path, 1.5 ml fluorimetry cuvette was obtained from Jencons Ltd, East Grinstead, West Sussex, UK. Recombinant human-RANTES, human IL-8 and human ENA-78 were obtained from Peprotech EC, London, UK.

Polyacrylamide mini-gels were cast using the Bio-Rad Protean II system and markers and reagents for electrophoresis were obtained and prepared as previously described in chapter 2. Primary 1C3 antibody from ascites was obtained as a gift from Yoji Kato, University of Hyogo, Japan. Secondary biotinylated rabbit anti-mouse $(Fab)_2$ antibodies and biotinylated primary rabbit anti-human RANTES antibodies were obtained from Peprotech EC, London, UK. Streptavidin-biotinylated horseradish peroxidase complex (StreptABC) was obtained from Dako UK Ltd, Ely, Cambridgeshire, UK. A commercial enhanced chemiluminescence (ECL) kit, SuperSignal, was obtained from Pierce Biotechnology Inc., Rockford, IL 61105, USA. Tween-20, PBS (-Ca^{2+}/Mg^{2+}) and Super RX Fuji medical X-Ray film were obtained from Fisher Scientific, Loughborough, Leicestershire, UK.

Dityrosine was a gift from Yoji Kato, University of Hyogo, JAPAN and was used to make the dityrosine-BSA standard for Western blotting. Normal tyrosine and stable isotopic tyrosine, horseradish peroxidise (HRP), borate buffer, trifluoroacetic acid (TFA), hydrochloric acid (HCl), methanol, L-methionine, ammonium acetate and acetic acid were used by Yoji Kato in the analysis of dityrosine by LCMS/MS.

3.3. Methods

3.3.1. Conjugation of dityrosine and BSA

A dityrosine-BSA standard was prepared as a positive control for Western blot analyses of dityrosine by dissolving dityrosine (1.7 mg) and BSA (2.4 mg) in 0.85 ml of 0.1 M phosphate buffer (pH 7.4). Glutaraldehyde solution (20 % (v/v), 200 µl) was added to the vessel, little by little with stirring (final concentration 3.8 % (v/v)). The reaction continued overnight with stirring at room temperature. The sample was then dialyzed against 500 ml PBS ($-Ca^{2+}/Mg^{2+}$) at 4 °C for 2 days changing the buffer on day 2. The concentration of albumin was finally adjusted to 1 mg/ml by diluting to 2.4 ml.

3.3.2. Preparation of samples for fluorimetry

Human recombinant RANTES was incubated for 2 days in PBS ($-Ca^{2+}/Mg^{2+}$) at 2.5 x 10^{-6} M (20 µg/ml) with 50 µM $CuCl_2$ plus 200 µM H_2O_2 in a total volume of 400 µl to allow the formation of cross-links in multimers.

3.3.3. Analysis of dityrosines by fluorimetry

40 µl of dityrosine-BSA standard (1 mg/ml) was diluted to 40 µg/ml in 1 ml of PBS ($-Ca^{2+}/Mg^{2+}$, Fisher UK, pH 7.4). Post-incubation samples containing RANTES (400 µl) were diluted to 10 µg/ml by the addition of 400 µl PBS ($-Ca^{2+}/Mg^{2+}$) and analysed at 37 ^{o}C using a Varian fluorescence spectrophotometer and Cary Eclipse Software. Analysis was performed using a Hellma far UV quartz 10 x 4 mm light path, 1.5 ml cuvette. The fluorescence spectra were scanned at different excitation wavelengths (table 3.2).

The following excitation wavelengths were used to detect dityrosines:

Excitation λ / nm	**Expected emission λ / nm**
280	Detection of singular tyrosine at 300-305
284	400
300	400 at pH 7.4
301	377-378 at high pH (pH 9)
315, 320	400 at high pH (pH 9)
325	407
355	460
485	538

Table 3.2. Excitation wavelengths suitable for the detection of dityrosines and the expected emission wavelengths (Ali *et al*, 2006; Atwood *et al*, 2004; Kato *et al*, 2000; Malencik *et al*, 1996).

3.3.4. Sample preparation for SDS-PAGE and Western blotting

In order to detect dityrosines by Western blotting, chemokines were incubated at higher concentrations than those used for the detection of the chemokines per se. RANTES, IL-8 and ENA-78 (2.5×10^{-6} M (20 μg/ml)) were incubated with $CuCl_2$ (1.25 - 100 μM), H_2O_2 (0.5 - 400μM) and HS (0.1 mg/ml) in PBS (-Ca^{2+}/Mg^{2+}), final volume 200 μl. RANTES was incubated for 2 days at 37 °C. IL-8 and ENA-78 were incubated for 1 day at 37 °C, since a 1 day incubation was found to be optimum for multimer formation. Incubated samples were frozen at -80 °C, freeze dried, reconstituted to 20 μl in 1x sample buffer (prepared as described in Chapter 2) and 15 μl of each sample analysed by SDS polyacrylamide gel electrophoresis and Western blotting as described in Chapter 2, Sections 2.3.4 and 2.3.5.

3.3.5. Guanidine hydrochloride treatment of samples

In order to establish the stability and covalent nature of dityrosine cross-links an equal volume of guanidine hydrochloride (G-HCl, 12 M) was added to samples (final concentration 6 M) following 1 or 2 day incubation at 37 °C, and removed by ethanol precipitation of proteins as previously described in Chapter 2, section 2.3.3.

3.3.6. 2-mercaptoethanol treatment of samples

Samples were reduced with 2-mercaptoethanol (2-ME) to investigate the presence of disulphide links. Following freeze drying of samples the lyophilised protein was re-constituted in 20 μl 1 x sample buffer containing 5 % (v/v) 2-mercaptoethanol (4.8 ml UHQ water, 0.4 ml 2-mercaptoethanol (2-ME), 0.8 ml glycerol, 1.6 ml 10 % (w/v) sodium dodecyl sulphate (SDS), 1 mg bromophenol blue) and boiled at 95 °C for 5 minutes. Once cooled, samples were loaded onto a 14 % polyacrylamide gel (15 μl per well).

3.3.7. SDS-PAGE and Western blotting

Proteins were separated on 14 % (w/v) polyacrylamide gels and transferred to 0.45 μm nitrocellulose as previously described in Chapter 2, sections 2.3.4 and 2.3.5.

3.3.8. Blocking Western blots

Following transfer to nitrocellulose membrane, Western blots were immersed in blocking buffer (PBS (phosphate buffered saline (-Ca/Mg)) / 2 % v/v Tween-20 at room

temperature) overnight prior to staining for RANTES as previously described in Chapter 2, section 2.3.5.

3.3.9. Dityrosine staining on Western blots

The membranes were first washed three times for 10 minutes each in 1x PBS / 0.05 % (v/v) Tween-20, and then incubated with primary antibody (mouse monoclonal anti-dityrosine (1C3) kept at -80 °C) at a working concentration of 1 μg/ml, 5 ml per blot in 5 % (v/v) rabbit serum for 90 minutes. Blots were again washed three times for 10 minutes each in PBS/0.05 % (v/v) Tween-20 and incubated for 60 minutes with biotinylated rabbit polyclonal anti-mouse $(Fab)_2$ antibody (Dako, UK) kept at 4 °C diluted 1:2000 v/v in PBS (-Ca/Mg) / 2 % Tween-20 (2.5 μl/5 ml per blot). The membranes were washed as before, 3 times for 10 minutes, and then incubated with a 1:20,000 (v/v) dilution (1 μl of each of tubes A and B in 10 ml) of a streptavidin-biotinylated horseradish peroxidase complex (StreptABC, DAKO) for 45 minutes at room temperature. Membranes were washed as before, 5 times for 10 minutes each and the blots developed using an ECL kit (Pierce) and placed against X-Ray film to visualise results. 2.5 ml of each of the developer and enhancer were mixed together (5 ml per blot).

3.3.10. Preparation of internal standard (IS) for liquid chromatography mass spectroscopy/mass spectroscopy (LCMS/MS)

The internal standard (IS) was prepared by Yoji Kato. As an IS, stable isotopic DiY (containing 18 x C^{13} atoms [$^{13}C_{18}$]) was prepared from stable isotopic tyrosine (contains 9 x C^{13} atoms [$^{13}C_9$]) by treatment with horseradish peroxidase (HRP) and H_2O_2. The IS had a different molecular weight than that of normal dityrosine (the IS parent ion had MW 379.2 whereas normal dityrosines have a parent ion MW 361.2). Therefore the IS and dityrosine were separately quantified.

L-tyrosine (5 mg) was incubated for 1 hr with 75 μg of horseradish peroxidase (HRP) in the presence of 5 μl of 30 % (v/v) H_2O_2 in 5 ml of 0.1 M borate buffer (pH 9.0). The mixture was acidified by the addition of 500 μl of 6 N HCl and 100 μl of trifluoroacetic acid (TFA) and then applied to a solid phase extraction (SPE) column (Supelco Spelclean ENVI-18, 500 mg solid). The column was then washed with 2 ml of 0.1 % (v/v) TFA, and the sample was eluted with 1 ml of 0.1 % (v/v) TFA/CH_3OH (1:3). The eluate was concentrated and then further purified by reverse-phase HPLC. The reaction

was terminated by the addition of L-methionine (final concentration 3 mM). The crude reaction mixture was acidified by the addition of a bolus of TFA solution. The reaction mixture was then applied to an SPE ENVI-18 column, which was washed with 2 ml of 0.1 % (v/v) TFA, and the sample was then eluted with 2 ml of methanol.

3.3.11. Sample preparation for LCMS/MS

Recombinant RANTES (Peprotech, UK) was incubated in triplicate for 2 days at 37 °C at a final concentration of 2.5 x 10^{-6}M (0.02 mg/ml) in the presence and absence of a final concentration of 50 μM $CuCl_2$, $NiCl_2$, $HgCl_2$, $FeCl_3$ or $ZnCl_2$ and in the presence and absence of final concentrations of either 25 or 200 μM H_2O_2. The final volume was 80 μl in 1x D-PBS (-Ca^{2+}/Mg^{2+}). Following 2 day incubation, samples were frozen at – 80 °C for 3 hours and freeze dried overnight. Freeze-dried samples were shipped to Hyogo University, JAPAN.

Each lyophilized sample was dissolved in 80 μl of water, and 40 μl was hydrolysed at 105 °C for 24 hours. Following hydrolysis the sample was dried and dissolved in 50 μl of 2 mM ammonium acetate in H_2O. For dityrosine analysis, 0.4 μl of IS was added to 40 μl of the sample. The analysis of dityrosines was done using 10 μl in duplicate. For tyrosine analysis, 5 μl was taken and diluted x 20, and 1 μl of IS was added to the 100 μl of solution for tyrosine analysis.

To identify and confirm that the peak is dityrosine, four traces were used for the analysis: two native dityrosine and two IS fragments. The IS allows quantification of the results.

3.3.12. LCMS/MS analysis for tyrosine and dityrosine

The LCMS/MS analysis was performed by Yoji Kato. Each sample was analysed using 10 μl in duplicate using an electrospray-ionisation quadrupole tandem mass spectrometer (API-3000, Applied Biosystems Co.) connected to an Agilent 1100 HPLC system. Data were calculated from the averages of two serial analyses of one sample. For the DiY and tyrosine analyses, HPLC was done by gradient systems using solvent A (0.1 % acetic acid) and solvent B (acetonitrile). The separation was performed using a reverse phase octadecyl silane (ODS-HG-3) high performance liquid chromatography (HPLC) column (2 x 50 mm).The gradient program was as follows: 0 min (A100 %), 2 min (A100 %), 7 min (A50 %), 7.1 min (A100 %), 15 min (A100 %). The positive

mode was used for the electrospray ionisation (ESI). To reduce possible contamination of the ion source, the flow was separated by a Valco switching valve using the following program: 0 min (waste), 2 min (mass), 7 min (waste).

The spectrometer had three serial quadrapoles. Using the first quadrapole, the parent ion 361 was formed by ionisation of dityrosine. The protonated dityrosine was fragmented by N_2 gas at the second quadrapole in the mass spectrometer. (This process is known as collision-induced dissociation or collision-induced fragmentation). The fragment ions were detected by the third quadrapole in the mass spectrometer.

Native dityrosine (DiY) [C^{12} x 18] has a MW of 360 (figure 3.2). To detect dityrosines by LCMS/MS, dityrosines were positively ionised and protonated (MW 360 --> 361, figure 3.2). The protonated parent ion, mass 361, can theoretically be detected by a mass spectrometer. However, many ionised molecules have a mass of 361 as the parent or fragment ion, therefore simple scanning of 361 will detect high background noise. To resolve this problem, multiple reaction monitoring (MRM) transitions were used, which involves scanning for both the parent ion and fragments of known mass simultaneously.

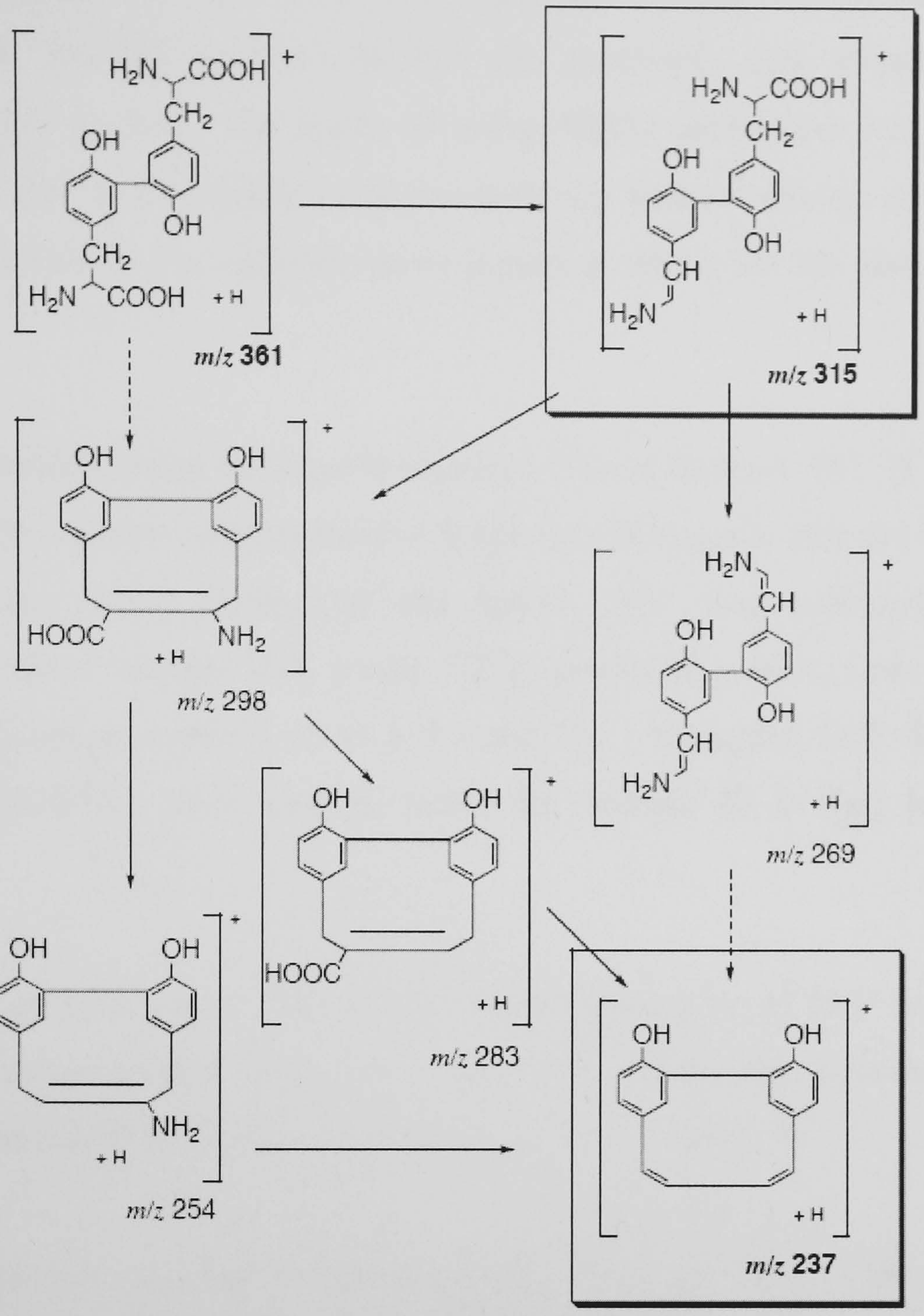

Figure 3.2. Proposed mechanism for Collision-Induced Dissociation of Dityrosine. These are the fragments of protonated dityrosine MW 361. The parent ion 361 is formed by ionisation of dityrosine. The observed protonated product ions were at m/z 315, 298, 283, 269, 254 and 237. The protonated dityrosine can be fragmented by N_2 gas in the mass spectrometer to form fragments of known size. Boxes indicate the selected MRM transitions (Takasaki *et al*, 2005).

Trace amounts of native DiY were analysed by LCMS/MS using stable isotopic methods. Several fragments, which occurred owing to the collision-induced fragmentation of native DiY, were observed. Of these, the combination of ions 361/237 and 361/315 (for native DiY) were similar and had good sensitivity.

Both fragments (MW 315 (de-carboxylated) and MW 237 (unknown structure)) were previously shown to be very suitable as MRMs for dityrosine (Takasaki *et al*, 2005) and both fragments had a good yield. Scanning for these two fragments (315 and 237) as well as the parent ion (MW 361) to detect dityrosines lowers the background compared

to a parent ion only scan at MW 361. For example, molecules with the MRM combination of MW 361/237 or MW 361/315 are extremely less abundant than molecules of MW 361 as ions. The result of using MRM transitions was that the background became very low resulting in high sensitivity and selectivity. The use of two MRMs (315 and 237) in one molecule gave greater accuracy for the identification of dityrosines.

Native DiY was quantified using an internal standard (IS) of isotopic DiY [C^{13} x 18]. The parent ion and subsequent collision induced fragments of isotopic DiY are of higher molecular weight than those formed by the native DiY. The collision-induced dissociation of protonated isotopic DiY (mass 379.2) produced product ions of 332.1 and 253.1 which correspond respectively to 315.1 and 237.1 for native DiY. MRMs of 379.2/332.1 and 379.2/253.1 were used to detect the isotopic IS as they had good sensitivity.

The detection limit of DiY was 1 nM and the calibration curve of DiY was linear (R=0.999) over a concentration range of 1–300 nM. Using the selected MRM transitions, the DiY in RANTES samples was estimated by LC/MS/MS.

Thus, the four multiple reaction monitoring (MRM) transitions used for the measurement of DiY were as follows: 379.2/332.1 (internal standard, [$^{13}C_{18}$] DiY-1), 379.2/253.1 (internal standard, [$^{13}C_{18}$] DiY-2), 361.2/315.1 (native [$^{12}C_{18}$] DiY-1), and 361.2/237.1 (native [$^{12}C_{18}$] DiY-2). The two MRM combinations for one molecule showed a similar sensitivity. The use of two MRMs on one molecule is meaningful for the identification of DiY. To estimate tyrosine [$^{12}C_9$], the analyte was diluted 100-fold by a solution of 2 mM ammonium formate with an additional IS (500 nM [$^{13}C_9$] tyrosine) and then analysed separately. Two MRMs 182.2/136.1 ([$^{12}C_9$] tyrosine) and 188.1/142.1 ([$^{13}C_9$] tyrosine) were used for the analysis. To check for artifact formation of DiY during sample preparation, the MRM of the [$^{13}C_9$] tyrosine-derived DiY [$^{13}C_{18}$] was also determined regularly. To avoid a decrease in the signal/noise ratio, the MRM scan program for the [$^{13}C_9$] tyrosine-derived DiY was omitted in routine analyses.

Importantly, the scanning of an MRM transition takes only about 100 msec. So many MRM combinations (and therefore many compounds) can be analysed in a single

experiment, almost simultaneously. The first MRM scans during the first 100 msec and then next MRM scans in the next 100 msec and this process is repeated.

3.4. Statistical analysis

Data were compared with a 1 or 2-way ANOVA followed by either a Dunnet's or Tukey's *post-hoc* test where $p < 0.05$ was the minimum accepted level of significance.

3.5. Results

3.5.1. Fluorimetry

The dityrosine-BSA standard was analysed by fluorimetry as a positive control. Of the excitation wavelengths used, 300 nm was found to give the best sensitivity for dityrosines in the dityrosine-BSA standard with an emission peak in the 390-420 nm range. This was similar to the findings of Atwood, *et al.* and Kato, *et al.* (Atwood *et al*, 2004; Kato *et al*, 2000). Therefore both the dityrosine standard and RANTES samples were analysed using an excitation wavelength of 300 nm.

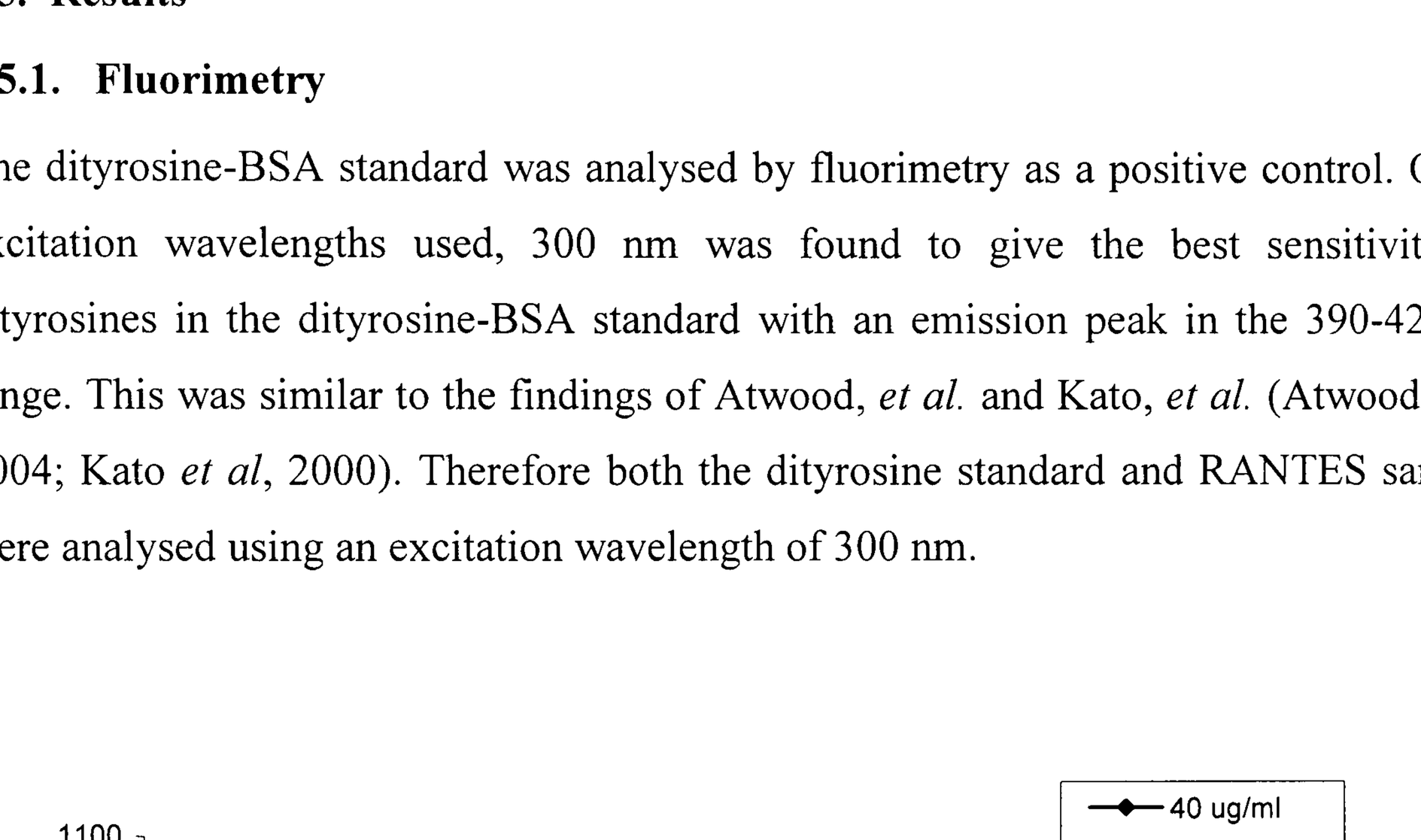

Figure 3.3. Emission spectra of dityrosine standard in PBS (0.625 – 40 μg/ml), analysed by fluorimetry at an excitation wavelength of 300 nm. Representative of two independent experiments. a.u. = arbitrary units.

The emission peak at 410 nm is characteristic of dityrosines (Atwood *et al*, 2004; Kato *et al*, 2000; Takasaki *et al*, 2005) and was detectable in the dityrosine standard at a limit of 1.25-2.5 μg/ml BSA. Recombinant human RANTES (Peprotech, UK) was incubated for 2 days in PBS ($-Ca^{2+}/Mg^{2+}$) at 2.5 x 10^{-6} M (20 μg/ml) with 50 μM $CuCl_2$ plus 200 μM H_2O_2 in a total volume of 400 μl, to generate multimers. Following 2 day incubation, the samples were diluted to 10 μg/ml in 800 μl PBS ($-Ca^{2+}/Mg^{2+}$) and samples were analysed by fluorimetry at an excitation wavelength of 300 nm.

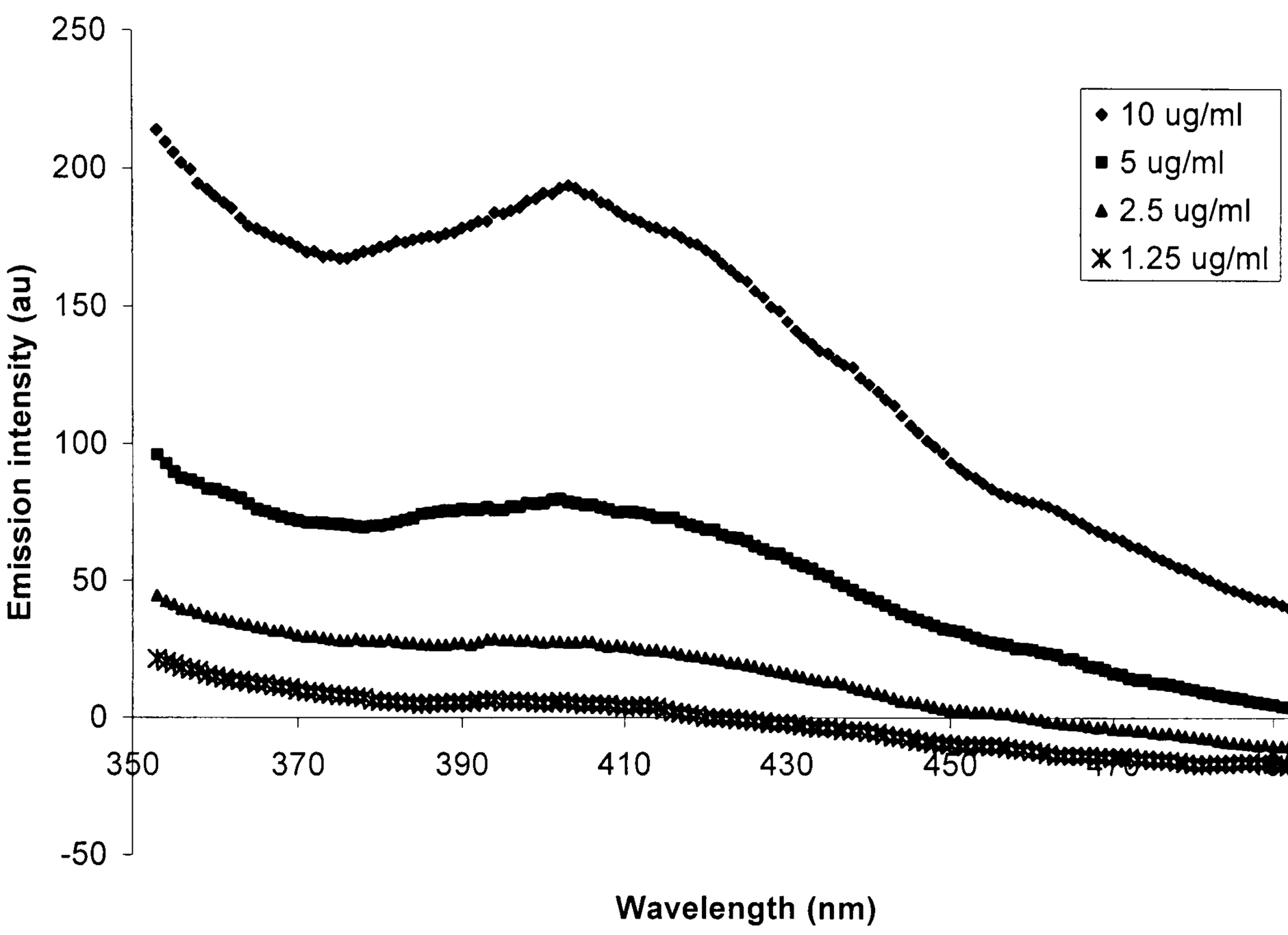

Figure 3.4. Fluorescence spectra for dityrosines detected in RANTES multimers. RANTES was incubated for 2 days in PBS at 2.5 x 10^{-6} M and 37 °C with $CuCl_2$ (50 μM) plus H_2O_2 (200 μM), diluted to 1.56 x 10^{-7} M - 1.25 x 10^{-6} M (1.25 - 10 μg/ml) following incubation and analysed by fluorimetry at an excitation wavelength of 300 nm.

The emission spectra observed at 404 nm is characteristic to dityrosines, indicating that dityrosines were present in RANTES multimers. The detection limit for dityrosines was 1.25 μg/ml. The concentration of dityrosines in RANTES multimers as detected by LCMS/MS was subsequently found to be small (Section 3.5.2.3). The peak at 404 nm was not detected in RANTES incubated for 2 days in PBS ($-Ca^{2+}/Mg^{2+}$) at 2.5 x 10^{-6} M (20 μg/ml) in the absence of $CuCl_2$ plus H_2O_2 (data not shown). This suggests that dityrosine cross-links are present in RANTES multimers formed in the presence of Cu/H_2O_2.

However, at the concentrations used and in the absence of $CuCl_2$ and H_2O_2, RANTES was dimeric (Chapter 2, Section 2.5.1), and it would be expected that some dityrosines would be detected in the dimer. It was suspected that in the absence of multimers, dityrosines in the RANTES dimer may be at very low concentrations that are not detectable by fluorimetry and therefore RANTES was analysed by Western blot and stained with the specific mouse monoclonal antibody IC3 to detect dityrosines.

3.5.2. SDS-PAGE and Western blotting

In order to determine the molecular weight of the RANTES multimers containing dityrosines, RANTES multimers were analysed using SDS-PAGE and Western blots were stained with the specific dityrosine antibody, IC3, a gift from Yoji Kato, University of Hyogo, JAPAN.

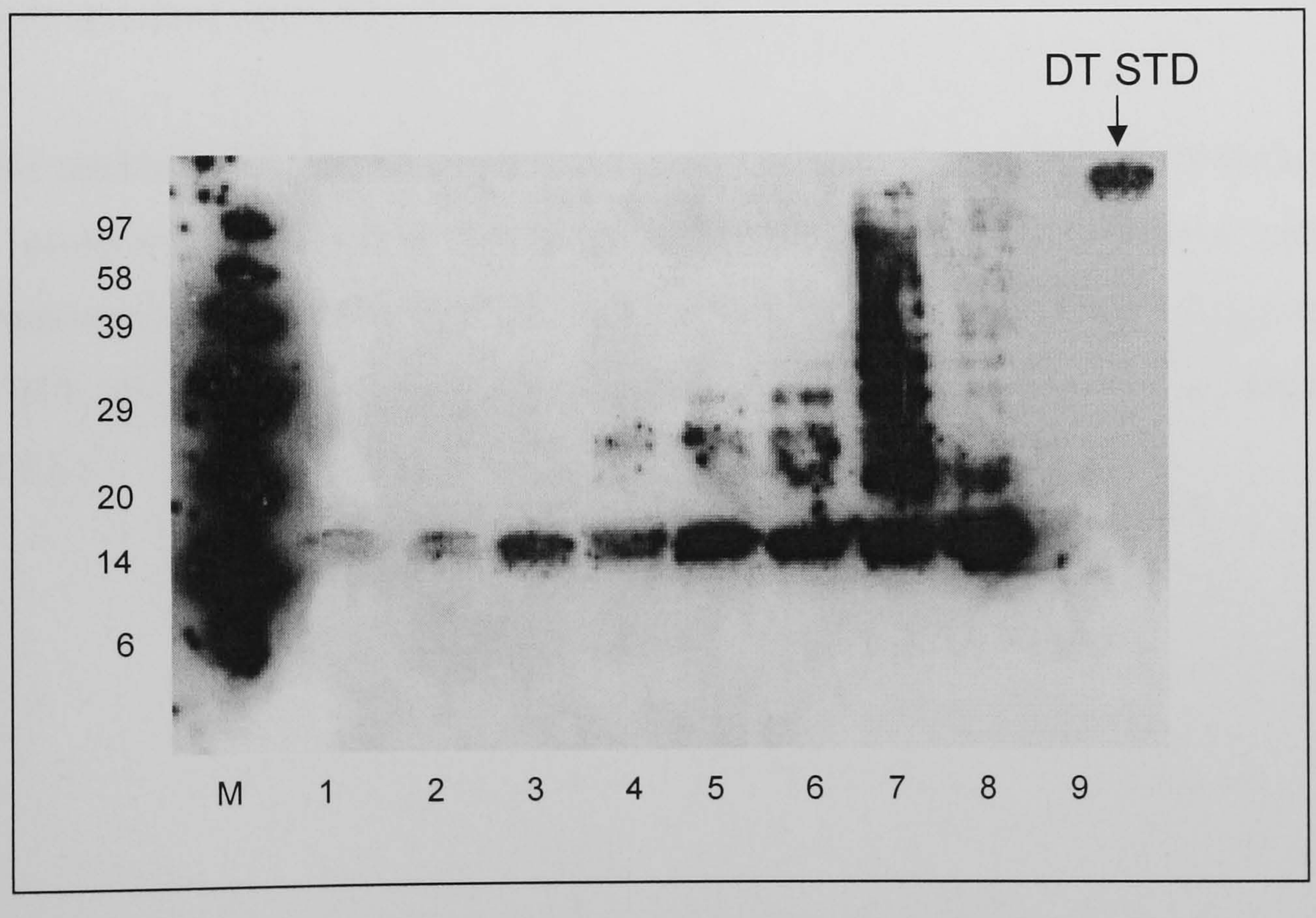

Figure 3.5. Dityrosines in RANTES multimers. RANTES (2.5×10^{-6} M) was incubated with copper (50 μM) alone, and copper (50 μM) plus 5 – 400 μM H_2O_2 for 2 days at 37 °C, analysed by SDS-PAGE on a 14 % polyacrylamide gel and Western blots were stained for dityrosines. M: molecular weight markers. Dityrosine standard (dityrosine cross-linked BSA) in lane 9. Lane 1: RANTES only, lane 2: RANTES + 50 μM $CuCl_2$, lane 3: RANTES + 50 μM $CuCl_2$ + 5 μM H_2O_2, lane 4: RANTES + 50 μM $CuCl_2$ + 25 μM H_2O_2, lane 5: RANTES + 50 μM $CuCl_2$ + 50 μM H_2O_2, lane 6: RANTES + 50 μM $CuCl_2$ + 100 μM H_2O_2, lane 7: RANTES + 50 μM $CuCl_2$ + 200 μM H_2O_2 and lane 8: RANTES + 50 μM $CuCl_2$ + 400 μM H_2O_2. Representative of two independent experiments, showing similar results.

Positive staining for dityrosines in RANTES multimers indicates the involvement of dityrosine cross-links in multimerisation of the chemokine, RANTES. The IC3 antibody stained RANTES dimers (16 KDa) in RANTES incubated alone (figure 3.5, lane 1) and in the presence of 50 μM $CuCl_2$ (lane 2). In the presence of 50 μM $CuCl_2$ plus 5 – 400 μM H_2O_2 the dimer appeared more strongly stained (lanes 3 – 8), with the maximum dityrosines detected in 16 KDa RANTES at 400 μM H_2O_2 (lane 8). Dityrosines were detected in higher order multimers of RANTES (trimer (24 KDa) and above) in the presence of 50 μM $CuCl_2$ plus 25 – 200 μM H_2O_2 (lanes 4 – 8), and maximum dityrosine formation was seen at 50 μM $CuCl_2$ plus 200 μM H_2O_2 (lane 7, up to approximately 100 KDa). RANTES tetramers (32 KDa) were detected in lanes 4 -7 (50 μM $CuCl_2$ plus 25 – 200 μM H_2O_2). H_2O_2 in the presence of 50 μM $CuCl_2$ promoted multimerisation in a dose dependent manner in lanes 4 – 7. However, at 50 μM $CuCl_2$ plus 400 μM H_2O_2, the higher order multimers were depleted (lane 8). Dityrosines were not detected in monomeric RANTES (8 KDa). The BSA-dityrosine standard was used as a positive control (lane 9), at a concentration of 25 μg/ml and 10 μl / lane. The dityrosine standard stained positively for dityrosines.

Since the multimers appear depleted by the high concentration (400 μM) of H_2O_2 in lane 8, the protective effect of HS, a free radical scavenger, on dityrosine cross-link formation was determined. RANTES was incubated as before, but in the presence of 0.1 mg/ml HS, analysed by SDS-PAGE, and Western blots were stained for dityrosines (figure 3.6).

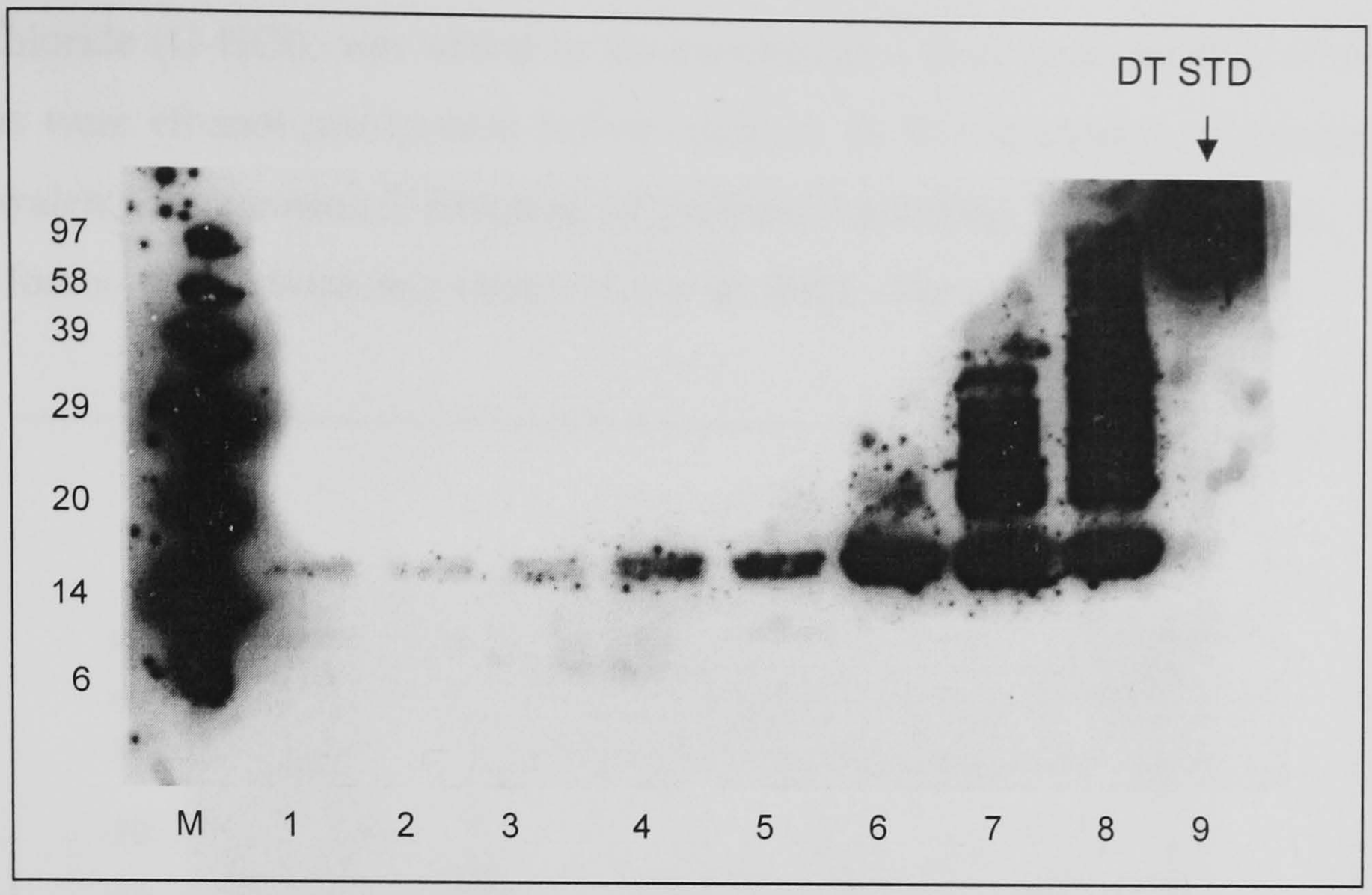

Figure 3.6. The protective effect of HS on dityrosines in RANTES. RANTES (2.5×10^{-6} M) was incubated with copper (50 μM) alone, and copper (50 μM) plus 5 – 400 μM H_2O_2 for 2 days at 37 °C in the presence of HS (0.1 mg/ml), analysed by SDS-PAGE on a 14 % polyacrylamide gel and Western blots were stained for dityrosines. M: molecular weight markers. Dityrosine standard (dityrosine cross-linked BSA) in lane 9. Lane 1: RANTES +HS, lane 2: RANTES + HS + 50 μM $CuCl_2$, lane 3: RANTES + HS + 50 μM $CuCl_2$ + 5 μM H_2O_2, lane 4: RANTES + HS + 50 μM $CuCl_2$ + 25 μM H_2O_2, lane 5: RANTES + HS + 50 μM $CuCl_2$ + 50 μM H_2O_2, lane 6: RANTES + HS + 50 μM $CuCl_2$ + 100 μM H_2O_2, lane 7: RANTES + HS + 50 μM $CuCl_2$ + 200 μM H_2O_2 and lane 8: RANTES + HS + 50 μM $CuCl_2$ + 400 μM H_2O_2. Representative of two independent experiments.

Positive staining for dityrosines in RANTES dimers and higher order complexes again indicates the involvement of dityrosine cross-links in RANTES multimer formation. However, higher concentrations of H_2O_2 were required to see this effect in the presence of HS (figure 3.6) compared to its absence (figure 3.5). In the absence of HS (figure 3.5), dityrosine was observed to form at 25 μM H_2O_2 (lane 4) and maximum dityrosine formation was seen at 50 μM $CuCl_2$ plus 200 μM H_2O_2 (lane 7). However, in the presence of 0.1 mg/ml HS, dityrosine formed at concentrations of H_2O_2 greater than 100 μM and the maximum effect was seen at 400 μM H_2O_2 (figure 3.6, lane 8). Higher order multimers were not depleted at the highest (400 μM) concentration of H_2O_2 in the presence of HS. The RANTES multimers can withstand higher concentrations of H_2O_2 (up to 400 μM) indicating that HS may be scavenging free radicals (figure 3.6). Again, the dityrosine standard stained positively for dityrosines (lane 9).

In order to investigate whether dityrosine cross-links were covalent links, RANTES was incubated for 2 days at 37 °C in the presence and absence of 50 μM $CuCl_2$, 25 μM H_2O_2 and 0.1 mg/ml HS, and following incubation, the chaotropic agent, guanidine

hydrochloride (G-HCl), was added to the samples at a final concentration of 6 M and proteins were ethanol precipitated before analysis. G-HCl is capable of disrupting the non-covalent 3-dimensional structure of proteins, including hydrogen bonds, van der Waals forces and hydrophobic effects (Lu *et al*, 2001; Neet & Timm, 1994).

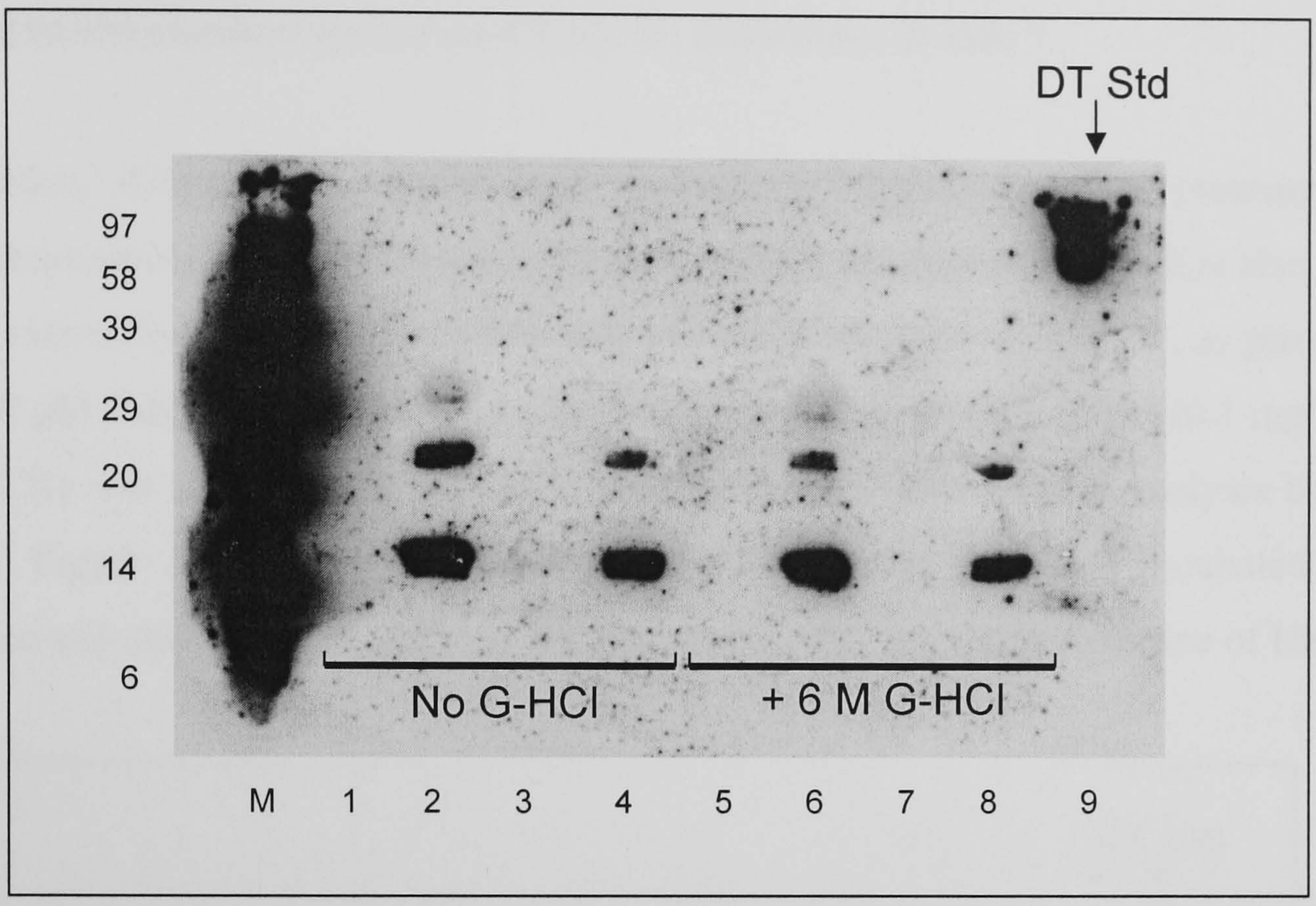

Figure 3.7. The stability of dityrosines to G-HCl. RANTES (2.5×10^{-6} M) was incubated in the presence and absence of copper (50 μM), ± H_2O_2 (25 μM) and ± HS (0.1 mg/ml), for 2 days at 37 °C. Samples were treated with 6 M G-HCl, analysed by SDS-PAGE on a 14 % polyacrylamide gel and Western blots were stained for dityrosines. M: molecular weight markers. Dityrosine standard (dityrosine cross-linked BSA) in lane 9. Lane 1: RANTES only, lane 2: RANTES + 50 μM $CuCl_2$ and 25 μM H_2O_2 , lane 3: RANTES + HS, lane 4: RANTES + HS + 50 μM $CuCl_2$ + 25 μM H_2O_2, lane 5: RANTES incubated with 6 M G-HCl,, lane 6: RANTES + 50 μM $CuCl_2$ + 25 μM H_2O_2, incubated with 6 M G-HCl , lane 7: RANTES + HS incubated with 6 M G-HCl and lane 8: RANTES + HS + 50 μM $CuCl_2$ + 25 μM H_2O_2 incubated with 6 M G-HCl. Representative of two independent experiments.

Dityrosines were not detected in RANTES incubated without Cu or H_2O_2 (figure 3.7, lane 1) which would normally be present as a dimer (figure 3.5, lane 1). This is likely due to the ethanol precipitation of the proteins, through which some of the dimer may have been lost, and therefore not detected by the antibody. As previously observed, RANTES dimers (16 KDa), trimers (24 KDa) and tetramers (32 KDa) were formed following 2 day incubation of RANTES with 50 μM $CuCl_2$ plus 25 μM H_2O_2 and stained positively for dityrosines in the absence of HS (figure 3.7, lane 2).

In the presence of HS, dimers (16 KDa) and trimers (24 KDa), but not tetramers (32 KDa) were detected (lane 4). Again, the result indicates a free radical scavenging effect upon the addition of HS. RANTES multimers generated following 2 day incubation

with 50 μM $CuCl_2$ plus 25 μM H_2O_2 in the presence and absence of HS (0.1 mg/ml) remained following the addition of 6 M G-HCl (lanes 6 and 8) when compared with the controls (RANTES incubated with 50 μM $CuCl_2$ plus 25 μM H_2O_2 in the presence and absence of HS (0.1 mg/ml) but in the absence of 6 M G-HCl in lanes 2 and 4.) The result indicates that RANTES multimers are covalently linked, and extremely stable. The dityrosine standard stained positively for dityrosines in lane 9.

In addition, RANTES multimers were stained for dityrosines in the presence of 2-mercaptoethanol (2-ME), a compound used to reduce disulphide bonds. It is also known for its antioxidant activity. RANTES was incubated for 2 days at 37 °C, as previously, with 50 μM $CuCl_2$ plus 25 μM H_2O_2 in the presence and absence of HS (0.1 mg/ml). 2-ME (5 %) was added to samples following incubation, and prior to analysis by SDS-PAGE. Figure 3.8 shows the effect of 2-ME (5 %) on RANTES incubated in the presence and absence of 50 μM $CuCl_2$ plus 5 - 400 μM H_2O_2 in the absence of HS.

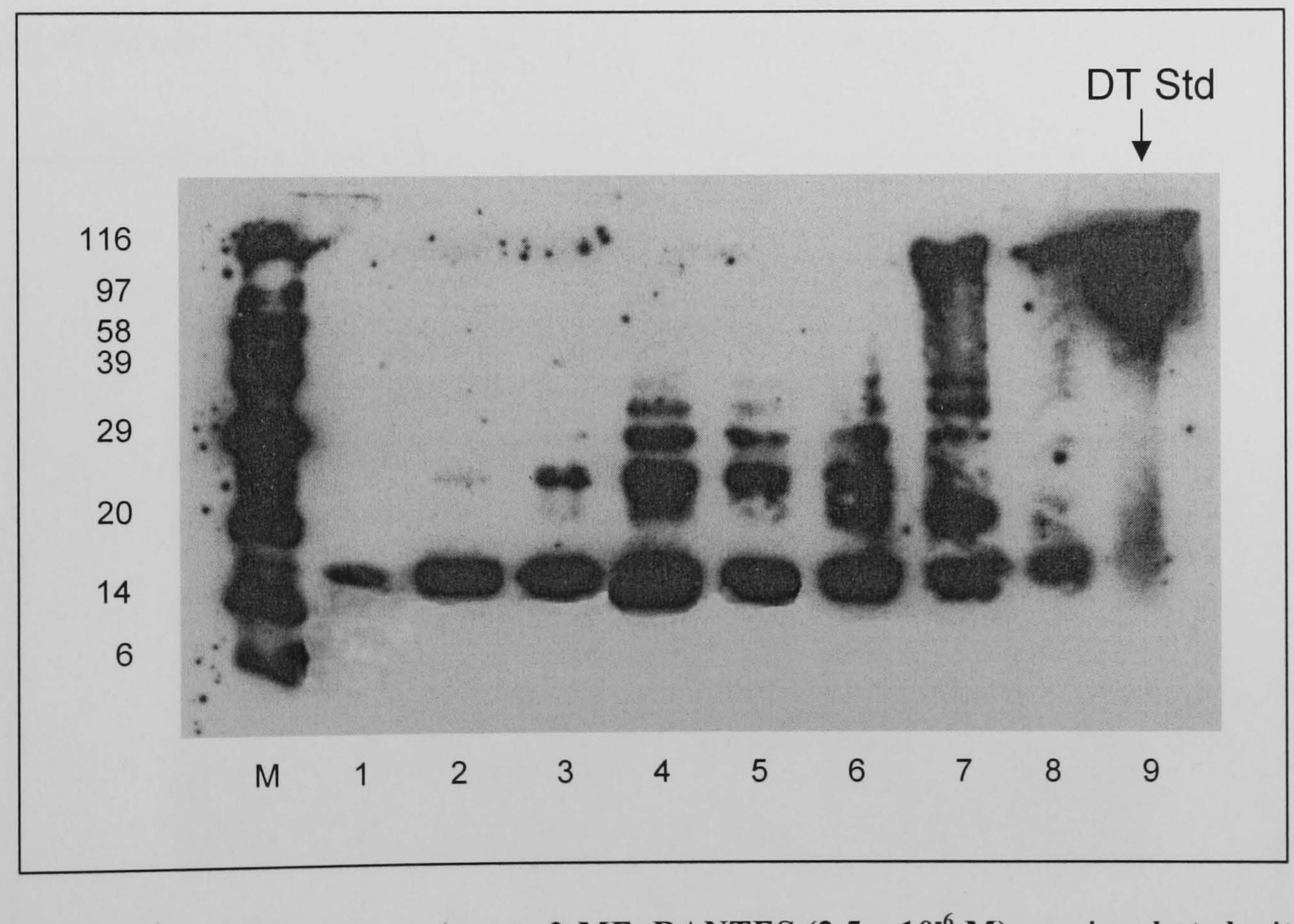

Figure 3.8. The stability of dityrosines to 2-ME. RANTES (2.5×10^{-6} M) was incubated with copper (50 μM) alone, and copper (50 μM) plus 5 – 400 μM H_2O_2 for 2 days at 37 °C, treated with 2-ME (5 % (v/v)), analysed by SDS-PAGE on a 14 % polyacrylamide gel and Western blots were stained for dityrosines. M: molecular weight markers. Dityrosine standard (dityrosine cross-linked BSA) in lane 9. Lane 1: RANTES only, lane 2: RANTES + 50 μM $CuCl_2$, lane 3: RANTES + 50 μM $CuCl_2$ + 5 μM H_2O_2, lane 4: RANTES + 50 μM $CuCl_2$ + 25 μM H_2O_2, lane 5: RANTES + 50 μM $CuCl_2$ + 50 μM H_2O_2, lane 6: RANTES + 50 μM $CuCl_2$ + 100 μM H_2O_2, lane 7: RANTES + 50 μM $CuCl_2$ + 200 μM H_2O_2 and lane 8: RANTES + 50 μM $CuCl_2$ + 400 μM H_2O_2. Representative of two independent experiments.

The RANTES multimers and dityrosine cross-links remained following treatment with 2-ME (figure 3.8), indicating that multimers were covalently linked, and that disulphide bonds were not responsible for multimer formation or dityrosine cross-linking. Higher order multimers appeared in the presence of 50 μM $CuCl_2$ only (24 KDa trimer in lane 2,), whereas in the absence of 2-ME, higher order multimers started to occur only in the presence of both 50 μM $CuCl_2$ and 25 μM H_2O_2 (figure 3.5, lane 4). Tetramers (32 KDa) also appeared at lower concentrations of H_2O_2 (25 μM, lane 4) in the presence of 2-ME than in the absence of 2-ME (figure 3.5, 100 μM H_2O_2, lane 6).

Maximum dityrosine formation occured at 50 μM $CuCl_2$ plus 200 μM H_2O_2 in both the absence (figure 3.5, lane 7), and presence (figure 3.8, lane 7) of 2-ME and dityrosines were diminished in the presence of at 50 μM $CuCl_2$ plus 400 μM H_2O_2 (lane 8) in both the absence and presence of 2-ME.

Figure 3.9 shows the effect of 2-ME (5 %) on RANTES incubated in the presence and absence of 50 μM $CuCl_2$ and 5 - 400 μM H_2O_2 in the presence of 0.1 mg/ml HS.

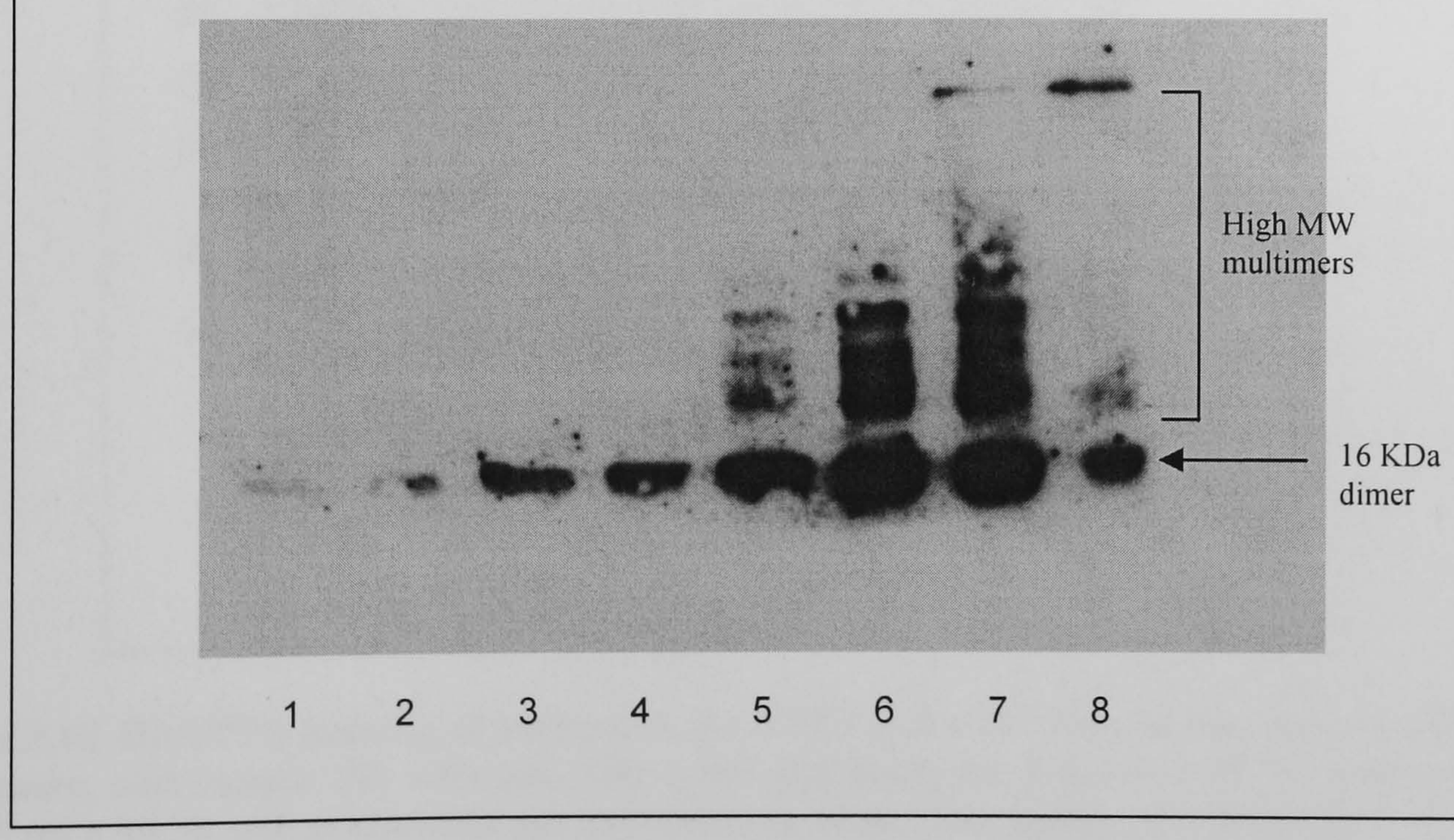

Figure 3.9. Dityrosine formation in the presence of HS. RANTES (2.5×10^{-6} M) was incubated with copper (50 μM) alone, and copper (50 μM) plus 5 – 400 μM H_2O_2 for 2 days at 37 °C in the presence of HS (0.1 mg/ml) and 2-ME (5 % (v/v)), analysed by SDS-PAGE on a 14 % polyacrylamide gel and Western blots were stained for dityrosines. M: molecular weight markers. Lane 1: RANTES +HS, lane 2: RANTES + HS + 50 μM $CuCl_2$, lane 3: RANTES + HS + 50 μM $CuCl_2$ + 5 μM H_2O_2, lane 4: RANTES + HS + 50 μM $CuCl_2$ + 25 μM H_2O_2, lane 5: RANTES + HS + 50 μM $CuCl_2$ + 50 μM H_2O_2, lane 6: RANTES + HS + 50 μM $CuCl_2$ + 100 μM H_2O_2, lane 7: RANTES + HS + 50 μM $CuCl_2$ + 200 μM H_2O_2 and lane 8: RANTES + HS + 50 μM $CuCl_2$ + 400 μM H_2O_2. Representative of two independent experiments.

In the presence of 0.1 mg/ml HS (figure 3.9), maximum dityrosine formation was still seen at 50 μM $CuCl_2$ plus 200 μM H_2O_2 (lane 7), but higher order multimerisation (24 KDa trimer and above) started to occur at higher concentrations of H_2O_2 in the presence of HS (figure 3.9, lane 5, 50 μM H_2O_2) than in the absence of HS (figure 3.8, lane 3, 5 μM H_2O_2). Although higher order multimers were depleted at 400 μM H_2O_2 (figure 3.9, lane 8), some high MW multimers appeared to be protected from degradation (MW approx 100 KDa). The effect was also seen at 200 μM H_2O_2 (lane 7). Again, this indicates that HS may be scavenging free radicals, allowing high order RANTES multimers to withstand high concentrations of H_2O_2.

Figure 3.10 shows RANTES incubated at 2.5 x 10^{-6} M and stained for RANTES rather than for dityrosines. The purpose was to compare the presence and absence of RANTES multimers and dityrosines in parallel, at the higher concentration of RANTES than used in experiments described in Chapter 2.

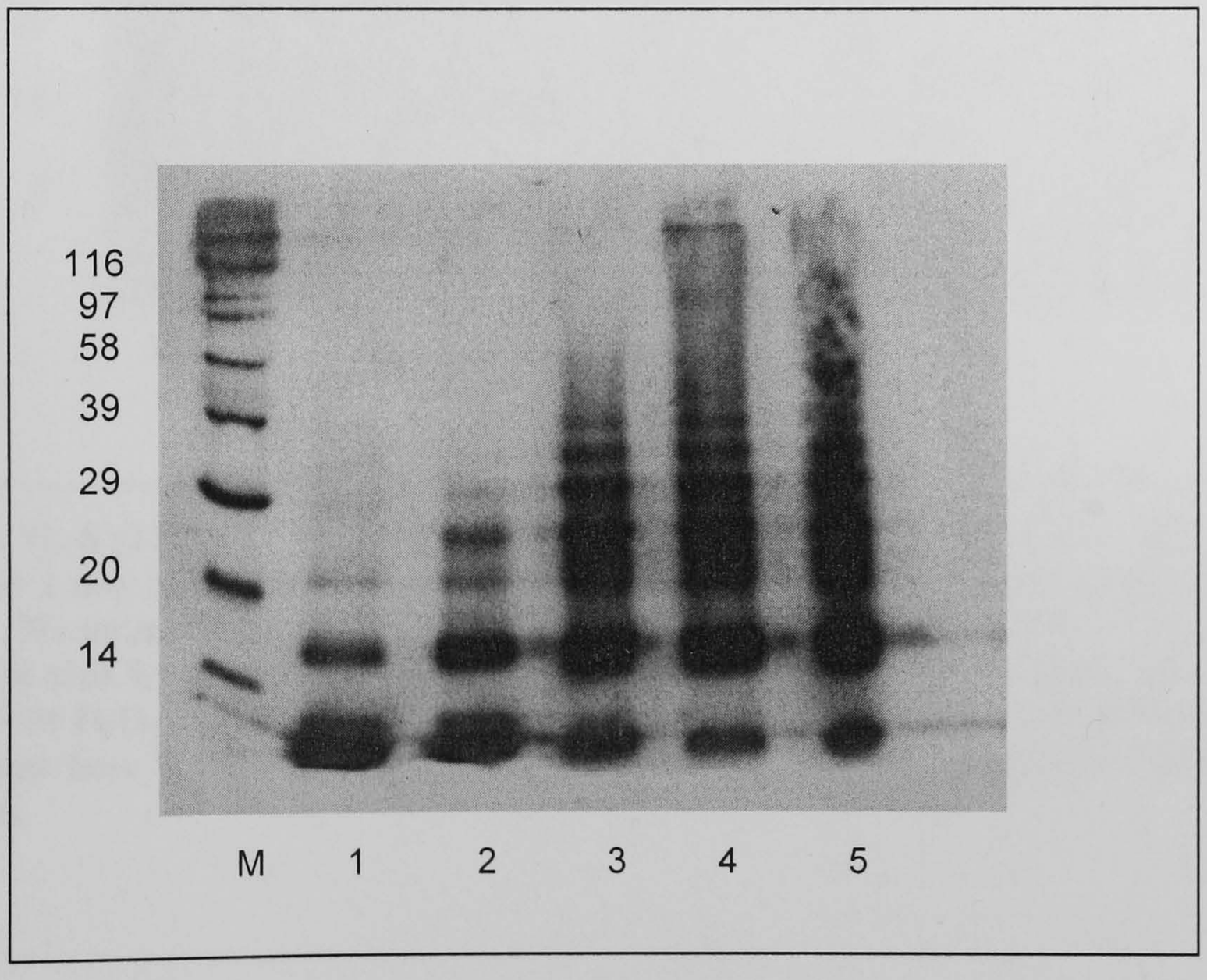

Figure 3.10. RANTES staining of multimers. RANTES (2.5 x 10^{-6} M) was incubated with copper (50 μM) alone, and copper (50 μM) plus 100 – 400 μM H_2O_2 for 2 days at 37 °C, analysed by SDS-PAGE on a 14 % polyacrylamide gel and Western blots were stained for RANTES. M: molecular weight markers. Lane 1: RANTES only, lane 2: RANTES + 50 μM $CuCl_2$, lane 3: RANTES + 50 μM $CuCl_2$ + 100 μM H_2O_2, lane 4: RANTES + 50 μM $CuCl_2$ + 200 μM H_2O_2 and lane 5: RANTES + 50 μM $CuCl_2$ + 400 μM H_2O_2. Representative of two independent experiments.

Maximum RANTES multimerisation occurred at 50 μM $CuCl_2$ plus 200 μM H_2O_2 in parallel with the observation that dityrosine formation occurred maximally under these conditions (figure 3.9). However, when staining for RANTES, the multimers appeared

relatively stable at 400 μM H_2O_2 (figure 3.10, lane 5) whereas dityrosines were depleted at this concentration of H_2O_2 (figure 3.5, lane 8). This indicates that another interaction is involved in RANTES multimerisation other than dityrosine cross-link formation.

Given that dityrosines were detected in RANTES multimers, IL-8 and ENA-78 multimers were also stained for dityrosines for comparison. Since ENA-78 has no tyrosine residues within its amino acid sequence, this made it useful as a negative control. IL-8 has only one tyrosine residue, whereas RANTES has five.

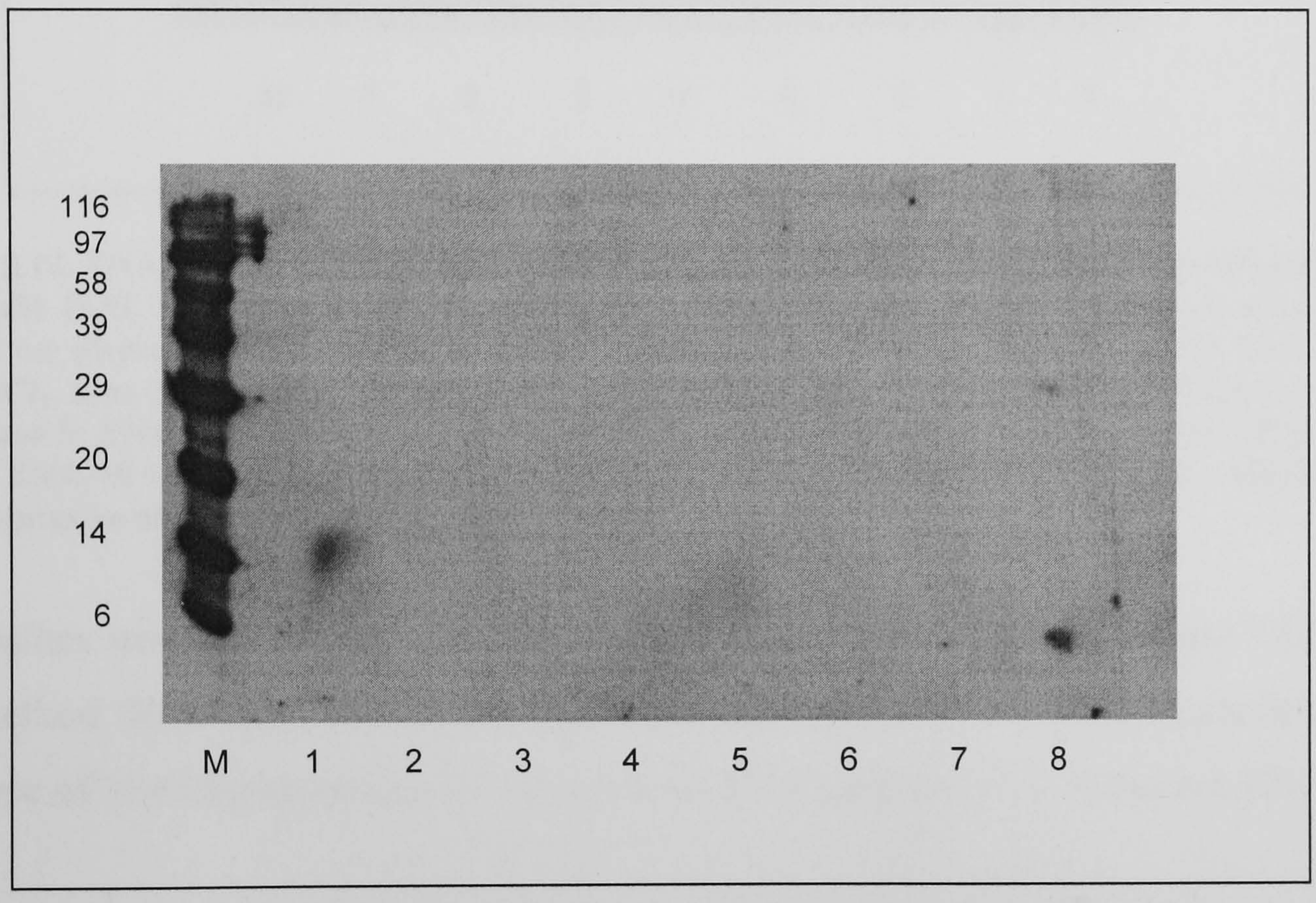

Figure 3.11. IL-8 (2.5×10^{-6} M) incubated with copper (50 μM) alone, copper (50 μM) plus 5 – 400 μM H_2O_2 for 1 day at 37 °C, analysed by SDS-PAGE on a 14 % polyacrylamide gel and stained for dityrosines. M: molecular weight markers. Lane 1: IL-8 only, lane 2: IL-8 + 50 μM $CuCl_2$, lane 3: IL-8 + 50 μM $CuCl_2$ + 5 μM H_2O_2, lane 4: IL-8 + 50 μM $CuCl_2$ + 25 μM H_2O_2, lane 5: IL-8 + 50 μM $CuCl_2$ + 50 μM H_2O_2, lane 6: IL-8 + 50 μM $CuCl_2$ + 100 μM H_2O_2, lane 7: IL-8 + 50 μM $CuCl_2$ + 200 μM H_2O_2 and lane 8: IL-8 + 50 μM $CuCl_2$ + 400 μM H_2O_2. Representative of two independent experiments.

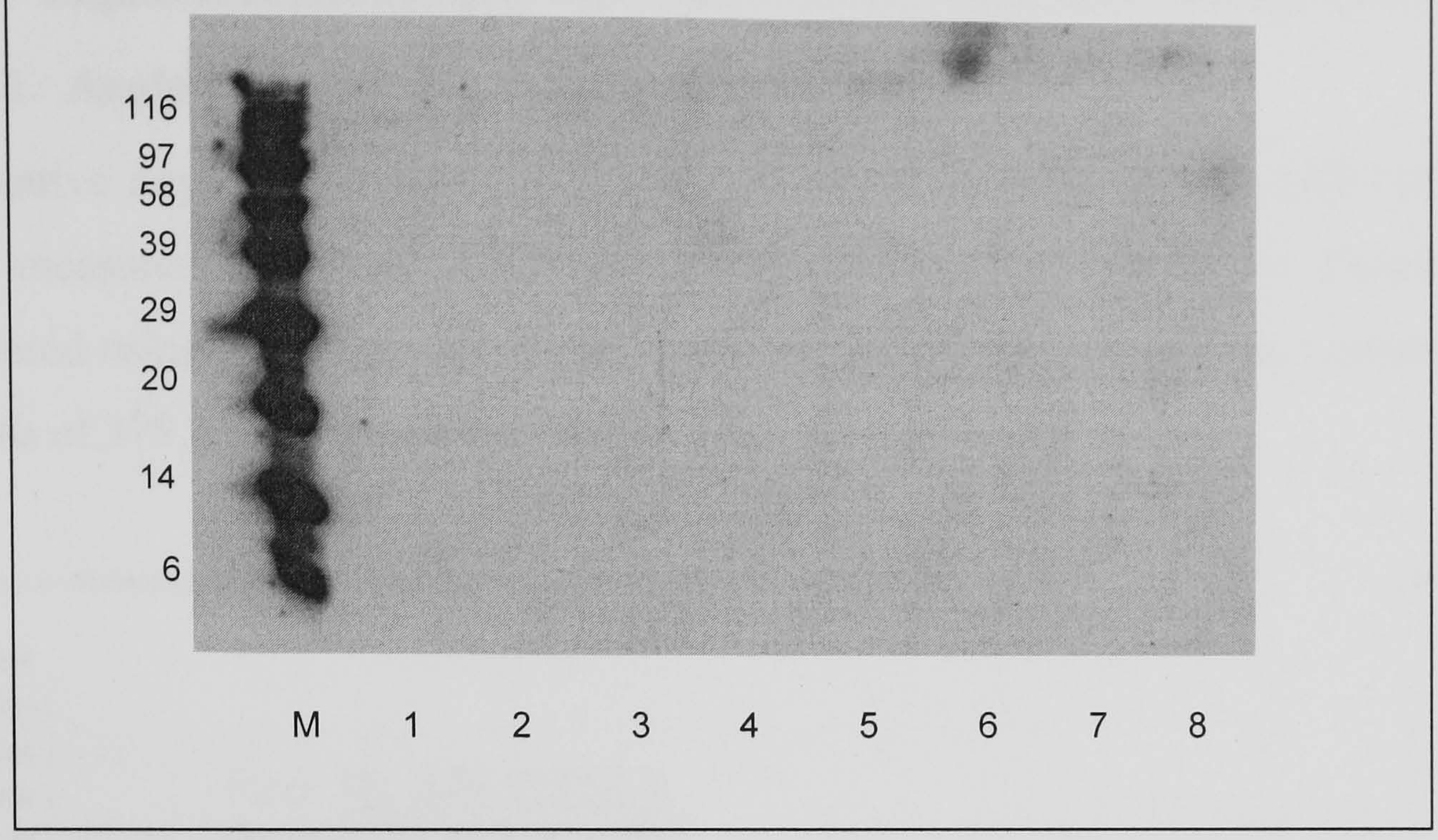

Figure 3.12. ENA-78 (2.5×10^{-6} M) incubated with copper (50 µM) alone, and copper (50 µM) plus 5 – 400 µM H_2O_2 for 1 day at 37 °C, analysed by SDS-PAGE on a 14 % polyacrylamide gel and stained for dityrosines. M: molecular weight markers. Lane 1: ENA-78 only, lane 2: ENA-78 + 50 µM $CuCl_2$, lane 3: ENA-78 + 50 µM $CuCl_2$ + 5 µM H_2O_2, lane 4: ENA-78 + 50 µM $CuCl_2$ + 25 µM H_2O_2, lane 5: ENA-78 + 50 µM $CuCl_2$ + 50 µM H_2O_2, lane 6: ENA-78 + 50 µM $CuCl_2$ + 100 µM H_2O_2, lane 7: ENA-78 + 50 µM $CuCl_2$ + 200 µM H_2O_2 and lane 8: ENA-78 + 50 µM $CuCl_2$ + 400 µM H_2O_2. Representative of two independent experiments.

Dityrosines were not detected in either IL-8 (figure 3.11) or ENA-78 (figure 3.12) using this method. However, subsequent analysis of dityrosines by LCMS/MS confirmed the presence of low concentrations of dityrosine in IL-8 (section 3.5.3.3) but not ENA-78.

3.5.3. Liquid chromatography mass spectroscopy/mass spectroscopy (LCMS/MS)

3.5.3.1. Analysis of native dityrosine-BSA standard

The native dityrosine standard [C^{12} x 18] and the IS (stable isotopic DiY) [C^{13} x 18] were measured using two MRM combinations for each. The native dityrosine was measured using MRMs of 361.2/315.1 and 361.2/237.1 and the IS was measured using MRMs of 379.2/332.1 and 379.2/253.1.

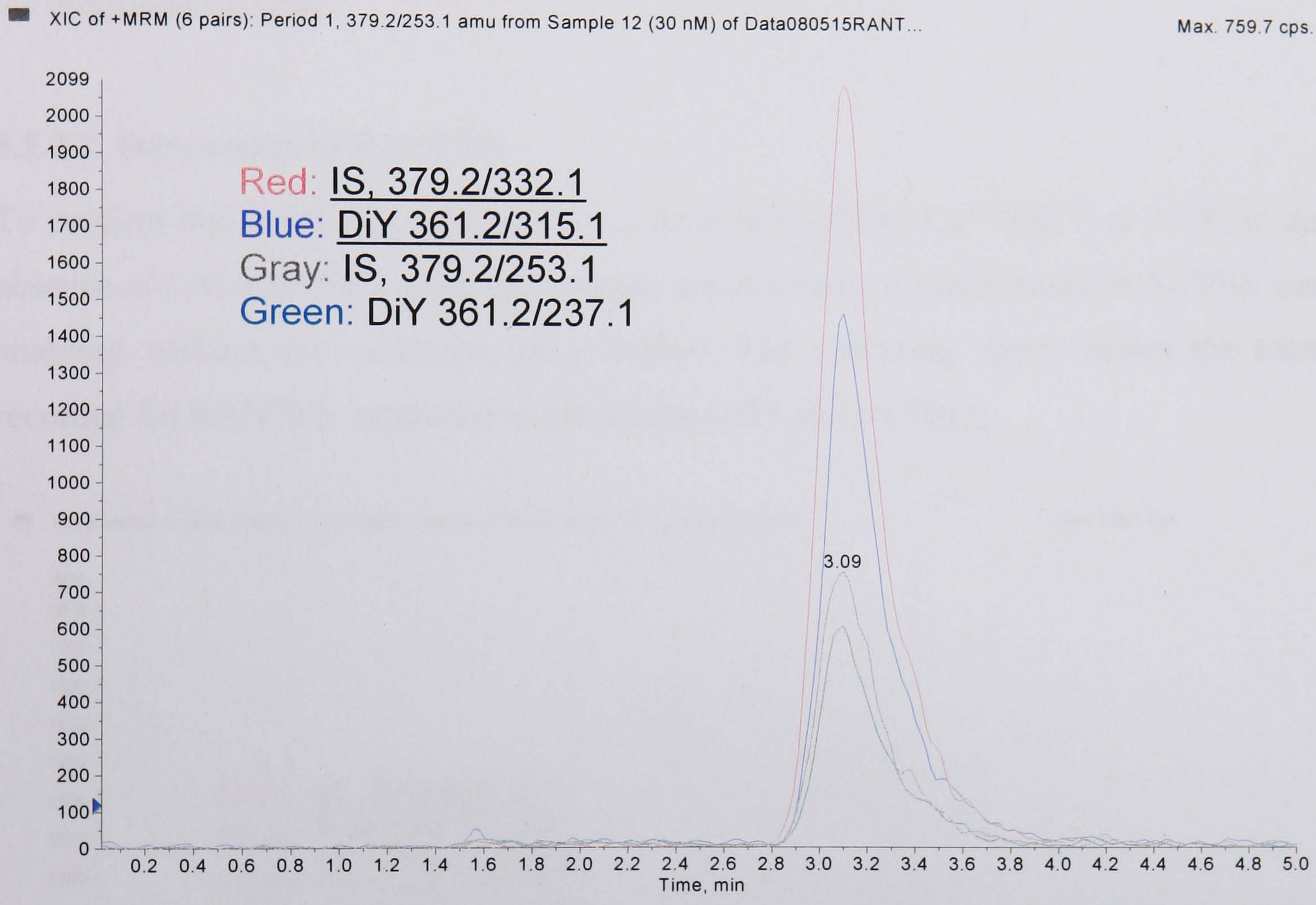

Figure 3.13. Trace showing dityrosine standards (both stable isotopic DiY standard and native DiY). The blue and green traces correlate to the native dityrosine-BSA standard which contained 18 x C^{12} [$^{12}C_{18}$] atoms. The red and gray traces correlate to the IS, which contained 18 x C^{13} [$^{13}C_{18}$] atoms. Both elute at 3 minutes.

The IS and dityrosine standard eluted at approximately 3 minutes. The two IS parent ion / fragment combinations (red and gray) are 'paired' to the two dityrosine parent ion / fragment combinations (blue and green.) Underlined and non-underlined numbers show a "pair" of fragments. For example, the IS with parent ion MW 379.2 / fragment MW 332.1 (red) and dityrosine parent ion MW 361.2 / fragment MW 315.1 (blue) show a similar pattern. Similarly, the IS with the dityrosine parent ion MW 379.2 / fragment MW 253.1 (gray) and dityrosine parent ion MW 361.2 / fragment MW 237.1 (green) show a similar pattern.

The problem with quantification when using mass spectroscopy with liquid chromatography is that the ionisation efficiency and therefore the incorporation of these ions into the sample mass can be variable, affecting the retention times which are also variable as a result. However, because the isotopic IS and native dityrosine eluted at the same retention time, it was concluded that the ionisation efficiency and the incorporation into the sample of both the native dityrosine ions and the IS were similar. Therefore the IS used was very suitable, since it was ionised at the same efficiency as the dityrosine sample.

3.5.3.2. Dityrosines in RANTES

To confirm that RANTES incubated for 2 days in 1x PBS (-Ca^{2+}/Mg^{2+}) at 37 °C in the absence of $CuCl_2$ or H_2O_2 does not contain any dityrosines, recombinant RANTES was analysed without any additions, as a control. The following figure shows the trace recorded for RANTES incubated in the absence of $CuCl_2$ or H_2O_2.

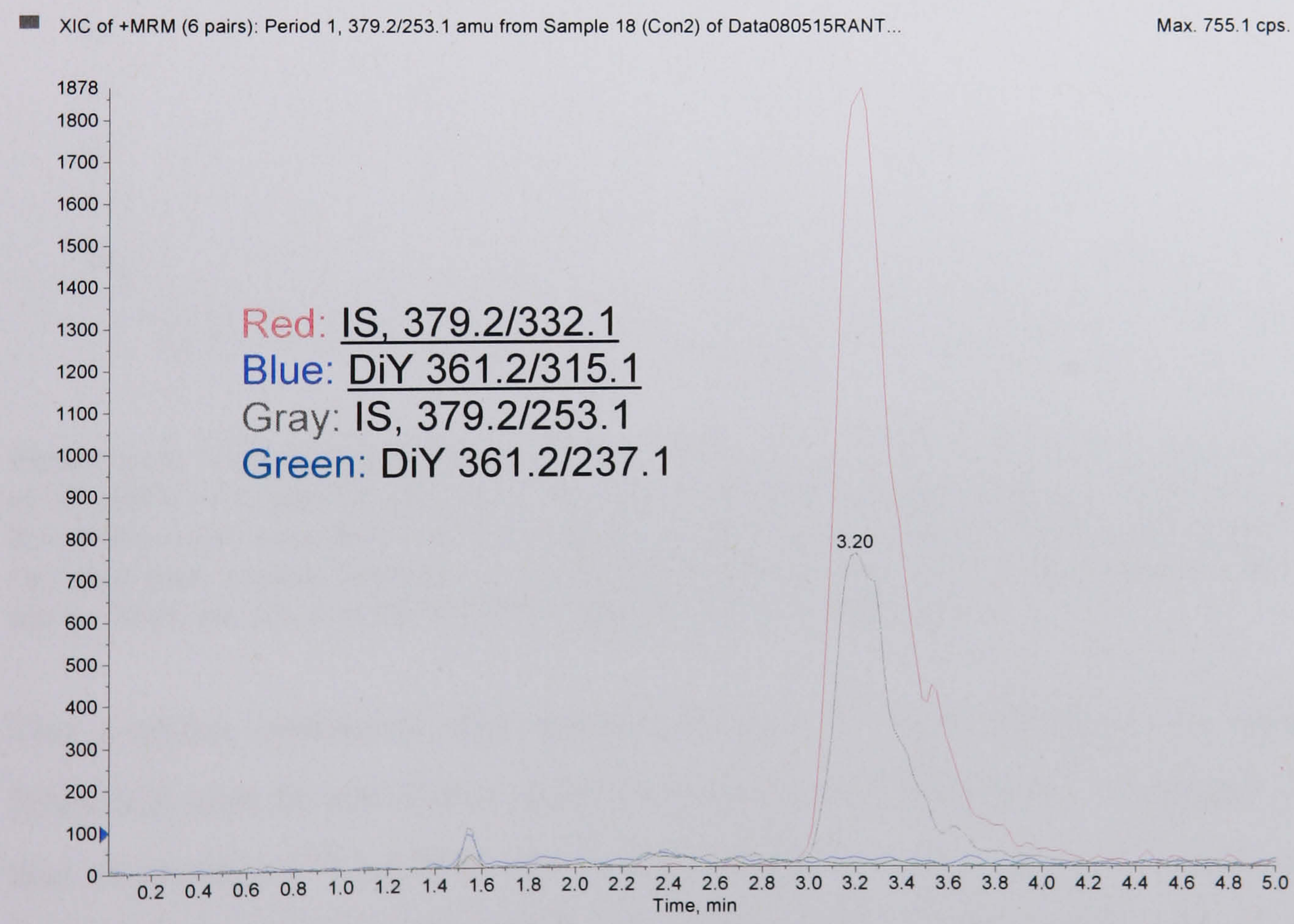

Figure 3.14. Trace showing RANTES (2.5 x 10^{-6}M) in the absence of $CuCl_2$ and H_2O_2. The blue and green traces correlate to RANTES. The red and gray traces correlate to the stable internal standard, which contained 18 x C^{13} [$^{13}C_{18}$] atoms. The IS elutes at 3 minutes

Figure 3.14 shows that no dityrosines were detected in the RANTES control (blue and green traces). The IS still elutes at 3 minutes.

3.5.3.3. Dityrosines in RANTES multimers

To determine whether dityrosines are present in RANTES multimers, recombinant RANTES was incubated for 2 days at 37 °C in 1x PBS ($-Ca^{2+}/Mg^{2+}$) in the presence of 50 μM $CuCl_2$ plus 25 μM H_2O_2. These are the concentrations at which RANTES is known to form multimers. The samples were freeze dried, and reconstituted in water, hydrolysed and analysed by LCMS/MS.

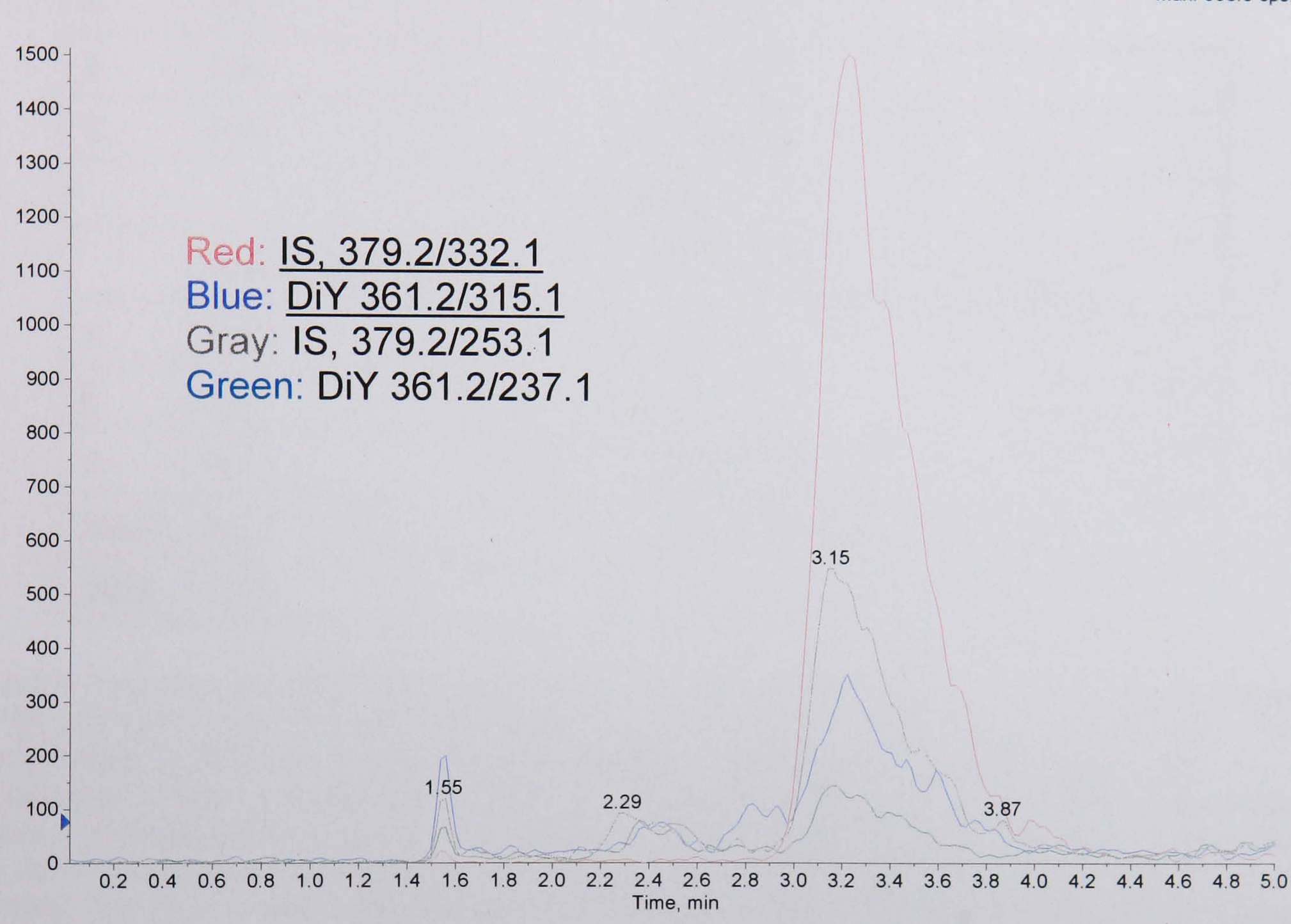

Figure 3.15. Trace showing dityrosines detected in RANTES (2.5×10^{-6}M) incubated in the presence of 50 μM $CuCl_2$ plus 25 μM H_2O_2. The blue and green traces correlate to dityrosines detected in RANTES multimers (RANTES incubated in the presence of 50 μM $CuCl_2$ plus 25 μM H_2O_2.) The red and gray traces correlate to the stable internal standard, which contained 18 x C^{13} [$^{13}C_{18}$] atoms. Both the I.S. and the RANTES sample eluted at 3 minutes.

The analysis confirmed that dityrosines were formed following the incubation of RANTES with 50 μM $CuCl_2$ and 25 μM H_2O_2 for 2 days at 37 °C. Figure 3.15 shows that dityrosines [$^{12}C_{18}$] MW 361.2 with fragments 315.1 and 237.1 were detected in RANTES multimers generated by incubation with 50 μM $CuCl_2$ and 25 μM H_2O_2. Dityrosines were detected using the two MRM combinations, MW 361.2/315.1, and MW 361.2/237.1. The IS was detected using two MRMs (MW 379.2/332.1 and MW 379.2/253.1), and used to quantify the data.

Dityrosine (nM)		
	Control (RANTES only)	RANTES + 50 μM $CuCl_2$ + 25 μM H_2O_2
A	0	2.4
B	0	9.4
C	0	19.3
Tyrosine (nM)		
	Control (RANTES only)	RANTES + 50 μM $CuCl_2$ + 25 μM H_2O_2
A	347	266
B	790	1605
C	676	7490
Tyr/DiY		
	Control (RANTES only)	RANTES + 50 μM $CuCl_2$ + 25 μM H_2O_2
A	NA	112
B	NA	171
C	NA	388
Mean	NA	224
SEM	N/A	83.9

Table 3.3. Tyrosine and dityrosine concentrations measured in RANTES (2.5 x 10^{-6}M) incubated with 50 μM $CuCl_2$ plus 25 μM H_2O_2. Data was calculated in triplicate using LCMS/MS. The detection limit of DiY was 1 nM and the calibration curve of DiY was linear (R=0.999) over a concentration range of 1–300 nM. Using the selected MRM transitions, the DiY in RANTES samples was estimated (n = 3). NA = not available (because the amount of dityrosine is zero). The table shows dityrosines and tyrosines, detected in RANTES incubated with 50 μM $CuCl_2$ plus 25 μM H_2O_2. The data is also expressed as a ratio of the number of tyrosine residues to dityrosines present (Y/DiY).

The number of dityrosines formed depends on the number of tyrosines present in the chemokine. In order to make allowances for this, the number of dityrosines present is expressed as a ratio of tyrosines (Y) / dityrosines (DiY). A lower ratio indicates that there are more dityrosines in the chemokine per one tyrosine residue.

Qualitative analysis of DiY by Western blotting indicated more DiY at higher concentrations of H_2O_2, up to 200 μM (figure 3.5). Therefore RANTES was incubated for 2 days at 37 °C in the presence of 50 μM $CuCl_2$ plus 200 μM H_2O_2 and analysed by LCMS/MS for quantitative analysis of DiY.

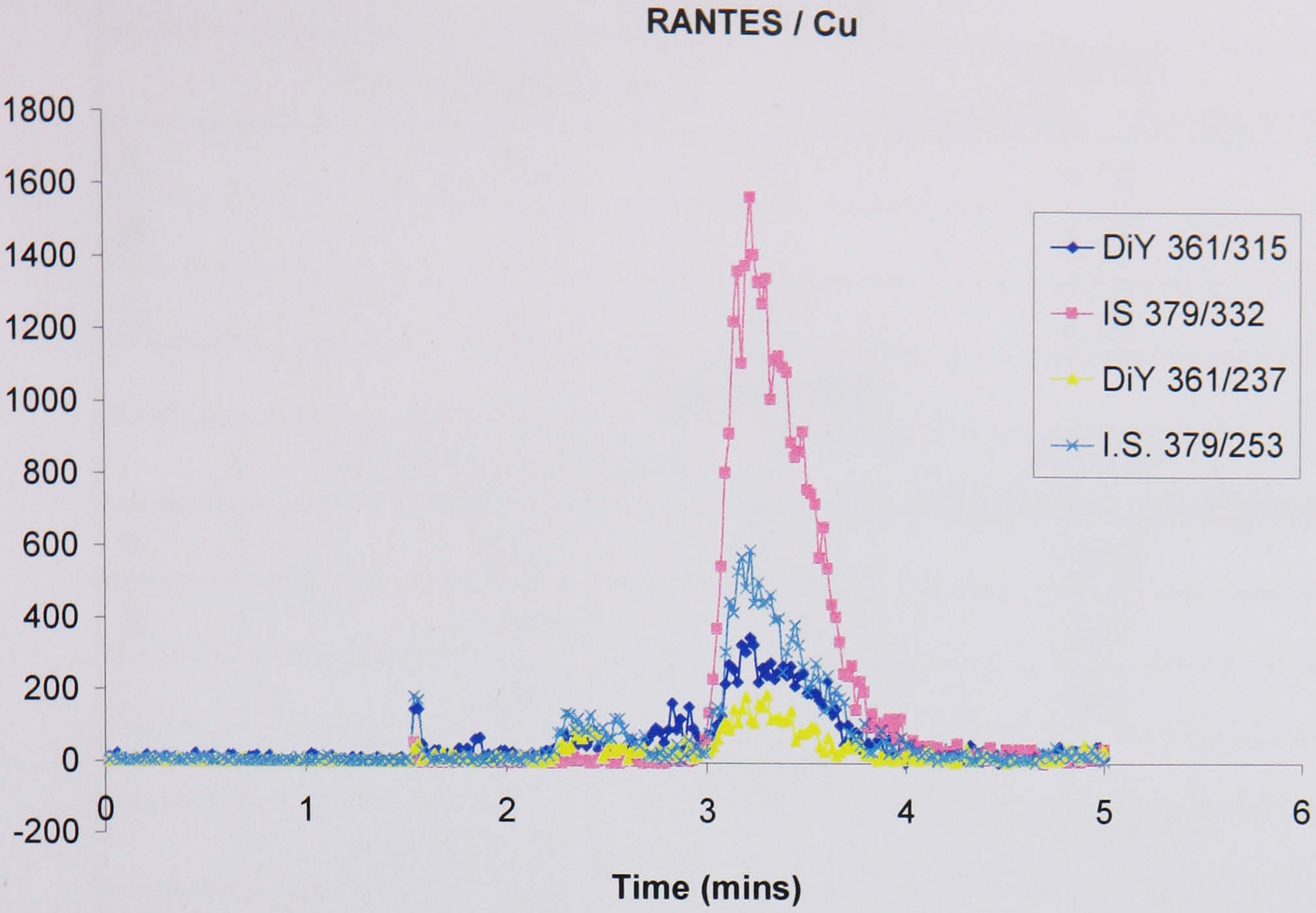

Figure 3.16. Trace showing dityrosines detected in RANTES (2.5 x 10^{-6}M) incubated in the presence of 50 µM $CuCl_2$ plus 200 µM H_2O_2. The trace shows dityrosines detected in RANTES with a parent ion MW 361.2/ fragment MW 315.1. The dityrosines in the sample eluted at 3 minutes.

Dityrosine (nM)		
	Control (RANTES only)	RANTES + 50 μM $CuCl_2$ + 200 μM H_2O_2
A	0	3.76
B	0	8.00
C	0	9.12
Tyrosine (nM)		
	Control (RANTES only)	RANTES + 50 μM $CuCl_2$ + 200 μM H_2O_2
A	347	118.9
B	790	800
C	676	506
Tyr/DiY		
	Control (RANTES only)	RANTES + 50 μM $CuCl_2$ + 200 μM H_2O_2
A	NA	32
B	NA	100
C	NA	55
Mean	NA	62.3
SEM	N/A	20

Table 3.4. Tyrosine and dityrosine concentrations measured in RANTES (2.5×10^{-6}M) incubated with 50 μM $CuCl_2$ plus 200 μM H_2O_2. Data was calculated in triplicate using LCMS/MS. The detection limit of DiY was 1 nM and the calibration curve of DiY was linear (R=0.999) over a concentration range of 1–300 nM. Using the selected MRM transitions, the DiY in RANTES samples was estimated (n = 3). NA = not available (because the amount of dityrosine is zero. Dityrosines and tyrosines were detected in RANTES incubated with 50 μM $CuCl_2$ plus 200 μM H_2O_2. The data is also expressed as a ratio of the number of tyrosine residues to dityrosines present (Y/DiY).

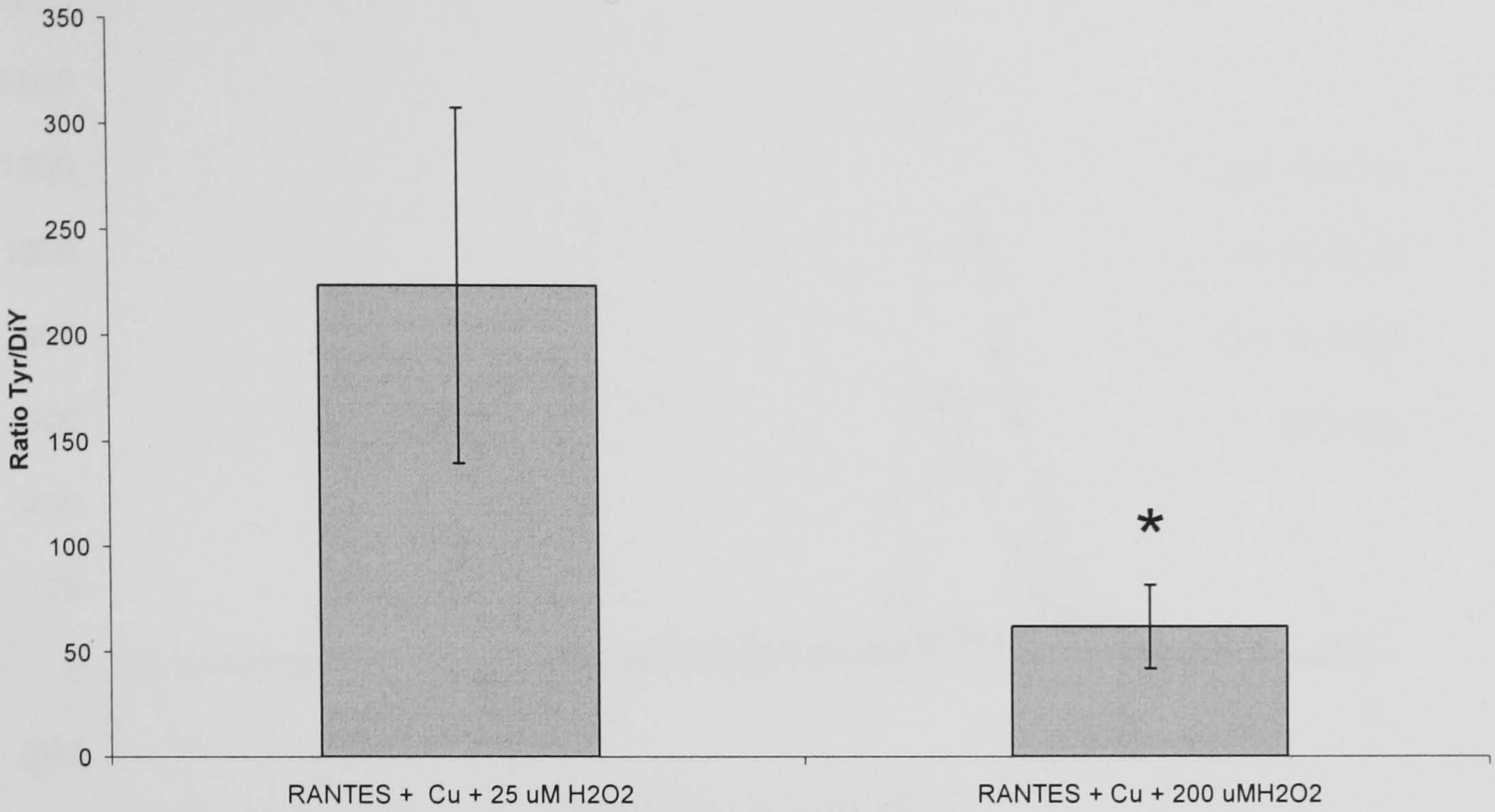

Figure 3.17. Ratio of tyrosines / dityrosines in RANTES incubated in the presence of 50 μM $CuCl_2$ plus 25 or 200 μM H_2O_2. The results are displayed as a ratio of the number of tyrosine residues to dityrosines present (Y/DiY). A lower ratio depicts a higher number of dityrosines present compared to the number of tyrosine residues. Values are expressed as means ± SEM. * indicates a significant difference between RANTES incubated with 50 μM $CuCl_2$ plus 25 μM H_2O_2 and RANTES incubated with 50 μM $CuCl_2$ plus 200 μM H_2O_2 (n=3, $p < 0.05$, one-tailed paired student's t-test).

The data confirmed that incubation with Cu plus H_2O_2 was necessary for dityrosine formation in RANTES. An increase in the H_2O_2 concentration from 25 to 200 μM resulted in significantly greater dityrosine formation ($p < 0.05$). The ratio of Tyr/DiY decreased from 239.7 ± 83.9 to 62.3 ± 20.0, indicating more dityrosine formation.

3.5.3.4. IL-8 and ENA-78

In order to investigate whether dityrosine formation correlates to the number of tyrosine residues in the amino acid sequence of chemokines, IL-8, which contains one tyrosine residue, and ENA-78 which contains no tyrosine residues were incubated with 50 μM $CuCl_2$ plus 200 μM H_2O_2 for comparison with RANTES which has five tyrosines.

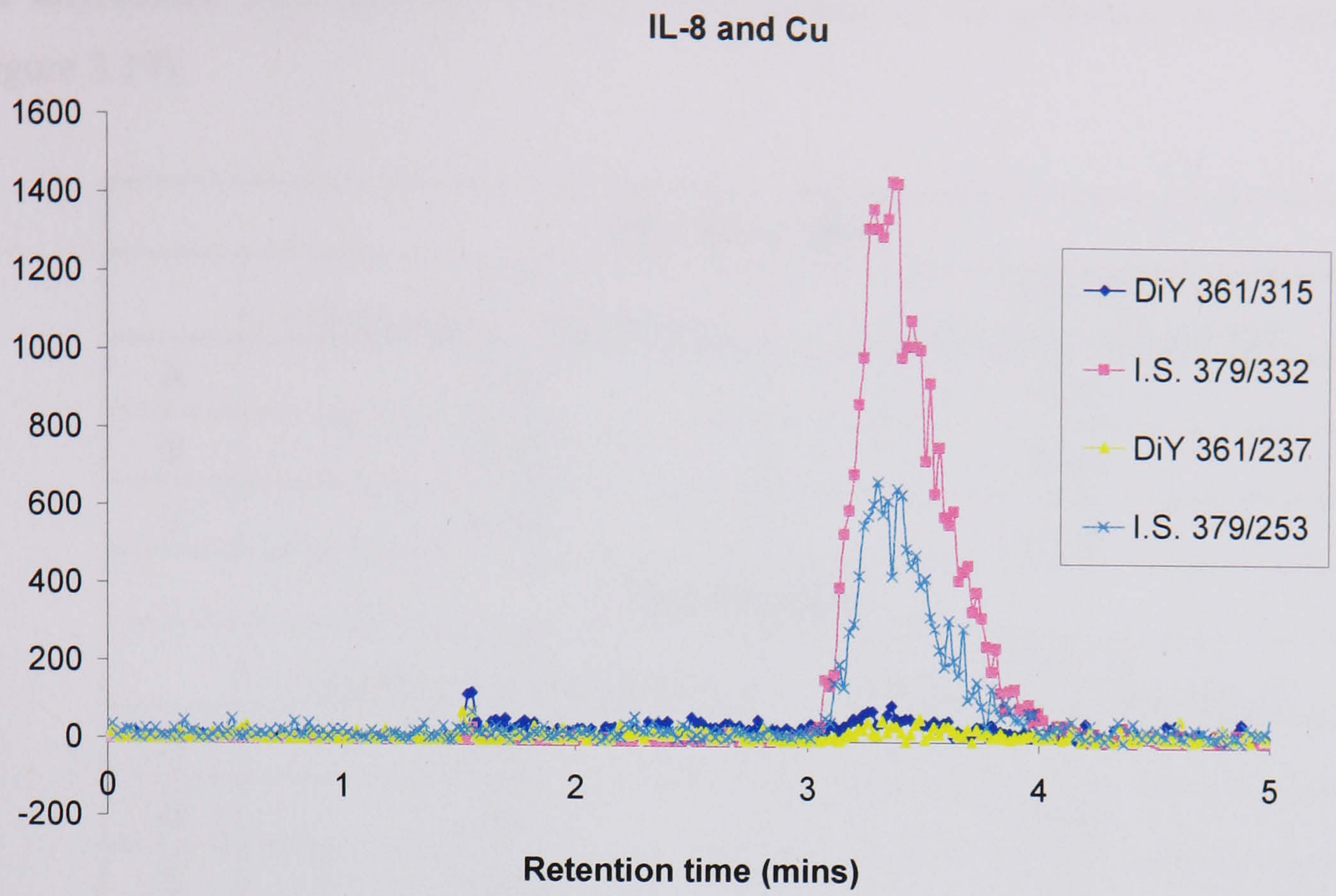

Figure 3.18. Trace showing dityrosines detected in IL-8 (2.5 x 10^{-6}M) incubated in the presence of 50 µM $CuCl_2$ plus 200 µM H_2O_2. The trace shows dityrosines analysed in IL-8 with a parent ion MW 361.2/ fragment MW 315.1. The dityrosines in the sample eluted at 3 minutes.

The trace shows minimal dityrosines detected in IL-8 incubated in the presence of 50 µM $CuCl_2$ plus 200 µM H_2O_2.

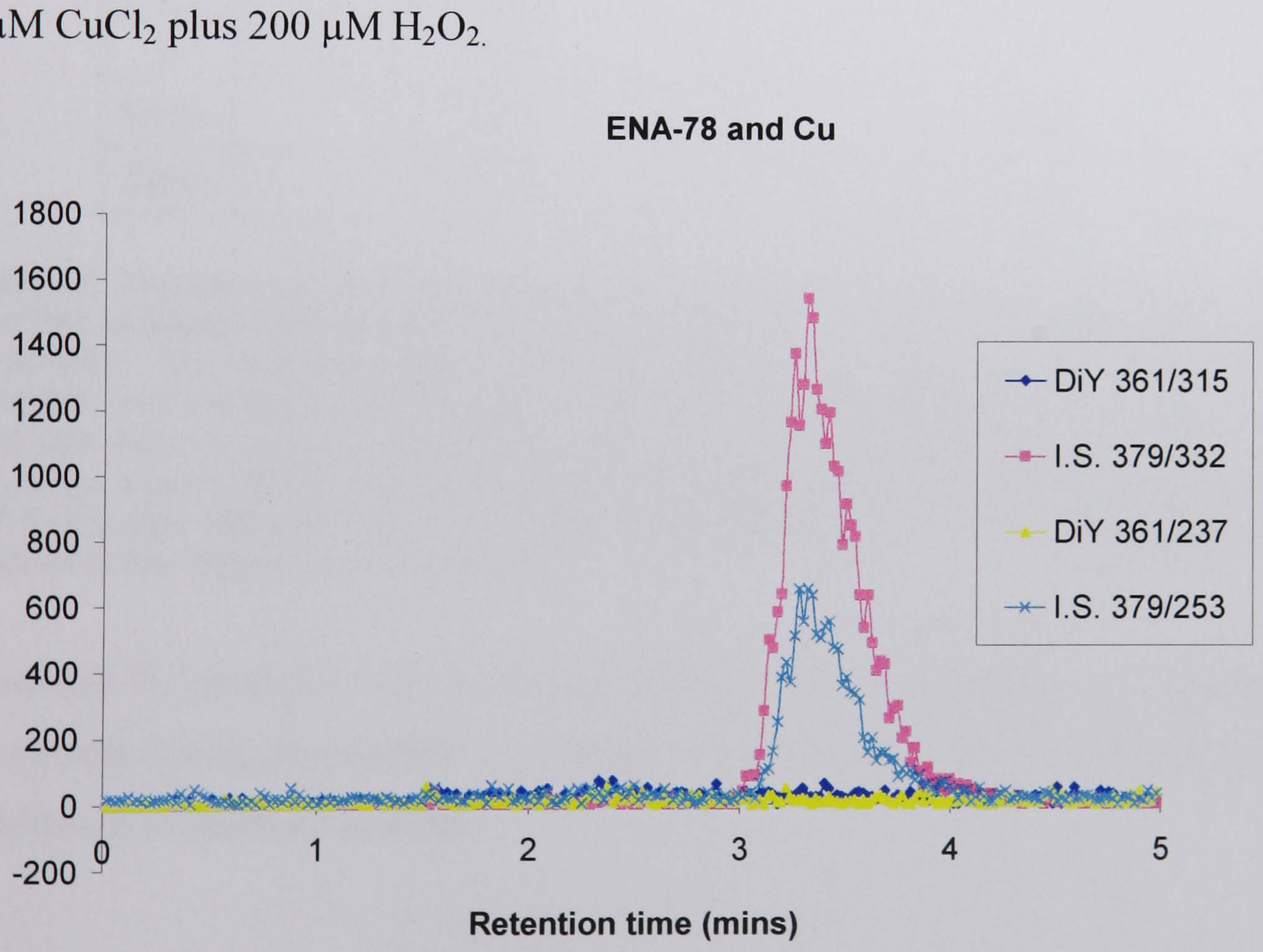

Figure 3.19. Trace showing dityrosines detected in ENA-78 (2.5 x 10^{-6}M) incubated in the presence of 50 µM $CuCl_2$ plus 200 µM H_2O_2. The trace shows no dityrosines detected in ENA-78 with a parent ion MW 361.2/ fragment MW 315.1.

No dityrosines were detected in ENA-78 incubated in the presence of Cu plus H_2O_2 (figure 3.19).

Dityrosine (nM)		
	IL-8 + 50 μM $CuCl_2$ + 200 μM H_2O_2	ENA-78 + 50 μM $CuCl_2$ + 200 μM H_2O_2
A	0.87	0.00
B	3.60	0.00
C	0.59	0.09
Tyrosine (nM)		
	IL-8 + 50 μM $CuCl_2$ + 200 μM H_2O_2	ENA-78 + 50 μM $CuCl_2$ + 200 μM H_2O_2
A	211.7	0
B	1811	229
C	188.3	0
Tyr/DiY		
	IL-8 + 50 μM $CuCl_2$ + 200 μM H_2O_2	ENA-78 + 50 μM $CuCl_2$ + 200 μM H_2O_2
A	244	NA
B	503	NA
C	322	0
Mean	356	N/A
SEM	76.7	N/A

Table 3.5. Tyrosine and dityrosine concentrations measured in IL-8 (2.5 x 10^{-6}M) and ENA-78 (2.5 x 10^{-6}M) incubated with 50 μM $CuCl_2$ plus 200 μM H_2O_2. Data was calculated in triplicate using LCMS/MS. The detection limit of DiY was 1 nM and the calibration curve of DiY was linear (R=0.999) over a concentration range of 1–300 nM. Using the selected MRM transitions, the DiY in IL-8 and ENA-78 samples was estimated (n = 3). NA = not available (because the amount of dityrosine is zero). Dityrosines and tyrosines were detected in IL-8 and ENA-78 incubated with 50 μM $CuCl_2$ plus 200 μM H_2O_2. The data is also expressed as a ratio of the number of tyrosine residues to dityrosines present (Y/DiY).

In sample B, tyrosines were detected in ENA-78. This is likely due to contamination of the sample during preparation or analysis, since ENA-78 does not contain any tyrosine residues in its primary structure.

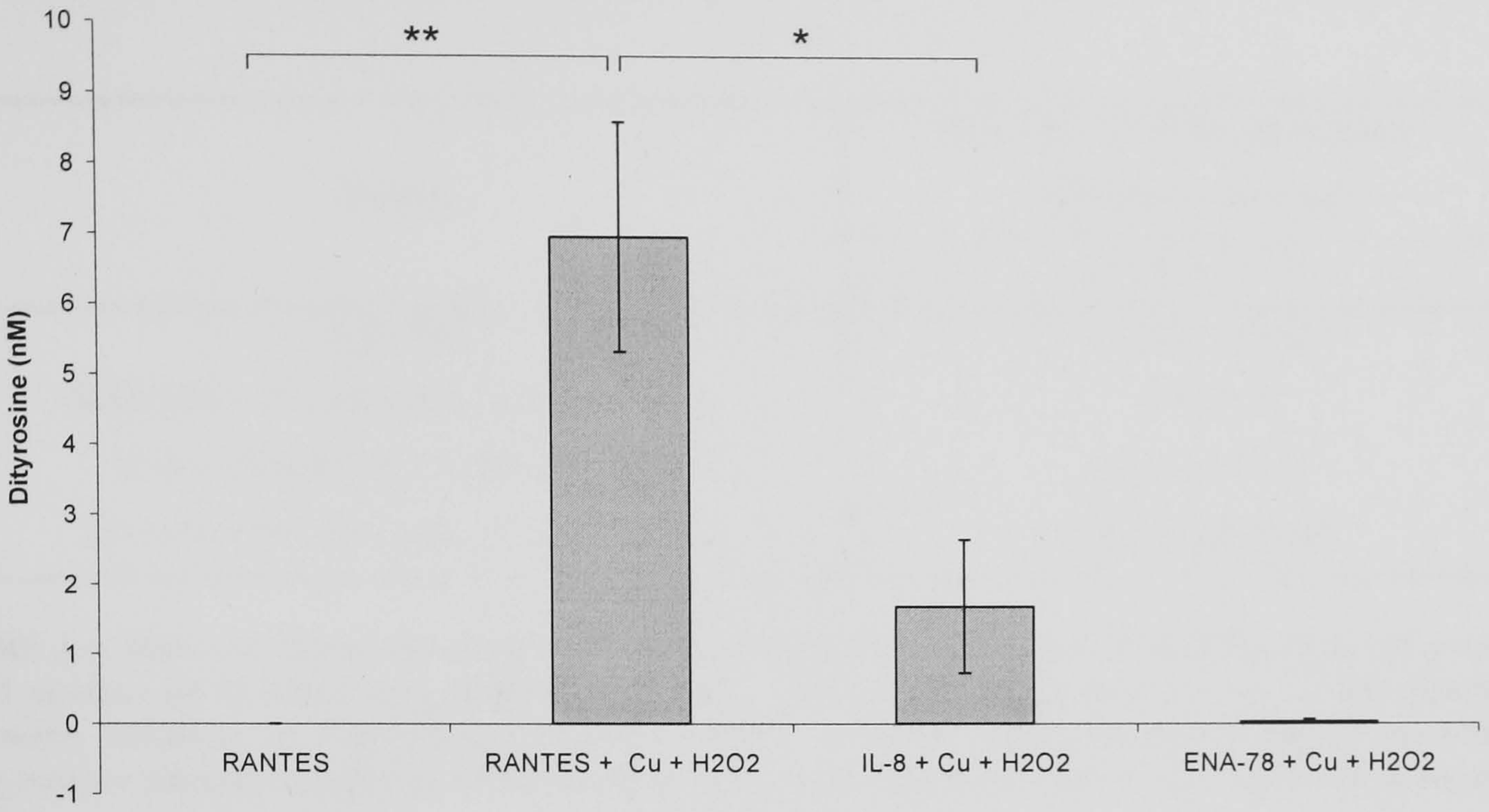

Figure 3.20. Dityrosines detected in RANTES (2.5 x 10^{-6}M), IL-8 (2.5 x 10^{-6}M) and ENA-78 (2.5 x 10^{-6}M) incubated with 50 μM $CuCl_2$ plus 200 μM H_2O_2. * indicates a significant difference between RANTES and IL-8 incubated with 50 μM $CuCl_2$ plus 200 μM H_2O_2 ($p < 0.05$). ** indicates a significant difference between RANTES alone and RANTES incubated with 50 μM $CuCl_2$ plus 200 μM H_2O_2 ($p < 0.01$). Values are expressed as means ± SEM (n =3). Data was compared using a 1-way ANOVA and Tukey's *post-hoc* test.

Copper (50 μM) plus H_2O_2 (200 μM) induced significant ($p < 0.01$) dityrosine formation in RANTES (6.96 ± 1.63 nM) compared to RANTES alone as a control (no dityrosines detected). Some dityrosine formation was observed in IL-8 under the same conditions, but it was not significantly higher than RANTES incubated alone as a control (1.69 ± 0.96 nM). No dityrosine formation was detected in ENA-78.

The following table summarises the results as a ratio of Y / DiY. These figures were calculated from nM concentrations of dityrosines and tyrosines detected in the samples.

Sample	Ratio (no. of Tyrosine residues : 1 Dityrosine detected)
	Mean (n = 3)
RANTES	No DiY detected
RANTES + 50 μM $CuCl_2$ + 200 μM H_2O_2	62.3 ± 20
IL-8 + 50 μM $CuCl_2$ + 200 μM H_2O_2	356.3 ± 76.7
ENA-78 + 50 μM $CuCl_2$ + 200 μM H_2O_2	No DiY detected

Table 3.6. Ratio of dityrosines / tyrosines in RANTES, IL-8 and ENA-78 incubated in the presence and absence of 50 μM $CuCl_2$ and 200 μM H_2O_2. The data is displayed as a ratio of the number of tyrosine residues to dityrosines present (Y/DiY). A lower ratio depicts a higher number of dityrosines present compared to the number of tyrosine residues. Values are expressed as means (n = 3).

3.5.3.5. The effect of other metals on dityrosine formation

Recombinant human RANTES was incubated in the presence of other metals in chloride form (50 μM), plus 200 μM H_2O_2 for 2 days at 37 °C. Samples were prepared as before, and analysed by LCMS/MS.

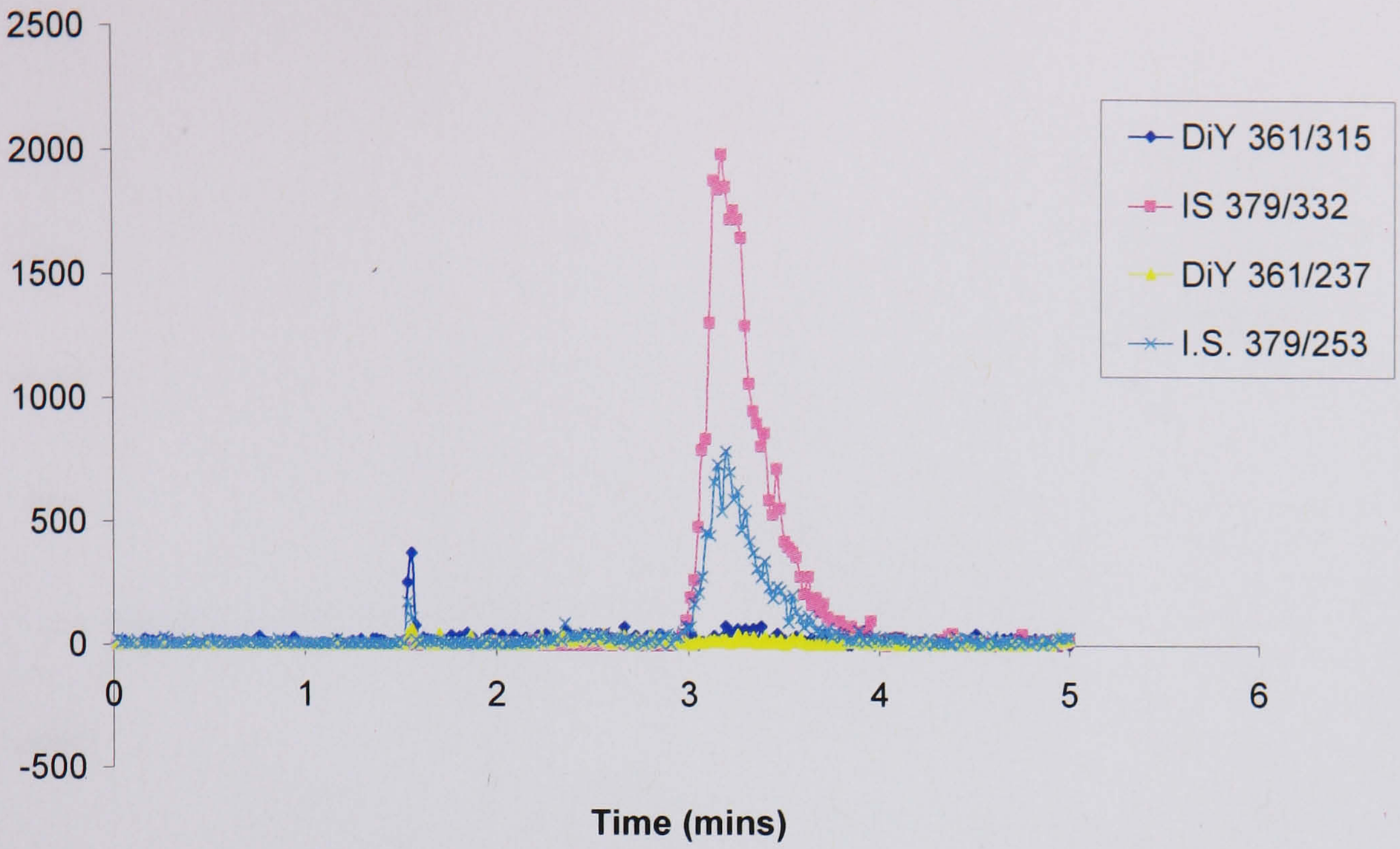

Figure 3.21. The effect of nickel on DiY formation. Trace showing dityrosines detected in RANTES (2.5×10^{-6}M) incubated in the presence of 50 µM $NiCl_2$ plus 200 µM H_2O_2. The trace shows dityrosines analysed in RANTES with a parent ion MW 361.2/ fragment MW 315.1. The dityrosines in the sample eluted at 3 minutes.

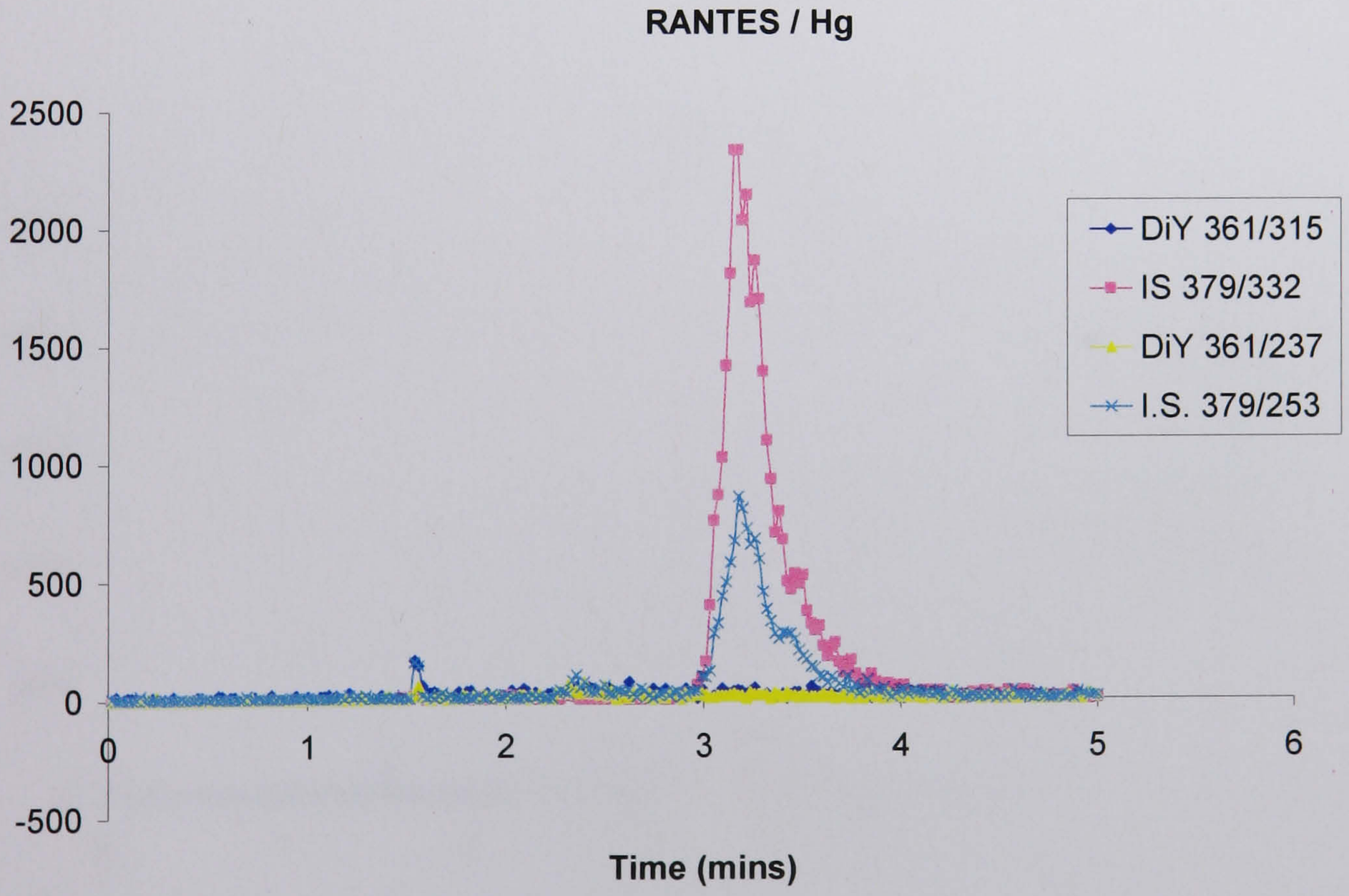

Figure 3.22. The effect of mercury on DiY formation. Trace showing dityrosines detected in RANTES (2.5×10^{-6}M) incubated in the presence of 50 µM $HgCl_2$ plus 200 µM H_2O_2. The trace shows dityrosines analysed in RANTES with a parent ion MW 361.2/ fragment MW 315.1. The dityrosines in the sample eluted at 3 minutes.

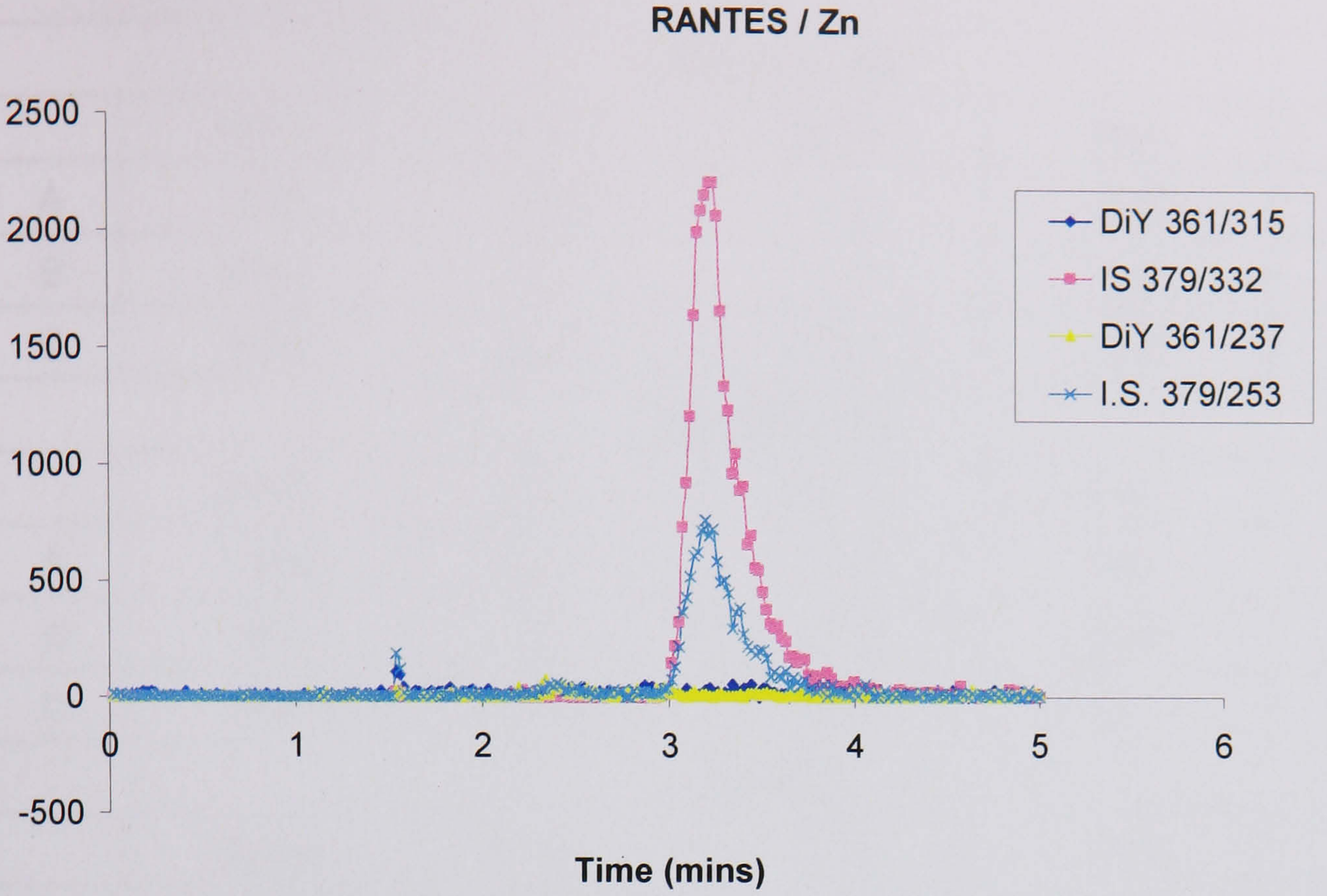

Figure 3.23. The effect of zinc on DiY formation. Trace showing dityrosines detected in RANTES (2.5×10^{-6}M) incubated in the presence of 50 µM $ZnCl_2$ plus 200 µM H_2O_2. The trace shows dityrosines analysed in IL-8 with a parent ion MW 361.2/ fragment MW 315.1. The dityrosines in the sample eluted at 3 minutes.

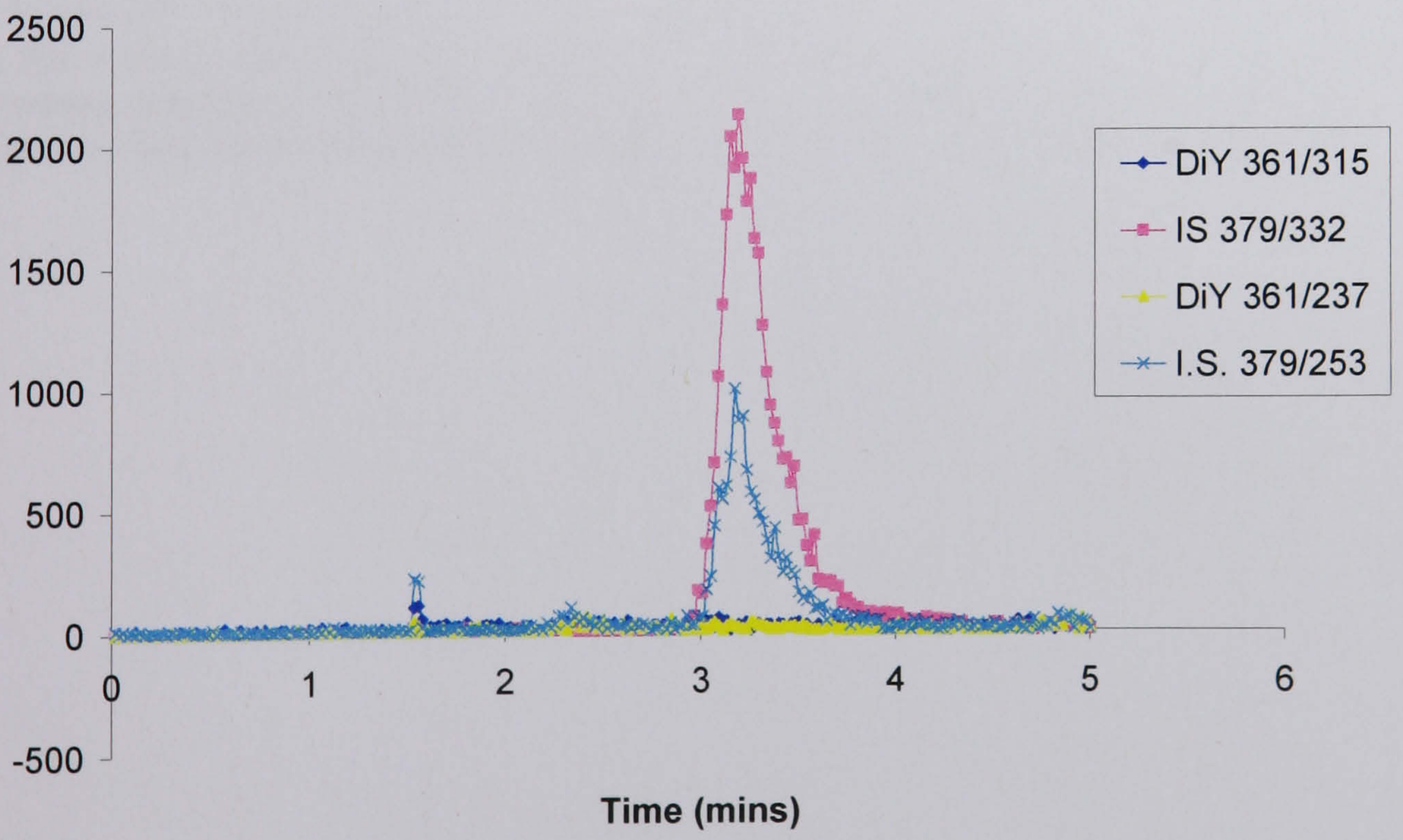

Figure 3.24. The effect of iron on DiY formation. Trace showing dityrosines detected in RANTES (2.5×10^{-6}M) incubated in the presence of 50 µM $FeCl_3$ plus 200 µM H_2O_2. The trace shows dityrosines analysed in RANTES with a parent ion MW 361.2/ fragment MW 315.1. The dityrosines in the sample eluted at 3 minutes.

Dityrosine, nM					
	$CuCl_2$	$NiCl_2$	$HgCl_2$	$FeCl_3$	$ZnCl_2$
A	3.76	0.69	0.00	0.00	0.00
B	8.00	2.31	0.00	0.84	0.00
C	9.12	0.00	0.00	0.00	0.00
Tyrosine, nM					
	$CuCl_2$	$NiCl_2$	$HgCl_2$	$FeCl_3$	$ZnCl_2$
A	118.9	1224	1168	1961	1411
B	800	1733	1114	2080	1302
C	506	1697	645	1617	1264
Tyr/DiY					
	$CuCl_2$	$NiCl_2$	$HgCl_2$	$FeCl_3$	$ZnCl_2$
A	32	1783	NA	NA	NA
B	100	750	NA	2245	NA
C	55	NA	NA	NA	NA
Mean	62.3	1266.5	N/A	2245	N/A
SEM	20	N/A	N/A	N/A	N/A

Table 3.7. Tyrosine and dityrosine concentrations measured in RANTES (2.5×10^{-6} M) incubated with Cu, Ni, Hg, Zn and Fe. Data was calculated in triplicate using LCMS/MS. The detection limit of DiY was 1 nM and the calibration curve of DiY was linear (R=0.999) over a concentration range of 1–300 nM. Using the selected MRM transitions, the DiY in RANTES samples was estimated (n = 3). NA = not available (because the amount of dityrosine is zero). The table shows dityrosines and tyrosines detected in RANTES incubated with metal chloride salts plus 200 μM H_2O_2. Data is also expressed as a ratio of the number of tyrosine residues to dityrosines present (Y/DiY).

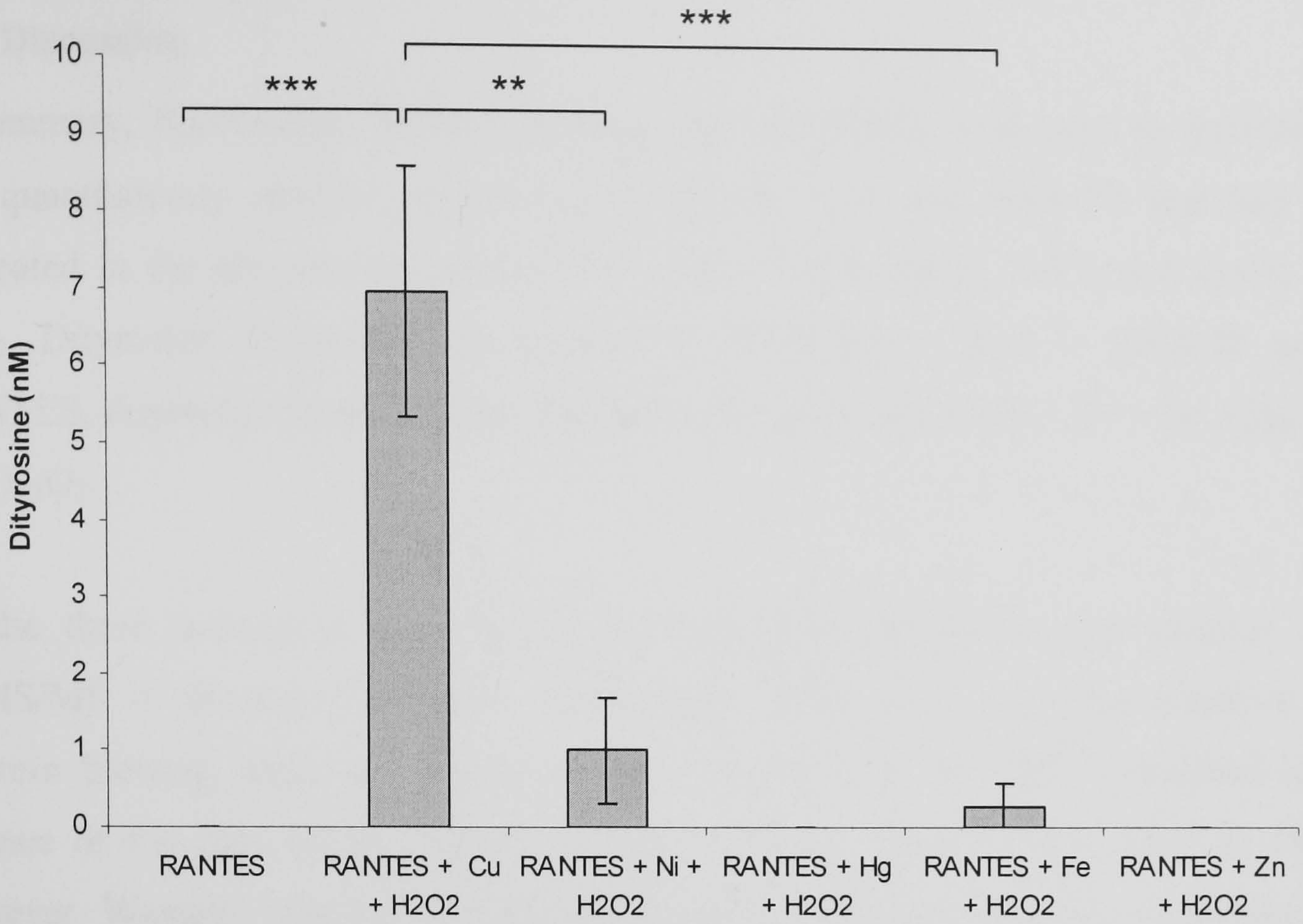

Figure 3.25. The effect of metal ions on DiY formation. RANTES incubated with 50 μM $CuCl_2$ $NiCl_2$ $HgCl_2$, $FeCl_3$ or $ZnCl_2$ plus 200 μM H_2O_2. ** indicates $p < 0.01$, * indicates $p < 0.001$. Values are expressed as means ± SEM (n = 3).**

Although Hg, and Zn did not induce dityrosine formation, Fe and Ni both induced dityrosine formation in RANTES but at levels significantly lower than those induced by Cu.

3.6. Discussion

In summary, fluorimetry, Western blotting and LCMS/MS were used to qualitatively and quantitatively analyse samples of RANTES, IL-8 and ENA-78 that had been incubated in the absence and presence of $CuCl_2$, $NiCl_2$, $HgCl_2$, $FeCl_3$ and $ZnCl_2$ plus H_2O_2. Dityrosine formation was greatest in RANTES > IL-8 > ENA-78 and in RANTES, dityrosine formation was greatest in the presence of Cu > Ni > Fe > Hg = Zn plus H_2O_2.

Of the three techniques used to detect dityrosines, sensitivity was greatest using LCMS/MS > Western blotting > fluorimetry. Fluorimetry was less sensitive than Western blotting, since no dityrosines were detected in RANTES incubated in the absence of Cu plus H_2O_2, whereas Western blotting detected dityrosines in dimers. However Western blotting did not detect any dityrosines in IL-8, indicating that LCMS/MS is a more sensitive technique. LCMS/MS is also quantitative and has previously been used to determine dityrosines in oxidised wheat-flour dough (Takasaki *et al*, 2005). The MRM pairings used in these previous studies showed outstanding sensitivity and selectivity, making this technique very useful for quantifying dityrosines in chemokine multimers.

Both fluorimetry and Western blotting have previously been used to detect dityrosines in Aβ-peptide multimers. Using an excitation wavelength of 300 nm, analysis of Aβ-peptide incubated with $CuCl_2$ (25 μM) plus H_2O_2 (250 μM) for 1 day resulted in an increase in the characteristic fluorescence signal at 400 nm for dityrosine cross-links (Atwood *et al*, 2004). Dityrosines were detected by fluorimetry in the dityrosine-BSA standard with an emission peak at 410 nm and in RANTES multimers with an emission peak of 404 nm. Although the emission peaks are not identical, they are present in a similar range. The incorporation of aromatic residues into peptides has little direct effect on their absorbance properties, but the aromatic residues are very sensitive to their immediate environment (Wetlaufer, 1962). This suggests that dityrosines may have slightly varied spectral properties due to minute differences in the peptide environment in which they were analysed, resulting in a shift in the emission peaks.

The IC3 antibody was previously used to detect dityrosines in Aβ-peptide multimers on Western blots. In these studies, Western blotting was also shown to be more sensitive than fluorimetry as Aβ-peptide multimers were detected both in the presence of $CuCl_2$ alone (without the addition of H_2O_2) and in the presence of $CuCl_2$ plus H_2O_2 (Atwood *et al*, 2004).

Positive staining for dityrosines in RANTES multimers on Western blots was dependent on the presence of Cu and H_2O_2 during incubation of the chemokine, indicating that these oxidative conditions promote dityrosine formation. RANTES multimers were not detected in the presence of H_2O_2 alone (Section 2.5.1) and similarly, dityrosines were not detected in Aβ-peptide oligomers in the presence of H_2O_2 alone (Atwood *et al*, 2004), suggesting that both RANTES multimers and Aβ-peptide multimers contain dityrosine cross-links that are generated in the presence of Cu plus H_2O_2. Dityrosines were detected in RANTES multimers (including the dimer) but not in monomeric RANTES indicating that dityrosines are associated with multimer formation. In the absence of Cu plus H_2O_2 dityrosines were detectable in the RANTES dimer but staining was very faint indicating that dityrosines are present at lower concentrations than in the presence of Cu plus H_2O_2.

While redox reactions contribute to the formation of dityrosines and multimerisation of RANTES, in excess, oxidative damage occurs to both RANTES (Section 2.5.1) and dityrosines (Section 3.5.2). The limiting effect of HS on dityrosine formation in RANTES multimers is similar to the effect observed with RANTES, IL-8 and ENA-78 multimer formation in the presence of Cu plus H_2O_2 (Section 2.5.1) and it is speculated that the effect is due to the known free radical scavenging properties of HS, as discussed in Section 2.6.

RANTES multimers are clearly linked by stable and covalent dityrosine links, as indicated by their resistance to SDS and both G-HCl and 2-ME treatment. The presence of dityrosine cross-linked residues confirms the formation of covalent links. This is similar to the result reported in section 2.5.1 where RANTES, IL-8 and ENA-78 multimers were resistant to G-HCl. Previous studies have shown that GAG binding and RANTES multimerisation are essential for the chemotactic properties of RANTES *in vivo*. The dimeric form of RANTES was shown to be devoid of activity, whereas the

tetramer was fully active, indicating that a tetramer is required for *in vivo* activity of this chemokine (Proudfoot *et al*, 2003). GAG interaction and multimerisation is thought to facilitate the retention of chemokines on cell surfaces, thereby maintaining a chemokine gradient and a high local concentration for cell activation (Proudfoot, 2006).

However, certain chemokines, such as MCP-3 and eotaxin which both have two tyrosine residues appear to be naturally occurring monomers, because structural and biophysical studies have failed to provide evidence of multimerisation and MCP-3 is fully active as a monomer but it is not known whether these chemokines multimerise on cell surface proteoglycans (Crump *et al*, 1998; Keizer *et al*, 2000; Kim *et al*, 1996).

Thus, multimerisation may be important only for some chemokines, and may have functional implications or depend on the site of production. It has been suggested that chemokines that are functional in recruiting cells from the circulation into the underlying tissue may require multimerisation to function under flow conditions, whereas those produced within the extravascular space may not (Proudfoot *et al*, 2003). It has also been hypothesised that chemokines whose GAG binding sites overlap with receptor binding sites, as is the case for RANTES and MCP-1, may require multimerisation to bind GAGs through some of the subunits while exposing other subunit binding sites to the receptor. Interaction of chemokines with leukocyte receptors through the exposed binding site could then trigger release of chemokine monomers from the multimer complex, allowing the entire binding site, which is partially buried in the multimers, to interact with the receptor (Paavola *et al*, 1998; Proudfoot *et al*, 2003).

The observation that RANTES multimers are covalently linked via dityrosine cross-links indicates that these multimers are highly stable and functionally relevant. The binding of stable RANTES multimers to endothelial expressed GAGs by electrostatic interaction may serve to concentrate RANTES on the endothelial cell surface, thereby maintaining a concentration gradient and a high local concentration of RANTES to facilitate leukocyte activation. In addition, the multimerisation and stabilisation of RANTES by covalent dityrosine cross-links may prevent proteolytic degradation, also facilitating the formation and maintenance of a stable chemotactic gradient, which is essential for leukocyte recruitment during inflammation.

The generation of dityrosine in proteins is a normal physiological process in specialised cases and a result of exposure to environmental agents in others (Malencik *et al*, 1996). Dityrosine cross-links are naturally occurring in certain proteins as discussed in Section 3.1.2, however, the formation of dityrosines *in vivo* is a generalised sign of oxidative stress, and may be a useful marker for assessing oxidative damage to proteins. The occurrence of dityrosines is relatively common during free radical reactions, due to the oxidative modification of proteins (Malencik *et al*, 1996; Smith *et al*, 2007). Agents that promote the *in vivo* formation of dityrosine include ultraviolet irradiation, hydroxyl radicals, peroxynitrite, and lipid hydroperoxides (Karam *et al*, 1984; Kikugawa *et al*, 1994; van der Vliet *et al*, 1997) and exposure to H_2O_2 results in the conversion of globin tyrosyl residues to dityrosine in the case of metmyoglobin or oxyhaemoglobin (Giulivi & Davies, 1993; Tew & Ortiz de Montellano, 1988). Thus, dityrosine formation may be more likely to occur under oxidative conditions, and the generation of H_2O_2 in oxidative stress during inflammation may promote dityrosine cross-link formation in chemokines, facilitating the formation and maintenance of stable chemotactic gradients.

The occurrence of higher order multimers at lower concentrations of H_2O_2 in the presence of 2-ME was unexpected. A possible explanation may be that 2-ME is a thiol capable of converting oxygen radicals to reactive sulphur radicals with subsequent generation of H_2O_2 (Kim *et al*, 1989) as follows:

$$HOCH_2CH_2SH + O2^- + H^+ \longrightarrow RS^- + H_2O_2$$

(2-ME)

This generation of H_2O_2 by 2-ME could contribute to redox cycling and result in dityrosine cross-linked multimer generation, at lower concentrations of added H_2O_2.

The antibody, IC3, has previously been shown to be highly specific for both protein dityrosine and free dityrosine (Kato *et al*, 2000). The specificity of the dityrosine antibody is confirmed since ENA-78 (which has no tyrosine residues) multimers did not stain positively for dityrosines, nor were dityrosines were detected by LCMS/MS in ENA-78 multimers, indicating the specificity of the technique. This indicates that ENA-78 multimers are not dityrosine cross-linked and that there is another interaction occurring in the formation of multimers in this chemokine that does not involve

dityrosines. In addition, RANTES multimers persist when dityrosines are degraded in the presence of high concentrations of H_2O_2 which also suggests that other links are also involved in RANTES multimer formation, in addition to dityrosine cross-links.

Using LCMS/MS, dityrosines were detectable in IL-8 (which has one tyrosine residue) multimers but were more abundant in RANTES (which has five tyrosine residues) multimers. Since RANTES multimers contained a mean ratio of 68.2 tyrosines : 1 dityrosine, this indicates that only a small proportion of the tyrosine residues within RANTES form dityrosine cross-links, adding to the evidence that other interactions are involved in RANTES multimerisation.

Non-dityrosine cross-links could form through the abstraction of hydrogen atoms from chemokines by free radicals. The sulphur containing amino acids are particularly susceptible. The amino acid radicals generated (such as cysteine or methionine radicals) can form disulphide bridges, protein-protein covalent bonds and cross-links (Horton & Fairhurst, 1987; Smith *et al*, 2007; Smith *et al*, 2006). In addition, non-dityrosine cross-linking could occur due to the formation of an intermolecular histidine bridge between Cu (II) atoms as discussed in Section 2.6.

It would be useful to study the involvement of histidine residues by using histidine blocking to investigate the formation of histidine bridges in chemokine multimers in addition to dityrosine cross-links, since ENA-78 contains one and RANTES and IL-8 have one and two histidine residues respectively, as described in Chapter 2, Section 2.6. Histidine blocking would involve the incubation of chemokines with compounds that are known to have histidine association capacity, such as imidazole (Arispe *et al*, 2008). Inhibited or diminished chemokine multimer formation would confirm the involvement of histidine residues in chemokine multimer formation.

A mechanism has been proposed for Cu-induced dityrosine cross-linking of Aβ1-28, Aβ1-40 and Aβ1-42 that is dependent on a Cu (II) mediated oxidative mechanism (Atwood *et al*, 2004; Kato *et al*, 2001; Liu *et al*, 2006) as discussed in Section 2.6. Similarly, dityrosine cross-links could be induced in chemokine multimers by a Cu (II) mediated oxidative mechanism.

The initial driving force for dityrosine cross-link formation may be the coordination of Cu ions to histidine residues of RANTES or IL-8. Histidine residues have been implicated in dityrosine cross-link formation in the Aβ-peptide (discussed in Section 2.6). This is a likely mechanism for the formation of dityrosine cross-links in chemokine multimers. It is proposed that the chemokine acts as the reductant, reducing Cu (II) to Cu (I) upon binding to histidine residues. Tyrosine residues in the vicinity can extract an electron from Cu (I) to form a carbon centred radical which can then covalently link to another adjacent tyrosyl radical, forming a stable dityrosine cross-link (Malencik *et al*, 1996).

It is postulated that Cu (I) can be oxidised to Cu (II) by molecular oxygen with the generation of the superoxide ion (figure 3.26, equation 1). Cu (II) is reduced to Cu (I) on interaction with RANTES or IL-8 histidine residues. The tyrosine oxidation that occurs from the interaction of Cu (I) with tyrosine residues would result in tyrosyl radical formation and subsequent dityrosine cross-link and RANTES or IL-8 multimer formation. It would also result in the oxidation of Cu (I) back to Cu (II) (2).

(1) $Cu^{1+} + O_2 \rightarrow Cu^{2+} + O_2^-$

(2) $CK + Cu^{2+} \rightarrow Cu^{1+} + CK : CK^+$

(3) $O_2^- + O_2^- + 2H^+ \rightarrow H_2O_2 + O_2$

(4) $H_2O_2 + Cu^{1+} \rightarrow Cu^{2+} + OH^- + OH^{\cdot}$

Figure 3.26. Suggested mechanism for the formation of Cu induced dityrosine cross-links in RANTES or IL-8 involving a Cu redox system. CK = chemokine.

However, Cu (I) could be oxidised back to Cu (II) through an interaction with molecular oxygen (1), or with H_2O_2, which if present, will enhance the recycling of Cu. An interaction with H_2O_2 would produce hydroxyl radicals as observed by (Kawanishi *et al*, 2002) (4). H_2O_2 can also form from the dismutation of superoxides (3).

It has previously been reported that the Cu/H_2O_2 oxidative system but not H_2O_2/Fe-EDTA, ascorbate/Cu and ascorbate/Fe-EDTA systems induces dityrosine cross-linking in lens proteins (Kato *et al*, 2001).

However, the Aβ-peptide aggregates in the presence of trace levels (< 0.8 μM) of Fe (III) (Huang *et al*, 2004), suggesting multimerisation effects are not restricted to Cu. The Aβ-peptide can bind Cu (II), Fe (III) and Zn (II) and both Cu (II) and Fe (III) induce Aβ-peptide aggregation. The interaction between the Aβ-peptide and Cu (II) or Fe (III) results in redox chemistry due to the redox activity of the Aβ-peptide that allows it to reduce Cu (II) to Cu (I) and Fe(III) to Fe(II). In the presence of oxygen, this leads to H_2O_2 production (Huang *et al*, 1999). It has also been suggested that other ions such as Ni (II) or Co (II) may cause Aβ-peptide multimerisation, although Ni (II) is present at trace levels compared to Cu, Fe and Zn which are more abundant in biological systems, and Co (II) is not present in an ionic form in biological systems (Huang *et al*, 2004).

Interestingly, both Ni and Fe were found to induce limited dityrosine formation in RANTES. It is possible that RANTES may bind Fe and Ni utilising a similar mechanism for dityrosine formation as that described for Cu, above. An interaction between RANTES and Fe (III) or Ni (II) could result in redox activity of RANTES and the reduction of Fe (III) to Fe (II) and Ni (II) to Ni (I) and in the presence of oxygen, this leads to H_2O_2 production which causes the redox to propagate.

The toxic effects resulting from iron overload generally have been attributed to the generation by iron of intracellular free radicals causing lipid peroxidation (Horton & Fairhurst, 1987). It is well known that Fe participates in redox cycling and generates free radicals through a reaction with H_2O_2 or molecular oxygen to generate the superoxide ion, and hydroxyl radical. The iron-dependent decomposition of H_2O_2 was originally postulated by Fenton, and has become known as the Fenton reaction (Imlay *et al*, 1988).

The Fenton reaction

$$Fe^{2+} + H_2O_2 \longrightarrow Fe^{3+} + OH^- + OH^{\cdot}$$

Generation of the superoxide radical

$$Fe^{3+} + H_2O_2 \longrightarrow Fe^{2+} + O_2^- + 2H^+$$

$$Fe^{2+} + O_2 \longrightarrow Fe^{3+} + O_2^-$$

The Fe catalysed generation and cycling of ROS leads to lipid peroxidation and cell damage. Furthermore, Fe^{3+} can react with H_2O_2 to generate metal-oxygen complexes that induce DNA damage (Kawanishi *et al*, 2002).

It has been reported than Fe generates Aβ-peptide oligomers (Huang *et al*, 2004) and although no Fe redox mechanism was suggested, the following may be a possible mechanism for the generation of dityrosine cross-linked multimers of RANTES in the presence of molecular oxygen. This is a similar mechanism to that described for Cu, above. The reaction is propagated by H_2O_2 production.

It is postulated that Fe (II) can be oxidised to Fe (III) by molecular oxygen with the generation of the superoxide ion (figure 3.27, equation 1). Fe (III) is reduced to Fe (II) on interaction with RANTES histidine residues. The tyrosine oxidation that occurs from the interaction of Fe (II) with tyrosine residues would result in tyrosyl radical formation and subsequent dityrosine cross-link and RANTES multimer formation (2).

(1) $Fe^{2+} + O_2 \rightarrow Fe^{3+} + O_2^-$

(2) $RANTES + Fe^{3+} \rightarrow Fe^{2+} + RANTES : RANTES^+$

(3) $O_2^- + O_2^- + 2H^+ \rightarrow H_2O_2 + O_2$

(4) $H_2O_2 + Fe^{2+} \rightarrow Fe^{3+} + OH^- + OH^{\cdot}$

Figure 3.27. Suggested mechanism for the formation of dityrosine cross-links in RANTES involving an iron redox system.

In order to cycle Fe (II) back to Fe (III), Fe (II) might interact again, with molecular oxygen (1), or with H_2O_2, which if present, will enhance the recycling of Fe. An interaction with H_2O_2 would produce hydroxyl radicals (4). H_2O_2 can also form from the dismutation of superoxides (3).

Ni (II) is known to cause oxidative DNA damage through the induction of DNA-DNA or DNA-protein cross-links (Wozniak & Blasiak, 2002). Ni (II) ions have been shown to bind DNA and subsequently react with H_2O_2 to cause strong DNA damage

(Kawanishi *et al*, 2002). It is also postulated that the genotoxic effects of Ni (II) can result from the generation of ROS in the reaction between metal and proteins. These radicals can subsequently interact with DNA, inducing damage to its bases, DNA strand breaks and DNA-protein cross-links (Wozniak & Blasiak, 2002). The DNA damage can be inhibited by hydroxyl radical scavengers such as DMSO, catalase or methionine (Kawanishi *et al*, 2002; M'Bemba-Meka *et al*, 2005), and Ni (II) induced DNA fragmentation and cell death is significantly diminished by the antioxidants ascorbic acid and N-acetyl cysteine (Jia & Chen, 2008). It is therefore generally accepted that ROS contribute to the carcinogenic and cytotoxic effect of Ni (II).

The cytotoxic mechanism is believed to involve hydrogen peroxide and other ROS which are generated as a result of the reaction between metals and proteins. The hydroxyl radical can be generated by the reaction of Ni (II) with cysteine in the presence of molecular oxygen (Wozniak & Blasiak, 2002). Ni (II) was also shown to react with H_2O_2 to produce hydroxyl free radicals, superoxide and metal-oxygen complexes that cause site specific oxidative damage (Kawanishi *et al*, 2002). In addition it has been shown that Ni induces NF-kB through the generation of H_2O_2 (Kennedy *et al*, 1998).

Since Ni (II) is capable of inducing DNA-protein cross-links, and can generate ROS on interaction with proteins (including the generation of the hydroxyl radical on interaction with cysteine residues, and the superoxide and hydroxyl radical on reaction with H_2O_2), it is proposed that Ni (II) may be able to induce cross-linking between the tyrosine residues of chemokines.

An obvious mechanism for protein cross-linking would be the interaction of Ni (II) with cysteine residues in RANTES to induce cross-linking, with the subsequent generation of free radicals. However, this does not explain the observation that dityrosines, specifically, were formed following the incubation of RANTES with $NiCl_2$.

A possible explanation is also a similar mechanism to that described for Cu. Fe is substituted for Cu and the reaction is propagated by H_2O_2.

Redox mechanism involving Nickel

(1) $Ni^{2+} + O_2 \rightarrow Ni^{3+} + O_2^-$

(2) $RANTES + Ni^{3+} \rightarrow Ni^{2+} + RANTES : RANTES^+$

(3) $O_2^- + O_2^- + 2H^+ \rightarrow H_2O_2 + O_2$

(4) $H_2O_2 + Ni^{2+} \rightarrow Ni^{3+} + OH^- + OH^{\cdot}$

Figure 3.28. Suggested mechanism for the formation of dityrosine cross-links in RANTES involving a nickel redox system.

Cu exists in oxidation states 1 and 2 and Zn exists only in oxidation state 2 and cannot be reduced. It appears that this oxidative property of Cu is important for the formation of dityrosines by means of a redox system, as previously proposed. Interestingly, although Hg has very similar oxidative properties to Cu, existing in oxidation states 1 and 2, it failed to induce dityrosine cross-linking. Zn (II) has been shown to bind and inhibit Aβ-peptide aggregation through the inhibition of Aβ-peptide mediated Cu (II) reduction and subsequent H_2O_2 production (Cuajungco *et al*, 2000). Therefore, it is possible that there is a similar effect where both Zn (II) and Hg (II) can bind RANTES but are unable to participate in redox reactions. A possible explanation for the failure of both Zn and Hg to induce dityrosine cross-linking is that both have a complete d sub-shell configuration (d^{10}) and therefore they are not true transition metals. Their ability to retain a complete d sub-shell configuration may render them more chemically unreactive than Cu, Ni and Fe and prevent them from participating in redox reactions.

Chapter 4

The role of copper in platelet-derived RANTES-induced T-cell chemotaxis and transendothelial migration

4. The role of copper in platelet-derived RANTES-induced T-cell chemotaxis and transendothelial migration

4.1. Introduction

4.1.1. Platelets in inflammation

4.1.1.1. Platelets in haemostasis and thrombosis

Platelets are anucleate cytoplasts of myeloid origin that have a life span of 8 -12 days and circulate in a resting state in the blood (Hartwig & Italiano, 2003). Two theories of platelet formation have been proposed based on studies conducted in model systems and *in vivo.* In one, platelets are produced in the bone marrow, following the cytoplasmic fragmentation of megakaryocytes which generates mature circulating platelets (Mandal *et al*, 2007; Zucker-Franklin & Philipp, 2000). A second model proposes that differentiated marrow megakaryocytes extend multiple elongated processes termed proplatelets. Platelets form at the ends of proplatelets after regulated translocation of intracellular constituents to proplatelet tips via microtubular tracks, and then bud off and circulate in the bloodstream (Hartwig & Italiano, 2003; Patel *et al*, 2005). Studies of differentiation of mouse and human haematopoietic stem cells to megakaryocytes *in vitro* support this second model (Choi *et al*, 1995; Cramer *et al*, 1997; Denis *et al*, 2005; Hartwig & Italiano, 2003; Patel *et al*, 2005; Weyrich *et al*, 2007). A study using intravital microscopy also reported proplatelet formation in mice *in vivo* (Junt *et al*, 2007).

The role of platelets in the coagulation cascade is mediated principally by thrombin. Thrombin is produced predominantly on the surface of circulating platelets as a result of the proteolytic activation of pro-thrombin which is constitutively synthesised by the liver and released into the circulation. Prothrombin binds to platelets and is proteolytically activated by factor Xa and its cofactor Va. The activation of Xa is mediated by both factor IV with its cofactor VIII and factor VII and its cofactor tissue factor, a membrane protein expressed at sites of vascular injury (Patterson *et al*, 2001).

Activated thrombin has a central role in the coagulation cascade, inducing clot formation via its serine protease activity, which cleaves fibrinogen to fibrin, thereby mediating fibrin deposition. Thrombin activates factor XI, factor V and factor VIII accelerating the production of thrombin in a positive feedback mechanism. Thrombin

also activates factor XIII, which catalyses the formation of covalent bonds between lysine and glutamine residues in fibrin increasing the stability of the fibrin clot (Coughlin, 2000).

In addition to its role in the coagulation cascade, thrombin also mediates the activation of platelets, facilitating thrombosis. Platelets can be activated by thrombin and ADP as well as antigens, platelet activating factor (PAF), collagen, antigen-antibody complexes, thromboxane A_2, epinephrine, serotonin, micro-organisms and bacterial endotoxins including lipopolysaccharides (Derian *et al*, 2002; O'Sullivan & Michelson, 2006). Once activated, platelets adhere to the vascular wall via the binding of platelet expressed glycoprotein to exposed endothelial collagen, recruit circulating platelets and mediate platelet aggregation through expression of the integrin $\alpha_{IIb}\beta_3$ and its interaction with fibrinogen or von Willebrand factor, and release proinflammatory mediators including further thrombin secretion. Activated platelets aggregate to form a thrombus which seals the damaged blood vessel (Johnson, 1999; Weyrich *et al*, 2003).

The cellular effects of thrombin are primarily mediated by protease-activated receptors (PARs). The PARs are a subfamily of related G-protein-coupled receptors that are activated by cleavage of the N-terminus of the receptor serine proteases. In the cleaved state, the newly formed N-terminus acts as the agonist, causing a physiological response (Coughlin, 2000).

There are 4 known PARs, numbered 1-4. These receptors are expressed throughout the body but highly expressed in platelets, endothelial cells, myocytes and neurons. Thrombin acts on PARs 1, 3 and 4, although thrombin mediated cleavage of PAR4 occurs at higher concentrations than are required for the activation of PAR1 and PAR3 (Patterson *et al*, 2001) and PAR2 is activated by multiple trypsin-like serine proteases including trypsin itself, mast cell tryptase, neutrophil proteinase 3, tissue factor, factor VIIa, factor Xa, and membrane-tethered serine protease-1 (Coughlin, 2000). Human platelets express PAR1 and PAR4, and activation of either is sufficient to trigger platelet activation, aggregation and degranulation causing the secretion of proinflammatory mediators. Thrombin signalling in platelets contributes to hemostasis and thrombosis whilst endothelial PARs 1 and 2 participate in the activation of the endothelium and promote vasodilatation, the adhesion and rolling of platelets and

leukocytes as well as leakage of plasma proteins to the extravascular space. Thrombin activation of endothelial PAR1 also triggers endothelial production of the neutrophil activator, platelet-activating factor, as well as the interleukins IL-6 and IL-8 (Coughlin, 2000).

4.1.1.2. The inflammatory role of platelets

Whilst platelets are well known to play an important role in haemostasis and thrombosis, it is also apparent that they have a function in inflammation, including the release of proinflammatory mediators, and interactions with leukocytes and endothelial cells. Platelets have long been known to play a role in the pathogenesis of asthma and humans with asthma have increased numbers of circulating platelets as compared with control subjects (Moritani *et al*, 1998). It has been reported that platelets promote leukocyte trafficking from blood vessels into lung tissue in allergen-sensitised mice through leukocyte-aggregate formation which is dependent on P-selectin expression on the surface of platelets (De Sanctis *et al*, 1997; Pitchford *et al*, 2005; Pitchford *et al*, 2003; Ulfman *et al*, 2003) and increased numbers of platelet-leukocyte aggregates were observed in the blood of human subjects with allergic asthma than healthy control subjects (Pitchford *et al*, 2003).

Selectin interactions are required to induce leukocyte rolling prior to the firm attachment and diapedesis of leukocytes across the endothelium. Although endothelial P-selectin expression alone can lead to leukocyte rolling, this process is much more efficient in the presence of platelet expressed P-selectin. Activated platelets can bind to leukocytes, forming leukocyte-platelet aggregates including T-cell-platelet aggregates (de Bruijne-Admiraal *et al*, 1992). The interaction of platelet expressed P-selectin with PSGL-1 expressed on leukocytes results in the formation of platelet-leukocyte aggregates (McEver, 2002). The subsequent activation of leukocytes and up-regulation of leukocyte expressed integrin adhesion molecules including CD11b and VLA-4, lead to tight leukocyte-platelet adhesion. Expression of these adhesion molecules allows for firm attachment of leukocytes to vascular endothelium followed by diapedesis (O'Sullivan & Michelson, 2006; Pitchford *et al*, 2005; Pitchford *et al*, 2003; Weyrich *et al*, 2003).

Platelets have been reported to undergo chemotaxis and can migrate out of blood vessels into lung tissue *in vivo* in allergen-sensitised mice in response to a sensitising

allergen (Pitchford *et al*, 2008; Pitchford *et al*, 2003). Platelets also contain and release adhesive proteins, activate other inflammatory cells and release vasoactive substances and pro-inflammatory mediators upon activation. Platelets contain three major secretory organelles: the lysosome, the dense granule, and the α-granule. Platelet-derived mediators are stored mainly in the α-granules of human platelets and released upon activation. Such mediators include interleukin-1 (IL-1) which activates the endothelium (Hawrylowicz *et al*, 1991), the prostaglandins and platelet activating factor as well as a host of chemokines (reviewed in O'Sullivan and Michelson, 2006). Among the mediators released from the α-granules is the chemokine RANTES (Kameyoshi et al, 1992; Kameyoshi et al, 1994; Klinger et al, 1995; Schroder et al, 1994; von Hundelshausen et al, 2001). The less abundant dense granules, numbering three to eight per platelet contain several mediators including calcium, polyphosphates, adenosine diphosphate (ADP), adenosine triphosphate (ATP), and serotonin and the relatively scarce lysosomes contain acidic hydrolases (Rendu & Brohard-Bohn, 2001).

Although platelets do not have nuclei, they do contain limited amounts of mRNA and, in addition, it has been shown that platelets are capable of protein synthesis and can not only release, but also synthesise RANTES (Power *et al*, 1995). Most importantly, platelet-derived RANTES has been shown to increase leukocyte arrest on the activated human lung microvascular endothelium and it was demonstrated that endothelial activation with IL-1 and TNF-α was essential to induce endothelial RANTES binding (Baltus *et al*, 2005; Schober *et al*, 2002; von Hundelshausen *et al*, 2001). In addition, platelets can secrete soluble GAGs. Platelet-derived chondroitin sulphate A has been shown to both increase the binding and presentation of RANTES on the microvascular endothelium and increase the interaction of RANTES with CCR5 bearing leukocytes, indicating another mechanism by which platelets may contribute to increased recruitment of leukocytes (Weingart *et al*, 2008).

It is speculated that RANTES released by infiltrated T-cells and platelets and possibly also by other cells, could contribute significantly to selective T-cell/basophil/eosinophil recruitment (Schroder *et al*, 1994). Thus platelet activation, P-selectin expression and platelet chemotaxis with subsequent chemokine release may enhance leukocyte recruitment to sites of vascular injury or inflammation, indicating an important role for platelets in leukocyte recruitment.

4.1.2. RANTES presentation on heparan sulphate proteoglycans in multimeric form

Heparan sulphate (HS) is the most ubiquitous glycosaminoglycan (GAG) (50 – 90 % of all GAGs) in the human body and is the most predominant GAG found in the lungs. It has been well documented that RANTES binds predominantly to HSPGs on human microvascular endothelial cells and HUVECs *in vitro* with a higher affinity than many other chemokines (Ali *et al*, 2002; Hillyer & Male, 2005; Hoogewerf *et al*, 1997; Proudfoot *et al*, 2001). RANTES must interact with GAGs to elicit cell migration *in vivo,* and it has been shown that RANTES multimerises on interaction with cell surface HS thereby increasing the local concentration, maintaining a chemotactic gradient and facilitating receptor binding on leukocytes. In addition it has been reported that RANTES has a minimal tetrameric structure for *in vivo* activity (reviewed in Sections 1.10 and 2.1.1) and Cu has been shown to induce RANTES multimerisation (Chapters 2 and 3).

It has been reported that the clearance of chemokines differs dramatically in lungs and skin, with slow clearance from lungs and rapid clearance from skin (Frevert *et al*, 2002). It was reported that dimerisation of the neutrophil chemoattractant IL-8 is an important mechanism that prolongs retention of IL-8 in lungs but not in skin. These differences in IL-8 retention may be due to tissue-specific differences in the composition of GAGs or the binding affinity of a specific subset of GAGs, such as heparan sulphate and chondroitin sulphate for IL-8. Thus, the mechanisms that govern the fate of IL-8 in tissue depend on the site at which IL-8 is deposited (Frevert *et al*, 2002; Frevert *et al*, 2003). It is speculated therefore that multimerisation may be an important mechanism for the retention of RANTES in lung tissue and that therapies that limit the multimerisation may be important for preventing excessive T-cell migration.

The presentation of RANTES on endothelial cells and the release of RANTES by endothelial cells, T-cells and platelets has been extensively reported, but so far there has been little investigation on the form, monomer or multimer, of RANTES released by these cells, nor the effect of Cu on this form. There have also been no reports on the effect of Cu on the endothelial bound form of RANTES.

4.1.3. Copper induced endothelial chemokine synthesis

Activated vascular endothelial cells are known to contribute to excessive inflammatory responses by secreting pro-inflammatory cytokines and chemokines including interleukin-1 (IL-1), IL-5, IL-6, IL-8, IL-11, IL-15, several colony-stimulating factors (CSF), granulocyte-CSF (G-CSF), macrophage CSF (M-CSF) and granulocyte-macrophage CSF (GM-CSF), and the chemokines, monocyte chemotactic protein-1 (MCP-1), RANTES, and growth-related oncogene protein-alpha (GRO-alpha) (Dinarello *et al*, 1993; Krishnaswamy *et al*, 1999; Marfaing-Koka *et al*, 1995). IL-8 in particular has been studied extensively since the chemotactic activity of IL-8 and neutrophil accumulation has been associated with several inflammatory diseases including systemic inflammatory response syndrome, adult respiratory distress syndrome, and multiple organ failure (Partrick *et al*, 1996; Sablotzki *et al*, 2002).

At physiologically relevant concentrations, cobalt, nickel and copper have been shown to stimulate greater IL-8 secretion from human endothelial cells than the proinflammatory cytokines TNF-α and IL-1β. Cu induces an increase in mRNA in HUVECs and HLMVECs within 24 hours, indicating early gene activation and new protein synthesis rather than IL-8 release from preformed storage sites (Bar-Or *et al*, 2003; Wagner *et al*, 1998b).

It has been shown that Cu activates the NF-kB pathway *in vitro* with subsequent TNF-α expression in the liver and lung tissues of rats (Persichini *et al*, 2006) and activation of NF-kB has been suggested as a possible mechanism for Cu induced endothelial IL-8 synthesis (Bar-Or *et al*, 2003). It has also been postulated that Cu may induce NF-kB and subsequent IL-8 synthesis through the activation of the phosphatidylinositol 3-kinase (PI3-kinase) pathway, which is activated by Cu independently of ROS generation in human fibroblasts (Bar-Or *et al*, 2003; Ostrakhovitch *et al*, 2002). PI3-kinase activates Akt which is involved in the activation of the NF-kB transcription factor (Ozes *et al*, 1999). Alternatively, Cu may activate NF-kB via mitogen-activated protein kinases (MAPKs) since Cu exposure has been shown to induce TNF-α expression and activate the MAPKs, c-Jun N-terminal kinase (JNK) and p38 MAP kinase in human bronchial epithelial cells (Samet et al, 1998).

Whilst Cu can induce NF-kB independently of ROS (Ostrakhovitch *et al*, 2002), it has become clear that Cu-induced oxidative stress may also contribute to NF-kB activation. Despite previous conflicting reports it has now been clearly demonstrated that increased serum Cu induces oxidative stress, with the generation of ROS resulting in the activation of NF-kB and subsequent TNF-α synthesis in the liver and lung tissues of rats (Persichini *et al*, 2006). H_2O_2, which is generated by Cu-redox mechanisms (Section 2.6) has also been shown to activate the PI3-kinase/Akt pathway via oxidation of the tumor suppressor PTEN, an inhibitor of the PI3-kinase/Akt pathway (Lee *et al*, 2002), but Cu^{2+} itself may also have the ability to oxidise PTEN and activate NF-kB via the PI3-kinase/Akt pathway. H_2O_2 is also a potent activator of MAPK (Fialkow *et al*, 1994) and therefore Cu-redox generated H_2O_2 may also activate NF-kB via MAPK pathways.

Additionally, Cu (II)-oxidised low-density lipoproteins have been shown to independently initiate the activation of activator protein-1 (AP-1), another transcription factor that has been associated with endothelial IL-8 expression in endothelial cells (Maziere *et al*, 1997).

The evidence that Cu induces cytokine and chemokine expression in human bronchial epithelial cells (Kennedy *et al*, 1998; Samet *et al*, 1998)(Section 1.20) and chemokine expression in HLMVECs *in vitro* (Bar-Or *et al*, 2003) together with evidence presented in this thesis to suggest that Cu promotes chemokine multimer formation (Chapters 2 and 3) indicates that Cu may have an important pro-inflammatory role and could influence leukocyte trafficking during lung inflammation. It has been reported that RANTES synthesis induced by IL-1β in human epithelial cells (Manni *et al*, 1996) and IFN-γ in HLMVECs (Sundstrom *et al*, 2001) is regulated by NF-kB, suggesting that RANTES synthesis in these cells may also be inducible by Cu, via the NF-kB pathway.

In addition, Cu-binding peptides have been shown to be effective in preventing Cu-redox and IL-8 release from endothelial cells (Rael *et al*, 2007), suggesting that Cu chelators may have therapeutic potential in inhibiting cytokine and chemokine synthesis, and subsequent leukocyte recruitment during inflammation.

4.1.4. Copper-dependent semicarbazide-sensitive amine oxidase

Lymphocyte trafficking is governed by adhesion molecules expressed both on lymphocytes and vascular endothelial cells (Section 1.1). One of the endothelial adhesion molecules involved in the multistep extravasation cascade is the copper-dependent ectoenzyme, vascular amine oxidase-1 (VAP-1).

VAP-1 is a dimeric sialoglycoprotein with a molecular mass of 170-180 kDa (Salmi & Jalkanen, 1992; Salmi & Jalkanen, 1995; Salmi & Jalkanen, 1996). VAP-1 contains two atoms of copper per dimer co-ordinated by three conserved histidines - one His-X-His motif and another histidine near the N-terminus (reviewed in Jalkanen and Salmi, 2001). VAP-1 is constitutively present in intracellular granules within endothelial cells (Salmi *et al*, 1993) but is only translocated lumenally from intracellular storage granules upon elicition of inflammation (Salmi *et al*, 1993). Animal studies, using an *in vivo* immunodetection method have provided convincing evidence that luminal VAP-1 is induced only upon elicitation of inflammation at lesion sites (Jaakkola et al, 2000).

It has been reported that VAP-1 is important for both the rolling phase and also the transmigration step of leukocyte extravasation (figure 4.1) (Jalkanen & Salmi, 2001; Salmi *et al*, 2001). On endothelial cells, VAP-1 can serve as a traditional adhesion molecule (Lalor *et al*, 2002; Salmi & Jalkanen, 1992; Salmi & Jalkanen, 1996) but VAP-1 belongs to a distinctive group of cell surface-expressed amine oxidases known as semicarbazide-sensitive amine oxidases (SSAOs) and it has been shown that the SSAO activity of VAP-1 is also important for leukocyte adhesion (Jalkanen & Salmi, 2001; Klinman & Mu, 1994; Salmi & Jalkanen, 2005).

Mechanistic analyses have revealed that VAP-1 displays both enzyme-activity-dependent and enzyme-activity-independent adhesive functions. Thus, anti-VAP-1 antibodies, which do not interfere with the SSAO activity of VAP-1, block leukocyte extravasation. On the other hand, SSAO inhibitors also suppress VAP-1-dependent extravasation without affecting the antibody-defined epitopes (Jalkanen & Salmi, 2001; Koskinen *et al*, 2004; Martelius *et al*, 2004).

It has been suggested that VAP-1 mediates adhesion and transmigration of lymphocytes through the binding of VAP-1 sialic acid residues to an unknown leukocyte-expressed lectin (Lalor *et al*, 2002; Salmi & Jalkanen, 1992; Salmi & Jalkanen, 1996).

Previous *in vitro* and *in vivo* studies have shown that the SSAO activity of VAP-1 mediates rolling, firm adhesion and transmigration of leukocytes under normal conditions and in inflammation (Koskinen *et al*, 2004; Marttila-Ichihara *et al*, 2006; Salmi & Jalkanen, 1996; Salmi & Jalkanen, 2001).

VAP-1 possesses MAO activity and it is generally agreed that *in vitro,* SSAOs only accept primary amines as substrates, with benzylamine and methylamine being the preferred substrates *in vitro* (Salmi *et al*, 2001). It has also been reported that VAP-1 binds to a primary amino group presented on the lymphocyte surface and oxidatively deaminates it in a reaction resulting in the formation of a transient covalent bond between the two cell types, which may be important in binding during the leukocyte rolling step (figure 4.1).

The SSAOs mediate oxidative deamination of primary amines in a reaction that results in the production of aldehyde, ammonium and H_2O_2. All end-products of the SSAO-catalysed reaction are biologically active compounds that may alter the function of the endothelial cells or affect other nearby cells in a paracrine manner (Jalkanen & Salmi, 2001).

Probably the most important of the end-products is H_2O_2 which, although toxic at high concentrations, is becoming increasingly recognised as a signal-transducing molecule at lower concentrations. H_2O_2 is known to up-regulate the function of transcription factors, such as NF-kB (Section 4.1.3), and hence the expression of many genes, including chemokines, adhesion molecules, cytokines and metalloproteinases (Bogdan *et al*, 2000; Finkel, 1998; Kunsch & Medford, 1999). In the vascular wall, H_2O_2 regulates the adhesive properties of endothelial cells and it has been shown that VAP-1 enzyme activity induces E- and P-selectin expression in human and mouse endothelial cells *in vitro* and that the induced selectins are induced by H_2O_2 and are functionally active in supporting leukocyte adhesion (Jalkanen *et al*, 2007).

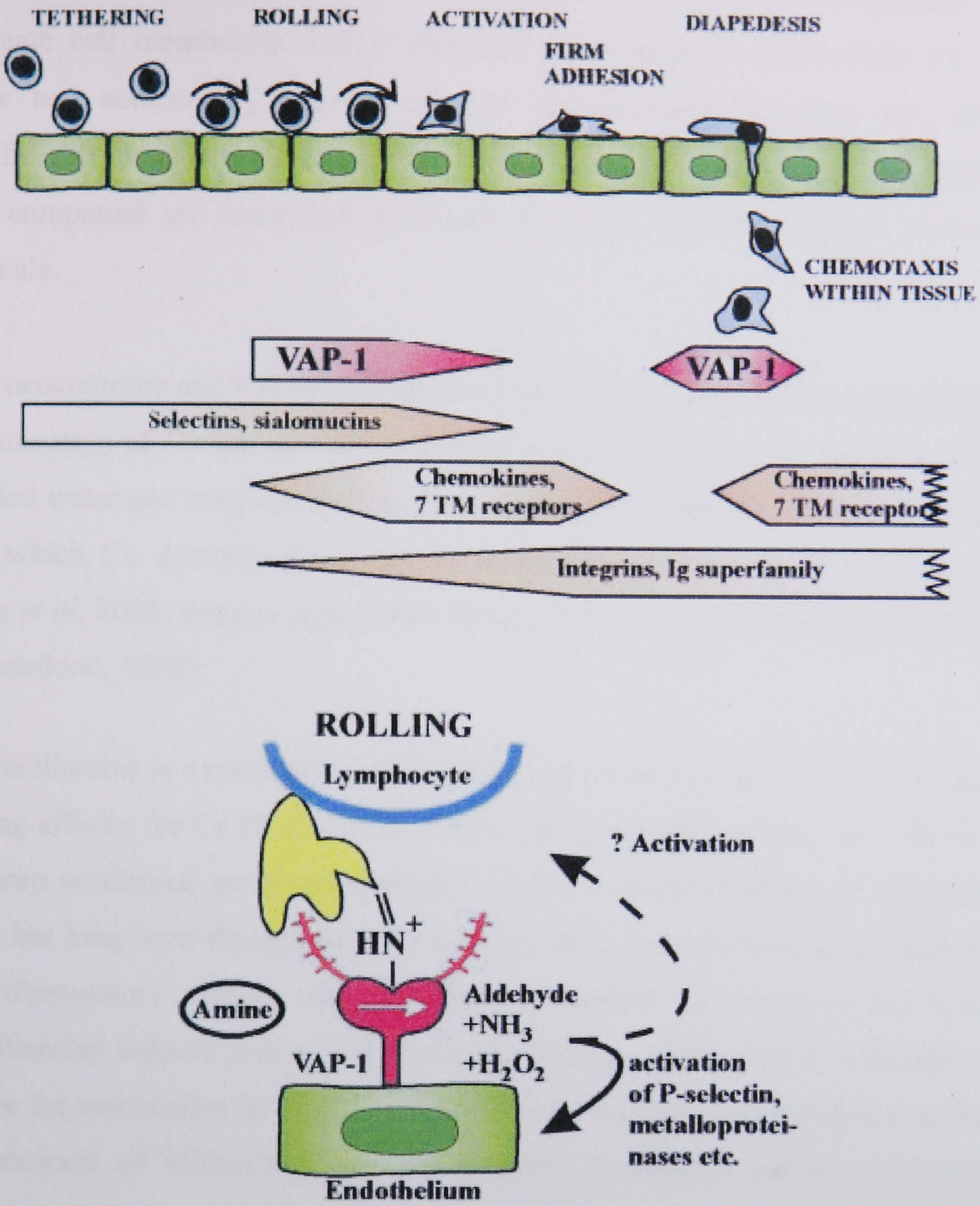

Figure 4.1. The leukocyte extravasation cascade. The different steps of the adhesion cascade and the involvement of VAP-1 are shown. The oligosaccharides of VAP-1 (purple extensions) can bind to an unknown lectin-like molecule (yellow) on lymphocytes. Alternatively, when endothelial VAP-1 uses a lymphocyte surface amine as a substrate the catalytic reaction results in the formation of a transient covalent bond between the two cell types. This enzymatic reaction seems to be involved in the binding during the rolling step (Jalkanen & Salmi, 2001).

4.1.5. Copper chelators

Neocuproine (2,9-dimethyl-1,10-phenanthroline) is an intracellular Cu chelator that can cross cellular membranes as indicated by studies that report the uptake of radio-labelled neocuproine into mycoplasmal cells (Smit *et al*, 1982). Neocuproine binds selectively to Cu (I) as confirmed by specrophotometric studies (Smith & McCurdy, 1952). Specrophotometric studies have also confirmed that the neocuproine derivative, bathocuproine disodium salt (4,7-diphenyl-2,9-dimethyl-1,10-phenanthroline), binds to

Cu (I) (Klemens *et al*, 1989; Smith & Wilkins, 1953), but this compound does not permeate cell membranes and is therefore considered an extracellular Cu chelator. These two compounds, neocuproine and bathocuproine disodium salt, are highly specific chromogens that bind to Cu to give coloured complexes. Two molecules of each compound are associated with each Cu atom, via two nitrogen atoms in each molecule.

Both neocuproine and bathocuproine disodium salt are useful in the spectrophotometric determination of Cu and also for extracting and concentrating Cu in the preparation of distilled water and reagents used in the analysis of Cu, thereby improving the certainty with which Cu determinations can be made (Buerge-Weiricht & Sulzberger, 2004; Guclu *et al*, 2005; Sozgen *et al*, 2006; Tutem *et al*, 1997; Williams *et al*, 1977; Yamini & Tamaddon, 1999).

D-penicillamine is a metabolite of penicillin and a well known Cu-chelating agent, with binding affinity for Cu (I) (Cui *et al*, 2005). The Cu binding affinity of D-penicillamine has been confirmed using spectroscopic studies (Mohanakrishnan & Chignell, 1985) and it has long been thought that this property of D-penicillamine may contribute to its anti-inflammatory effects. Although the mechanism of action is not known, D-penicillamine induces urinary Cu excretion (Walshe, 1956), and it is thought that this may be the mechanism by which D-penicillamine exerts its anti-inflammatory effects in the treatment of Wilson's disease and possibly rheumatoid arthritis (McQuaid *et al*, 1992).

Tobramycin is an aminoglycaside antibiotic used to treat bacterial infections, particularly gram positive infections. Tobramycin works by binding to a site on the bacterial 30S and 50S ribosome, preventing formation of the 70S complex. As a result, mRNA cannot be translated into protein and cell death ensues. Using potentiometric and spectroscopic studies is has been shown that tobramycin binds Cu (II) via several distinct binding sites to form strong complexes (Jezowska-Bojczuk et al, 1998), however, as yet the role of transition metal ions in the biological activity of aminoglycoside antibiotics has not been determined.

4.1.6. Objectives

The objectives of the experiments described in this chapter were to investigate:

1. The form (monomer or multimer) of RANTES expressed by endothelial cells under basal and stimulated conditions
2. The effect of $CuCl_2/H_2O_2$ on the form of RANTES expressed by endothelial cells
3. The effect of copper chelators on the form of RANTES expressed by endothelial cells
4. The effect of $CuCl_2/H_2O_2$ on the amount of RANTES expressed by endothelial cells
5. The concentration and form of RANTES released by unactivated and thrombin activated platelets
6. The concentration of RANTES released by T-cells activated *in vitro*
7. The response of T-cells to RANTES multimers, and definition of which receptors were involved
8. The role of platelet-derived RANTES in T-cell transendothelial migration
9. The effect of copper chelators on platelet-dependent T-cell transendothelial migration

4.2. Materials

Human lung microvascular endothelial cells (HLMVECs) were obtained from Clonetics (Lonza Ltd., Slough, Berkshire, UK). EGM-2MV cell growth medium was prepared by supplementing 500 ml EGM-2 Basal Medium (CC-3156, Lonza, UK) with EGM-2MV BulletKit (CC-3202, Lonza, UK) (includes Basal Medium and SingleQuots). Trypsin/EDTA (TE) containing 0.025 % trypsin and 0.02 % EDTA and trypsin neutralising solution (TNS) were also obtained from Lonza, UK. Uncoated 75 cm^2 culture vessels and 24-well companion plates were obtained from Triple Red Ltd., Long Crendon, Buckinghamshire, UK. 5μm, PVP-free polycarbonate filters were obtained from Fisher Scientific, Loughborough, Leicestershire, UK and 3 μm fibronectin coated and uncoated cell culture inserts were obtained from BD Biosciences, Oxford, Oxfordshire, UK.

Boyden chambers (48-well with 50 μl upper and 25 μl lower wells) were obtained from Neuro Probe, Maryland, USA. Anti-CCR3, anti-CCR5 neutralising antibodies, and isotype control (rat IgG2a and mouse IgG2b) antibodies were obtained from R & D Systems, Ltd., Abingdon, Oxfordshire, UK.

Lymphoprep was obtained from Axis-Shield UK, Kimbolton, Cambridgeshire, UK. Phytohaemagglutinin (PHA), fetal calf serum (FCS, heat inactivated), antibiotics, L-glutamine, bovine serum albumin (30 %, cell culture tested), sodium pyruvate (1 M), trypan blue (0.4 % (w/v) in 0.9 % (w/v) NaCl), collagen IV, thrombin, NaCl, Tris base, EDTA, sodium dodecyl sulphate (SDS), tergitol nonidet P-40, copper chloride ($CuCl_2$), hydrogen peroxide (H_2O_2), catalase, sodium phosphate (Na_2HPO_4), citric acid, dithiothreitol (DTT), sodium acetate, glacial acetic acid, tetramethylbenzidine (TMB), 2,2'-Azino-bis(3-ethylbenzthiazoline-6-sulfonic acid) (ABTS), dimethyl sulphoxide (DMSO), triton-X-100, sodium chlorate and the lactate dehydrogenase (LDH) (TOX-7) and plasmin enzyme assay kits were obtained from Sigma-Aldrich Inc., Poole, Dorset, UK. 10X Hanks balanced salt solution (HBSS) (-Ca^{2+}/Mg^{2+}), RPMI 1640 containing 25 mM HEPES, and L-Glutamine and phosphate buffered saline (PBS) (-Ca^{2+}/Mg^{2+}) were obtained from Invitrogen Ltd, Paisley, UK.

Recombinant human RANTES, interferon (IFN)-γ, tumor necrosis factor (TNF)-α, human interleukin-2 (IL-2) and the IFN-γ and TNF-α enzyme-linked immunosorbant assay (ELISA) antibody duosets were obtained from Peprotech EC, London, UK. The RANTES enzyme linked immunosorbent assay (ELISA) duoset was obtained from R & D Systems, Ltd., Abingdon, Oxfordshire, UK. 0.2 μm sterile filters were obtained from BD Biosciences, Oxford, Oxfordshire, UK. All copper chelators were supplied by Sigma, UK. The PAI-1 inhibitor, XR5118 was a gift from Xenova.

Polyacrylamide mini-gels were cast using the Bio-Rad Protean II system and markers and reagents for electrophoresis were obtained and prepared as previously described in Section 2.3.4. Gradient (4 – 15 %) polyacrylamide ready-gels were obtained from Bio-Rad Laboratories Ltd, Hemel Hempstead, Hertfordshire, UK.

Non-biotinylated goat polyclonal anti-duffy antigen receptor complex (DARC) was obtained from Abcam plc., Cambridge, UK. Biotinylated primary polyclonal rabbit anti-human RANTES antibodies and rabbit polyclonal anti-RANTES (non-biotinylated) antibodies were obtained from Peprotech EC, London, UK. Rabbit anti-goat secondary biotinylated antibodies (for DARC staining) and the streptavidin-biotinylated horseradish peroxidase complex (StreptABC) were obtained from Dako UK Ltd, Ely, Cambridgeshire, UK. A commercial enhanced chemiluminescence (ECL) kit, SuperSignal, Restore Plus Western Blot Stripping Buffer and the FOX-2 assay kit were obtained from Pierce Biotechnology Inc., Chester, UK. Tween-20, Super RX Fuji medical X-Ray film, Hema Gurr staining reagents and 24 and 6-well culture plates were obtained from Fisher Scientific, Loughborough, Leicestershire, UK.

Complete mini® Protease inhibitor tablets which when dissolved at double strength in 5 ml of water contain (EDTA (2 mM, inhibits metalloproteases), aprotinin (0.6 μM, inhibits plasmin, kallikrein, trypsin, and chymotrypsin with high activity), bestatin [(2S, 3R)-3-Amino-2-hydroxy-4-phenylbutanoyl]-L-leucine hydrochloride, (260 μM, an inhibitor of amino peptidases), calpain inhibitor I (N-Acetyl-Leu-Leunorleucinal, 34 μg/ml, inhibits activity of Calpain I), calpain inhibitor II (N-Acetyl-Leu-Leumethioninal, 14 μg/ml, inhibits activity of Calpain II), chymostatin (200 μM, specific inhibitor of α, β, γ and δ-chymotrypsin), E-64 (N-(N-(L-3-Transcarboxirane-2-carbonyl)-Lleucyl)-agmatine. 56 μM, inhibits papain and other cysteine proteases such

as cathepsin B and L), leupeptin (Ac-Leu-Leu argininal x 1/2 H_2SO_4, 2 μM, inhibits serine and cysteine proteases such as trypsin, papain, plasmin, and cathepsin B), α_2 macroglobulin (25 Inh.U, inhibits most endoproteinases, unit definition: One inhibitor unit inhibits 9.1 μg of trypsin), pefabloc SC 4-(2-Aminoethyl)-benzenesulfonyl-fluoride hydrochloride (AEBSF), 8 mM, irreversibly inhibits serine proteases. including trypsin, chymotrypsin, plasmin, plasma kallikrein, and thrombin, pepstatin (2 μM, inhibits aspartic (acid) proteases such as pepsin, renin, cathepsin D, chymosin, and many microbial acid proteases), Phenyl methyl sulfonyl fluoride (PMSF), 2 mM, inhibits serine proteases (chymotrypsin, trypsin, and thrombin) and also inhibits cysteine proteases such as papain, L-1-Chloro-3-(4-tosylamido)-7-amino-2-heptanone hydrochloride N-α-Tosyl-Llysine chloromethyl ketone (TLCK-HCl), 270 μM, irreversibly and specifically inhibits trypsin and also inhibits many other serine and cysteine proteases such as bromelain, ficin, and papain, trypsin inhibitor from chicken egg white (200 μg/ml) and trypsin inhibitor from soyabean (200 μg/ml, also inhibits factor Xa, plasmin, and plasma kallikrein) were obtained from Roche Ltd., Welwyn Garden City, Hertfordshire, UK. A protein A agarose bead suspension was obtained from Merck Chemicals Ltd., Nottingham, Nottinghamshire, UK. Vacutainers (9 ml) containing EDTA for blood collection were obtained from Greiner-Bio-One Ltd., Stonehouse, Gloucestershire, UK. Plasmin substrate; S2251 (25 mg/vial) was purchased from Chromogenix (Lexington, MA, USA).

4.3. Methods

4.3.1. Cell culture

4.3.1.1. Growth medium for endothelial cell culture

Endothelial full growth medium type 2 for microvascular cells (EGM-2MV) is optimised for use with human lung microvascular endothelial cells. The full medium was prepared from endothelial basal medium type 2 (EBM-2) and the EGM-2MV BulletKit supplements supplied by Lonza, UK. The final fully supplemented growth medium contained heat inactivated FBS (5 %), hydrocortisone (0.04 %), human fibroblastic growth factor (hFGF-2, 0.4 %), vascular endothelial growth factor (VEGF, 0.1 %), insulin-like growth factor (R^3-IGF-1, 0.1 %), ascorbic acid (0.1 %), human epidermal growth factor (hEGF, 0.1 %), gentamycin (50 ng/ml) and amphotericin-B (50 µg/ml). The contents of each supplement vial was split into 5 aliquots and frozen at -20 ^{o}C. 1 aliquot was added to 100 ml of the basal media in a sterile glass bottle, and the full medium stored at 4 ^{o}C for up to 1 week.

4.3.1.2. Culture setup/seeding

HLMVECs were seeded at 5000 cells / cm^2 in 75 cm^2 flasks with vented caps. The number of vessels to be set up was calculated with reference to the certificate of analysis and technical information supplied with the cryovial by Lonza, UK. Each flask was labelled with the passage number, cell type, lot number and date. Supplemented growth medium was aseptically transferred to uncoated culture vessels (Triple Red, UK), adding 1 ml growth medium for every 5 cm^2 flask surface area. Vented caps were applied and culture vessels allowed equilibrate at 37 ^{o}C and 5 % CO_2 in a humidified incubator for at least 30 minutes. Cryovials were thawed one at a time. Once removed from liquid nitrogen storage, vials were sterilised and opened a quarter turn to relieve the internal pressure before retightening. The bottom ¾ of the cryovial was dipped in the 37 ^{o}C water bath and swirled gently for 1 – 2 minutes until the contents were thawed, and then wiped dry. The cap was removed and the thawed cells in the vial (1 ml) were resuspended with a pipette set to 800 µl. An equal amount of cells was dispensed into each of the flasks to be set up (number of flasks calculated from the certificate of analysis supplied with the cryovial for a final seeding density of 5000 cells/ cm^2) and the vented caps replaced. Flasks were returned to the incubator and cells allowed to adhere overnight.

4.3.1.3. Feeding

The growth medium was changed one day after seeding to remove residual dimethyl sulphoxide (DMSO) from the freezing medium in which the cells were shipped and any unattached cells, and then every other day thereafter, examining them daily. Fully supplemented growth medium was warmed to 37 °C for 30 minutes. Old medium was removed from flasks by aspirating with a sterile pipette on the opposite side of the flask from where the cells were attached. New medium (15 ml) was added down the same side.

The cells were fed a larger volume of medium as they became more confluent, according to the table below.

Feeds:

Under 25 % confluent	Feed 0.67 ml per 5 cm^2 (10 ml)
From 25 – 45 % confluent	Feed 1 ml per 5 cm^2 (15 ml)
Exceeding 45 % confluence	Feed 1.5 ml per 5 cm^2 (22.5 ml)

Feeding was continued until cells were 60 – 90 % confluent.

4.3.1.4. Subculture

Cells were sub-cultured when they were 60 – 90 % confluent and displayed many mitotic figures throughout the flask. For each 75 cm^2 of cells to be sub-cultured 2 ml of trypsin/EDTA (TE) (Lonza, UK) and 4 ml trypsin neutralising solution (TNS) (Lonza, UK) was thawed and allowed to reach room temperature. EGM-2MV growth medium was pre-warmed at 37 °C and 1 ml growth medium transferred to the flasks for every 5 cm^2 surface area. Flasks were equilibrated for 30 minutes in a humidified 37 °C incubator with 5 % CO_2. Medium was aspirated from one culture vessel at a time, and the adhered cells rinsed with 5 ml 1x Hanks Balanced Salt Solution (HBSS) – Ca^{2+}/Mg^{2+} (Invitrogen, UK) The HBSS was aspirated from the flask and the cells covered with 2 ml TE solution per 75 cm^2. The cap was tightened and the cells monitored under a microscope. Trypsinisation continued until approximately 90 % of cells were rounded up. Cells were released from the culture surface by rapping the flask. The trypsin was neutralised with 4 ml of TNS per flask. The detached cells were transferred to a sterile 15 ml centrifuge tube and the flask rinsed with 2 ml of HBSS (-Ca^{2+}/Mg^{2+}) to collect residual cells which were added to the centrifuge tube. Cells were

centrifuged at 220 g for 5 minutes, and the supernatant aspirated. The pellet was re-suspended in 1-2 ml full growth medium and cells counted with a haemocytometer (10 µl suspension was added to 90 µl Trypan Blue and 10 µl was loaded onto the haemocytometer). The total number of cells was calculated and cell viability assessed.

The total number of viable cells was counted using the following formula:

Total cell count x % viability = Total no. of viable cells

Cells were diluted and seeded at the recommended seeding density (5000 cells/cm^2 for HLMVECs.) Flasks were labelled with the passage number, cell type, lot number and date and incubated at 37 ^{o}C, and 5% CO_2 until 60 – 90 % confluent.

4.3.1.5. Collagen coating 24 and 6-well plates

The method for collagen coating was adapted from the supplier's instructions. Lyophilised collagen IV (Sigma, C5533) was reconstituted to 0.1 mg/ml in 3 % (v/v) acetic acid and dissolved for several hours at 4 ^{o}C. 2 ml of collagen IV solution was added to each well of a 6-well plate, 500 µl per well for a 24-well plate. Plates were incubated for 1 hour at room temperature. Excess collagen IV was removed, the plates dried and the wells washed 3 or more times with 1x HBSS (-Ca/Mg) (Sigma) containing phenol red to remove acetic acid. Finally, plates were rinsed in 70 % (v/v) ethanol, air dried and stored at 4 °C under sterile conditions.

4.3.1.6. Subculture of HLMVECs into collagen IV coated 6-well and 24-well plates

Collagen IV coated 24-well and 6-well plates (Fisher Scientific, UK) were incubated at 37 ^{o}C and 5 % CO_2 for a minimum of 30 minutes prior to subculture. One 75 cm^2 culture flask (1 – 2 x 10^6 cells) was harvested per 24/6-well plate to be seeded. Cell medium was aspirated from flasks, followed by washing with 5 ml 1x HBSS (-Ca^{2+}/Mg^{2+}) and trypsinisation with 2 ml TE solution / 75 cm^2flask. Flasks were incubated at 37 ^{o}C and 5 % CO_2 for 10 minutes to lift cells from the culture surface. Flasks were either rapped or scraped with a cell scraper to release remaining attached cells and trypsin was neutralised with 4 ml TNS / 75 cm^2 flask. Harvested cells were aspirated, and flasks washed with 5 ml 1x HBSS (-Ca^{2+}/Mg^{2+}) which was added to the harvested cells. Cells were centrifuged at 220 g for 5 minutes, the supernatant aspirated

and the pellet re-suspended in 1 ml growth medium (EGM-2MV, Lonza, UK.) The total number of cells was calculated using a haemocytometer slide as previously described.

24-well plates

Cells were diluted to 2 x 10^5 cells / ml in 6 ml growth medium per 24- well plate and seeded at 250 µl per well. The total number of cells was 50,000 per well. Plates were covered and incubated overnight at 37 °C and 5 % CO_2. Before use in an assay, the cells were examined for mitotic figures to ensure that they had resumed active growth.

6-well plates

Cells were diluted to 2 x 10^5/ml and seeded at 1.5 ml / well. This corresponded to a total cell number of 300,000 per well. Plates were covered and incubated overnight at 37 °C and 5 % CO_2. Before use in an assay, the cells were examined for mitotic figures to ensure that they had resumed active growth.

4.3.1.7. Cryopreservation of cells

Cells were harvested as previously described in section 4.3.1.4 and centrifuged at 220 g for 5 minutes. The supernatant was aspirated leaving 100-200 µl. The pellet was re-suspended in cold freezing solution composed of EGM-2MV (Lonza, UK) containing 10 % (v/v) DMSO. Cells were counted and diluted to 500,000 – 2,000,000 cells/ml and aliquotted into freezing vials or ampoules and sealed. Cryovials were insulated in a Styrofoam or propanol freezing canister and stored at -80 °C overnight. Within 12-24 hours, cells were placed in liquid nitrogen (-200 °C) for long term storage.

4.3.1.8. Sodium chlorate

HLMVECs were grown in full growth medium supplemented with 30 mM sodium chlorate for 3 days to inhibit glycosaminoglycan (GAG) synthesis. A 10x stock solution (300 mM) was prepared in EGM-2 MV medium. The stock solution was diluted to a final concentration of 30 mM in EGM-2 MV medium (1:10 dilution). HLMVECs were re-suspended and diluted in the medium before seeding.

4.3.2. Induction of RANTES expression in HLMVECs and analysis by SDS-PAGE and Western blotting

4.3.2.1. Subculture

HLMVECs were subcultured as previously described (Section 4.3.1.6) into collagen IV coated 6-well plates in EGM-2MV culture medium, 1.5 ml / well and 2 x 10^5/ml. This corresponded to a total cell number of 300,000 per well. Plates were covered and incubated for 24 hours at 37 ^{o}C and 5 % CO_2.

4.3.2.2. Induction of RANTES synthesis

Following incubation, spent medium was aspirated from wells, and adherent cells washed once with 1x HBSS (-Ca^{2+}/Mg^{2+}) to remove non-adherent cells. New full culture medium (EGM-2MV) containing 100 U/ml IFN-γ plus 10 ng/ml TNF-α was added to each well, total volume 1380 µl. The plates were incubated for 24 hours at 37 ^{o}C and 5 % CO_2.

4.3.2.3. HLMVEC culture in 6-well plates with 12.5 – 200 µM $CuCl_2$

A 1.25 mM $CuCl_2$ (MW 134.45, Sigma, UK) solution was also prepared in serum and ascorbic acid free EGM-2MV. This was to prevent the removal of Cu through binding to serum components and the protective effects of ascorbic acid against oxidative stress, as observed by Bar-Or *et al*, 2003 (Bar-Or *et al*, 2003). The solution was filter-sterilised using a 0.2 µm filter (BD Biosciences, UK.) Following incubation of HLMVECs for 24 hours, spent medium was aspirated from wells, and adherent cells washed once with 1x HBSS (-Ca^{2+}/Mg^{2+}) to remove non-adherent cells. Serum and ascorbic acid free EGM-2MV was added to the cells. $CuCl_2$ was added to the wells (15, 30, 60, 120 and 240 µl) and wells were adjusted to 1500 µl of medium per well resulting in final concentrations of 12.5, 25, 50, 100 and 200 µM $CuCl_2$. Culture medium alone was added to the control wells. The plates were covered and incubated for a further 24 hours at 37 ^{o}C and 5 % CO_2.

4.3.2.4. HLMVEC culture in 6-well plates with 50 µM $CuCl_2$ and 100 – 400 µM H_2O_2

A 1.25 mM $CuCl_2$ (MW 134.45, Sigma, UK) solution was prepared in full culture medium. The solution was filter-sterilised using a 0.2 µm filter (BD Biosciences, UK), and 60 µl added to the wells resulting in a final concentration of 50 µM $CuCl_2$. Culture medium was added to the control wells.

A 10 mM H_2O_2 (MW 34, Sigma, UK) solution was prepared in full culture medium. The 10 mM stock solution was diluted 1:2 to 5 mM, and a further 1:2 to 2.5 mM. The solutions were filter-sterilised using a 0.2 μm filter. The addition of each solution (60 μl) to the wells resulted in final concentrations of 400, 200, and 100 μM H_2O_2 in the presence of 50 μM $CuCl_2$.Culture medium alone was added to control wells. The plates were covered and incubated for 24 hours at 37 °C and 5 % CO_2.

4.3.2.5. Harvesting

Following incubation, the plates were placed onto ice and 1500 μl of cell supernatants was harvested. Cell debris was cleared by centrifuging at 900 g for 10 minutes at 4 °C. The supernatant was retained and stored at -80 °C for analysis by Western blotting or ELISA. The cells in the plate were washed twice with 1000 μl ice cold 1x PBS (-Ca^{2+}/Mg^{2+}), and 500 μl of ice cold 1 % Triton-X-100 (v/v) containing double strength protease inhibitors (Roche, UK) was added to each well. Double strength protease inhibitors were used since 1x strength protease inhibitors failed to prevent the proteolysis of RANTES in the samples. The plate was stored at -80 °C and subjected to 2 freeze-thaw cycles. The cell lysates were removed from the plate and stored at -80 °C in 1.5 ml eppendorf tubes for analysis by SDS-PAGE or ELISA.

4.3.2.6. Freeze drying for SDS-PAGE analysis

500 μl lysate and 1500 μl supernatant samples were freeze dried for a minimum of 6 hours using a Thermo Scientific Modulyo freeze drier.

4.3.2.7. Immunoprepitation of human RANTES for SDS-PAGE analysis

Freeze dried samples were reconstituted to 40 μl in 1 x PBS (-Ca^{2+}/Mg^{2+}). Samples were then diluted 1/5 in immunoprecipitation buffer (150 mM NaCl, 50 mM Tris, 5 mM EDTA, 0.1 % (w/v) SDS, 0.5 % (v/v) Tergitol Nonidet P-40, and protease inhibitor cocktail (2 x tablets in 10 ml, double strength) (Roche, UK)). Affinity purified rabbit polyclonal anti-RANTES (non-biotinylated) was added at 1 μg/ml (4 μl of 50 μg/ml stock was added to a 200 μl sample). Protein A agarose bead suspension (3 μl) was added to the samples followed by incubation with shaking at 4°C overnight.

Following overnight incubation, samples were centrifuged at 3000 g and 4°C for 5 minutes. The supernatant was removed and the pellet washed 3 times with ice-cold immunoprecipitation buffer with centrifugation at 3000 g. To release the immunoprecipitated protein from the primary antibody-protein A agarose complex, samples were incubated with 40 µl/sample 5x Laemmli sample buffer (8 ml 5x running buffer, 2.5 ml glycerol and 1.25 mg bromophenol blue) containing 100 mM DTT at room temperature for 30 minutes, or in the absence of DTT with boiling at 95 °C for 5 minutes. Samples were then centrifuged for 5 minutes at 3000 g before analysis by Western blotting.

4.3.2.8. Analysis by SDS-PAGE and Western blotting

Samples were analysed by SDS-PAGE on either 14 %, or 4 - 15 % gradient polyacrylamide gels, transferred, blocked overnight in 2 % (v/v) Tween-20 / PBS (-Ca^{2+}/Mg^{2+}) and Western blots were stained for RANTES as previously described in Chapter 2, Sections 2.3.4 and 2.3.5.

4.3.2.9. Quantification of human RANTES by ELISA

The ELISA was performed according to the manufacturer's instructions (R & D Systems, UK)

Wells of a 96-well plate were coated with 100 µl of mouse anti-human RANTES capture antibody (R & D Systems, UK) at 1 µg/ml in PBS -Ca^{2+}/Mg^{2+}, sealed and incubated overnight at room temperature. Following overnight incubation, the capture antibody was aspirated and each well washed three times with 200 µl wash buffer (0.05 % Tween-20 (Fisher, Scientific, UK) / PBS -Ca^{2+}/Mg^{2+}).

Plates were blocked by adding 300 µl reagent diluent / well (sterile filtered (0.2 µM) 1 % (w/v) BSA (Sigma, UK) / PBS -Ca^{2+}/Mg^{2+}), sealed and incubated for 1 hour at room temperature. Following incubation, wells were washed three times with 200 µl wash buffer (0.05 % Tween-20/ PBS -Ca^{2+}/Mg^{2+}) and 100 µl of samples or standards (50 ng/ml) diluted in reagent diluent in the range 0-500 pg/ml were added to the wells.

Plates were sealed and incubated for 2 hours at room temperature. Following incubation, wells were washed three times with 200 µl wash buffer (0.05 % Tween-20/ PBS -Ca^{2+}/Mg^{2+}).

The detection antibody (biotinylated goat anti-human RANTES – R & D Systems, UK) was diluted in reagent diluent to 20 ng/ml, and 100 µl added per well. Plates were sealed and incubated for 2 hours at room temperature. Following incubation, wells were washed three times with 200 µl wash buffer (0.05 % Tween-20). Streptavidin-HRP (R & D Systems, UK, kept at 4°C) was diluted 1:200 to working strength in reagent diluent, and 100 µl added per well. Plates were incubated for 20 minutes at room temperature, avoiding direct sunlight. Following incubation, wells were washed three times with 200 µl wash buffer (0.05 % Tween-20/ PBS -Ca^{2+}/Mg^{2+}).

A substrate solution was prepared using the following formula per one plate:

12 ml substrate buffer (1.8 mM, pH 5.5)
200 µl Tetramethylbenzidine (TMB) stock solution (6 mg/ml in DMSO)
1.2 µl H_2O_2 stock solution (30 % (v/v), Sigma, UK).
The solution was stored for up to 1 month at room temperature, protecting against light. 100 µl of the substrate solution was added per well and plates were incubated for 20 minutes at room temperature (or until the top standard had developed a strong colour). To stop the reaction, 50 µl of 2 M H_2SO_4, (Fisher Scientific, UK) was added to each well. The optical density at 450 nm for each well was determined immediately using a micro-plate reader.

4.3.3. Analysis of T-cell derived RANTES

4.3.3.1. T-cell isolation

Normal venous blood was collected by venepuncture from healthy volunteers into vacutainers containing EDTA and diluted 1:1 with PBS -Ca/Mg in sterile conditions. Diluted blood was layered onto an equal volume of sterile Lymphoprep using a long necked Pasteur pipette and centrifuged at 438 g for 30 minutes at 20 °C. The peripheral blood mononuclear cell (PBMC) layer was harvested using a plastic pipette and diluted to 50 ml in Falcon tubes with HBSS - Ca^{2+}/Mg^{2+}. PBMCs were centrifuged at 760 g for 10 minutes and the supernatant discarded. The pellet was re-suspended and diluted to 50 ml with HBSS - Ca^{2+}/Mg^{2+}, and centrifuged at 190 g for 5 minutes to remove platelets and erythrocytes. The supernatant was discarded and the PBMC pellet re-suspended in RPMI/10 % FCS, 0.5 ml per 9 -10 ml of blood collected. Re-suspended pellets were

combined before counting. The number of viable cells was counted, and the purity of the final preparation was assessed by microscopic observation with x400 magnification. 10 µl of cell suspension was mixed with 90 µl Trypan blue stain and 2 x 10 µl was loaded onto a haemocytometer slide.

The following formula was used to estimate the number of viable cells:

No. of cells/ml = n x 10 x 10^4 (where n = no. of cells in the 25 square field)

PBMCs were diluted to 2 x 10^6/ml in warm RPMI/10 % (v/v) FCS containing 2 mM l glutamine, 1 mM sodium pyruvate, 100 units/ml penicillin, 100 µg/ml streptomycin and 250 ng/ml amphotericin B. The PBMC suspension was transferred into 25 ml Petri dishes (10 ml / dish) and incubated overnight at 37 °C and 5 % CO_2 to remove adherent monocytes.

Non-adherent T-cells were harvested and the Petri dishes washed with warm RPMI containing 10 % (v/v) FCS. The wash was combined with the T-cell suspension and centrifuged at 760 g for 10 minutes. The supernatant was discarded and the pellet re-suspended in RPMI / 10 % FCS. T-cells were counted and diluted to 2 x 10^6/ml in RPMI/10 % FCS, supplemented with 2 mM 1-glutamine, 1 mM sodium pyruvate, 100 units/ml penicillin, 100 µg/ml streptomycin and 250 ng/ml amphotericin B.

4.3.3.2. T-cell activation

The mitogen, phytohaemagglutinin (PHA), was added to activate T-cells at a final concentration of 1 µg/ml. The T-cell suspension was transferred to 75 cm^2 tissue culture flasks (8-10 ml / flask) and cultured for 2 days at 37 °C and 5 % CO_2. Following 2 day incubation, interleukin-2 (IL-2) was added to the medium, final concentration 200 units/ml. Culture was continued for 3 days at 37 °C and 5 % CO_2 to allow cells to proliferate.

4.3.3.3. Induction of RANTES expression following T-cell activation

Following activation, T-cells were harvested and diluted to 2 x 10^6, 5 x 10^6 and 1 x 10^7 cells/ml in RPMI/ 10 % FCS supplemented with L-glutamine, sodium pyruvate and antibiotics as described above. T-cells were incubated in 24-well plates (0.25 ml/well)

in the presence and absence of IFN-γ (100 U/ml) plus TNF-α (10 ng/ml) for 2 days to induce RANTES production.

Conditioned medium from activated T-cells was collected for analysis 4 hours, 1 and 2 days following the addition of IFN-γ plus TNF-α. Cell suspensions were centrifuged at 760 g for 10 minutes and cell-free supernatants were collected and stored at -80 °C. The samples were quantitatively analysed by ELISA to detect RANTES as previously described in section 4.3.2.9.

4.3.4. Purification of platelets and induction of platelet derived RANTES release

4.3.4.1. Platelet isolation

Normal venous blood was collected from healthy volunteers into vacutainers containing EDTA, diluted 1:1 with 1x PBS (-Ca/Mg), layered onto lymphoprep and centrifuged at 438 g for 30 minutes at 20 °C. The platelet-rich plasma layer was extracted and centrifuged at 2500 g for 15 minutes to obtain platelet-rich pellets. The platelets were washed twice with sterile PBS ($-Ca^{2+}/Mg^{2+}$) containing 10 mM EDTA, with centrifugation at 2500 g for 15 minutes and re-suspended in RPMI 1640/ 0.5 % (w/v) BSA. Platelets were counted using a haemocytometer as previously described and diluted to 10^7, 10^8 and 10^9 / ml in RPMI 1640/ 0.5 % BSA (833 µl 30 % (w/v) sterile BSA solution / 50 ml RPMI 1640). The purity of the final preparation was assessed by microscopic observation.

4.3.4.2. Induction of RANTES release from platelets

Purified platelets were incubated in suspension at 10^7, 10^8 and 10^9 / ml in RPMI 1640 (Invitrogen) / 0.5 % (w/v) BSA (Sigma, UK), 250 µl per well and cultured in a 24-well plate (Triple Red, UK) at 37 °C for 1 hour in the absence and presence of thrombin at 0.5, 1 and 2 U/ml. 100 U of lyophilised thrombin (Sigma, UK) was reconstituted in 1 ml RPMI/ 0.1 % BSA (166 ul 30% BSA / 50 ml RPMI 1640) and stored in 30 µl aliquots at -20 °C. 5 µl of 100, 50 and 25 U/ml stock solution was added per well (24-well plate, 0.25 ml/well) to give final concentrations of 2, 1 and 0.5 U/ml.

Conditioned medium from purified platelets was collected 1 hour after treatment with thrombin. Following centrifugation at 2500 g for 15 minutes at 4 °C, cell-free supernatants were collected, stored at -80 °C and quantified for RANTES by ELISA as

previously described (Section 4.3.2.9), or freeze dried and analysed by SDS-PAGE and Western blotting as described in Sections 4.3.2.6 and 4.3.2.8.

4.3.5. Endothelial cell and platelet co-culture

4.3.5.1. Co-culture

Platelets were isolated as previously described in Section 4.3.4.1 and diluted to 10^8 / ml in RPMI 1640 / 0.5 % (w/v) BSA and added (1500 µl / well) in the absence/presence of thrombin at 1 U/ml (Sigma, UK) (Mack, *et al.* 2002) to confluent HLMVECs that were incubated in the presence and absence of IFN-γ plus TNF-α for 24 hours in a 6-well plate. Following the addition of platelets and thrombin to HLMVECs, the plates were incubated for 1 hour at 37 °C and 5 % CO_2.

4.3.5.2. Harvesting

Following incubation the plates were placed onto ice and cell supernatants and lysates were harvested. Cell debris was cleared by centrifuging at 2500 g for 15 minutes at 4 °C. The supernatant (1500 µl) was retained and stored at -80 °C for analysis by ELISA. The cells in the plate were washed twice with 1000 µl ice cold 1x PBS (-Ca^{2+}/Mg^{2+}), and 500 µl of ice cold 1 % Triton-X-100 (v/v) (Sigma, UK) containing double strength protease inhibitors (Roche, UK) was added to each well. The plate was stored at -80 °C and subjected to 2 freeze-thaw cycles. The cell lysates were removed from the plate and stored in 1.5 ml Eppendorf tubes for analysis by ELISA.

4.3.5.3. Analysis by ELISA

The cell supernatants and lysates were quantified for RANTES by ELISA as described in section 4.3.2.9.

4.3.6. Analysis of lipid peroxidation in HLMVECs

The effect of Cu/H_2O_2 on lipid peroxidation was investigated as an indicator of oxidative stress in HLMVECs in the absence and presence of sodium chlorate to inhibit GAG synthesis.

4.3.6.1. Seeding HLMVECs in 24-well plates

The HLMVECs were seeded into collagen IV coated 24-well plates (Triple Red, UK) at $2x10^5$/ml in EGM-2MV culture medium and 500 µl well (this corresponds to a total cell number of 100,000 per well) in the absence and presence of 30 mM sodium chlorate (Sigma, UK.)

Sodium chlorate:

A 10X solution (300 mM) was made up in full culture medium by dissolving 319 mg in 10 ml culture medium. The 10X solution was diluted to give a 30 mM solution in which the cells were seeded.The plates were covered and incubated for 24 hours at 37 °C and 5 % CO_2.

4.3.6.2. Induction of RANTES release

The adherence and confluence of seeded cells was checked. The growth medium was changed, this also removes non-adherent cells. The old medium was aspirated from wells, and the cells washed once with 1x HBSS (-Ca^{2+}/Mg^{2+}). 460 µl new full culture medium, +/- sodium chlorate (30 mM) containing 100 U/ml IFN-γ and 10 ng/ml TNF-α was added per well. Cells were incubated for 24 hours at 37 °C and 5 % CO_2.

4.3.6.3. Addition of $CuCl_2$ and H_2O_2

Following incubation, $CuCl_2$ and H_2O_2 were added to wells. A 1.25 mM $CuCl_2$ solution was made up in growth medium, filter sterilised using a 0.2 µm filter (BD Biosciences), and 20 µl added in triplicate wells to give a final concentration of 50 µM $CuCl_2$. 20 µl of growth medium was added to control wells (no $CuCl_2$).

A 10 mM H_2O_2 stock solution was made up in growth medium (5.67 µl of 30 % H_2O_2 (kept at 4 °C) in 5 ml) and diluted to 5 mM, 1.25 mM and 0.625 mM in full growth medium.

All solutions were filter-sterilised using a 0.2 µm filter. 20 µl of each solution was added to the wells, in triplicate to give final concentrations of 400, 200, 50 and 25 µM H_2O_2. 20 µl of growth medium was added to control wells (no H_2O_2). The plates were covered and incubated for 24 hours at 37 °C and 5 % CO_2.

4.3.6.4. FOX-2 assay for the quantification of lipid peroxides

Lipid peroxides were assayed in endothelial cell lysates using the PeroXOquant Quantitative Peroxide Assay Kit (lipid-compatible formulation) (Pierce, Chester, UK) according to the manufacturers instructions.

The working reagent (WR) was prepared by mixing 1 volume of reagent A with 100 volumes of reagent C (150 µl of A and 15 ml of reagent C per microplate). 30 % (v/v)

hydrogen peroxide stock solution (Sigma, UK) was serially diluted in UHQ water to achieve 8 standards in duplicate in the concentration range 0-1000 μM. The high standard (1000 μM) was prepared by adding 10 μl of the stock to 88 ml of water.

Cell supernatants were removed from each well and stored at -80 °C for analysis for RANTES by ELISA. Cells were washed in cell medium and 60 μl of cell medium and 600 μl of WR were added to each well (10 volumes of WR were added to 1 volume of sample). The samples were incubated at room temperature for 15-20 minutes in order to reach the endpoint. For each well, 2 x 275 μl samples were removed and pipetted into a 96-well microplate. Sample absorbances were measured at 595 nm using a plate reader, and the peroxide concentrations calculated by reference to the standard curve absorbance values.

4.3.7. T-cell chemotaxis assays

4.3.7.1. RANTES preparation for chemotaxis assay

Samples containing RANTES multimers were prepared in duplicate, in the presence and absence of 50 μM $CuCl_2$ and 25 μM H_2O_2, as described in Chapter 2, section 2.3.1, and incubated for 2 days at 37 °C. The final concentration of RANTES in the samples was 5 x 10^{-7} M. Following incubation, samples were diluted to 1.25 x 10^{-8} M (125 ng/ml) in Hanks Balanced salt Solution (HBSS) with Ca^{2+}/Mg^{2+} supplemented with 20 mM HEPES (0.48 g/100 ml and adjusted to pH 7.4, and used in a chemotaxis assay. Fresh unincubated RANTES was used as a positive control, final concentration 1.25 x 10^{-8} M in HBSS ($+Ca^{2+}/Mg^{2+}$) supplemented with 20 mM HEPES, pH 7.4. $CuCl_2$ and H_2O_2 alone were added to lower wells as a negative control.

4.3.7.2. Modified Boyden Chamber technique for T-cell chemotaxis assay

The method for chemotaxis was modified from the methods of Harvath *et al.* and Richards *et al.* (Harvath *et al*, 1980; Richards & McCullough, 1984).

Activated T-cells were re-suspended in HBSS with Ca^{2+}/Mg^{2+} supplemented with 20 mM HEPES (0.48 g/100 ml and adjusted to pH 7.4). T-cells were counted and diluted to 2 x 10^{6} /ml in this buffer. RANTES was initially diluted to a concentration range of

1.25 – 500 ng/ml (1.56 x 10^{-10} M – 6.25 x 10^{-8} M) in HBSS (+Ca^{2+}/Mg^{2+}) containing 20 mM HEPES, pH 7.4.

All components of the microchambers were washed thoroughly for 1h in distilled water, rinsed and dried prior to use. Samples and standards (25 µl) were diluted in HBSS (+Ca^{2+}/Mg^{2+}), containing 20 mM HEPES, pH 7.4 and added to the lower wells. The buffer was added to lower wells as a negative control. Fresh unincubated RANTES was used as a positive control, at a concentration of 1.56 x 10^{-8} M (125 ng/ml). All samples were analysed in duplicate.

A 5µm pore-size, PVP-free polycarbonate filter was placed over the lower wells, with no cross contamination between wells. The top gasket was placed over the filter and the top plate on the filter and the thumb nuts secured and tightened. The upper wells were filled with the T-cell suspension, 50 µl per well, and the chambers were incubated at 37 °C in an incubator with 5 % CO_2 for 30 minutes under humidified conditions.

Following incubation, the thumb nuts were removed and each chamber inverted. The lower plate and gasket were removed so that the underside of the filter was exposed with the migrated cells adhered. Both ends of the filter were held firmly with clamps. Keeping the underside facing upwards, the topside (with non-migrated T-cells) was washed in 1x HBSS with Ca^{2+}/Mg^{2} and wiped on a plate at an angle of 45 ° to remove non-migrated cells. Washing was repeated three times, to ensure non-migrated cells were removed. The filter was allowed to dry before staining.

4.3.7.3. Anti-CCR3 and CCR5 antibodies

RANTES samples and isolated T-cells were incubated with 100 µg/ml anti-CCR3, anti-CCR5 neutralising antibodies or isotype controls (rat IgG2a and mouse IgG2b) for 30 minutes before they were used in the chemotaxis assay.

4.3.7.4. Hema-Gurr staining

Filters were stained using Hema Gurr stain (BDH). Filters were fixed in methanol for 10 seconds and stained for 10 seconds with eosin red followed by methylene blue for 10 seconds. Finally, filters were washed in 1x PBS without Ca^{2+}/Mg^{2+} and allowed to dry. Filters were placed on a glass slide with migrated cells facing up.

When dry, filters were covered with immersion oil and the total number of cells counted using a light microscope at x 400 magnification in five high power fields (hpf) per well. Data was presented as the mean number of cells in one hpf.

4.3.8. Transendothelial migration assays

4.3.8.1. Subculture of HLMVECs into fibronectin coated and uncoated Transwells

The method was adapted from the supplier's instructions and that of (Sundstrom *et al*, 2001); (Broughton-Head, 2005; Carr *et al*, 1994; Kanda *et al*, 2004).

HLMVEC cells were seeded in T-75 flasks at a density of 5000 cells/cm^2 and grown for 1 week in 15 ml EGM-2MV fully supplemented culture medium. HLMVEC subcultures were used in experiments when they reached 60 – 70 % confluence at passage 5-11. Cells were harvested by trypsinisation as previously described in Chapter 4, Section 4.3.1.6 (2 ml of Trypsin/EDTA / 75 cm^2 of cells to be sub-cultured on Transwells.) Trypsin/EDTA was neutralised with trypsin neutralisng solution as previously described (4 ml / 75 cm^2 of cells.) Fully supplemented EGM-2MV growth medium was pre-warmed to 37 ^{o}C in a water bath. In a tissue culture hood, sterile 3 µm uncoated and fibronectin coated polyethylene terephthalate (PET) BD Biosciences) culture inserts were placed into a 24-well companion plate (BD Biosciences, UK.) Growth medium was transferred to the 24-well culture inserts (800 µl into the lower wells, and 300 µl into the upper wells) before they were placed in a humidified 37 ^{o}C incubator with 5 % CO_2 to equilibrate for 30 minutes.

Harvested HLMVEC cells were centrifuged at 220 g for 5 minutes to pellet the cells. The supernatant was aspirated and the cells counted using a haemocytometer slide (naubayer bright line), adding 10 µl cell suspension + 90 µl trypan blue (Sigma, UK) and loading 10 µl onto the slide. The cells were counted and diluted to 2 x 10^5 cell / ml in EGM-2MV (Lonza, UK.)

Growth medium was removed from the upper wells and the cells seeded onto the Transwell inserts at 60,000 cells / 300 µl per well. Cells were grown on Transwells for 2 weeks, and confluency established by microscopic observation and staining with Hema

Gurr stain (BDH) as described in Section 4.3.7.4. When confluent, the cells were ready for use in a transmigration assay.

4.3.8.2. Induction of HLMVEC RANTES synthesis

RANTES synthesis was induced in HLMVEC monolayers using a method adapted from that of Hashimoto *et al*, 2000, Sundstrom *et al*, 2001 and Terada *et al*, 1996.

The confluence of HLMVEC monolayers was observed and the culture medium changed to remove non-adherent cells. Old medium was aspirated from the wells, and adherent cells washed once with 1x HBSS (-Ca^{2+}/Mg^{2+}). New full culture medium (EGM-2MV) containing 100 U/ml IFN-γ plus 10 ng / ml TNF-α was added to each well. The HLMVEC monolayers were incubated for 1 day at 37 °C and 5 % CO_2.

4.3.9. Purification of platelets and induction of platelet derived RANTES release

Platelets were isolated as previously described in Section 4.3.4.1 and diluted to 10^8/ml in RPMI/ 10 % (v/v) FCS. Isolated platelets were activated with 1 U/ml thrombin (Mack, *et al.* 2002).

4.3.10. T-cell transendothelial migration assay

HLMVECs were grown to confluence in EGM-2MV growth medium for 2 weeks in monolayers on Transwells as previously described. T-cells were isolated and activated with PHA and IL-2 for 5 days as previously described in Chapter 4, Sections 4.3.3.1 and 2. Platelets were isolated as previously described in Section 4.3.4.1. HLMVECs were used in transendothelial migration assays at passage 5 - 10. Where indicated, HLMVECs were pre-treated with copper chelators overnight prior to the migration assay. Chelators were added to both the apical and basal wells. Neocuproine (NC) or bathocuproine disodium salt (BCDS) were added at a final concentration of 0.1, 0.25, and 0.5 mM, and D-penicillamine or tobramycin were added at a final concentration of 0.01, 0.1 and 0.5 mM.

On the day of the transendothelial migration assay, 30 minutes before T cells are added, confluent HLMVEC layers were washed with RPMI 1640. The lower wells of the plate were filled either with isolated platelets at a final concentration of 1 x 10^8/ml in RPMI 1640 containing 25 mM HEPES and 2 mM l-glutamine (Invitrogen, UK) supplemented with 10 % FCS serum (Sigma, UK) and activated with 1 U/ml thrombin, 1.25 x 10^{-8} M

recombinant RANTES (Peprotech, UK) in RPMI/10 % FCS or RPMI/10 % FCS alone as a control. Cu chelators were added to the basal wells containing platelets 30 minutes before the start of the assay. The final volume in all basal wells was 800 µl.

Activated T-cells were counted and diluted to 2 x 10^6/ml in RPMI 1640 containing 25 mM HEPES and 2 mM L-glutamine (Invitrogen, UK) and supplemented with 10 % FCS serum (Sigma, UK) (Kawai *et al*, 1999). Anti-RANTES (Peprotech, UK) was added to T-cells (final concentration 10 µg/ml) 30 minutes before the transendothelial migration assay and at the start of the assay to basal wells at a final concentration of 10 µg/ml. The PAI-1 inhibitor XR5118 (a gift from Xenova, UK) was added at final concentration 1, 10 and 100 µM and catalase was added at a final concentration of 500 U/ml, to basal wells 30 minutes before the start of the assay and to the apical wells at the start of the assay. Cu chelators were also added to the apical wells at the start of the assay. The confluent HLMVEC layers were overlaid with pre-treated or untreated activated T cells in the upper wells (in RPMI 1640 / 10 % FCS) at 2 x 10^5/ml and in a final volume of 300 µl / well (Kawai *et al*, 1999). Transwells were incubated at 37 °C and 5 % CO_2 for 5 hours (Kawai *et al*, 1999).

4.3.11. Harvesting

Following incubation, the plates were removed from the incubator and placed on ice for 10 minutes. 80 µl of 100 mM EDTA (Sigma, UK) was added to each lower well, resulting in a final concentration of 10 mM. The plate was incubated for 5 minutes at room temperature. The inserts were shaken gently to loosen adherent cells. All cells from the basal wells were collected, and the wells washed once with 600 µl RPMI 1640. This was added to the cells recovered from each well. The cell suspensions were centrifuged at 2500 g for 15 minutes. The supernatant was retained and stored at -80 °C for analysis by ELISA and Western blotting, and the pellet re-suspended in 100 µl PBS –Ca^{2+}/Mg^{2+}. 10 µl cell of the cell suspension was added to 10 µl Trypan Blue and the total number of cells migrated was calculated by loading 10 µl onto a haemocytometer slide and using the following formula:

No. of cells/ml = n x 2 x 10^4 (where n = no. of cells in the 25 square field)

The apical supernatants were harvested, cleared at 2500 g and stored at -80 °C for immunoprecipitation and analysis by ELISA and Western blotting. The HLMVECs in

the Transwells were washed twice with 200 µl ice cold 1x PBS (-Ca^{2+}/Mg^{2+}). and 200 µl of ice cold 1 % (v/v) Triton-X-100 in UHQ water containing double strength protease inhibitors (Roche, UK) was added to each well. The plate was stored at -80 °C and subjected to 2 freeze-thaw cycles. The cell lysates were removed from the plate and stored at -80 °C in 1.5 ml eppendorf tubes for analysis by SDS-PAGE and Western blotting.

4.3.12. Immunoprecipitation of human RANTES from HLMVEC lysates and supernatants for SDS-PAGE analysis

Lysates (200 µl) and supernatants (300 µl of apical and 500 µl of basal supernatant) were freeze dried and immunoprecipitated for RANTES as previously described in Sections 4.3.2.6 and 4.3.2.7.

4.3.13. Analysis of supernatants and HLMVEC monolayer lysates by SDS-PAGE and Western blotting

Cell lysates and supernatants were analysed by SDS-PAGE on 4 - 15 % gradient polyacrylamide gels, transferred and blocked overnight in 2 % (v/v) Tween-20 / PBS (-Ca^{2+}/Mg^{2+}) as previously described in Chapter 2, Section 2.3.4. Western blots were stained for RANTES as previously described in Chapter 2, Section 2.3.5.

4.3.14. Quantification of human IFN-γ in apical supernatants by ELISA

The ELISA was performed according to the manufacturer's instructions supplied with the duoset (Peprotech EC, UK)

Wells of a 96-well plate were coated with 100 µl rabbit anti-human IFN-γ capture antibody (Peprotech EC, UK) at 1 µg/ml in PBS -Ca^{2+}/Mg^{2+}, sealed and incubated overnight at room temperature. Following overnight incubation, the capture antibody was aspirated and each well washed three times with 200 µl wash buffer (0.05 % Tween-20 (Fisher, Scientific, UK) / PBS -Ca^{2+}/Mg^{2+}).

Plates were blocked by adding 300 µl reagent diluent / well (sterile filtered (0.2 µM) 1 % (w/v) BSA (Sigma, UK) / PBS -Ca^{2+}/Mg^{2+}), sealed and incubated for 1 hour at room temperature. Following incubation, wells were washed three times with 200 µl wash buffer (0.05 % Tween-20/ PBS -Ca^{2+}/Mg^{2+}) and 100 µl of samples or standards (1 µg/ml) were diluted in reagent diluent in the range 0 – 1000 pg/ml. Supernatants from

transendothelial migration experiments (apical side) were assayed at a dilution of 1:10 in reagent diluent.

Plates were sealed and incubated for 2 hours at room temperature. Following incubation, wells were washed three times with 200 µl wash buffer (0.05 % Tween-20/ PBS -Ca^{2+}/Mg^{2+}).

The detection antibody (biotinylated rabbit anti-human IFN-γ (Peprotech EC, UK) was diluted to a working concentration of 0.25 µg/ml in reagent diluent, and 100 µl added per well. Plates were sealed and incubated for 2 hours at room temperature. Following incubation, wells were washed three times with 200 µl wash buffer (0.05 % Tween-20). Avidin-HRP (Peprotech EC, UK), kept at -20°C) was diluted 1:2000 to working strength in reagent diluent, and 100 µl added per well. Plates were incubated for 30 minutes at room temperature, avoiding direct sunlight. Following incubation, wells were washed three times with 200 µl wash buffer (0.05 % Tween-20/ PBS -Ca^{2+}/Mg^{2+}).

A substrate solution was prepared using the following formula per one plate: 10 ml of 2,2'-Azino-bis(3-ethylbenzthiazoline-6-sulfonic acid) (ABTS) solution (prepared by dissolving 1 x ABTS tablet (Sigma, UK) in 100 ml 50 mM phosphate-citrate buffer, adjusted to pH 5.0) and 25 µl H_2O_2 stock solution (30 % (v/v), Sigma, UK).

The phosphate-citrate buffer (50 mM) was prepared by dissolving 0.71 g sodium phosphate (Na_2HPO_4, Sigma, UK) in 100 ml of UHQ water and 0.961 g citric acid (Sigma, UK) in 100 ml distilled water, and adjusting the sodium phosphate to pH 5.0 by adding the citric acid.

Substrate solution was added 100 µl per well, and plates were incubated for 20 minutes at room temperature (or until the top standard had developed a strong colour). To stop the reaction, 50 µl of 1 % SDS (in water) was added to each well. The optical density for each well was determined immediately using a micro-plate reader set to 405 nm.

4.3.15. Quantification of human TNF-α in apical supernatants by ELISA

The ELISA was performed according to the manufacturer's instructions supplied with the duoset (Peprotech EC, UK)

Wells of a 96-well plate were coated with 100 µl of rabbit anti-human TNF-α capture antibody (Peprotech EC, UK) at 1 µg/ml in PBS -Ca^{2+}/Mg^{2+}, sealed and incubated overnight at room temperature. Following overnight incubation, the capture antibody was aspirated and each well washed three times with 200 µl wash buffer (0.05 % Tween-20 (Fisher, Scientific, UK) / PBS -Ca^{2+}/Mg^{2+}

Plates were blocked by adding 300 µl reagent diluent / well (sterile filtered (0.2 µM) 1 % (w/v) BSA (Sigma, UK) / PBS -Ca^{2+}/Mg^{2+}), sealed and incubated for 1 hour at room temperature. Following incubation, wells were washed three times with 200 µl wash buffer (0.05 % Tween-20/ PBS -Ca^{2+}/Mg^{2+}) and 100 µl of samples or standards (1 µg/ml) were diluted in reagent diluent in the range 0-1000 pg/ml. Supernatants from transendothelial migration experiments (apical side) were assayed at a dilution of 1:10 in reagent diluent.

Plates were sealed and incubated for 2 hours at room temperature. Following incubation, wells were washed three times with 200 µl wash buffer (0.05 % Tween-20/ PBS -Ca^{2+}/Mg^{2+}).

The detection antibody (biotinylated rabbit anti-human TNF- α (Peprotech EC, UK) was diluted in reagent diluent to a working concentration of 0.5 µg/ml and 100 µl added per well. Plates were sealed and incubated for 2 hours at room temperature. Following incubation, wells were washed three times with 200 µl wash buffer (0.05 % Tween-20). Avidin-HRP (Peprotech EC, UK), kept at -20°C) was diluted 1:2000 to working strength in reagent diluent, and 100 µl added per well. Plates were incubated for 30 minutes at room temperature, avoiding direct sunlight. Following incubation, wells were washed three times with 200 µl wash buffer (0.05 % Tween-20/ PBS -Ca^{2+}/Mg^{2+}).

A substrate solution was prepared using the following formula per one plate: 10 ml of 2,2'-Azino-bis(3-ethylbenzthiazoline-6-sulfonic acid) (ABTS) solution (prepared by

dissolving 1 x ABTS tablet (Sigma, UK) in 100 ml 50 mM phosphate-citrate buffer, adjusted to pH 5.0) and 25 µl H_2O_2 stock solution (30 % (v/v), Sigma, UK).

The phosphate-citrate buffer (50 mM) was prepared by dissolving 0.71 g sodium phosphate (Na_2HPO_4, Sigma, UK) in 100 ml of UHQ water and 0.961 g citric acid (Sigma, UK) in 100 ml distilled water, and adjusting the sodium phosphate to pH 5.0 by adding the citric acid.

Substrate solution was added 100 µl per well, and plates were incubated for 20 minutes at room temperature (or until the top standard had developed a strong colour). To stop the reaction, 50 µl of 1 % SDS (in water) was added to each well. The optical density for each well was determined immediately using a micro-plate reader set to 405 nm.

4.3.16. Quantification of human RANTES in supernatants from transendothelial migration assays by ELISA

Apical and basal supernatants were analysed by RANTES ELISA as previously described in Section 4.3.2.9.

4.3.17. Lactate dehydrogenase (LDH) assay

The lactate dehydrogenase (LDH) assay (TOX-7, Sigma, Dorset, UK) was used to determine whether the effects of Cu chelators was due to cytotoxicity. LDH is an intracellular cytoplasmic protein that is released into cell culture supernatants when cells become non-viable and sustain damage to their membrane (Legrand, C. et al., 1992). The assay works on the principle that LDH released from cells will reduce NAD to NADH. The NADH can then convert a tetrazolium dye into a coloured compound. The assay was adapted for use in a microtitre plate and 5 µl of cell culture supernatant was added to 45 µl 1x PBS. The LDH assay solution was prepared by mixing equal volumes of substrate, enzyme and dye together. 100 µl of the mixture was added per well. The plate was incubated for 30 minutes at room temperature, protected from light. To stop the reaction, 8.33 µl of 1M HCl was added to each well and the absorbance was measured at 490 nm using a microplate reader (Dynex microplate reader, West Sussex, UK).

4.3.18. Plasmin activity assay

The assay was based on methods in the Chromogenix catalogue.

The plasmin substrate stock solution was prepared by dissolving 25 mg plasmin substrate (S2251, Chromagenix, UK) in 11.33 ml UHQ. The stock was stored at 4 °C. The enzyme standard (plasmin from human plasma, Sigma, UK) was prepared by dissolving 0.5 mg (3.2 U/ml protein) in 0.5 ml assay buffer (50 mM Tris-HCl with 130 mM NaCl, pH 8.5) giving a final concentration of 1 mg/ml. The enzyme standard was aliquotted and stored at -20 °C. Standards were diluted in assay buffer from the 1 mg/ml stock to a range of 0 -100 µg/ml.

Supernatant samples and standards were assayed by adding 25 µl of sample to 75 µl assay buffer in a 96-well plate. The reaction was initiated by adding 25 µl of substrate (final concentration 0.8 mM) to the wells. The plate was incubated at 37 °C for 60 minutes and read on a plate reader at 405 nm.

4.3.19. Vascular amine oxidase activity assay

HLMVECs were grown to confluence in 75 cm^2 flasks and 1 flask of cells was treated overnight either with neocuproine, bathocuproine disodium salt, D-penicillamine or tobramycin (0.5 mM). Following overnight incubation, the flasks were treated for 5 hours with IFN-γ (100 U/ml) and TNF-α (10 ng/ml) before harvesting. Medium was aspirated from one culture vessel at a time, and the adhered cells rinsed with 5 ml 1x HBSS (-Ca^{2+}/Mg^{2+}). The HBSS was aspirated from the flask and the cells covered with 10 ml 1x HBSS (-Ca^{2+}/Mg^{2+}) containing EDTA (10 mM) per 75 cm^2 flask. The cap was tightened and the cells monitored under a microscope until approximately 90 % of cells were rounded up. Cells were released from the culture surface by rapping the flask. The detached cells were transferred to sterile 50 ml centrifuge tubes and the flasks rinsed with 5 ml of 1x HBSS (-Ca^{2+}/Mg^{2+}) to collect residual cells which were added to the centrifuge tubes. Cells were centrifuged at 220 g for 5 minutes, and the supernatants aspirated. Each pellet was re-suspended in 300 µl physiological HEPES buffer solution (UHQ water containing HEPES (50 mM), KCl (5 mM), $CaCl_2$ (2 mM), $MgCl_2$ (1.4 mM) and adjusted to pH 7.4 with NaOH (approximately 20 mM) with NaCl subsequently added such that the final concentration of sodium in the buffer is 140 mM).

Whole cell samples were assayed by adding half (150 µl) of each cell suspension to 150 µl of physiological HEPES buffer containing the SSAO inhibitors semicarbazide (100 µM) and hydroxylamine (5 µM), and half (150 µl) of each cell suspension to 150 µl physiological HEPES buffer alone without inhibitors in a 24-well plate. Plates were incubated for 30 minutes at 37 °C. The reaction was initiated by adding 150 µl of chromagenic solution (physiological HEPES buffer containing 4-aminoantipyrine, (500 µM), 2-4-dichlorophenol (1 mM) and horseradish peroxidise (40 U/ml)) and 150 µl of methylamine substrate (16 mM in physiological HEPES buffer) to the wells. The final assay volume was 600 µl. The plate was incubated at 37 °C for 24 hours and read on a plate reader at 510 nm.

4.4. Statistical analysis

Data were compared with a paired student's t-test, or a 1 or 2-way ANOVA followed by either a Dunnet's or Tukey's *post-hoc* test where appropriate, as indicated in the figure legends. $p < 0.05$ was the minimum accepted level of significance.

4.5. Results

4.5.1. The effect of copper plus H_2O_2 on RANTES expression by HLMVECs

Whilst it is known that endothelial cells synthesise RANTES, experiments were carried out to analyse the form, monomer or multimer, of RANTES expressed by HLMVECs under basal conditions and following stimulation with IFN-γ plus TNF-α. Further, in view of the evidence presented in Chapters 2 and 3, the effect of $CuCl_2$ plus H_2O_2 on the multimerisation of RANTES expressed by HLMVECs was investigated.

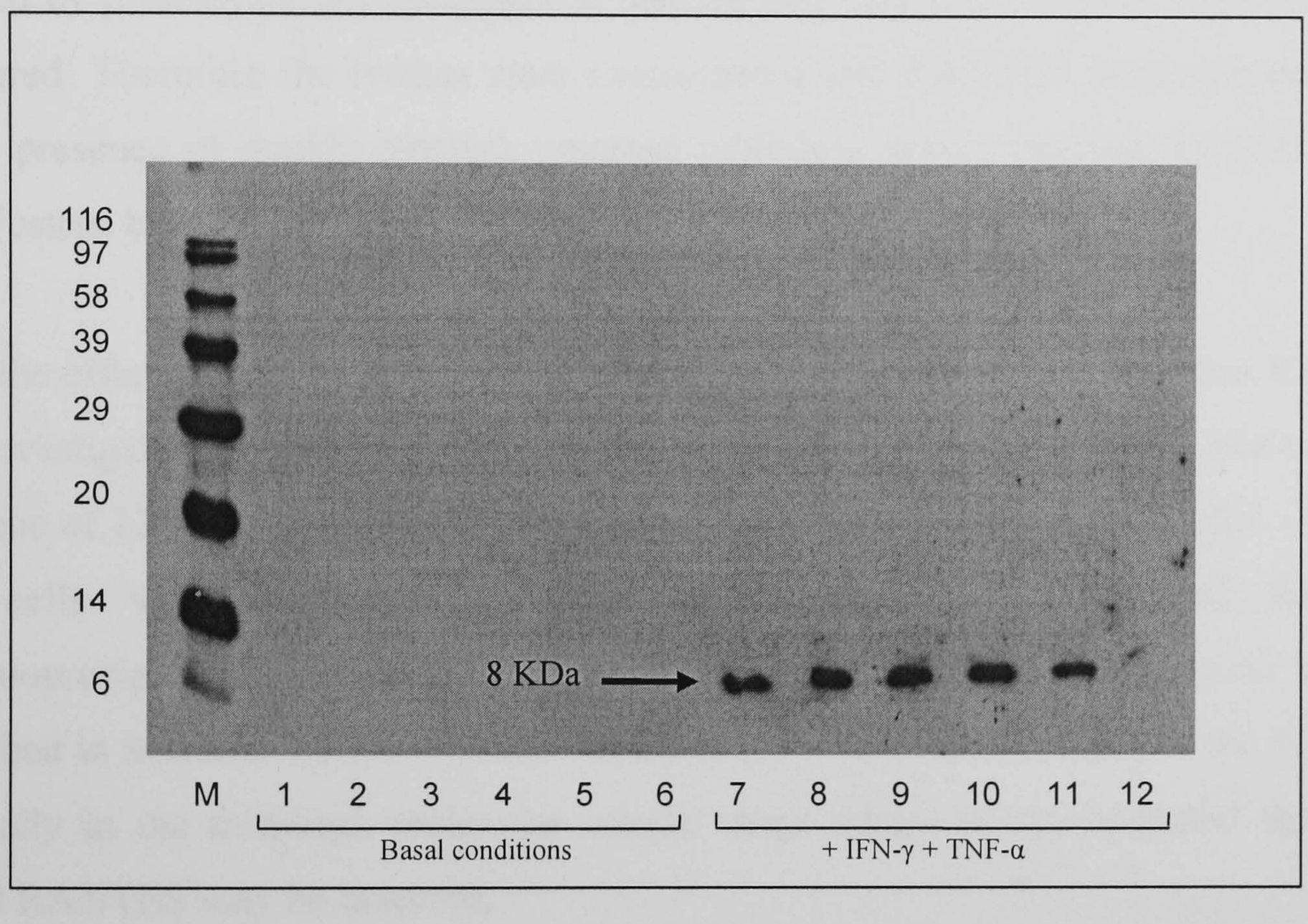

Figure 4.1. RANTES synthesised by HLMVECs and released into supernatants. RANTES in supernatants from HLMVECs grown for 24 hours in collagen IV coated 6-well plates followed by incubation for 24 hours in the absence and presence of 50 μM $CuCl_2$, 25 – 400 μM H_2O_2, IFN-γ (100 U/ml) and TNF-α (10 ng/ml). M: molecular weight markers. Lanes 1-6 show HLMVEC supernatants in the absence of IFN-γ plus TNF-α, and in Lane 1: in the absence of $CuCl_2$ and H_2O_2, lane 2: in the presence of 50 μM $CuCl_2$, lane 3: 50 μM $CuCl_2$ and 25 μM H_2O_2, lane 4: 50 μM $CuCl_2$ plus 50 μM H_2O_2, lane 5: 50 μM $CuCl_2$ and 200 μM H_2O_2 and lane 6: 50 μM $CuCl_2$ and 400 μM H_2O_2. Lanes 7-12 show HLMVEC supernatants in the presence of IFN-γ (100 U/ml) plus TNF-α (10 ng/ml) and in lane 7: no $CuCl_2$ or H_2O_2, lane 8: 50 μM $CuCl_2$, lane 9: 50 μM $CuCl_2$ and 25 μM H_2O_2, lane 10: 50 μM $CuCl_2$ and 50 μM H_2O_2, lane 11: 50 μM $CuCl_2$ and 200 μM H_2O_2 and lane 12: 50 μM $CuCl_2$ and 400 μM H_2O_2. Representative of two independent experiments.

RANTES was not detectable in supernatants from HLMVECs incubated in the absence of IFN-γ plus TNF-α (figure 4.1, lanes 1 - 6). However, monomeric (8 KDa) endogenous RANTES was detected in supernatants from HLMVECs incubated in the presence of IFN-γ (100 U/ml) plus TNF-α (10 ng/ml) (lanes 7 – 11). The addition of 50 μM $CuCl_2$ alone and in the presence of 25 – 400 μM H_2O_2 had no effect on the form of

RANTES detected in the supernatant (lanes 8-11), when compared to the control (no $CuCl_2$ or H_2O_2, lane 7), RANTES remains monomeric. However, high concentrations (400 μM) of H_2O_2 appear to destroy the RANTES monomer (lane 12).

It was speculated that if there were any multimers of RANTES formed in the presence of 50 μM $CuCl_2$ and 25 – 400 μM H_2O_2 they may remain bound to glycosaminoglycans (GAGs) on the endothelial cell surface, rather than appear free in the supernatant. Therefore, endothelial cell lysates were analysed for the presence of RANTES. Preliminary experiments indicated that analysis of RANTES in whole cell lysates was affected by proteolysis and non-specific binding and very low levels of RANTES were recovered. Therefore the lysates were concentrated and RANTES immunoprecipitated in the presence of double strength protease inhibitors before analysis by SDS-PAGE and Western blotting.

First, the effect of $CuCl_2$ alone on the form of endothelial bound endogenous RANTES was investigated. HLMVECs were grown in collagen IV coated 6-well plates in the presence of 12.5 – 200 μM $CuCl_2$ as previously described in Sections 4.3.2.1 - 4.3.2.3. The cells were harvested as described in Section 4.3.2.5 and RANTES immunoprecipitated from cell lysates was analysed on 4-15 % gradient gels as described in Sections 4.3.2.6 - 4.3.2.8. Gradient gels were used to separate the RANTES optimally in the mid-high molecular weight range where it was expected that GAG bound RANTES may be detected.

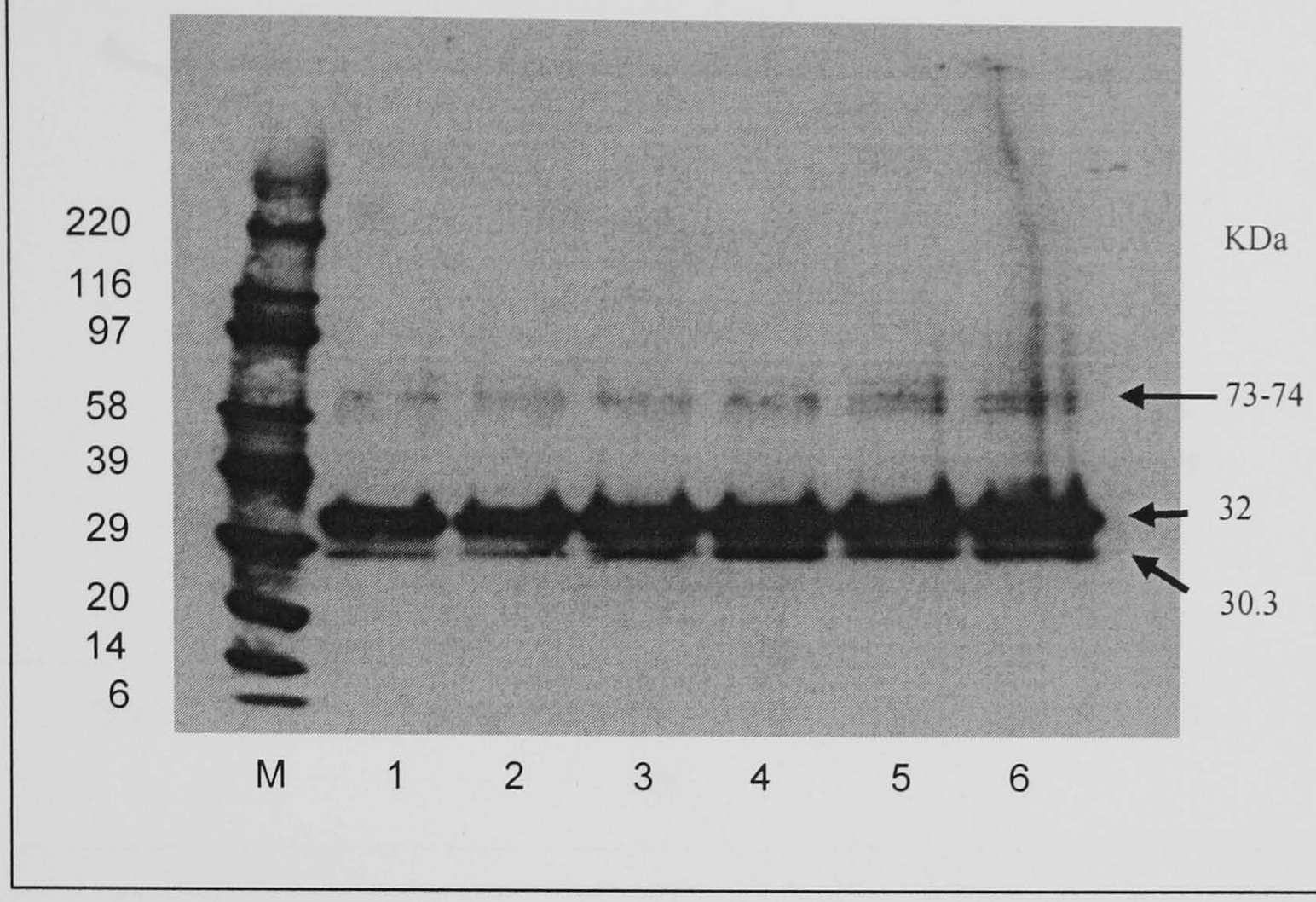

Figure 4.2. The effect of Cu on RANTES multimerisation in HLMVECs. Lysates from HLMVECs grown in collagen IV coated 6-well plates and incubated for 24 hours in the presence of IFN-γ (100 U/ml) plus TNF-α (10 ng/ml) and a further 24 hours in the presence of 12.5 - 200 μM $CuCl_2$. Lysates were freeze-dried from 500 μl, reconstituted in 40 μl 1x sample buffer, immunoprecipitated for human RANTES, analysed by SDS-PAGE on a 4-15 % gradient polyacrylamide gel and stained for RANTES. M: molecular weight markers. Lanes 1-6 show HLMVEC lysates in the presence of IFN-γ (100 U/ml), TNF-α (10 ng/ml), and in Lane 1: 0 μM $CuCl_2$ (control), lane 2: 12.5 μM $CuCl_2$, lane 3: 25 μM $CuCl_2$, lane 4: 50 μM $CuCl_2$, lane 5: 100 μM $CuCl_2$ and lane 6: 200 μM $CuCl_2$. Representative of two independent experiments.

In the presence of IFN-γ (100 U/ml) plus TNF-α (10 ng/ml) and absence of $CuCl_2$ RANTES was detected in HLMVEC lysates predominantly in 32 KDa form, which may be tetrameric RANTES. In addition, resistance to SDS and the disulphide reducing agent, dithiothreitol (DTT), during immunoprecipitation indicates that the RANTES tetramer is covalently linked as shown for recombinant human RANTES (Sections 2.5.1 and 3.5.2). Using a standard curve (figure 4.3) a high molecular weight form of RANTES was detected with an estimated molecular weight of 73-74 KDa (arrowhead, figure 4.2, lanes 1-6). This Western blot shows clearly the RANTES stained band at 73-74 KDa which may be a RANTES complex or RANTES bound to another protein. However, further higher molecular weight complexes of RANTES could be seen following over-exposure of the Western blot (not shown). These complexes are seen clearly in figures 4.5 and 4.7 which show the results of other experiments.

$CuCl_2$ in the range 12.5 – 200 μM had no effect on the form of RANTES (lanes 2-6) compared to the no $CuCl_2$ control, (lane 1). However, a dose-dependent increase in the amount of tetrameric RANTES was observed (figure 4.2, lanes 2 – 6).

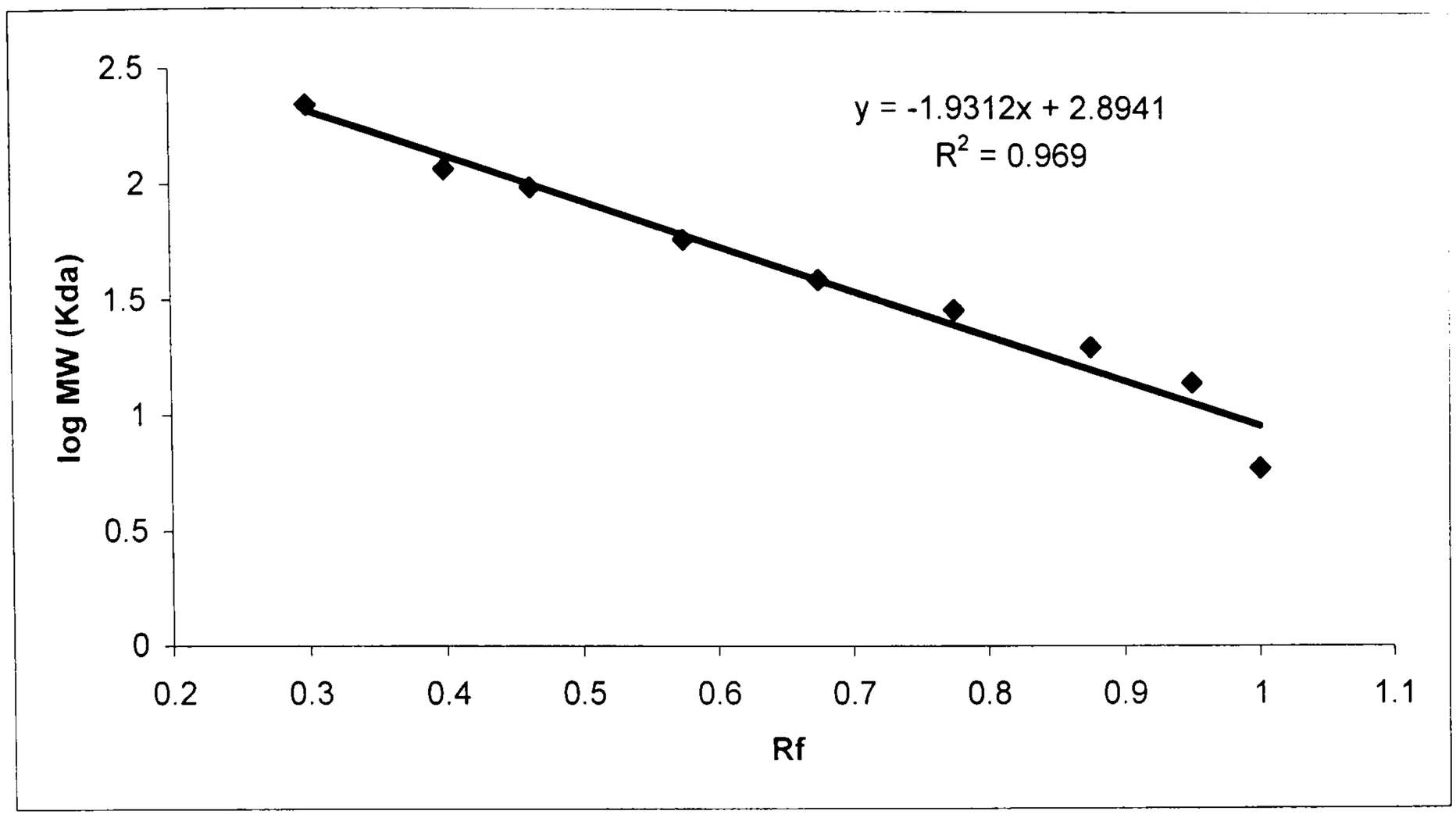

Figure 4.3. A standard curve of log molecular weight markers plotted against rf value where the rf value = distance moved by the protein / total distance moved by the bromophenol blue dye front and the RANTES complex had an rf value of 0.53. The RANTES band below the tetramer had an rf value of 0.73.

The rf value of 0.73 correlates to a molecular weight of 30.3 KDa for the RANTES band observed below the tetramer. It is likely that despite the presence of protease inhibitors upon lysis of the cells, this is a post-translational proteolytically processed form of RANTES.

In order to investigate whether the 73-74 KDa RANTES was a complex with GAGs in the cell lysates (figure 4.2), HLMVECs were grown in a collagen IV coated 6-well plate as before, stimulated with IFN-γ (100 U/ml) plus TNF-α (10 ng/ml) for 24 hours in the presence of 12.5 – 200 μM $CuCl_2$ and sodium chlorate (30 mM) to inhibit glycosaminoglycan (GAG) synthesis. The agent inhibits GAG sulphation and has been shown to abolish chemokine presentation on the endothelial cell surface (Davies *et al*, 2001; Humphries & Silbert, 1988; Humphries *et al*, 1989; Qiao *et al*, 2003; Safaiyan *et al*, 1999).

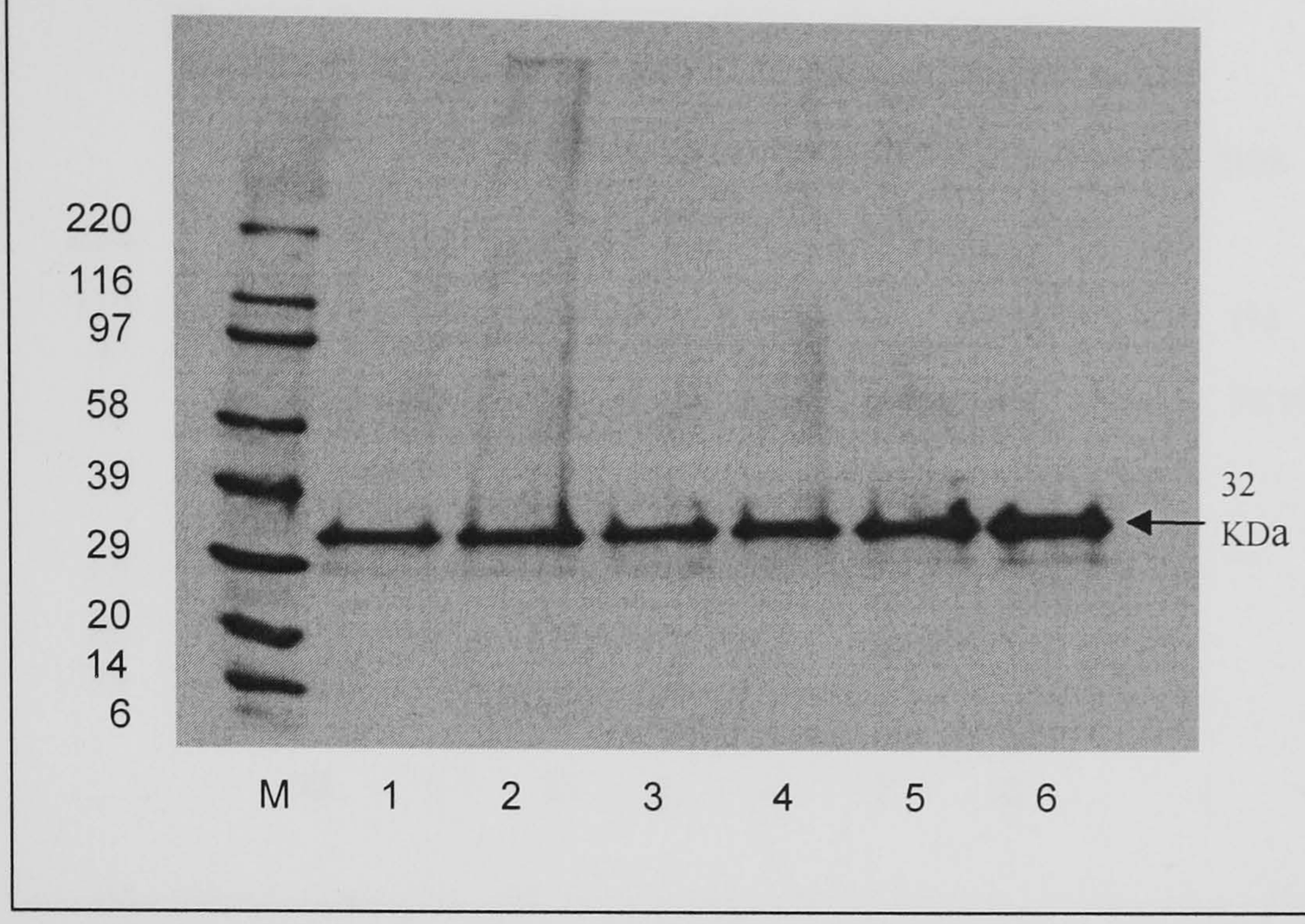

Figure 4.4. The effect of sodium chlorate on RANTES multimers in the presence of copper alone. HLMVECs were grown in collagen IV coated 6-well plates with 30 mM sodium chlorate and incubated for 24 hours in the presence of IFN-γ (100 U/ml) plus TNF-α (10 ng/ml) and a further 24 hours with 12.5 - 200 μM $CuCl_2$. Lysates were freeze-dried from 500 μl, reconstituted in 40 μl 1x sample buffer, immunoprecipitated for human RANTES, analysed by SDS-PAGE on a 4-15 % gradient polyacrylamide gel and stained for RANTES. M: molecular weight markers. Lanes 1-6 show HLMVEC lysates in the presence of IFN-γ (100 U/ml), TNF-α (10 ng/ml), sodium chlorate (30 mM) and in Lane 1: 0 μM $CuCl_2$ (control), lane 2: 12.5 μM $CuCl_2$, lane 3: 25 μM $CuCl_2$, lane 4: 50 μM $CuCl_2$, lane 5: 100 μM $CuCl_2$ and lane 6: 200 μM $CuCl_2$. Representative of two independent experiments.

In the presence of 30 mM sodium chlorate (figure 4.4, lanes 1 - 6) the RANTES complex (MW 73-74 KDa, figure 4.2) observed following HLMVEC stimulation with IFN-γ (100 U/ml) plus TNF-α (10 ng/ml) for 1 day was not observed. The result suggests that this form of RANTES was bound to a sulphated GAG on the endothelial cell surface (figure 4.2), which was not synthesised in the presence of sodium chlorate (figure 4.4). The tetrameric form of RANTES remains, and there is an increase in expression with increasing $CuCl_2$ as previously observed in figure 4.2.

In the presence of sodium chlorate, RANTES was detected only as a tetramer in cell lysates in the absence and presence of $CuCl_2$ alone. The effect of $CuCl_2$ plus H_2O_2 was subsequently investigated. HLMVECs were grown in collagen IV coated 6-well plates as before and incubated for 24 hours in the presence and IFN-γ (100 U/ml) plus TNF-α (10 ng/ml) to stimulate RANTES synthesis, and in the presence of 50 μM $CuCl_2$ plus 25 – 400 μM H_2O_2.

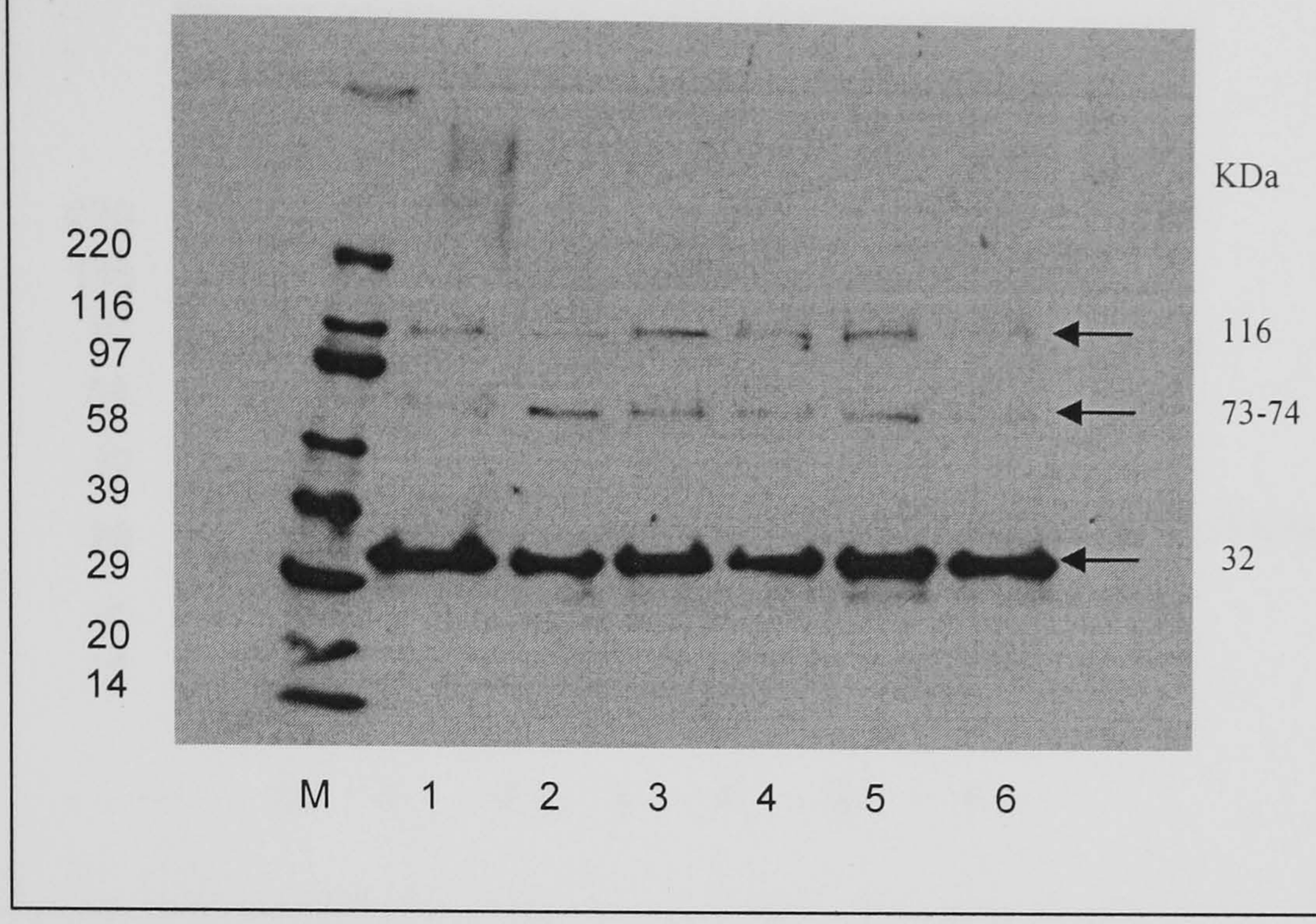

Figure 4.5. The effect of $CuCl_2$ and H_2O_2 on RANTES multimers. HLMVECs were grown in collagen IV coated 6-well plates and incubated for 24 hours in the presence of IFN-γ (100 U/ml) plus TNF-α (10 ng/ml), and a further 24 hours in the presence and absence of 50 μM $CuCl_2$ and 25 – 400 μM H_2O_2. Lysates were freeze-dried from 500 μl, reconstituted in 40 μl 1x sample buffer, immunoprecipitated for human RANTES, analysed by SDS-PAGE on a 4-15 % gradient polyacrylamide gel and stained for RANTES. M: molecular weight markers. Lanes 1-6 show HLMVEC lysates in the presence of IFN-γ (100 U/ml) plus TNF-α (10 ng/ml) and in Lane 1: 0 μM $CuCl_2$ (control), lane 2: 50 μM $CuCl_2$, lane 3: 50 μM $CuCl_2$ plus 25 μM H_2O_2, lane 4: 50 μM $CuCl_2$ plus 50 μM H_2O_2, lane 5: 50 μM $CuCl_2$ plus 200 μM H_2O_2 and lane 6: 50 μM $CuCl_2$ plus 400 μM H_2O_2. Representative of two independent experiments.

H_2O_2 (25 – 400 μM) had no effect on the form of RANTES in the presence of 50 μM $CuCl_2$ (figure 4.5, lanes 2-6) compared to the control (no $CuCl_2$ or H_2O_2, lane 1). The tetramer remained in the presence of 400 μM H_2O_2, unlike the monomeric RANTES which was destroyed in the supernatant (figure 4.1). This indicates that the tetramer in cell lysates is more stable than the monomer in supernatants.

Another high MW complex was observed that was not due to an effect of $CuCl_2$ or H_2O_2, since it was observed in the control (lane 1). This RANTES complex was estimated to be approximately 116 KDa (figure 4.5). This 116 KDa RANTES complex is likely to be a HSPG-RANTES complex. In order to investigate further the 116 KDa RANTES complex, HLMVECs were grown in a collagen IV coated 6-well plate as before, stimulated with IFN-γ (100 U/ml) and TNF-α (10 ng/ml) for 1 day in the presence of 50 μM $CuCl_2$, 25 – 400 μM H_2O_2 and 30 mM sodium chlorate to inhibit glycosaminoglycan (GAG) synthesis.

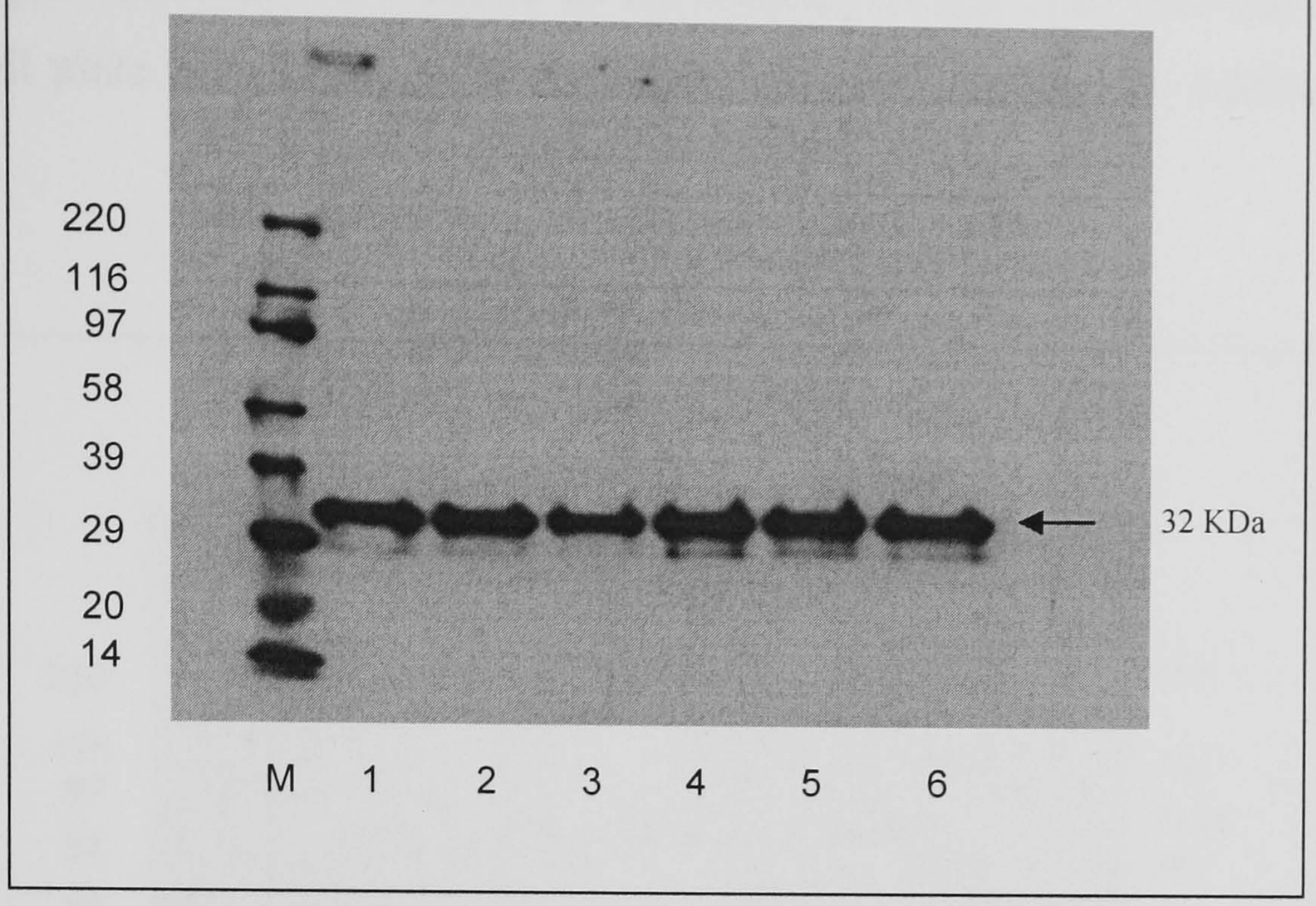

Figure 4.6. The effect of sodium chlorate on higher order forms of RANTES in the presence of $CuCl_2$ plus H_2O_2. HLMVECs were grown in collagen IV coated 6-well plates with sodium chlorate (30 mM) , incubated for 24 hours in the presence of IFN-γ (100 U/ml) plus TNF-α (10 ng/ml, and a further 24 hours in the presence and absence of 50 μM $CuCl_2$ and 25 – 400 μM H_2O_2. Lysates were freeze-dried from 500 μl, reconstituted in 40 μl 1x sample buffer, immunoprecipitated for human RANTES, analysed by SDS-PAGE on a 4-15 % gradient polyacrylamide gel and stained for RANTES. M: molecular weight markers. Lanes 1-6 show HLMVEC lysates in the presence of IFN-γ (100 U/ml plus TNF-α (10 ng/ml), sodium chlorate (30 mM), and Lane 1: 0 μM $CuCl_2$ (control), lane 2: 50 μM $CuCl_2$, lane 3: 50 μM $CuCl_2$ plus 25 μM H_2O_2, lane 4: 50 μM $CuCl_2$ plus 50 μM H_2O_2, lane 5: 50 μM $CuCl_2$ plus 200 μM H_2O_2 and lane 6: 50 μM $CuCl_2$ plus 400 μM H_2O_2. Representative of two independent experiments.

In the presence of sodium chlorate (30 mM, figure 4.6, lanes 1 - 6) the RANTES complexes observed following HLMVEC stimulation with IFN-γ (100 U/ml) plus TNF-α (10 ng/ml) for 1 day (MW 73-74 KDa and 116 KDa, figure 4.5) were both abolished. The result again suggests that RANTES was bound to a protein or a proteoglycan on the endothelial cell surface in figure 4.5, which was not synthesised in the presence of sodium chlorate in figure 4.6. Again, both $CuCl_2$ and H_2O_2 had no effect on the form of RANTES compared to the control (no $CuCl_2$ or H_2O_2, lane 1).

Since added $CuCl_2$ and H_2O_2 had no effect, and RANTES has so far been detected at a minimum MW of 30.3 KDa, it was speculated that there may already be sufficient physiological levels of $CuCl_2$ and H_2O_2 in the endothelial model to induce covalently linked tetramer formation, which has been shown to be the form which induces leukocyte migration *in vivo* (Proudfoot, 2006). To investigate this possibility, HLMVECs were incubated with IFN-γ (100 U/ml) plus TNF-α (10 ng/ml) for 1 day as before, but in the presence of the intracellular copper chelator, neocuproine (NC) and

the extracellular copper chelator bathocuproine disodium salt (BCDS), to chelate free copper. Copper chelators were added at the seeding of the cells into the collagen IV coated 6-well plate for maximum effect. This was 2 days before the addition of IFN-γ plus TNF-α.

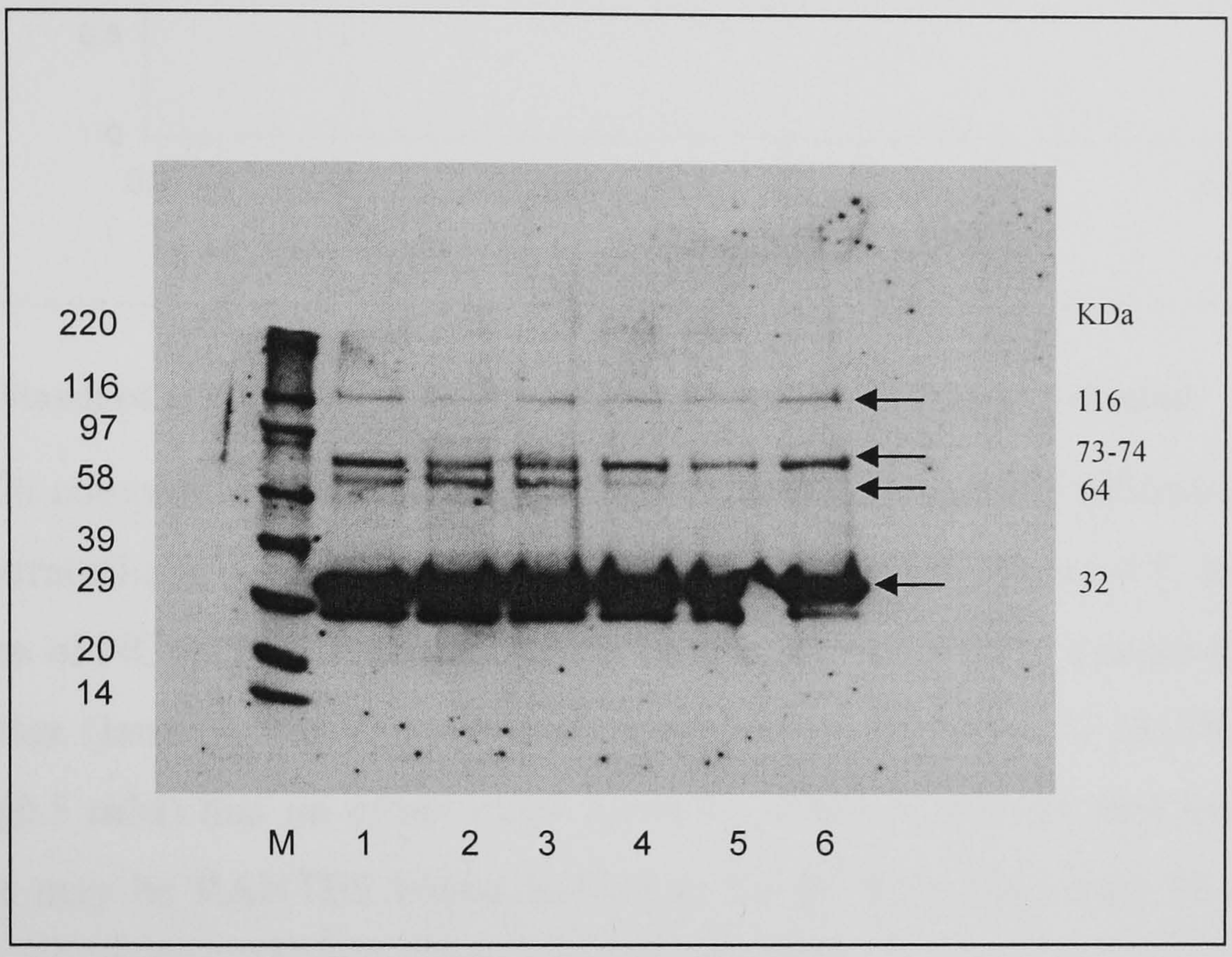

Figure 4.7. The effect of copper chelators on RANTES multimers. HLMVECs were grown in collagen IV coated 6-well plates in the presence of copper chelators, and incubated for 48 hours in the presence of IFN-γ (100 U/ml) plus TNF-α (10 ng/ml) and Cu chelators. Lysates were freeze-dried from 500 µl, reconstituted in 40 µl 1x sample buffer, immunoprecipitated for human RANTES, analysed by SDS-PAGE on a 4-15 % gradient polyacrylamide gel and stained for RANTES. M: molecular weight markers. Lanes 1-6 show HLMVEC lysates of cells grown in the presence of IFN-γ (100 U/ml plus TNF-α (10 ng/ml) and Lane 1: no copper chelators (control), lane 2: 0.1 mM neocuproine, lane 3: 0.5 mM neocuproine, lane 4: 0.1 mM bathocuproine disodium salt, lane 5: 0.5 mM bathocuproine disodium salt and lane 6: 0.5 mM neocuproine plus 0.5 mM bathocuproine disodium salt. Representative of two independent experiments.

NC (0.1 and 0.5 mM) had no effect on the tetrameric (32 KDa) or complexed form of RANTES (figure 4.7, lanes 2 and 3) compared to the control (no copper chelators, lane 1). In addition to the RANTES complex observed at 73-74 KDa, another RANTES complex was observed that was not due to the presence of copper chelators, since it appears in the control (lane 1) and the RANTES complex had an rf value of 0.6. The complex was estimated to be approximately 64 KDa, calculated using a standard curve (figure 4.8).

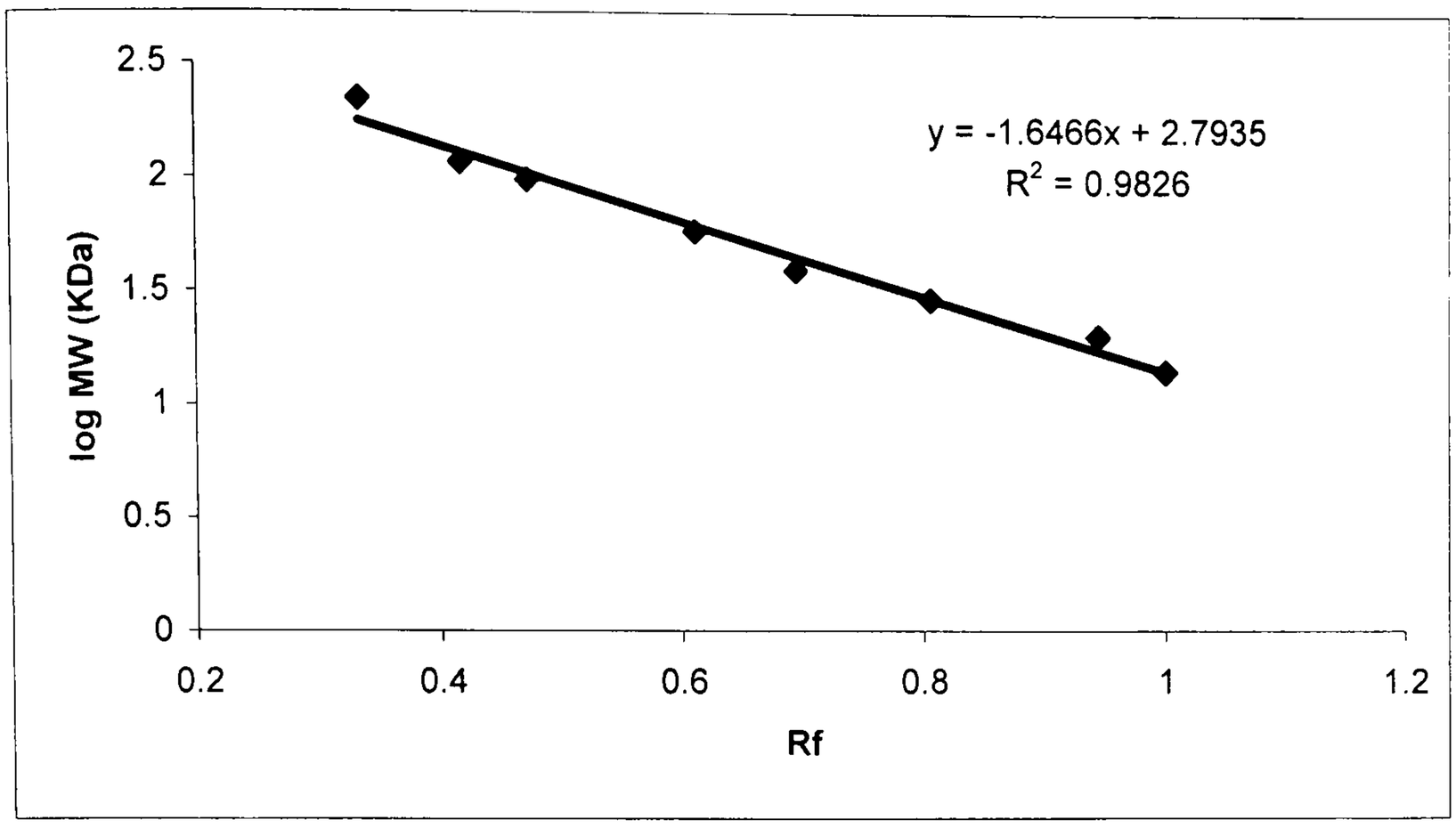

Figure 4.8. Standard curve of log molecular weight markers plotted against rf value.

The 64 KDa complex was diminished in a dose-dependent manner following treatment with the extracellular copper chelator, BCDS (0.1 – 0.5 mM) (figure 4.7, lanes 4-5). A combination of NC (0.5 mM) and BCDS (0.5 mM) also resulted in attenuation of the 64 KDa complex (lane 6), but this was only attributed to the effect of BCDS (0.5 mM), since NC (0.5 mM) had no effect alone (lane 3). While it appears that the 73/74-116 KDa bands may be RANTES bound to GAGs, the 64 KDa band may be a RANTES dimer bound to duffy antigen receptor complex (DARC).

RANTES was observed predominantly in tetrameric form (figures 4.2, 4.4 4.5 4.6 and 4.7). It was proposed that the tetramer may have been non-covalently bound to a GAG, and that the denaturing of the samples abolishes the GAG-RANTES interaction with the subsequent release of the tetramer. One suggestion was that dithiothreitol (DTT), a reagent which reduces disulfides, may have caused this denaturing during recovery of the immunoprecipitated proteins. Therefore, the recovery was performed in the absence and presence of DTT, with boiling at 95 ^{o}C for 5 minutes used as an alternative to DTT for the release of the RANTES from the agarose beads following immunoprecipitation.

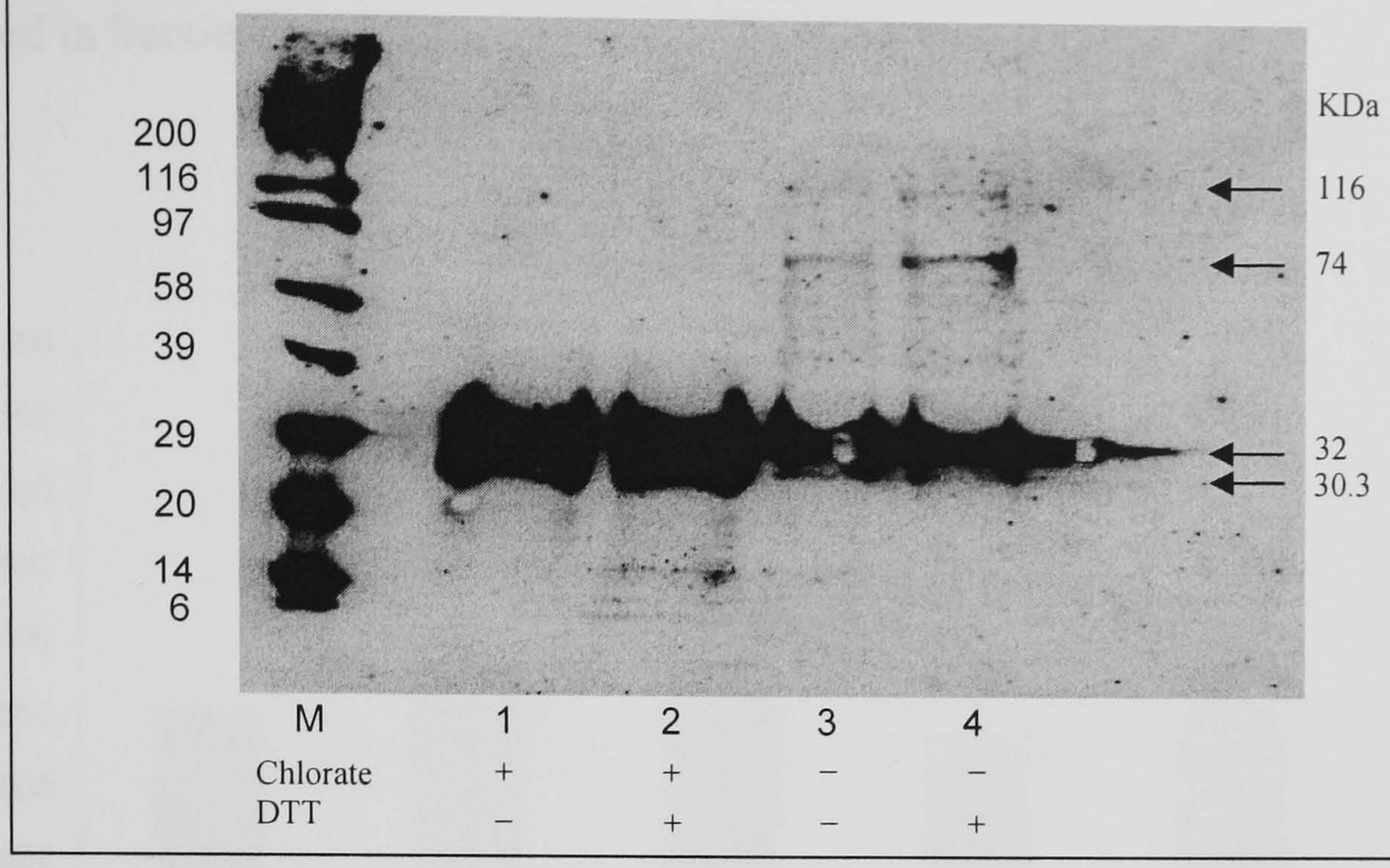

Figure 4.9. The effect of DTT on the form of RANTES. HLMVECs were grown in collagen IV coated 6-well plates in the absence and presence of sodium chlorate (30 mM) and incubated for 24 hours in the presence of IFN-γ (100 U/ml) plus TNF-α (10 ng/ml). Lysates were freeze-dried from 500 µl, reconstituted in 40 µl 1x sample buffer, immunoprecipitated for human RANTES in the absence of DTT with boiling at 95 °C for 5 minutes or in the presence of DTT (100 µM) for 30 minutes, analysed by SDS-PAGE on a 4-15 % gradient polyacrylamide gel and stained for RANTES. M: molecular weight markers. Lanes 1-4 show HLMVEC lysates of cells grown in the presence of IFN-γ (100 U/ml plus TNF-α (10 ng/ml) and Lane 1: 30 mM sodium chlorate and immunoprecipitation in the absence of DTT, lane 2: 30 mM sodium chlorate with immunoprecipitation in the presence DTT, lane 3: immunoprecipitation in the absence of DTT, lane 4: immunoprecipitation in the presence of DTT. Representative of two independent experiments.

In the presence of sodium chlorate (30 mM, figure 4.9, lanes 1 - 2) the high MW RANTES complexes observed following HLMVEC stimulation with IFN-γ (100 U/ml) plus TNF-α (10 ng/ml) for 1 day (MW 73-74 KDa and 116 KDa, lanes 3 and 4) were both abolished. Again, the results (lanes 3 and 4) suggest that RANTES was bound to a protein or a proteoglycan on the endothelial cell surface, which was not synthesised in the presence of sodium chlorate (lanes 1 and 2). The 30.3 KDa post-translational proteolytically processed form of RANTES was observed in the presence (lanes 1 and 2), but not the absence (lanes 3 and 4) of sodium chlorate, indicating that the inhibition of GAG synthesis by sodium chlorate also leads to a reduced protective effect against proteolytic degradation. In addition, the presence of DTT (lane 4) had no effect on the form of RANTES recovered compared to the absence of DTT (lane 3) which was found to be predominantly tetrameric.

Subsequent experiments investigated the concentration of RANTES synthesised by HLMVECs in response to $CuCl_2$, as measured by ELISA. HLMVECs were cultured as described in Section 4.3.2.

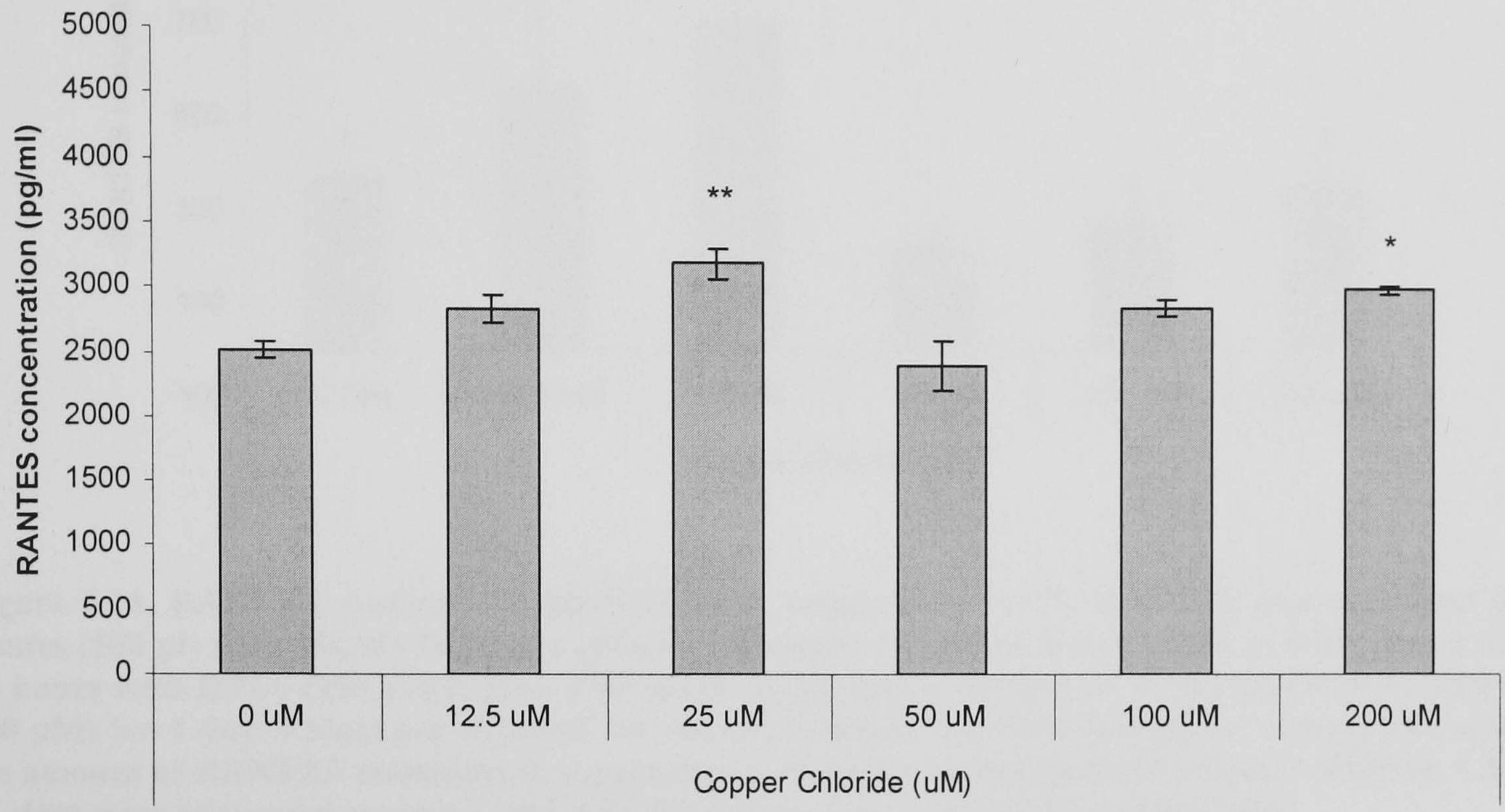

Figure 4.10. RANTES released into supernatants in response to $CuCl_2$. RANTES was measured in supernatants (1500 µl) from HLMVECs grown on collagen IV coated 6-well plates and incubated for 24 hours with IFN-γ (100 U/ml) plus TNF-α (10 ng/ml) and a further 24 hours with $CuCl_2$ (12.5 – 200 µM). RANTES was quantified by ELISA. Results are represented as mean ± SEM (* $p < 0.05$, ** $p < 0.01$ compared to the no Cu control, n = 4), data were compared using a 1-way ANOVA followed by a Dunnett's *post-hoc* test.

The addition of $CuCl_2$ in the range 12.5 – 25 µM resulted in a significant dose-dependent increase in RANTES synthesis and release into the HLMVEC supernatant as detected by ELISA (figure 4.10). The greatest increase ($p < 0.01$) in RANTES release was detected in the presence of 25 µM $CuCl_2$ (3189.8 ± 124.4 pg/ml) compared to the no $CuCl_2$ control (2508.3 ± 58.1). The effect was biphasic with another significant dose-dependent increase ($p < 0.05$) in RANTES synthesis and release in the presence of 200 µM $CuCl_2$ (2993.6 ± 35.8 pg/ml).

The concentration of RANTES in HLMVEC lysates was also measured by ELISA (figure 4.11).

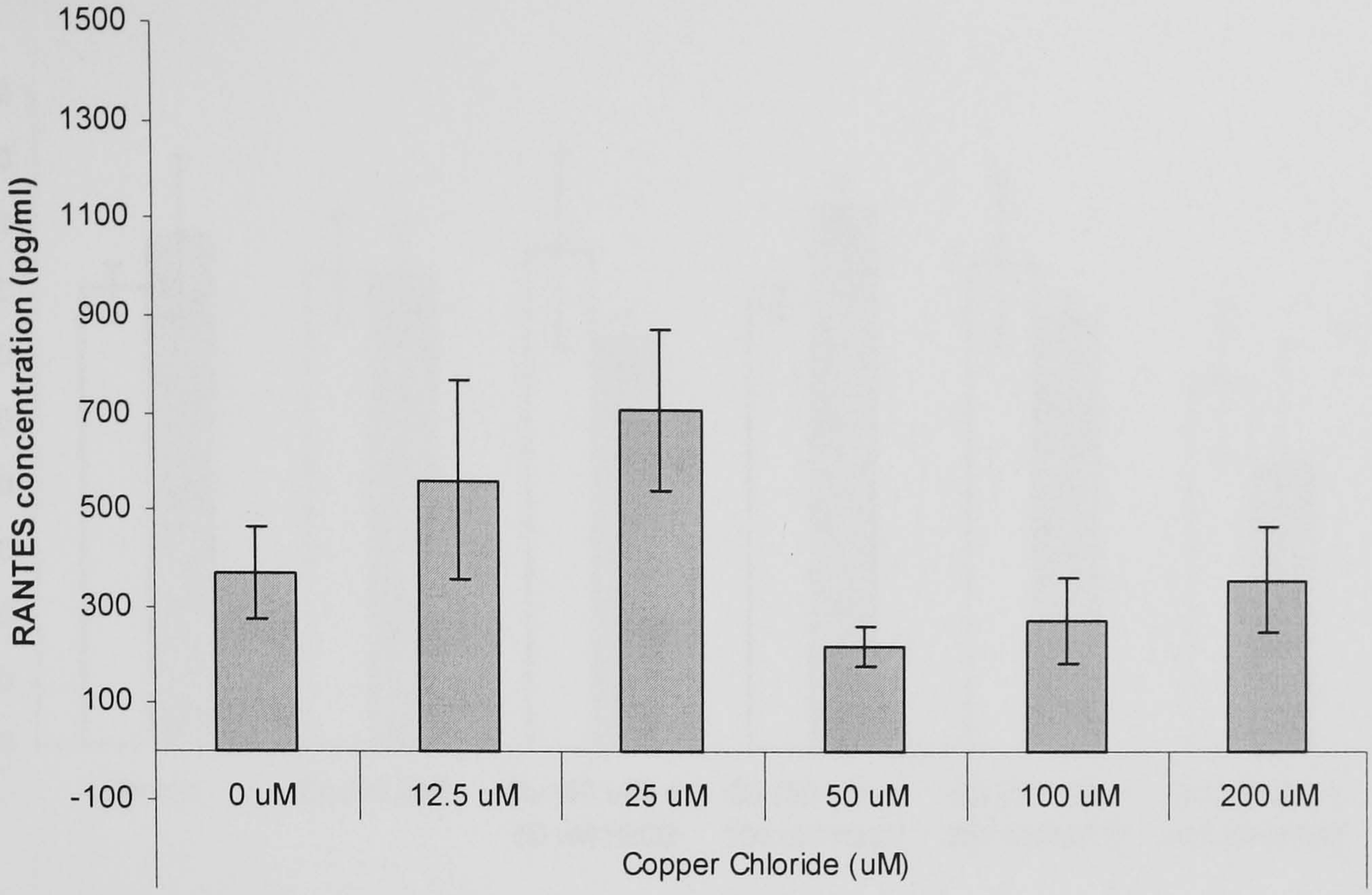

Figure 4.11. RANTES synthesis by HLMVECs in response to $CuCl_2$. RANTES was measured in lysates (500 µl) from HLMVECs were grown on collagen IV coated 6-well plates and incubated for 24 hours with IFN-γ (100 U/ml) plus TNF-α (10 ng/ml) and a further 24 hours with $CuCl_2$ (12.5 – 200 µM) for 1 day. Values are adjusted for relative volumes (i.e. 500/1500 µl) for comparison with the amount of RANTES measured in supernatants. Results are represented as mean ± SEM (n = 3 - 4), data were compared using a 1-way ANOVA followed by a Dunnett's *post-hoc* test.

The addition of $CuCl_2$ in the range 12.5 – 25 µM resulted in a dose-dependent increase in RANTES synthesis as detected by ELISA. A non-significant increase in RANTES was detected in the lysates (figure 4.11) at 25 µM $CuCl_2$ (709.2 ± 168.6 pg/ml) compared to the no $CuCl_2$ control (369.9 ± 95). At 50 µM $CuCl_2$ the RANTES concentration fell to 220.1 ± 41.4 pg/ml), with another dose-dependent increase in RANTES synthesis and release from 50 - 200 µM $CuCl_2$ to levels not significantly different to the control. The levels of RANTES detected in the lysates (figure 4.11) were lower than those detected in the supernatants (figure 4.10). RANTES was detected at 369.9 ± 95 pg/ml in the HLMVEC lysate control (0 µM $CuCl_2$, 500 µl) compared to 2508.3 ± 58.1 pg/ml in the HLMVEC supernatant control (0 µM $CuCl_2$, 1500 µl). The result suggests that under the incubation conditions more RANTES is released into the supernatant than is bound to the endothelial cell surface.

Subsequently, the effect of H_2O_2 together with 50 µM $CuCl_2$ on the concentration of RANTES in HLMVEC supernatants and lysates was investigated.

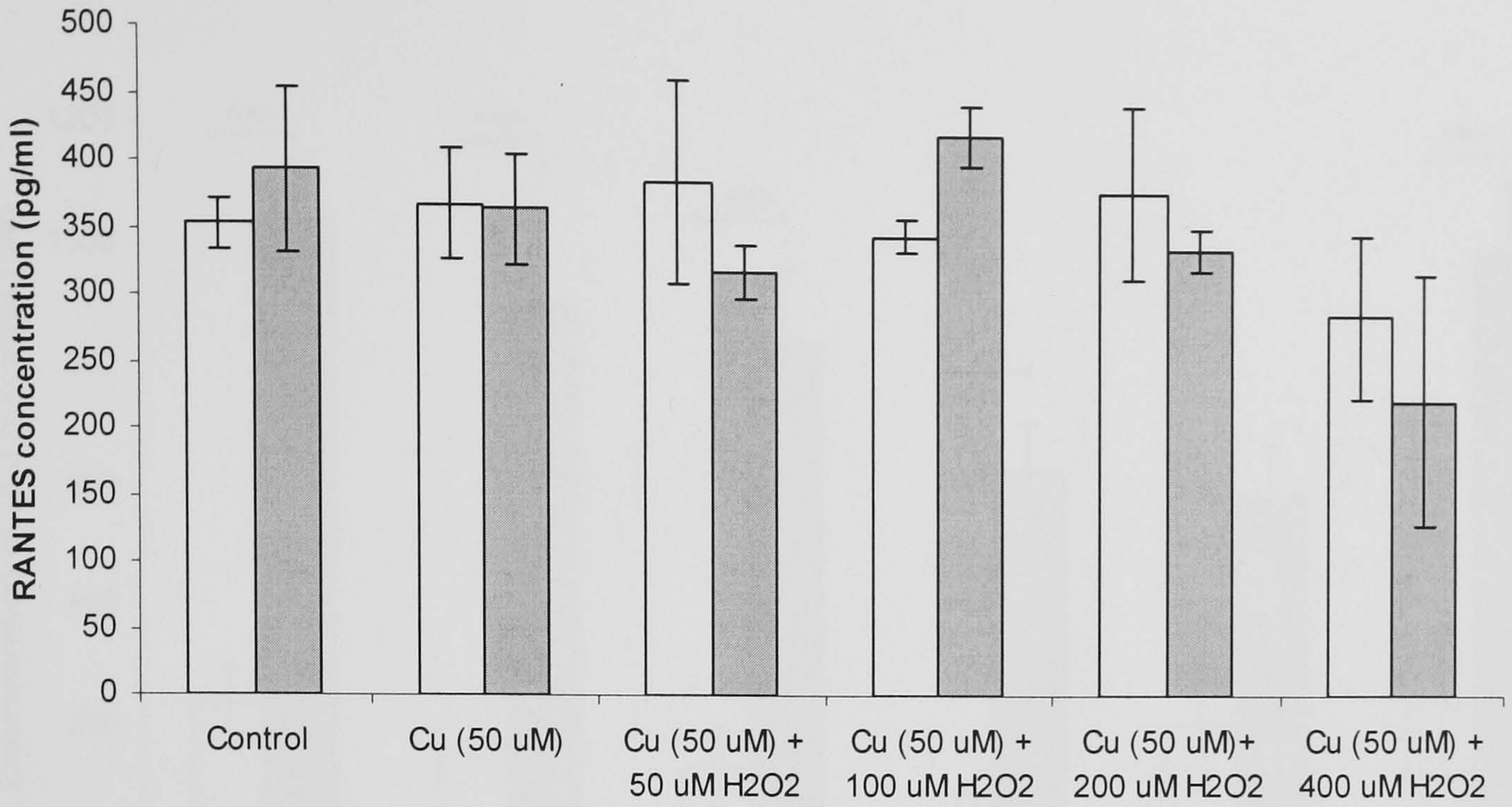

Figure 4.12. RANTES released into supernatants in the presence of $CuCl_2$ plus H_2O_2. RANTES was measured in supernatants from HLMVECs grown on collagen IV coated 6-well plates and incubated for 24 hours with IFN-γ (100 U/ml) plus TNF-α (10 ng/ml) and a further 24 hours with the addition of $CuCl_2$ (50 μM) plus H_2O_2 (50 – 400 μM). The experiment was carried out in the absence (□) and in the presence (▨) of sodium chlorate (30 mM). RANTES was quantified by ELISA. Results are represented as mean ± SEM (n = 3), data were compared using a 2-way ANOVA followed by a Tukey's *post-hoc* test.

As seen in these experiments (figure 4.12) 50 μM $CuCl_2$ had no effect on RANTES levels in supernatants as previously shown (figure 4.10). Additionally, there was no significant difference in RANTES release into HLMVEC supernatants following treatment with 50 – 400 μM H_2O_2 in the presence of 50 μM $CuCl_2$ compared to the control (EGM-2MV growth medium). The addition of sodium chlorate also had no effect, which was unexpected.

To confirm an effect of chlorate on GAG synthesis under these conditions, the effect of $CuCl_2$ plus H_2O_2 on lipid peroxidation was investigated. HLMVECs were grown as before, in collagen IV coated 6-well plates and incubated in the presence of IFN-γ (100 U/ml) plus TNF-α (10 ng/ml) to stimulate RANTES synthesis, in the presence of 50 μM $CuCl_2$ plus 50 – 400 μM H_2O_2 and in the absence and presence of sodium chlorate. Cell lysates were analysed for lipid peroxides using a quantitative FOX-2 assay kit.

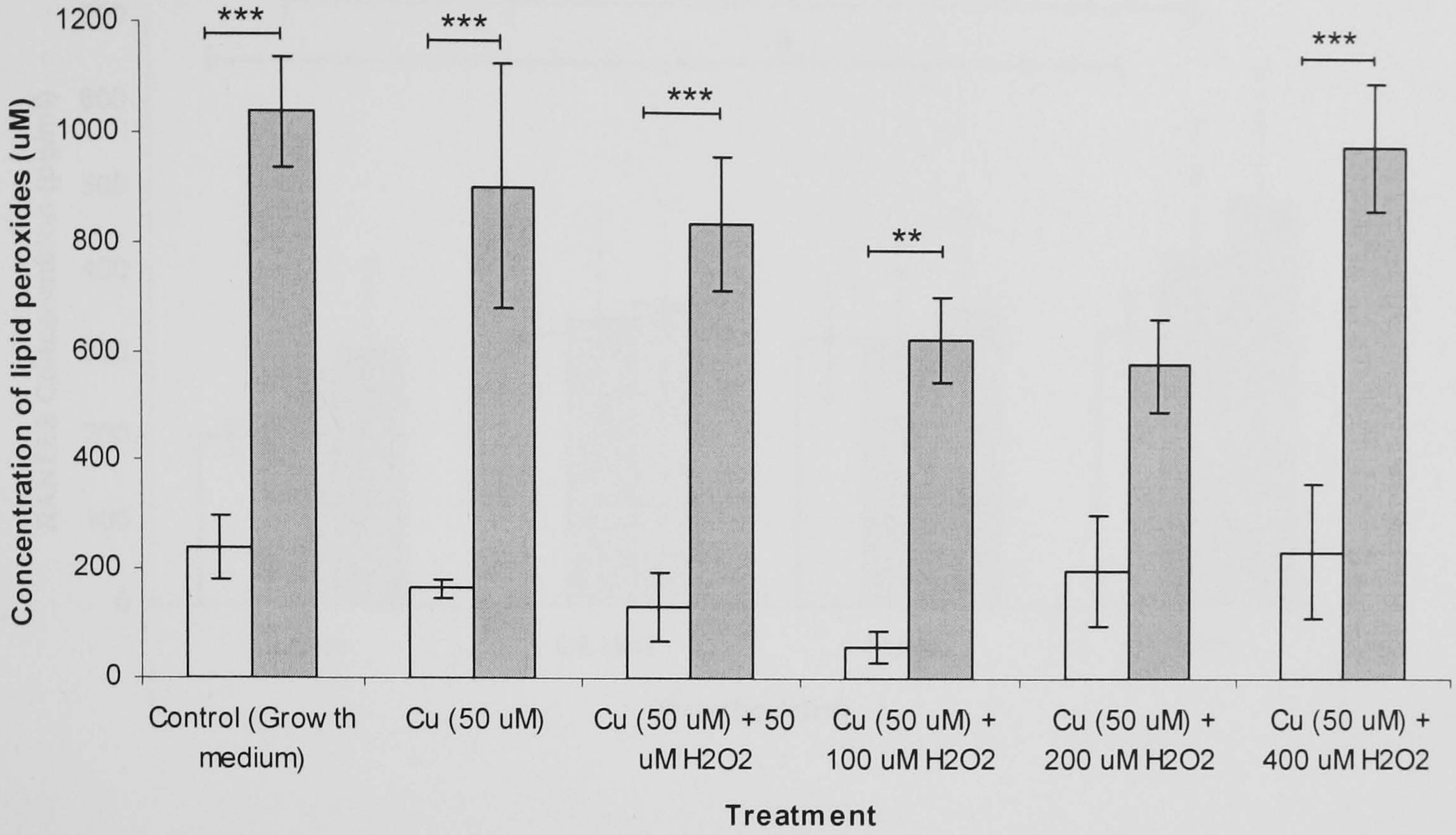

Figure 4.13. Lipid peroxides measured in lysates in the presence of $CuCl_2$ plus H_2O_2. HLMVECs were grown in collagen IV coated 6-well plates and incubated for 24 hours with IFN-γ (100 U/ml) plus TNF-α (10 ng/ml) and a further 24 hours with the addition of $CuCl_2$ (50 μM) plus H_2O_2 (50 – 400 μM) in the absence (□) and in the presence of sodium chlorate (30 mM) (▩). Lipid peroxides were quantified by FOX-2 assay. Results are represented as mean ± SEM (* $p < 0.001$ and ** $p < 0.01$ (2-way ANOVA, Tukey's *post-hoc* test), n = 4).**

There was no significant difference in lipid peroxide measured in HLMVEC supernatants following treatment with 50 – 400 μM H_2O_2 in the presence of 50 μM $CuCl_2$ compared to the control (EGM-2MV growth medium) either in the presence or absence of sodium chlorate (figure 4.13). However, in the presence of sodium chlorate (30 mM), there was a significant increase in lipid peroxides under all conditions tested. The maximum increase in lipid peroxides occurred in the EGM-2MV control group (increase from 238.7 ± 58.6 μM in the absence of sodium chlorate to 1037.2 ± 101.3 μM in the presence of sodium chlorate, $p < 0.001$).

4.5.2. Platelets

Initial experiments quantified RANTES release by thrombin-stimulated normal platelets using ELISA. Platelets were isolated and incubated as described in Section 4.3.4.

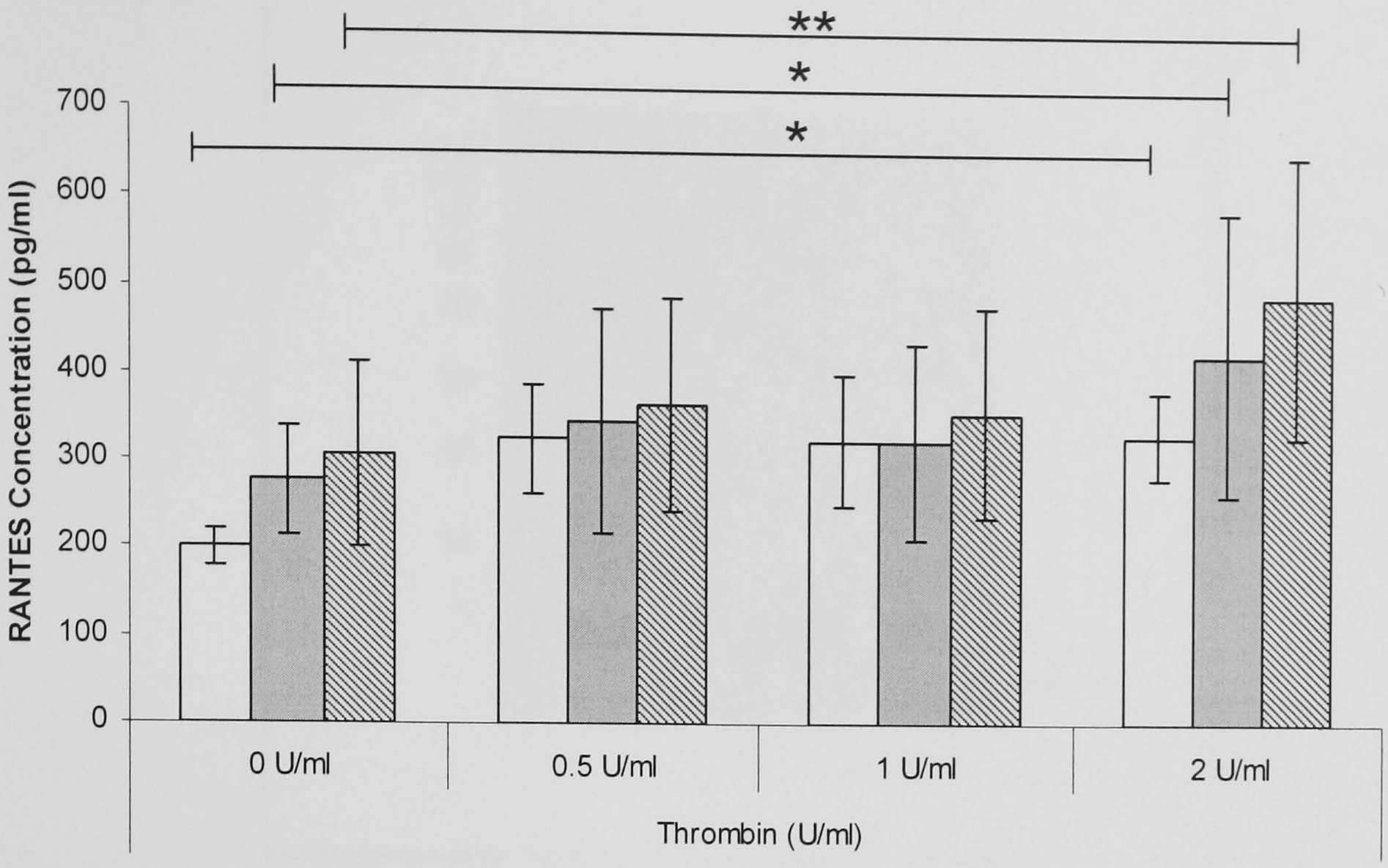

Figure 4.14. RANTES release by thrombin-activated platelets. RANTES was measured in supernatants (250 µl) from isolated platelets diluted to 10^7/ml (□), 5 x 10^7/ml (▒) and 10^8/ml (▨) and incubated in an uncoated 24-well plate for 1 hour with 0.5 – 2 U/ml thrombin. Results are represented as mean ± SEM (2-way ANOVA, Tukey's *post-hoc* test, n = 5).

An increase in RANTES release into supernatants was observed with increasing concentrations of thrombin (figure 4.14). Concentrations were significantly higher than unstimulated control values at 2 U/ml at platelet concentrations 10^7 (increase from 200.3 ± 47.5 to 330.3 ± 110.6), 5 x 10^7 (increase from 276.7 ± 139.1 to 422.9 ± 361.1 pg/ml ($p < 0.05$)) and 10^8/ml (increase from 306.1 ± 236.3 to 489 ± 357.9 pg/ml ($p < 0.01$)). The increase in RANTES release in response to thrombin therefore appears to be dose-dependent. There was no significant increase in RANTES concentration as the platelet concentration was increased from 10^7 through to 10^8/ml at all concentrations of thrombin. The data suggests that RANTES is released spontaneously from platelets and in response to thrombin, but that there is a limiting factor at high cell density.

To determine the form of platelet-derived RANTES, isolated platelets were suspended at 10^8/ml and cultured in an uncoated 6-well plate for 1 hour in the presence of thrombin (1 U/ml). For comparison, HLMVECs were grown on collagen IV coated 6-well plates and incubated in the presence and absence of thrombin. The form of RANTES in platelet supernatants was analysed by SDS-PAGE on a 14 % polyacrylamide gel and Western blotting.

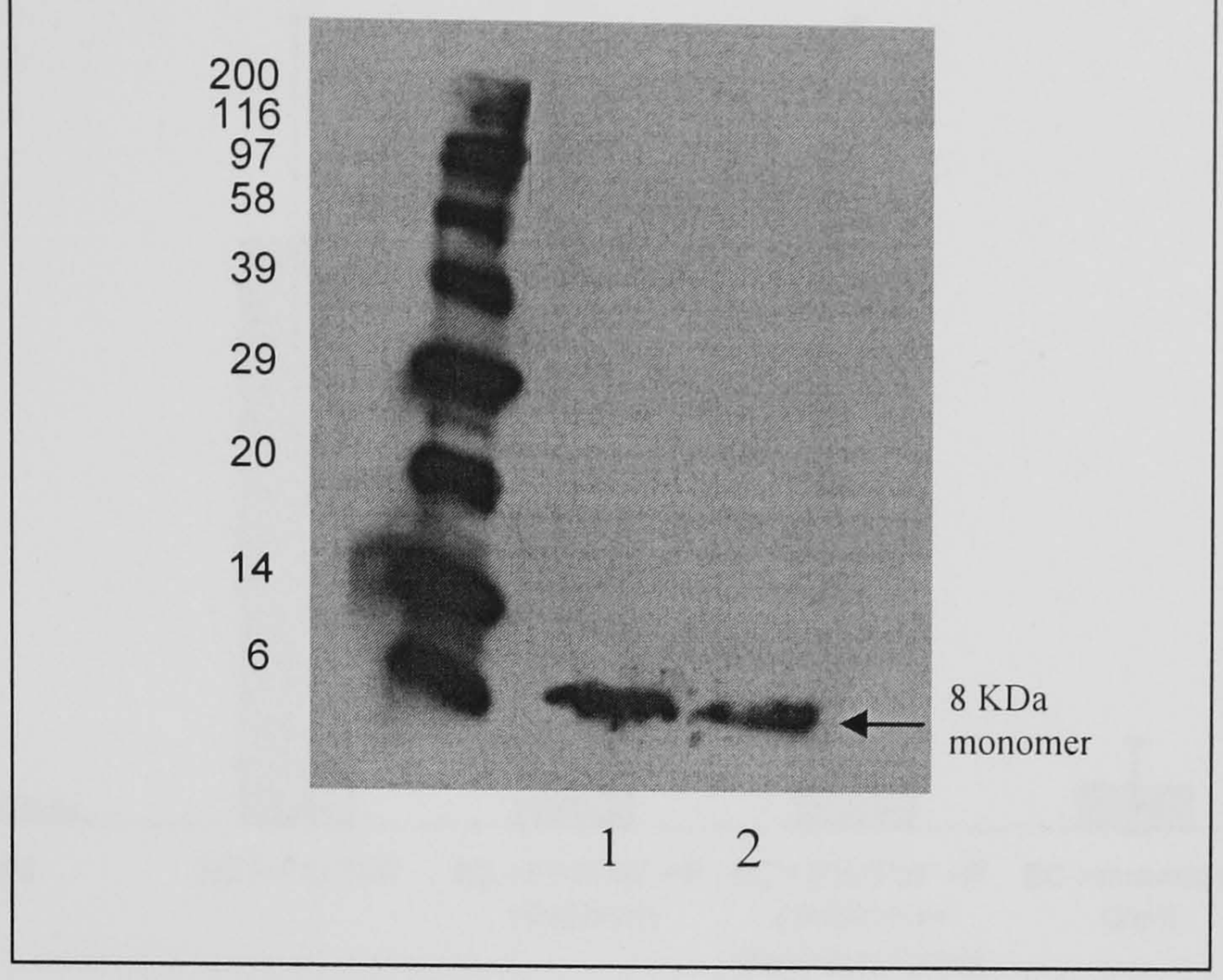

Figure 4.15. Platelet-derived RANTES. Platelets (10^8/ml) were incubated in a 6-well plate (lanes 1 and 2) for 1 hour in the presence and absence of IFN-γ (100 U/ml) plus TNF-α (10 ng/ml) and in the presence of thrombin (1 U/ml). Supernatants were freeze-dried from 1500 µl, reconstituted in 40 µl 1x sample buffer, analysed by SDS-PAGE on a 14 % polyacrylamide gel and stained for RANTES. M: molecular weight markers. Lane 1: isolated platelets in the presence of thrombin and lane 2: isolated platelets in the presence of IFN-γ plus TNF-α and thrombin. Representative of two independent experiments.

In the presence of thrombin (1 U/ml), platelet-derived RANTES was monomeric (figure 4.15, lane 1). IFN-γ (100 U/ml) plus TNF-α (10 ng/ml) had no effect on the form of RANTES released by thrombin stimulated platelets (lane 2), which remained monomeric. The results indicate that platelets release monomeric RANTES following stimulation with thrombin (1 U/ml), (figure 4.15).

Whilst platelet and HLMVEC-derived RANTES has separately been determined by ELISA, the extent of RANTES release when platelets and HLMVECs are cocultured together was not known. To investigate the contribution of each, HLMVECs and platelets were cultured alone and together in the presence and absence of IFN-γ (100 U/ml) plus TNF-α (10 ng/ml) and thrombin (1 U/ml). RANTES was quantified by ELISA in both supernatants and cell lysates, which were prepared as previously described (Section 4.3.5).

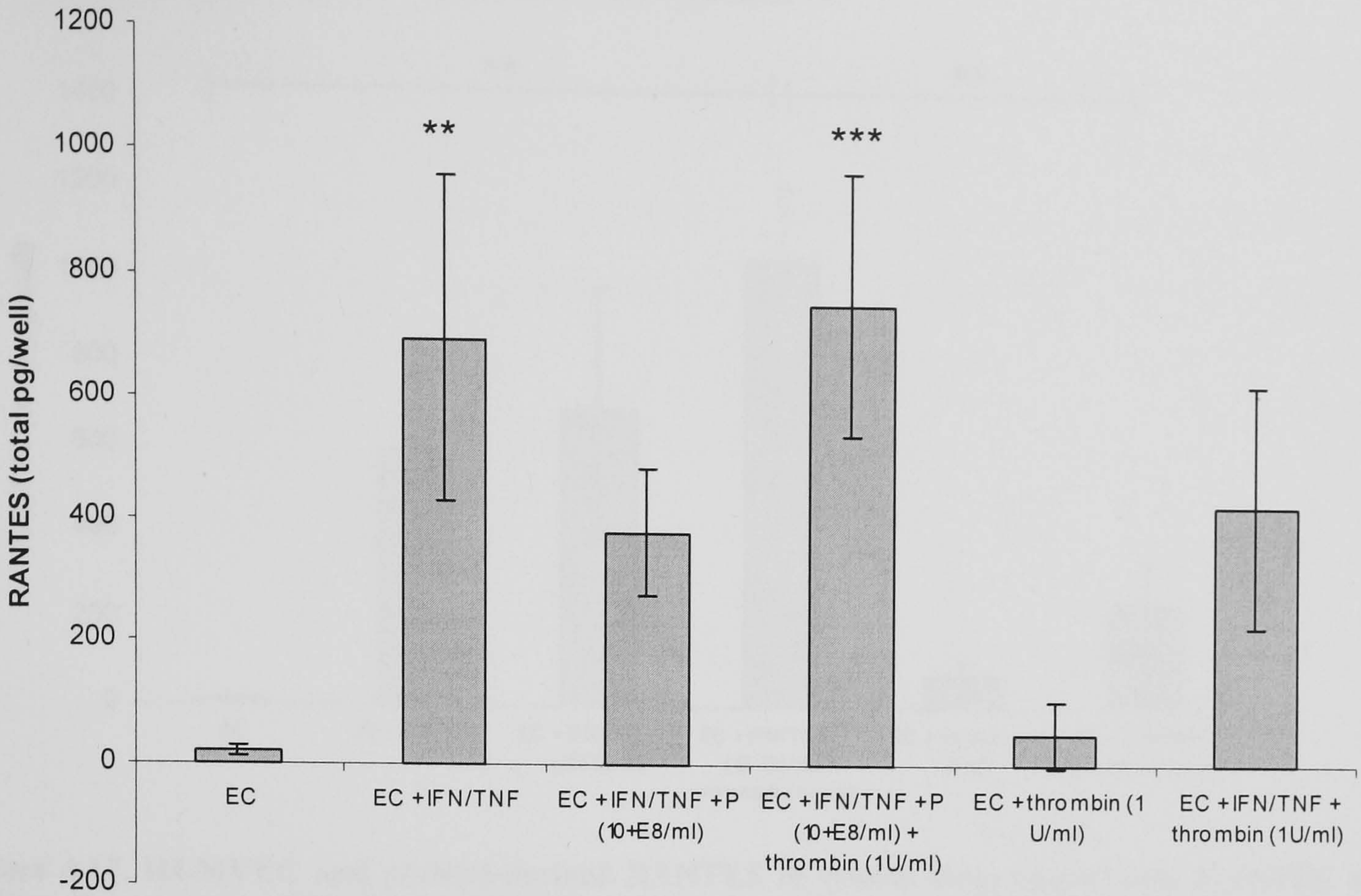

Figure 4.16. HLMVEC and platelet-derived RANTES release in supernatants from co-cultures. RANTES was measured in supernatants from isolated platelets (10^8/ml) and HLMVECs co-cultured in collagen IV coated 6-well plates. HLMVECs were incubated for 1 day in the presence and absence of IFN-γ (100 U/ml), TNF-α (10 ng/ml) and following incubation, platelets and thrombin (1 U/ml) were added to the wells for 1 hour. Supernatants (1500 µl) were analysed by ELISA. EC: endothelial cells, P: platelets (10^8/ml). Results are represented as mean ± SEM (* p < 0.001, ** p< 0.01 compared to EC control). Data was compared using a 1-way ANOVA and Tukey's *post-hoc* test, n = 5).**

HLMVEC activation with IFN-γ plus TNF-α significantly ($p < 0.01$) increased RANTES release into supernatants in the absence of platelets (from 18.7 ± 8.4 in the control (endothelial cells only) to 694.4 ± 264.5 pg/well. Reduced levels of RANTES in the presence of platelets and activated HLMVECs suggests either that the platelets are binding RANTES synthesised by the endothelial cells, or that the addition of platelets results in increased binding of RANTES to the endothelium thus removing it from the supernatant.

RANTES was also measured in HLMVEC lysates.

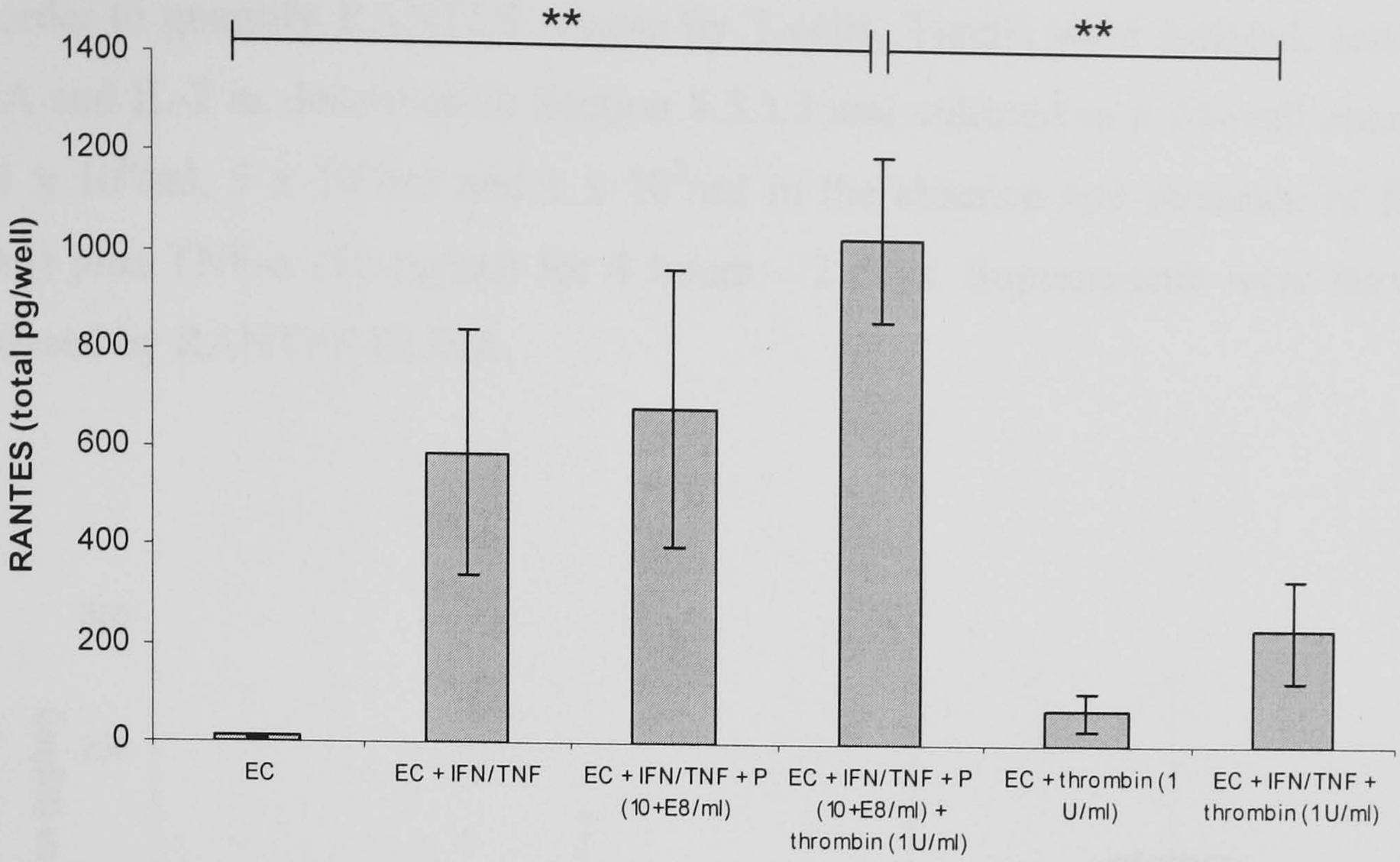

Figure 4.17. HLMVEC and platelet-derived RANTES in lysates from co-cultures. RANTES was measured in lysates (500 µl) from isolated platelets (10^8/ml) and HLMVECs co-cultured in a collagen IV coated 6-well plate. HLMVECs were incubated for 1 day in the presence and absence of IFN-γ (100 U/ml), TNF-α (10 ng/ml). Following incubation, platelets and thrombin (1 U/ml) were added to the wells for 1 hour. Values are adjusted for relative volumes (i.e. 500/1500 µl) for comparison with the amount of RANTES measured in supernatants. Lysates were analysed by RANTES ELISA. EC: endothelial cells, P: platelets (10^8/ml). Results are represented as mean ± SEM ($p < 0.01$). Data was compared using a 1-way ANOVA and Tukey's *post-hoc* test, n = 3).**

Treatment with IFN-γ plus TNF-α increased RANTES in HLMVEC lysates in the presence and absence of platelets but the effect was not significant compared to HLMVECs alone as a control (figure 4.17). The presence of unactivated platelets also did not significantly increase the amount of RANTES in the activated endothelium.

However, the addition of thrombin activated platelets to HLMVECs activated with IFN-γ plus TNF-α results in a significant increase in endothelial RANTES (from 238.3 ± 105.1 to 1035.8 ± 168.5 pg/well ($p < 0.01$) indicating a requirement for thrombin activated platelets for RANTES binding to the activated endothelium.

The results indicate that in both the supernatants and lysates, RANTES is measured at the highest concentrations in the presence of activated HLMVECs and platelets. In addition, under these conditions there appears to be more RANTES bound to the endothelium than free in the supernatant (1035.8 ± 168.5 pg/well bound compared to 753.6 ± 213.7 pg/well free in the supernatant).

4.5.3. T-cells

In order to quantify RANTES release by T-cells, T-cells were isolated, activated with PHA and IL-2 as described in Section 4.3.3.2 and cultured in a 24-well uncoated plate at 1 x 10^6/ml, 5 x 10^6/ml and 1 x 10^7/ml in the absence and presence of IFN-γ (100 U/ml) plus TNF-α (10 ng/ml) for 4 hours – 2 days. Supernatants were harvested and analysed by RANTES ELISA.

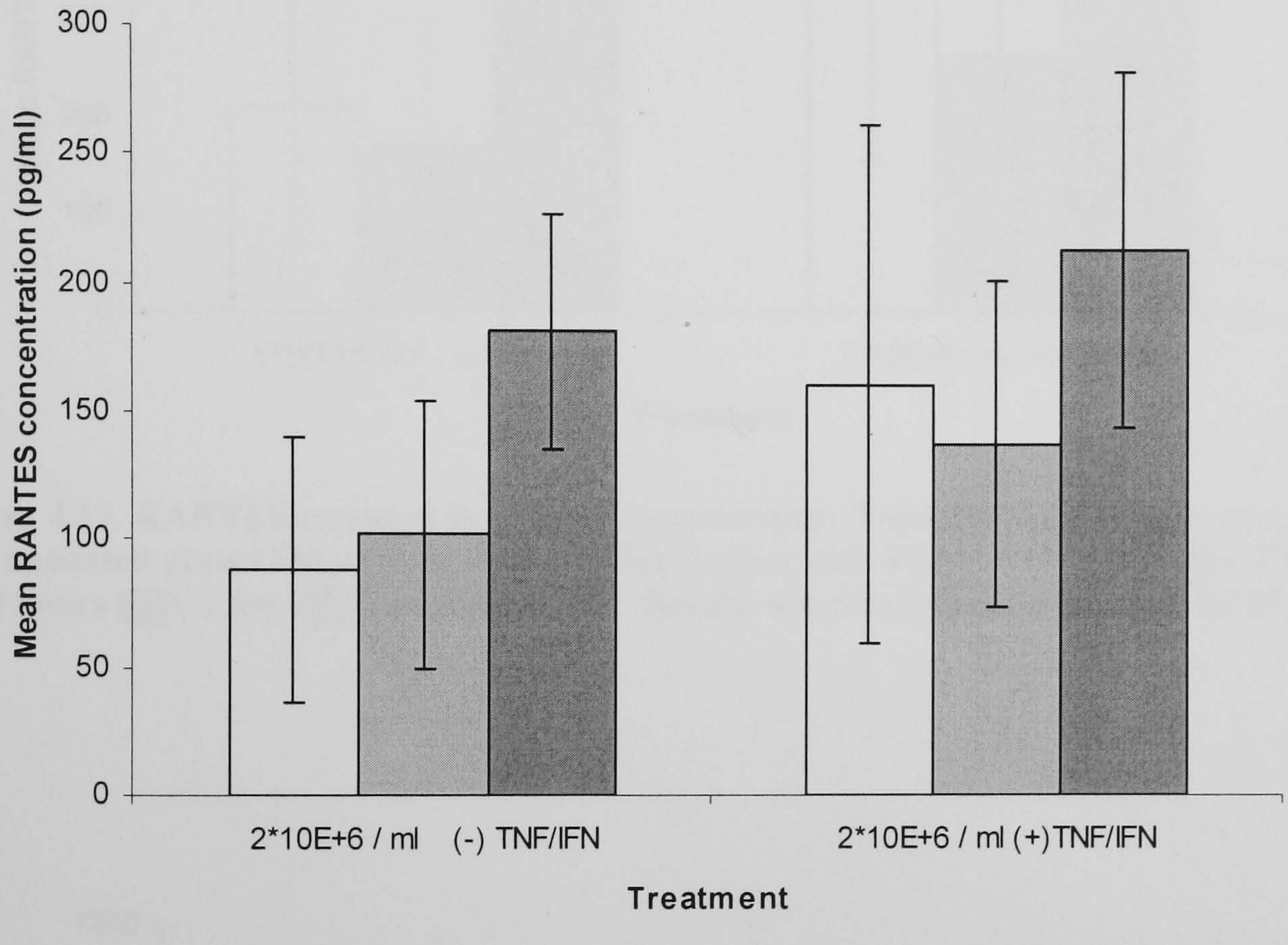

Figure 4.18. RANTES released into T-cell supernatants. T-cells (2 x 10^6/ml) were cultured in a 24-well uncoated plate (250 µl/well) following incubation with IFN-γ (100 U/ml) plus TNF-α (10 ng/ml) for 4 hours (□), 1 day (■) and 2 days (□). Results are represented as mean ± SEM, n = 3.

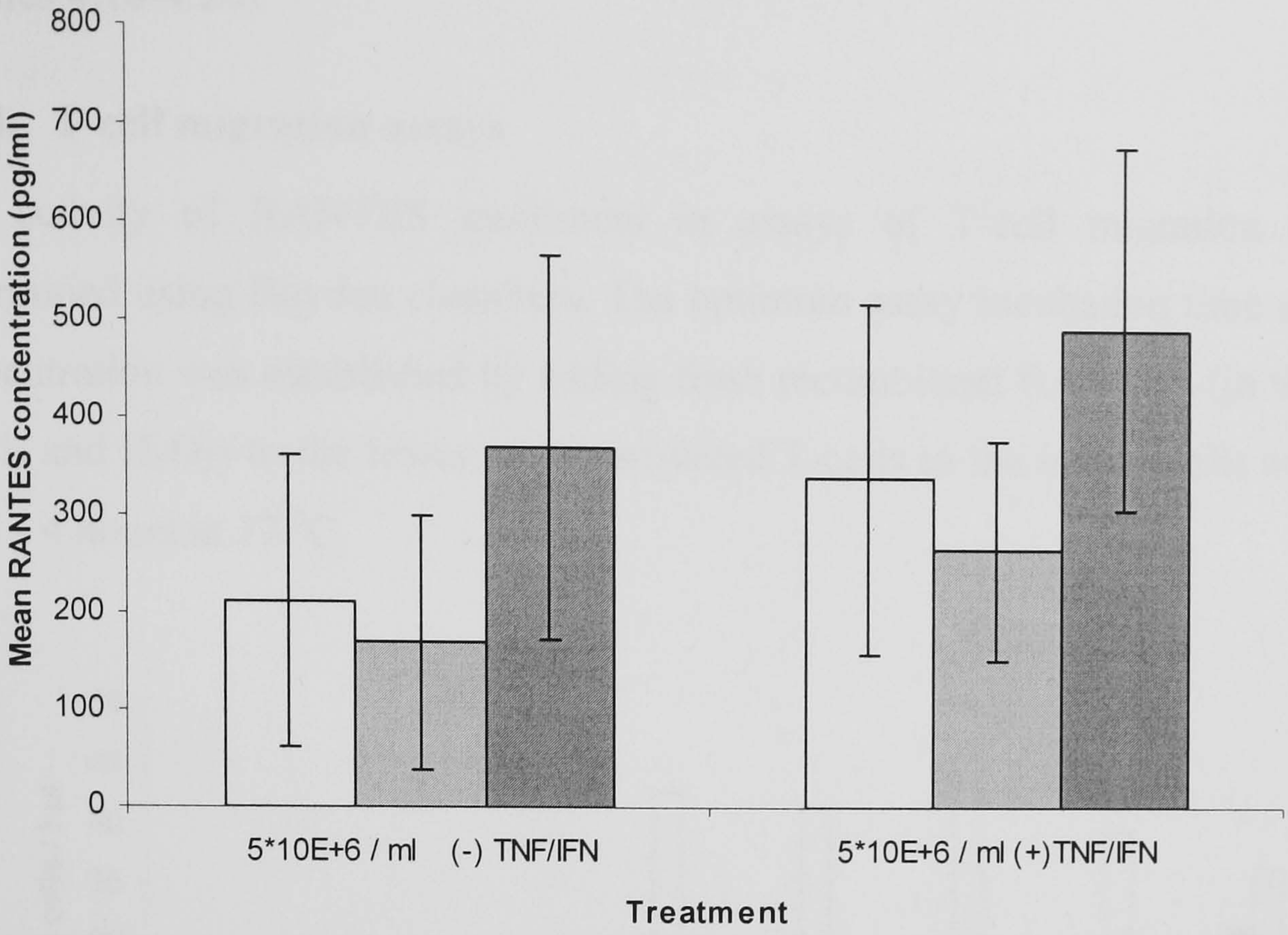

Figure 4.19. RANTES released into T-cell supernatants. T-cells (5 x 10^6/ml) were cultured in a 24-well uncoated plate (250 µl/well) following incubation with IFN-γ (100 U/ml) plus TNF-α (10 ng/ml) for 4 hours (□), 1 day (■) and 2 days (□). Results are represented as mean ± SEM, n = 3.

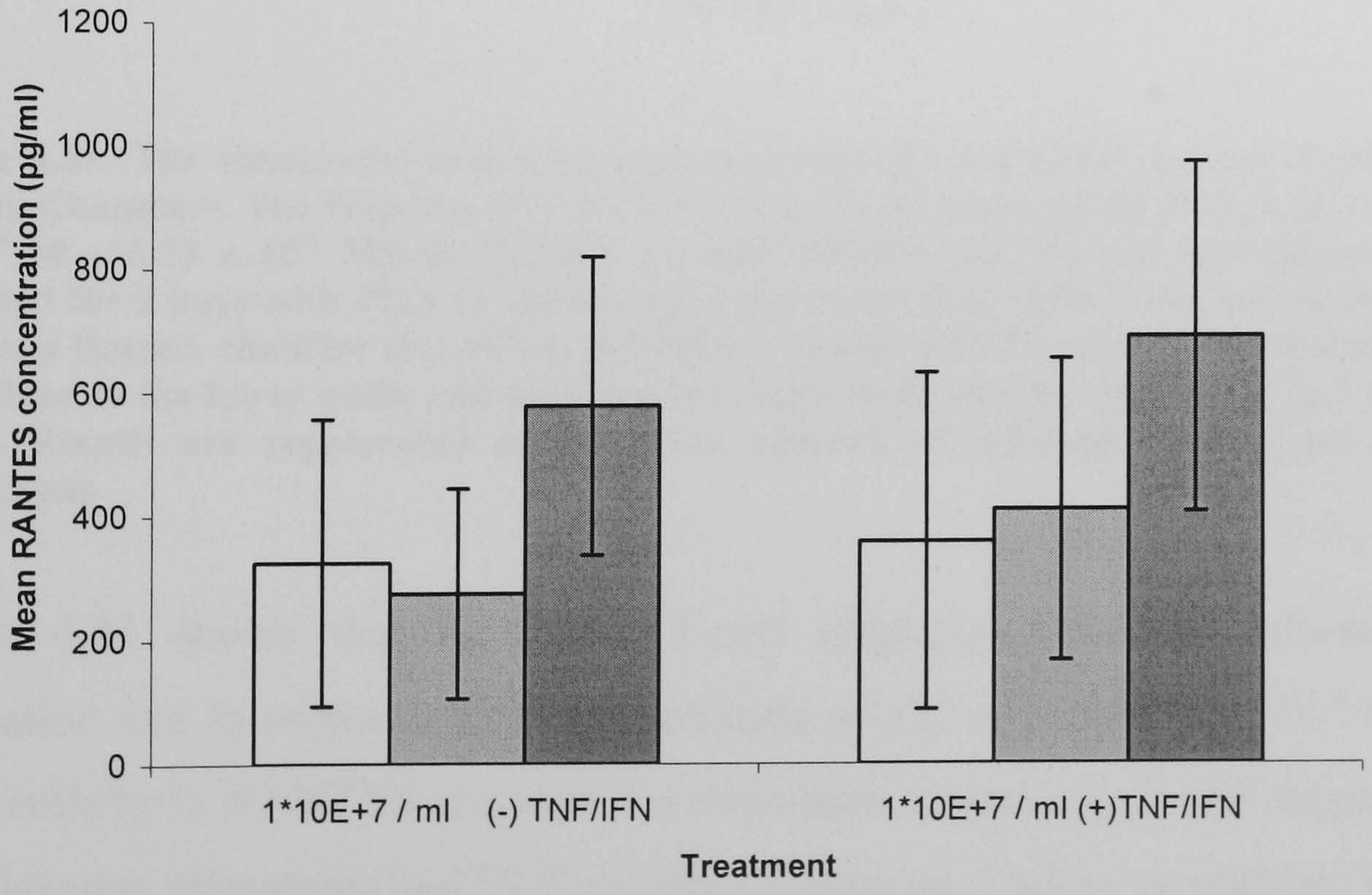

Figure 4.20. RANTES released into T-cell supernatants. T-cells (1 x 10^7/ml) were cultured in a 24-well uncoated plate (250 µl/well) following incubation with IFN-γ (100 U/ml) plus TNF-α (10 ng/ml) for 4 hours (□), 1 day (■) and 2 days (□). Results are represented as mean ± SEM, n = 3.

There was no significant effect of IFN-γ (100 U/ml) plus TNF-α (10 ng/ml) stimulation and no significant time-dependent increase in RANTES release at any T-cell density (figures 4.18-4.20).

4.5.4. T-cell migration assays

The activity of RANTES multimers in assays of T-cell migration was initially determined using Boyden chambers. The optimum assay incubation time and RANTES concentration was established by adding fresh recombinant RANTES (in the absence of $CuCl_2$ and H_2O_2) to the lower wells, activated T-cells to the upper wells and incubating for 1 - 4 hours at 37 °C.

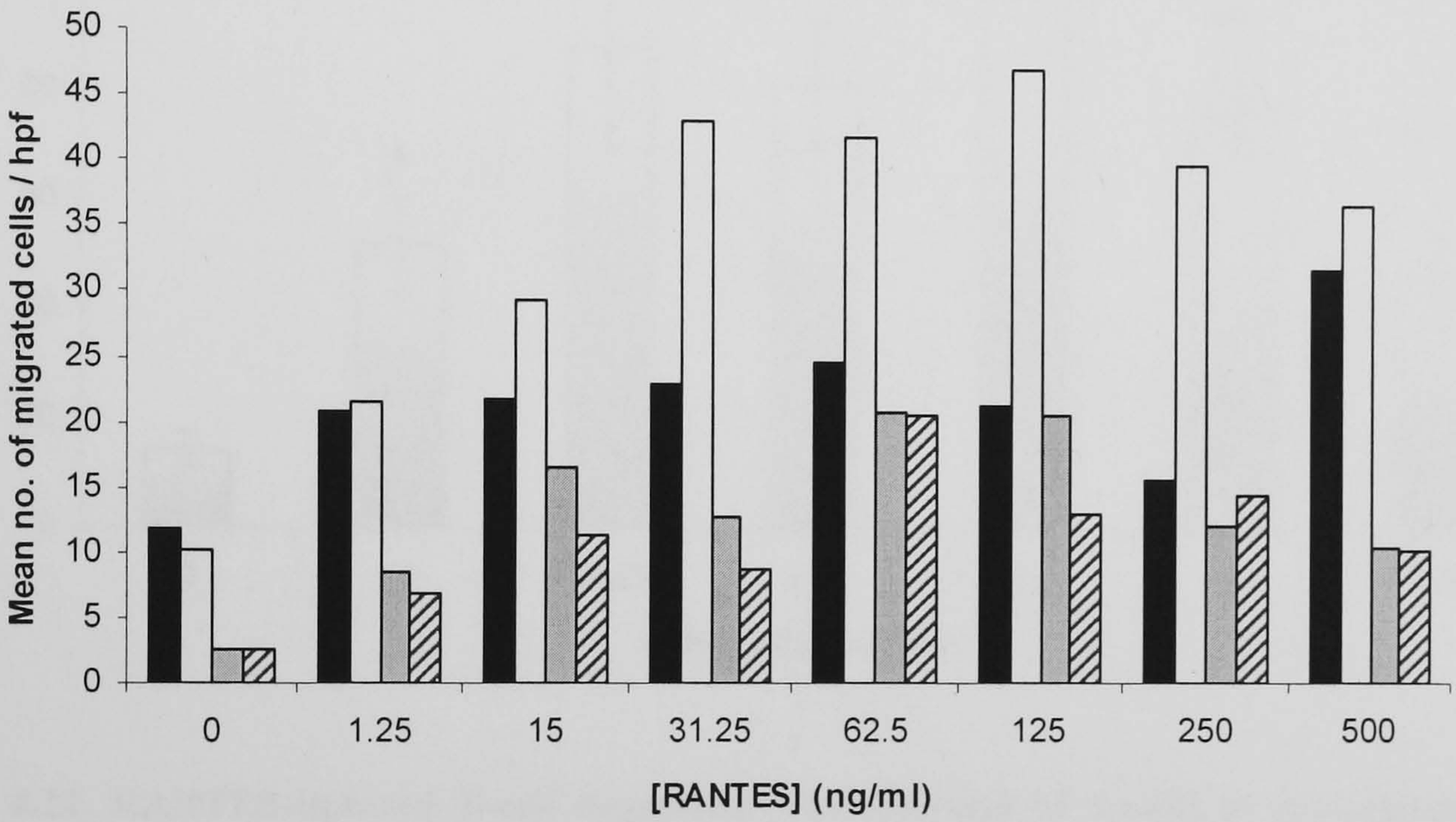

Figure 4.21. The timecourse and dose-response curve for RANTES-induced T-cell migration in Boyden Chambers. The response of T-cells to recombinant human RANTES (1.25 - 500 ng/ml (1.56 x 10^{-10} M – 6.25 x 10^{-8} M)) in HBSS + 20 mM HEPES, pH 7.4 was investigated. T-cells were activated for 2 days with PHA (1 μg/ml) and 3 days with IL-2 (200 U/ml) and added to the upper wells of a Boyden chamber (2 x 10^6/ml in HBSS + 20 mM HEPES, pH 7.4). Recombinant RANTES was added to the lower wells, and the chambers were incubated for 1(■), 2 (□), 3 (▒) and 4 (▨) hours. Results are represented as the mean number of cells/hpf. Results are from a single experiment.

Figure 4.21 shows that maximum T-cell migration occurred following 2 hours incubation and in response to a concentration of 125 ng/ml (1.56 x 10^{-8} M) RANTES (47.2 cells/hpf). RANTES stimulated a maximum increase in T-cell migration from 12 (spontaneous migration) to 47.2 T-cells/hpf following 2 hours incubation, indicating the most appropriate RANTES concentration and time for sensitive assay of RANTES-induced T-cell migration in Boyden chambers. After 3 - 4 hours, T-cells had begun to die, confirmed by the uptake of Trypan blue by T-cells from the lower chambers

analysed by cytospin (data not shown). This reflects the lower numbers of migrated cells at these timepoints.

Migration of T-cells over 2 hours was measured using multiple T-cell donors and due to donor variability, the results normalised to the response observed for 125 ng/ml RANTES which was designated as 100 % response.

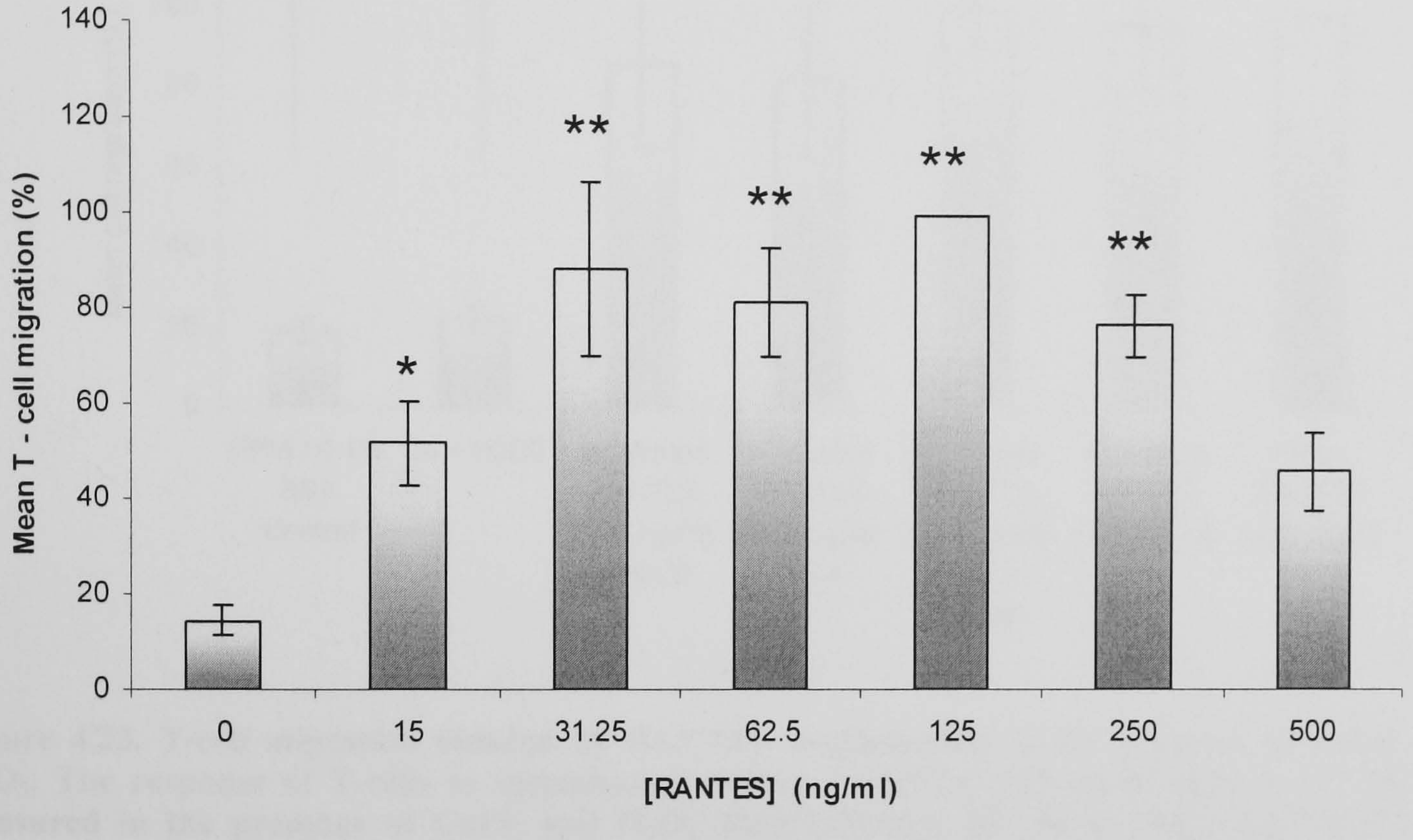

Figure 4.22. RANTES-induced T-cell migration. The response of T-cells to recombinant human RANTES (15 - 500 ng/ml (1.88 x 10^{-9} M – 6.25 x 10^{-8} M)) in HBSS + 20 mM HEPES, pH 7.4 was measured. T-cells were activated as before and added to the upper wells of a Boyden chamber. Recombinant RANTES was added to the lower wells and the chamber was incubated for 2 hours. Following incubation, migrated cells were stained and counted as before. Results are presented as the mean number of cells/hpf. The results were normalised to the maximum migration at 125 ng/ml (151.3 ± 43.8 T-cells/hpf,) which was designated as 100 %. Results represent mean ± SEM, and were compared using a 1-way ANOVA and Dunnett's *post-hoc* test (control = 0 ng/ml RANTES, *p < 0.05, ** p < 0.01 compared to the no RANTES control, n = 6).

Maximum migration occurred at 125 ng/ml RANTES (151.3 ± 43.8 T-cells/hpf, 100 %, $p < 0.01$), compared to the control (14.5 ± 3.1 %, figure 4.22).

The activity of RANTES multimers in T-cell migration assays was then investigated. Recombinant RANTES was incubated for 2 days in the presence and absence of $CuCl_2$ (50 μM) and H_2O_2 (25 μM) (as described in Chapter 2, Section 2.3.1) to induce RANTES multimerisation, diluted to 125 ng/ml (1.56 x 10^{-8} M), and used in a T-cell migration assay.

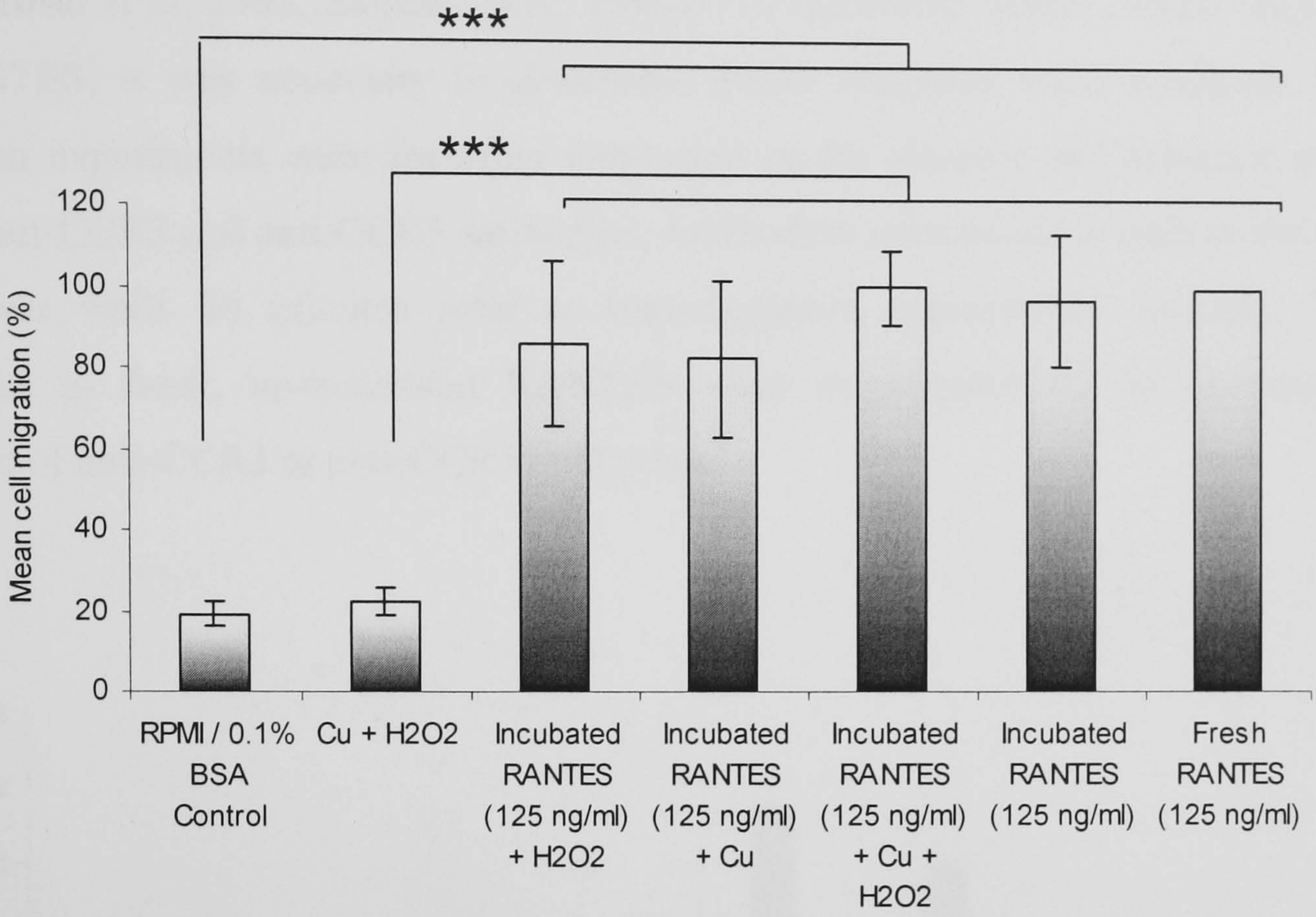

Figure 4.23. T-cell migration induced by RANTES multimerised in the presence of $CuCl_2$ plus H_2O_2. The response of T-cells to recombinant human RANTES (125 ng/ml (1.56×10^{-8} M) was measured in the presence of $CuCl_2$ and H_2O_2. RANTES (5×10^{-7} M in PBS $-Ca^{2+}/Mg^{2+}$) was incubated for 2 days in the presence and absence of 50 µM $CuCl_2$ and 25 µM H_2O_2 and diluted to 125 ng/ml in RPMI/0.1 % (w/v) BSA. T-cells were activated as before and added to the upper wells of a Boyden chamber. RANTES multimers were added to the lower wells and the chamber was incubated for 2 hours. Following incubation, migrated cells were stained and counted as before. Results are presented as mean number of cells/hpf. The results were normalised to the positive control (fresh/unincubated RANTES at 125 ng/ml (150.8 ± 39.4 T-cells/hpf) which was designated as 100 %. Results represent mean ± SEM, and data was compared using a 1-way ANOVA and Tukey's *post-hoc* test (* $p < 0.001$ compared to the RPMI/BSA control, n = 5).**

RANTES multimers generated in the presence of $CuCl_2$ and H_2O_2 over 2 days were shown to be chemotactically active, inducing 100 % migration compared to the RPMI/0. 1 % (w/v) BSA control (19.3 ± 6.7 % migration, $p < 0.001$). RANTES multimers were chemotactically as active (100 ± 19.9 %) as the fresh un-incubated RANTES control (100 %, figure 4.23). There was no observed difference between the chemoattractant activity of fresh un-incubated RANTES (100 % migration) and incubated RANTES in the absence of $CuCl_2$ and H_2O_2 (96.8 ± 36 % migration). In addition, $CuCl_2$ and H_2O_2 alone neither induced nor attenuated T-cell migration compared to the RPMI/0.1 % BSA control (22.2 ± 7.5 % migration).

Although Th1 and Th2 T-cells both signal through CCR1 in response to RANTES, RANTES recruits Th1 T-cells through CCR5 and Th2 T-cells through CCR3 receptors. In addition, $CD8^+$ cytotoxic T-cells also express CCR-1 and CCR-3, and CCR-1 and CCR-5 receptors on Tc type-1 and Tc type-2 cytotoxic T-cells respectively (D'Ambrosio *et al*, 1998; Sallusto *et al*, 1998a). To determine which T-cells responded to RANTES, it was necessary to determine which receptors were involved. T-cell migration experiments were therefore conducted in the absence and presence of 100 µg/ml anti-CCR3 and anti CCR5 antibodies. Antibodies were added to both to the upper and lower wells 30 minutes prior to transmigration experiments. Initially, T-cell responses to fresh, un-incubated RANTES were investigated in the absence and presence of anti-CCR3 or anti-CCR5 antibodies.

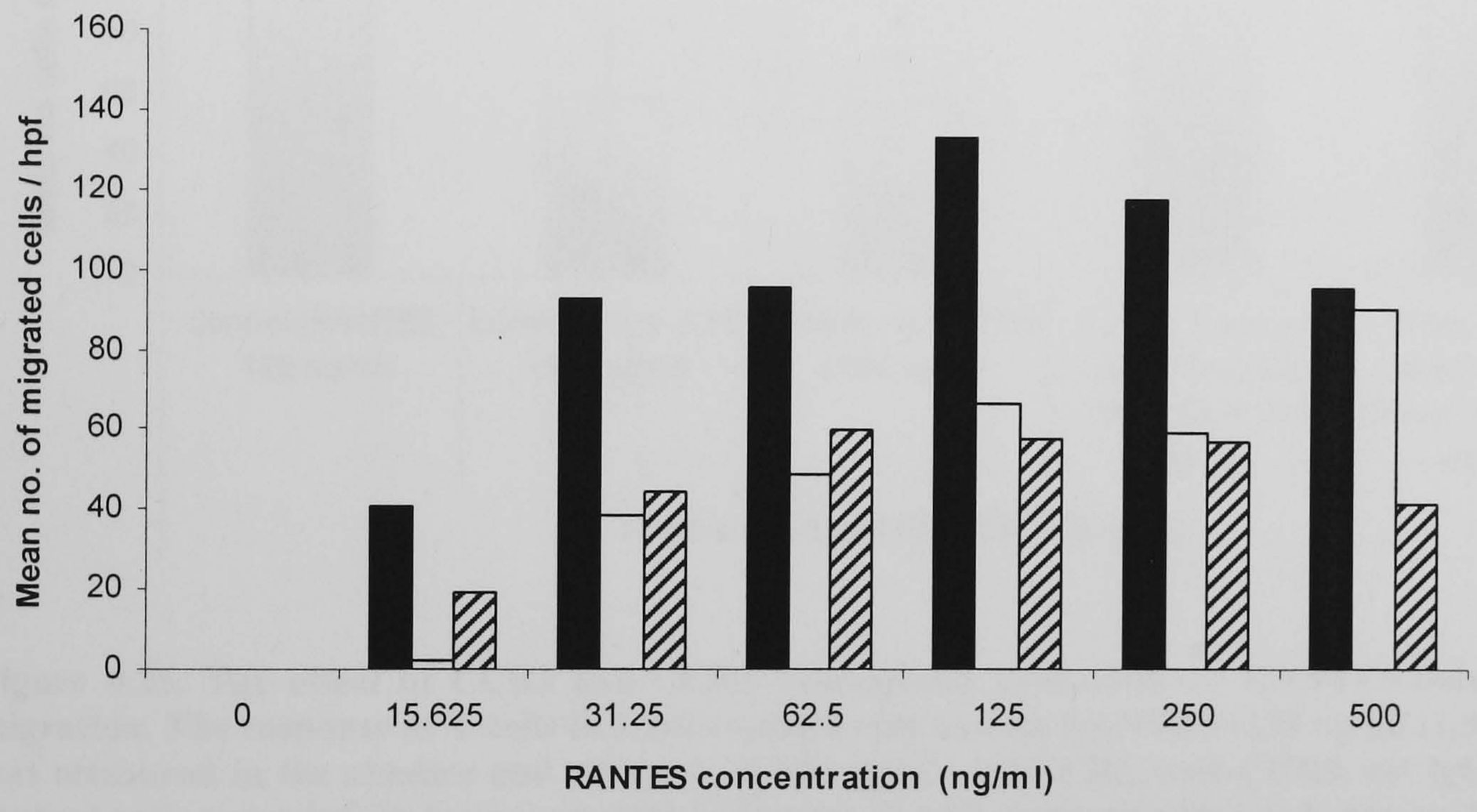

Figure 4.24. The effect of CCR3 and CCR5 neutralising antibodies on RANTES-induced T-cell migration. The response of T-cells to fresh recombinant human RANTES (■) (125 ng/ml (1.56 x 10^{-8} M) was measured in the presence of 100 µg/ml anti-CCR3 (□) and anti-CCR5 (▨) antibodies. T-cells were activated as before and incubated for 30 minutes with anti-CCR3 or anti-CCR5 antibodies before they were added to the upper wells of a Boyden chamber. RANTES was incubated for 30 minutes with anti-CCR3/5 antibodies before adding to the lower wells and the chamber was incubated for 2 hours. Following incubation, migrated cells were stained and counted as before. Results are presented as the mean number of cells/hpf. Results are the mean of two independent experiments.

Maximum T-cell migration occurred, as before, in response to 125 ng/ml RANTES (134 T-cells/hpf, figure 4.24). The addition of anti-CCR3 antibody (100 µg/ml) resulted in a 50.1 % reduction in T-cell migration (reduction from 134 to 66.8 T-cells/hpf). Similarly, the addition of anti-CCR5 antibody (100 µg/ml) resulted in a 56.5 % reduction in T-cell migration (reduction from 134 to 58.3 T-cells/hpf). The results

suggest that both CCR3 ($CD4^+$, Th2 and $CD8^+$ Tc2) and CCR5 bearing T-cells ($CD4^+$ Th1, and $CD8^+$ Tc1) may be involved in the response to fresh/unincubated RANTES (125 ng/ml). The results also show that there was an equal response of T-cells expressing either CCR3 or CCR5 receptors.

Figure 4.25 shows the effect of anti-CCR3 and anti-CCR5 antibodies on the responses of T-cells from different donors to fresh, unincubated RANTES at an optimum concentration, and also compares the effect of isotype control antibodies.

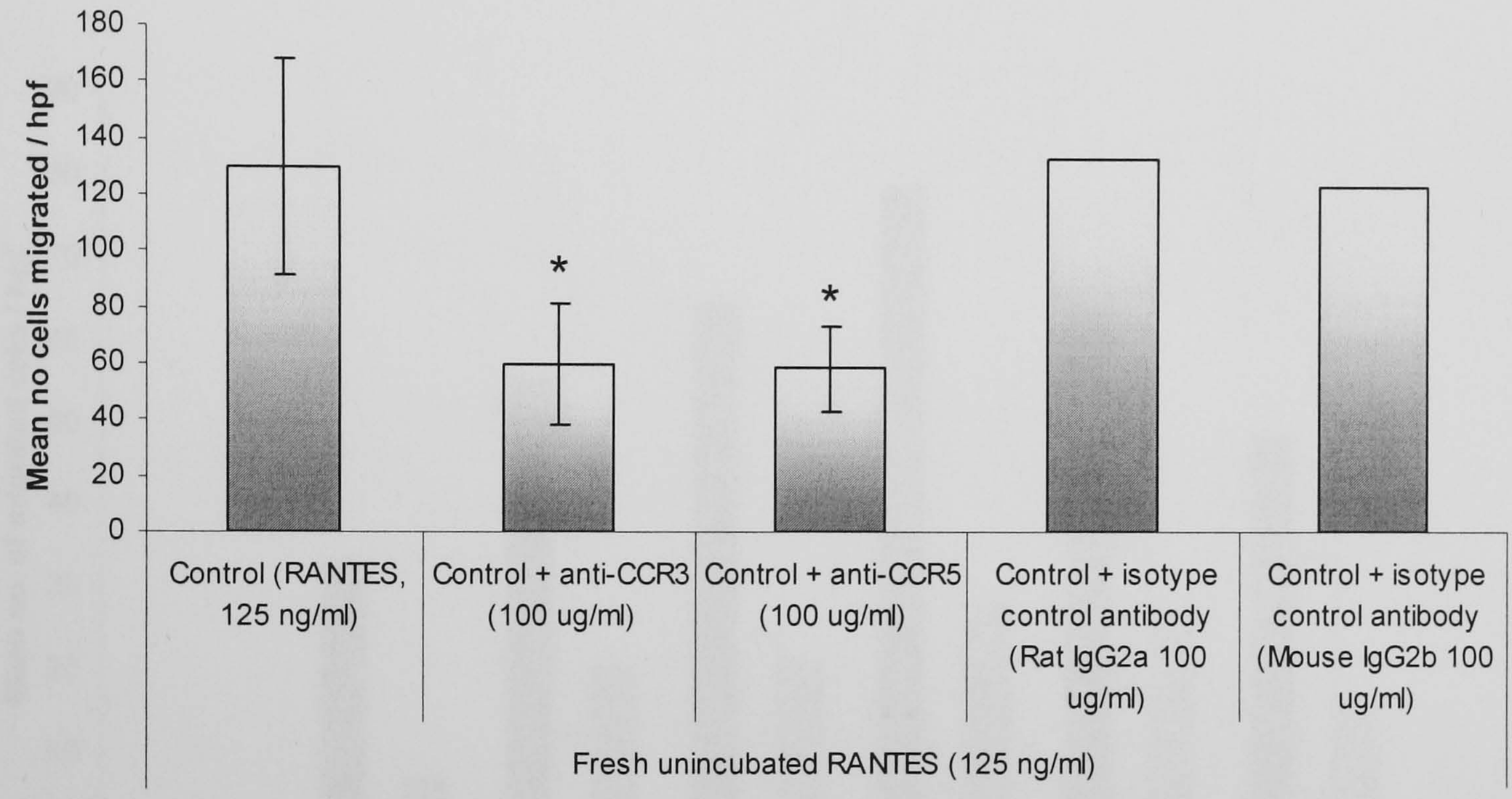

Figure 4.25. The effect of CCR3 and CCR5 neutralising antibodies on RANTES-induced T-cell migration. The response of T-cells to fresh recombinant human RANTES (125 ng/ml (1.56×10^{-8} M) was measured in the absence and presence of 100 µg/ml anti-CCR3, anti-CCR5, rat IgG2a isotype control and mouse IgG2b isotype control antibodies. T-cells were activated as before and incubated for 30 minutes with anti-CCR3, anti-CCR5 (n = 4) or isotype control antibodies (n = 2) before they were added to the upper wells of a Boyden chamber. RANTES was incubated for 30 minutes with anti-CCR3, anti-CCR5 or isotype control antibodies before adding to the lower wells and the chamber was incubated for 2 hours. Following incubation, migrated cells were stained and counted as before. Results are represented as the mean number of cells/hpf. Results are presented as mean ± SEM, and were compared using a 1-way ANOVA and Tukey's *post-hoc* test (* $p < 0.05$ compared to RANTES control, n = 4).

A concentration of 125 ng/ml RANTES induced a T-cell response of 130.2 ± 38.5 cells/hpf (figure 4.25). The addition of anti-CCR3 (100 µg/ml) caused a 56.3 ± 4.2 % reduction in T-cell migration to 60.4 ± 21.6 T-cells/hpf ($p < 0.05$). The cells that did not migrate were attributed to CCR3 bearing T-cells. The addition of anti-CCR5 (100 µg/ml) caused a 53.3 ± 3.3 % reduction in T-cell migration to 58.7 ± 15.6 T-cells/hpf ($p < 0.05$) and the T-cells that did not migrate can be attributed to CCR5 bearing T-cells.

Since the isotype controls had no effect on T-cell migration, the results suggest that two T-cell populations are responding to fresh RANTES through CCR3 and CCR5 receptors.

To determine whether RANTES multimers stimulate a response through CCR3 or CCR5 bearing T-cells, RANTES multimers were generated in the presence of $CuCl_2$ (50 μM) and H_2O_2 (25 μM), and used in T-cell migration assays in the absence and presence of anti-CCR3 and anti-CCR5 antibodies.

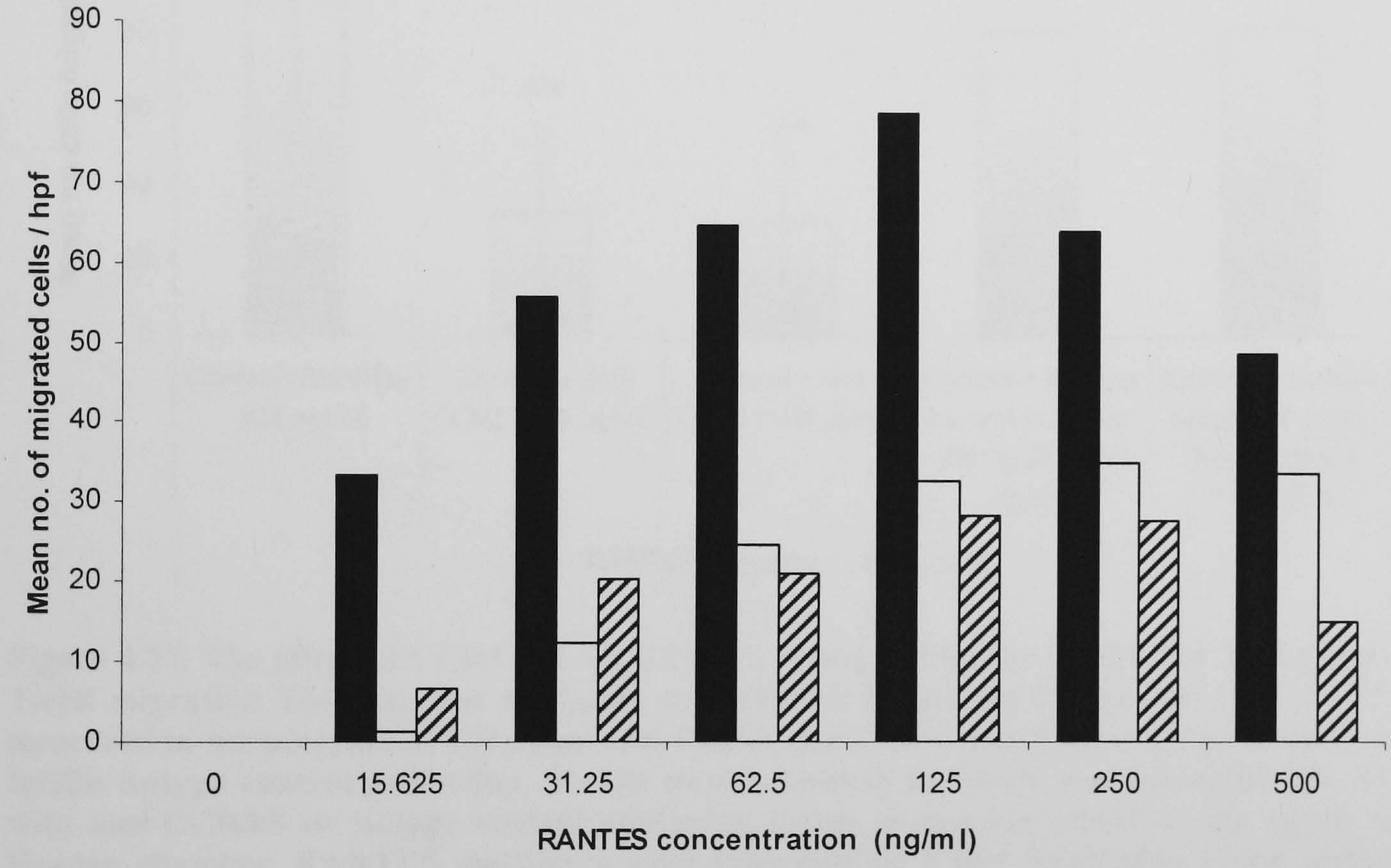

Figure 4.26. The effect of CCR3 and CCR5 neutralising antibodies on RANTES multimer-induced T-cell migration. The response of T-cells to RANTES multimers (■) (125 ng/ml (1.56×10^{-8} M) was measured in the presence of 100 μg/ml anti-CCR3 (□) and anti-CCR5 (▨) antibodies. T-cells were activated as before and incubated for 30 minutes with anti-CCR3 and anti-CCR5 antibodies before they were added to the upper wells of a Boyden chamber. RANTES multimers were generated by 2 day incubation in the presence of 50 μM $CuCl_2$ and 25 μM H_2O_2 and incubated for 30 minutes with anti-CCR3 and anti-CCR5 antibodies before adding to the lower wells and the chamber was incubated for 2 hours. Following incubation, migrated cells were stained and counted as before. Results are presented as the mean number of cells/hpf. Results represent the mean of two independent experiments.

Maximum T-cell migration occurred, as before, in response to 125 ng/ml RANTES multimers (78.9 T-cells/hpf, figure 4.26). The addition of anti-CCR3 antibody (100 μg/ml) resulted in a 58.4 % reduction in T-cell migration to 32.8 T-cells/hpf. Similarly, the addition of anti-CCR5 antibody (100 μg/ml) resulted in a 64 % reduction in T-cell

migration to 28.4 T-cells/hpf. The results suggest that T-cells are responding to RANTES multimers (125 ng/ml) through both CCR3 and CCR5 receptors.

Figure 4.27 shows the effect of anti-CCR3 and anti-CCR5 antibodies on the response of T-cells from different donors to RANTES multimers, and compares the effect of isotype control antibodies.

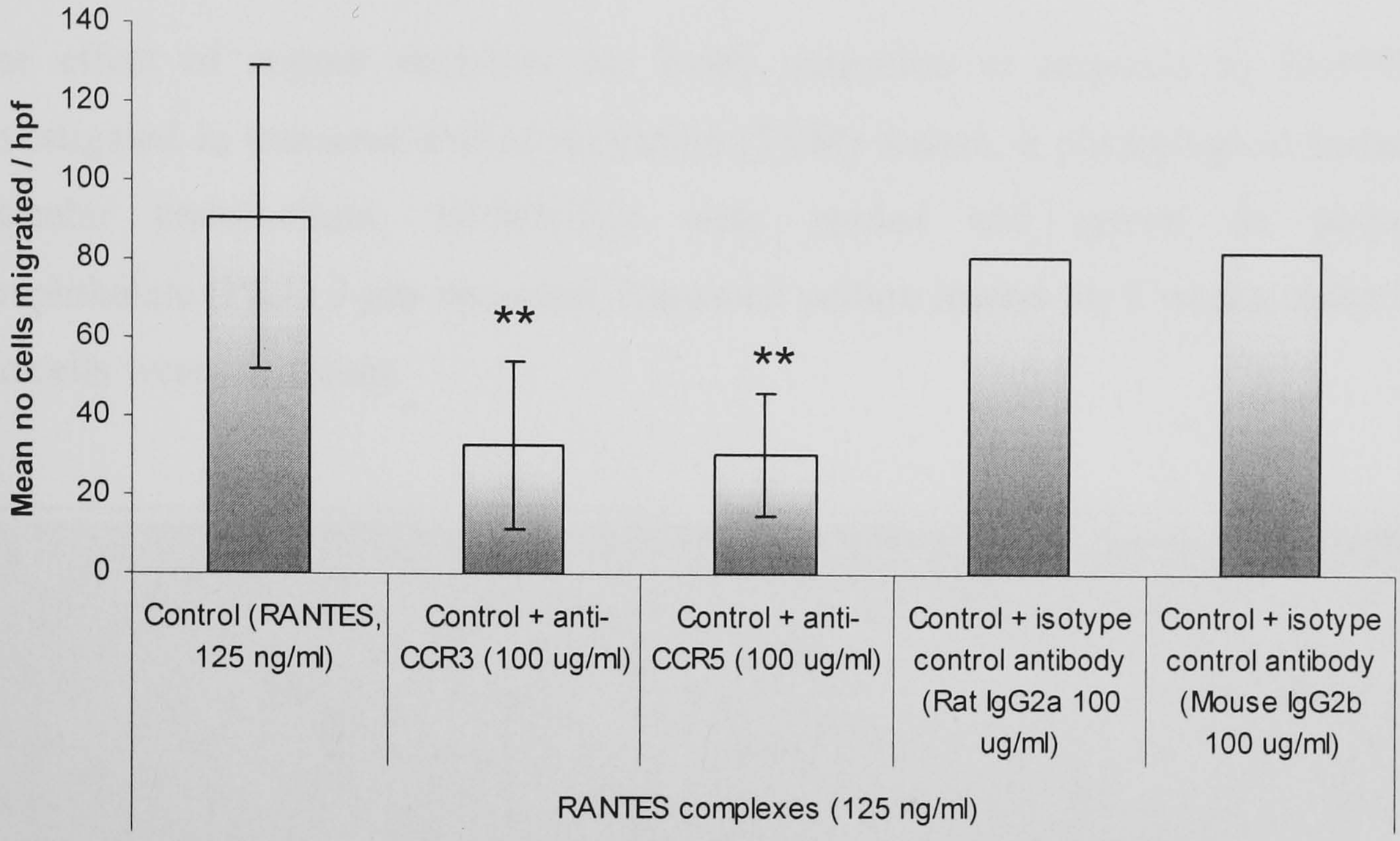

Figure 4.27. The effect of CCR3 and CCR5 neutralising antibodies on RANTES multimer-induced T-cell migration The response of T-cells to RANTES multimers (125 ng/ml (1.56 x 10^{-8} M) was measured in the presence of 100 μg/ml anti-CCR3, anti-CCR5, rat IgG2a isotype control and mouse IgG2b isotype control antibodies. T-cells were activated as before and incubated for 30 minutes with anti-CCR3/5 or isotype control antibodies before they were added to the upper wells of a Boyden chamber. RANTES multimers were generated by 2 day incubation in the presence of 50 μM $CuCl_2$ and 25 μM H_2O_2 and incubated for 30 minutes with anti-CCR3, anti-CCR5 (n = 4) or isotype control antibodies (n = 2) before adding to the lower wells and the chamber was incubated for 2 hours. Following incubation, migrated cells were stained and counted as before. Results are presented as the mean number of cells/hpf. Results represent mean ± SEM, and were compared using a 1-way ANOVA and Tukey's *post-hoc* test ($p < 0.01$ compared to RANTES control, n = 4).**

A concentration of 125 ng/ml RANTES caused a T-cell response of 90.8 ± 21.5 cells/hpf (figure 4.27). The addition of anti-CCR3 (100 μg/ml) caused a 66.3 ± 5.5 % reduction in T-cell migration to 32.9 ± 11.1 T-cells/hpf ($p < 0.01$). The cells that did not migrate were attributed to CCR3 bearing T-cells. The addition of anti-CCR5 (100 μg/ml) caused a 70.6 ± 7.04 % reduction in T-cell migration to 30.6 ± 12.4 T-cells/hpf ($p < 0.01$). The cells that did not migrate were attributed to CCR5 bearing T-cells. Since the isotype controls had no effect on T-cell migration, the results suggest that T-cells are responding to RANTES multimers through both CCR3 and CCR5 receptors.

4.5.5. RANTES-induced T-cell transendothelial migration.

It has been shown by others that RANTES has a minimal tetrameric quaternary structure for cell attractant activity *in vivo* and that both the monomeric and dimeric forms of RANTES are devoid of chemotactic activity *in vivo* (Czaplewski *et al*, 1999; Proudfoot *et al*, 2003). Since it appears that $CuCl_2$ is important for RANTES multimer formation *in vitro*, it is possible that copper is required under physiological conditions for T-cell recruitment and accumulation during inflammation.

The effect of copper chelators on T-cell migration in response to RANTES was investigated in transendothelial migration (TEM) assays, a physiological model of the vascular endothelium. HLMVECs were seeded and grown on polyethylene terephthalate (PET) 3 μm uncoated Transwell culture inserts for 2 weeks. After 2 weeks the cells were confluent.

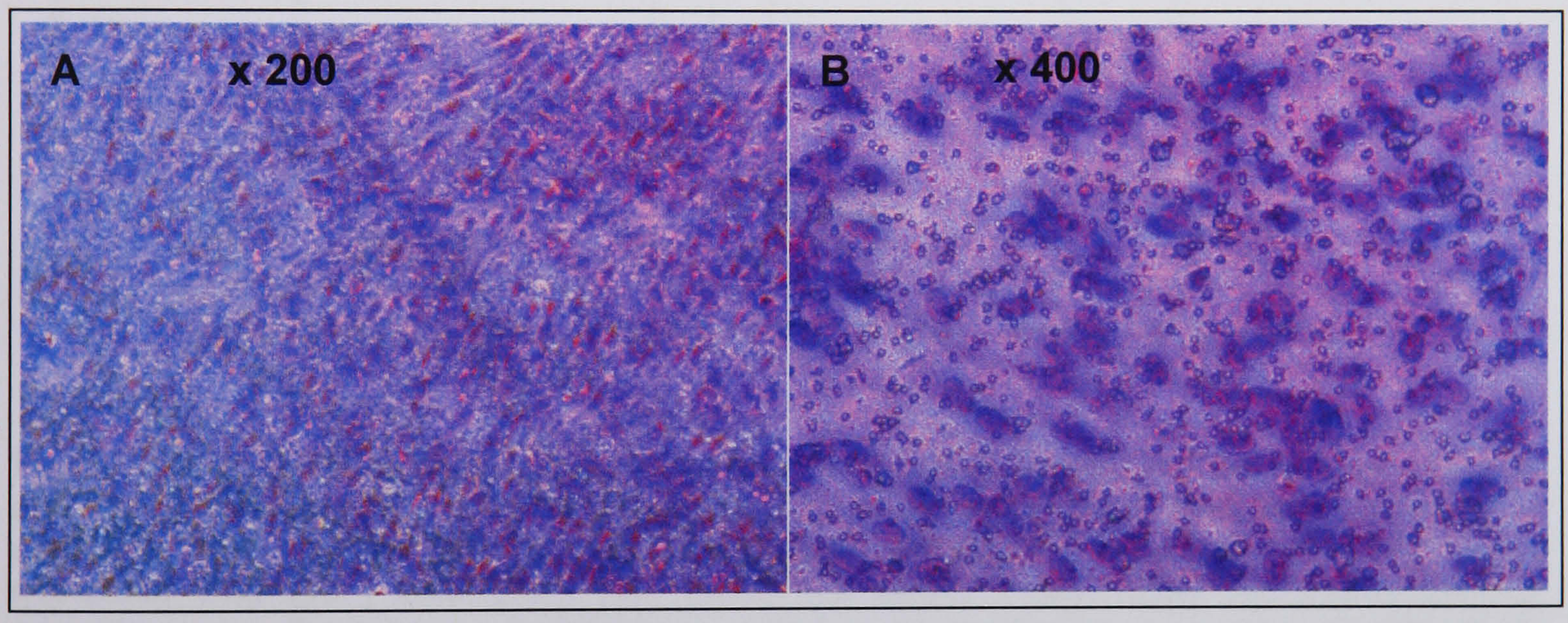

Figure 4.28A and B.

A: HLMVECs grown on polyethylene terephthalate (PET) 3 μm uncoated Transwell culture inserts, stained with Hema-Gurr stain and photographed after 2 weeks at x200 magnification on a light microscope.

B: HLMVECs grown on polyethylene terephthalate (PET) 3 μm uncoated Transwell culture inserts, stained with Hema-Gurr stain and photographed after 2 weeks at x400 magnification on a light microscope.

Figure 4.28A shows confluent HLMVECs grown for 2 weeks on PET 3 μm uncoated Transwell culture inserts at x200 magnification. Figure 4.28B shows the same cells at x400 magnification. The photographs show that the cells were confluent after 2 weeks of culture, and ready to use in a transmigration assay.

Initially, to find the best endothelial model, HLMVECs were seeded and grown for 2 weeks on both fibronectin coated and uncoated 3 μm PET membranes. The T-cell response to both endogenous RANTES synthesised by IFN-γ plus TNF-α activated endothelium and exogenously added recombinant RANTES was investigated.

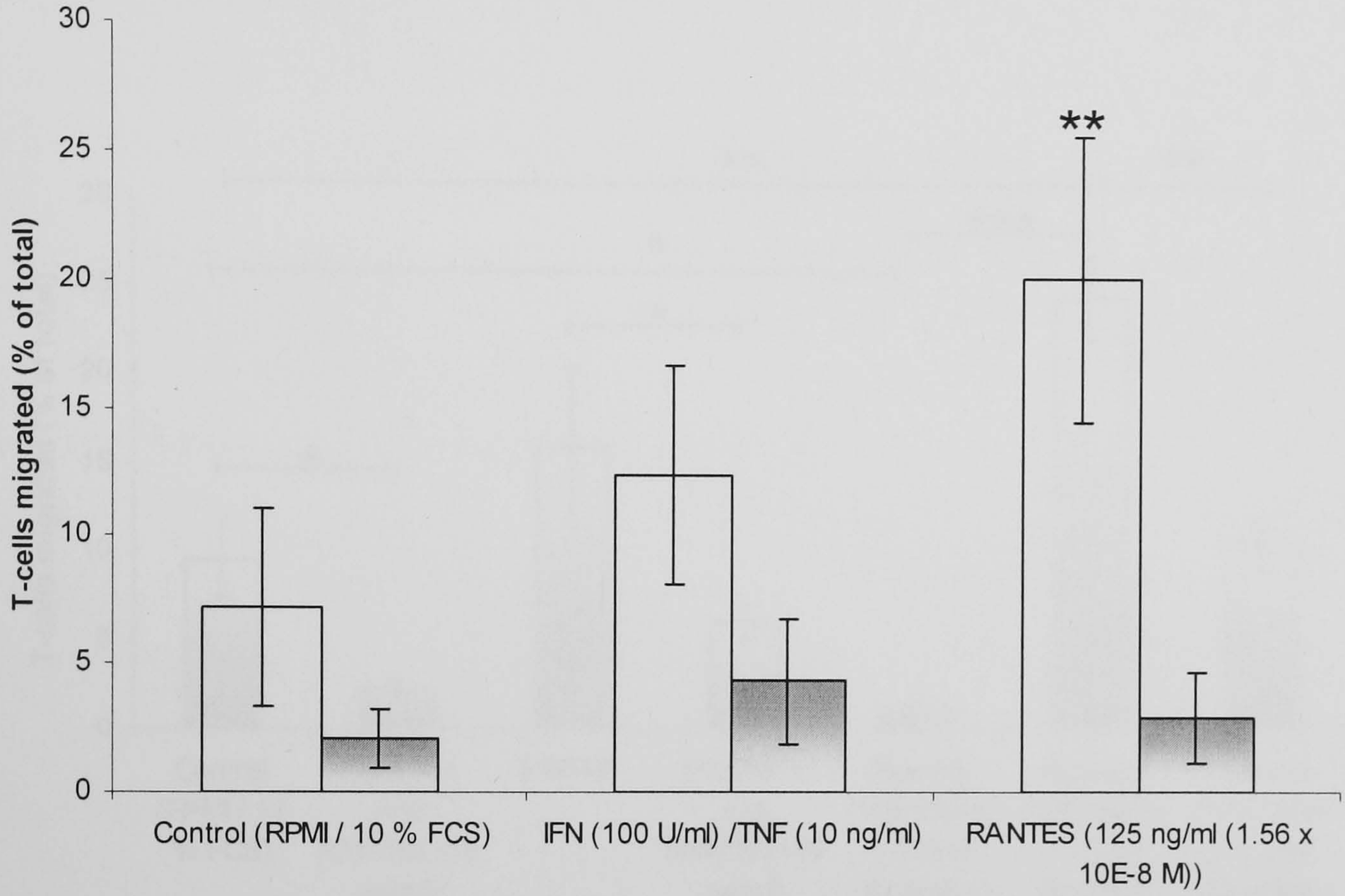

Figure 4.29. Transendothelial migration of activated T-cells in response to endogenous RANTES and recombinant RANTES. HLMVECs were grown on uncoated (□) and fibronectin coated (▩) 3 μm PET membranes for 2 weeks. To induce endogenous RANTES synthesis, HLMVECs were stimulated with IFN-γ (100 U/ml) plus TNF-α (10 ng/ml) 1 day before the transendothelial migration assay. Recombinant RANTES was added to the medium in the basal wells (800 μl) 30 minutes before the assay. Activated T-cells (2 x 10^6/ml) were added to the apical wells (300 μl), and plates were incubated for 5 hours. Following incubation, migrated cells were removed and counted using a haemocytometer. Results are represented as mean ± SEM, n = 3. Data was compared using a 1-way ANOVA and Dunnett's *post-hoc* test (control = RPMI/10 % FCS, ** $p < 0.01$).

Endogenous RANTES synthesised by endothelial cells in response to IFN-γ (100 U/ml) and TNF-α (10 ng/ml) did not induce significant T-cell migration (figure 4.29), despite the evidence that IFN-γ plus TNF-α induces HLMVEC RANTES synthesis (Section 4.5.1, figures 4.1, 4.16 and 4.17.) The addition of recombinant RANTES (125 ng/ml) below the endothelial monolayer induced a significant increase in T-cell migration across endothelium grown on uncoated 3 μm PET membranes compared to the RPMI/10 % FCS control (increase from 7.2 ± 3.9 % to 20.1 ± 5.5 % of the total T-cells added at the start of the assay, $p < 0.01$). There was no significant migration across

endothelial monolayers grown on fibronectin coated 3 μm PET membranes in response to recombinant RANTES.

Platelets added to the lower well were activated with 1 U/ml thrombin, which had previously been shown to induce significant RANTES release (Section 4.5.2, figure 4.16). Platelets with 1 U/ml thrombin were added to either apical or basal wells, 30 minutes before the TEM assay.

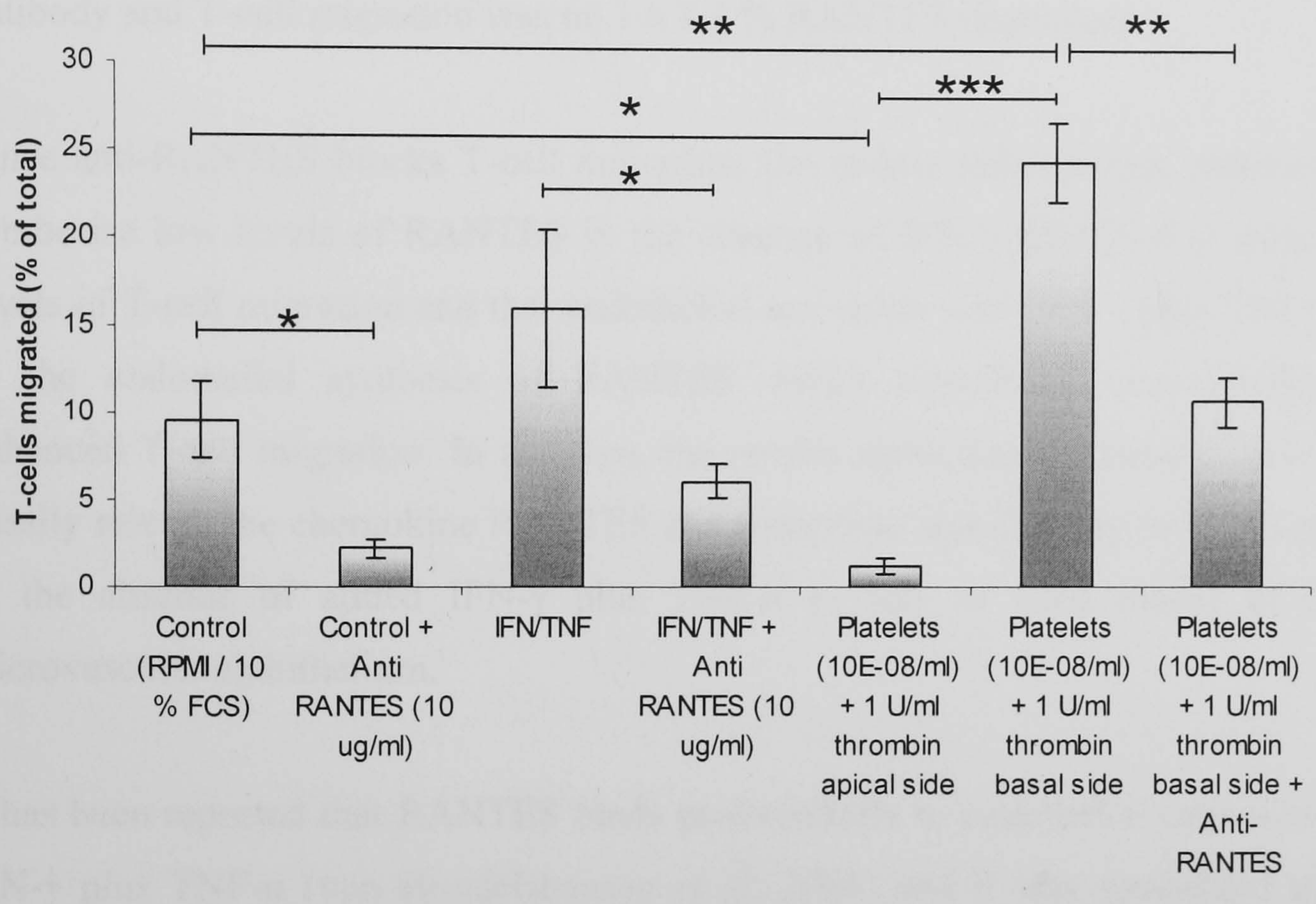

Figure 4.30. Transendothelial migration of activated T-cells in response to endogenous RANTES and platelet derived RANTES. HLMVECs were grown on uncoated 3 μm PET membranes for 2 weeks. To induce endogenous RANTES synthesis, where indicated, HLMVECs were stimulated with IFN-γ (100 U/ml) plus TNF-α (10 ng/ml) 1 day before the transendothelial migration assay. Isolated platelets (10^8/ml) were activated with 1 U/ml thrombin and then immediately added to the basal wells (800 μl) 30 minutes before the assay. Activated T-cells (2 x 10^6/ml) were added to the apical wells (300 μl), and plates were incubated for 5 hours. Following incubation, migrated cells were removed and counted using a haemocytometer. Anti-RANTES (10 μg/ml) was added to T-cells and basal wells at the start of the assay. Results are represented as mean ± SEM, n = 3. Data was compared using a 1-way ANOVA and Tukey's *post-hoc* test, * $p < 0.05$, ** $p < 0.01$ and *** $p < 0.001$.

The addition of anti-RANTES antibody caused a significant ($p < 0.05$) reduction in spontaneous T-cell migration in the control from 9.56 ± 2.2 % to 2.2 ± 0.6 % which indicated constitutive RANTES expression. In response to IFN-γ plus TNF-α stimulated RANTES synthesis, T-cell migration was not significantly increased, as also seen in figure 4.29. However, the anti-RANTES antibody significantly ($p < 0.05$) reduced

migration from 16 ± 4.5 % to 6.1 ± 1 %, which was not significantly different from the control value (figure 4.30).

Platelets in the lower wells activated with 1 U/ml thrombin induced a significant ($p < 0.01$) increase in T-cell migration (24.4 ± 2.2 %) compared to the RPMI/10 % FCS control (9.56 ± 2.2 %). However, activated platelets added apically significantly inhibited T-cell migration when compared to the RPMI/10 % FCS control (1.2 ± 0.5 %, $p < 0.05$). T-cell migration in response to activated platelets added basally was reduced significantly ($p < 0.01$) from 24.4 ± 2.2 % to 10.7 ± 1.4 % by the anti-RANTES antibody and T-cell migration was 66.1 ± 8.1 % RANTES dependent.

Since anti-RANTES blocks T-cell migration, the results indicate that endothelial cells synthesise low levels of RANTES in the absence of IFN-γ plus TNF-α inducing low levels of T-cell migration and that endothelial activation with IFN-γ plus TNF-α results in the endothelial synthesis of RANTES which contributes non-significantly to enhanced T-cell migration. In addition, the results show that activated platelets added basally release the chemokine RANTES and contribute significantly to T-cell migration in the absence of added IFN-γ plus TNF-α in this *in vitro* model of the lung microvascular endothelium.

It has been reported that RANTES binds preferentially to endothelial cells activated by IFN-γ plus TNF-α (von Hundelshausen *et al*, 2001) and it was speculated that these cytokines may be released by T-cells, platelets and HLMVECs *in vitro* which would promote the binding of platelet-derived RANTES to the endothelium. It has previously been reported that TNF-α is stored by platelets (Muylle *et al*, 1993) and both IFN-γ and TNF-α are released by naïve $CD45RA^+$ T-cells, $CD4^+$ memory Th1 type T-cells and at low levels by Th2 type T-cells (Conlon *et al*, 1995; Mosmann & Coffman, 1989; Tsicopoulos *et al*, 1992). Therefore, IFN-γ and TNF-α were measured in apical supernatants from experiments in which T-cell transmigration was induced by platelets in the basal compartment, and in which these cytokines had not been added exogenously to activate the endothelium.

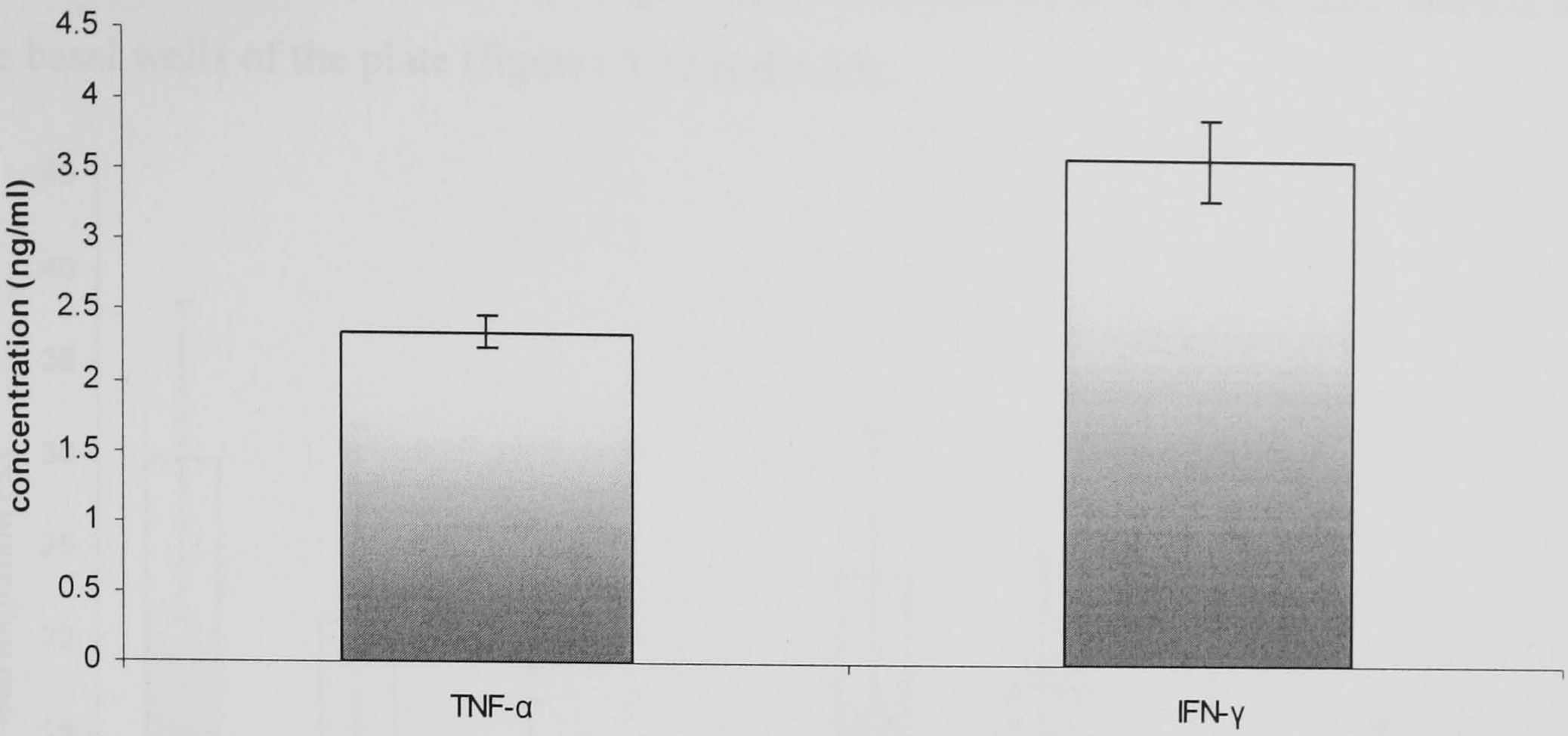

Figure 4.31. IFN-γ and TNF-α detected in apical supernatants from HLMVECs grown on Transwell inserts and used in a TEM assay. Isolated platelets (10^8/ml) were activated with 1 U/ml thrombin and added to the basal wells (800 µl) 30 minutes before the assay. Activated T-cells (2 x 10^6/ml) were added to the apical wells (300 µl), and plates were incubated for 5 hours. Following incubation, apical wells were cleared (2500 g) and cytokines analysed by ELISA. Results are expressed as mean ± SEM, n = 3.

Figure 4.31 shows that both IFN-γ and TNF-α were released into the supernatants. IFN-γ was detected at 3.6 ± 0.3 ng/ml and TNF-α was detected at 2.4 ± 1.1 ng/ml. The amount of IFN-γ (2 x 10^7 U/mg) and TNF-α added exogenously to activate HLMVECs was 100 U/ml (or 5 pg/ml) and 10 ng/ml respectively. Thus, the amount of endogenous IFN-γ detected by ELISA was higher than the amount that was used to induce endothelial RANTES release when added in combination with TNF-α. This indicates that the concentration of endogenous IFN-γ released in the presence of platelets and T-cells was sufficiently high to remove the need to add exogenous IFN-γ in the model of the endothelium. The amount of endogenous TNF-α detected by ELISA was of the same order as that which was used to induce endothelial RANTES release when added exogenously (10 ng/ml). Therefore, in subsequent experiments, exogenous IFN-γ plus TNF-α was not added.

Platelets are essential for leukocyte recruitment and have been shown to induce T-cell migration in the vascular endothelial model when activated with thrombin (1 U/ml) and added basally (figure 4.30). Since this was a physiological model, it was used to investigate the anti-inflammatory potential of the copper chelators neocuproine (NC), bathocuproine disodium salt (BCDS), D-penicillamine (D-pen) and tobramycin (Tob). In order to determine whether these copper chelators could attenuate T-cell migration, HLMVECs grown on Transwells were exposed to these copper chelators for 24 hours

before the TEM assay and T-cell migration was induced by adding activated platelets to the basal wells of the plate (figures 4.32 and 4.33).

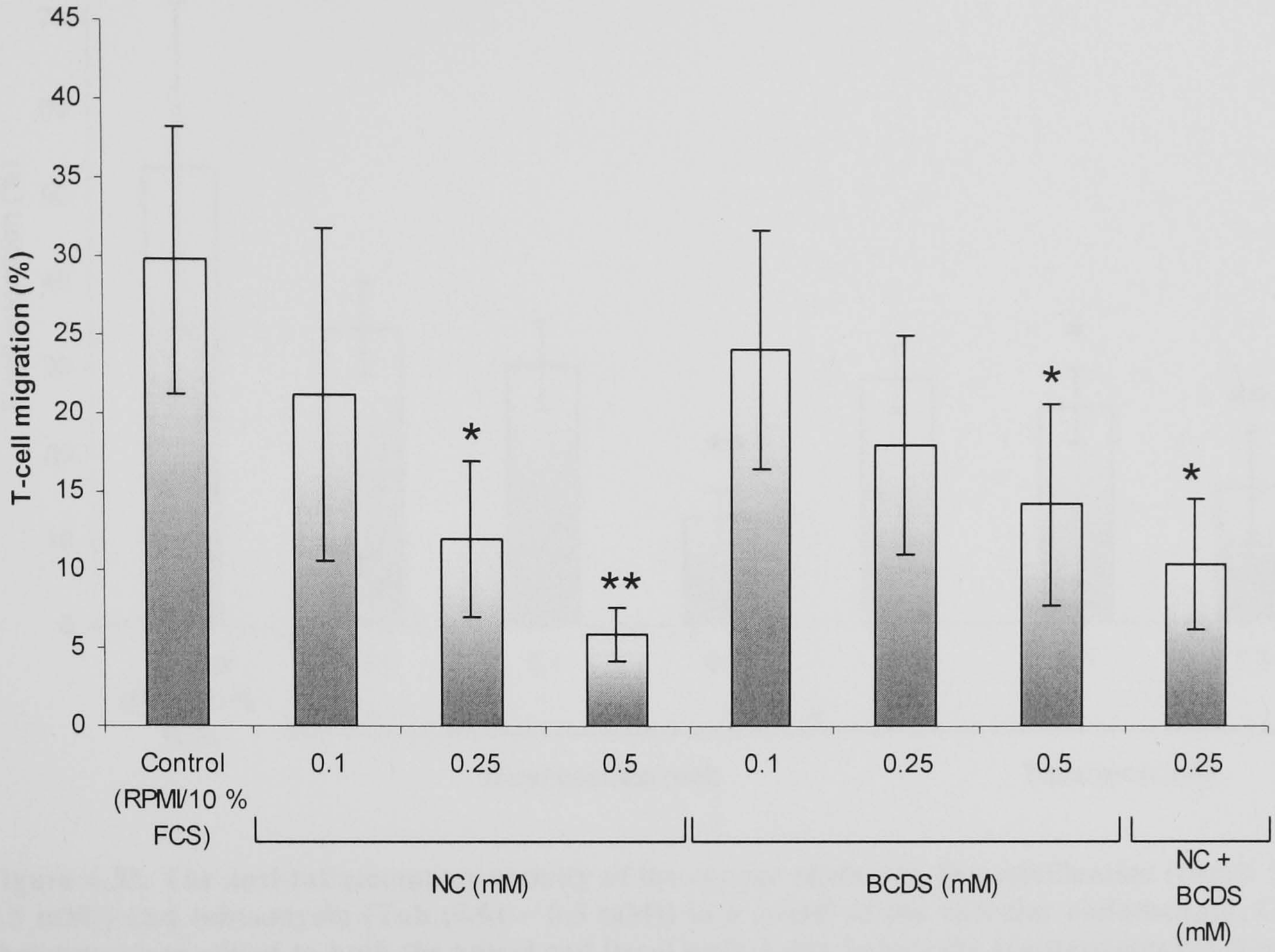

Figure 4.32. The anti-inflammatory activity of the copper chelators, neocuproine (NC (0.1 – 0.5 mM)) and bathocuproine disodium salt (BCDS (0.1 – 0.5 mM)) in a model of the vascular endothelium. Copper chelators were added to both the apical and basal wells 1 day before the transendothelial migration (TEM) assay. T-cells (2 x 10^6/ml) were added to the apical wells (300 µl) and T-cell migration was induced by the addition of activated platelets (10^8/ml + 1 U/ml thrombin) to the basal wells (800 µl) 30 minutes before the assay. Results are represented as mean ± SEM, n = 3. Data was compared using a 1-way ANOVA and Dunnett's *post-hoc* test, * $p < 0.05$, ** $p < 0.01$ compared to RPMI/10 % FCS control.

Treatment with NC (0.1 – 0.5 mM) induced a significant ($p < 0.05$) dose-dependent decrease in T-cell migration from a control value of 29.8 ± 8.5 % to 12.1 ± 5 % at 0.25 mM, and 5.9 ± 1.7 at 0.5 mM ($p < 0.01$), (figure 4.32). Similarly, BCDS (0.1 - 0.5 mM) induced a significant ($p < 0.05$) dose-dependent decrease in T-cell migration from the control value to 14.3.1 ± 6.4 % at 0.5 mM.

The addition of 0.25 mM NC and BC together did not result in an additive effect and T-cell migration (10.4 ± 4.2 %) was not significantly lower than the migration in the presence of 0.25 mM NC or BCDS alone.

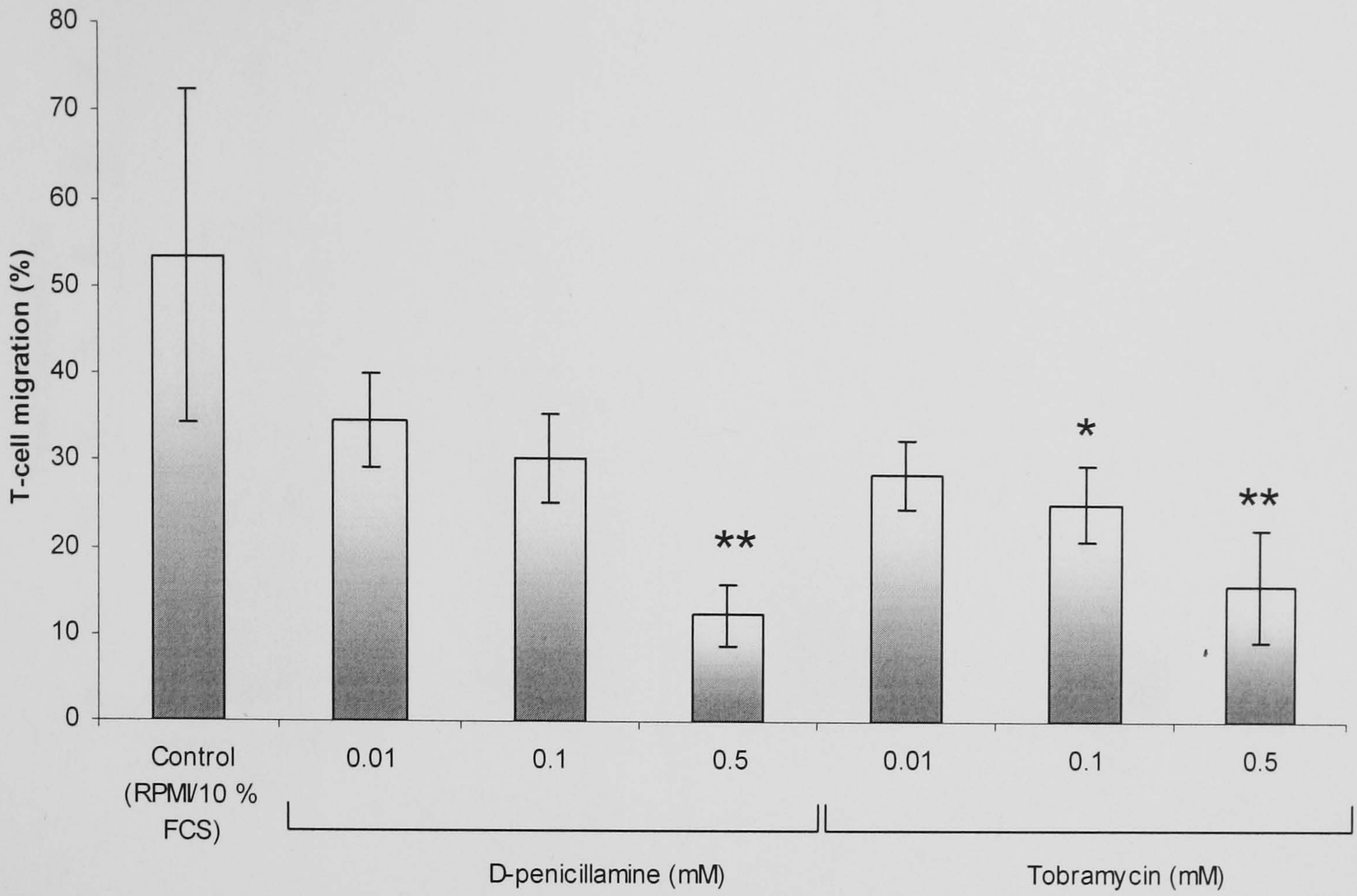

Figure 4.33. The anti-inflammatory activity of the copper chelators, D-penicillamine (D-pen (0.01 – 0.5 mM)) and tobramycin (Tob (0.01 – 0.5 mM)) in a model of the vascular endothelium. Copper chelators were added to both the apical and basal wells 1 day before the transendothelial migration (TEM) assay. T-cells (2 x 10^6/ml) were added to the apical wells (300 µl) and T-cell migration was induced by the addition of activated platelets (10^8/ml + 1 U/ml thrombin) to the basal wells (800 µl) 30 minutes before the assay. Results are represented as mean ± SEM, n = 3. Data was compared using a 1-way ANOVA and Dunnett's *post-hoc* test, * $p < 0.05$, ** $p < 0.01$ compared to RPMI/ 10 % FCS control.

Treatment with D-penicillamine (0.01 – 0.5 mM) induced a significant ($p < 0.01$) dose-dependent decrease in T-cell migration from a control value of 53.3 ± 19 % to 12.4 ± 3.6 % at 0.5 mM (figure 4.33). Similarly, tobramycin (0.01 – 0.5 mM) induced a significant ($p < 0.05$) dose-dependent decrease in T-cell migration from the control value to to 25.3 ± 4.3 % at 0.1 mM and 15.8 ± 6.5 % at 0.5 mM ($p < 0.01$).

The inhibitory effect of the PAI-1 inhibitor, XR5118 (Einholm *et al*, 2003), a gift from Xenova, on T-cell migration was also investigated since inhibition of PAI-1 was previously shown to induce shedding of IL-8 and inhibit neutrophil migration (Marshall *et al*, 2003). It was expected that XR5118 would increase plasmin activity and induce the shedding of proteoglycan-bound RANTES on the endothelial cell surface, thereby inhibiting T-cell migration. XR5118 (1-100 µM) was added to apical and basal wells at the start of the TEM assay.

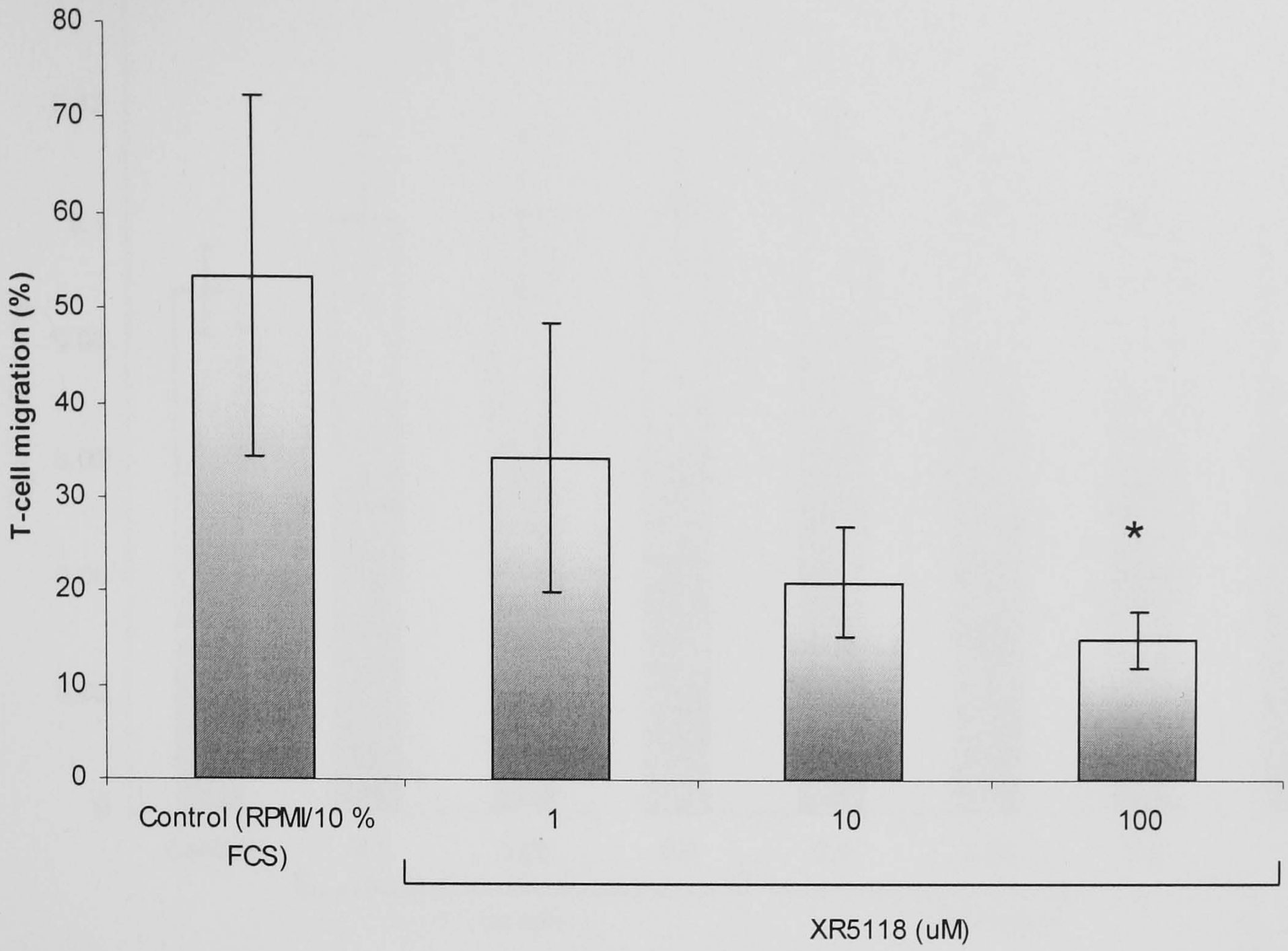

Figure 4.34. The anti-inflammatory activity of the PAI-1 inhibitor, XR5118 (1 – 100 μM) in a model of the vascular endothelium. XR5118 was added to both the apical and basal wells at the start of the transendothelial migration (TEM) assay. T-cells (2 x 10^6/ml) were added to the apical wells (300 μl) and T-cell migration was induced by the addition of activated platelets (10^8/ml + 1 U/ml thrombin) to the basal wells (800 μl) 30 minutes before the assay. Results are represented as mean ± SEM, n = 4. Data was compared using a paired student's t-test, * $p < 0.05$.

Treatment with the PAI-1 inhibitor, XR5118 (1 – 100 μM) induced a significant ($p < 0.05$) dose-dependent decrease in T-cell migration from a control value of 53.3 ± 19 % to 15 ± 3 % at at 100 μM, figure 4.34. The reduction in T-cell migration at 100 μM X5118 was associated with an increase in plasmin activity in the basal supernatants from 6.3 ± 1.4 in the control to 7.7 ± 0.9 μg/ml following treatment with 100 μM XR5118 ($n = 4$, $p < 0.05$).

The analysis of basal supernatants for lactate dehydrogenase (LDH) enzyme activity confirmed that T-cell migration was not attenuated due to the toxicity of copper chelators, PAI-1 inhibititor or XR5118 (figures 4.35 – 4.37).

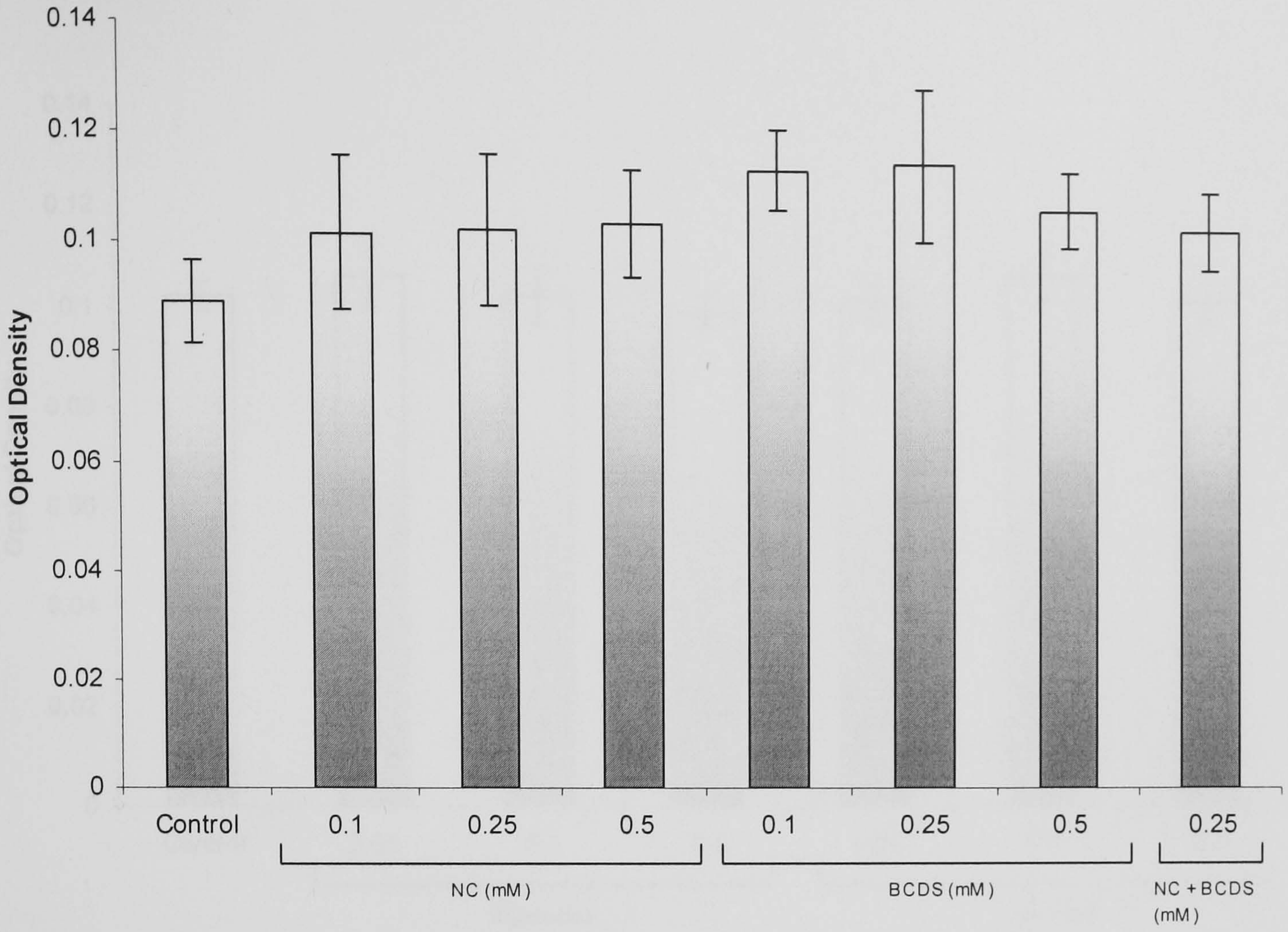

Figure 4.35. LDH release measured in basal supernatants (total volume 1400 µl) following treatment with NC (0.1 – 0.5 mM), BCDS (0.1 – 0.5 mM) and NC + BCDS (0.25 mM). Results are expressed as mean ± SEM, n = 3.

Figure 4.35 shows that there was no significant increase in LDH release after treatment with NC, BCDS, or both NC and BCDS together. The result indicates that NC and BCDS did not cause toxicity and cell death as a mechanism for the reduction in T-cell migration.

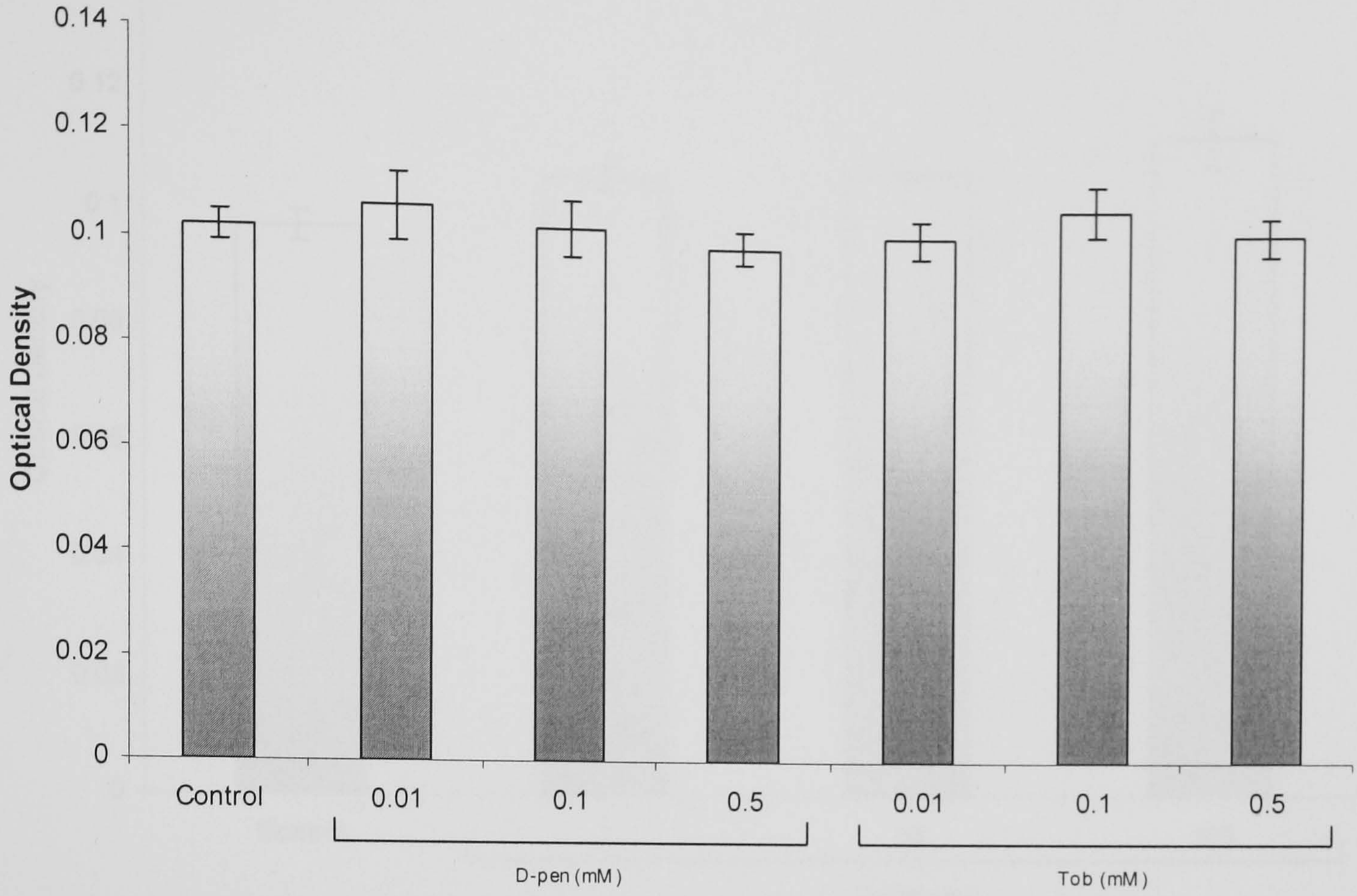

Figure 4.36. LDH release measured in basal supernatants (total volume 1400 µl) following treatment with D-penicillamine (0.01 – 0.5 mM) and tobramycin (0.01 – 0.5 mM). Results are expressed as mean ± SEM, n = 3.

Figure 4.36 shows that treatment with D-penicillamine or tobramycin caused no increase in LDH release. The result indicates that these copper chelators were not toxic to cells, and that cell toxicity did not contribute to the observed reduction in T-cell migration following treatment with these copper chelators.

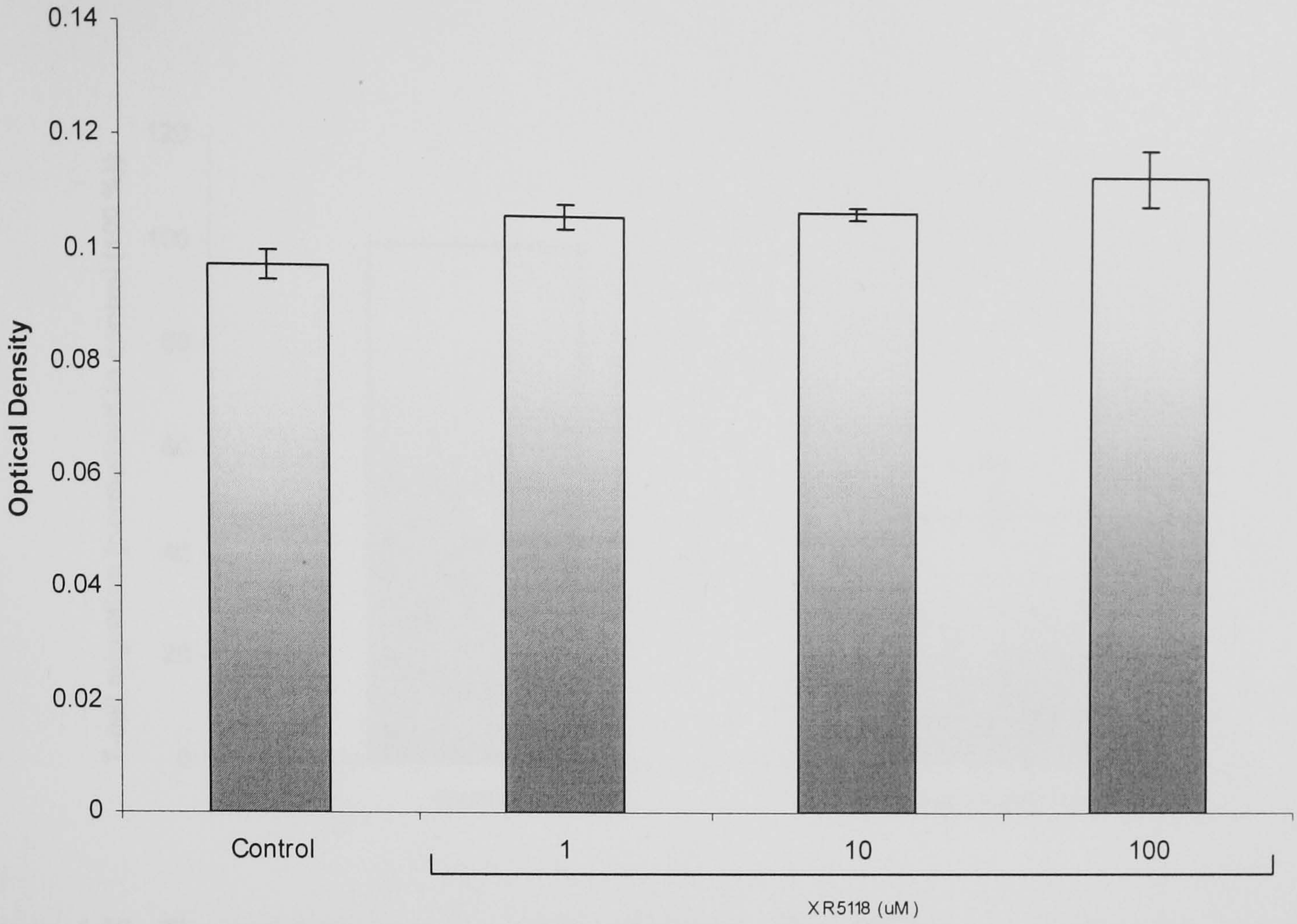

Figure 4.37. LDH release measured in basal supernatants (total volume 1400 µl) following treatment with the PAI-1 inhibitor, XR5118 (1 – 100 µM). Results are expressed as mean ± SEM, n = 3.

Figure 4.37 shows that treatment with XR5118 did not cause an increase in LDH release, and again, the result indicates that XR5118 does not exert its inhibitory effects on T-cell migration through cell toxicity and death.

Since it was established that both copper and H_2O_2 are involved in multimer formation (Chapters 2 and 3), the involvement of H_2O_2 in RANTES induced T-cell migration was investigated. Catalase is an endogenous enzyme that catalyses the dismutation of H_2O_2 to O_2 and H_2O and protects cells from peroxidation and damage induced by free radicals.

HLMVECs were treated with catalase (500 U/ml) at the start of transendothelial migration assays.

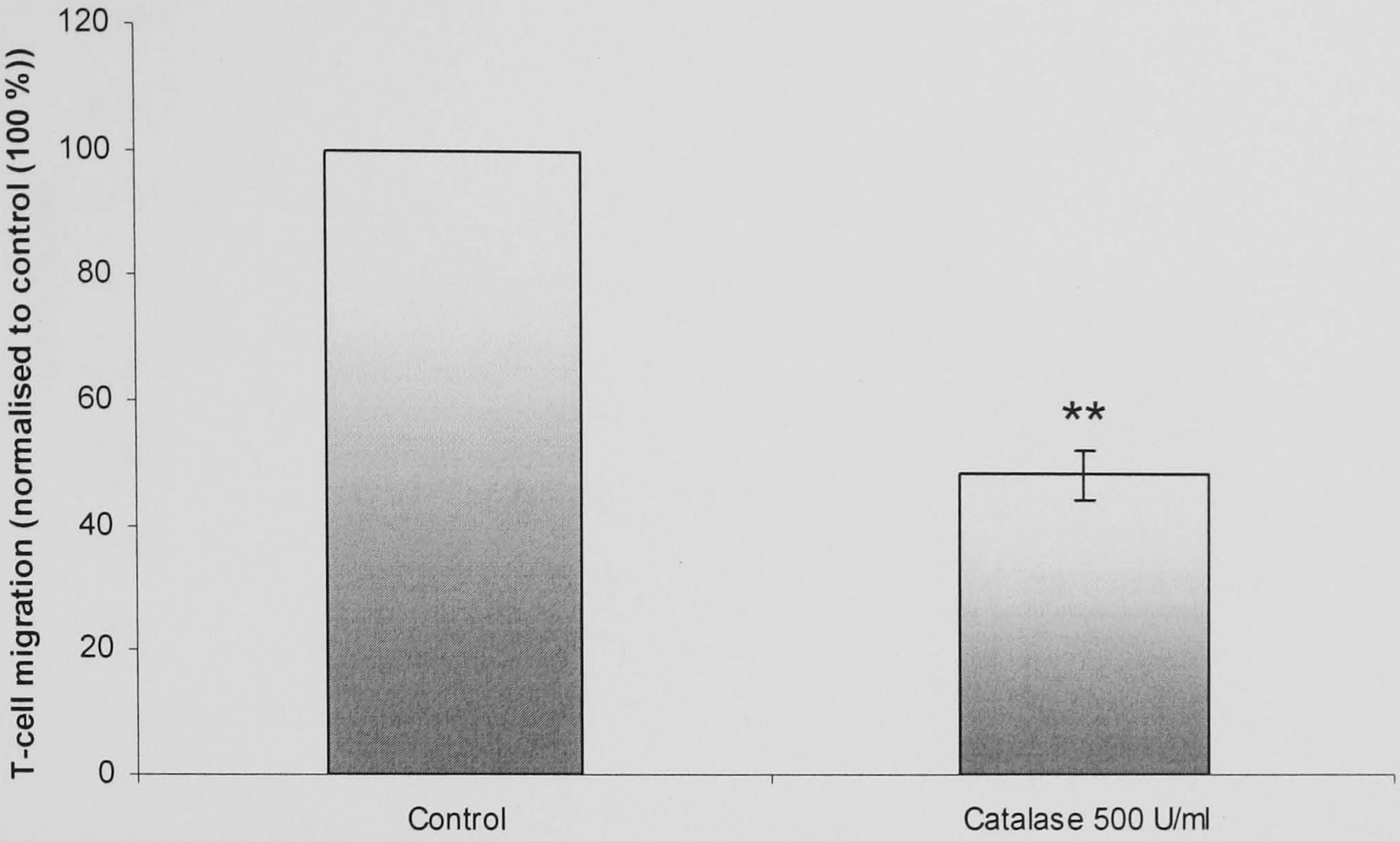

Figure 4.38. The anti-inflammatory activity of catalase (500 U/ml) in a model of the vascular endothelium. Catalase (500 U/ml) was added to both the apical and basal wells at the start of the transendothelial migration (TEM) assay. T-cells (2 x 10^6/ml) were added to the apical wells (300 µl) and T-cell migration was induced by the addition of activated platelets (10^8/ml + 1 U/ml thrombin) to the basal wells (800 µl) 30 minutes before the assay. Results were normalised to the control (mean = 24.3 % of total T-cells added, 100 %) and are represented as mean ± SEM, n = 3. Data was compared using a paired student's t-test, ** $p < 0.01$.

The addition of catalase (500 U/ml) induced a significant reduction in T-cell migration from 100 % to 48.6 ± 3.9 % ($p < 0.01$, figure 4.38) indicating that H_2O_2 may be involved in the mechanism of RANTES induced T-cell migration.

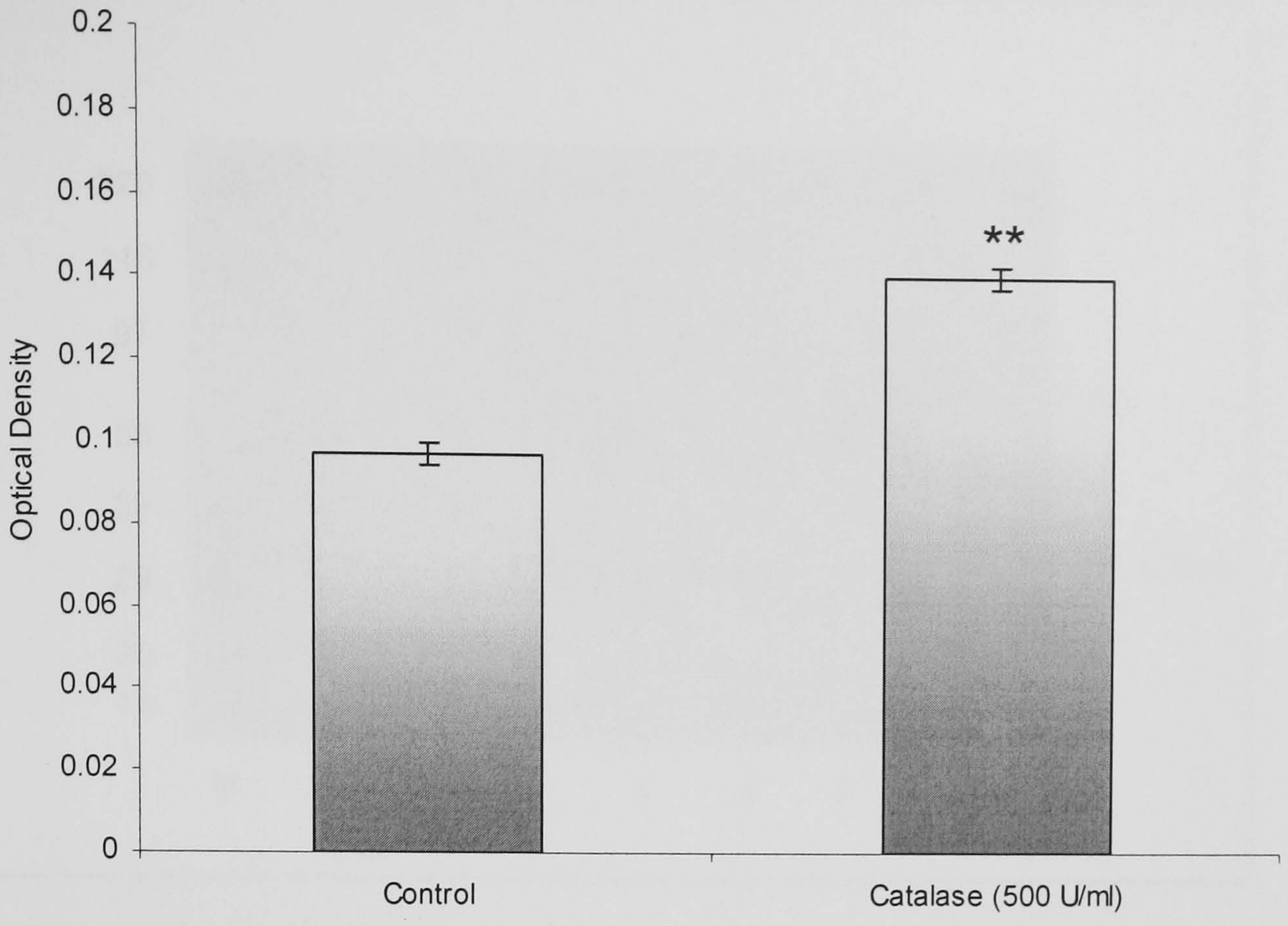

Figure 4.39. LDH release measured in basal supernatants (total volume 1400 µl) following treatment with catalase (500 U/ml). Results are expressed as mean ± SEM, n = 3. Data was compared using a paired student's t-test, ** $p < 0.01$.

Figure 4.39 shows that treatment with catalase (500 U/ml) caused a significant increase in LDH release. The result indicates that toxicity and cell death may have contributed to the reduction in T-cell migration observed following treatment with catalase. However, 100 % Trypan blue dye exclusion of HLMVECs, platelets and T-cells at the end of the transmigration assay indicated that these cells were still viable.

In order to investigate the mechanism of action of copper chelators, HLMVECs were lysed following a transmigration assay, and the cell lysates were analysed by SDS-PAGE, Western blotting and staining for RANTES. It was expected that the addition of copper chelators and catalase may alter the form of RANTES bound to the endothelium.

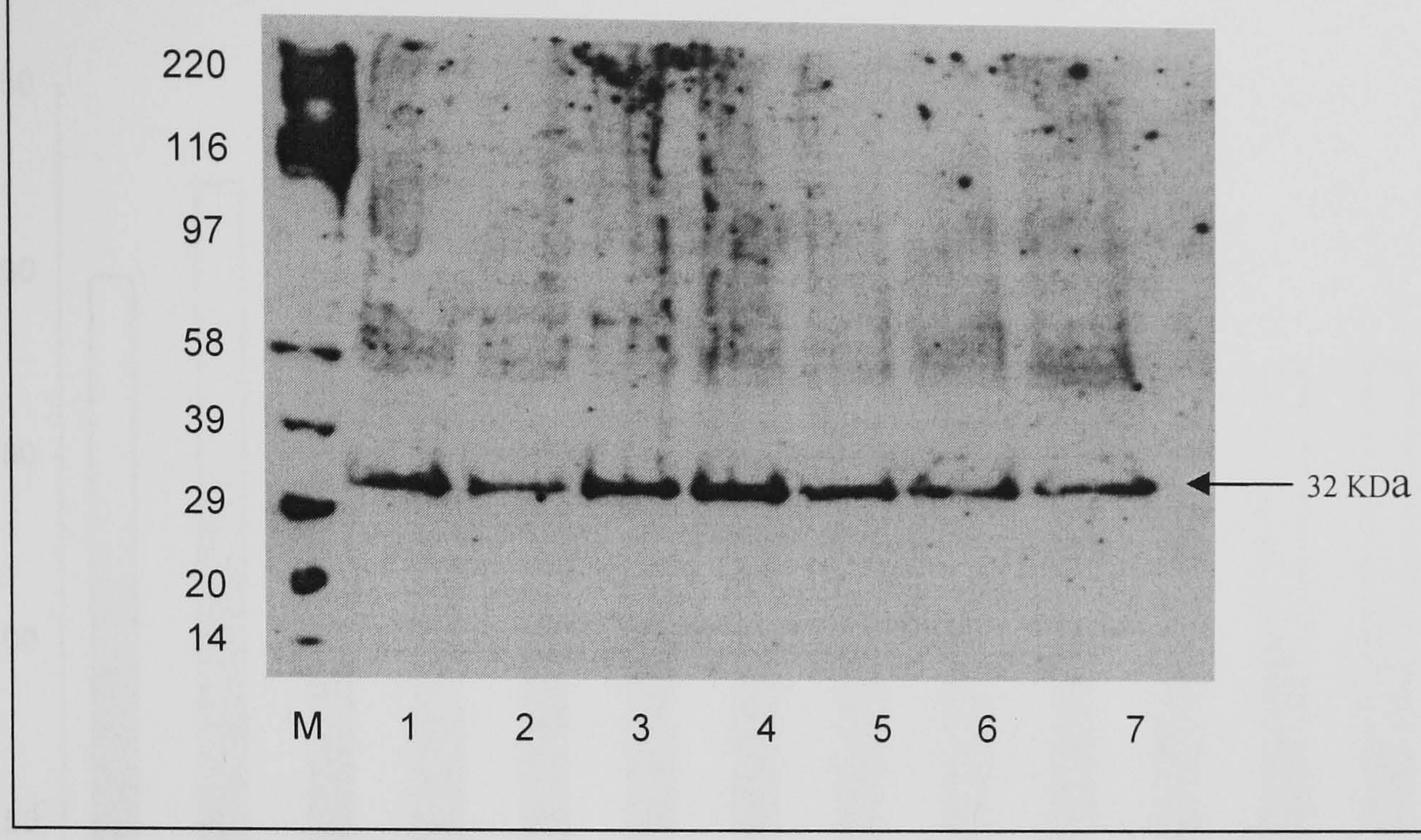

Figure 4.40. Lysates from HLMVECs grown for 2 weeks on uncoated 3 μm PET cell culture inserts, treated with copper chelators, the PAI-1 inhibitor XR5118 and catalase and used in a TEM assay. Lysates were freeze-dried from 200 μl 1 % (v/v) triton-X-100 with protease inhibitors, reconstituted in 40 μl 1x sample buffer, immunoprecipitated for human RANTES, analysed by SDS-PAGE on a 4-15 % gradient polyacrylamide gel and stained for RANTES. M: molecular weight markers. Lane 1: HLMVECs only, Lane 2: HLMVECs treated with 0.5 mM NC, lane 3: HLMVECs treated with 0.5 mM BCDS, Lane 4: HLMVECs treated with 0.5 mM D-pen, lane 5: HLMVECs treated with 0.5 mM tobramycin, lane 6: HLMVECs treated with catalase (500 U/ml) and lane 7: HLMVECs treated with 100 μM XR5118. Results from a single experiment.

Figure 4.40 shows that RANTES was predominantly present as the 32 KDa tetramer and there was no change in the form of RANTES following treatment with the copper chelators NC, BCDS, D-pen or tobramycin, the PAI-1 inhibitor XR5118 (100 μM) or the preotective enzyme catalase (500 U/ml) indicating that the form of RANTES was not changed as a mechanism of action for the anti-inflammatory activity of copper chelators, XR5118 or catalase.

Since it has already been shown that the addition of $CuCl_2$ induces production of RANTES by HLMVECs (Section 4.5.1) it may be that copper chelators reduce the amount of RANTES synthesised by the endothelium as a mechanism for decreased T-cell recruitment. Basal supernatants were cleared following a TEM assay and analysed for RANTES by ELISA.

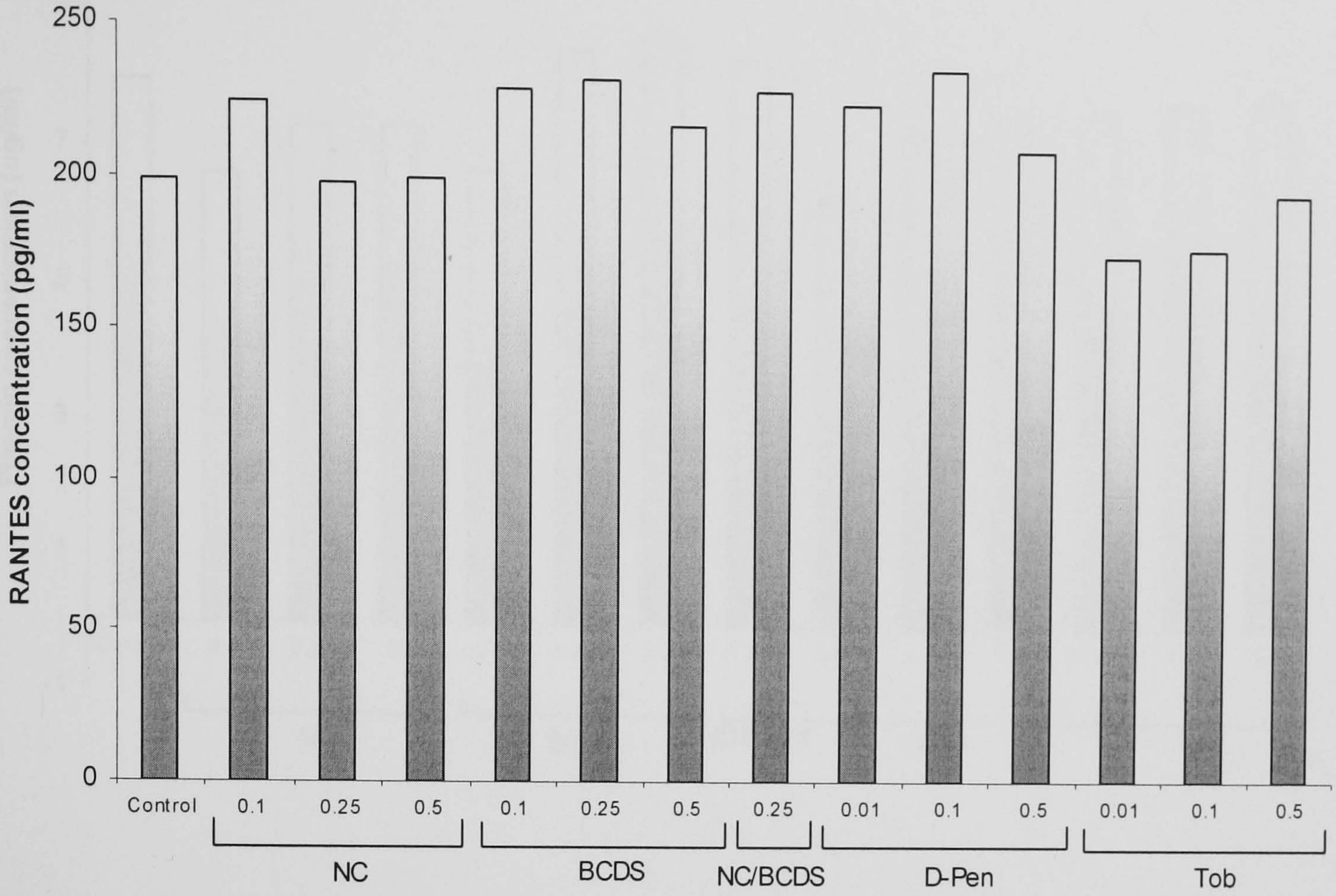

Figure 4.41. Basal supernatants from a TEM assay analysed for RANTES by ELISA. Representative of 2 independent experiments.

Figure 4.41 shows that there was no change in the amount of RANTES present in the basal supernatants following treatment with the copper chelators, NC, BCDS, D-pen and tobramycin indicating that copper chelators did not alter RANTES synthesis or release through the removal of copper.

A further possible mechanism of action of copper chelators is through PAI-1 inhibition. The subsequent activation of plasminogen by plasminogen activator results in plasmin accumulation and increased shedding of endothelial bound proteoglycans.

A plasmin enzyme assay was used to confirm activity levels in basal supernatants from TEM assays in response to treatment with copper chelators.

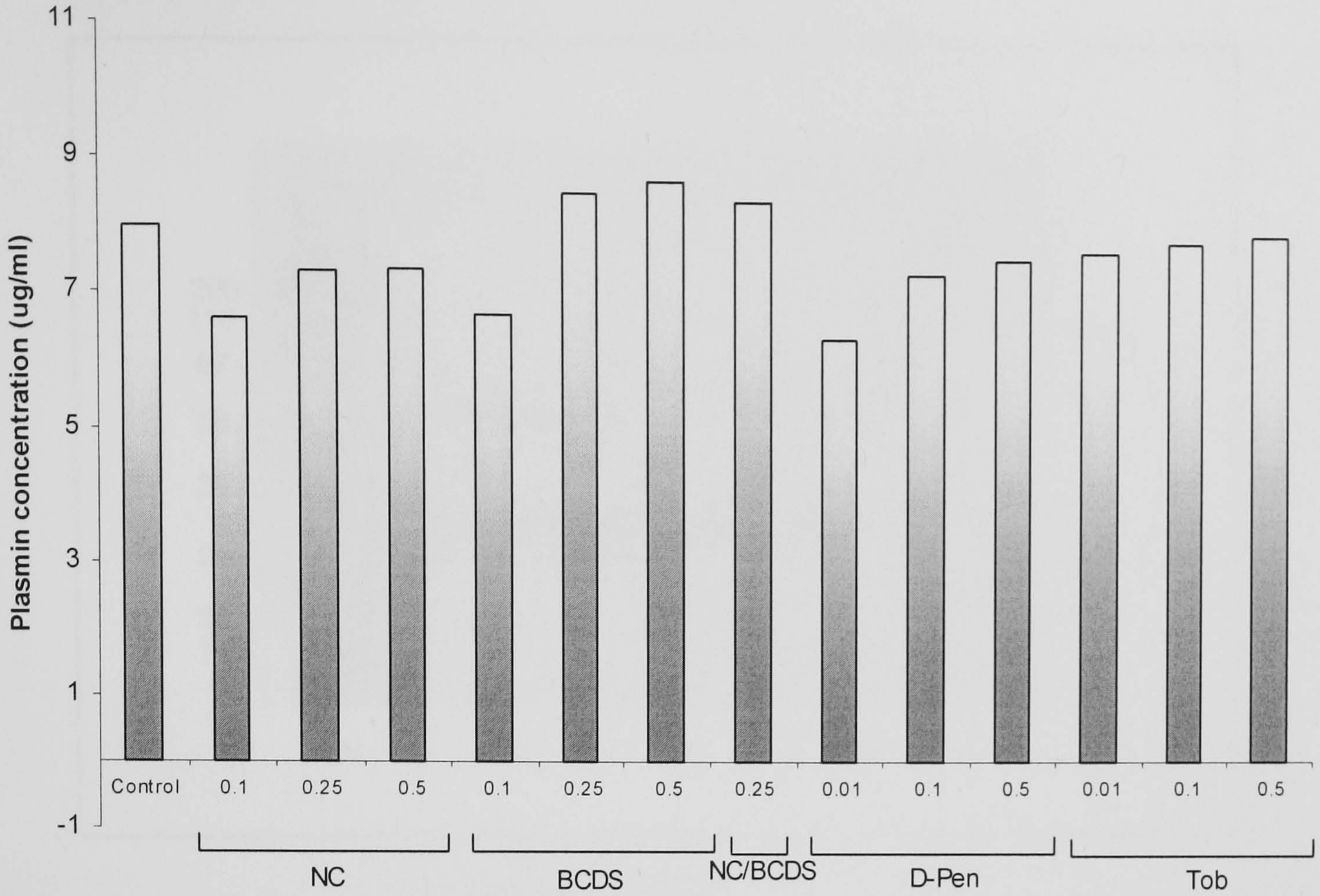

Figure 4.42. Basal supernatants from a TEM assay analysed for plasmin. Representative of 2 independent experiments.

Figure 4.42 confirms that there was no change in plasmin activity levels as a result of treatment with copper chelators.

Figures 4.43-4.45 show RANTES released into the apical and basal supernatants from transmigration assays in the absence and presence of the Cu chelators NC, BCDS, D-penicillamine and tobramycin and the PAI-1 inhibitor XR5118. Platelet-derived RANTES was the T-cell chemoattractant in the lower compartment in the absence of exogenously added IFN-γ plus TNF-α.

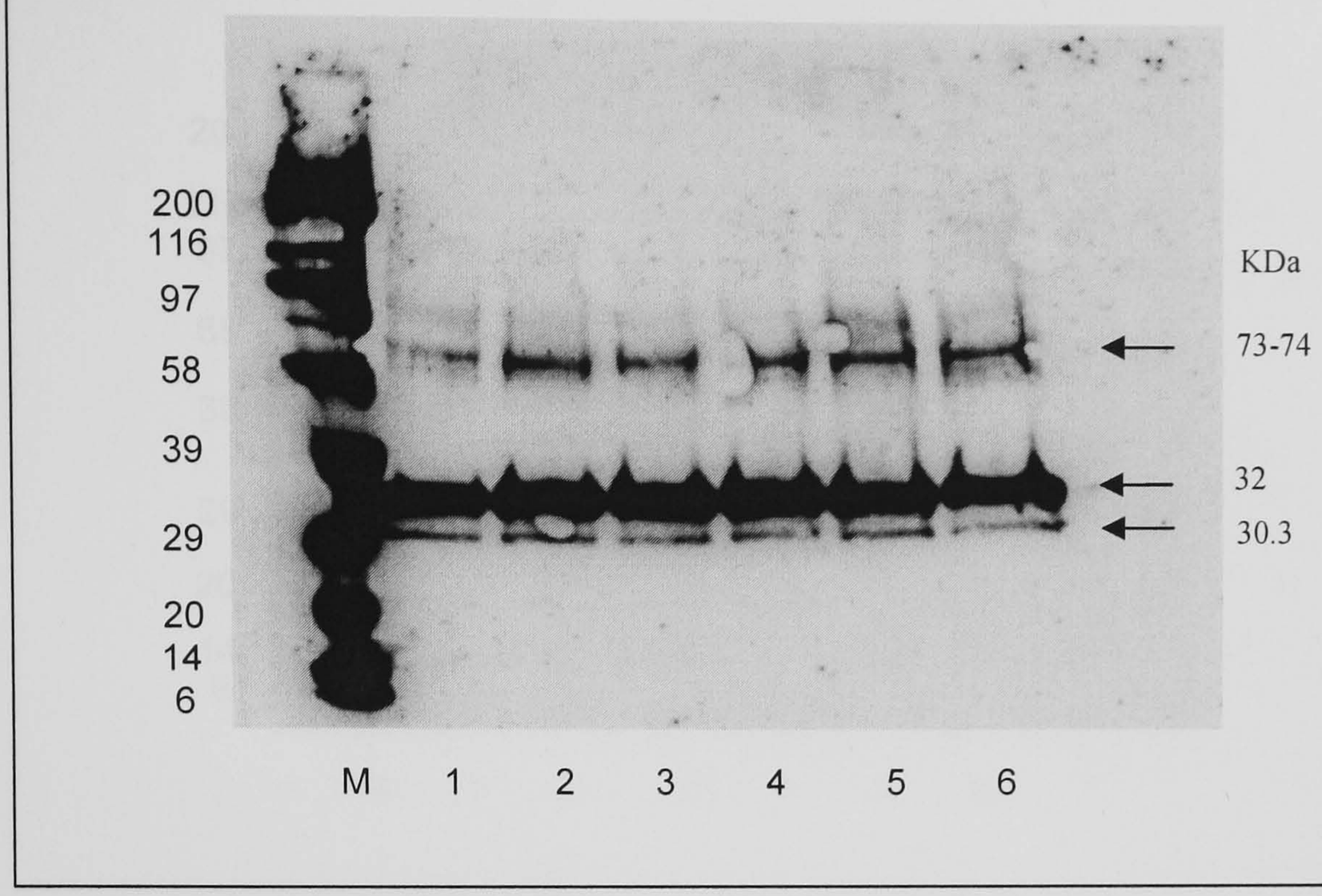

Figure 4.43. Apical supernatants from transmigration experiments in the absence and presence of Cu chelators. HLMVECs were grown for 2 weeks on uncoated 3 µm PET cell culture inserts, treated with copper chelators or the PAI-1 inhibitor XR5118 overnight and used in a TEM assay.. Apical supernatants were freeze-dried from 300 µl, reconstituted in 40 µl 1x PBS (-Ca^{2+}/Mg^{2+}), immunoprecipitated for human RANTES, analysed by SDS-PAGE on a 4-15 % gradient polyacrylamide gel and stained for RANTES. M: molecular weight markers. Lane 1: HLMVECs no Cu chelators, Lane 2: 0.5 mM NC, lane 3: 0.5 mM BCDS, Lane 4: 0.5 mM D-pen, lane 5: 0.5 mM tobramycin, lane 6: 100 µM XR5118. Representative of two independent experiments.

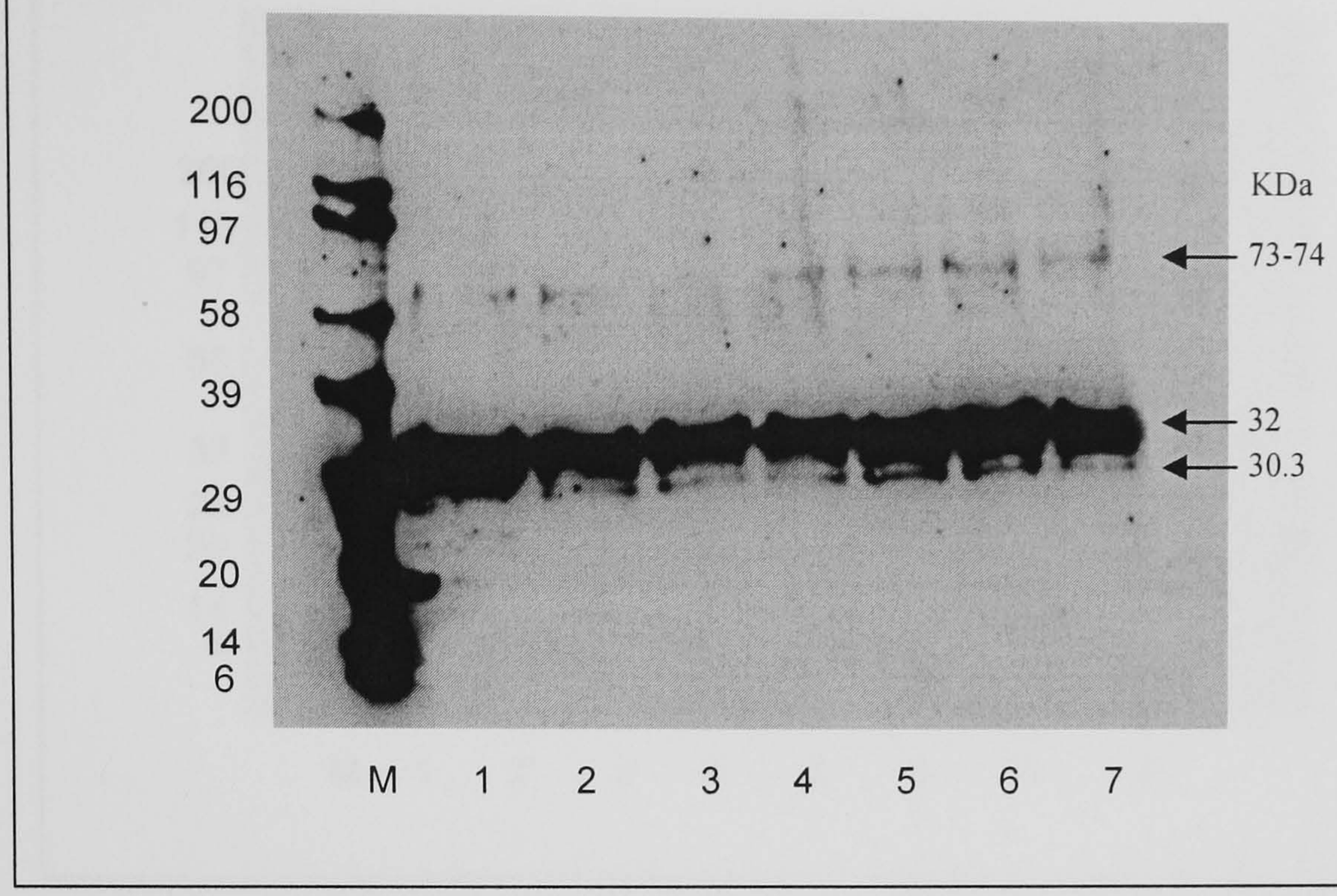

Figure 4.44. Basal supernatants from transmigration experiments in the absence and presence of Cu chelators. HLMVECs were grown for 2 weeks on uncoated 3 µm PET cell culture inserts, treated with copper chelators or the PAI-1 inhibitor XR5118 overnight and used in a TEM assay. Basal supernatants were freeze-dried from 500 µl, reconstituted in 40 µl 1x PBS (-Ca^{2+}/Mg^{2+}), immunoprecipitated for human RANTES, analysed by SDS-PAGE on a 4-15 % gradient polyacrylamide gel and stained for RANTES. M: molecular weight markers. Lane 1: no Cu chelators, Lane 2: 0.1 mM NC, lane 3: 0.25 mM NC, Lane 4: 0.5 mM NC, lane 5: 0.1 mM BCDS, lane 6: 0.25 mM BCDS and Lane 7: 0.5 mM BCDS. Representative of two independent experiments.

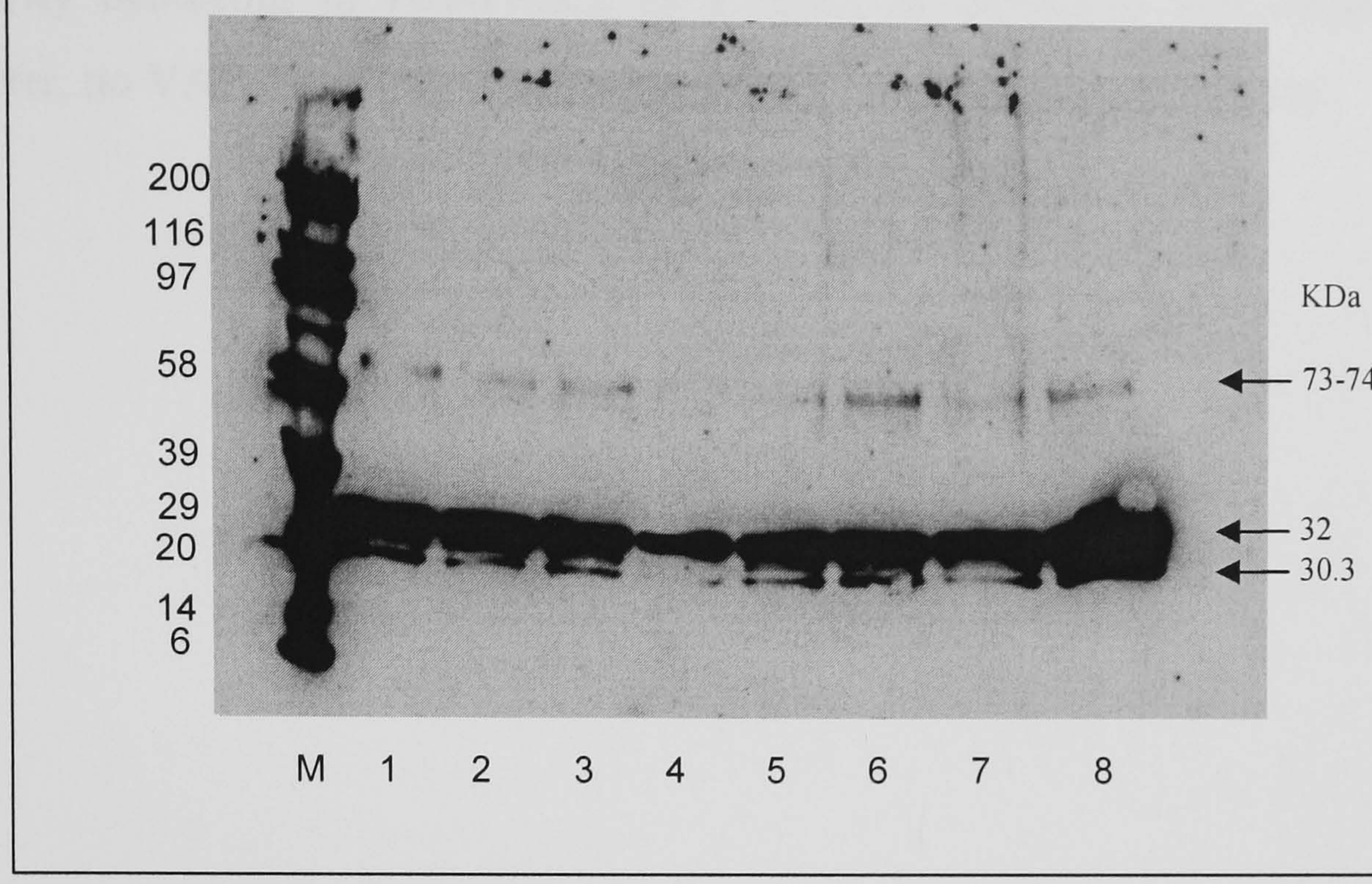

Figure 4.45. Basal supernatants from transmigration experiments in the absence and presence of Cu chelators. HLMVECs were grown for 2 weeks on uncoated 3 µm PET cell culture inserts, treated with copper chelators or the PAI-1 inhibitor XR5118 overnight and used in a TEM assay. Basal supernatants were freeze-dried from 500 µl, reconstituted in 40 µl 1x PBS (-Ca^{2+}/Mg^{2+}), immunoprecipitated for human RANTES, analysed by SDS-PAGE on a 4-15 % gradient polyacrylamide gel and stained for RANTES. M: molecular weight markers. Lane 1: no Cu chelators, Lane 2: 0.01 mM D-pen, lane 3: 0.1 mM D-pen, Lane 4: 0.5 mM D-pen, lane 5: 0.01 mM tobramycin, lane 6: 0.1 mM tobramycin, lane 7: 0.5 mM tobramycin and lane 8: 100 µM XR5118. Representative of two independent experiments.

Despite significantly inhibited T-cell migration following treatment with the Cu chelators NC, BCDS, D-penicillamine and tobramycin (figures 4.32 and 4.33) there was no detectable change in the form of RANTES in the apical (figure 4.43) or basal supernatants (figures 4.44 and 4.45) from these transmigration experiments. Unexpectedly, RANTES was present predominantly in tetrameric form in both the apical and basal supernatants. The 73-74 KDa form of RANTES appeared more strongly in the apical supernatants than the basal supernatants. In addition, a proteolytically cleaved form of RANTES was also detected in both apical and basal supernatants (30.3 KDa) as seen previously (Section, 4.5.1, figure 4.2).

Although NC (0.1-0.5 mM), BCDS (0.1-0.5 mM), D-penicillamine (0.01-0.5 mM) and tobramycin (0.01-0.5 mM) had no effect on the amount of soluble forms of RANTES released into apical or basal supernatants (figures 4.43 – 4.45), treatment with XR5118 (100 µM) increased the shedding of the soluble tetrameric form of RANTES from the cell surface into the basal supernatant as shown clearly in figure 4.45, lane 8.

A VAP-1 enzyme assay (Section 4.3.1.9) was used to determine any inhibition in VAP-1 activity occurring in HLMVECs as a result of treatment with copper chelators. However, no VAP-1 activity was detected in HLMVECs using this assay.

4.6. Discussion

In summary, RANTES multimers were chemotactically active, inducing T-cell migration via both CCR3 and CCR5 receptors suggesting the involvement of $CD4^+$ Th2 and Th1 T-cells as well as $CD8^+$ type 1 (Tc1) and type 2 (Tc2) T-cells. In addition, platelet-derived RANTES was demonstrated to be a T-cell chemoattractant when added to the basal compartment in a model of the lung microvascular endothelium. Platelets added apically induced T-cell arrest. RANTES in HLMVEC lysates was found predominantly present as a covalently-linked tetramer, which may have been bound to a HLMVEC surface-GAG via an electrostatic interaction prior to analysis. Similarly, the RANTES tetramer was the predominant form present in supernatants following transendothelial migration even though activated platelets and HLMVECs were shown to release monomeric RANTES. The treatment of the endothelium with Cu chelators and catalase inhibited T-cell migration indicating a requirement for both Cu and H_2O_2 in the T-cell chemotactic response to platelet-derived RANTES.

T-cell responses to both fresh un-incubated recombinant RANTES and RANTES multimers generated in the presence of $CuCl_2$ and H_2O_2 were mediated through both CCR3 and CCR5 receptors, indicating the possible involvement of $CD4^+$ Th2 and Th1 T-cells as well as $CD8^+$ type 1 (Tc1) and type 2 (Tc2) T-cells. Others have reported that RANTES induces both Th2 and Th1 T-cell migration through CCR1, and CCR3, and CCR1 and CCR5 receptors respectively (Baltus *et al*, 2003; Gerber *et al*, 1997; Kawai *et al*, 1999; Sallusto *et al*, 1998a; Sallusto *et al*, 1998b; Sallusto *et al*, 1997) and that RANTES induces cytotoxic $CD8^+$ T-cell migration through both CCR3 and CCR5 receptors found on Tc2 and Tc1 $CD8^+$ cytotoxic cells, respectively (Hadida *et al*, 1998; Iijima *et al*, 2003; Luangsay *et al*, 2003; Ohtani *et al*, 2004). There is no evidence to suggest that $CD8^+$ cytotoxic T-cell migration is mediated by CCR1 receptors in response to RANTES, therefore it is speculated that any $CD8^+$ T-cell migration would be predominantly mediated by CCR3 and CCR5 receptors.

The result also indicates that T-cell responses to both fresh unincubated recombinant RANTES and RANTES multimers were mediated equally by CCR3 and CCR5 receptors. It is unlikely that T-cells responded through CCR1 mediated chemotaxis, since 100 % of the responses were blocked by CCR3 and CCR5 neutralising antibodies.

CCR3 and CCR5 are also expressed on other inflammatory cells and in other tissues. CCR3 is also expressed by eosinophils and basophils, and CCR5 is also expressed by monocytes and dendritic cells (Sallusto *et al*, 1998b) and in addition, CCR3 is expressed by microvascular endothelial cells and mediates vessel wall remodelling and angiogenesis (Salcedo *et al*, 2001). There is also evidence to suggest that CCR3 may influence key epithelial cell functions including wound repair, and the amplification of profibrogenic and chemokine transcript expression (Beck *et al*, 2006). Therefore neutralising these receptors using specific antibodies may effectively limit T-cell migration and inflammation but not without affecting other fundamental functions that are mediated through CCR3 and CCR5 receptors.

The T-cell chemotactic response to platelet-derived RANTES in transendothelial migration experiments indicates a role for platelets in human leukocyte recruitment during inflammation. It is well known that platelets release chemokines including RANTES upon activation with thrombin (Kameyoshi *et al*, 1992; Kameyoshi *et al*, 1994; Klinger *et al*, 1995; Schroder *et al*, 1994) and platelets have previously been shown to migrate into tissues and influence the pulmonary recruitment of eosinophils and lymphocytes in murine allergic inflammation (Pitchford *et al*, 2005; Pitchford *et al*, 2003). In addition, RANTES deposition by platelets has been shown to induce monocyte arrest in human atherosclerotic endothelium (von Hundelshausen *et al*, 2001) and platelet-derived RANTES has been shown to induce monocyte arrest on inflamed microvascular endothelium under flow conditions (Baltus *et al*, 2005).

RANTES released from platelets on the apical side of the endothelium is likely to bind to the apical surface of the endothelial monolayer and prevent the formation of a chemotactic gradient, inducing the arrest of T-cell migration. Importantly, the requirement for platelets to be present and activated on the subluminal side of the endothelium for T-cell migration indicates that platelets must first undergo transendothelial migration themselves and become activated in the tissues in order to induce T-cell recruitment. Platelets have been reported to undergo chemotaxis *in vitro* in response to prostaglandins, autoantibodies, fMLP or necrotic cells (Clancy, 1972; Czapiga *et al*, 2005; Valone *et al*, 1974) and platelets have been reported to undergo diapedesis in sections of lung from asthmatic patients and have been detected in

bronchoalveolar lavage fluid from asthmatic patients (Jeffery *et al*, 1989; Metzger *et al*, 1987). Platelets have also been detected in the bronchoalveolar lavage fluid of allergen-challenged mice (Pitchford *et al*, 2004) and have been reported to migrate out of blood vessels into lung tissue *in vivo* in allergen-sensitised mice in response to a sensitising allergen (Pitchford *et al*, 2008). Degranulated platelets have been identified in the bronchoalveolar lavage fluid of asthmatic individuals (Metzger *et al*, 1986) and it has also been reported that platelets promote leukocyte trafficking from blood vessels into lung tissue in allergen-sensitised mice (Pitchford *et al*, 2005; Pitchford *et al*, 2003). Furthermore, platelet depletion has been shown to reduce leukocyte accumulation in alveolar compartments in a murine model of lung injury (Zimmerman *et al*, 1984). This evidence demonstrates that platelets can migrate out of blood vessels into murine lung tissue and both murine and human alveolar spaces during inflammation and also that platelets influence leukocyte recruitment into the alveolar spaces in murine models. However, it has not yet been fully demonstrated that platelets influence leukocyte migration into human lung tissue or alveolar spaces or that platelets migrate into human lung tissue *in vivo* during inflammation.

Platelet activation occurs during antigen-induced airway reactions in asthmatic subjects. The mechanism for platelet chemotaxis is thought to involve allergen-specific IgEs produced after contact with the sensitising antigen (Pitchford *et al*, 2008; Yoshida *et al*, 2002). The IgE binds to platelet IgE receptors and, upon exposure to allergen, the allergen induces cross-linking of contiguous receptors and the consequent triggering of platelet migration (Pitchford *et al*, 2008). In addition, platelets of patients with asthma have been shown to release RANTES upon activation via IgE (Hasegawa *et al*, 1999), indicating that both platelet migration and platelet-derived mediator release may be triggered via an IgE dependent mechanism. However, in considering the mechanisms involved in murine models it must be remembered that the number of circulating platelets is higher in mice compared to humans (Mestas & Hughes, 2004; Tsakiris *et al*, 1999).

It is also feasible that platelet recruitment to sites of inflammation is directed by a number of chemokines, since SDF-1, CXCL12, macrophage-derived chemokine (MDC), RANTES, CCL22, and CCL17 (TARC) can activate platelets via their receptors CXCR4, CCR3 and CCR4, although no migratory response has yet been

demonstrated *in vivo* or *in vitro* (Abi-Younes *et al*, 2000; Abi-Younes *et al*, 2001; Clemetson *et al*, 2000; Kowalska *et al*, 2000). It is not known whether platelets migrate from blood vessels into lung tissue prior to, or in conjunction with leukocyte migration. However, an interesting proposition is that during inflammation, platelets may initially migrate into lung tissue and become activated, resulting in platelet degranulation and release of inflammatory mediators such as the chemokine RANTES, which subsequently promote leukocyte migration into lung tissue. Platelet activation may occur in response to a variety of inflammatory stimuli including chemokines, cytokines, antigens, platelet activating factor (PAF), collagen, antigen-antibody complexes and bacterial endotoxins including lipopolysaccharides (reviewed in section 4.1.1.1). Following the recruitment of leukocytes into lung tissue, migrated leukocytes may be influenced by another epithelial derived chemotactic signal which induces leukocyte homing and migration across the epithelium into the alveolar spaces, such as TARC. TARC is synthesised by airway epithelial cells in response to IL-4, and TGF-β (Heijink *et al*, 2007). Alternatively, platelets may migrate from lung tissue into the alveolar spaces themselves via an allergen-specific mechanism or in response to a chemotactic signal and induce subsequent leukocyte migration into alveolar spaces via degranulation and inflammatory mediator release.

Interestingly, platelets are not only a source of RANTES, but also a source of plasminogen activator inhibitor-1 (PAI-1) and Cu. Plasmin can induce syndecan shedding and release of bound chemokines (Marshall *et al*, 2003), and is cleaved from plasminogen in the presence of plasminogen activator (PA). The activation of plasminogen is inhibited by plasminogen activator inhibitors including platelet derived PAI-1. Therefore PAI-1 is pro-inflammatory, its activity resulting in longer association of syndecan-chemokine complexes with the endothelium. Platelets have been shown to synthesise and release PAI-1 in response to thrombin stimulation (Booth *et al*, 1988; Brogren *et al*, 2004; Nordenhem & Wiman, 1997; Pawlowska *et al*, 2001), and Cu has been measured in platelets at 1.1 ± 1.0 μg/g dry weight (Hallgren *et al*, 1987) and 24.4 ±10.7 ng/10^9 cells (Milne & Nielsen, 1996). This evidence suggests that not only do platelets migrate into tissues and synthesise and release RANTES, but they may also have a role in maintaining the presentation of RANTES on proteoglycans through the synthesis and release of PAI-1. Since platelets also contain Cu they may also have an important role in inducing chemokine multimerisation.

In addition to the release of inflammatory mediators, the mechanism of platelet induced leukocyte recruitment *in vivo* may also be contact-dependent, involving surface CD11b, which is up-regulated on leukocytes interacting with platelets. It is possible that platelet aggregation with leukocytes may prime and activate leukocytes for subsequent adhesion to and transmigration across the endothelium (Pitchford *et al*, 2003) (reviewed in Section 4.1.1.2). Cooperation between platelets and leukocytes has been observed in both cardiovascular disease and tumor metastasis (Karpatkin & Pearlstein, 1981; Mickelson *et al*, 1996) and activated platelets have previously been shown to bind to leukocytes, including T-cells (de Bruijne-Admiraal *et al*, 1992).

Interestingly, endothelial progenitor cell (EPC) recruitment during new blood vessel formation and angiogenesis in the asthmatic inflammatory response has been reported to be both Th1 and Th2 dependent (Asosingh *et al*, 2007). This finding indicates that the migration of platelets into tissues may induce T-cell recruitment leading to subsequent EPC recruitment. Thus, platelets may be central not only to the recruitment of T-cells and other inflammatory cells but may also be important for angiogenesis at sites of inflammation.

Although as shown in Section 4.5.1, figure 4.1 and Section 4.5.2, figure 4.15, platelet-derived RANTES, and RANTES released into HLMVEC culture medium is monomeric, RANTES was predominantly found as a tetramer in HLMVEC lysates and in supernatants from transmigration experiments. These tetramers were found to be covalently-linked as reported for isolated recombinant RANTES exposed to Cu plus H_2O_2 (Chapters 2 and 3). The release of RANTES from platelets and HLMVECs in monomeric form has not previously been reported. However, it appears that when platelets are activated by thrombin in the transendothelial migration model, monomeric RANTES is released and binds to the endothelium to induce T-cell migration. The binding of RANTES to the endothelium is dependent on endothelial activation (von Hundelshausen *et al*, 2001) and in the transendothelial migration model, both IFN-γ and TNF-α were present and may have been derived from T-cells or platelets at concentrations sufficient to activate the endothelium (discussed later) and induce platelet-derived RANTES binding to the endothelium with the formation of tetramers. This suggests that if Cu and H_2O_2 are involved in RANTES tetramer formation they

must be present endogenously at concentrations sufficient to induce covalent cross-linking.

During T-cell transendothelial migration it is evident that there is shedding of the tetramer, since the tetramer appears in the supernatants from transendothelial migration experiments at levels as high as in the cell lysates. The shedding of the tetramer into the supernatants may be due to plasmin activity and increased syndecan turnover. Plasmin may have been activated by thrombin which was added to platelets during the transmigration experiments.

In addition, it is possible that the 74 KDa RANTES-GAG complex (discussed later) was more predominant in the apical supernatants than basal supernatants due to the requirement for RANTES presentation on the apical endothelial cell surface for transendothelial migration of T-cells to occur. It is possible that pro-inflammatory cytokines released by T-cells such as IFN-γ and TNF-α up-regulate GAG expression during endothelial activation, and that this occurs more strongly on the apical surface of HLMVECs, the site at which T-cells were added. It is also possible that RANTES is directed to GAGs on the apical endothelial cell surface by transcytosis, which may involve DARC (discussed later).

HLMVEC lysates contained a 30.3 KDa RANTES multimer, and despite the presence of protease inhibitors upon lysis of the cells, it is likely that this is a post-translational proteolytically processed form of RANTES. A 3-68 or 4-68 truncated amino acid variant with a monomeric mass of 7663 or 7515 KDa has previously been reported (Lim *et al*, 2005) and the formation of a tetramer with these truncated RANTES monomers would result in a mass of 30.7 or 30.1 KDa.

Both RANTES (3-68) and RANTES (1-68) have been detected in the cell culture medium of dermal fibroblasts stimulated with TNF- α or IL-1β and the study showed that the loss of the two residues does not affect the eosinophil chemotactic activity towards RANTES (Noso *et al*, 1996). It has also been shown that both full-length and truncated RANTES induce a similar chemotactic response in T-cells and that RANTES (3-68) has impaired binding and signalling capacity through CCR1 and CCR3 but retains activity on CCR5 (Oravecz *et al*, 1997). This would suggest that both the

tetramer of full length and truncated RANTES should be chemotactically active. This is in agreement with previous findings that have shown that chemotactic inactivity occurs only in the absence of the first 8 amino-terminus amino acids (Vives *et al*, 2002; Wells *et al*, 1995).

Sodium chlorate has previously been shown to abolish GAG sulphation, including HSPG sulphation by competing with sulphate for sulphotransferase enzymes and therefore blocking the sulphation of new glycosaminoglycan chains, and subsequently inhibiting GAG synthesis (Davies *et al*, 2001; Humphries & Silbert, 1988; Humphries *et al*, 1989; Qiao *et al*, 2003; Safaiyan *et al*, 1999). Thus, treatment of HLMVECs with sodium chlorate depleted GAG synthesis as indicated by increases in both lipid peroxidation (Section 4.5.1, figure 4.13) and the post-translational proteolytic modification of RANTES (figure 4.9). GAGs are well known as free radical scavengers and have been shown to have protective effects against the degradation of chemokine multimers (Chapters 2 and 3). Others have reported the protective effects of GAGs against lipid peroxidation and oxidative damage in liposome and fibroblast cultures (reviewed in Section 2.6).

An increase in lipid peroxidation in the presence of sodium chlorate therefore occurs as a result of the reduced protective effect of GAGs against ROS which are generated by the dismutation of the superoxide radical (O_2^-) and produced by the endothelium under normal physiological conditions. This experiment (figure 4.13) also indicated that exogenously added Cu and H_2O_2 did not induce further increases in lipid peroxidation and therefore activated HLMVECs are producing ROS at levels sufficient to induce maximum lipid peroxidation in the absence of GAGs.

The activation of HLMVECs by TNF-α and IFN-γ may have contributed to the generation of ROS resulting in lipid peroxidation, since it has been reported that ROS, including superoxide radicals and H_2O_2 are generated by fibroblasts in response to TNF-α (0.28 nM-10 nM) and IL-1 (0.145 nM-50 nM) (Meier et al, 1989). In addition, TNF-α (10 pM-1 nM) has also been reported to stimulate superoxide radical generation by neutrophils (Ferrante *et al*, 1988; Tsujimoto *et al*, 1986).

Vascular endothelial cells have a capacity to produce superoxide anions and H_2O_2 from several intracellular sources, including eNOS, cyclooxygenase, lipoxygenase, cytochrome P450 enzymes and NAD(P)H oxidases (Kinnula *et al*, 1992c; Kunsch & Medford, 1999; Matoba *et al*, 2002; Matoba *et al*, 2000). Levels of H_2O_2 at or below 20-50 μM appear to have limited cytotoxicity to many cell types (Halliwell *et al*, 2000a) and previous studies have claimed normal physiological levels of H_2O_2 of up to 35 μM in human plasma (Deskur *et al*, 1998; Lacy *et al*, 1998; Varma & Devamanoharan, 1991). However in the absence of protective mechanisms, these otherwise harmless levels of H_2O_2 may become toxic, and result in DNA, protein and lipid peroxidation. In addition, pathophysiological levels of H_2O_2 have been reported of up to 100 μM, released by activated granulocytes during inflammation (Bucchieri *et al*, 2002).

The toxic effects of H_2O_2 have been attributed to the spontaneous generation of highly reactive hydroxyl radicals from H_2O_2 (Halliwell *et al*, 2000a). The generation of reactive oxygen species (ROS) causes peroxidative damage to membrane lipids and cellular nucleic acids and the direct oxidation of proteins (Campo *et al*, 2004).

Lipid peroxidation is initiated by the attack of any chemical species that has sufficient reactivity to abstract a hydrogen atom from a methylate carbon in the side chain, including the hydroxyl radical ($OH^{\cdot}$) (Gutteridge & Halliwell, 1990).

The hydrogen atom is a free radical since it has a single unpaired electron and its removal leaves behind an unpaired electron on the carbon atom to which it was originally attached.

$$\text{Lipid-H} + OH^{\cdot} \longrightarrow \text{Lipid}^{\cdot} + H_2O$$

In aerobic cells the resulting carbon centred radical undergoes molecular rearrangement followed by reaction with molecular oxygen to give a peroxyl radical.

$$\text{Lipid}^{\cdot} + O_2 \longrightarrow \text{Lipid-}O_2^{-}$$

Peroxyl radicals can attack membrane proteins but can also propagate lipid peroxidation by abstracting hydrogen from adjacent fatty acid side chains in a membrane. Once initiated, the process of peroxidation proceeds as a free radical chain reaction.

$$\text{Lipid-}O_2^{\cdot} + \text{Lipid-H} \longrightarrow \text{Lipid-}O_2H + \text{Lipid}\cdot$$

The occurrence of lipid peroxidation in biological membranes causes impairment of membrane functioning, decreased fluidity, inactivation of membrane-bound receptors and enzymes ans increased non-specific permeability to ions (Gutteridge & Halliwell, 1990). As well as lipid peroxidation, oxidative stress can also lead to protein and DNA oxidation, leading to oxidative damage.

O_2 can be reduced to the superoxide radical $O_2^{\cdot}$ in inflammation. Mast cells, macrophages, eosinophils and neutrophils recruited and activated at sites of tissue injury are a major source of $O_2^{\cdot}$ radicals which can dismutase to H_2O_2 (van der Vliet *et al*, 1997).

$$2O_2^{\cdot} + 2H^{+} \longrightarrow H_2O_2 + O_2$$

The mechanism for the oxidation of proteins is similar to that of lipid peroxidation. Free radicals can also abstract hydrogen ions from proteins generating amino acid radicals that can form disulphide bridges, protein-lipid and protein-protein covalent bonds. The cross-linking of proteins in this manner can give rise to high molecular weight aggregates (Horton & Fairhurst, 1987).

$$\text{Protein-H} + OH\cdot \longrightarrow \text{Protein}\cdot + H_2O$$

$$\text{Protein}\cdot + \text{Lipid}\cdot \longrightarrow \text{Protein-Lipid}$$

$$\text{Protein}\cdot + \text{Protein}\cdot \longrightarrow \text{Protein-Protein / High molecular weight aggregates}$$

HLMVEC-associated RANTES is predominantly tetrameric (32 KDa) in the presence of the anionic surfactant, SDS. It is possible though that the the RANTES tetramer may have been bound to a HLMVEC surface GAG through a non-covalent interaction such as ionic or Van der Waals forces. The loss of higher molecular weight forms of

RANTES in the presence of sodium chlorate indicates that RANTES is indeed presented on HLMVECs as a GAG-bound RANTES complex, but it may be that separation of proteins in the presence of SDS disrupts the complexes. In support of the finding that RANTES was not covalently bound to HLMVEC-expressed GAGs, the HS-RANTES interaction has previously been shown by others to be due to specific electrostatic interactions including hydrogen bonds, salt bridges and van der Waals forces involving the classical BBXB cluster in the 40s loop of RANTES (described in section 1.9) that is also implicated in CC receptor binding (Martin *et al*, 2001; Proudfoot *et al*, 2003; Rek, 2009).

These findings are in contrast to reports of IL-8 bound to HS expressed by HUVECs through an interaction that is resistant to both SDS and the sulphydryl reducing agent, DTT (Marshall *et al*, 2003), suggesting that the interaction of IL-8 with HUVEC-expressed HSPG is covalent unlike the RANTES interaction with HLMVEC-expressed HSPG which appears to be electrostatic. Alternatively it may be that the form of chemokines presented on HUVECs differs to that on HLMVECs.

The weak bands of complexed RANTES at MW 73-74 and 116 KDa are likely a RANTES-heparan sulphate proteoglycan (HSPG) complex since HS is the most ubiquitous GAG (50 – 90 % of all GAGs) found on the endothelium and is the most predominant GAG found in the lungs, followed by chondroitin sulphate/dermatan sulphate, hyaluronan and heparin (Cockwell *et al*, 1996; Frevert *et al*, 2003; Ihrcke *et al*, 1993). HS is considered the most ubiquitous and physiologically relevant cell-surface GAG. In addition, it has been well documented that RANTES binds to HSPGs on human microvascular endothelial cells and HUVECs *in vitro* and with a higher affinity than many other chemokines (Ali *et al*, 2002; Carter *et al*, 2003; Hillyer & Male, 2005; Hoogewerf *et al*, 1997; Kuschert *et al*, 1999; Proudfoot *et al*, 2001). So far, RANTES has been reported to bind both syndecan-1 and syndecan-4 proteoglycans (Bartlett *et al*, 2007; Slimani *et al*, 2003).

The suggestion that RANTES binds to HSPG as a tetramer agrees with previous reports that have demonstrated RANTES binding to heparin as a tetramer (Hoogewerf *et al*, 1997) with a minimal tetrameric structure for chemotactic activity *in vivo* and that both the monomeric and dimeric forms of RANTES are devoid of chemotactic activity.

Heparin was deemed structurally and chemically similar enough to serve as a good substitute for HS in these studies (Proudfoot *et al*, 2003). It has also been shown that RANTES binding to HS and subsequent oligomerisation is required for the chemotactic activity of RANTES *in vitro* as shown using oligomerisation-deficient RANTES mutants which were unable to induce leukocyte chemotaxis (Rek, 2009).

In addition, the HS binding and oligomerisation domain of RANTES have been found to be structurally and functionally coupled. The binding of RANTES to HS was found to be positively cooperative – the binding of RANTES to HS promotes further RANTES binding and oligomerisation. Upon binding to HS, RANTES undergoes a conformational change which is dependent on a HS length greater than 6dp and this induced structural fit has been interpreted to be responsible for the GAG-promoted oligomerisation of RANTES (Rek, 2009).

The predominance and higher stability of the tetrameric form of RANTES, indicated by resistance to higher concentrations of H_2O_2 than the monomeric form, suggests that the tetramer is the most likely form presented to circulating leukocytes since it will not be degraded, but will remain during inflammation which can generate high concentrations of H_2O_2 up to 100 μM.

The observation that RANTES occurred as a 64 KDa complex (Chapter 4) indicates that in addition to GAG binding, RANTES may also bind to the Duffy antigen receptor for chemokines (DARC) expressed on the endothelium. RANTES can bind to DARC (Choe *et al*, 2005; Neote *et al*, 1994) and since DARC is 48 KDa, and the predominant form of RANTES detected in HLMVEC lysates is the tetramer (32 KDa) (Section 4.5.1), it is speculated that a RANTES tetramer-DARC complex would be 80 KDa and a RANTES dimer-DARC complex would be 64 KDa. It has previously been reported that RANTES binds to DARC and that DARC is expressed on both apical and basal membrane domains of the endothelium of large venules and capillaries *ex vivo* (Chaudhuri et al, 1997; Peiper et al, 1995). DARC expression has also been demonstrated on the endothelium using HUVECs *in vitro* (Lee *et al*, 2003) and the expression of DARC has been reported on the endothelium of postcapillary venules in all tissues except for the liver (Hadley *et al*, 1994). DARC is also expressed on erythrocyte surfaces and it has been shown that RANTES also binds to erythrocyte

expressed DARC (Neote *et al*, 1994). In addition, it has previously been shown that IL-8 binds to erythrocyte DARC as a dimer (Leong *et al*, 1997).

It has been shown that DARC plays a role in the transport of chemokines to the apical surface of the endothelium. Using HUVECs it has been shown that DARC facilitates the movement of IL-8 and GRO-α across the endothelium *in vitro*, promoting neutrophil transmigration both *in vitro* and *in vivo* (Lee *et al*, 2003). Since DARC has been shown to transport chemokines unidirectionally from the basolateral to the apical side of the endothelium (Pruenster & Rot, 2006) it is likely that RANTES is transported to the apical surface by endothelial expressed DARC.

Thus DARC may intercept chemokines that are passing from the tissue into the plasma and may salvage their activity by redirecting these chemokines to GAGs on the luminal endothelial cell surface. It has been suggested that by preventing chemokines from entering the circulation, the surface retention of chemokines by DARC prevents leukocyte desensitisation in the circulation by soluble plasma chemokines leading to the enhancement of chemokine induced leukocyte recruitment (Rot, 2005).

However, the weak staining of the 64 KDa RANTES complex (Section 4.5.1) indicates that there may be very low levels of DARC expression in cultured HLMVECs. This is most likely due to the lack of DARC expression in cultured endothelial cells. It has previously been reported that microvascular endothelial cells rapidly lose their DARC expression in the process of their culture *in vitro* (Rot, 2003) and DARC is almost undetectable in cultured HUVECS (Hoogewerf *et al*, 1997). Since others have reported the strong expression of DARC in the postcapillary venules of all tissues, and also in HUVECs, it is likely that HLMVECs do indeed also strongly express DARC, but that this expression has been lost during the culturing process. Further work using a DARC antibody to stain Western blots would confirm the presence of DARC in cultured HLMVECs and also whether RANTES forms a complex with DARC on the surface of these cells.

Although Cu and H_2O_2 were not found to have any effect on the form of RANTES detected in HLMVEC lysates and supernatants, it is possible that the activation of the endothelium with IFN-γ and TNF-α had already induced maximal ROS generation by

HLMVECs, as previously discussed. This may prevent Cu/H_2O_2 from having any further effect on multimer formation via redox and subsequent ROS generation. In support of this notion, RANTES tetramers were already formed prior to the addition of Cu/H_2O_2 (figure 4.5). However, 24 hour exposure to Cu was found to induce the synthesis and release of RANTES from HLMVECs. In support of this finding, others have reported the synthesis and release of IL-8 from HUVECs and HLMVECs similarly within 24 hours, indicating early gene activation and new protein synthesis rather than IL-8 release from preformed storage sites (Bar-Or *et al*, 2003).

It has been suggested that Cu may induce NF-kB and subsequent IL-8 synthesis through the activation of the phosphatidylinositol 3-kinase (PI3-kinase)/Akt/NF-kB pathway independently of ROS, possibly through the oxidation of the tumor suppressor PTEN, an inhibitor of the PI3-kinase/Akt pathway (Bar-Or *et al*, 2003; Ostrakhovitch *et al*, 2002) (Ozes *et al*, 1999) or alternatively through a MAPK (JNK, p38) / NF-kB pathway (Samet et al, 1998) (reviewed in Section 4.1.3).

It has also been reported that Cu-induced ROS generation by Cu/redox mechanisms induces oxidative stress resulting in NF-kB activation (Persichini *et al*, 2006). ROS have also been shown to activate the PI3-kinase/Akt pathway via oxidation of the tumor suppressor PTEN (Lee *et al*, 2002) and also via MAPK (Fialkow *et al*, 1994) (reviewed in Section 4.1.3). Additionally it has been suggested that Cu (II)-oxidised low-density lipoproteins may independently initiate the activation of activator protein-1 (AP-1), a transcription factor associated with endothelial IL-8 expression in endothelial cells (Maziere *et al*, 1997).

RANTES synthesis is inducible by IL-1β in human bronchial epithelial cells (Manni *et al*, 1996) and IFN-γ in HLMVECs (Sundstrom *et al*, 2001) through the regulation of NF-kB. Since it has been suggested that Cu-induced IL-8 synthesis in HLMVECs is regulated by the NF-kB pathway, and Cu has been shown to induce NF-kB independently of ROS through the activation of PI3-kinase/Akt and MAPK pathways (Ostrakhovitch *et al*, 2002; Samet *et al*, 1998) and through the generation of ROS via Cu/redox (Persichini *et al*, 2006) and subsequent activation of the PTEN/PI3-kinase/Akt and MAPK pathways (Fialkow *et al*, 1994; Lee *et al*, 2002; Pelaia *et al*, 2004), this suggests that Cu induced RANTES synthesis in HLMVECs most likely occurs via the

NF-kB pathway. The activation of RANTES transcription may also occur through PI3-kinase/Akt or MAPK (JNK or p38) activation, either independently of ROS or possibly through the generation of ROS via Cu/redox mechanisms.

A possible explanation for the failure of increased concentrations of H_2O_2 to induce further RANTES synthesis in the presence of Cu is that in biological systems, H_2O_2 is present transiently and may immediately dismutate in the presence of antioxidants generated by HLMVECs in culture. Therefore in the presence of H_2O_2, RANTES synthesis would be regulated by Cu, generating a Cu-redox system as a constant source of H_2O_2 and ROS in order to activate NF-kB and transcription of RANTES mRNA.

The biphasic manner in which Cu induced the synthesis of HLMVEC-derived RANTES can be explained in terms of the regulation of NF-kB and its inhibitor IkB. In most cells, the majority of NF-kB resides in the cytoplasm, bound to the IkB inhibitory protein family, which include IkBα, IkBβ, IkBε, Bcl-3, p100, and p105. These proteins function as inhibitors through ankyrin repeats, which bind to the REL domain of NF-kB and prevent NF-kB nuclear translocation (Beg & Baldwin, 1993).

Activation of NF-kB is mediated through the IkB kinase complex (IKK), which functions to phosphorylate two serine residues on IkB proteins. Phosphorylation of these residues causes the ubiquitination and subsequent degradation of IkB proteins. Upon loss of IkB, NF-kB is free to translocate to the nucleus where it binds to its cognate DNA sequence and interacts with the basal transcription machinery and transcriptional co-activators to stimulate gene expression (Karin & Ben-Neriah, 2000). One of the numerous genes induced by NF-kB is the ankyrin repeat containing proteins that serve to recapture and inactivate NF-kB, including the IkB family (Brasier, 2006). Once resynthesised, IkB is transported to the nucleus where it binds and inhibits NF-kB DNA binding (Arenzana-Seisdedos et al, 1995). NF-kB is sequestered back to the cytoplasm through a nuclear export signal located in the amino terminus of IkB (Huang *et al*, 2000a).

Therefore the activation of NF-kB by Cu would result in the transcription of both RANTES and the NF-kB inhibitory IkB proteins. It is possible that low doses (up to 25 μM) of Cu induce RANTES transcription in a dose-dependent manner, but at a dose of

50 μM, the transcription of the NF-kB inhibitor, IkB, reaches a level sufficient to inhibit NF-kB, resulting in reduced RANTES synthesis. Additional increases in Cu would then result in further dose-dependent NF-kB mediated synthesis of RANTES.

Although multimers of recombinant RANTES generated in the presence of Cu plus H_2O_2 were chemotactically active, the finding that neither the addition of either Cu plus H_2O_2 nor the addition of Cu chelators had any effect on the form of RANTES detected in HLMVEC lysates indicated that Cu is not involved in RANTES multimer formation and presentation in HLMVECs. However, the ability of Cu to induce RANTES synthesis and the Cu-dependence of the vascular adhesion protein VAP-1 (reviewed in Section 4.1.4) indicated that Cu may still have an important pro-inflammatory role and could influence leukocyte trafficking during lung inflammation. In addition, studies by others indicated that Cu-binding peptides were effective in preventing both Cu-redox and IL-8 release from endothelial cells (Rael *et al*, 2007), suggesting that Cu chelators may have therapeutic potential in inhibiting cytokine and chemokine synthesis, and subsequent leukocyte recruitment during inflammation.

Much of the evidence presented in this chapter suggested that platelets may migrate into tissues and contribute to leukocyte recruitment, as a source of not only RANTES but also PAI-1 and Cu, all of which may play a role in inducing T-cell migration during the inflammatory response, especially in the lungs where raised levels of RANTES, PAI-1 and excessive T-cell accumulation have been implicated in asthma, COPD and CF (reviewed in Sections 1.5 and 1.17). Raised levels of PAI-1 have been reported in both sputum and plasma from patients suffering with CF, COPD and asthma compared to control subjects (Ashitani *et al*, 2002; Kowal *et al*, 2007; Xiao *et al*, 2005). PAI-1 may also be derived from the HLMVECs themselves, since PAI-1 synthesis and release has been reported to occur in HUVECs in response to thrombin and in bovine aortic endothelial cells in response to TNF-α (Dichek & Quertermous, 1989; Gelehrter & Sznycer-Laszuk, 1986; Sawdey *et al*, 1989). Platelets have also been reported as a source of chondroitin sulphate A, which increases the binding of RANTES to endothelial cells (reviewed in Section 4.1.1.2). In addition, in lung tissue there is a high exposure to oxygen which promotes the generation of ROS through Cu/redox mechanisms (Section 2.6) which are known to activate NF-kB as a regulator of cytokine and chemokine expression. Therefore, a model of the vascular endothelium was used to

investigate the therapeutic potential of Cu chelators as inhibitors of T-cell transendothelial migration in response to platelet-derived RANTES.

Thrombin is well known as a coagulation factor, generated by the coagulation cascade factors and cofactors, but also induces platelet activation and degranulation (Section 4.1.1.1). At different phases of blood coagulation, thrombin is generated in an extremely wide range of concentrations, varying from pM and nM amounts to the maximal level of 0.8–1.4 μM (Brummel-Ziedins et al, 2004; Mann et al, 2003). Hence, during blood coagulation, platelets can be exposed to very low and very high thrombin concentrations. Studies have shown that at low thrombin concentrations of 0.5–1 nM, almost all platelets become activated, whereas high doses (10 – 100 nM) trigger platelet apoptosis (Leytin et al, 2007). In addition, the low molecular weight phospholipid, platelet activating factor (PAF), released from inflammatory cells including neutrophils, eosinophils, macrophages and platelets (Barnes *et al*, 1988) has been shown to induce human platelet aggregation and degranulation including the secretion of serotonin from human platelets (Henson, 1976; O'Donnell *et al*, 1978) and to activate rabbit platelets at a concentration of 1 μM. This concentration, which is around 6 orders of magnitude above the concentration needed to induce platelet activation and aggregation, was required to degranulate and remove most of the releasable ATP from the platelets (Vargaftig et al, 1982). Although PAF has a central role in the pathogenesis of asthma (Barnes *et al*, 1988), it appears that PAF is a less potent inducer of platelet degranulation than thrombin, indicating that thrombin may be more important as an inducer of platelet degranulation than PAF during the inflammatory response. Thrombin was used at a concentration of 1 U/ml which correlates to 0.019 - 7.94 nM (activity of thrombin was 1500 - 3500 NIH Units/mg) which is of an order sufficient to activate platelets without triggering apoptosis.

It was expected that HLMVECs grown on Transwells would synthesise their own basement membrane following 2 weeks of culture as an important physiological component of the transendothelial migration model (Butler *et al*, 2008; Butler *et al*, 2005). Platelets can become activated during coagulation through interaction with collagen in basement membranes. In healthy, undamaged tissues, collagens which support the blood vessel wall and surrounding tissue are concealed by endothelial cell layers and cannot come into contact with the circulating platelets. However, should the

endothelial cell layer be removed either in disease or upon tissue injury, then collagens are revealed which can interact with the cellular components of the blood as well as with proteins in blood plasma (reviewed in Farndale, 2006).

Collagen can bind directly to several receptors on the platelet surface, notably integrin α2β1 and Glycoprotein VI (GpVI) which is considered the primary activatory collagen receptor expressed on the platelet surface. Indirect interactions can also occur, as when von Willebrand Factor (VWF) binds to the platelet surface through the Glycoprotein Ib/ V/IX complex, interacting directly with GpIbα through its A1 domain and also to specific sites within the collagens through its A3 domain. Thus, a series of platelet receptors contribute to the interaction of the platelet with the collagens and subsequent platelet activation (Farndale, 2006). However, in the lung microvascular endothelial model, it was not expected that platelets would be exposed to collagen, and therefore thrombin was preferentially used as a platelet activator. Thrombin has been previously used to activate platelets and cause degranulation in studies of RANTES release and platelet-induced monocyte arrest (von Hundelshausen *et al*, 2001) and platelet-induced eosinophil recruitment (Kameyoshi *et al*, 1992; Kameyoshi *et al*, 1994).

Whilst unstimulated platelets spontaneously released RANTES, thrombin induced a dose-dependent increase in platelet-derived RANTES release but there appears to be a limiting factor at high cell density. One suggestion is that this may be due to the binding of RANTES to platelets. The high level of spontaneous RANTES release may be due to activation during platelet isolation, which could be minimised by using a rapid, one-step density gradient (Bagamery *et al*, 2005).

During transendothelial migration experiments, HLMVECs constitutively produced RANTES, as indicated by the inhibition of spontaneous T-cell migration by anti-RANTES neutralising antibodies (Section 4.5.5, figure 4.30). However, RANTES-dependent T-cell migration was enhanced in the presence of IFN-γ plus TNF-α, which increased the synthesis of RANTES as indicated by ELISA measurements. This finding is in agreement with previous studies that have reported IFN-γ plus TNF-α induced RANTES synthesis in HUVECs and human mucosal microvascular endothelial cells (HMMECs) (Marfaing-Koka *et al*, 1995; Terada *et al*, 1996). This may also explain the

finding that in platelet-HLMVEC co-cultures, RANTES release was maximal in the presence of the activated endothelium.

However, more RANTES was bound to the endothelium and detectable in the lysates than free in the supernatant under these conditions. In support of this result, it has previously been reported that greater amounts of platelet-derived RANTES bind to HLMVECs following endothelial activation with IFN-γ and TNF-α when compared with non-activated HLMVECs (von Hundelshausen *et al*, 2001). It is thought that endothelial activation up-regulates the synthesis of many endothelial cell surface proteins including proteoglycans and induces specific endothelial binding sites for RANTES, explaining the enhanced binding of platelet-derived RANTES to the activated endothelium (von Hundelshausen *et al*, 2001). This may also explain the binding of monomeric RANTES released from platelets and HLMVECs to the activated endothelium in the presence of IFN-γ, TNF-α and thrombin (Section 4.5.2, figure 4.17).

Some previous studies have also shown enhanced RANTES-induced T-cell migration across IFN-γ plus TNF-α activated endothelium (Ding et al, 2000; May & Ager, 1992) and the mechanism is thought to be due to the up-regulation of endothelial adhesion molecules. Endothelial activation also up-regulates the synthesis of E-selectin, P-selectin, VCAM-1 and ICAM-1 (Carlos & Harlan, 1994; Ding et al, 2000; Pober & Cotran, 1990; Springer, 1994), and IL-1 and TNF-α have been reported to induce GAG synthesis in human synovial fibroblast, human cervical fibroblasts and human lung fibroblast cultures. In particular, the up-regulation of hyularonic acid synthesis has been reported (Daireaux *et al*, 1990; Elias *et al*, 1988; Ogawa *et al*, 1998; Yaron *et al*, 1989). It is thought that the up-regulation of GAG synthesis occurs via the activation of NF-kB and induction of cyclo-oxygenase-2 and prostaglandin E2 pathway (Schmitz *et al*, 2003). Therefore it is speculated that endothelial activation may be important for the up-regulation of cell-adhesion molecules and the binding of RANTES to the endothelium. Thus, pro-inflammatory cytokines may play a role in T-cell transendothelial migration.

The cytokines IFN-γ and TNF-α were both present endogenously in the transendothelial migration model, eliminating the need to add them exogenously in order to activate the endothelium. A likely source for these cytokines is synthesis by T-cells, including naïve $CD45RA^+$ T-cells, $CD4^+$ memory Th1 type T-cells and low levels of synthesis by Th2

type T-cells (Barnes, 2008; Conlon et al, 1995; Mosmann & Coffman, 1989; Tsicopoulos et al, 1992). It is also speculated that activated platelets may also release IFN-γ and TNF-α upon degranulation. Although there is no evidence for platelet release of these cytokines, TNF-α has previously been detected in stored platelet concentrates (Muylle *et al*, 1993). In addition, activated human platelets also synthesise and release IL-1β which may play a role in endothelial activation (Denis *et al*, 2005).

Since T-cells have been shown to release RANTES upon activation with the mitogen phytohaemagglutinin (PHA) (Section 4.5.3) (Mire-Sluis *et al*, 1987; Mizel, 1982; Palacios, 1982), in addition to platelet derived RANTES, T-cells may also contribute to RANTES release in the transendothelial migration model. The inability of IFN-γ and TNF-α to induce T-cell RANTES release (Section 4.5.3, figures 4.18-4.20) is likely due to the prior activation of T-cells by PHA. However, there is little previous evidence to suggest that IFN- γ and TNF-α can induce RANTES release by T-cells. A comparison of the relative amounts of RANTES released by IFN-γ and TNF-α stimulated HLMVECs, PHA activated T-cells and thrombin stimulated platelets (not shown) indicated that are all likely to contribute equally to overall RANTES release in the proposed model of transendothelial migration.

Although the intracellular Cu chelator neocuproine and the extracellular Cu chelator bathocuproine both inhibited T-cell transendothelial migration in response to platelet-derived RANTES in a dose-dependent manner, there was no synergistic effect when both were added together, indicating that extracellular chelation is more important for the inhibition of T-cell migration.

Similarly, D-penicillamine and tobramycin also inhibited T-cell migration in response to platelet-derived RANTES in a dose-dependent manner and both had an effect at therapeutic concentrations (6.7 – 13 μM for D-penicillamine for and 4.3 – 21 μM for tobramycin) (British National Formulary, No. 56, September 2008).

D-penicillamine is a metabolite of penicillin. Although it has no antibiotic properties, D-penicillamine is a Cu chelating agent (Section 4.1.5). D-penicillamine is currently used therapeutically for rheumatoid arthritis, cystinuria, autimmune hepatitis, Wilson's disease and emergency treatment of copper and lead poisoning (British National

Formulary, No. 56, September 2008). Although the mechanism of action in the treatment of Wilson's disease and hepatitis remains unknown, it has been suggested that the Cu-binding properties of D-penicillamine may increase urinary Cu excretion, preventing hepatic Cu accumulation (Klein *et al*, 2000; McQuaid *et al*, 1992; Togashi *et al*, 1992). Several mechanisms have also been suggested for the anti-inflammatory action of D-penicillamine in rheumatoid arthritis. It has again been proposed that D-penicillamine increases the urinary excretion of Cu (McQuaid *et al*, 1992) and it has also been suggested that D-penicillamine inhibits macrophage-derived IL-1 and collagen-inhibiting factors with a subsequent increase in synovial collagen synthesis (Brisset et al, 1986). It is also thought that the thiol group may be a key structural feature of this drug (Wood et al, 2008). In the treatment of rheumatoid arthritis, D-penicillamine may act by directly sequestering reactive aldehydes released by inflammatory cells and also by restoring intracellular thiol pools that can also act to sequester aldehydes, which damage collagen and cartilage and ultimately result in joint deterioration.

Tobramycin is an aminoglycaside antibiotic used to treat bacterial infections (Section 4.1.5). Tobramycin is preferred over gentamicin for *Pseudomonas aeruginosa* pneumonia due to better lung penetration and bactericidal activity (Vakulenko & Mobashery, 2003) and is currently used as an inhaled antibiotic for the treatment of *Pseudomonas aeruginosa* infection in cystic fibrosis (CF) patients and also for the treatment of local infection in the eye (British National Formulary, No. 56, September 2008).

The finding that tobramycin inhibits T-cell transendothelial migration indicates that tobramycin may have potential both as an indirect (antibiotic) and direct (non-antibiotic) anti-inflammatory agent. In addition, the aminoglycoside vancomycin may also have potential to inhibit T-cell transendothelial migration, since vancomycin has been shown to be a highly effective copper chelator (Swiatek *et al*, 2005). This could be confirmed by using this drug in further transmigration experiments.

It was expected that treatment with copper chelators would inhibit RANTES production through the inhibition of the NF-kB pathway and possibly also via the inhibition of Cu/redox, and alter the form of RANTES presented on the endothelial cell surface

through interference with the Cu-redox mechanisms that have been shown to mediate RANTES multimer formation (Chapters 2 and 3). However, RANTES concentrations were not altered as a result of Cu chelation. Cu chelation also did not induce any alteration in the multimeric form of RANTES or increase plasmin activity which indicates that Cu chelators did not induce syndecan shedding as a mechanism for the inhibition of T-cell migration. Although Cu chelation did not alter the form of RANTES detected in HLMVEC lysates, this was only associated with overnight treatment of the endothelial cells, which would likely only affect the form of newly synthesised RANTES and not RANTES multimers that had already formed and bound to the endothelial cell surface prior to treatment with Cu chelators. Since Cu has been shown to induce RANTES multimerisation via the formation of dityrosine cross-links (Chapters 2 and 3), it is possible that Cu chelation may still have a long-term effect, preventing RANTES multimerisation to the tetramer which is the predominant and active form of RANTES detected in HLMVEC lysates. This effect may occur in addition to the short-term inhibitory effect on T-cell transendothelial migration seen in this chapter, suggesting further work which would involve the incubation of HLMVECs with Cu chelators in longer term experiments.

The PAI-1 inhibitor, XR5118 inhibited T-cell migration in response to platelet-derived RANTES a dose-dependent manner, and this was associated with an increase in soluble tetrameric RANTES and an increase in plasmin activity confirming that the anti-inflammatory action of XR5118 occurs through the inhibition of PAI-1. The inhibition of PAI-1 by the neutralising antibody MAI-12 has previously been shown to induce syndecan shedding in HUVECs with an associated increase in soluble HSPG-bound IL-8 (Marshall *et al*, 2003). It therefore follows that treatment with XR5118 induces syndecan shedding as a consequence of PAI-1 inhibition resulting in reduced RANTES presentation to T-cells and reduced T-cell migration.

In addition, the enzyme catalase also inhibited T-cell migration in response to platelet-derived RANTES, suggesting the involvement of H_2O_2 in T-cell migration, in addition to the involvement of Cu. H_2O_2 is produced by the endothelium and as a known second messenger, can upregulate endothelial E- and P-selectin, VCAM-1, ICAM-1, TNF-α and chemokine expression via NF-kB (discussed later), which may explain the inhibition of T-cell migration upon treatment of HLMVECs with catalase. However,

treatment with catalase induced a significant increase in LDH release, although 100 % Trypan blue exclusion of platelets, T-cells and HLMVECs indicated that these cells were still viable.

However, by way of explanation of the conflicting results, the enzyme LDH is known to be sensitive to Cu-mediated inactivation (Pamp *et al*, 2005). Cu is associated with many oxidation processes. The ability of Cu to exchange between stable oxidised Cu (II) and unstable, reduced Cu (I) states is used by cuproenzymes involved in redox reactions, e.g. Cu/Zn superoxide dismutase or cytochrome oxidase (Camakaris *et al*, 1999). However, the Cu (II) to Cu (I) or vice versa transitions also results in the generation of reactive oxygen species (ROS) and oxidative stress (Halliwell & Gutteridge, 1988).

Multivalent metal ions are fundamental to redox chemistry as they facilitate electron transfers during the redox process (Smith *et al*, 2007). The oxidised form, Cu (II), in the presence of a reducing agent, such as ascorbate, is reduced to Cu (I) which subsequently catalyses the generation of reactive oxygen species (ROS). Cu (I) reductively activates H_2O_2 to form OH radicals in a mechanism analogous to the metal-driven Haber Weiss reaction, or Fenton reaction (Zhu *et al*, 2002). In addition to OH radicals, the other ROS generated in the presence of Cu ions are: $\cdot O_2^-$ $\cdot RO_2$ and $\cdot ONOO^-$ (peroxynitrite formed by the reaction of $NO\cdot$ (nitric oxide) with O_2-. H_2O_2 can be generated by the free radical scavenger superoxide dismutase in the following reaction:

$$O_2 + 2H_2O \longrightarrow 2H_2O_2$$

Cu (I) reductively activates H_2O_2 to form OH radicals

$$H_2O_2 + Cu^+ \longrightarrow Cu^{2+} + OH^- + OH\cdot$$

Consequently a paradoxical situation arises where reducing agents, such as ascorbate can amplify oxidative damage in the presence of Cu (I) (Balogh *et al*, 2003). Thus, free radicals generated in the presence of Cu ions can result in lipid, DNA and protein peroxidation. It is therefore possible that free radicals may play a role in Cu-mediated inactivation of LDH. Catalase scavenges H_2O_2 and will therefore be expected to

influence redox cycling. If free radicals are removed it may be possible that LDH inactivation is reversed, resulting in increased LDH activity. This may be a mechanism whereby treatment with catalase could result in increased LDH activity through H_2O_2 scavenging.

The overnight treatment of HLMVECs with Cu chelators or XR5118 did not cause toxicity to endothelial cells as confirmed by lactate dehydrogenase (LDH) assay, indicating that cytotoxicity was not the cause of reduced T-cell migration upon treatment with Cu chelators. Therefore, VAP-1, a Cu-dependent membrane bound enzyme that can influence leukocyte transendothelial migration was investigated as a mechanism for the inhibitory effects of Cu chelators. VAP-1 acts as a traditional adhesion molecule through the binding of sialic acid residues to a leukocyte-expressed lectin and also oxidatively deaminates leukocyte surface primary amines via its semicarbazide-sensitive amine oxidase activity with a resulting transient covalent bond that is thought to influence leukocyte-endothelial binding during leukocyte rolling with important end products including H_2O_2, aldehyde and ammonium which may regulate NF-kB and the adhesive properties of endothelial cells including the upregulation of P- and E-selectin (reviewed in Section 4.1.4).

However, failure to detect HLMVEC VAP-1 activity indicates that this enzyme is either not present or expressed at levels beyond the detection limit of the assay, despite reports that VAP-1 is expressed in the endothelium of large and mid-sized pulmonary vessels of normal human lungs (Singh *et al*, 2003) and that VAP-1 SSAO-mediated deamination is involved in the recruitment of leukocytes during lipopolysachharide-induced pulmonary inflammation in transgenic mice that overexpress VAP-1 (Yu *et al*, 2006). Some reports have shown that VAP-1 is only up-regulated in response to inflammation (Jaakkola *et al*, 2000; Merinen *et al*, 2005) but the activation of HLMVECs with IFN-γ and TNF-α did not appear to induce VAP-1 expression.

VAP-1 has so far only been detectable intracellularly in the cytoplasm of cultured HUVECs, and it has been reported that cultured endothelial cells including HUVECs lack detectable surface VAP-1. VAP-1 in HUVECs was not translocated onto the endothelial cell surface after stimulation with multiple cytokines including IFN-γ and TNF-α, mitogens or secretagogues which induced expression of other known

endothelial adhesion molecules including ICAM-1, E-selectin, and VCAM-1 (Arvilommi *et al*, 1997; Salmi & Jalkanen, 1995). VAP-1 detected in HUVECs also lacks several types of common post-translational modifications such as sialic acids in contrast to naturally occurring VAP-1 in HEV, which may preclude its surface expression in cultured endothelial cells and also render VAP-1 functionally inactive. The authors of these studies have suggested that populations of cultured primary endothelial cell types commonly used as a model in studying lymphocyte-endothelial cell interactions lack surface expression of VAP-1 compared to peripheral lymph node-type high endothelial venules (HEV), and hence are inherently of limited use in analyses of lymphocyte transendothelial migration (Salmi & Jalkanen, 1995).

It may be possible to detect HLMVEC-expressed VAP-1 using a more sensitive radiochemical method, such as that used by Yu, *et* al., 2006, to detect VAP-1 SSAO activity in lung tissue from transgenic mice. The method involves the use of ^{14}C-labelled benzylamine or methylamine as the substrate with the use of chlorgyline and deprenyl to block MAO activity. The enzyme reaction was terminated with citric acid and the oxidised products were extracted and quantified using a liquid scintillation counter. SSAO activity was detected as low as 0.1 nMol/min/mg protein using this method.

Endothelial cells are known to produce H_2O_2 which is involved in redox cycling and the subsequent generation of ROS as described. A possible mechanism for the anti-inflammatory effects of copper chelators on T-cell transendothelial migration is via the inhibition of Cu-redox mechanisms resulting in impaired redox cycling and lowered levels of ROS. ROS are known to act as second messengers, upregulating gene expression in the vasculature, via NF-kB including the expression of VCAM-1 (Kunsch & Medford, 1999), ICAM-1 (Cheng *et al*, 1998), TNF-α (Valen *et al*, 1999), E- and P-selectin (Jalkanen *et al*, 2007) and chemokines (Chen *et al*, 2004; Lakshminarayanan *et al*, 1997) and consequently may play an important role in endothelial activation, cytokine and chemokine production and adhesion molecule upregulation.

Therefore, it is postulated that Cu chelators may exert their anti-inflammatory effects via the impairment of redox cycling and subsequent inhibition of gene expression for important vascular adhesion molecules, cytokines and chemokines. In support of this

notion, the impairment of leukocyte-endothelial adhesion has been reported in the muscle microcirculation of the copper-deficient rat (Schuschke *et al*, 2001) and in addition, copper-deficiency has been reported to attenuate endothelial cell Ca^{2+} mobilisation (Schuschke *et al*, 2000) and suppress the expression of cell surface molecules in human promonocytic cells and neutrophils (Huang & Failla, 2000; Karimbakas *et al*, 1998). Furthermore, the anti-inflammatory effects of the drug enoxaparin (EP) were shown to occur via its antioxidant potential (Manduteanu *et al*, 2007). It was demonstrated that in cultured endothelial cells exposed to non-toxic levels of H_2O_2, treatment with EP reduced monocyte adhesion, ICAM-1 and P-selectin expression, decreased the nuclear levels of c-Jun and p65 proteins, and diminished the phosphorylation of c-Jun protein, MAPK p38 and JNK. Thus the report demonstrates impaired leukocyte adhesion with the reduced expression of adhesion molecules via the MAPK (both p38 and JNK) / NF-kB pathway in response to antioxidant therapy. In addition, it has been shown that D-penicillamine has anti-oxidative properties, preventing hyaluronan degradation induced by Cu/redox ROS generation (Valachova *et al*, 2008). The anti-oxidative effects of D-penicillamine are likely dependent on its ability to impair redox cycling and may also be dependent on its ability to bind Cu, indicating that other Cu-binding drugs may also have anti-oxidative potential.

Since enoxaparin is a low molecular weight heparin, other GAGs may also have anti-oxidant potential, as demonstrated by the increases in lipid peroxidation and post-translational proteolytic modification of RANTES upon treatment with sodium chlorate, which inhibits GAG synthesis, and the protective effects of HS against the degradation of chemokine multimers (Chapters 2 and 3). As discussed, the protective effects of GAGs against lipid peroxidation and oxidative damage have also been reported in liposome and fibroblast cultures (reviewed in Section 2.6).

Chapter 5

General Discussion

5. General Discussion

This thesis provides evidence that Cu has *pro*-inflammatory effects and that Cu chelators have anti-inflammatory properties that indicate their therapeutic potential. However, the use of copper *per se* as a therapeutic agent is well documented and probably dates to the beginning of recorded history and even earlier as a folk remedy for arthritis. The use of Cu by transdermal delivery in the form of the metal from Cu bracelets has been a time-honoured practice since antiquity, when it was recognised for its *anti*-inflammatory activity. The potential for the use of Cu as an *anti*-inflammatory agent remains subject to controversy, because scientific studies designed to demonstrate therapeutic benefits for arthritic conditions through dermal contact with metallic Cu or its compounds have been inadequate.

Interestingly, raised Cu levels and mildly acidic conditions are common during inflammation and raised Cu serum levels that correlate with disease activity have been reported in particular in patients with rheumatoid arthritis (Strecker, 2005)(reviewed in Section 1.20). Furthermore, both acute and chronic inflammation have been characterised by a significant increase in total serum Cu, which can be regarded as a factor capable of worsening pathological processes, including oxidative stress (Milanino & Buchner, 2006).

Many studies have extensively claimed that there is little benefit from the use of Cu bracelets in the therapy of rheumatoid arthritis (Camara & Danao-Camara, 1999; Herman *et al*, 2004; Kestin *et al*, 1985; Rao *et al*, 2003; Rao *et al*, 1999; Struthers *et al*, 1983). However, several studies reported a significantly greater number of the patients who stated that their condition improved while wearing a Cu bracelet compared to wearing an aluminium bracelet. The effect was attributed to the supply of a steady supplemental amount of Cu from the bracelets. Cu bracelets were reported to have lost an average of 13 mg in a month of use and the lost Cu was assumed to have dissolved into the wearers' sweat and then to have been absorbed into their skin (Bratton *et al*, 2002; Walker *et al*, 1981; Walker & Keats, 1976).

It has been discovered that upon contact with skin, and in the presence of O_2 and H_2O, Cu metal oxidises and dissolves in sweat. Subsequent laboratory experiments showed that Cu bracelets could slowly release Cu ions that form complexes with amino acids

and fatty acids, which will permeate both the surrounding skin and eventually also the body (Walker & Griffin, 1976; Walker & Keats, 1976; Walker & Reeves, 1977). In samples of artificial sweat where initial copper concentration was of the order of 2 x 10^{-5} M, after 24 hours of incubation with Cu turnings the samples turned blue and the concentration had increased to 2 x 10^{-3}M Cu. However, quantitative data for percutaneous penetration of the metal's putative oxidation products, which may be generated in contact with skin in humans, is not available, and because no beneficial effect could be statistically documented for skin contact with Cu devices, the mechanism of action of Cu bracelets in rheumatoid arthritis, if it occurs at all, is still poorly understood.

Cu is an essential trace element, present in the mammalian organism only in minimal concentration as free ionic Cu (10^{-18} M, with a range between 10^{-11} and 10^{-19} M) and is predominantly complexed with proteins and amino acids (reviewed in Hostynek & Maibach, 2006). Some studies have reported anti-inflammatory activity upon the parenteral administration of Cu-complexes in carrageenin rat paw oedema models including several tetrachlorocuprate (II) complexes (Jimenez-Hernandez *et al*, 1995), and salicylic acid Cu complexes (Beveridge *et al*, 1980; Beveridge *et al*, 1982; Walker *et al*, 1980). In addition, Cu complexes of anti-arthritic drugs, including salicylic acid, acetylsalicylic acid, penicillamine, and several corticoids, were found to be more active than the parent drugs. A comparison of Cu, gold, and silver thiomalate and thiosulfate complexes in models of inflammation revealed that the Cu complexes were effective, while the gold and silver complexes were virtually inactive (Aaseth *et al*, 1998). As a general rule, Cu complexes are less toxic and suppress the ulcerogenic effect of many of the ligand drugs themselves. The modern use of Cu complexes to treat arthritis dates from the 1940s, and the theory that Cu complexes of nonsteroidal anti-inflammatory drugs are more active and less toxic than the parent compounds is supported by a substantial body of literature (Hostynek & Maibach, 2006).

Based on this evidence, compounds that have subsequently been investigated include Cu complexes of well-known antiarthritic drugs, including steroidal and nonsteroidal anti-inflammatory drugs niflumic acid, D-penicillamine, hydrocortisone, dexamethasone, dimethylsulfoxide, clopirac, ketoprofen, naproxen, indomethacin. mefenamic acid, diclofenaca and ibuprofen among a number of others. All the Cu

complexes of those drugs have been found to be active or more effective anti-inflammatory agents than the parent drug (Hostynek & Maibach, 2006).

The anti-inflammatory activity of Cu-complexes has been attributed to superoxide dismutase (SOD) activity exhibited by these compounds (Santini *et al*, 2003), resulting in the dismutation of the superoxide anion (O_2^-) to the less potent H_2O_2 and O_2. Catalase or glutathione peroxidise can then decompose H_2O_2 into H_2O and O_2 (Rahman *et al*, 2006). The superoxide dismutase activity of Cu-complexes occurs due the ability of Cu to participate in electron transfer reactions. Cu can accept and donate single electrons as it changes valency between the reduced Cu (I) and oxidised Cu (II) states, assisting in the catalysis of oxidation-reduction reactions involving oxygen radicals (Leary & Winge, 2007; Osterberg, 1980). This is used by cuproenzymes involved in redox reactions such as CuZnSOD and cytochrome *c* oxidase (Camakaris *et al*, 1999). Reports have shown that Cu-complexes have a potent inhibitory effect on the production of superoxide anions in serum and in tumor cell lines *in vitro* (Huber *et al*, 1987; Saczewski *et al*, 2007; Weser & Schubotz, 1981). These inhibitory effects could explain, at least in part, the anti-inflammatory activity of Cu-complexes (Frechilla *et al*, 1990a; Frechilla *et al*, 1990b), since oxidative stress can determine alterations at the cellular level via oxidant-induced activation of signalling pathways.

Reactive oxygen species (ROS), either directly or via the formation of lipid peroxidation products such as acrolein, 4-hydroxy-2-nonenal and F(2)-isoprostanes, may play a role in enhancing inflammation through the activation of stress kinases (JNK, MAPK, p38, phosphoinositide 3 (PI-3)-kinase/PI-3K-activated serine-threonine kinase Akt) and redox sensitive transcription factors such as NF-kB and AP-1 (Rahman, 2002)(reviewed in Sections 4.1.3 and 4.6). Oxidative stress also causes disruption of membrane lipids and cellular destruction as a result of lipid peroxidation induced by ROS. The end products of lipid peroxidation can also activate p44/42 (ERK 1/2) and c-Jun MAPK pathways (Ciencewicki *et al*, 2008). In addition, oxidative stress can lead to rises in intracellular calcium ions, cytoskeleton disruption and DNA damage (Halliwell, 1991). Recent data have also indicated that oxidative stress and pro-inflammatory mediators can alter nuclear histone acetylation/deacetylation allowing access for transcription factor binding to DNA, leading to enhanced pro-inflammatory gene expression in various lung cells (Rahman, 2002).

Oxidative stress is associated with a host of inflammatory diseases, particularly those associated with the lung (Ciencewicki *et al*, 2008). This is because of all the organs in the human body, the lungs are by far the most susceptible to attack by free radicals due to the highest exposure to oxygen and oxidants in inhaled air, and large surface area and blood supply to the lungs. Homeostasis of the oxidation/reduction (redox) state is imperative for cell viability, activation, proliferation and survival, all of which are necessary for the proper functioning of all organs (Rahman *et al*, 2006). The lungs defend against oxidative challenge with efficient antioxidant defenses such as glutathione (GSH), albumin, uric acid, vitamins C and E, SOD and catalase (Mak & Chan-Yeung, 2006). However, during inflammation, infiltrated phagocytic cells including neutrophils, eosinophils and macrophages release large amounts of ROS (Kinnula *et al*, 1995) and there is evidence that as well as inflammatory cells, non-inflammatory cells including the alveolar and bronchial epithelium and the endothelium release ROS (Folkerts *et al*, 2001; Holland *et al*, 1990; Kinnula *et al*, 1992a; Kinnula *et al*, 1992b). An imbalance of the redox system in the lungs leads to lung tissue damage and fibrosis. Oxidative stress has been increasingly recognised as one of the major factors contributing to the chronic inflammatory process in the lungs (Mak, 2008) and is well known to contribute to the inflammatory response in pulmonary hypertension (Bowers *et al*, 2004), cystic fibrosis (CF) (Brown *et al*, 1996; Reid *et al*, 2007), asthma (Mak & Chan-Yeung, 2006), adult respiratory distress syndrome (ARDS) (Cross *et al*, 1990) and chronic obstructive pulmonarty disease (COPD) (Psarras *et al*, 2005).

Antioxidant therapy using a novel antioxidant rich formulation for oral administration containing beta-carotene (30 mg), tocopherols (vitamin E) including alpha-tocopherol (200 IU) and gamma-tocopherol (94 mg) and other tocopherols (31 mg), coenzyme Q10 (CoQ10) (30 mg) vitamin D3 400 IU and vitamin K1 (300 mg) has been shown to reduce airway inflammation in CF (Papas et al, 2008) and antioxidant thiol molecules, polyphenol salts erdosteine and carbocysteine lysine salt have been reported to reduce inflammation in COPD (Rahman, 2006). It has also been suggested that antioxidant therapy may be useful in the treatment of asthma (Garcia-Larsen et al, 2009; Nadeem et al, 2008; Riccioni et al, 2007).

As well as increased oxidative stress, raised Cu levels have also been reported in many disease states including rheumatoid and osteoarthritis, cancer and angiogenesis, cardiovascular disease, Alzheimer's disease, chronic wounds, vasculitis and chronic hepatitis (reviewed in Section 1.20). Raised Cu levels induce pulmonary inflammation and many inflammatory diseases of the lung are associated with raised Cu status including COPD, CF, ARDS and asthma (Karadag *et al*, 2004; Percival *et al*, 1999; Rice *et al*, 2001).

The evidence suggests that especially in the lung, inflammation is exacerbated by oxidative stress, and that Cu may also contribute to oxidative stress in these diseases due to its well documented role in redox reactions resulting in ROS generation (Section 2.6). This evidence leads to the suggestion that Cu-binding compounds may be of therapeutic value in the treatment of pulmonary inflammation including COPD, CF, ARDS and asthma, both through the removal of Cu, preventing its involvement in redox cycling and ROS generation leading to suppressed NF-kB activation and also by acting directly as an antioxidant via superoxide dismutase activity. In support of this notion, Cu-complexes have been shown to exhibit anti-inflammatory activity which has been attributed to the SOD activity of these Cu-binding compounds. In addition, Cu-binding drugs that also have antibiotic activity may prove even more effective, such as gentamycin, tobramycin or vancomycin.

Wilson's disease, an inherited disease of Cu toxicity has been the driving force in the development of anti-copper drugs. The genetic defect is caused by a mutation or deletion of the gene, ATP7B, encoding a P-type ATPase of 1411 amino acids. ATP7B is essential for Cu transport and elimination of Cu from the body (Bull *et al*, 1993). Wilson's disease is characterised by low ceruloplasmin concentrations in blood and a marked increase in the Cu contents of the liver and brain (Brewer & Yuzbasiyan-Gurkan, 1992). Absorbed Cu is brought to the liver by the Cu transporters albumin and transcuprein (reviewed in Section 1.18). Following uptake by the hepatocyte, a portion of the Cu is normally incorporated into ceruloplasmin and another portion is excreted in the bile. A third portion is incorporated into Cu-dependent intracellular enzymes such as CuZnSOD and cytochrome oxidase. In the liver of patients with Wilson disease the process of Cu incorporation into ceruloplasmin appears to be impaired, as is excretion of Cu into the bile.

Because the Cu cannot enter the bile nor participate in ceruloplasmin synthesis, the result is an accumulation of Cu by the liver. Prolonged accumulation of Cu in liver cells results in cirrhosis and subsequent deposition of excess Cu in extra-hepatic tissues as well as brain damage as a result of Cu accumulation in the brain (Linder & Hazegh-Azam, 1996). The accumulation results in neurologic symptoms of tremors, spasticity. rigidity and chorea, dystonia, unsteady gait and psychosis (Cui *et al*, 2005). The disease is very treatable with Cu-binding drugs with excellent clinical results (Brewer, 2008).

D-penicillamine was the first drug developed for oral administration in Wilson's disease. The Cu chelator induces the excretion of a large amount of Cu in the urine (Walshe, 1956). Although highly effective, D-penicillamine has a long list of side effects including the worsening of neurological symptoms in newly diagnosed patients and many patients who worsen never recover (Brewer, 2008). The second drug developed was trientine (Walshe, 1982), another Cu chelator that increases the urinary excretion of Cu. Although trientine causes fewer side effects than D-penicillamine, it shares the propensity to cause worsening of neuralgia.

Zinc was developed as the third treatment option (Brewer *et al*, 1998), and this treatment has very few side effects. Zinc acts by inducing intestinal cell metallothionein which then binds Cu from food and endogenous secretions and holds the Cu in the intestinal tract. The fourth drug which is not yet in the market is tetrathiomolybdate (TMB). This drug has been shown in clinical trials to be excellent for the stabilistation of neurologic status and preventing worsening. It acts by forming a tripartite complex with Cu and protein that is very tight. Taken with food, the drug complexes with food protein and endogenously secreted Cu and preventing its absorption. Taken without food, TMB is absorbed and binds free Cu and albumin so that the Cu is no longer available for cellular uptake. The TMB complex is metabolised by the liver, and excreted into the urine (Brewer, 2008).

Cu-binding drugs are also used in the treatment of rheumatoid arthritis. Rheumatoid arthritis is a chronic destructive inflammatory joint disease, characterised by massive synovial proliferation and subintimal infiltration of inflammatory cells, which along with angiogenesis leads to the formation of a very aggressive tissue called pannus

(Feldmann *et al*, 1996; Koch, 1998). Expansion of the pannus induces bone erosion and cartilage thinning leading to the loss of joint function. Rheumatoid arthritis is characterised by increased production of inflammatory cytokines including TNF-α, IL-1-α and IL-1-β (Feldmann *et al*, 1996) as well as raised serum Cu (Honkanen *et al*, 1991) which may correlate with the increased cytokine production seen in rheumatoid arthritis patients (Zoli *et al*, 1998).

D-penicillamine has been used in the therapy of rheumatoid arthritis for many years but the mechanism of the effect of D-penicillamine is still unknown, although it is thought that D-penicillamine may induce the excretion of endogenous Cu in the urine (McQuaid *et al*, 1992). However, TMB is much more effective in inducing Cu excretion into the urine than D-penicillamine and has also proved effective in suppressing adjuvant-induced arthritis and inflammation-associated cachexia in rats (Omoto *et al*, 2005), suggesting that the two drugs may have a similar mechanism of action that in part involves increasing the urinary excretion of Cu. As described above, the mechanism of these Cu-binding drugs likely also involves the inhibition of redox cycling and ROS generation. NF-kB can be activated directly by Cu but can also be activated by ROS that are generated by Cu-redox mechanisms. This indicates both a direct and indirect mechanism for the inhibition of Cu-induced NF-kB activation by Cu-binding drugs, leading to suppressed inflammatory cytokine production since NF-kB is the master regulator of many proinflammatory cytokines. This effect could occur in addition to the superoxide dismutase activity exhibited by Cu-complexes.

It is likely that neocuproine, bathocuproine, D-penicillamine and tobramycin inhibit T-cell recruitment in response to platelet-derived RANTES in the transendothelial migration model via the binding and removal of free Cu, since all four of these compounds were effective in inhibiting T-cell recruitment (Chapter 4) and in this Chapter, one common property of all these compounds is their ability to bind Cu. As discussed here and in Section 4.6, the anti-inflammatory mechanism is likely due to the antioxidant potential of Cu-binding compounds with the subsequent impairment of redox cycling which may result in the inhibition of gene expression for important vascular adhesion molecules, cytokines and chemokines.

Beyond the treatment of Wilson's disease and rheumatoid arthritis, as discussed, Cu-binding compounds may prove useful for the treatment of pulmonary inflammatory diseases via the lowering of oxidative stress which occurs in particular in the lungs, and this may also result in suppressed leukocyte recruitment. Cu-binding compounds may prove useful in the treatment of COPD, CF, ARDS, asthma, and pulmonary fibrosis, but could also be beneficial in the treatment of cancer and angiogenesis, prion disease and Alzheimer's disease (reviewed in Section 1.22) (Squitti *et al*, 2005). The pathogenesis of these diseases may be dependent on the availability of free Cu and could be inhibited by lowering levels of free Cu.

Cu has been shown to play a role in Aβ-peptide aggregation and plaque formation in the pathophysiology of Alzheimer's disease (reviewed in Section 1.21), suggesting that a therapy aimed at lowering free Cu levels in Alzheimer's disease might be beneficial to patients. Cu chelators are effective in solubilising brain Aβ (Cherny et al, 2000) and in addition, the metal chelation of Cu with clioquinol markedly inhibits Aβ aggregation in Alzheimer's disease transgenic mice (Cherny et al, 2001). However, during clinical trials, although clioquinol has been shown to steady the cognitive ability of patients with Alzheimer's disease, the drug was also associated with serious neurologic side effects known as subacute myelo-optic neuropathy (SMON), the symptoms of which included numbness, pain and intestinal distress, paralysis and blindness. Clinical trials are on-going in order to assess the therapeutic potential of clioquinol, since it is thought that the toxic effects of clioquinol may have been due to the formation of a toxic biproduct during the manufacture of clioquinol (Cahoon, 2009). It has also been found that Cu chelation delays the onset of prion disease in mice (Sigurdsson et al, 2003) (reviewed in Section 1.22).

In phase I/II trials, TMB has also been shown to be effective in idiopathic pulmonary fibrosis patients (Flaherty *et al*, 2007) and TMB also inhibits liver and heart inflammation in mouse models via the inhibition of TNF-α, IL-1β and IL-2 expression (Hou *et al*, 2005; Ma, 2004). The growth of cancers involves angiogenesis and the development of a blood supply for the growing tumor. Angiogenesis is stimulated by many cytokines and the upregulation and activity of these cytokines is dependent on Cu. Preclinical studies have strongly indicated that TMB inhibits angiogenesis in mouse models, including squamous carcinoma, mammary cancer. head and neck cancer

models and TMB also showed efficacy in a study of advanced cancers in pet dogs (reviewed in Brewer, 2008). It has been asserted that the anti-angiogenic action of TMB occurs via the inhibition of Cu-dependent effects on NF-kB activity (Khan & Merajver, 2009; Pan *et al*, 2003; Pan *et al*, 2002).

However, it is important to consider the side effects of Cu-binding drugs when evaluating their potential for the treatment of diseases where Cu-lowering therapy may be beneficial. Of all the Cu-binding drugs discussed so far, D-penicillamine has the highest risk with regard to side effects and toxicity. As discussed, D-penicillamine has in particular been associated with side effects neurological symptoms, but it has also been associated with reduced platelet count, proteinuria associated with immune complex nephritis, nausea, loss of taste and rash outbreak (British National Formulary, No. 56, September 2008) (Dubois *et al*, 1998; Magnus *et al*, 1987).

The aminoglycoside antibiotics including kanamycin, gentamycin and tobramycin are associated with vestibular and auditory damage, nephrotoxicity, antibiotic-associated colitis, stomatitis, nausea, vomiting, rash and muscular weakness (British National Formulary, No. 56, September 2008) and the aminoglycosides are also not absorbed via oral administration and therefore must be administered intravenously to achieve effective serum concentrations. In addition, the aminoglycosides do not readily cross the blood-brain barrier and therefore are unlikely to be of use in the treatment of Alzheimer's disease (Bruckner *et al*, 1981; Moellering *et al*, 1981).

However, so far clinical trials have shown that orally administered TMB is effective in the treatment of Wilson's disease (Brewer *et al*, 2006; Brewer *et al*, 2003; Brewer *et al*, 1996), rheumatoid arthritis (Omoto *et al*, 2005) and also has antiangiogenic effects in malignant pleural mesothelioma patients after resection of gross disease (Pass *et al*, 2008), patients with advanced kidney cancer (Redman *et al*, 2003) and patients with hormone-refractory prostate cancer (Henry *et al*, 2006). The trials have shown that TMB exhibits minimal toxicity. Side effects included anaemia, neutropaenia, leukopaenia and transaminase elevations but these side effects were generally resolved with either a dose adjustment or temporary suspension of the dosing regimen (Medici & Sturniolo, 2008). The evidence indicates that TMB has greater potential for use as an

anti-inflammatory agent than some of the Cu-binding drugs used in the past since it can be administered orally and is highly effective with minimal toxicity risks.

It is also important to consider the effective targeting of Cu-binding drugs to the site of inflammation. Whilst systemic administration of Cu-binding drugs via the oral or intravenous route is effective in the treatment of Wilson's disease and some cancers, local inflammation may be more difficult to target. As discussed, the lung could be an important target for Cu-lowering therapy since many of the inflammatory diseases of the lung are associated with raised Cu and the infiltration of phagocytes, both of which contribute to oxidative stress and exacerbate inflammation. In order to target the lung, it may be more beneficial to use an inhaled formulation which would directly target the bronchial airways and alveolar spaces, the sites at which excessive inflammation can be life threatening. Previous studies have reported that a formulation of aerosolised tobramycin is effective in the treatment of CF and *Pseudomonas aeruginosa* infection, significantly improving pulmonary function, and the inhaled formulation was well tolerated by patients (Chuchalin *et al*, 2007). Aerosolised antibiotics including tobramycin, gentamycin, neomycin, amikacin, aztreonam, colistin, carbenicillin, amphoteracin, ticarcillin and ceftazidime have also been used for non-cystic fibrosis bronchiectasis which has been shown to decrease sputum bacterial density (Rubin, 2008).

However, this route of administration of Cu-binding drugs may result in toxic side effects that could occur upon the removal of Cu as an essential cofactor for many proteins and enzymes, including the intracellular proteins cytochrome *c* oxidase and CuZnSOD and the extracellular proteins ceruloplasmin, lysyl oxidase, transcuprein and amine oxidases (Linder & Hazegh-Azam, 1996). Cytochrome *c* oxidase is the terminal enzyme of the electron transport chain in mitochondria and the site where oxygen is utilised in respiration, catalysing the reduction of O_2 to $2H_2O_2$. CuZnSOD is important for the dismutation of superoxide anions and therefore the loss of the SOD activity of this enzyme would likely affect oxidative stress levels and exacerbate inflammation. Ceruloplasmin is also a Cu-dependent ROS scavenger, protecting against oxidative damage. As with CuZnSOD, loss of this scavenging activity would also result in increased oxidative stress, which could exacerbate inflammation. Inhibition of ceruloplasmin would also have detrimental effects on the transport of essential Cu from

the liver to other tissues. However it is likely that the activity of these anti-oxidative enzymes would be replaced with the anti-oxidative Cu-antibiotic complex.

Lysyl oxidase is another Cu-dependent enzyme critical for the formation and function of connective tissue throughout the body. Its function is to catalyse cross-linking of newly formed collagen and tropoelastin fibres through the oxidative deamination of lysine side chains on these proteins. Cu deficiency leads to a lack of collagen maturation and defective sheathing of blood vessels by elastic fibres, which can result in aneurisms (reviewed in Linder and Hazegh-Azam, 1996).

It was shown that Cu induces the multimerisation of isolated recombinant RANTES, IL-8 and ENA-78 (Chapter 2) and RANTES multimerisation was shown to occur via the formation of Cu-induced dityrosine cross-links (Chapter 3). Although Cu chelation had no effect on the multimerisation of RANTES *in vitro*, as discussed in Section 4.6, RANTES may already have formed tetramers during culture prior to the addition of the Cu chelators for 24 hours. The treatment of HLMVECs with Cu chelators in longer term experiments may prevent the formation of tetramers prior to transendothelial migration assays. The tetrameric form was predominant form of RANTES bound to the endothelium and was found to be highly stable (Chapter 4). This highly stable form of RANTES may be important *in vivo* under shear flow conditions and it is possible that Cu may be important *in vivo* for the formation of the tetramer and retention of RANTES on the endothelium during inflammation, and perhaps also other chemokines such as IL-8 and ENA-78 which also multimerise in the presence of Cu (Chapter 2). Therefore, although it has not yet been demonstrated *in vitro*, it is possible that Cu chelation may reduce the retention and presentation of chemokines on the endothelium *in vivo* under flow conditions in the bloodstream. The presentation of chemokines on the endothelium not only directs leukocyte recruitment but also induces the firm adhesion of leukocytes to the endothelium prior to transcytosis and migration to the site of inflammation (reviewed in Section 1.1). Therefore Cu chelation may be a useful strategy to target the accumulation of leukocytes as an essential response during inflammation.

The endothelium controls the selectivity of invasive processes via its phenotype and its physiological or pathological state. Thus endothelial cells select populations of circulating cells via a multi-step process leading to leukocyte recruitment. The

specificity is regulated by the arrangement of cytokines, chemokines and adhesion molecules that guide circulating leukocytes to specific locations. The presentation of chemokines via GAGs on the endothelial cell surface plays an essential role in the selective regulation of leukocyte homing by attracting circulating cells via a gradient and activating integrins upon binding to specific GPCRs on leukocytes (reviewed in Section 1.1).

The profile of chemokine expression varies between different endothelial types. As the focus of this thesis, RANTES is implicated in many diseases of the lung (reviewed in sections 1.5 and 1.16), but since RANTES presentation on the endothelium occurs predominantly via HSPGs (Hillyer & Male, 2005) and HSPGs are ubiquitously expressed, it is not surprising that RANTES expression has been reported in many endothelial types. RANTES binds strongly to several endothelia including human lung and dermal microvascular endothelium, saphenous and umbilical vein endothelium, appendix endothelium, brain endothelium, skin endothelium, bone marrow endothelium and mesenteric lymph node endothelium (Crola Da Silva *et al*, 2009; Hillyer & Male, 2005). As a chemokine involved in T-cell recruitment, it is most likely that RANTES is involved ubiquitously in inflammation, as an important chemotactic signal in the adaptive immune response.

Binding sites for several chemokines including RANTES have been demonstrated on the endothelial cells of dermal venules and small veins but not arteries or capillaries (Hub & Rot, 1998; Rot, 1992), in the afferent lymphatic vessels in the upper and lower dermis of human skin (Hub & Rot, 1998) and also in the lining of high endothelial venules (HEV) suggesting that RANTES may be implicated in directing the trafficking of T-cells through the afferent lymphatic vessels to the lymph nodes. It is thought that during clearance, chemokines are channelled and redistributed to the lymph nodes where they can induce leukocyte recruitment after association with HEV (Rot, 2003). The chemokines CCL19 and CCL21 have been shown to be essential in the transmigration of T-cells across HEVs via binding to CCR7, the shared receptor for these two chemokines. CCR7 is uniformly expressed by all naïve T-cells as well as subsets of resting memory T-cells (Ebert *et al*, 2005). However, RANTES may be involved in the recirculation of activated T-cells expressing the receptors CCR3 and CCR5.

Therefore a strategy such as Cu-lowering therapy for altering RANTES presentation on the endothelium may not only be important for lung inflammation where RANTES has been implicated with several inflammatory diseases, but also in a wide range of other diseases involving other major organs. However, because in addition to Cu, oxidative stress has also been implicated in inflammation, required both for redox cycling and also inducing chemokine multimer formation, as the most susceptible organ to oxidative stress the lungs may be the most important target for Cu chelation therapy.

Further work:

Possible suggestions for further work include investigating the Cu chelators TMB and vancomycin for anti-inflammatory activity, anti-oxidant activity and therapeutic potential using transmigration assays and FOX-2 assays to determine whether these Cu chelators inhibit T-cell migration or protect lipids from peroxidation in cell cultures.

The effect of Cu-tobramycin or Cu-vancomycin complexes, which are easily synthesised by overnight incubation of tobramycin or vancomycin with $CuCl_2$ followed by ethanol precipitation could also be investigated using a FOX-2 assay to determine whether Cu-tobramycin or Cu-vancomycin protect lipids from peroxidation or have any effect on the redox state of cells in culture.

The effect of Cu on RANTES NFkB/IkB expression could be determined at the mRNA level.

Further longer-term experiments could be used to evaluate the effect of Cu depletion on chemokine multimer formation and binding to the endothelium in conjunction with the effect on leukocyte migration.

Transmigration experiments using several different endothelial types would facilitate the speculation of which tissues could be targeted with Cu-binding drugs to the greatest anti-inflammatory effect.

In addition, treatment of immunoprecipitated cell lysates with GAG-lyases would also give an indication as to which GAGs the chemokines are binding in different

endothelia, and this could parallel the use of Western blotting and immunostaining for GAGs including HSPG, chondroitin sulphate and dermatan sulphate.

Furthermore, to determine the mechanism of action of Cu chelators in the suppression of leukocyte migration it would be necessary to investigate the expression of endothelial expressed adhesion molecules including ICAM-1, VCAM-1, P-selectin and E-selectin and also the nuclear levels of NF-kB, and the phosphorylation of proteins associated with the MAPK pathway such as c-Jun, p65, p38 and JNK.

Aaseth J, Haugen M, Forre O (1998) Rheumatoid arthritis and metal compounds--perspectives on the role of oxygen radical detoxification. *Analyst* **123:** 3-6

Abi-Younes S, Sauty A, Mach F, Sukhova GK, Libby P, Luster AD (2000) The stromal cell-derived factor-1 chemokine is a potent platelet agonist highly expressed in atherosclerotic plaques. *Circ Res* **86:** 131-8

Abi-Younes S, Si-Tahar M, Luster AD (2001) The CC chemokines MDC and TARC induce platelet activation via CCR4. *Thromb Res* **101:** 279-89

Albertini R, Passi A, Abuja PM, De Luca G (2000) The effect of glycosaminoglycans and proteoglycans on lipid peroxidation. *Int J Mol Med* **6:** 129-36

Albertini R, Rindi S, Passi A, Pallavicini G, De Luca G (1996) Heparin protection against Fe2+ -and Cu2+ -mediated oxidation of liposomes. *FEBS Lett* **383:** 155-8

Ali FE, Leung A, Cherny RA, Mavros C, Barnham KJ, Separovic F, Barrow CJ (2006) Dimerisation of N-acetyl-L-tyrosine ethyl ester and Abeta peptides via formation of dityrosine. *Free Radic Res* **40:** 1-9

Ali FE, Separovic F, Barrow CJ, Cherny RA, Fraser F, Bush AI, Masters CL, Barnham KJ (2005) Methionine regulates copper/hydrogen peroxide oxidation products of Abeta. *J Pept Sci* **11:** 353-60

Ali S, Fritchley SJ, Chaffey BT, Kirby JA (2002) Contribution of the putative heparan sulfate-binding motif BBXB of RANTES to transendothelial migration. *Glycobiology* **12:** 535-43

Andersen SO (1963) Characterization of a new type of cross-linkage in resilin, a rubber-like protein. *Biochim Biophys Acta* **69:** 249-62

Andersen SO (1964) The Cross-Links in Resilin Identified as Dityrosine and Trityrosine. *Biochim Biophys Acta* **93:** 213-5

Appay V, Rowland-Jones SL (2001) RANTES: a versatile and controversial chemokine. *Trends Immunol* **22:** 83-7

Arenzana-Seisdedos F, Thompson J, Rodriguez MS, Bachelerie F, Thomas D, Hay RT (1995) Inducible nuclear expression of newly synthesized I kappa B alpha negatively regulates DNA-binding and transcriptional activities of NF-kappa B. *Mol Cell Biol* **15:** 2689-96

Arispe N, Diaz JC, Flora M (2008) Efficiency of histidine-associating compounds for blocking the alzheimer's Abeta channel activity and cytotoxicity. *Biophys J* **95:** 4879-89

Arvilommi AM, Salmi M, Jalkanen S (1997) Organ-selective regulation of vascular adhesion protein-1 expression in man. *Eur J Immunol* **27:** 1794-800

Ashitani J, Mukae H, Arimura Y, Matsukura S (2002) Elevated plasma procoagulant and fibrinolytic markers in patients with chronic obstructive pulmonary disease. *Intern Med* **41:** 181-5

Asosingh K, Swaidani S, Aronica M, Erzurum SC (2007) Th1- and Th2-dependent endothelial progenitor cell recruitment and angiogenic switch in asthma. *J Immunol* **178:** 6482-94

Atwood CS, Huang X, Khatri A, Scarpa RC, Kim YS, Moir RD, Tanzi RE, Roher AE, Bush AI (2000a) Copper catalyzed oxidation of Alzheimer Abeta. *Cell Mol Biol (Noisy-le-grand)* **46:** 777-83

Atwood CS, Moir RD, Huang X, Scarpa RC, Bacarra NM, Romano DM, Hartshorn MA, Tanzi RE, Bush AI (1998) Dramatic aggregation of Alzheimer abeta by Cu(II) is induced by conditions representing physiological acidosis. *J Biol Chem* **273:** 12817-26

Atwood CS, Perry G, Zeng H, Kato Y, Jones WD, Ling KQ, Huang X, Moir RD, Wang D, Sayre LM, Smith MA, Chen SG, Bush AI (2004) Copper mediates dityrosine cross-linking of Alzheimer's amyloid-beta. *Biochemistry* **43:** 560-8

Atwood CS, Scarpa RC, Huang X, Moir RD, Jones WD, Fairlie DP, Tanzi RE, Bush AI (2000b) Characterization of copper interactions with alzheimer amyloid beta peptides: identification of an attomolar-affinity copper binding site on amyloid beta1-42. *J Neurochem* **75:** 1219-33

Bagamery K, Kvell K, Barnet M, Landau R, Graham J (2005) Are platelets activated after a rapid, one-step density gradient centrifugation? Evidence from flow cytometric analysis. *Clin Lab Haematol* **27:** 75-7

Baggiolini M, Dahinden CA (1994) CC chemokines in allergic inflammation. *Immunol Today* **15:** 127-33

Balogh GT, Illes J, Szekely Z, Forrai E, Gere A (2003) Effect of different metal ions on the oxidative damage and antioxidant capacity of hyaluronic acid. *Arch Biochem Biophys* **410:** 76-82

Baltus T, von Hundelshausen P, Mause SF, Buhre W, Rossaint R, Weber C (2005) Differential and additive effects of platelet-derived chemokines on monocyte arrest on inflamed endothelium under flow conditions. *J Leukoc Biol* **78:** 435-41

Baltus T, Weber KS, Johnson Z, Proudfoot AE, Weber C (2003) Oligomerization of RANTES is required for CCR1-mediated arrest but not CCR5-mediated transmigration of leukocytes on inflamed endothelium. *Blood* **102:** 1985-8

Bar-Or D, Thomas GW, Yukl RL, Rael LT, Shimonkevitz RP, Curtis CG, Winkler JV (2003) Copper stimulates the synthesis and release of interleukin-8 in human endothelial cells: a possible early role in systemic inflammatory responses. *Shock* **20:** 154-8

Barnes PJ (2008) The cytokine network in asthma and chronic obstructive pulmonary disease. *J Clin Invest* **118:** 3546-56

Barnes PJ, Chung KF, Page CP (1988) Platelet-activating factor as a mediator of allergic disease. *J Allergy Clin Immunol* **81:** 919-34

Bartlett AH, Hayashida K, Park PW (2007) Molecular and cellular mechanisms of syndecans in tissue injury and inflammation. *Mol Cells* **24:** 153-66

Beck LA, Tancowny B, Brummet ME, Asaki SY, Curry SL, Penno MB, Foster M, Bahl A, Stellato C (2006) Functional analysis of the chemokine receptor CCR3 on airway epithelial cells. *J Immunol* **177:** 3344-54

Beg AA, Baldwin AS, Jr. (1993) The I kappa B proteins: multifunctional regulators of Rel/NF-kappa B transcription factors. *Genes Dev* **7:** 2064-70

Bernfield M, Gotte M, Park PW, Reizes O, Fitzgerald ML, Lincecum J, Zako M (1999) Functions of cell surface heparan sulfate proteoglycans. *Annu Rev Biochem* **68:** 729-77

Beveridge SJ, Walker WR, Whitehouse MW (1980) Anti-inflammatory activity of copper salicylates applied to rats percutaneously in dimethyl sulphoxide with glycerol. *J Pharm Pharmacol* **32:** 425-7

Beveridge SJ, Whitehouse MW, Walker WR (1982) Lipophilic copper(II) formulations: some correlations between their composition and anti-inflammatory/anti-arthritic activity when applied to the skin of rats. *Agents Actions* **12:** 225-31

Bleul CC, Wu L, Hoxie JA, Springer TA, Mackay CR (1997) The HIV coreceptors CXCR4 and CCR5 are differentially expressed and regulated on human T lymphocytes. *Proc Natl Acad Sci U S A* **94:** 1925-30

Bogdan C, Rollinghoff M, Diefenbach A (2000) Reactive oxygen and reactive nitrogen intermediates in innate and specific immunity. *Curr Opin Immunol* **12:** 64-76

Booth NA, Simpson AJ, Croll A, Bennett B, MacGregor IR (1988) Plasminogen activator inhibitor (PAI-1) in plasma and platelets. *Br J Haematol* **70:** 327-33

Bopp SK, Abicht HK, Knauer K (2008) Copper-induced oxidative stress in rainbow trout gill cells. *Aquat Toxicol* **86:** 197-204

Bowers R, Cool C, Murphy RC, Tuder RM, Hopken MW, Flores SC, Voelkel NF (2004) Oxidative stress in severe pulmonary hypertension. *Am J Respir Crit Care Med* **169:** 764-9

Brasier AR (2006) The NF-kappaB regulatory network. *Cardiovasc Toxicol* **6:** 111-30

Bratton RL, Montero DP, Adams KS, Novas MA, McKay TC, Hall LJ, Foust JG, Mueller MB, O'Brien PC, Atkinson EJ, Maurer MS (2002) Effect of "ionized" wrist bracelets on musculoskeletal pain: a randomized, double-blind, placebo-controlled trial. *Mayo Clin Proc* **77:** 1164-8

Brewer GJ (2005) Anticopper therapy against cancer and diseases of inflammation and fibrosis. *Drug Discov Today* **10:** 1103-9

Brewer GJ (2007) A brand new mechanism for copper toxicity. *J Hepatol* **47:** 621-2

Brewer GJ (2008) The risks of free copper in the body and the development of useful anticopper drugs. *Curr Opin Clin Nutr Metab Care* **11:** 727-32

Brewer GJ, Askari F, Lorincz MT, Carlson M, Schilsky M, Kluin KJ, Hedera P, Moretti P, Fink JK, Tankanow R, Dick RB, Sitterly J (2006) Treatment of Wilson disease with ammonium tetrathiomolybdate: IV. Comparison of tetrathiomolybdate and trientine in a double-blind study of treatment of the neurologic presentation of Wilson disease. *Arch Neurol* **63:** 521-7

Brewer GJ, Dick RD, Johnson VD, Brunberg JA, Kluin KJ, Fink JK (1998) Treatment of Wilson's disease with zinc: XV long-term follow-up studies. *J Lab Clin Med* **132:** 264-78

Brewer GJ, Hedera P, Kluin KJ, Carlson M, Askari F, Dick RB, Sitterly J, Fink JK (2003) Treatment of Wilson disease with ammonium tetrathiomolybdate: III. Initial therapy in a total of 55 neurologically affected patients and follow-up with zinc therapy. *Arch Neurol* **60:** 379-85

Brewer GJ, Johnson V, Dick RD, Kluin KJ, Fink JK, Brunberg JA (1996) Treatment of Wilson disease with ammonium tetrathiomolybdate. II. Initial therapy in 33 neurologically affected patients and follow-up with zinc therapy. *Arch Neurol* **53:** 1017-25

Brewer GJ, Yuzbasiyan-Gurkan V (1992) Wilson disease. *Medicine (Baltimore)* **71:** 139-64

Brisset M, Pujol JP, Arenzana-Seisdedos F, Virelizier JL, Penfornis H, Farjanel J, Rattner A, Bocquet J, Beliard R, Loyau G (1986) D-penicillamine inhibition of interleukin-1 production: a possible mechanism for its effect on synovial collagen synthesis? *Int J Tissue React* **8:** 279-87

Brogren H, Karlsson L, Andersson M, Wang L, Erlinge D, Jern S (2004) Platelets synthesize large amounts of active plasminogen activator inhibitor 1. *Blood* **104:** 3943-8

Broughton-Head VJ (2005) Novel Anti-Inflammatory and Mucolytic Effects of Heparin, PhD thesis, University of Portsmouth.

Brown DR, Guantieri V, Grasso G, Impellizzeri G, Pappalardo G, Rizzarelli E (2004) Copper(II) complexes of peptide fragments of the prion protein. Conformation changes induced by copper(II) and the binding motif in C-terminal protein region. *J Inorg Biochem* **98:** 133-43

Brown RK, Wyatt H, Price JF, Kelly FJ (1996) Pulmonary dysfunction in cystic fibrosis is associated with oxidative stress. *Eur Respir J* **9:** 334-9

Brozyna S, Ahern J, Hodge G, Nairn J, Holmes M, Reynolds PN, Hodge S (2009) Chemotactic mediators of Th1 T-cell trafficking in smokers and COPD patients. *COPD* **6:** 4-16

Bruckner O, Alexander M, Collmann H (1981) Tobramycin levels in cerebrospinal fluid of patients with slightly and severely impaired blood-cerebrospinal barrier. *Chemotherapy* **27:** 303-8

Brummel-Ziedins KE, Pouliot RL, Mann KG (2004) Thrombin generation: phenotypic quantitation. *J Thromb Haemost* **2:** 281-8

Bucchieri F, Puddicombe SM, Lordan JL, Richter A, Buchanan D, Wilson SJ, Ward J, Zummo G, Howarth PH, Djukanovic R, Holgate ST, Davies DE (2002) Asthmatic bronchial epithelium is more susceptible to oxidant-induced apoptosis. *Am J Respir Cell Mol Biol* **27:** 179-85

Buerge-Weiricht D, Sulzberger B (2004) Formation of Cu(I) in estuarine and marine waters: application of a new solid-phase extraction method to measure Cu(I). *Environ Sci Technol* **38:** 1843-8

Bull PC, Thomas GR, Rommens JM, Forbes JR, Cox DW (1993) The Wilson disease gene is a putative copper transporting P-type ATPase similar to the Menkes gene. *Nat Genet* **5:** 327-37

Burrows SD, Doyle ML, Murphy KP, Franklin SG, White JR, Brooks I, McNulty DE, Scott MO, Knutson JR, Porter D, et al. (1994) Determination of the monomer-dimer equilibrium of interleukin-8 reveals it is a monomer at physiological concentrations. *Biochemistry* **33:** 12741-5

Bush AI, Pettingell WH, Jr., Paradis MD, Tanzi RE (1994) Modulation of A beta adhesiveness and secretase site cleavage by zinc. *J Biol Chem* **269:** 12152-8

Butcher EC (1991) Leukocyte-endothelial cell recognition: three (or more) steps to specificity and diversity. *Cell* **67:** 1033-6

Butler LM, Khan S, Ed Rainger G, Nash GB (2008) Effects of endothelial basement membrane on neutrophil adhesion and migration. *Cell Immunol* **251:** 56-61

Butler LM, Rainger GE, Rahman M, Nash GB (2005) Prolonged culture of endothelial cells and deposition of basement membrane modify the recruitment of neutrophils. *Exp Cell Res* **310:** 22-32

Cahoon L (2009) The curious case of clioquinol. *Nat Med* **15:** 356-9

Camakaris J, Voskoboinik I, Mercer JF (1999) Molecular mechanisms of copper homeostasis. *Biochem Biophys Res Commun* **261:** 225-32

Camara K, Danao-Camara T (1999) Awareness of, use and perception of efficacy of alternative therapies by patients with inflammatory arthropathies. *Hawaii Med J* **58:** 329-32

Campo GM, D'Ascola A, Avenoso A, Campo S, Ferlazzo AM, Micali C, Zanghi L, Calatroni A (2004) Glycosaminoglycans reduce oxidative damage induced by copper (Cu+2), iron (Fe+2) and hydrogen peroxide (H2O2) in human fibroblast cultures. *Glycoconj J* **20:** 133-41

Carlos TM, Harlan JM (1994) Leukocyte-endothelial adhesion molecules. *Blood* **84:** 2068-101

Carr MW, Roth SJ, Luther E, Rose SS, Springer TA (1994) Monocyte chemoattractant protein 1 acts as a T-lymphocyte chemoattractant. *Proc Natl Acad Sci U S A* **91:** 3652-6

Carter NM, Ali S, Kirby JA (2003) Endothelial inflammation: the role of differential expression of N-deacetylase/N-sulphotransferase enzymes in alteration of the immunological properties of heparan sulphate. *J Cell Sci* **116:** 3591-600

Catalfamo M, Karpova T, McNally J, Costes SV, Lockett SJ, Bos E, Peters PJ, Henkart PA (2004) Human CD8+ T cells store RANTES in a unique secretory compartment and release it rapidly after TcR stimulation. *Immunity* **20:** 219-30

Chaudhuri A, Nielsen S, Elkjaer ML, Zbrzezna V, Fang F, Pogo AO (1997) Detection of Duffy antigen in the plasma membranes and caveolae of vascular endothelial and epithelial cells of nonerythroid organs. *Blood* **89:** 701-12

Chen XL, Zhang Q, Zhao R, Medford RM (2004) Superoxide, H2O2, and iron are required for TNF-alpha-induced MCP-1 gene expression in endothelial cells: role of Rac1 and NADPH oxidase. *Am J Physiol Heart Circ Physiol* **286:** H1001-7

Cheng JJ, Wung BS, Chao YJ, Wang DL (1998) Cyclic strain-induced reactive oxygen species involved in ICAM-1 gene induction in endothelial cells. *Hypertension* **31:** 125-30

Cherny RA, Atwood CS, Xilinas ME, Gray DN, Jones WD, McLean CA, Barnham KJ, Volitakis I, Fraser FW, Kim Y, Huang X, Goldstein LE, Moir RD, Lim JT, Beyreuther K, Zheng H, Tanzi RE, Masters CL, Bush AI (2001) Treatment with a copper-zinc chelator markedly and rapidly inhibits beta-amyloid accumulation in Alzheimer's disease transgenic mice. *Neuron* **30:** 665-76

Cherny RA, Barnham KJ, Lynch T, Volitakis I, Li QX, McLean CA, Multhaup G, Beyreuther K, Tanzi RE, Masters CL, Bush AI (2000) Chelation and intercalation: complementary properties in a compound for the treatment of Alzheimer's disease. *J Struct Biol* **130:** 209-16

Choe H, Moore MJ, Owens CM, Wright PL, Vasilieva N, Li W, Singh AP, Shakri R, Chitnis CE, Farzan M (2005) Sulphated tyrosines mediate association of chemokines and Plasmodium vivax Duffy binding protein with the Duffy antigen/receptor for chemokines (DARC). *Mol Microbiol* **55:** 1413-22

Choi ES, Nichol JL, Hokom MM, Hornkohl AC, Hunt P (1995) Platelets generated in vitro from proplatelet-displaying human megakaryocytes are functional. *Blood* **85:** 402-13

Chuchalin A, Csiszer E, Gyurkovics K, Bartnicka MT, Sands D, Kapranov N, Varoli G, Monici Preti PA, Mazurek H (2007) A formulation of aerosolized tobramycin (Bramitob) in the treatment of patients with cystic fibrosis and Pseudomonas aeruginosa

infection: a double-blind, placebo-controlled, multicenter study. *Paediatr Drugs* **9 Suppl 1:** 21-31

Chung CW, Cooke RM, Proudfoot AE, Wells TN (1995) The three-dimensional solution structure of RANTES. *Biochemistry* **34:** 9307-14

Ciencewicki J, Trivedi S, Kleeberger SR (2008) Oxidants and the pathogenesis of lung diseases. *J Allergy Clin Immunol* **122:** 456-68; quiz 469-70

Clancy R (1972) Cellular immunity to autologous platelets and serum-blocking factors in idiopathic thrombocytopenic purpura. *Lancet* **1:** 6-9

Clayton A, Evans RA, Pettit E, Hallett M, Williams JD, Steadman R (1998) Cellular activation through the ligation of intercellular adhesion molecule-1. *J Cell Sci* **111 (Pt 4):** 443-53

Clemetson KJ, Clemetson JM, Proudfoot AE, Power CA, Baggiolini M, Wells TN (2000) Functional expression of CCR1, CCR3, CCR4, and CXCR4 chemokine receptors on human platelets. *Blood* **96:** 4046-54

Clore GM, Appella E, Yamada M, Matsushima K, Gronenborn AM (1990) Three-dimensional structure of interleukin 8 in solution. *Biochemistry* **29:** 1689-96

Clore GM, Gronenborn AM (1995) Three-dimensional structures of alpha and beta chemokines. *Faseb J* **9:** 57-62

Cockwell P, Adams DH, Savage CO (1996) Glycosaminoglycans contribute to multiple functions of vascular endothelial cells. *Clin Exp Immunol* **104:** 1-3

Colditz IG, Schneider MA, Pruenster M, Rot A (2007) Chemokines at large: in-vivo mechanisms of their transport, presentation and clearance. *Thromb Haemost* **97:** 688-93

Conlon K, Lloyd A, Chattopadhyay U, Lukacs N, Kunkel S, Schall T, Taub D, Morimoto C, Osborne J, Oppenheim J, et al. (1995) CD8+ and CD45RA+ human peripheral blood lymphocytes are potent sources of macrophage inflammatory protein 1 alpha, interleukin-8 and RANTES. *Eur J Immunol* **25:** 751-6

Conti P, Barbacane RC, Feliciani C, Reale M (2001) Expression and secretion of RANTES by human peripheral blood CD4+ cells are dependent on the presence of monocytes. *Ann Clin Lab Sci* **31:** 75-84

Conti P, DiGioacchino M (2001) MCP-1 and RANTES are mediators of acute and chronic inflammation. *Allergy Asthma Proc* **22:** 133-7

Coughlin SR (2000) Thrombin signalling and protease-activated receptors. *Nature* **407:** 258-64

Cramer EM, Norol F, Guichard J, Breton-Gorius J, Vainchenker W, Masse JM, Debili N (1997) Ultrastructure of platelet formation by human megakaryocytes cultured with the Mpl ligand. *Blood* **89:** 2336-46

Crola Da Silva C, Lamerant-Fayel N, Paprocka M, Mitterrand M, Gosset D, Dus D, Kieda C (2009) Selective human endothelial cell activation by chemokines as a guide to cell homing. *Immunology* **126:** 394-404

Cross CE, Forte T, Stocker R, Louie S, Yamamoto Y, Ames BN, Frei B (1990) Oxidative stress and abnormal cholesterol metabolism in patients with adult respiratory distress syndrome. *J Lab Clin Med* **115:** 396-404

Crump MP, Rajarathnam K, Kim KS, Clark-Lewis I, Sykes BD (1998) Solution structure of eotaxin, a chemokine that selectively recruits eosinophils in allergic inflammation. *J Biol Chem* **273:** 22471-9

Cuajungco MP, Faget KY, Huang X, Tanzi RE, Bush AI (2000) Metal chelation as a potential therapy for Alzheimer's disease. *Ann N Y Acad Sci* **920:** 292-304

Cui Z, Lockman PR, Atwood CS, Hsu CH, Gupte A, Allen DD, Mumper RJ (2005) Novel D-penicillamine carrying nanoparticles for metal chelation therapy in Alzheimer's and other CNS diseases. *Eur J Pharm Biopharm* **59:** 263-72

Culley FJ, Pennycook AM, Tregoning JS, Dodd JS, Walzl G, Wells TN, Hussell T, Openshaw PJ (2006) Role of CCL5 (RANTES) in viral lung disease. *J Virol* **80:** 8151-7

Czapiga M, Gao JL, Kirk A, Lekstrom-Himes J (2005) Human platelets exhibit chemotaxis using functional N-formyl peptide receptors. *Exp Hematol* **33:** 73-84

Czaplewski LG, McKeating J, Craven CJ, Higgins LD, Appay V, Brown A, Dudgeon T, Howard LA, Meyers T, Owen J, Palan SR, Tan P, Wilson G, Woods NR, Heyworth CM, Lord BI, Brotherton D, Christison R, Craig S, Cribbes S, Edwards RM, Evans SJ, Gilbert R, Morgan P, Randle E, Schofield N, Varley PG, Fisher J, Waltho JP, Hunter MG (1999) Identification of amino acid residues critical for aggregation of human CC chemokines macrophage inflammatory protein (MIP)-1alpha, MIP-1beta, and RANTES. Characterization of active disaggregated chemokine variants. *J Biol Chem* **274:** 16077-84

D'Ambrosio D, Iellem A, Bonecchi R, Mazzeo D, Sozzani S, Mantovani A, Sinigaglia F (1998) Selective up-regulation of chemokine receptors CCR4 and CCR8 upon activation of polarized human type 2 Th cells. *J Immunol* **161:** 5111-5

Dairaghi DJ, Soo KS, Oldham ER, Premack BA, Kitamura T, Bacon KB, Schall TJ (1998) RANTES-induced T cell activation correlates with CD3 expression. *J Immunol* **160:** 426-33

Daireaux M, Redini F, Loyau G, Pujol JP (1990) Effects of associated cytokines (IL-1, TNF-alpha, IFN-gamma and TGF-beta) on collagen and glycosaminoglycan production by cultured human synovial cells. *Int J Tissue React* **12:** 21-31

Davenpeck KL, Sterbinsky SA, Bochner BS (1998) Rat neutrophils express alpha4 and beta1 integrins and bind to vascular cell adhesion molecule-1 (VCAM-1) and mucosal addressin cell adhesion molecule-1 (MAdCAM-1). *Blood* **91:** 2341-6

Davies JA, Fisher CE, Barnett MW (2001) Glycosaminoglycans in the study of mammalian organ development. *Biochem Soc Trans* **29:** 166-71

de Bruijne-Admiraal LG, Modderman PW, Von dem Borne AE, Sonnenberg A (1992) P-selectin mediates Ca(2+)-dependent adhesion of activated platelets to many different types of leukocytes: detection by flow cytometry. *Blood* **80:** 134-42

De Sanctis GT, Wolyniec WW, Green FH, Qin S, Jiao A, Finn PW, Noonan T, Joetham AA, Gelfand E, Doerschuk CM, Drazen JM (1997) Reduction of allergic airway responses in P-selectin-deficient mice. *J Appl Physiol* **83:** 681-7

Denis MM, Tolley ND, Bunting M, Schwertz H, Jiang H, Lindemann S, Yost CC, Rubner FJ, Albertine KH, Swoboda KJ, Fratto CM, Tolley E, Kraiss LW, McIntyre TM, Zimmerman GA, Weyrich AS (2005) Escaping the nuclear confines: signal-dependent pre-mRNA splicing in anucleate platelets. *Cell* **122:** 379-91

Derian CK, Damiano BP, D'Andrea MR, Andrade-Gordon P (2002) Thrombin regulation of cell function through protease-activated receptors: implications for therapeutic intervention. *Biochemistry (Mosc)* **67:** 56-64

Deskur E, Przywarska I, Dylewicz P, Szczesniak L, Rychlewski T, Wilk M, Wysocki H (1998) Exercise-induced increase in hydrogen peroxide plasma levels is diminished by endurance training after myocardial infarction. *Int J Cardiol* **67:** 219-24

Devalia JL, Bayram H, Abdelaziz MM, Sapsford RJ, Davies RJ (1999) Differences between cytokine release from bronchial epithelial cells of asthmatic patients and non-asthmatic subjects: effect of exposure to diesel exhaust particles. *Int Arch Allergy Immunol* **118:** 437-9

Devergne O, Marfaing-Koka A, Schall TJ, Leger-Ravet MB, Sadick M, Peuchmaur M, Crevon MC, Kim KJ, Schall TT, Kim T, et al. (1994) Production of the RANTES chemokine in delayed-type hypersensitivity reactions: involvement of macrophages and endothelial cells. *J Exp Med* **179:** 1689-94

Dichek D, Quertermous T (1989) Thrombin regulation of mRNA levels of tissue plasminogen activator and plasminogen activator inhibitor-1 in cultured human umbilical vein endothelial cells. *Blood* **74:** 222-8

Dinarello CA, Gelfand JA, Wolff SM (1993) Anticytokine strategies in the treatment of the systemic inflammatory response syndrome. *JAMA* **269:** 1829-35

Ding Z, Xiong K, Issekutz TB (2000) Regulation of chemokine-induced transendothelial migration of T lymphocytes by endothelial activation: differential effects on naive and memory T cells. *J Leukoc Biol* **67:** 825-33

Dubois B, D'Hooghe MB, De Lepeleire K, Ketelaer P, Opdenakker G, Carton H (1998) Toxicity in a double-blind, placebo-controlled pilot trial with D-penicillamine and metacycline in secondary progressive multiple sclerosis. *Mult Scler* **4:** 74-8

Ebert LM, Schaerli P, Moser B (2005) Chemokine-mediated control of T cell traffic in lymphoid and peripheral tissues. *Mol Immunol* **42:** 799-809

Ebnet K, Simon MM, Shaw S (1996) Regulation of chemokine gene expression in human endothelial cells by proinflammatory cytokines and Borrelia burgdorferi. *Ann N Y Acad Sci* **797:** 107-17

Einholm AP, Pedersen KE, Wind T, Kulig P, Overgaard MT, Jensen JK, Bodker JS, Christensen A, Charlton P, Andreasen PA (2003) Biochemical mechanism of action of a diketopiperazine inactivator of plasminogen activator inhibitor-1. *Biochem J* **373:** 723-32

Elias JA, Krol RC, Freundlich B, Sampson PM (1988) Regulation of human lung fibroblast glycosaminoglycan production by recombinant interferons, tumor necrosis factor, and lymphotoxin. *J Clin Invest* **81:** 325-33

Farndale RW (2006) Collagen-induced platelet activation. *Blood Cells Mol Dis* **36:** 162-5

Fattal-German M, Le Roy Ladurie F, Cerrina J, Lecerf F, Berrih-Aknin S (1998) Expression and modulation of ICAM-1, TNF-alpha and RANTES in human alveolar macrophages from lung-transplant recipients in vitro. *Transpl Immunol* **6:** 183-92

Feldmann M, Brennan FM, Maini RN (1996) Rheumatoid arthritis. *Cell* **85:** 307-10

Ferrante A, Nandoskar M, Bates EJ, Goh DH, Beard LJ (1988) Tumour necrosis factor beta (lymphotoxin) inhibits locomotion and stimulates the respiratory burst and degranulation of neutrophils. *Immunology* **63:** 507-12

Fialkow L, Chan CK, Rotin D, Grinstein S, Downey GP (1994) Activation of the mitogen-activated protein kinase signaling pathway in neutrophils. Role of oxidants. *J Biol Chem* **269:** 31234-42

Finkel T (1998) Oxygen radicals and signaling. *Curr Opin Cell Biol* **10:** 248-53

Fitzgerald KA, O'Neill, L. A. J., Gearing, A. J. H. and Callard, R. E. (2001) The Cytokine Facts Book, second edition.**:** 444-447

Fitzgerald ML, Wang Z, Park PW, Murphy G, Bernfield M (2000) Shedding of syndecan-1 and -4 ectodomains is regulated by multiple signaling pathways and mediated by a TIMP-3-sensitive metalloproteinase. *J Cell Biol* **148:** 811-24

Flaherty KR, Brewer GJ, Andrei A (2007) A phase I/II trial of tetrathiomolybdate for patients with idiopathic pulmonary fibrosis refractory to previous therapy. *Am Thorac Soc***:** A497

Foerder CA, Shapiro BM (1977) Release of ovoperoxidase from sea urchin eggs hardens the fertilization membrane with tyrosine crosslinks. *Proc Natl Acad Sci U S A* **74:** 4214-8

Folkerts G, Kloek J, Muijsers RB, Nijkamp FP (2001) Reactive nitrogen and oxygen species in airway inflammation. *Eur J Pharmacol* **429:** 251-62

Frechilla D, Lasheras B, Ucelay M, Parrondo E, Craciunescu G, Cenarruzabeitia E (1990a) Anti-inflammatory activity of some copper(II) complexes. *Arzneimittelforschung* **40:** 914-7

Frechilla D, Lasheras B, Ucelay M, Parrondo E, Craciunescu G, Cenarruzabeitia E (1990b) On the mechanism of the anti-inflammatory activity of some copper (II) complexes. *Arzneimittelforschung* **40:** 1008-10

Frevert CW, Goodman RB, Kinsella MG, Kajikawa O, Ballman K, Clark-Lewis I, Proudfoot AE, Wells TN, Martin TR (2002) Tissue-specific mechanisms control the retention of IL-8 in lungs and skin. *J Immunol* **168:** 3550-6

Frevert CW, Kinsella MG, Vathanaprida C, Goodman RB, Baskin DG, Proudfoot A, Wells TN, Wight TN, Martin TR (2003) Binding of interleukin-8 to heparan sulfate and chondroitin sulfate in lung tissue. *Am J Respir Cell Mol Biol* **28:** 464-72

Garcia-Larsen V, Chinn S, Rodrigo R, Amigo H, Bustos P, Rona RJ (2009) Relationship between oxidative stress-related biomarkers and antioxidant status with asthma and atopy in young adults: a population-based study. *Clin Exp Allergy* **39:** 379-86

Garrow JS, James, W. P. T. and Ralph, A. (2000) Human Nutrition and Dietetics. In, pp 197 - 200.

Gelehrter TD, Sznycer-Laszuk R (1986) Thrombin induction of plasminogen activator-inhibitor in cultured human endothelial cells. *J Clin Invest* **77:** 165-9

Gerber BO, Zanni MP, Uguccioni M, Loetscher M, Mackay CR, Pichler WJ, Yawalkar N, Baggiolini M, Moser B (1997) Functional expression of the eotaxin receptor CCR3 in T lymphocytes co-localizing with eosinophils. *Curr Biol* **7:** 836-43

Gimbrone MA, Jr. (1987) Vascular endothelium: nature's blood-compatible container. *Ann N Y Acad Sci* **516:** 5-11

Gimbrone MA, Jr. (1999) Endothelial dysfunction, hemodynamic forces, and atherosclerosis. *Thromb Haemost* **82:** 722-6

Giulivi C, Davies KJ (1993) Dityrosine and tyrosine oxidation products are endogenous markers for the selective proteolysis of oxidatively modified red blood cell hemoglobin by (the 19 S) proteasome. *J Biol Chem* **268:** 8752-9

Giulivi C, Davies KJ (1994) Dityrosine: a marker for oxidatively modified proteins and selective proteolysis. *Methods Enzymol* **233:** 363-71

Goger B, Halden Y, Rek A, Mosl R, Pye D, Gallagher J, Kungl AJ (2002) Different affinities of glycosaminoglycan oligosaccharides for monomeric and dimeric interleukin-8: a model for chemokine regulation at inflammatory sites. *Biochemistry* **41:** 1640-6

Gonzalez-Iglesias R, Pajares MA, Ocal C, Espinosa JC, Oesch B, Gasset M (2002) Prion protein interaction with glycosaminoglycan occurs with the formation of oligomeric complexes stabilized by Cu(II) bridges. *J Mol Biol* **319:** 527-40

Gonzalez C, Martin T, Cacho J, Brenas MT, Arroyo T, Garcia-Berrocal B, Navajo JA, Gonzalez-Buitrago JM (1999) Serum zinc, copper, insulin and lipids in Alzheimer's disease epsilon 4 apolipoprotein E allele carriers. *Eur J Clin Invest* **29:** 637-42

Gonzalo JA, Lloyd CM, Wen D, Albar JP, Wells TN, Proudfoot A, Martinez AC, Dorf M, Bjerke T, Coyle AJ, Gutierrez-Ramos JC (1998) The coordinated action of CC chemokines in the lung orchestrates allergic inflammation and airway hyperresponsiveness. *J Exp Med* **188:** 157-67

Guclu K, Sozgen K, Tutem E, Ozyurek M, Apak R (2005) Spectrophotometric determination of ascorbic acid using copper(II)-neocuproine reagent in beverages and pharmaceuticals. *Talanta* **65:** 1226-32

Gupte A, Mumper RJ (2007) An investigation into copper catalyzed D-penicillamine oxidation and subsequent hydrogen peroxide generation. *J Inorg Biochem* **101:** 594-602

Gutteridge JM, Halliwell B (1990) The measurement and mechanism of lipid peroxidation in biological systems. *Trends Biochem Sci* **15:** 129-35

Hadida F, Vieillard V, Autran B, Clark-Lewis I, Baggiolini M, Debre P (1998) HIV-specific T cell cytotoxicity mediated by RANTES via the chemokine receptor CCR3. *J Exp Med* **188:** 609-14

Hadley TJ, Lu ZH, Wasniowska K, Martin AW, Peiper SC, Hesselgesser J, Horuk R (1994) Postcapillary venule endothelial cells in kidney express a multispecific chemokine receptor that is structurally and functionally identical to the erythroid isoform, which is the Duffy blood group antigen. *J Clin Invest* **94:** 985-91

Hallgren R, Feltelius N, Lindh U (1987) Redistribution of minerals and trace elements in chronic inflammation--a study on isolated blood cells from patients with ankylosing spondylitis. *J Rheumatol* **14:** 548-53

Halliwell B (1991) Reactive oxygen species in living systems: source, biochemistry, and role in human disease. *Am J Med* **91:** 14S-22S

Halliwell B, Clement MV, Long LH (2000a) Hydrogen peroxide in the human body. *FEBS Lett* **486:** 10-3

Halliwell B, Clement MV, Ramalingam J, Long LH (2000b) Hydrogen peroxide. Ubiquitous in cell culture and in vivo? *IUBMB Life* **50:** 251-7

Halliwell B, Gutteridge JM (1988) Free radicals and antioxidant protection: mechanisms and significance in toxicology and disease. *Hum Toxicol* **7:** 7-13

Hartwig J, Italiano J, Jr. (2003) The birth of the platelet. *J Thromb Haemost* **1:** 1580-6

Harvath L, Falk W, Leonard EJ (1980) Rapid quantitation of neutrophil chemotaxis: use of a polyvinylpyrrolidone-free polycarbonate membrane in a multiwell assembly. *J Immunol Methods* **37:** 39-45

Hasegawa S, Pawankar R, Suzuki K, Nakahata T, Furukawa S, Okumura K, Ra C (1999) Functional expression of the high affinity receptor for IgE (FcepsilonRI) in human platelets and its' intracellular expression in human megakaryocytes. *Blood* **93:** 2543-51

Hausler M, Schweizer K, Biesterfel S, Opladen T, Heimann G (2002) Peripheral decrease and pulmonary homing of CD4+CD45RO+ helper memory T cells in cystic fibrosis. *Respir Med* **96:** 87-94

Hawrylowicz CM, Howells GL, Feldmann M (1991) Platelet-derived interleukin 1 induces human endothelial adhesion molecule expression and cytokine production. *J Exp Med* **174:** 785-90

Hebert CA, ed. (1999) Chemokines in disease.

Heeger P, Wolf G, Meyers C, Sun MJ, O'Farrell SC, Krensky AM, Neilson EG (1992) Isolation and characterization of cDNA from renal tubular epithelium encoding murine Rantes. *Kidney Int* **41:** 220-5

Heijink IH, Marcel Kies P, van Oosterhout AJ, Postma DS, Kauffman HF, Vellenga E (2007) Der p, IL-4, and TGF-beta cooperatively induce EGFR-dependent TARC expression in airway epithelium. *Am J Respir Cell Mol Biol* **36:** 351-9

Henry NL, Dunn R, Merjaver S, Pan Q, Pienta KJ, Brewer G, Smith DC (2006) Phase II trial of copper depletion with tetrathiomolybdate as an antiangiogenesis strategy in patients with hormone-refractory prostate cancer. *Oncology* **71:** 168-75

Henson PM (1976) Activation and desensitization of platelets by platelet-activating factor (PAF) derived from IgE-sensitized basophils. I. Characteristics of the secretory response. *J Exp Med* **143:** 937-52

Herman CJ, Allen P, Hunt WC, Prasad A, Brady TJ (2004) Use of complementary therapies among primary care clinic patients with arthritis. *Prev Chronic Dis* **1:** A12

Herzog V, Berndorfer U, Saber Y (1992) Isolation of insoluble secretory product from bovine thyroid: extracellular storage of thyroglobulin in covalently cross-linked form. *J Cell Biol* **118:** 1071-83

Hileman RE, Fromm JR, Weiler JM, Linhardt RJ (1998) Glycosaminoglycan-protein interactions: definition of consensus sites in glycosaminoglycan binding proteins. *Bioessays* **20:** 156-67

Hillyer P, Male D (2005) Expression of chemokines on the surface of different human endothelia. *Immunol Cell Biol* **83:** 375-82

Hirano S, Ebihara H, Sakai S, Kodama N, Suzuki KT (1993) Pulmonary clearance and toxicity of intratracheally instilled cupric oxide in rats. *Arch Toxicol* **67:** 312-7

Hirano S, Sakai S, Ebihara H, Kodama N, Suzuki KT (1990) Metabolism and pulmonary toxicity of intratracheally instilled cupric sulfate in rats. *Toxicology* **64:** 223-33

Holland JA, Pritchard KA, Pappolla MA, Wolin MS, Rogers NJ, Stemerman MB (1990) Bradykinin induces superoxide anion release from human endothelial cells. *J Cell Physiol* **143:** 21-5

Honkanen V, Konttinen YT, Sorsa T, Hukkanen M, Kemppinen P, Santavirta S, Saari H, Westermarck T (1991) Serum zinc, copper and selenium in rheumatoid arthritis. *J Trace Elem Electrolytes Health Dis* **5:** 261-3

Hoogewerf AJ, Kuschert GS, Proudfoot AE, Borlat F, Clark-Lewis I, Power CA, Wells TN (1997) Glycosaminoglycans mediate cell surface oligomerization of chemokines. *Biochemistry* **36:** 13570-8

Horton AA, Fairhurst S (1987) Lipid peroxidation and mechanisms of toxicity. *Crit Rev Toxicol* **18:** 27-79

Hostynek JJ, Maibach HI (2006) *Copper and the skin*. Edited by Hostynek, J. J, and Maibach, H. I. New York, USA: Informa Healthcare

Hou G, Dick R, Abrams GD, Brewer GJ (2005) Tetrathiomolybdate protects against cardiac damage by doxorubicin in mice. *J Lab Clin Med* **146:** 299-303

Huang TT, Kudo N, Yoshida M, Miyamoto S (2000a) A nuclear export signal in the N-terminal regulatory domain of IkappaBalpha controls cytoplasmic localization of inactive NF-kappaB/IkappaBalpha complexes. *Proc Natl Acad Sci U S A* **97:** 1014-9

Huang X, Atwood CS, Moir RD, Hartshorn MA, Tanzi RE, Bush AI (2004) Trace metal contamination initiates the apparent auto-aggregation, amyloidosis, and oligomerization of Alzheimer's Abeta peptides. *J Biol Inorg Chem* **9:** 954-60

Huang X, Cuajungco MP, Atwood CS, Hartshorn MA, Tyndall JD, Hanson GR, Stokes KC, Leopold M, Multhaup G, Goldstein LE, Scarpa RC, Saunders AJ, Lim J, Moir RD, Glabe C, Bowden EF, Masters CL, Fairlie DP, Tanzi RE, Bush AI (1999) Cu(II) potentiation of alzheimer abeta neurotoxicity. Correlation with cell-free hydrogen peroxide production and metal reduction. *J Biol Chem* **274:** 37111-6

Huang X, Cuajungco MP, Atwood CS, Moir RD, Tanzi RE, Bush AI (2000b) Alzheimer's disease, beta-amyloid protein and zinc. *J Nutr* **130:** 1488S-92S

Huang ZL, Failla ML (2000) *FASEB J* **14:** A794

Hub E, Rot A (1998) Binding of RANTES, MCP-1, MCP-3, and MIP-1alpha to cells in human skin. *Am J Pathol* **152:** 749-57

Hubeau C, Lorenzato M, Couetil JP, Hubert D, Dusser D, Puchelle E, Gaillard D (2001) Quantitative analysis of inflammatory cells infiltrating the cystic fibrosis airway mucosa. *Clin Exp Immunol* **124:** 69-76

Huber KR, Sridhar R, Griffith EH, Amma EL, Roberts J (1987) Superoxide dismutase-like activities of copper(II) complexes tested in serum. *Biochim Biophys Acta* **915:** 267-76

Humphries DE, Silbert JE (1988) Chlorate: a reversible inhibitor of proteoglycan sulfation. *Biochem Biophys Res Commun* **154:** 365-71

Humphries DE, Sugumaran G, Silbert JE (1989) Decreasing sulfation of proteoglycans produced by cultured cells. *Methods Enzymol* **179:** 428-34

Ihrcke NS, Wrenshall LE, Lindman BJ, Platt JL (1993) Role of heparan sulfate in immune system-blood vessel interactions. *Immunol Today* **14:** 500-5

Iijima W, Ohtani H, Nakayama T, Sugawara Y, Sato E, Nagura H, Yoshie O, Sasano T (2003) Infiltrating CD8+ T cells in oral lichen planus predominantly express CCR5 and CXCR3 and carry respective chemokine ligands RANTES/CCL5 and IP-10/CXCL10 in their cytolytic granules: a potential self-recruiting mechanism. *Am J Pathol* **163:** 261-8

Imlay JA, Chin SM, Linn S (1988) Toxic DNA damage by hydrogen peroxide through the Fenton reaction in vivo and in vitro. *Science* **240:** 640-2

Jaakkola K, Nikula T, Holopainen R, Vahasilta T, Matikainen MT, Laukkanen ML, Huupponen R, Halkola L, Nieminen L, Hiltunen J, Parviainen S, Clark MR, Knuuti J, Savunen T, Kaapa P, Voipio-Pulkki LM, Jalkanen S (2000) In vivo detection of vascular adhesion protein-1 in experimental inflammation. *Am J Pathol* **157:** 463-71

Jackson GS, Murray I, Hosszu LL, Gibbs N, Waltho JP, Clarke AR, Collinge J (2001) Location and properties of metal-binding sites on the human prion protein. *Proc Natl Acad Sci U S A* **98:** 8531-5

Jalkanen S, Karikoski M, Mercier N, Koskinen K, Henttinen T, Elima K, Salmivirta K, Salmi M (2007) The oxidase activity of vascular adhesion protein-1 (VAP-1) induces endothelial E- and P-selectins and leukocyte binding. *Blood* **110:** 1864-70

Jalkanen S, Salmi M (2001) Cell surface monoamine oxidases: enzymes in search of a function. *EMBO J* **20:** 3893-901

Jeffery PK (1999) Differences and similarities between chronic obstructive pulmonary disease and asthma. *Clin Exp Allergy* **29 Suppl 2:** 14-26

Jeffery PK, Wardlaw AJ, Nelson FC, Collins JV, Kay AB (1989) Bronchial biopsies in asthma. An ultrastructural, quantitative study and correlation with hyperreactivity. *Am Rev Respir Dis* **140:** 1745-53

Jezowska-Bojczuk M, Karaczyn A, Kozlowski H (1998) Copper(II) binding to tobramycin: potentiometric and spectroscopic studies. *Carbohydr Res* **313:** 265-9

Jia J, Chen J (2008) Chronic nickel-induced DNA damage and cell death: the protection role of ascorbic acid. *Environ Toxicol* **23:** 401-6

Jimenez-Hernandez RM, Frechilla D, Lasheras B, Gutierrez-Rios MT, Parrondo E. Craciunescu G, Cenarruzabeita E (1995) Inhibition of inflammation and gastric damage in rats by copper (II) complexes. *Arzneimittelforschung* **45:** 277-81

Jobling MF, Huang X, Stewart LR, Barnham KJ, Curtain C, Volitakis I, Perugini M, White AR, Cherny RA, Masters CL, Barrow CJ, Collins SJ, Bush AI, Cappai R (2001) Copper and zinc binding modulates the aggregation and neurotoxic properties of the prion peptide PrP106-126. *Biochemistry* **40:** 8073-84

Johnson WT (1999) Copper and signal transduction: platelets as a model to determine the role of copper in stimulus-response coupling. *Biofactors* **10:** 53-9

Jose PJ, Griffiths-Johnson DA, Collins PD, Walsh DT, Moqbel R, Totty NF, Truong O, Hsuan JJ, Williams TJ (1994) Eotaxin: a potent eosinophil chemoattractant cytokine detected in a guinea pig model of allergic airways inflammation. *J Exp Med* **179:** 881-7

Junt T, Schulze H, Chen Z, Massberg S, Goerge T, Krueger A, Wagner DD, Graf T, Italiano JE, Jr., Shivdasani RA, von Andrian UH (2007) Dynamic visualization of thrombopoiesis within bone marrow. *Science* **317:** 1767-70

Kaburagi Y, Shimada Y, Nagaoka T, Hasegawa M, Takehara K, Sato S (2001) Enhanced production of CC-chemokines (RANTES, MCP-1, MIP-1alpha, MIP-1beta, and eotaxin) in patients with atopic dermatitis. *Arch Dermatol Res* **293:** 350-5

Kadota J, Mukae H, Tomono K, Kohno S (2001) High concentrations of beta-chemokines in BAL fluid of patients with diffuse panbronchiolitis. *Chest* **120:** 602-7

Kainulainen V, Wang H, Schick C, Bernfield M (1998) Syndecans, heparan sulfate proteoglycans, maintain the proteolytic balance of acute wound fluids. *J Biol Chem* **273:** 11563-9

Kameyoshi Y, Dorschner A, Mallet AI, Christophers E, Schroder JM (1992) Cytokine RANTES released by thrombin-stimulated platelets is a potent attractant for human eosinophils. *J Exp Med* **176:** 587-92

Kameyoshi Y, Schroder JM, Christophers E, Yamamoto S (1994) Identification of the cytokine RANTES released from platelets as an eosinophil chemotactic factor. *Int Arch Allergy Immunol* **104 Suppl 1:** 49-51

Kanda A, Adachi T, Kayaba H, Yamada Y, Ueki S, Yamaguchi K, Hamada K, Fujita M, Chihara J (2004) Red blood cells regulate eosinophil chemotaxis by scavenging RANTES secreted from endothelial cells. *Clin Exp Allergy* **34:** 1621-6

Karadag F, Cildag O, Altinisik M, Kozaci LD, Kiter G, Altun C (2004) Trace elements as a component of oxidative stress in COPD. *Respirology* **9:** 33-7

Karam LR, Dizdaroglu M, Simic MG (1984) OH radical-induced products of tyrosine peptides. *Int J Radiat Biol Relat Stud Phys Chem Med* **46:** 715-24

Karimbakas J, Langkamp-Henken B, Percival SS (1998) Arrested maturation of granulocytes in copper deficient mice. *J Nutr* **128:** 1855-60

Karin M, Ben-Neriah Y (2000) Phosphorylation meets ubiquitination: the control of NF-[kappa]B activity. *Annu Rev Immunol* **18:** 621-63

Karpatkin S, Pearlstein E (1981) Role of platelets in tumor cell metastases. *Ann Intern Med* **95:** 636-41

Kato Y, Kitamoto N, Kawai Y, Osawa T (2001) The hydrogen peroxide/copper ion system, but not other metal-catalyzed oxidation systems, produces protein-bound dityrosine. *Free Radic Biol Med* **31:** 624-32

Kato Y, Wu X, Naito M, Nomura H, Kitamoto N, Osawa T (2000) Immunochemical detection of protein dityrosine in atherosclerotic lesion of apo-E-deficient mice using a novel monoclonal antibody. *Biochem Biophys Res Commun* **275:** 11-5

Kawai T, Seki M, Hiromatsu K, Eastcott JW, Watts GF, Sugai M, Smith DJ, Porcelli SA, Taubman MA (1999) Selective diapedesis of Th1 cells induced by endothelial cell RANTES. *J Immunol* **163:** 3269-78

Kawanishi S, Oikawa S, Inoue S, Nishino K (2002) Distinct mechanisms of oxidative DNA damage induced by carcinogenic nickel subsulfide and nickel oxides. *Environ Health Perspect* **110 Suppl 5:** 789-91

Keizer DW, Crump MP, Lee TW, Slupsky CM, Clark-Lewis I, Sykes BD (2000) Human CC chemokine I-309, structural consequences of the additional disulfide bond. *Biochemistry* **39:** 6053-9

Kennedy T, Ghio AJ, Reed W, Samet J, Zagorski J, Quay J, Carter J, Dailey L, Hoidal JR, Devlin RB (1998) Copper-dependent inflammation and nuclear factor-kappaB activation by particulate air pollution. *Am J Respir Cell Mol Biol* **19:** 366-78

Kestin M, Miller L, Littlejohn G, Wahlqvist M (1985) The use of unproven remedies for rheumatoid arthritis in Australia. *Med J Aust* **143:** 516-8

Khan G, Merajver S (2009) Copper chelation in cancer therapy using tetrathiomolybdate: an evolving paradigm. *Expert Opin Investig Drugs* **18:** 541-8

Kikugawa K, Kato T, Okamoto Y (1994) Damage of amino acids and proteins induced by nitrogen dioxide, a free radical toxin, in air. *Free Radic Biol Med* **16:** 373-82

Kim IH, Kim K, Rhee SG (1989) Induction of an antioxidant protein of Saccharomyces cerevisiae by O2, Fe3+, or 2-mercaptoethanol. *Proc Natl Acad Sci U S A* **86:** 6018-22

Kim KS, Rajarathnam K, Clark-Lewis I, Sykes BD (1996) Structural characterization of a monomeric chemokine: monocyte chemoattractant protein-3. *FEBS Lett* **395:** 277-82

Kinnula VL, Chang L, Everitt JI, Crapo JD (1992a) Oxidants and antioxidants in alveolar epithelial type II cells: in situ, freshly isolated, and cultured cells. *Am J Physiol* **262:** L69-77

Kinnula VL, Chang LY, Ho YS, Crapo JD (1992b) Hydrogen peroxide release from alveolar macrophages and alveolar type II cells during adaptation to hyperoxia in vivo. *Exp Lung Res* **18:** 655-73

Kinnula VL, Crapo JD, Raivio KO (1995) Generation and disposal of reactive oxygen metabolites in the lung. *Lab Invest* **73:** 3-19

Kinnula VL, Whorton AR, Chang LY, Crapo JD (1992c) Regulation of hydrogen peroxide generation in cultured endothelial cells. *Am J Respir Cell Mol Biol* **6:** 175-82

Klein D, Lichtmannegger J, Heinzmann U, Summer KH (2000) Dissolution of copper-rich granules in hepatic lysosomes by D-penicillamine prevents the development of fulminant hepatitis in Long-Evans cinnamon rats. *J Hepatol* **32:** 193-201

Klemens FK, Fanwick PE, Bibler JK, McMillin DR (1989) Crystal and molecular structure of [Cu(bcp)2]BF4.cntdot.CH3OH (bcp = 2,9-dimethyl-4,7-diphenyl-1,10-phenanthroline). *Inorganic Chemistry* **28:** 3076-79

Klinger MH, Wilhelm D, Bubel S, Sticherling M, Schroder JM, Kuhnel W (1995) Immunocytochemical localization of the chemokines RANTES and MIP-1 alpha within human platelets and their release during storage. *Int Arch Allergy Immunol* **107:** 541-6

Klinman JP, Mu D (1994) Quinoenzymes in biology. *Annu Rev Biochem* **63:** 299-344

Koch AE (1998) Review: angiogenesis: implications for rheumatoid arthritis. *Arthritis Rheum* **41:** 951-62

Koskinen K, Vainio PJ, Smith DJ, Pihlavisto M, Yla-Herttuala S, Jalkanen S, Salmi M (2004) Granulocyte transmigration through the endothelium is regulated by the oxidase activity of vascular adhesion protein-1 (VAP-1). *Blood* **103:** 3388-95

Kowal K, Bodzenta-Lukaszyk A, Pampuch A, Szmitkowski M, Donati MB, Iacoviello L (2007) Plasminogen activator inhibitor-1 plasma concentration in allergic asthma patients during allergen challenge. *Int Arch Allergy Immunol* **144:** 240-6

Kowalska MA, Ratajczak MZ, Majka M, Jin J, Kunapuli S, Brass L, Poncz M (2000) Stromal cell-derived factor-1 and macrophage-derived chemokine: 2 chemokines that activate platelets. *Blood* **96:** 50-7

Kramer ML, Kratzin HD, Schmidt B, Romer A, Windl O, Liemann S, Hornemann S, Kretzschmar H (2001) Prion protein binds copper within the physiological concentration range. *J Biol Chem* **276:** 16711-9

Krishnaswamy G, Kelley J, Yerra L, Smith JK, Chi DS (1999) Human endothelium as a source of multifunctional cytokines: molecular regulation and possible role in human disease. *J Interferon Cytokine Res* **19:** 91-104

Kucharewicz I, Kowal K, Buczko W, Bodzenta-Lukaszyk A (2003) The plasmin system in airway remodeling. *Thromb Res* **112:** 1-7

Kunsch C, Medford RM (1999) Oxidative stress as a regulator of gene expression in the vasculature. *Circ Res* **85:** 753-66

Kurashima K, Mukaida N, Fujimura M, Yasui M, Shinagawa T, Matsuda T, Ohmoto Y, Matsushima K (1997) A specific elevation of RANTES in bronchoalveolar lavage fluids of patients with chronic eosinophilic pneumonia. *Lab Invest* **76:** 67-75

Kuschert GS, Coulin F, Power CA, Proudfoot AE, Hubbard RE, Hoogewerf AJ, Wells TN (1999) Glycosaminoglycans interact selectively with chemokines and modulate receptor binding and cellular responses. *Biochemistry* **38:** 12959-68

LaBella F, Keeley F, Vivian S, Thornhill D (1967) Evidence for dityrosine in elastin. *Biochem Biophys Res Commun* **26:** 748-53

LaBella F, Waykole P, Queen G (1968) Formation of insoluble gels and dityrosine by the action of peroxidase on soluble collagens. *Biochem Biophys Res Commun* **30:** 333-8

Lacy F, O'Connor DT, Schmid-Schonbein GW (1998) Plasma hydrogen peroxide production in hypertensives and normotensive subjects at genetic risk of hypertension. *J Hypertens* **16:** 291-303

Lakshminarayanan V, Beno DW, Costa RH, Roebuck KA (1997) Differential regulation of interleukin-8 and intercellular adhesion molecule-1 by H2O2 and tumor necrosis factor-alpha in endothelial and epithelial cells. *J Biol Chem* **272:** 32910-8

Lalor PF, Edwards S, McNab G, Salmi M, Jalkanen S, Adams DH (2002) Vascular adhesion protein-1 mediates adhesion and transmigration of lymphocytes on human hepatic endothelial cells. *J Immunol* **169:** 983-92

Lane BR, Markovitz DM, Woodford NL, Rochford R, Strieter RM, Coffey MJ (1999) TNF-alpha inhibits HIV-1 replication in peripheral blood monocytes and alveolar macrophages by inducing the production of RANTES and decreasing C-C chemokine receptor 5 (CCR5) expression. *J Immunol* **163:** 3653-61

Laurence JS, Blanpain C, Burgner JW, Parmentier M, LiWang PJ (2000) CC chemokine MIP-1 beta can function as a monomer and depends on Phe13 for receptor binding. *Biochemistry* **39:** 3401-9

Leary SC, Winge DR (2007) The Janus face of copper: its expanding roles in biology and the pathophysiology of disease. Meeting on Copper and Related Metals in Biology. *EMBO Rep* **8:** 224-7

Lee JS, Frevert CW, Wurfel MM, Peiper SC, Wong VA, Ballman KK, Ruzinski JT, Rhim JS, Martin TR, Goodman RB (2003) Duffy antigen facilitates movement of chemokine across the endothelium in vitro and promotes neutrophil transmigration in vitro and in vivo. *J Immunol* **170:** 5244-51

Lee SR, Yang KS, Kwon J, Lee C, Jeong W, Rhee SG (2002) Reversible inactivation of the tumor suppressor PTEN by H2O2. *J Biol Chem* **277:** 20336-42

Leong SR, Lowman HB, Liu J, Shire S, Deforge LE, Gillece-Castro BL, McDowell R, Hebert CA (1997) IL-8 single-chain homodimers and heterodimers: interactions with chemokine receptors CXCR1, CXCR2, and DARC. *Protein Sci* **6:** 609-17

Ley K, Laudanna C, Cybulsky MI, Nourshargh S (2007) Getting to the site of inflammation: the leukocyte adhesion cascade updated. *Nat Rev Immunol* **7:** 678-89

Leytin V, Allen DJ, Lyubimov E, Freedman J (2007) Higher thrombin concentrations are required to induce platelet apoptosis than to induce platelet activation. *Br J Haematol* **136:** 762-4

Lim JK, Burns JM, Lu W, DeVico AL (2005) Multiple pathways of amino terminal processing produce two truncated variants of RANTES/CCL5. *J Leukoc Biol* **78:** 442-52

Linder MC, Hazegh-Azam M (1996) Copper biochemistry and molecular biology. *Am J Clin Nutr* **63:** 797S-811S

Liu G, Huang W, Moir RD, Vanderburg CR, Lai B, Peng Z, Tanzi RE, Rogers JT, Huang X (2006) Metal exposure and Alzheimer's pathogenesis. *J Struct Biol* **155:** 45-51

Loetscher P, Seitz M, Baggiolini M, Moser B (1996) Interleukin-2 regulates CC chemokine receptor expression and chemotactic responsiveness in T lymphocytes. *J Exp Med* **184:** 569-77

Loetscher P, Uguccioni M, Bordoli L, Baggiolini M, Moser B, Chizzolini C, Dayer JM (1998) CCR5 is characteristic of Th1 lymphocytes. *Nature* **391:** 344-5

Lominadze DG, Saari JT, Miller FN, Catalfamo JL, Justus DE, Schuschke DA (1996) Platelet aggregation and adhesion during dietary copper deficiency in rats. *Thromb Haemost* **75:** 630-4

Lu BY, Beck PJ, Chang JY (2001) Oxidative folding of murine prion mPrP(23-231). *Eur J Biochem* **268:** 3767-73

Luangsay S, Kasper LH, Rachinel N, Minns LA, Mennechet FJ, Vandewalle A, Buzoni-Gatel D (2003) CCR5 mediates specific migration of Toxoplasma gondii-primed CD8 lymphocytes to inflammatory intestinal epithelial cells. *Gastroenterology* **125:** 491-500

Lumpkins K, Bochicchio GV, Zagol B, Ulloa K, Simard JM, Schaub S, Meyer W, Scalea T (2008) Plasma levels of the beta chemokine regulated upon activation, normal T cell expressed, and secreted (RANTES) correlate with severe brain injury. *J Trauma* **64:** 358-61

M'Bemba-Meka P, Lemieux N, Chakrabarti SK (2005) Role of oxidative stress, mitochondrial membrane potential, and calcium homeostasis in nickel sulfate-induced human lymphocyte death in vitro. *Chem Biol Interact* **156:** 69-80

Ma S, Hou, G, Dick, R, Brewer, G. J. (2004) Tetrathiomolybdate protects against liver injury from acetaminophen in mice. *J Appl Res Clim Exp Ther* **4:** 419-426

Madaric A, Ginter E, Kadrabova J (1994) Serum copper, zinc and copper/zinc ratio in males: influence of aging. *Physiol Res* **43:** 107-11

Magnus JH, Gran JT, Mikkelsen K, Nygaard H, Brath HK (1987) Toxicity to D-penicillamine in rheumatoid arthritis. *Scand J Rheumatol* **16:** 441-4

Mak JC (2008) Pathogenesis of COPD. Part II. Oxidative-antioxidative imbalance. *Int J Tuberc Lung Dis* **12:** 368-74

Mak JC, Chan-Yeung MM (2006) Reactive oxidant species in asthma. *Curr Opin Pulm Med* **12:** 7-11

Malencik DA, Sprouse JF, Swanson CA, Anderson SR (1996) Dityrosine: preparation, isolation, and analysis. *Anal Biochem* **242:** 202-13

Mandal RV, Mark EJ, Kradin RL (2007) Megakaryocytes and platelet homeostasis in diffuse alveolar damage. *Exp Mol Pathol* **83:** 327-31

Manduteanu I, Dragomir E, Voinea M, Capraru M, Simionescu M (2007) Enoxaparin reduces H2O2-induced activation of human endothelial cells by a mechanism involving cell adhesion molecules and nuclear transcription factors. *Pharmacology* **79:** 154-62

Mann KG, Brummel K, Butenas S (2003) What is all that thrombin for? *J Thromb Haemost* **1:** 1504-14

Manni A, Kleimberg J, Ackerman V, Bellini A, Patalano F, Mattoli S (1996) Inducibility of RANTES mRNA by IL-1beta in human bronchial epithelial cells is associated with increased NF-kappaB DNA binding activity. *Biochem Biophys Res Commun* **220:** 120-4

Marelli-Berg FM, Cannella L, Dazzi F, Mirenda V (2008) The highway code of T cell trafficking. *J Pathol* **214:** 179-89

Marfaing-Koka A, Devergne O, Gorgone G, Portier A, Schall TJ, Galanaud P, Emilie D (1995) Regulation of the production of the RANTES chemokine by endothelial cells. Synergistic induction by IFN-gamma plus TNF-alpha and inhibition by IL-4 and IL-13. *J Immunol* **154:** 1870-8

Marshall LJ, Ramdin LS, Brooks T, PC DP, Shute JK (2003) Plasminogen activator inhibitor-1 supports IL-8-mediated neutrophil transendothelial migration by inhibition of the constitutive shedding of endothelial IL-8/heparan sulfate/syndecan-1 complexes. *J Immunol* **171:** 2057-65

Martelius T, Salaspuro V, Salmi M, Krogerus L, Hockerstedt K, Jalkanen S, Lautenschlager I (2004) Blockade of vascular adhesion protein-1 inhibits lymphocyte infiltration in rat liver allograft rejection. *Am J Pathol* **165:** 1993-2001

Martin L, Blanpain C, Garnier P, Wittamer V, Parmentier M, Vita C (2001) Structural and functional analysis of the RANTES-glycosaminoglycans interactions. *Biochemistry* **40:** 6303-18

Marttila-Ichihara F, Smith DJ, Stolen C, Yegutkin GG, Elima K, Mercier N, Kiviranta R, Pihlavisto M, Alaranta S, Pentikainen U, Pentikainen O, Fulop F, Jalkanen S, Salmi M (2006) Vascular amine oxidases are needed for leukocyte extravasation into inflamed joints in vivo. *Arthritis Rheum* **54:** 2852-62

Matoba T, Shimokawa H, Kubota H, Morikawa K, Fujiki T, Kunihiro I, Mukai Y, Hirakawa Y, Takeshita A (2002) Hydrogen peroxide is an endothelium-derived hyperpolarizing factor in human mesenteric arteries. *Biochem Biophys Res Commun* **290:** 909-13

Matoba T, Shimokawa H, Nakashima M, Hirakawa Y, Mukai Y, Hirano K, Kanaide H, Takeshita A (2000) Hydrogen peroxide is an endothelium-derived hyperpolarizing factor in mice. *J Clin Invest* **106:** 1521-30

Matsushima K, Larsen CG, DuBois GC, Oppenheim JJ (1989) Purification and characterization of a novel monocyte chemotactic and activating factor produced by a human myelomonocytic cell line. *J Exp Med* **169:** 1485-90

May MJ, Ager A (1992) ICAM-1-independent lymphocyte transmigration across high endothelium: differential up-regulation by interferon gamma, tumor necrosis factor-alpha and interleukin 1 beta. *Eur J Immunol* **22:** 219-26

Mayo KH, Chen MJ (1989) Human platelet factor 4 monomer-dimer-tetramer equilibria investigated by 1H NMR spectroscopy. *Biochemistry* **28:** 9469-78

Maziere C, Djavaheri-Mergny M, Frey-Fressart V, Delattre J, Maziere JC (1997) Copper and cell-oxidized low-density lipoprotein induces activator protein 1 in fibroblasts, endothelial and smooth muscle cells. *FEBS Lett* **409:** 351-6

McEver RP (2002) P-selectin and PSGL-1: exploiting connections between inflammation and venous thrombosis. *Thromb Haemost* **87:** 364-5

McFadden G, Kelvin D (1997) New strategies for chemokine inhibition and modulation: you take the high road and I'll take the low road. *Biochem Pharmacol* **54:** 1271-80

McQuaid A, Lamand M, Mason J (1992) The interactions of penicillamine with copper in vivo and the effect on hepatic metallothionein levels and copper/zinc distribution: the implications for Wilson's disease and arthritis therapy. *J Lab Clin Med* **119:** 744-50

Medici V, Sturniolo GC (2008) Tetrathiomolybdate, a copper chelator for the treatment of Wilson disease, pulmonary fibrosis and other indications. *IDrugs* **11:** 592-606

Meier B, Radeke HH, Selle S, Younes M, Sies H, Resch K, Habermehl GG (1989) Human fibroblasts release reactive oxygen species in response to interleukin-1 or tumour necrosis factor-alpha. *Biochem J* **263:** 539-45

Mellado M, Rodriguez-Frade JM, Manes S, Martinez AC (2001) Chemokine signaling and functional responses: the role of receptor dimerization and TK pathway activation. *Annu Rev Immunol* **19:** 397-421

Merinen M, Irjala H, Salmi M, Jaakkola I, Hanninen A, Jalkanen S (2005) Vascular adhesion protein-1 is involved in both acute and chronic inflammation in the mouse. *Am J Pathol* **166:** 793-800

Mestas J, Hughes CC (2004) Of mice and not men: differences between mouse and human immunology. *J Immunol* **172:** 2731-8

Metzger WJ, Richerson HB, Worden K, Monick M, Hunninghake GW (1986) Bronchoalveolar lavage of allergic asthmatic patients following allergen bronchoprovocation. *Chest* **89:** 477-83

Metzger WJ, Sjoerdsma K, Richerson HB, Moseley P, Zavala D, Monick M, Hunninghake GW (1987) Platelets in bronchoalveolar lavage from asthmatic patients and allergic rabbits with allergen-induced late phase responses. *Agents Actions Suppl* **21:** 151-9

Meyer JE, Berner I, Teran LM, Bartels J, Sticherling M, Schroder JM, Maune S (1998) RANTES production by cytokine-stimulated nasal fibroblasts: its inhibition by glucocorticoids. *Int Arch Allergy Immunol* **117:** 60-7

Mickelson JK, Lakkis NM, Villarreal-Levy G, Hughes BJ, Smith CW (1996) Leukocyte activation with platelet adhesion after coronary angioplasty: a mechanism for recurrent disease? *J Am Coll Cardiol* **28:** 345-53

Milanino R, Buchner V (2006) Copper: role of the 'endogenous' and 'exogenous' metal on the development and control of inflammatory processes. *Rev Environ Health* **21:** 153-215

Milne DB, Nielsen FH (1996) Effects of a diet low in copper on copper-status indicators in postmenopausal women. *Am J Clin Nutr* **63:** 358-64

Mire-Sluis AR, Wickremasinghe RG, Hoffbrand AV, Timms AM, Francis GE (1987) Human T lymphocytes stimulated by phytohaemagglutinin undergo a single round of cell division without a requirement for interleukin-2 or accessory cells. *Immunology* **60:** 7-12

Mizel SB (1982) Interleukin 1 and T cell activation. *Immunol Rev* **63:** 51-72

Moellering RC, Jr., Krogstad DJ, Greenblatt DJ (1981) Pharmacokinetics of vancomycin in normal subjects and in patients with reduced renal function. *Rev Infect Dis* **3 suppl:** S230-5

Mohanakrishnan P, Chignell CF (1985) Difference circular dichroism studies of copper and nickel binding to D-penicillamine in the presence of human serum albumin. *Biochem Pharmacol* **34:** 675-7

Moritani C, Ishioka S, Haruta Y, Kambe M, Yamakido M (1998) Activation of platelets in bronchial asthma. *Chest* **113:** 452-8

Mosmann TR, Coffman RL (1989) TH1 and TH2 cells: different patterns of lymphokine secretion lead to different functional properties. *Annu Rev Immunol* **7:** 145-73

Murphy PM (2002) Chemokine/chemokine receptor nomenclature. *J Immunol Methods* **262:** 1-3

Murphy PM, Baggiolini M, Charo IF, Hebert CA, Horuk R, Matsushima K, Miller LH, Oppenheim JJ, Power CA (2000) International union of pharmacology. XXII. Nomenclature for chemokine receptors. *Pharmacol Rev* **52:** 145-76

Murphy PM, Baggiolini M, Charo IF, Hebert CA, Horuk R, Matsushima K, Miller LH, Oppenheim JJ, Power CA (2003) Chemokine/chemokine receptor nomenclature. *Cytokine* **21:** 48-9

Muylle L, Joos M, Wouters E, De Bock R, Peetermans ME (1993) Increased tumor necrosis factor alpha (TNF alpha), interleukin 1, and interleukin 6 (IL-6) levels in the plasma of stored platelet concentrates: relationship between TNF alpha and IL-6 levels and febrile transfusion reactions. *Transfusion* **33:** 195-9

Nadeem A, Masood A, Siddiqui N (2008) Oxidant--antioxidant imbalance in asthma: scientific evidence, epidemiological data and possible therapeutic options. *Ther Adv Respir Dis* **2:** 215-35

Neet KE, Timm DE (1994) Conformational stability of dimeric proteins: quantitative studies by equilibrium denaturation. *Protein Sci* **3:** 2167-74

Nelson PJ, Kim HT, Manning WC, Goralski TJ, Krensky AM (1993) Genomic organization and transcriptional regulation of the RANTES chemokine gene. *J Immunol* **151:** 2601-12

Neote K, Mak JY, Kolakowski LF, Jr., Schall TJ (1994) Functional and biochemical analysis of the cloned Duffy antigen: identity with the red blood cell chemokine receptor. *Blood* **84:** 44-52

Nordenhem A, Wiman B (1997) Plasminogen activator inhibitor-1 (PAI-1) content in platelets from healthy individuals genotyped for the 4G/5G polymorphism in the PAI-1 gene. *Scand J Clin Lab Invest* **57:** 453-61

Noso N, Sticherling M, Bartels J, Mallet AI, Christophers E, Schroder JM (1996) Identification of an N-terminally truncated form of the chemokine RANTES and granulocyte-macrophage colony-stimulating factor as major eosinophil attractants released by cytokine-stimulated dermal fibroblasts. *J Immunol* **156:** 1946-53

O'Donnell MC, Henson PM, Fiedel BA (1978) Activation of human platelets by platelet activating factor (PAF) derived from sensitized rabbit basophils. *Immunology* **35:** 953-8

O'Donnell R, Breen D, Wilson S, Djukanovic R (2006) Inflammatory cells in the airways in COPD. *Thorax* **61:** 448-54

O'Neill DW, Adams S, Bhardwaj N (2004) Manipulating dendritic cell biology for the active immunotherapy of cancer. *Blood* **104:** 2235-46

O'Sullivan BP, Michelson AD (2006) The inflammatory role of platelets in cystic fibrosis. *Am J Respir Crit Care Med* **173:** 483-90

Ogawa M, Hirano H, Tsubaki H, Kodama H, Tanaka T (1998) The role of cytokines in cervical ripening: correlations between the concentrations of cytokines and hyaluronic acid in cervical mucus and the induction of hyaluronic acid production by inflammatory cytokines by human cervical fibroblasts. *Am J Obstet Gynecol* **179:** 105-10

Ohtani N, Ohtani H, Nakayama T, Naganuma H, Sato E, Imai T, Nagura H, Yoshie O (2004) Infiltration of CD8+ T cells containing RANTES/CCL5+ cytoplasmic granules in actively inflammatory lesions of human chronic gastritis. *Lab Invest* **84:** 368-75

Olszewska-Pazdrak B, Casola A, Saito T, Alam R, Crowe SE, Mei F, Ogra PL, Garofalo RP (1998) Cell-specific expression of RANTES, MCP-1, and MIP-1alpha by lower airway epithelial cells and eosinophils infected with respiratory syncytial virus. *J Virol* **72:** 4756-64

Omoto A, Kawahito Y, Prudovsky I, Tubouchi Y, Kimura M, Ishino H, Wada M, Yoshida M, Kohno M, Yoshimura R, Yoshikawa T, Sano H (2005) Copper chelation with tetrathiomolybdate suppresses adjuvant-induced arthritis and inflammation-associated cachexia in rats. *Arthritis Res Ther* **7:** R1174-82

Opazo C, Huang X, Cherny RA, Moir RD, Roher AE, White AR, Cappai R, Masters CL, Tanzi RE, Inestrosa NC, Bush AI (2002) Metalloenzyme-like activity of Alzheimer's disease beta-amyloid. Cu-dependent catalytic conversion of dopamine, cholesterol, and biological reducing agents to neurotoxic H(2)O(2). *J Biol Chem* **277:** 40302-8

Oravecz T, Pall M, Roderiquez G, Gorrell MD, Ditto M, Nguyen NY, Boykins R, Unsworth E, Norcross MA (1997) Regulation of the receptor specificity and function of the chemokine RANTES (regulated on activation, normal T cell expressed and secreted) by dipeptidyl peptidase IV (CD26)-mediated cleavage. *J Exp Med* **186:** 1865-72

Ortiz BD, Nelson PJ, Krensky AM (1997) Switching gears during T-cell maturation: RANTES and late transcription. *Immunol Today* **18:** 468-71

Osterberg R (1980) Physiology and pharmacology of copper. *Pharmacol Ther* **9:** 121-46

Ostrakhovitch EA, Lordnejad MR, Schliess F, Sies H, Klotz LO (2002) Copper ions strongly activate the phosphoinositide-3-kinase/Akt pathway independent of the generation of reactive oxygen species. *Arch Biochem Biophys* **397:** 232-9

Ozes ON, Mayo LD, Gustin JA, Pfeffer SR, Pfeffer LM, Donner DB (1999) NF-kappaB activation by tumour necrosis factor requires the Akt serine-threonine kinase. *Nature* **401:** 82-5

Paavola CD, Hemmerich S, Grunberger D, Polsky I, Bloom A, Freedman R, Mulkins M, Bhakta S, McCarley D, Wiesent L, Wong B, Jarnagin K, Handel TM (1998) Monomeric monocyte chemoattractant protein-1 (MCP-1) binds and activates the MCP-1 receptor CCR2B. *J Biol Chem* **273:** 33157-65

Palacios R (1982) Mechanism of T cell activation: role and functional relationship of HLA-DR antigens and interleukins. *Immunol Rev* **63:** 73-110

Pamp K, Bramey T, Kirsch M, De Groot H, Petrat F (2005) NAD(H) enhances the Cu(II)-mediated inactivation of lactate dehydrogenase by increasing the accessibility of sulfhydryl groups. *Free Radic Res* **39:** 31-40

Pan Q, Bao LW, Merajver SD (2003) Tetrathiomolybdate inhibits angiogenesis and metastasis through suppression of the NFkappaB signaling cascade. *Mol Cancer Res* **1:** 701-6

Pan Q, Kleer CG, van Golen KL, Irani J, Bottema KM, Bias C, De Carvalho M, Mesri EA, Robins DM, Dick RD, Brewer GJ, Merajver SD (2002) Copper deficiency induced by tetrathiomolybdate suppresses tumor growth and angiogenesis. *Cancer Res* **62:** 4854-9

Panoskaltsis-Mortari A, Strieter RM, Hermanson JR, Fegeding KV, Murphy WJ, Farrell CL, Lacey DL, Blazar BR (2000) Induction of monocyte- and T-cell-attracting chemokines in the lung during the generation of idiopathic pneumonia syndrome following allogeneic murine bone marrow transplantation. *Blood* **96:** 834-9

Papas KA, Sontag MK, Pardee C, Sokol RJ, Sagel SD, Accurso FJ, Wagener JS (2008) A pilot study on the safety and efficacy of a novel antioxidant rich formulation in patients with cystic fibrosis. *J Cyst Fibros* **7:** 60-7

Parish CR (2005) Heparan sulfate and inflammation. *Nat Immunol* **6:** 861-2

Partrick DA, Moore FA, Moore EE, Biffl WL, Sauaia A, Barnett CC, Jr. (1996) Jack A. Barney Resident Research Award winner. The inflammatory profile of interleukin-6, interleukin-8, and soluble intercellular adhesion molecule-1 in postinjury multiple organ failure. *Am J Surg* **172:** 425-9; discussed 429-31

Pass HI, Brewer GJ, Dick R, Carbone M, Merajver S (2008) A phase II trial of tetrathiomolybdate after surgery for malignant mesothelioma: final results. *Ann Thorac Surg* **86:** 383-9; discussion 390

Patel SR, Hartwig JH, Italiano JE, Jr. (2005) The biogenesis of platelets from megakaryocyte proplatelets. *J Clin Invest* **115:** 3348-54

Patterson C, Stouffer GA, Madamanchi N, Runge MS (2001) New tricks for old dogs: nonthrombotic effects of thrombin in vessel wall biology. *Circ Res* **88:** 987-97

Pattison JM, Nelson PJ, Huie P, Sibley RK, Krensky AM (1996) RANTES chemokine expression in transplant-associated accelerated atherosclerosis. *J Heart Lung Transplant* **15:** 1194-9

Pawlowska Z, Chabielska E, Kobylanska A, Maciaszek A, Swiatkowska M, Buczko W, Stec WJ, Cierniewski CS (2001) Regulation of PAI-1 concentration in platelets by systemic administration of antisense oligonucleotides to rats. *Thromb Haemost* **85:** 1086-9

Peiper SC, Wang ZX, Neote K, Martin AW, Showell HJ, Conklyn MJ, Ogborne K, Hadley TJ, Lu ZH, Hesselgesser J, Horuk R (1995) The Duffy antigen/receptor for chemokines (DARC) is expressed in endothelial cells of Duffy negative individuals who lack the erythrocyte receptor. *J Exp Med* **181:** 1311-7

Pelaia G, Cuda G, Vatrella A, Gallelli L, Fratto D, Gioffre V, D'Agostino B, Caputi M, Maselli R, Rossi F, Costanzo FS, Marsico SA (2004) Effects of hydrogen peroxide on MAPK activation, IL-8 production and cell viability in primary cultures of human bronchial epithelial cells. *J Cell Biochem* **93:** 142-52

Percival SS, Kauwell GP, Bowser E, Wagner M (1999) Altered copper status in adult men with cystic fibrosis. *J Am Coll Nutr* **18:** 614-9

Persichini T, Percario Z, Mazzon E, Colasanti M, Cuzzocrea S, Musci G (2006) Copper activates the NF-kappaB pathway in vivo. *Antioxid Redox Signal* **8:** 1897-904

Petrek M, Pantelidis P, Southcott AM, Lympany P, Safranek P, Black CM, Kolek V, Weigl E, du Bois RM (1997) The source and role of RANTES in interstitial lung disease. *Eur Respir J* **10:** 1207-16

Pitchford SC, Momi S, Baglioni S, Casali L, Giannini S, Rossi R, Page CP, Gresele P (2008) Allergen induces the migration of platelets to lung tissue in allergic asthma. *Am J Respir Crit Care Med* **177:** 604-12

Pitchford SC, Momi S, Giannini S, Casali L, Spina D, Page CP, Gresele P (2005) Platelet P-selectin is required for pulmonary eosinophil and lymphocyte recruitment in a murine model of allergic inflammation. *Blood* **105:** 2074-81

Pitchford SC, Riffo-Vasquez Y, Sousa A, Momi S, Gresele P, Spina D, Page CP (2004) Platelets are necessary for airway wall remodeling in a murine model of chronic allergic inflammation. *Blood* **103:** 639-47

Pitchford SC, Yano H, Lever R, Riffo-Vasquez Y, Ciferri S, Rose MJ, Giannini S, Momi S, Spina D, O'Connor B, Gresele P, Page CP (2003) Platelets are essential for leukocyte recruitment in allergic inflammation. *J Allergy Clin Immunol* **112:** 109-18

Pober JS, Cotran RS (1990) Cytokines and endothelial cell biology. *Physiol Rev* **70:** 427-51

Pope CA, 3rd (1989) Respiratory disease associated with community air pollution and a steel mill, Utah Valley. *Am J Public Health* **79:** 623-8

Pope CA, 3rd, Dockery DW, Spengler JD, Raizenne ME (1991) Respiratory health and PM10 pollution. A daily time series analysis. *Am Rev Respir Dis* **144:** 668-74

Power CA, Clemetson JM, Clemetson KJ, Wells TN (1995) Chemokine and chemokine receptor mRNA expression in human platelets. *Cytokine* **7:** 479-82

Proudfoot AE (2006) The biological relevance of chemokine-proteoglycan interactions. *Biochem Soc Trans* **34:** 422-6

Proudfoot AE, Fritchley S, Borlat F, Shaw JP, Vilbois F, Zwahlen C, Trkola A, Marchant D, Clapham PR, Wells TN (2001) The BBXB motif of RANTES is the principal site for heparin binding and controls receptor selectivity. *J Biol Chem* **276:** 10620-6

Proudfoot AE, Handel TM, Johnson Z, Lau EK, LiWang P, Clark-Lewis I, Borlat F, Wells TN, Kosco-Vilbois MH (2003) Glycosaminoglycan binding and oligomerization are essential for the in vivo activity of certain chemokines. *Proc Natl Acad Sci U S A* **100:** 1885-90

Pruenster M, Rot A (2006) Throwing light on DARC. *Biochem Soc Trans* **34:** 1005-8

Psarras S, Caramori G, Contoli M, Papadopoulos N, Papi A (2005) Oxidants in asthma and in chronic obstructive pulmonary disease (COPD). *Curr Pharm Des* **11:** 2053-62

Qiao D, Meyer K, Mundhenke C, Drew SA, Friedl A (2003) Heparan sulfate proteoglycans as regulators of fibroblast growth factor-2 signaling in brain endothelial cells. Specific role for glypican-1 in glioma angiogenesis. *J Biol Chem* **278:** 16045-53

Qin K, Coomaraswamy J, Mastrangelo P, Yang Y, Lugowski S, Petromilli C, Prusiner SB, Fraser PE, Goldberg JM, Chakrabartty A, Westaway D (2003) The PrP-like protein Doppel binds copper. *J Biol Chem* **278:** 8888-96

Qin K, Yang Y, Mastrangelo P, Westaway D (2002) Mapping Cu(II) binding sites in prion proteins by diethyl pyrocarbonate modification and matrix-assisted laser desorption ionization-time of flight (MALDI-TOF) mass spectrometric footprinting. *J Biol Chem* **277:** 1981-90

Rael LT, Rao NK, Thomas GW, Bar-Or R, Curtis CG, Bar-Or D (2007) Combined cupric- and cuprous-binding peptides are effective in preventing IL-8 release from endothelial cells and redox reactions. *Biochem Biophys Res Commun* **357:** 543-8

Rahman I (2002) Oxidative stress and gene transcription in asthma and chronic obstructive pulmonary disease: antioxidant therapeutic targets. *Curr Drug Targets Inflamm Allergy* **1:** 291-315

Rahman I (2006) Antioxidant therapies in COPD. *Int J Chron Obstruct Pulmon Dis* **1:** 15-29

Rahman I, Biswas SK, Kode A (2006) Oxidant and antioxidant balance in the airways and airway diseases. *Eur J Pharmacol* **533:** 222-39

Rajarathnam K, Sykes BD, Kay CM, Dewald B, Geiser T, Baggiolini M, Clark-Lewis I (1994) Neutrophil activation by monomeric interleukin-8. *Science* **264:** 90-2

Rao JK, Kroenke K, Mihaliak KA, Grambow SC, Weinberger M (2003) Rheumatology patients' use of complementary therapies: results from a one-year longitudinal study. *Arthritis Rheum* **49:** 619-25

Rao JK, Mihaliak K, Kroenke K, Bradley J, Tierney WM, Weinberger M (1999) Use of complementary therapies for arthritis among patients of rheumatologists. *Ann Intern Med* **131:** 409-16

Rao RM, Yang L, Garcia-Cardena G, Luscinskas FW (2007) Endothelial-dependent mechanisms of leukocyte recruitment to the vascular wall. *Circ Res* **101:** 234-47

Reale M, Intorno R, Tenaglia R, Feliciani C, Barbacane RC, Santoni A, Conti P (2002) Production of MCP-1 and RANTES in bladder cancer patients after bacillus Calmette-Guerin immunotherapy. *Cancer Immunol Immunother* **51:** 91-8

Redman BG, Esper P, Pan Q, Dunn RL, Hussain HK, Chenevert T, Brewer GJ, Merajver SD (2003) Phase II trial of tetrathiomolybdate in patients with advanced kidney cancer. *Clin Cancer Res* **9:** 1666-72

Reid DW, Misso N, Aggarwal S, Thompson PJ, Walters EH (2007) Oxidative stress and lipid-derived inflammatory mediators during acute exacerbations of cystic fibrosis. *Respirology* **12:** 63-9

Reinhardt PH, Elliott JF, Kubes P (1997) Neutrophils can adhere via alpha4beta1-integrin under flow conditions. *Blood* **89:** 3837-46

Rek AB, B. Geretti, E. Kungl, A.J. (2009) A biophysical insight into the RANTES-glycosaminoglycan interaction. *Biochimica et Biophysica Acta* **1794:** 577-582

Rendu F, Brohard-Bohn B (2001) The platelet release reaction: granules' constituents, secretion and functions. *Platelets* **12:** 261-73

Riccioni G, Barbara M, Bucciarelli T, di Ilio C, D'Orazio N (2007) Antioxidant vitamin supplementation in asthma. *Ann Clin Lab Sci* **37:** 96-101

Rice TM, Clarke RW, Godleski JJ, Al-Mutairi E, Jiang NF, Hauser R, Paulauskis JD (2001) Differential ability of transition metals to induce pulmonary inflammation. *Toxicol Appl Pharmacol* **177:** 46-53

Richards KL, McCullough J (1984) A modified microchamber method for chemotaxis and chemokinesis. *Immunol Commun* **13:** 49-62

Rot A (1992) Binding of neutrophil attractant/activation protein-1 (interleukin 8) to resident dermal cells. *Cytokine* **4:** 347-52

Rot A (1993) Neutrophil attractant/activation protein-1 (interleukin-8) induces in vitro neutrophil migration by haptotactic mechanism. *Eur J Immunol* **23:** 303-6

Rot A (1996) Inflammatory and Physiological Roles of Chemokines. *Pathol Oncol Res* **2:** 16-20

Rot A (2003) In situ binding assay for studying chemokine interactions with endothelial cells. *J Immunol Methods* **273:** 63-71

Rot A (2005) Contribution of Duffy antigen to chemokine function. *Cytokine Growth Factor Rev* **16:** 687-94

Rot A, Hub E, Middleton J, Pons F, Rabeck C, Thierer K, Wintle J, Wolff B, Zsak M, Dukor P (1996) Some aspects of IL-8 pathophysiology. III: Chemokine interaction with endothelial cells. *J Leukoc Biol* **59:** 39-44

Rot A, Krieger M, Brunner T, Bischoff SC, Schall TJ, Dahinden CA (1992) RANTES and macrophage inflammatory protein 1 alpha induce the migration and activation of normal human eosinophil granulocytes. *J Exp Med* **176:** 1489-95

Rubin BK (2008) Aerosolized antibiotics for non-cystic fibrosis bronchiectasis. *J Aerosol Med Pulm Drug Deliv* **21:** 71-6

Sablotzki A, Friedrich I, Muhling J, Dehne MG, Spillner J, Silber RE, Czeslik E (2002) The systemic inflammatory response syndrome following cardiac surgery: different expression of proinflammatory cytokines and procalcitonin in patients with and without multiorgan dysfunctions. *Perfusion* **17:** 103-9

Saczewski F, Dziemidowicz-Borys E, Bednarski PJ, Gdaniec M (2007) Synthesis, crystal structure, cytotoxic and superoxide dismutase activities of copper(II) complexes of N-(4,5-dihydroimidazol-2-yl)azoles. *Arch Pharm (Weinheim)* **340:** 333-8

Saetta M, Di Stefano A, Turato G, Facchini FM, Corbino L, Mapp CE, Maestrelli P, Ciaccia A, Fabbri LM (1998) CD8+ T-lymphocytes in peripheral airways of smokers with chronic obstructive pulmonary disease. *Am J Respir Crit Care Med* **157:** 822-6

Safaiyan F, Kolset SO, Prydz K, Gottfridsson E, Lindahl U, Salmivirta M (1999) Selective effects of sodium chlorate treatment on the sulfation of heparan sulfate. *J Biol Chem* **274:** 36267-73

Salcedo R, Young HA, Ponce ML, Ward JM, Kleinman HK, Murphy WJ, Oppenheim JJ (2001) Eotaxin (CCL11) induces in vivo angiogenic responses by human CCR3+ endothelial cells. *J Immunol* **166:** 7571-8

Sallusto F, Baggiolini M (2008) Chemokines and leukocyte traffic. *Nat Immunol* **9:** 949-52

Sallusto F, Lanzavecchia A, Mackay CR (1998a) Chemokines and chemokine receptors in T-cell priming and Th1/Th2-mediated responses. *Immunol Today* **19:** 568-74

Sallusto F, Lenig D, Mackay CR, Lanzavecchia A (1998b) Flexible programs of chemokine receptor expression on human polarized T helper 1 and 2 lymphocytes. *J Exp Med* **187:** 875-83

Sallusto F, Mackay CR, Lanzavecchia A (1997) Selective expression of the eotaxin receptor CCR3 by human T helper 2 cells. *Science* **277:** 2005-7

Salmi M, Jalkanen S (1992) A 90-kilodalton endothelial cell molecule mediating lymphocyte binding in humans. *Science* **257:** 1407-9

Salmi M, Jalkanen S (1995) Different forms of human vascular adhesion protein-1 (VAP-1) in blood vessels in vivo and in cultured endothelial cells: implications for lymphocyte-endothelial cell adhesion models. *Eur J Immunol* **25:** 2803-12

Salmi M, Jalkanen S (1996) Human vascular adhesion protein 1 (VAP-1) is a unique sialoglycoprotein that mediates carbohydrate-dependent binding of lymphocytes to endothelial cells. *J Exp Med* **183:** 569-79

Salmi M, Jalkanen S (2001) VAP-1: an adhesin and an enzyme. *Trends Immunol* **22:** 211-6

Salmi M, Jalkanen S (2005) Cell-surface enzymes in control of leukocyte trafficking. *Nat Rev Immunol* **5:** 760-71

Salmi M, Kalimo K, Jalkanen S (1993) Induction and function of vascular adhesion protein-1 at sites of inflammation. *J Exp Med* **178:** 2255-60

Salmi M, Yegutkin GG, Lehvonen R, Koskinen K, Salminen T, Jalkanen S (2001) A cell surface amine oxidase directly controls lymphocyte migration. *Immunity* **14:** 265-76

Samet JM, Graves LM, Quay J, Dailey LA, Devlin RB, Ghio AJ, Wu W, Bromberg PA, Reed W (1998) Activation of MAPKs in human bronchial epithelial cells exposed to metals. *Am J Physiol* **275:** L551-8

Santini C, Pellei M, Lobbia GG, Fedeli D, Falcioni G (2003) Synthesis and characterization of new copper(I) complexes containing 4-(diphenylphosphane)benzoic acid and "scorpionate" ligands with "in vitro" superoxide scavenging activity. *J Inorg Biochem* **94:** 348-54

Sawdey M, Podor TJ, Loskutoff DJ (1989) Regulation of type 1 plasminogen activator inhibitor gene expression in cultured bovine aortic endothelial cells. Induction by transforming growth factor-beta, lipopolysaccharide, and tumor necrosis factor-alpha. *J Biol Chem* **264:** 10396-401

Schall TJ (1991) Biology of the RANTES/SIS cytokine family. *Cytokine* **3:** 165-83

Schall TJ, Bacon K, Toy KJ, Goeddel DV (1990) Selective attraction of monocytes and T lymphocytes of the memory phenotype by cytokine RANTES. *Nature* **347:** 669-71

Schall TJ, Jongstra J, Dyer BJ, Jorgensen J, Clayberger C, Davis MM, Krensky AM (1988) A human T cell-specific molecule is a member of a new gene family. *J Immunol* **141:** 1018-25

Schilsky ML (1996) Wilson disease: genetic basis of copper toxicity and natural history. *Semin Liver Dis* **16:** 83-95

Schmitz T, Leroy MJ, Dallot E, Breuiller-Fouche M, Ferre F, Cabrol D (2003) Interleukin-1beta induces glycosaminoglycan synthesis via the prostaglandin E2 pathway in cultured human cervical fibroblasts. *Mol Hum Reprod* **9:** 1-8

Schnitzel W, Monschein U, Besemer J (1994) Monomer-dimer equilibria of interleukin-8 and neutrophil-activating peptide 2. Evidence for IL-8 binding as a dimer and oligomer to IL-8 receptor B. *J Leukoc Biol* **55:** 763-70

Schober A, Manka D, von Hundelshausen P, Huo Y, Hanrath P, Sarembock IJ, Ley K, Weber C (2002) Deposition of platelet RANTES triggering monocyte recruitment requires P-selectin and is involved in neointima formation after arterial injury. *Circulation* **106:** 1523-9

Schroder JM, Kameyoshi Y, Christophers E (1994) RANTES, a novel eosinophil-chemotactic cytokine. *Ann N Y Acad Sci* **725:** 91-103

Schuschke DA (1997) Dietary copper in the physiology of the microcirculation. *J Nutr* **127:** 2274-81

Schuschke DA, Falcone JC, Saari JT, Fleming JT, Percival SS, Young SA, Pass JM, Miller FN (2000) Endothelial cell calcium mobilization to acetylcholine is attenuated in copper-deficient rats. *Endothelium* **7:** 83-92

Schuschke DA, Saari JT, Miller FN (2001) Leukocyte-endothelial adhesion is impaired in the cremaster muscle microcirculation of the copper-deficient rat. *Immunol Lett* **76:** 139-44

Schwiebert LM, Estell K, Propst SM (1999) Chemokine expression in CF epithelia: implications for the role of CFTR in RANTES expression. *Am J Physiol* **276:** C700-10

Sekine Y, Yasufuku K, Heidler KM, Cummings OW, Van Rooijen N, Fujisawa T, Brown J, Wilkes DS (2000) Monocyte chemoattractant protein-1 and RANTES are chemotactic for graft infiltrating lymphocytes during acute lung allograft rejection. *Am J Respir Cell Mol Biol* **23:** 719-26

Sigurdsson EM, Brown DR, Alim MA, Scholtzova H, Carp R, Meeker HC, Prelli F, Frangione B, Wisniewski T (2003) Copper chelation delays the onset of prion disease. *J Biol Chem* **278:** 46199-202

Singh B, Tschernig T, van Griensven M, Fieguth A, Pabst R (2003) Expression of vascular adhesion protein-1 in normal and inflamed mice lungs and normal human lungs. *Virchows Arch* **442:** 491-5

Skelton NJ, Aspiras F, Ogez J, Schall TJ (1995) Proton NMR assignments and solution conformation of RANTES, a chemokine of the C-C type. *Biochemistry* **34:** 5329-42

Slimani H, Charnaux N, Mbemba E, Saffar L, Vassy R, Vita C, Gattegno L (2003) Binding of the CC-chemokine RANTES to syndecan-1 and syndecan-4 expressed on HeLa cells. *Glycobiology* **13:** 623-34

Smail EH, Briza P, Panagos A, Berenfeld L (1995) Candida albicans cell walls contain the fluorescent cross-linking amino acid dityrosine. *Infect Immun* **63:** 4078-83

Smit H, van der Goot H, Nauta WT, Timmerman H, de Bolster MW, Stouthamer AH, Vis RD (1982) Mechanism of action of the copper(I) complex of 2,9-dimethyl-1,10-phenanthroline on Mycoplasma gallisepticum. *Antimicrob Agents Chemother* **21:** 881-6

Smith DG, Cappai R, Barnham KJ (2007) The redox chemistry of the Alzheimer's disease amyloid beta peptide. *Biochim Biophys Acta* **1768:** 1976-90

Smith DP, Smith DG, Curtain CC, Boas JF, Pilbrow JR, Ciccotosto GD, Lau TL, Tew DJ, Perez K, Wade JD, Bush AI, Drew SC, Separovic F, Masters CL, Cappai R, Barnham KJ (2006) Copper-mediated amyloid-beta toxicity is associated with an intermolecular histidine bridge. *J Biol Chem* **281:** 15145-54

Smith GF, McCurdy WH (1952) 2,9-Dimethyl-1,10-phenanthroline. *Analytical Chemistry* **24:** 371-73

Smith GF, Wilkins DH (1953) New Colorimetric Reagent Specific for Cooper. *Analytical Chemistry* **25:** 510-11

Sozgen K, Cekic SD, Tutem E, Apak R (2006) Spectrophotometric total protein assay with copper(II)-neocuproine reagent in alkaline medium. *Talanta* **68:** 1601-9

Spillmann D, Witt D, Lindahl U (1998) Defining the interleukin-8-binding domain of heparan sulfate. *J Biol Chem* **273:** 15487-93

Springer TA (1994) Traffic signals for lymphocyte recirculation and leukocyte emigration: the multistep paradigm. *Cell* **76:** 301-14

Squitti R, Lupoi D, Pasqualetti P, Dal Forno G, Vernieri F, Chiovenda P, Rossi L, Cortesi M, Cassetta E, Rossini PM (2002) Elevation of serum copper levels in Alzheimer's disease. *Neurology* **59:** 1153-61

Squitti R, Pasqualetti P, Dal Forno G, Moffa F, Cassetta E, Lupoi D, Vernieri F, Rossi L, Baldassini M, Rossini PM (2005) Excess of serum copper not related to ceruloplasmin in Alzheimer disease. *Neurology* **64:** 1040-6

Stanczak P, Valensin D, Juszczyk P, Grzonka Z, Migliorini C, Molteni E, Valensin G, Gaggelli E, Kozlowski H (2005a) Structure and Stability of the Cu(II) Complexes with Tandem Repeats of the Chicken Prion. *Biochemistry* **44:** 12940-54

Stanczak P, Valensin D, Juszczyk P, Grzonka Z, Valensin G, Bernardi F, Molteni E, Gaggelli E, Kozlowski H (2005b) Fine tuning the structure of the Cu(2+) complex with the prion protein chicken repeat by proline isomerization. *Chem Commun (Camb)*: 3298-300

Strecker D (2005) [Copper content in rheumatoid arthritis patients]. *Ann Acad Med Stetin* **51 Suppl 1:** 129-33

Struthers GR, Scott DL, Scott DG (1983) The use of 'alternative treatments' by patients with rheumatoid arthritis. *Rheumatol Int* **3:** 151-2

Sugasawa H, Ichikura T, Tsujimoto H, Kinoshita M, Morita D, Ono S, Chochi K, Tsuda H, Seki S, Mochizuki H (2008) Prognostic significance of expression of CCL5/RANTES receptors in patients with gastric cancer. *J Surg Oncol* **97:** 445-50

Sundstrom JB, McMullan LK, Spiropoulou CF, Hooper WC, Ansari AA, Peters CJ, Rollin PE (2001) Hantavirus infection induces the expression of RANTES and IP-10 without causing increased permeability in human lung microvascular endothelial cells. *J Virol* **75:** 6070-85

Swiatek M, Valensin D, Migliorini C, Gaggelli E, Valensin G, Jezowska-Bojczuk M (2005) Unusual binding ability of vancomycin towards Cu2+ ions. *Dalton Trans*: 3808-13

Takasaki S, Kato Y, Murata M, Homma S, Kawakishi S (2005) Effects of peroxidase and hydrogen peroxide on the dityrosine formation and the mixing characteristics of wheat-flour dough. *Biosci Biotechnol Biochem* **69:** 1686-92

Tapiero H, Townsend DM, Tew KD (2003) Trace elements in human physiology and pathology. Copper. *Biomed Pharmacother* **57:** 386-98

Taylor KR, Gallo RL (2006) Glycosaminoglycans and their proteoglycans: host-associated molecular patterns for initiation and modulation of inflammation. *Faseb J* **20:** 9-22

Terada N, Maesako K, Hamano N, Ikeda T, Sai M, Yamashita T, Fukuda S, Konno A (1996) RANTES production in nasal epithelial cells and endothelial cells. *J Allergy Clin Immunol* **98:** S230-7

Teran LM, Mochizuki M, Bartels J, Valencia EL, Nakajima T, Hirai K, Schroder JM (1999) Th1- and Th2-type cytokines regulate the expression and production of eotaxin and RANTES by human lung fibroblasts. *Am J Respir Cell Mol Biol* **20:** 777-86

Tew D, Ortiz de Montellano PR (1988) The myoglobin protein radical. Coupling of Tyr-103 to Tyr-151 in the H2O2-mediated cross-linking of sperm whale myoglobin. *J Biol Chem* **263:** 17880-6

Thienel U, Loike J, Yellin MJ (1999) CD154 (CD40L) induces human endothelial cell chemokine production and migration of leukocyte subsets. *Cell Immunol* **198:** 87-95

Togashi Y, Li Y, Kang JH, Takeichi N, Fujioka Y, Nagashima K, Kobayashi H (1992) D-penicillamine prevents the development of hepatitis in Long-Evans Cinnamon rats with abnormal copper metabolism. *Hepatology* **15:** 82-7

Tripathy D, Thirumangalakudi L, Grammas P (2008) RANTES upregulation in the Alzheimer's disease brain: A possible neuroprotective role. *Neurobiol Aging*

Tsakiris DA, Scudder L, Hodivala-Dilke K, Hynes RO, Coller BS (1999) Hemostasis in the mouse (Mus musculus): a review. *Thromb Haemost* **81:** 177-88

Tsicopoulos A, Hamid Q, Varney V, Ying S, Moqbel R, Durham SR, Kay AB (1992) Preferential messenger RNA expression of Th1-type cells (IFN-gamma+, IL-2+) in classical delayed-type (tuberculin) hypersensitivity reactions in human skin. *J Immunol* **148:** 2058-61

Tsujimoto M, Yokota S, Vilcek J, Weissmann G (1986) Tumor necrosis factor provokes superoxide anion generation from neutrophils. *Biochem Biophys Res Commun* **137:** 1094-100

Tsukishiro S, Suzumori N, Nishikawa H, Arakawa A, Suzumori K (2006) Elevated serum RANTES levels in patients with ovarian cancer correlate with the extent of the disorder. *Gynecol Oncol* **102:** 542-5

Tutem E, Apak R, Gunaydi E, Sozgen K (1997) Spectrophotometric determination of vitamin E (alpha-tocopherol) using copper(II)-neocuproine reagent. *Talanta* **44:** 249-255

Twomey PJ, Wierzbicki AS, House IM, Viljoen A, Reynolds TM (2007) Percentage non-caeruloplasmin bound copper. *Clin Biochem* **40:** 749-50

Ulfman LH, Joosten DP, van Aalst CW, Lammers JW, van de Graaf EA, Koenderman L, Zwaginga JJ (2003) Platelets promote eosinophil adhesion of patients with asthma to endothelium under flow conditions. *Am J Respir Cell Mol Biol* **28:** 512-9

Vaday GG, Peehl DM, Kadam PA, Lawrence DM (2006) Expression of CCL5 (RANTES) and CCR5 in prostate cancer. *Prostate* **66:** 124-34

Vakulenko SB, Mobashery S (2003) Versatility of aminoglycosides and prospects for their future. *Clin Microbiol Rev* **16:** 430-50

Valachova K, Hrabarova E, Gemeiner P, Soltes L (2008) Study of pro- and anti-oxidative properties of D-penicillamine in a system comprising high-molar-mass hyaluronan, ascorbate, and cupric ions. *Neuro Endocrinol Lett* **29:** 697-701

Valen G, Erl W, Eriksson P, Wuttge D, Paulsson G, Hansson GK (1999) Hydrogen peroxide induces mRNA for tumour necrosis factor alpha in human endothelial cells. *Free Radic Res* **31:** 503-12

Valone FH, Austen KF, Goetzl EJ (1974) Modulation of the random migration of human platelets. *J Clin Invest* **54:** 1100-6

van der Vliet A, Eiserich JP, Marelich GP, Halliwell B, Cross CE (1997) Oxidative stress in cystic fibrosis: does it occur and does it matter? *Adv Pharmacol* **38:** 491-513

Vargaftig BB, Joseph D, Marlas G, Chevance LG (1982) Degranulation of rabbit platelets with PAF-acether: a new procedure for unravelling the mode of action of platelet-activating substances. *Thromb Haemost* **48:** 67-71

Varma SD, Devamanoharan PS (1991) Hydrogen peroxide in human blood. *Free Radic Res Commun* **14:** 125-31

Venge J, Lampinen M, Hakansson L, Rak S, Venge P (1996) Identification of IL-5 and RANTES as the major eosinophil chemoattractants in the asthmatic lung. *J Allergy Clin Immunol* **97:** 1110-5

Versieck JaC, R (1980) Normal levels of trace elements in human blood plasma or serum. *Analytica Chimica Acta* **116:** 217-254

Vives RR, Sadir R, Imberty A, Rencurosi A, Lortat-Jacob H (2002) A kinetics and modeling study of RANTES(9-68) binding to heparin reveals a mechanism of cooperative oligomerization. *Biochemistry* **41:** 14779-89

Volin MV, Shah MR, Tokuhira M, Haines GK, Woods JM, Koch AE (1998) RANTES expression and contribution to monocyte chemotaxis in arthritis. *Clin Immunol Immunopathol* **89:** 44-53

Volpi N, Tarugi P (1999) The protective effect on Cu2+- and AAPH-mediated oxidation of human low-density lipoproteins depends on glycosaminoglycan structure. *Biochimie* **81:** 955-63

von Hundelshausen P, Weber KS, Huo Y, Proudfoot AE, Nelson PJ, Ley K, Weber C (2001) RANTES deposition by platelets triggers monocyte arrest on inflamed and atherosclerotic endothelium. *Circulation* **103:** 1772-7

Wadsworth JD, Hill AF, Joiner S, Jackson GS, Clarke AR, Collinge J (1999) Strain-specific prion-protein conformation determined by metal ions. *Nat Cell Biol* **1:** 55-9

Wagner JG, Roth RA (2000) Neutrophil migration mechanisms, with an emphasis on the pulmonary vasculature. *Pharmacol Rev* **52:** 349-74

Wagner L, Yang OO, Garcia-Zepeda EA, Ge Y, Kalams SA, Walker BD, Pasternack MS, Luster AD (1998a) Beta-chemokines are released from HIV-1-specific cytolytic T-cell granules complexed to proteoglycans. *Nature* **391:** 908-11

Wagner M, Klein CL, van Kooten TG, Kirkpatrick CJ (1998b) Mechanisms of cell activation by heavy metal ions. *J Biomed Mater Res* **42:** 443-52

Walker WR, Beveridge SJ, Whitehouse MW (1980) Anti-inflammatory activity of a dermally applied copper salicylate preparation (Alcusal). *Agents Actions* **10:** 38-47

Walker WR, Beveridge SJ, Whitehouse MW (1981) Dermal copper drugs: the copper bracelet and cu(II) salicylate complexes. *Agents Actions Suppl* **8:** 359-67

Walker WR, Griffin BJ (1976) The solubility of copper in human sweat. *Search* **7:** 100

Walker WR, Keats DM (1976) An investigation of the therapeutic value of the 'copper bracelet'-dermal assimilation of copper in arthritic/rheumatoid conditions. *Agents Actions* **6:** 454-9

Walker WR, Reeves RR (1977) Perfusion of intact skin by a saline solution of bis(glycinato) copper(II). *Bioinorg Chem* **7:** 271-6

Walshe JM (1956) Penicillamine, a new oral therapy for Wilson's disease. *Am J Med* **21:** 487-95

Walshe JM (1982) Treatment of Wilson's disease with trientine (triethylene tetramine) dihydrochloride. *Lancet* **1:** 643-7

Walz A, Peveri P, Aschauer H, Baggiolini M (1987) Purification and amino acid sequencing of NAF, a novel neutrophil-activating factor produced by monocytes. *Biochem Biophys Res Commun* **149:** 755-61

Ward SG, Bacon K, Westwick J (1998) Chemokines and T lymphocytes: more than an attraction. *Immunity* **9:** 1-11

Ward SG, Westwick J (1998) Chemokines: understanding their role in T-lymphocyte biology. *Biochem J* **333 (Pt 3):** 457-70

Warner RG, Hundt C, Weiss S, Turnbull JE (2002) Identification of the heparan sulfate binding sites in the cellular prion protein. *J Biol Chem* **277:** 18421-30

Weber C, Weber KS, Klier C, Gu S, Wank R, Horuk R, Nelson PJ (2001) Specialized roles of the chemokine receptors CCR1 and CCR5 in the recruitment of monocytes and T(H)1-like/CD45RO(+) T cells. *Blood* **97:** 1144-6

Weingart C, Nelson PJ, Kramer BK, Mack M (2008) Dose dependent effects of platelet derived chondroitinsulfate A on the binding of CCL5 to endothelial cells. *BMC Immunol* **9:** 72

Wells TN, Guye-Coulin F, Bacon KB (1995) Peptides from the amino-terminus of RANTES cause chemotaxis of human T-lymphocytes. *Biochem Biophys Res Commun* **211:** 100-5

Wells TN, Power CA, Lusti-Narasimhan M, Hoogewerf AJ, Cooke RM, Chung CW, Peitsch MC, Proudfoot AE (1996) Selectivity and antagonism of chemokine receptors. *J Leukoc Biol* **59:** 53-60

Weser U, Schubotz LM (1981) Catalytic reaction of copper complexes with superoxide. *Agents Actions Suppl* **8:** 103-20

Wetlaufer DB (1962) Ultraviolet spectra of proteins and amino acids. *Adv Protein Chem* **17:** 303-390

Weyrich AS, Denis MM, Schwertz H, Tolley ND, Foulks J, Spencer E, Kraiss LW, Albertine KH, McIntyre TM, Zimmerman GA (2007) mTOR-dependent synthesis of Bcl-3 controls the retraction of fibrin clots by activated human platelets. *Blood* **109:** 1975-83

Weyrich AS, Lindemann S, Zimmerman GA (2003) The evolving role of platelets in inflammation. *J Thromb Haemost* **1:** 1897-905

White AR, Huang X, Jobling MF, Barrow CJ, Beyreuther K, Masters CL, Bush AI. Cappai R (2001) Homocysteine potentiates copper- and amyloid beta peptide-mediated toxicity in primary neuronal cultures: possible risk factors in the Alzheimer's-type neurodegenerative pathways. *J Neurochem* **76:** 1509-20

Williams HL, Johnson DJ, Haut MJ (1977) Simultaneous spectrophotometry of Fe2+ and Cu2+ in serum denatured with guanidine hydrochloride. *Clin Chem* **23:** 237-40

Williams MA, Cave CM, Quaid G, Robinson C, Daly TJ, Witt D, Lentsch AB, Solomkin JS (2005) Interleukin 8 dimerization as a mechanism for regulation of neutrophil adherence-dependent oxidant production. *Shock* **23:** 371-6

Wood PL, Khan MA, Moskal JR (2008) Mechanism of action of the disease-modifying anti-arthritic thiol agents D-penicillamine and sodium aurothiomalate: restoration of cellular free thiols and sequestration of reactive aldehydes. *Eur J Pharmacol* **580:** 48-54

Wozniak K, Blasiak J (2002) Free radicals-mediated induction of oxidized DNA bases and DNA-protein cross-links by nickel chloride. *Mutat Res* **514:** 233-43

Xiao W, Hsu YP, Ishizaka A, Kirikae T, Moss RB (2005) Sputum cathelicidin, urokinase plasminogen activation system components, and cytokines discriminate cystic fibrosis, COPD, and asthma inflammation. *Chest* **128:** 2316-26

Yamini Y, Tamaddon A (1999) Solid-phase extraction and spectrophotometric determination of trace amounts of copper in water samples. *Talanta* **49:** 119-24

Yanagishita M, Hascall VC (1992) Cell surface heparan sulfate proteoglycans. *J Biol Chem* **267:** 9451-4

Yaron I, Meyer FA, Dayer JM, Bleiberg I, Yaron M (1989) Some recombinant human cytokines stimulate glycosaminoglycan synthesis in human synovial fibroblast cultures and inhibit it in human articular cartilage cultures. *Arthritis Rheum* **32:** 173-80

Ying S, Meng Q, Taborda-Barata L, Corrigan CJ, Barkans J, Assoufi B, Moqbel R, Durham SR, Kay AB (1996) Human eosinophils express messenger RNA encoding RANTES and store and release biologically active RANTES protein. *Eur J Immunol* **26:** 70-6

Yoshida A, Ohba M, Wu X, Sasano T, Nakamura M, Endo Y (2002) Accumulation of platelets in the lung and liver and their degranulation following antigen-challenge in sensitized mice. *Br J Pharmacol* **137:** 146-52

Yoshimura T, Matsushima K, Tanaka S, Robinson EA, Appella E, Oppenheim JJ, Leonard EJ (1987) Purification of a human monocyte-derived neutrophil chemotactic factor that has peptide sequence similarity to other host defense cytokines. *Proc Natl Acad Sci U S A* **84:** 9233-7

Yoshimura T, Yuhki N, Moore SK, Appella E, Lerman MI, Leonard EJ (1989) Human monocyte chemoattractant protein-1 (MCP-1). Full-length cDNA cloning, expression in mitogen-stimulated blood mononuclear leukocytes, and sequence similarity to mouse competence gene JE. *FEBS Lett* **244:** 487-93

Yu PH, Lu LX, Fan H, Kazachkov M, Jiang ZJ, Jalkanen S, Stolen C (2006) Involvement of semicarbazide-sensitive amine oxidase-mediated deamination in lipopolysaccharide-induced pulmonary inflammation. *Am J Pathol* **168:** 718-26

Zhu BZ, Antholine WE, Frei B (2002) Thiourea protects against copper-induced oxidative damage by formation of a redox-inactive thiourea-copper complex. *Free Radic Biol Med* **32:** 1333-8

Zimmerman GA, Renzetti AD, Hill HR (1984) Granulocyte adherence in pulmonary and systemic arterial blood samples from patients with adult respiratory distress syndrome. *Am Rev Respir Dis* **129:** 798-804

Ziora D, Dworniczak S, Niepsuj G, Krol W, Oklek K (1999) [Chemokine RANTES in bronchoalveolar lavage fluid(BAL)from two different lung segments indicated by high resolution tomography (HRCT) in patients with sarcoidosis]. *Pneumonol Alergol Pol* **67:** 525-35

Zoli A, Altomonte L, Caricchio R, Galossi A, Mirone L, Ruffini MP, Magaro M (1998) Serum zinc and copper in active rheumatoid arthritis: correlation with interleukin 1 beta and tumour necrosis factor alpha. *Clin Rheumatol* **17:** 378-82

Zucker-Franklin D, Philipp CS (2000) Platelet production in the pulmonary capillary bed: new ultrastructural evidence for an old concept. *Am J Pathol* **157:** 69-74